CONTENTS

Vol. 3, Issues Nos. 1–12

Journal of Polymer Science
Part A: General Papers

ISSUE No. 4, APRIL

Issue No. 5, May

Book Reviews

Notes

Issue No. 7, July

Notes

ISSUE No. 9, SEPTEMBER

ISSUE NO. 10, OCTOBER

ISSUE No. 12, DECEMBER

Some Remarks on Amorphous and Atactic α-Olefin Polymers and Random Ethylene–Propylene Copolymers

G. NATTA, A. VALVASSORI, F. CIAMPELLI, and G. MAZZANTI,
Institute of Industrial Chemistry, Polytechnic of Milan, Milan, Italy, and
*Milan Research Institute "G. Donegani" of Montecatini S.p.A.,
Milan, Italy*

Synopsis

The necessity is pointed out to distinguish between an "amorphous" α-olefin polymer and an "atactic" α-olefin polymer. It is convenient to limit the term "atactic" only to those amorphous linear regularly head-to-tail polymers which possess the same chemical regularity as the corresponding tactic polymers, from which they differ only for the lack of steric regularity. A clear interpretation is given of the presence of bands at 1155 and 915 cm.$^{-1}$ in the IR spectra of isotactic and atactic polypropylenes. The presence of these bands is due to the —CH$_2$—CH— monomeric unit, with a regular head
$$\quad\quad\quad\quad\quad\quad |$$
$$\quad\quad\quad\quad\quad CH_3$$
to-tail arrangement. The absence of these bands in the propylene polymers obtained with the aid of cationic-type catalysts depends on the presence of a very small content of monomeric units of this type. Finally the conclusion is drawn that the presence of the two above-mentioned bands in the IR spectrum of the ethylene–propylene copolymers does not indicate the presence of long propylene sequences of the isotactic type, and therefore the existence of a block copolymer, but only the presence of the monomeric unit mentioned above.

Tactic polymers of α-olefins were discovered more than ten years ago[1] and their nomenclature was defined in detail shortly thereafter.[2] However, there is still some confusion when it comes to defining actual polymers in terms of their steric structure. One reason for this is probably the fact that actual α-olefin polymers can be classified according to the definitions of tacticity which were established with reference to ideal macromolecules. Furthermore, the degree of tacticity of α-olefin polymers is not determined, in general, through actual, direct measurements of the number of steric inversions or permanences, but is derived indirectly through the measure of certain physical properties,[2] such as solubility and crystallinity. This indirect method is obviously only approximate and does not allow one to establish the actual number of steric inversions which may occur along the polymer chains.

A particular state of confusion seems to exist with regard to "atactic" and of "amorphous" α-olefin polymers. An ideal atactic α-olefin polymer

can be defined[2] as a macromolecular compound in which monomer units of enantiomorphous steric configuration are distributed at random.   In reality, for an α-olefin polymer to have the properties (solubility in certain organic solvents, lack of crystallinity) of an atactic polymer it will not be absolutely necessary that such a perfect random distribution exists;   as shown by one of us[2] the presence of tactic blocks (stereoblocks) will not alter those properties, provided these blocks are sufficiently short (see also recent NMR studies of amorphous polypropylene[3]).

What we would like to stress particularly here is the need to draw a distinction between an "amorphous" α-olefin polymer in general and an "atactic" α-olefin polymer.

An α-olefin polymer can be amorphous (noncrystalline) not only because of irregular steric structure but also because of the presence in its macromolecules of irregularities and inversions in the enchainment of the monomer units, and also of monomer units which may be chemically different from each other, although derived from a single monomer.

In α-olefin polymers obtained through anionic coordinated polymerization no such chemical irregularities exist; amorphous α-olefin polymers thus obtained are amorphous only because of lack or insufficiency of steric regularity.   They are linear, regular head-to-tail polymers, which possess the same chemical regularity as the cooresponding tactic polymers, from which they differ only because of lack of steric regularity.   (Steric regularity presupposes the existence of chemical regularity in the polymer macromolecules.)   Therefore it is convenient to limit the term "atactic" only to such amorphous polymers.   Some authors,[4,5] however, have not taken this into account, and have recently considered as atactic polymers those which possess no chemical regularity at all.

This has led to an incorrect interpretation of certain bands of the infrared spectrum of polypropylene, and consequently to incorrect considerations on the structure of ethylene–propylene copolymers obtained through anionic coordinated polymerization.   These authors,[4,5] in fact, have noticed that propylene polymers obtained through cationic polymerization do not show in the infrared spectrum the bands at 1155 and 975 cm.$^{-1}$ which are always present in the infrared spectra of both crystalline and amorphous polypropylenes (ether extract or polymers in the molten state) obtained through anionic coordinated polymerization.   The bands at 1155 and 975 cm.$^{-1}$ were attributed to isotactic polypropylene, and it was concluded[4,5] that their presence in an ethylene–propylene copolymer was indicative of the presence of isotactic polypropylene sequences and therefore the existence of a block copolymer instead of a random copolymer.   These conclusions arc completely contrary to what can be derived from other experimental data, which we have accurately collected.

Bands at 1155 cm.$^{-1}$ and in the range 975–930 cm.$^{-1}$ are cited in the literature[6,7] as characteristic of the group

$$\begin{array}{c} CH_3 \\ | \\ -CH_2-CH-CH_2- \end{array}$$
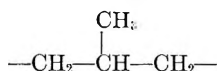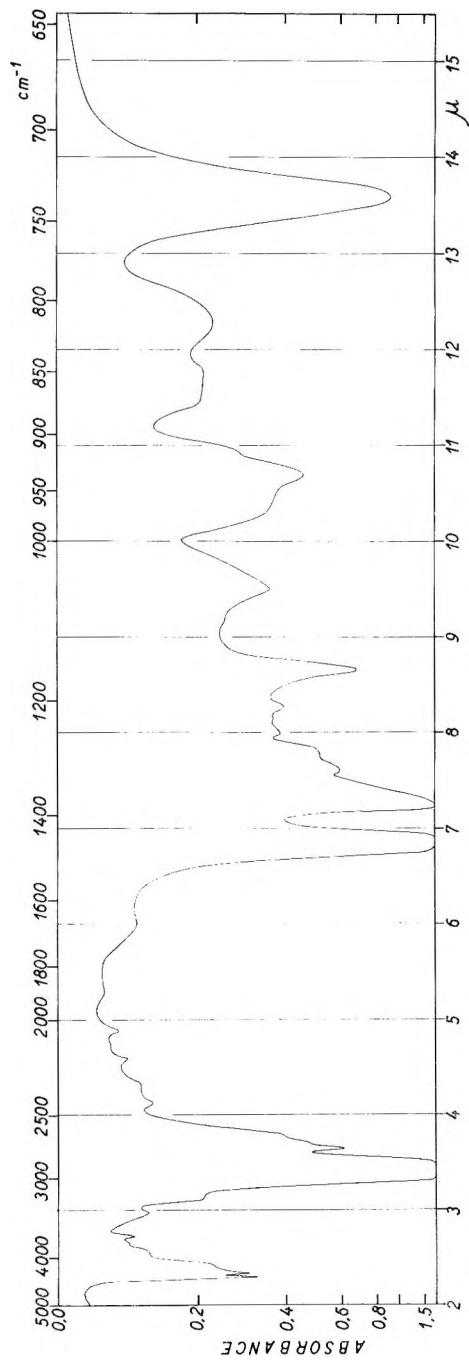
Fig. 1. Infrared spectrum of the ethylene–propylene alternating copolymer obtained by hydrogenation of polyisoprene.

TABLE I

Polymer	Content of various monomeric units by infrared, %					
	$-CH-CH_2-$ $\quad\ \ CH_3$ (1155 cm.$^{-1}$)	$-CH_2-CH-CH-CH_2-$ $\qquad CH_3\ \ CH_3$ (750, 1120 cm.$^{-1}$)	$-CH-$ CH_2-CH_3 (775 cm.$^{-1}$)	$-CH_2-CH_2-CH_2-$ (735 cm.$^{-1}$)	$\qquad CH_3$ $-C-$ $\qquad CH_3$ (1378, 1245 cm.$^{-1}$)	$-(CH_2)_n-$ for $n > 3$ (723 cm.$^{-1}$)
Polypropylenes obtained by fraction-ation of a crude polymer containing isotactic portions						
A. Boiling n-heptane-insoluble fraction: isotactic polypro-pylene	~100	Traces	—	—	—	—
B. Boiling ethyl ether-insoluble, but boiling n-heptane-soluble fraction: isotactic stereoblock polypropylene	~98	~2	—	—	—	—
C. Boiling ethyl ether-soluble fraction atactic polypropylene	~95	~5	—	—	—	—

Polypropylenes obtained in the presence of catalysts acting through an anionic coordinated mechanism, able to polymerize propylene with syndiotactic enchainment[15]						
A. Crystalline syndiotactic polypropylene	98–100%	0–2	—	—	—	—
B. Atactic polypropylene	~95	~5	—	Traces	—	—
Polypropylenes obtained in the presence of catalytic systems acting with cationic mechanism						
A. Polypropylene obtained in the presence of the catalytic system Al(C₂H₅)Cl₂ + TiCl₄ (Al/Ti molar ratio = 1.5)[20]	~15	~20	~20	~30	~10	~5
B. Polypropylene obtained in the presence of AlCl₃[14]	~10	~25	~25	~30	~5	~5
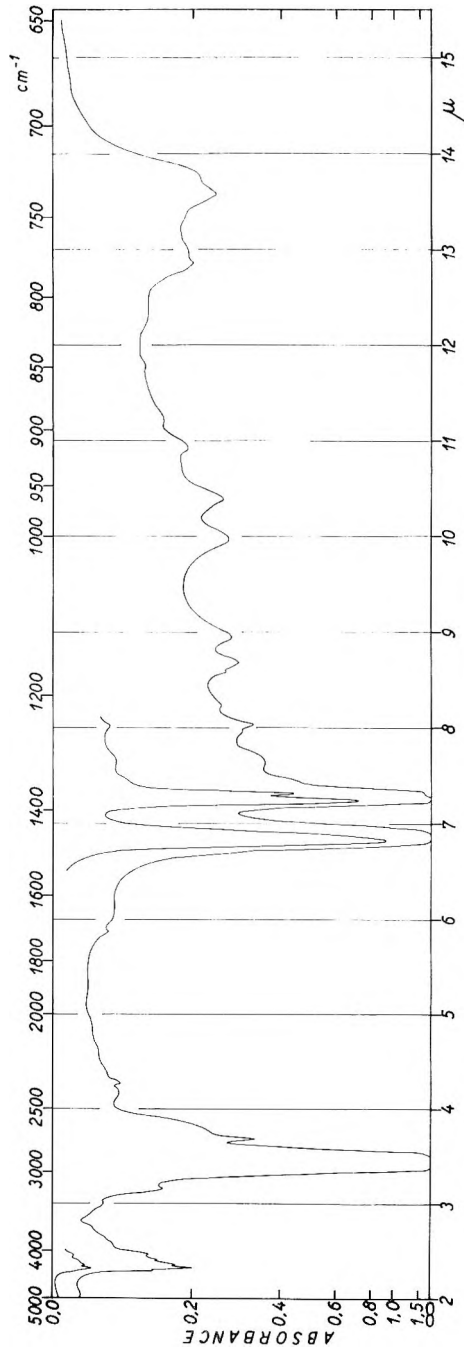
Fig. 2. Infrared spectrum of propylene polymer obtained in the presence of TiCl$_4$ and Al(C$_2$H$_5$) Cl$_2$ (Al/Ti molar ratio = 1.5).

The band at 1155 cm.$^{-1}$ is in a very constant position, both for 3-methyl paraffins and 4-methyl paraffins and other substances containing the group

$$R\text{---}(CH_2)_{n1}\text{---}\overset{\displaystyle CH_3}{\underset{\displaystyle |}{CH}}\text{---}(CH_2)_{n2}\text{---}R$$
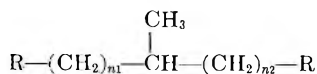
These include squalane (2,6,10,15,19,23-hexamethyltetracosane; API infrared spectrum no. 2290) and the polymer having the structure of the alternating ethylene–propylene copolymer obtainable by hydrogenation of 1,4-polyisoprene (Fig. 1).[8]   The position of this 1155 cm.$^{-1}$ band is independent of the values of n_1 and n_2, provided they are both equal to or higher than one.   On the contrary, the position of the second band shifts in the range between 975 and 930 cm.$^{-1}$, depending on the values of n_1 and n_2.

In 3-methyl paraffins and in such substances as 2,2,4-trimethylhexane and 3,3,5-trimethylpentane this band can be observed at about 965 cm.$^{-1}$, for 4-methyl paraffins it is seen at about 955 cm.$^{-1}$; in squalane the band is at 930 cm.$^{-1}$, a position near that observed for the polymer, obtained by hydrogenation of polyisoprene (Fig. 1), having the structure of an alternating ethylene–propylene copolymer.

It is therefore evident that the shift of this band when observed in ethylene–propylene copolymers can give some indication of the distribution of propylene sequences in the copolymer.   (Some experiments on this relationship presently being carried out appear quite promising.)

These bands, however, are not at all related to the isotacticity of polypropylene.   (In fact, they are present also in the infrared spectrum of syndiotactic polypropylene.[9])   The fact that they are not practically present in propylene polymers obtained in the presence of cationic-type catalysts can be easily explained by the fact that the propylene units of these polymers do not have a regular head-to-tail enchainment and that such polymers contain many different units that, although derived from propylene, do not have the —CH$_2$—CH(CH$_3$)— structure (Table I).

Figure 2 shows the spectrum of a propylene polymer obtained in the presence of a catalytic system formed by Al(C$_2$H$_5$)Cl$_2$ and TiCl$_4$ (Al/Ti ratio = 1.5) which, as is well known,[10,11] is supposed to act through a cationic mechanism, due to the low Al/Ti ratio.

A band at 735 cm.$^{-1}$ is noted which can be attributed to sequences of the —(CH$_2$)$_3$— type, the concentration of which, on the basis of a comparison between the intensity of this band and of the band present in the spectrum of hydrogenated polyisoprene, can be calculated to be about 30%.

The band at 775 cm.$^{-1}$ can be ascribed to structures of the —CH(CH$_2$CH$_3$)— type.   If the intensity of this band is compared with that present in the spectrum of polybutene-1, a concentration of about 20% can be calculated   The bands at 1120 and 750 cm.$^{-1}$ can be attributed to structures of the CH$_2$—CH(CH$_3$)—CH(CH$_3$)—CH$_2$— type; by comparing the intensity of these bands with those present in the spectrum of an alternating ethylene–butene-2 copolymer,[12] a concentration of about 20% can

be calculated. From the bands at 1378 and 1245 cm.$^{-1}$ the presence of about 10% of units of the —C(CH$_3$)$_2$— type can be deduced.

These measures, although being only of an approximate character, lead to the conclusion that in the cationic type polymer under examination there are comparatively few propylene units of the —CH(CH$_3$)—CH$_2$— type, having a regular head-to-tail enchainment.

By adopting a method of analysis used for ethylene–propylene copolymers[13] based on the measurement of the band at 1155 cm.$^{-1}$, the presence of only 15% of these units can be deduced. We have obtained similar results also on examining a polymer obtained from propylene in the presence of AlCl$_3$ as catalyst (see Table I).[4,14]

The results of the infrared examination of certain propylene polymers obtained through cationic polymerization are reported in Table I and compared with results for crystalline and amorphous polypropylenes obtained through anionic coordinated polymerization.

These considerations with respect to polypropylene can be applied also to ethylene–propylene copolymers. The presence of bands at 1155 cm.$^{-1}$ and at about 970 cm.$^{-1}$ does not indicate the presence of long sequences of isotactic propylene units, but only of propylene units of the —CH(CH$_3$)—CH$_2$— type regularly enchained with other propylene units or with ethylene units.

In the infrared spectra of copolymers obtained through anionic coordinated polymerization, bands are present at 1155 cm.$^{-1}$ and in the range 970–930 cm.$^{-1}$ The intensity of these bands decreases with a decrease of the propylene content in the copolymer.

In copolymers which we have prepared using the catalytic system VCl$_4$ + SnPh$_4$ + AlBr$_3$ according to Phillips and Carrick,[16] we have observed that these bands (comparatively weak) have an intensity corresponding to low propylene contents. But, in ethylene–propylene copolymers obtained with the aid of free radical catalysts[17] these bands are not observed; this is because the number of —CH(CH$_3$)—CH$_2$— groups in these copolymers is very small, much smaller in fact than the number that would result from the propylene content in the copolymers.

In ethylene–propylene copolymers obtained with the aid of catalysts formed by alkyl aluminum compounds and transition metal salts, the bands at 1155 and at about 970 cm.$^{-1}$ should be considered as characteristic of the —CH(CH$_3$)—CH$_2$— propylene units in random or block distribution. While variations in the propylene sequence distribution do not influence the position of the first band, they influence both position and form of the second band (Fig. 3).

As for the possibility of employing the band at 1155 cm.$^{-1}$ to determine the propylene content in an ethylene–propylene copolymer, we have noted[13] a relationship, not very far from linearity, between absorbance of the band at 1155 cm.$^{-1}$ and contents —CH(CH$_3$)—CH$_2$— propylene units.

The examination of different series of ethylene–propylene copolymers obtained by use of different anionic coordinated catalyst systems is now in
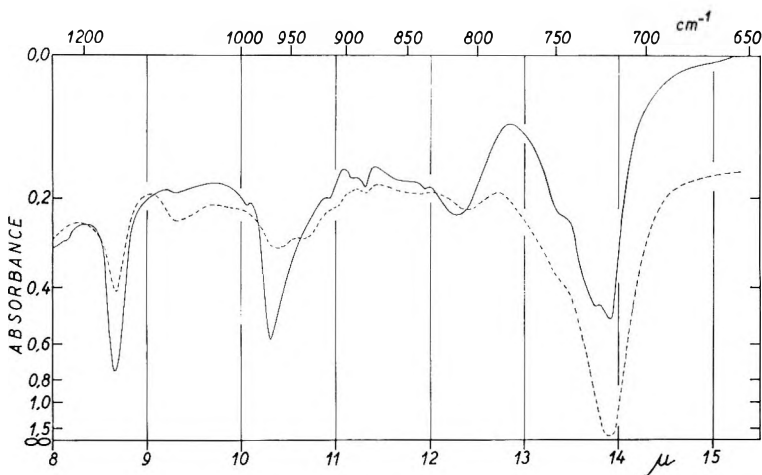
Fig. 3. Infrared spectra of ethylene–propylene copolymers having propylene sequences of different lengths. (———) long propylene sequences: (- -) short propylene sequences.

progress, in order to establish whether and to what extent the absorbance of the band at 1155 cm.$^{-1}$ is influenced by possible variations in the enchainment and distribution of the various monomer units.

We are also examining the absorbance of the bands used in other infrared methods of analysis of ethylene–propylene copolymers.[18-21] We have noticed that the absorbance of the band at 1155 cm.$^{-1}$ varies somewhat with the copolymerization catalyst used; however, the variations determined so far do not appear sufficient to prevent the possibility of using infrared methods of analysis based on this band.

References

1. Natta, G., *J. Polymer Sci.*, **16**, 143 (1955); G. Natta, P. Pino, P. Corradini, F. Danusso, E. Mantica, G. Mazzanti, and G. Moraglio, *J. Am. Chem. Soc.*, **77**, 1708 (1955).

2. Natta, G., G. Mazzanti, G. Crespi, and G. Moraglio, *Chim. Ind. (Milan)*, **39**, 275 (1957); G. Natta, G. Mazzanti, and P. Longi, *Chim. Ind. (Milan)*, **40**, 183 (1958); G. Natta, *J. Polymer Sci.*, **34**, 531 (1959); G. Natta and F. Danusso, *J. Polymer Sci.*, **34**, 3 (1959).

3. Woodbrey, J. C., *J. Polymer Sci.*, **B2**, 315 (1964).

4. Falt, V. L., J. T. Shipman, and S. Krimm, *J. Polymer Sci.*, **61**, S17 (1962).

5. Lomonte, J. M., *J. Polymer Sci.*, **B1**, 645 (1963).

6. Smith, D. C., Naval Research Laboratory Report C2274, May 6, 1948.

7. McMurry, H. L., and V. Thornton, *Anal. Chem.*, **24**, 318 (1952).

8. Van Schooten, J., E. W. Duck, and R. Berkenbosch, *Polymer*, **2**, 357 (1961); F. L. Ramp, E. J. De Witt, and L. E. Trapasso, *J. Org. Chem.*, **27**, 4368 (1962).

9. Natta, G., I. Pasquon, P. Corradini, M. Peraldo, M. Pegoraro, and A. Zambelli, *Atti Accad. Nazl. Lincei, Rend. Classe Sci. Fis. Mat. Nat.* [8], **28**, 539 (1960); M. Peraldo and M. Cambini, in press.

10. Liang, C. Y., and W. R. Watt, *J. Polymer Sci.*, **51**, S14 (1961).

11. Natta, G., *SPE J.*, **15**, 373 (1959).

12. Natta, G., G. Dall'Asta, G. Mazzanti, and F. Ciampelli, *Kolloid Z.*, **182**, 50 (1962).

13. Ciampelli, F., G. Bucci, T. Simonazzi, and A. Santambrogio, *Chim. Ind. (Milan)*, **44**, 489 (1962).

14. Immergut, E. H., G. Kollmanan, and A. Malatesta, *J. Polymer Sci.*, **51**, S57 (1961).

15. Zambelli, A., G. Natta, and I. Pasquon, *J. Polymer Sci.*, **C4**, 411 (1964).

16. Phillips, G. W., and W. L. Carrick; *J. Am. Chem. Soc.*, **84**, 920 (1962).

17. Boghetic, L., G. A. Mortimer, and G. W. Danes, *J. Polymer Sci.*, **61**, 3 (1962).

18. Gössl, T., *Makromol. Chem.*, **42**, 1 (1960).

19. Bucci, G., and T. Simonazzi, *Chim. Ind. (Milan)*, **44**, 263 (1962).

20. Drusel, H. V., and F. A. Iddings, *Anal. Chem.*, **35**, 29 (1963).

21. Corish, P. J., and M. E. Tunicliffe, *J. Polymer Sci.*, **C7**, 187 (1964).

Résumé

Il est nécessaire de faire une distinction entre un polymère alpha-oléfinique "amorphe" et un polymère alpha-oléfinique "atactique". Le terme "atactique" doit s'appliquer uniquement aux polymères amorphes qui possèdent une régularité linéaire tête-à-queue et qui ont la même régularité chmique que les polymères tactiques correspondants dont ils diffèrent seulement par le manque de régularité stérique. On peut en avoir une interprétation claire par la présence de bandes à 1155 et 915 cm.$^{-1}$ dans le spectre infrarouge des polypropylènes isotactique et atactique. La présence de ces bandes est due à l'unité monomérique —CH$_2$—CH— qui possède un arrangement régulier tête-à-queue.
    |
   CH$_3$
L absence de ces bandes dans les polymères de propylène obtenus au moyen de catalyseurs de type cationique dépend de la présence d'une très petite quantité d'unités monomériques de ce type. On peut conclure que la présence des deux bandes mentionnées ci-dessus dans le spectre infra-rouge des copolymères éthylène-propylène n'indiquent pas la présence de longues séquences de propylène du type isotactique, et par conséquent l'existence du copolymère à bloc, mais seulement la présence de l'unité monomérique mentionnée ci-dessus.

Zusammenfassung

Die Notwendigkeit, zwischen einem "amorphen" und einem "ataktischen" α-Olefinpolymeren zu unterscheiden, wird betont. Es ist angebracht, den Audruck "ataktisch" nur auf diejenigen amorphen, linearen, regelmässigen Kopf-Schwanzpolymeren zu beschränken, welche dieselbe chemische Regelmässigkeit wie die entsprechenden ataktischen Polymeren besitzen, von welchen sie sich nur durch den Mangel an sterischer Regelmässigkeit unterscheiden. Eine klare Zuordnung der Anwesenheit von Banden bei 1155 und 915 cm.$^{-1}$ im IR-Sprektrum von isotaktischen und ataktischen Polypropylenen wird gegeben. Die Anwesenheit dieser Banden ist durch die —CH$_2$—CH— mono-
    |
   CH$_3$
mereinheit mit einer regelmässigen Kopf-Schwanzanordnung bedingt. Das Fehlen dieser Banden in Propylenpolymeren, die mit Hilfe kationischer Katalysatoren erhalten wurden, wird auf die Gegenwart einer nur sehr geringen Menge von Monomereinheiten dieses Typs zurückgeführt. Schliesslich kommt man zu dem Schluss, dass die Anwesenheit der oben erwähnten Banden im IR-Spektrum von Äthylen–Propylencopolymeren nicht für das Vorhandensein langer Propylensequenzen vom isotaktischen Typ und daher auch nicht für die Existenz eines Blockcopolymeren spricht, sondern nur für die Anwesenheit der oben erwähnten Monomereinheit.

X-Ray Study of Some Isotactic Substituted Poly-Carboalkoxybutadienes

G. NATTA, *Istituto di Chimica Industriale del Politecnico di Milano, Centro Nazionale di Chimica delle Macromolecole, Sez. I, Milan*, and P. CORRADINI and P. GANIS, *Istituto di Chimica Generale, Universita di Napoli, Centro Nazionale di Chimica delle Macromolecole, Sez.VII, Naples, Italy*

Synopsis

The chain conformation and configuration of some polysorbates and poly-β-styryl-acrylates is discussed in this paper. From x-ray fiber spectra of these polymers we obtained the identity period of 4.80 ± 0.05 A. The conformation of the main chain is the same as that of 1,4 *trans* polybutadiene and isotactic 1-4 *trans* polypentadiene. From considerations of the mode of packing of the chains and of the encumbrance of the side groups in respect to the main chain it was possible to assign an *erythro* configuration in regard to the relative placement of lateral groups. The examined polymers are tritactic and have a *trans-erythro*-isotactic configuration.

A new series of crystalline polymers has been obtained at the Department of Industrial Chemistry of the Polytechnic of Milan by Natta and Farina[1] starting from substituted carboalkoxybutadienes. In particular, crystalline polymers have been obtained from various alkyl esters of the *trans-trans* isomer of sorbic acid and β-styrylacrylic acid. The monomer units with 1,4 enchainment are of the type —CHR—CH=CH—CHCOOR′—. They show three sites of possible stereoisomerism, i.e., the double bond and the two tertiary carbon atoms of the chain. In this paper we shall report the results of an x-ray analysis of these polymers. Some of the corresponding preliminary results have been reported previously.[2]

X-Ray Data

The powder spectra of five typical polymers recorded with a Geiger counter are shown in Figure 1. From the fiber spectra of all polysorbates and of the poly(β-styryl *n*-butylacrylate) we obtained the same value of the identity period along the fiber axis, i.e., $c = 4.80 \pm 0.05$ A. The spacings of the two most intense equatorial reflections are shown in Table I.

The spacing of the first line varies regularly with an increase in the encumbrance of the lateral group; the spacing of the second line is about the same for all the polymers studied.

The reconstruction of the reciprocal lattice has been possible for the equatorial reflections of poly(*n*-butyl sorbate); the reciprocal axes, which
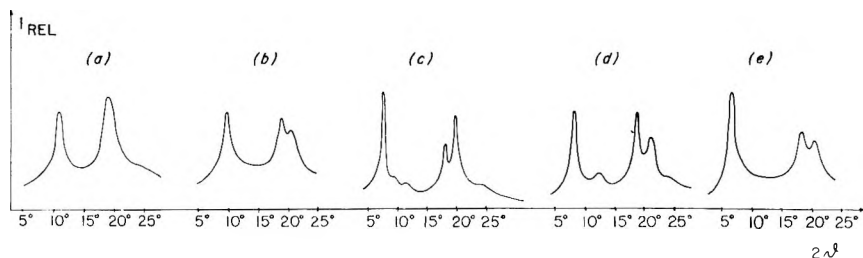
Fig. 1. Powder spectra (CuKα) of the crystalline polymers: (a) poly(methyl sorbate);
(b) poly(ethyl sorbate); (c) poly(n-butyl sorbate); (d)poly(methyl-β-styrylacrylate);
(e) poly(n-butyl-β-styrylacrylate).

are perpendicular to each other are: $a^* = 1/(11.36 \pm 0.10)$ A.$^{-1}$; $b^* = 1/(9.70 \pm 0.10)$ A.$^{-1}$. On the first layer line only four reflections are observed; therefore no complete reconstruction of the reciprocal lattice has been attempted.

TABLE I

	2θ (CuKα)	d, A.	2θ (CuKα)	d, A.
Poly(methyl sorbate)	10.95	8.07 ± 0.10	19.00	4.67 ± 0.05
Poly(ethyl sorbate)	9.90	9.90 ± 0.10	19.00	4.67 ± 0.05
Poly(isopropyl sorbate)	8.40	10.52 ± 0.10	18.80	4.71 ± 0.05
Poly(n-butyl sorbate)	7.75	11.40 ± 0.10	18.10	4.92 ± 0.05
Poly(isobutyl sorbate)	7.40	11.94 ± 0.10	19.40	4.57 ± 0.05
Poly(isoamyl sorbate)	6.80	12.99 ± 0.10	18.10	4.92 ± 0.05
Poly(methyl-β styrylacrylate)	7.60	11.62 ± 0.10	18.30	4.83 ± 0.05
Poly(n-butyl-β styrylacrylate)	6.25	14.00 ± 0.15	18.10	4.92 ± 0.05

Possible Configurational Models

Each chain should be ordered in respect to the three centers of stereoisomerism, at least for long sequences of monomeric units. In fact, the x-ray crystallinity is high, and the infrared spectrum of the polymer in the solid state is very different from the corresponding spectrum of the melt.

Accordingly, at least for long sequences of monomeric units, we shall expect the following regularities: (1) the double bond must be always of the cis or always of the trans type; (2) the relative configuration of successive monomeric units must be either isotactic or syndiotactic; (3) the relative configuration of two adjacent tetrahedral centers of stereoisomerism must be either of the threo or of the erythro type.

The possible configurational models are shown in Figure 2.

Chain Conformation

The identity period along the fiber axis is identical to that found for 1,4-trans-polybutadiene.[3] The identity unit contains only one monomer unit, as shown by the equatorial dimensions found for poly(n-butyl sor-

bate) and by the distribution of diffracted intensity on the meridian of the successive layer lines.

Accordingly, the chain conformation should be characterized by a succession of internal rotation angles very close to the sequence:...*trans*, $\sigma_1 = 120°$, $\sigma_2 = 180°$, $\sigma_3 = -120°$, *trans*... (Fig. 3). The assignment of a *trans* configuration to the double bonds is confirmed by the appearance in the infrared spectra, of a band at 10.52 μ.
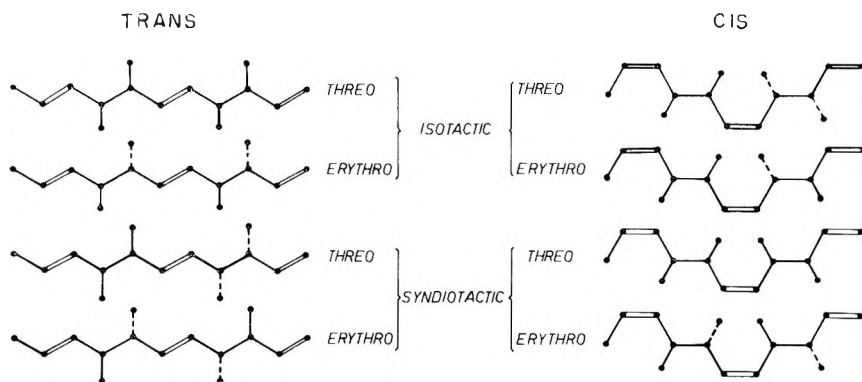
Fig. 2. Possible configurational models of the examined polymers.
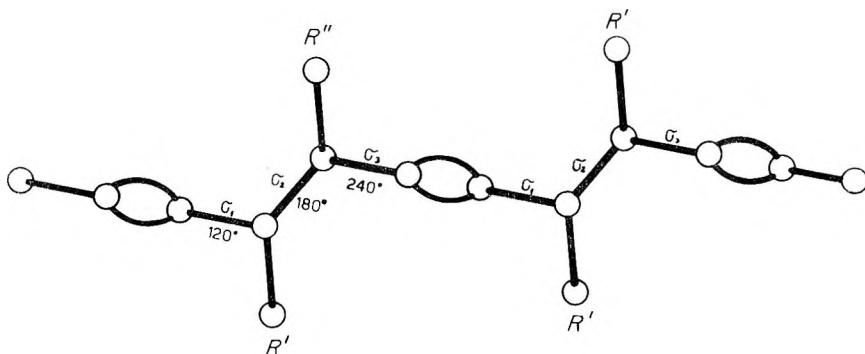
Fig. 3. Chain conformation of the examined polymers.   R' = CH_3, C_6H_5;   R" = —COOR.

Moreover, the successive monomeric units must necessarily be of the isotactic type. Thus, for the examined polymers, the knowledge of the identity period along the fiber axis and very simple considerations on the intensity distribution are sufficient to permit the type of tacticity of two of the centers of stereoisomerism to be assigned with certainty. The situation is analogous to that of ditactic polymers such as poly-1,4-*trans*-pentadiene.[4]

A qualitative model of the packing of the macromolecules is shown in Figure 4 for poly(n-butyl sorbate). We have assumed a plane group *pg*, owing to the fact that the a^* and b^* axes are perpendicular to each other.
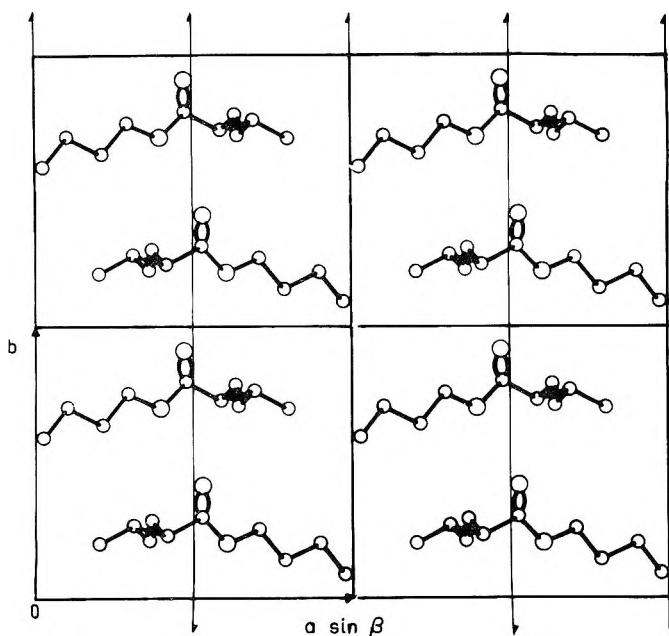
Fig. 4. Qualitative packing model of poly(n-butyl sorbate).
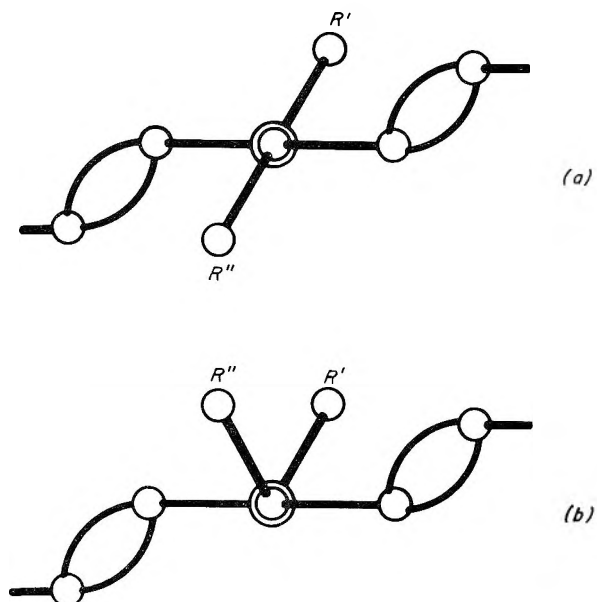
Fig. 5. Models of (a) *erythro* configuration of two tertiary carbon atoms, the lateral groups having a *trans* arrangement; (b) *threo* configuration with a *gauche* arrangement of the lateral groups.

The plane group *pm* may be discarded on the basis of elementary considerations on the intensity of the reflections.

Since the space group was unknown, this model was regarded as a first approximation and therefore was not refined further, though there was reasonable agreement between calculated and observed structure factors.

The mode of packing of the chains for the other polymers should be in some way similar to that of poly(*n*-butyl sorbate), with chain packing side by side, with parallel orientation of the direction of maximum encumbrance. This is in agreement with the main features of the equatorial spectra of all the investigated polymers.

As already remarked, the spacing of one of the two strongest equatorial reflections varies regularly with an increase of the bulkiness of the side groups; accordingly it arises from planes perpendicular to the direction of maximum encumbrance. The spacing of the other strong equatorial reflection is almost invariant in the polymer series studied; thus it should arise from planes nearly parallel to the direction of maximum encumbrance.

The fact that the equatorial encumbrance of the chains varies practically only in one direction points to a *trans* arrangement, and hence to an *erythro* placement of the lateral groups (Fig. 5).

Further Considerations on Poly(β-styryl Acrylates)

Although it was not possible to obtain oriented fibers of poly(methyl-β styrylacrylate), oriented crystalline fibers were obtained in the case of poly-(*n*-butyl-β-styrylacrylate).

The main features of the spectrum are very similar to those of the various studied polysorbates. However, for the polysorbates polymers, some double could remain about a possible *gauche* (instead of *trans*) placement of the methyl group with respect to the carboxylic group, but it is impossible to build a stereochemically reasonable model of the chain of poly(*n*-butyl-β-styrylacrylate) with a *gauche* arrangement of the benzene and carboxylic group (Fig. 6).

This fact is strongly indicative of an *erythro* isotactic configuration of the polymer. Simple calculations of the internal conformation energy for a *threo* and an *erythro* configuration of the side group associated with the known conformation of the chain gives rise for poly(*n*-butyl-β-styryl-acrylate) to a very large internal energy difference.

A *trans* conformational arrangement (and hence an *erythro* placement) of the side groups is indicated also by the nuclear magnetic resonance spectra, which have been recorded for all the studied polymers.[6]

Conclusions

The examination of the x-ray spectra of some polysorbates and poly(β-styrylacrylates) allows a unequivocal assignment of a *trans*-isotactic configuration to the studied polymers. From considerations on the mode
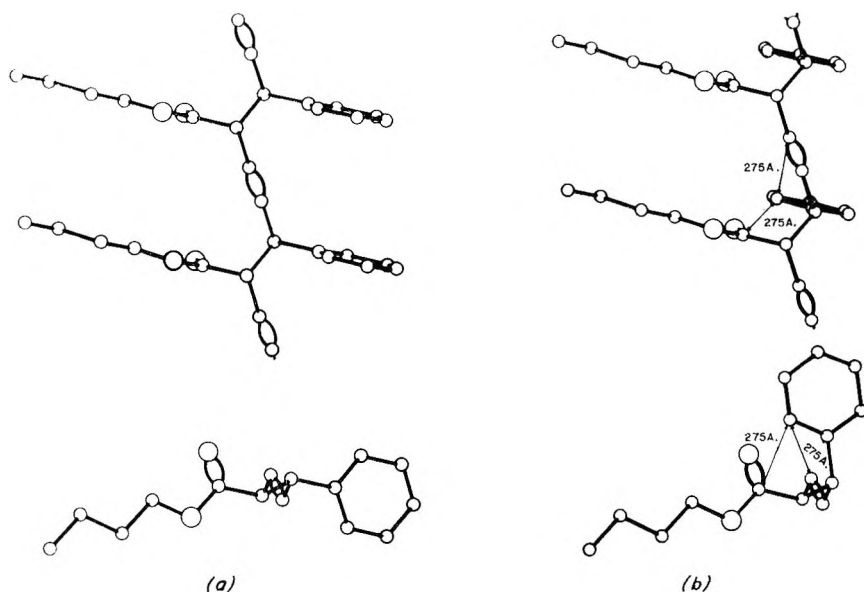
Fig. 6. Chain models of poly(n-butyl-β-styrylacrylate): (a) with a *trans* arrangement of the benzene and carboxylic group (*erythro* configuration); (b) with a *gauche* arrangement of the benzene andc arboxylic group (*threo* configuration); in this case the worst intramolecular atomic distances are shown.

of packing of the chains and on the encumbrance of the side groups as regard to the main chain permits one to assign an *erythro* configuration with respect to the relative placement of lateral groups.

The polymers we have studied are tritactic and have, at least for long sequences of monomeric units, a *trans-erythro*-isotactic configuration.

References

1. Natta, G., M. Farina, M. Donati, and M. Peraldo, *Chim. Ind. (Milan)*, **42**, 1363 (1960); G. Natta, M. Farina, and M. Donati, *Makromol. Chem.*, **43**, 251 (1961).

2. Natta, G., M. Farina, P. Corradini, M. Peraldo, M. Donati, and P. Ganis, *Chim. Ind. (Milan)*, **42**, 1361 (1960).

3. Natta, G., P. Corradini, L. Porri, D. Morero, *Chim. Ind. (Milan)*, **40**, 362 (1958).

4. Natta, G., L. Porri, P. Corradini, G. Zannini, and F. Ciampelli, *J. Polymer Sci.*, **51**, 463 (1961).

5. Natta, G., P. Corradini, and P. Ganis, *J. Polymer Sci.*, **58**, 1191 (1962); *Atti Accad. Nazl. Lincei, Rend. Classe Sci. Fis. Mat. Nat.*, **33**, 200 (1962).

6. Lombardi, E., and A. Segre, *Atti Accad. Nazl. Lincei, Rend. Classe Sci. Fis. Mat. Nat.*, **34**, 547 (1963).

Résumé

Cet article traite de la conformation et de la configuration de quelques polysorbates et poly-β-styrylacrylates. Ces polymères ont été examinés sous forme de fibres aux rayons-X; on a trouvé la valeur de 4.80 ± 0.05 A. comme longueur du motif périodique. La conformation de la chaîne principale est égale à celle du polybutadiène-1-4-*trans* et du polypentadiène-1-4-*trans* isotactique. En considérant la manière d'empaquettement des chaînes et l'encombrement des groupes latéraux par rapport à la chaîne principale,

il a été possible de déterminer une configuration *érythro* du point de vue de la localisation des groupes latéraux. Les polymères étudiés sont pourtant tritactiques et leur configuration est *trans-érythro*-isotactique.

Zusammenfassung

In der vorliegenden Arbeit wird die Kettenkonformation und Konfiguration einiger Polysorbate und Poly-β-styrylacrylate diskutiert. Das Röntgenfaserdiagramm dieser Polymeren zeigt eine Identitätsperiode von 4,80 ± 0,05 A. Diese Polymeren besitzen daher die gleiche Kettenkonformation wie das 1,4-*trans*-Polybutadien und das isotaktische 1,4-*trans*-Polypentadien. Die relative Stellung der seitlichen Gruppen entspricht einer Erythrokonfiguration, wie durch einer Untersuchung der Kettenpackung und die Hinderung der seitlichen Gruppen in Bezug auf die Hauptkette bewiesen wird. Die Polymeren sind tritaktisch und besitzen eine *trans-erythro*-isotaktische Konfiguration.

Polyamides of 1,4-Cyclohexanebis(methylamine)

ALAN BELL, JAMES G. SMITH,* and CHARLES J. KIBLER,†
Research Laboratories, Tennessee Eastman Company, Division of Eastman Kodak Company, Kingsport, Tennessee

Synopsis

Polyamides of both *cis*- and *trans*-1,4-cyclohexanebis(methylamine) with aliphatic dicarboxylic acids and copolyamides of *trans*-1,4-cyclohexanebis(methylamine) with *p*-xylene-α,α'-diamine were prepared in order to discover the effect of cycloalkane rings on melting point. Analogous polyamides of *p*-xylene-α,α'-diamine were prepared for comparison. The polyamides of *trans*-1,4-cyclohexanebis(methylamine) had higher melting points than the analogous polyamides of *p*-xylene-α,α'-diamine. This result is believed to be due to the slightly contracted conformation which *trans*-1,4-cyclohexanebis(methylamine) can adopt in the polymer chain. The polyamides of *cis*-1,4-cyclohexanebis(methylamine) melted lower than those of the *trans* isomer. The lower symmetry of the *cis*-diamine accounts for this result. The melting points of the copolyamides of *trans*-1,4-cyclohexanebis(methylamine) and *p*-xylene-α,α'-diamine were higher than expected. It is suggested that these compositions are examples of partially isomorphous copolyamides.

INTRODUCTION

In spite of the considerable amount of literature dealing with the relationship of the chemical structure of polyamides to their physical properties, relatively little of it deals with the effect of cycloalkane rings on melting point. It was of interest, therefore, to prepare polyamides from 1,4-cyclohexanebis(methylamine)[1] and compare their melting points with those of their aromatic analogs prepared from *p*-xylene-α,α'-diamine.

Aromatic dicarboxylic acids, such as terephthalic acid, produce high-melting polyamides[2] with aliphatic diamines due to the combined effects of the hydrogen bonding of the amide groups and the chain stiffening resulting from the conjugation of the carbonyl groups with the aromatic ring. Polyamides from *p*-xylene-α,α'-diamine and aliphatic dicarboxylic acids have only the rigidity and symmetry of the benzene ring to influence the polymer melting point. Consequently, as the reports in the literature[3-7] indicate, these polyamides melt much lower. In addition, some interesting isomorphous copolyamide systems involving *p*-xylene-α,α'-diamine have been reported.[3,4]

* Present address: Dow Chemical Co., Sarnia, Ontario, Canada.
† To whom all inquiries should be sent.

DISCUSSION

While p-xylene-α,α'-diamine polyamides have been described in the past, particularly in the patent literature, no list of the melting points of the various reported polyamides is available. The melting points of the p-xylene-α,α'-diamine polyamides prepared during the course of this work are summarized in Table I. It should be noted that two different melting points have been reported for the polysebacamide, one at approximately 270°C.[4] and another at approximately 300°C.[7] The authors of the latter report also state that the polyadipamide melts at 280°C. Since experience indicates that the polyadipamide would melt at a temperature higher than the polysebacamide, it is suspected that the 300°C. melting point is in error and that the 270°C. is the correct one.

The melting points of the polyamides of trans-1,4-cyclohexanebis-(methylamine) and a series of dicarboxylic acids prepared in the course of this work are also recorded in Table I.

A graphical presentation of these melting points versus the number of carbon atoms in the dicarboxylic acids is given in Figure 1. This shows the alternating character of the melting points—first high, then low—as the number of carbon atoms in the aliphatic dicarboxylic acid is progressively increased by one. This alternating effect is well known,[8] and various explanations have been suggested.[9,10]

It is apparent from a comparison of the two polyamide series of Table I that the polyamides from trans-1,4-cyclohexanebis(methylamine) melt at a somewhat higher temperature than the corresponding polyamides from p-xylene-α,α'-diamine. It must be concluded that the trans-1,4-cyclohexylene ring is at least equivalent to the p-phenylene ring insofar as its effect on the melting point of the polymer is concerned. Indeed, it even appears to be slightly more effective in producing high-melting polyamides. This is consistent with similar observations in the case of polyesters prepared from trans-1,4-cyclohexanedimethanol and p-xylene-α,α'-diol.[11]

TABLE I
Melting Points of Polyamides

Dicarboxylic acid	trans-1,4-Cyclohexanebis(methylamine)		p-Xylene-α,α'-diamine	
	[η]	M.p., °C.	[η]	M.p., °C.
Glutaric	0.29	280–290	—	—
Adipic	0.85	345[a]	1.02	333[a]
Pimelic	1.45	290–293	1.00	280–284
Suberic	1.34	308–311	0.93	300–305
Azelaic	1.04	270–275	0.68	259–263
Sebacic	1.68	295–300	0.82	279–281
Dodecanedioic	1.38	275–278	0.89	268–272
Isophthalic	0.58	305–310	Insol.	270–290

[a] Obtained by the extrapolation of the m.p. of a copolyamide series with 1,6-hexanediamine.
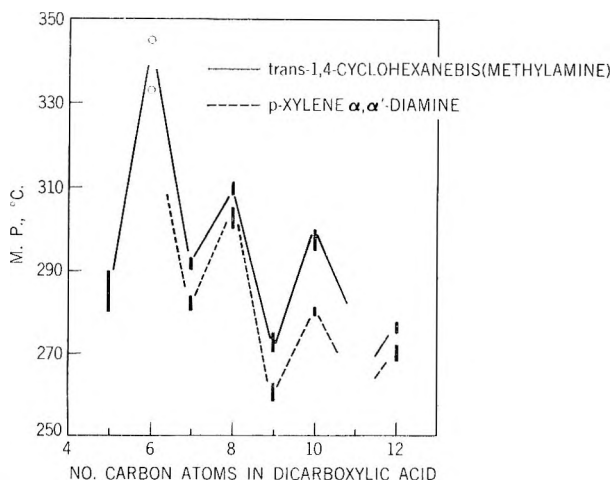
Fig. 1. Melting points of polyamides from *trans*-1,4-cyclohexanebis(methylamine) and *p*-xylene-α,α'-diamine.

Fisher-Herschfelder-Stuart models of the two polyamide series were compared. The models were so arranged that the aliphatic chain of the dicarboxylic acid moiety was planar zigzag and coplanar with the amide linkage.[12]

The model of poly(*p*-phenylenedimethylene adipamide) is shown schematically as structure I. An examination of this model revealed that rota-
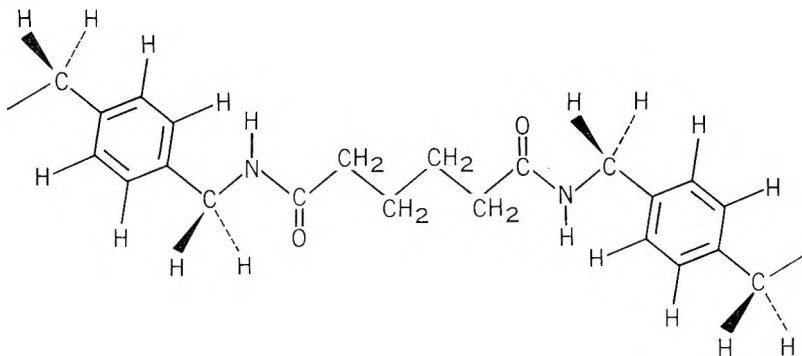
I

tion of the benzene ring about the axis joining the two methylene carbon atoms to the aromatic ring produces no change in the repeat distance of the polyamide. The conformation adopted by the aromatic ring is probably determined by the steric interaction of the hydrogen atoms on the benzene ring and those on the methylene groups attached to this ring. This interaction is at a minimum when the plane of the benzene ring is perpendicular to that of the amide group; i.e., in structure I, when the plane of the benzene ring is perpendicular to the plane of the paper. Such a conformation has been suggested[13] on the basis of x-ray diffraction studies.

The model of poly(*trans*-1,4-cyclohexylenedimethylene adipamide) is shown schematically as structure II; the cyclohexane ring is assumed to have the chair conformation, and the substituents in the 1 and 4 positions
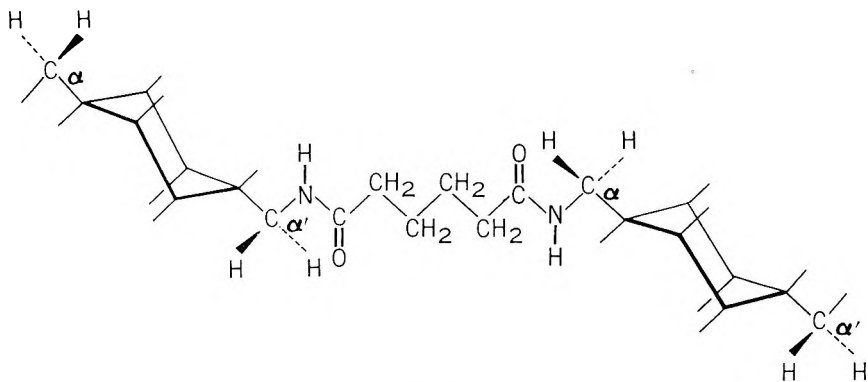
II

are assumed to be attached by equatorial bonds. In contrast to the ring in poly(*p*-phenylenedimethylene adipamide), rotation of the *trans*-1,4-cyclohexylene ring about the $C\alpha$—$C\alpha'$ axis has a pronounced effect on the repeat distance. As approximated by measurements on the models, the maximum length of the repeat unit is 17.9 cm. when conformation IIIA is adopted and the minimum length is 16.8 cm. when conformation IIIB is adopted. At its minimum length, the repeat distance is 0.5 cm. shorter than the repeat distance of poly(*p*-phenylenedimethylene adipamide) (17.3 cm.).
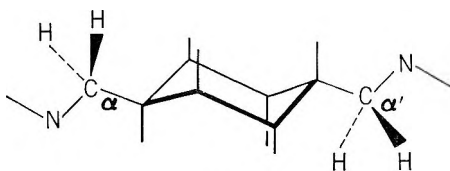
IIIA
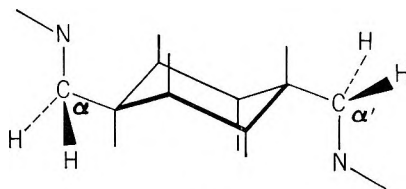
IIIB

The conformation adopted by the cyclohexane ring is determined by the steric interaction of the hydrogen atoms on the C_α and $C_{\alpha'}$ carbon atoms with the hydrogen atoms on the ring. This steric interaction is at a maximum in conformation IIIA and at a minimum in conformation IIIB.
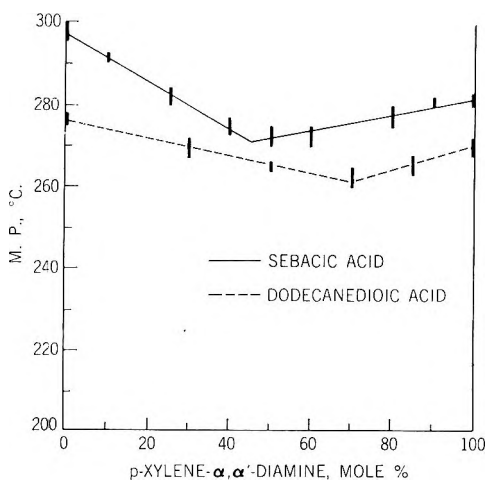
Fig. 2. Melting points of copolyamides of *trans*-1,4-cyclohexanebis(methylamine) and *p*-xylene-α,α'-diamine.
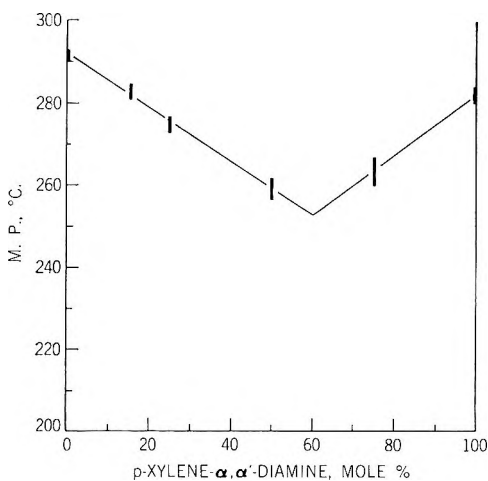
Fig. 3. Melting points of copolyamides of *trans*-1,4-cyclohexanebis(methylamine) and *p*-xylene-α,α'-diamine with pimelic acid.

It is suggested that the higher melting points of the polyamides derived from *trans*-1,4-cyclohexanebis(methylamine) compared to those of the polyamides derived from *p*-xylene-α,α'-diamine are due to the ability of the former moiety to adopt the slightly contracted conformation IIIB. As a consequence, a polyamide derived from *trans*-1,4-cyclohexanebis-(methylamine) has a slightly smaller repeat distance than the analogous polyamide derived from *p*-xylene-α,α'-diamine, and the ring system occurs more frequently per unit length of polymer chain. Thus, the former polyamide is more rigid and symmetrical.   These factors, symmetry and rigidity, contribute to high melting points.

Copolyamides of *trans*-1,4-cyclohexanebis(methylamine) and *p*-xylene-α,α'-diamine were prepared in an effort to gain information on the similarities or differences in the molecular structures of the two. As may be seen from Figures 2 and 3, the copolyamides do show the usual V-shaped curves when the melting points are plotted as a function of composition. However, the maximum depression of the melting point curves is surprisingly small.

The copolyamides derived from sebacic acid were studied further. Copolyamides were also prepared from mixtures of *trans*-1,4-cyclohexanebis-(methylamine) and 1,6-hexanediamine and from mixtures of *p*-xylene-α,α'-diamine and 1,6-hexanediamine. Data from these copolyamide systems are presented graphically in Figure 4; curve *ABC* represents the melting
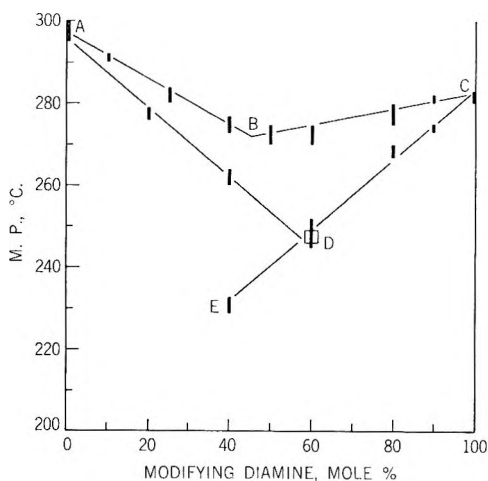
Fig. 4. Melting points of copolyamides of sebacic acid: (*ABC*) polyamide of *trans*-1,4-cyclohexanebis(methylamine) modified with *p*-xylene-α,α'-diamine; (*AD*) polyamide of *trans*-1,4-cyclohexanebis(methylamine) modified with 1,6-hexanediamine; (*EDC*) polyamide of 1,6-hexanediamine modified with *p*-xylene-α,α'-diamine.

points of the *trans*-1,4-cyclohexanebis(methylamine)/*p*-xylene-α,α'-diamine system, curve *AD* represents the *trans*-1,4-cyclohexanebis(methylamine)/1,6-hexanediamine system, and curve *EDC* represents the 1,6-hexanediamine/*p*-xylene-α,α'-diamine system.

In a nonisomorphous copolyamide system, the melting point of the major component is depressed by an amount proportional to the mole percent of the modifier. Furthermore, the nature of the modifier has little effect on the extent of this depression.[14] On the basis of this it was expected that a combination of the melting point-composition curve of the *trans*-1,4-cyclohexanebis(methylamine)/1,6-hexanediamine copolyamide system with that of the *p*-xylene-α,α'-diamine/1,6-hexanediamine system would provide the complete melting point-composition curve for the *trans*-1,4-cyclohexanebis(methylamine)/*p*-xylene-α,α'-diamine copolyamide system.
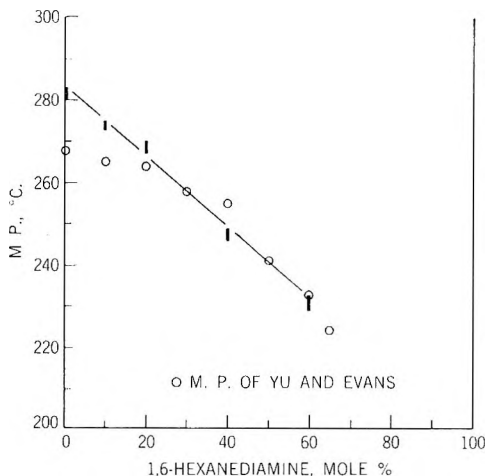
Fig. 5. Melting points of copolyamides of p-xylene-α,α'-diamine and 1,6-hexanediamine with sebacic acid.

As may be seen from Figure 4, this expectation was not realized. 1,6-Hexanediamine effected a greater depression of the melting points of the *trans*-1,4-cyclohexanebis(methylamine) and p-xylene-α,α'-diamine polyamides than was observed in the sebacic acid/*trans*-1,4-cyclohexanebis-(methylamine)/p-xylene-α,α'-diamine copolyamide system at equivalent degrees of modification.

Yu and Evans[4] proposed a lattice model for nonisomorphous copolyamides. The modifying component interrupts the chain structure so that the subsequent amide linkage of the polymer chain does not fall upon the dipole planes formed by the amide linkages of the assembly of polymer chains. This can occur when the repeat unit of the modifying component has a different length than that of the major repeat unit. Such a situation prevails when 1,6-hexanediamine is used to modify the *trans*-1,4-cyclohexanebis(methylamine) or p-xylene-α,α'-diamine polyamides.

Yu and Evans also described partially isomorphous copolyamides in which the initial addition of the modifying component did not immediately produce a linear depression of the melting point of the base polyamide. A plot of the melting point of the copolyamide against the composition showed a curve which increased in slope as the degree of modification increased. The copolyamide system sebacic acid/p-xylene-α,α'-diamine/1,6-hexanediamine was cited as one example.

In our work, the p-xylene-α,α'-diamine/1,6-hexanediamine copolyamide system did not show this behavior. Instead, the copolyamide behavior as a nonisomorphous system and a linear depression of melting point with composition was observed. A comparison of our data with that of Yu and Evans is shown in Figure 5; the open circles represent the reported melting points and the heavy lines represent the melting points found in this work. It should be noted that the discrepancy in melting
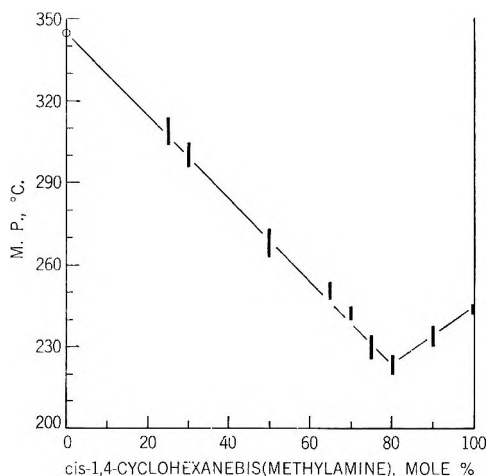
Fig 6. Melting points of copolyamides of *cis*- and *trans*-1,4-cyclohexanebis(methyl-amine) with adipic acid.

points is confined to the homopolymer and to the lower degrees of modification. At high degrees of modification there is good agreement between the two sets of data.

It is suggested that the copolyamide system sebacic acid/*trans*-1,4-cyclo-hexanebis(methylamine)/*p*-xylene-α,α'-diamine shows the characteristic feature of a partially isomorphous system (Figs. 2 and 4). That is, across the entire compositional spectrum, a smaller depression of the melting point of the base polyamide is obtained than would be expected from the observations of the depression of the melting point by modification with a nonisomorphous modifier.

The similarity in size and shape of the two diamines, *trans*-1,4-cyclo-hexanebis(methylamine) and *p*-xylene-α,α'-diamine, is, doubtlessly, responsible for the partially isomorphous nature of the copolyamide system. Due to the slightly contracted conformation which the former diamine can adopt, an exact replacement in the polyamide chain of one diamine by another cannot occur without some degree of disturbance. However, the degree of disturbance is small and, consequently, the melting point depression is minimized.

Copolyamides of *cis*- and *trans*-1,4-cyclohexanebis(methylamine) were prepared to observe the effect of the *cis–trans* ratio on the melting points. The melting point–composition curve in Figure 6 shows that a definite eutectic composition was formed. This would indicate that the repeat distances of the two polyamides differ markedly so that copolyamides of the two stereoisomers are members of a nonisomorphous system.

A series of polyamides was also prepared from *cis*-1,4-cyclohexanebis-(methylamine) and various aliphatic dicarboxylic acids. Their compositions and melting points are summarized in Table II. As expected from the lower symmetry of the *cis*-diamine, the polyamides of the *cis* isomer

TABLE II
Polyamides of *cis*-1,4-Cyclohexanebis(methylamine)

Dicarboxylic acid	Polyamide	
	$[\eta]$	M.p., °C.
Glutaric	0.27	163–167
Adipic	0.88	242–246
Pimelic	1.17	188–191
Suberic	0.97	210–215
Azelaic	0.98	190–195
Sebacic	1.06	205–208
Dodecanedioic	0.87	205–215

melt lower than the corresponding polyamides of the *trans* isomer. Indeed, the melting points observed resemble closely those obtained from the linear aliphatic diamines such as 1,6-hexanediamine.

EXPERIMENTAL

Materials

Glutaric, adipic, pimelic, suberic, azelaic, sebacic, and dodecanedioic acids and 1,6-hexanediamine were obtained from commercial sources.

p-Xylene-α,α'-diamine and *trans*-1,4-cyclohexanebis(methylamine) were obtained from Eastman Chemical Products, Inc.

A mixture of *cis* and *trans* isomers of 1,4-cyclohexanebis(methylamine) (approximately 60% *cis*) was also obtained from Eastman Chemical Products, Inc. The isomers can be separated by careful fractional vacuum distillation through a 4-ft. column packed with Podbielniak Heli-pak. *trans*-1,4-Cyclohexanebis(methylamine) showed b.p. 238°C. at 734 mm. Hg and 98–99°C. at 5 mm. Hg; m.p. 27°C., n_D^{20} 1.4890 (super-cooled). For *cis*-1,4-cyclohexanebis(methylamine) these data were b.p. 243°C. at 734 mm. Hg and 79–79.5°C. at 2 mm. Hg; n_D^{20} 1.4959.

Methods

Inherent Viscosities. Phenol–tetrachloroethane (60/40) solutions at 25°C. containing the polyamides in 0.25% concentration were used for inherent viscosity determinations. The polyamides generally were soluble after being heated at 145°C. for 1 hr.

Melting Points. The melting points were determined on a Fisher-Johns melting point apparatus. Near the melting point, the sample was repeatedly pressed with a pencil point and the temperature at which the sample flowed freely under this pressure was taken as the melting point. Usually, there was a preliminary softening of the polymer sample from 2 to 5°C. below the melting point but no liquefaction was noted.

It was found advisable to take a preliminary melting point and then place a second sample on the melting point apparatus at a temperature

from 5 to 10°C. below the observed melting point. This procedure avoided much of the possibility of thermal degradation or oxidation of the sample before it melted.

However, it was also found that the copolyamides of *cis*- and *trans*-1,4-cyclohexanebis(methylamine) crystallized slowly. For these polyamides, it was expedient to heat-crystallize the sample at 180–190°C. for a few minutes before the melting point was taken.

The polyamides of *trans*-1,4-cyclohexanebis(methylamine) or *p*-xylene-α,α'-diamine with adipic acid melted above 325°C. Consequently, decompositions occurred so rapidly that accurate melting points could not be obtained. The melting points were estimated by extrapolation of the melting points of a copolyamide series with 1,6-hexanediamine. The data used are tabulated in Table III.

TABLE III
Melting Points of Adipic Acid Copolyamides

1,6-Hexane-diamine, mole %	Polyamide with trans-1,4-cyclohexanebis-(methylamine)		Polyamide with p-xylene-α,α'-diamine	
	[η]	M.p., °C.	[η]	M.p., °C.
10	0.48	332–337	0.97	325–327
20	—	—	1.08	322–325
25	1.32	317–320	—	—
30	—	—	0.81	310–313
33		307–311	—	—
40	—	—	1.33	305–309
50	1.58	290–293	—	—
70	1.29	270–275	—	—

Experiments

The polyamides were prepared by well-known methods[15] which involved the initial preparation of a polyamide salt followed by its conversion to the polyamide by dehydration in a phenolic solvent. The preparation of the polyamide from *trans*-1,4-cyclohexanebis(methylamine) and pimelic acid is given as a typical procedure.

Preparation of *trans*-1,4-Cyclohexylenedimethylenebis[ammonium pimelate]. A solution of 110 g. (0.688 mole) of pimelic acid in 800 ml. of 2B ethyl alcohol was prepared by heating the mixture to approximately 50°C. To this solution, a solution of 99.4 g. (0.70 mole) of *trans*-1,4-cyclohexanebis(methylamine) in 50 ml. of 2B ethyl alcohol was added rapidly with stirring. An exothermic reaction occurred and the ammonium salt precipitated rapidly. The mixture was cooled, filtered, and washed with 2B ethyl alcohol. After drying, the recovered salt weighed 423 g. (98.5% yield).

The salt (150 g.) was dissolved in a heated solution of 150 ml. of water in 250 ml. of 2B ethyl alcohol. A 2-g. portion of Norite SG II was

added and the solution was filtered while hot. The filtrate was treated with 600 ml. of 2B ethyl alcohol to precipitate the salt. After being cooled, filtered, and dried, the salt weighed 121 g. (80.6% recovery).

Preparation of Poly(*trans*-1,4-cyclohexylenedimethylene pimelamide). A 10-g. portion of *trans*-1,4-cyclohexylenedimethylenebis[ammonium pimelate] was placed in a reaction flask which was shaped like a large test tube (approximately 6 in. long and 1 in. in diameter) and was equipped with an inlet for nitrogen, a take-off, and a stirrer. To this was added 15 ml. of distilled *m*-cresol, and the tube was immersed in a heated Wood's metal bath. The mixture was heated to 200°C. while being stirred in the presence of nitrogen. The salt dissolved rapidly and water was evolved. Heating at 200°C. was continued for 1 hr. and then the temperature of the metal bath was increased at the rate of 25°C. every 15 min. until a temperature of 290°C. was reached. During this heating period, *m*-cresol distilled off. At 290°C., the pressure was reduced to less than 1 mm. of mercury for a period of 10 min. This vacuum treatment removed the last traces of *m*-cresol. The final molten polymer was cooled in a vacuum and isolated by breaking the tube. The inherent viscosity of the polymer was 1.45 and the melting point was 290–293 °C.

In the majority of cases the product was a viscous, molten mass. With high melting polymers (m.p. >310°C.), the product was obtained as a dry powder which formed during the heating period as the cresol distilled off. No attempt was made to fuse such polymers at metal bath temperatures above 315–320 °C.

References

1. Bell, A., J. G. Smith, and C. J. Kibler (to Eastman Kodak Co.), U. S. Pat. 3,012,-994 (1961).

2. Bunn, C. W., in *Fibres From Synthetic Polymers*, R. Hill, Ed., Elsevier, Amsterdam, 1953, pp. 316, 327.

3. Frunze, T. M., and V. V. Korshak, *Vysokomol. Soedin.*, **1**, 287 (1959); T. M. Frunze, V. V. Korshak, and E. A. Krasnyanskaya, *Vysokomol. Soedin.*, **1**, 495 (1959).

4. Yu, A. J., and R. D. Evans, *J. Am. Chem. Soc.*, **81**, 5361 (1959); A. J. Yu, and R. D. Evans (to American Viscose Corporation), U. S. Pat. 3,053,813 (1962).

5. California Research Corporation, British Pat. 766,927 (1957).

6. Perfogit Società per Azioni, Italian Pat. 538,850 (1956).

7. Losen, I. P., O. Ya. Fedotova, and M. L. Kerber, *Zh. Obsch. Khim.*, **26**, 548 (1956).

8. See for example, R. J. W. Reynolds, in *Fibres From Synthetic Polymers*, R. Hill, Ed., Elsevier, Amsterdam, 1953, p. 135; C. W. Bunn, *ibid.*, p. 312.

9. Bunn, C. W., *J. Polymer Sci.*, **16**, 323 (1955).

10. Slichter, W. P., *J. Polymer Sci.*, **35**, 77 (1959).

11. Kibler, C. J., A. Bell, and J. G. Smith, *J. Polymer Sci.*, **A2**, 2115 (1964).

12. Bunn, C. W., in *Fibres From Synthetic Polymers*, R. Hill, Ed., Elsevier, Amsterdam, 1953, p. 206 ff.

13. Vogelsong, D. C., *J. Polymer Sci.*, **57**, 895 (1962).

14. Bunn, C. W., in *Fibres From Synthetic Polymers*, R. Hill, Ed., Elsevier, Amsterdam, 1953, p. 320.

15. Coffman, D. D., G. J. Brechet, W. R. Peterson, and E. W. Spanagel, *J. Polymer Sci.*, **2**, 306 (1947).

Résumé

Dans le but d'étudier l'influence de la présence d'anneaux alicycliques sur le point de fusion, on a préparé des polyamides *cis* et *trans* 1,4-cyclohexanebis(méthylamine) avec des acides aliphatiques dicarboxyliques. On a également préparé des copolyamides du 1,4-*trans*-cyclohexanebis(méthylamine) avec le α,α'-diamino *p*-xylène de même que les polyamides du α,α'-diamino *p*-xylène comme base de comparaison. Les polyamides du *trans*-1,4-cyclohexenebis(méthylamine) ont des points de fusion plus élevés que les polyamides analogues du α,α'-diamino *p*-xylène. On admet que ce résultat est dû au fait que le *trans*-1,4-cyclohexanebis(méthylamine) peut adopter une conformation légèrement contractée dans une chaîne polymérique. Les polymères du *cis*-1,4-cyclohexanebisméthylamine fondent plus bas que ceux de l'isomère *trans*. Ceci est dû à une symmétrie moins élevée de la *cis*-diamine. Les points de fusion des copolyamides du *trans*-1,4-cyclohexanebis(méthylamine) et du α,α'-diamine *p*-xylène sont plus élevés que prévus. On suppose que ces polyamides sont des exemples de système partiellement isomorphes.

Zusammenfassung

Polyamide von *cis*- und *trans*-1,4-Zyklohexanbis(methylamin) mit aliphatischen Dicarbonsäuren und Copolyamide von *trans*-1,4-Zyklohexanbis(methylamin) mit *p*-Xylol-α,α'-diamin wurden dargestellt, um den Einfluss von Zykloalkanringen auf den Schmelzpunkt zu untersuchen. Zum Vergleich wurden analoge Polyamide aus *p*-Xylol-α,α'-diamin dargestellt. Die Polyamide von *trans*-1,4-Zyklohexanbis(methylamin) besassen höhere Schmelzpunkte als die analogen Polyamide von *p*-Xylol-α,α'-diamin. Es wird angenommen, dass dieses Ergebnis auf die schwach kontrahierte Konformation, welche *trans*-1,4-Zyklohexanbis(methylamin) in der Polymerkette annehmen kann, zurückzuführen ist. Die Polyamide von *cis*-1,4-Zyklohexanbis(methylamin) besitzen einen niedrigeren Schmelzpunkt als die des *trans*-Isomeren. Die niedrige Symmetrie des *cis*-Diamins ist für dieses Ergebnis verantwortlich. Die Schmelzpunkte der Copolyamide von *trans*-1,4-Zyklohexanbis(methylamin) und *p*-Xylol-α,α'-diamin waren unerwartet hoch. Es wird angenommen, dass hier Beispiele für partiell isomorphe Copolyamide vorliegen.

Certain Characteristics of the Polymerization of Butadiene-1,3 in Presence of Soluble Cobalt Complex Catalyst

A. I. DIACONESCU* and S. S. MEDVEDEV, *Institute for Fine Chemical Technology, Moscow, U.S.S.R.*

Synopsis

Studies were carried out on the kinetics of the process for producing 1,4-*cis*-polybutadiene in the presence of the catalytic system formed of monochlordiisobutylaluminum and the alcoholic complex of cobalt chloride. The experiments, carried out in homogenneous benzene solution at room temperature, pointed out the predominant role of water; when water is absent butadiene forms oligomers. Under the given conditions, the rate of polymerization of butadiene increases with the increase in the concentration of cobalt or aluminum compound and varies in a strange way when the water concentration changes. The dependence of the rate of polymerization on water concentration accounts for the difficulties in the reproductibility of experiments. The molecular weights of the polymers obtained increase linearly with the increase in water concentration and decrease with the decrease in the concentration of aluminum or cobalt compound. No dependence was noticed between the microstructure of polymers and the conditions of working.

The soluble (especially in aromatic hydrocarbons) systems consisting of a cobalt compound and alkylaluminum halides are known to be quite efficient catalysts for the polymerization of butadiene-1,3, particularly in the 1,4-*cis* position.[1−4] Despite the importance of the problem it seems that, except for a few partial data,[2,4−8] no systematic investigations enabling us to elucidate the kinetics and mechanism of this difficult polymerization process have been published.

Our researches demonstrated that the study of the kinetics of butadiene polymerization in the presence of a mixture of the alcoholic complex of cobalt chloride ($CoCl_2 \cdot xC_2H_5OH$) and monochlorodiisobutylaluminum in benzene solution may be carried out only if one takes into account the quantity of water, whose presence was also proved by other authors[4,9] to be necessary in the polymerization system. In the absence of water, although the rate of polymerization is not zero (this being probably due to the surplus of ethyl alcohol in the system), the butadiene forms low molecular weight liquid polymers. It is also probable that the presence of certain impurities in the monomer—for example, butenes—usually associated with

* Present address: Chemical Research Institute, Bucharest, Rumania.

commercial butadiene influences the progress of polymerization.[2] For this reason we preferred to utilize a butadiene purified by the tetrabromobutane method and finally by prepolymerization on ethyllithium. The final purification of the solvent was carried out by a prolonged treatment with liquid Na–K alloy. i-Bu_2AlCl treated with NaCl at about 150°C. and freshly rectified was used. Both the preparation of monomer and the polymerization experiments were carried out in entirely silvered glass equipment under high vacuum. The water was introduced in the benzene. The progress of the polymerization was followed dilatometrically. The dilatometers were filled as follows: first solvent was added with water, then monomer, then the i-Bu_2AlCl, and then the cobalt complex. The concentration of butadiene was 1.58 moles/l. and the temperature was 22°C. In absence of cobalt complex, butadiene does not polymerize in this mentioned system even after a long time.

Influence of Water

The experiments carried out at constant concentrations of i-Bu_2AlCl and cobalt complex (17 and 0.038 mmoles/l., respectively) in a range between 0 and 5.1 mmoles water per liter, showed that the addition of water and its increasing concentration led, first, to a rapid increase of the rate of polymerization up to a well marked maximum; subsequently, there was a decrease of rate, in some cases to values below the level of those corresponding
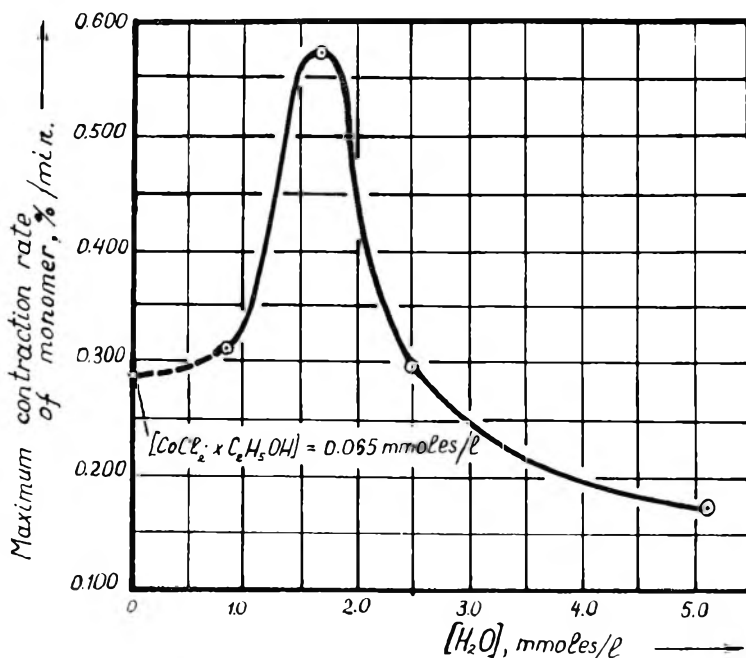
Fig. 1. Dependence of maximum contraction rate of monomer on water concentration. [i-Bu_2AlCl] = 17 mmoles/l.; [$CoCl_2 \cdot xC_2H_5OH$] = 0.038 mmoles/l.

to a water-free system (Fig. 1). At the same time the viscosity measurements showed a direct proportionality between the molecular weights of the polymers obtained and the concentration of water in the given interval. It is important to mention the high content of 1,4-*cis* structures in polymer (above 96%) even at the maximum water concentration of 5.1 mmoles/l. $(Al/H_2O = 3.3, H_2O/Co = 134)$.

Influence of the Alcoholic Complex of Cobalt Chloride

Taking into account the influence of the presence of water, the influence of cobalt complex was studied at i-Bu$_2$AlCl concentration of 17 mmoles/l. and water concentrations of 0.85, 1.67, and 2.5 mmoles/l., which correspond to points on the ascending curve, to the maximum, and the decreasing curve, respectively, in plots of the polymerization rate with increasing of the water concentration (Fig. 1). Under these conditions
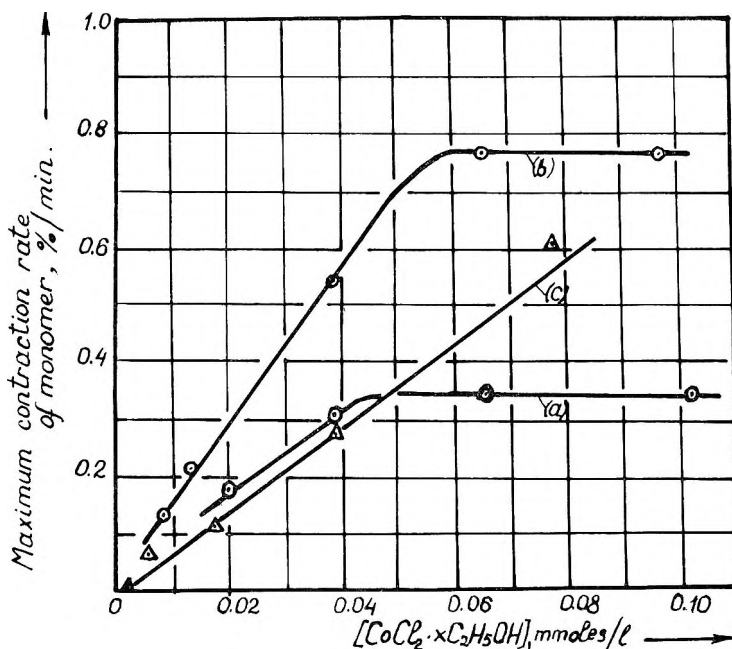
Fig. 2. Dependence of maximum contraction rate of monomer on Co-complex concentration: (a) [H$_2$O] = 0.85 mmoles/l.; (b) [H$_2$O] = 1.67 mmoles/l., (c) [H$_2$O] = 2.5 mmoles/l. [i-Bu$_2$AlCl] = 17 mmoles/l.

the increase of cobalt complex concentration resulted in a proportional increase of the rate of polymerization, but only at low concentrations of the Co-complex (Fig. 2). The flat portion of the curves corresponds to high values of cobalt complex concentration; the higher the concentration of water and therefore the ratio of H$_2$O/Al, the higher is the value of the flat portion of the curves (see Fig. 2, curves a and b).

In our experiments with water concentrations of 2.5 mmoles/l. (mole ratio $Al/H_2O = 7$) the range of variation for the cobalt complex concentration did not reach the domain of independence of the rate of polymerization (Fig. 2, curve c). The molecular weights of the polymers obtained at a water concentration of 1.67 mmoles/l. ($Al/H_2O = 10$) proved to be dependent on the cobalt complex concentration throughout the studied range, in conformity with the approximate relation

$$\overline{M}_a = K_{Co}[Co]^{-0.45} \tag{1}$$

where K_{Co} is a constant under the given conditions, but is probably variable when the H_2O and i-Bu_2AlCl concentration changes).

Influence of Monochlorodiisobutylaluminum

The influence of monochlorodiisobutylaluminum in the range of concentration from 1.45 to 21.7 mmoles/l. at a constant water and cobalt complex concentrations (0.85 and 0.038 mmoles/l., respectively) proved to be similar
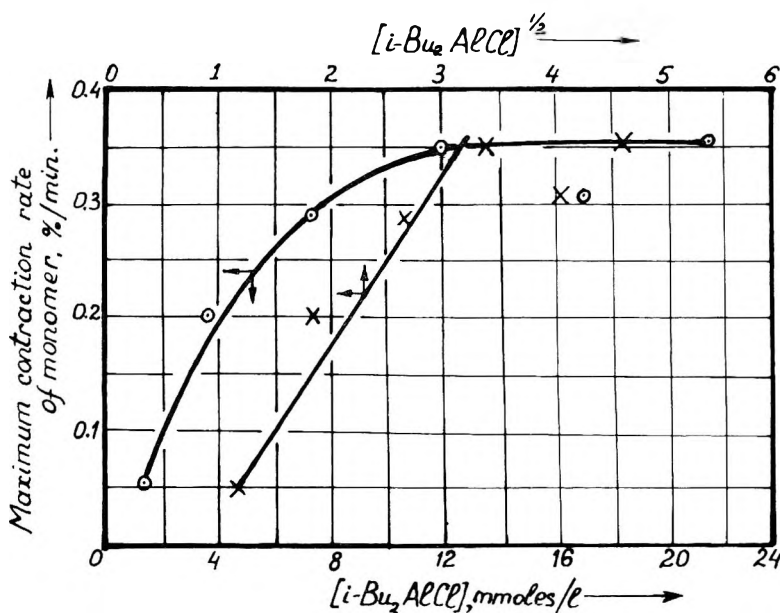
Fig. 3. Dependence of maximum contraction rate of monomer on i-Bu_2AlCl concentration. $[CoCl_2 \cdot xC_2H_5OH] = 0.038$ mmoles/l.; $[H_2O] = 0.85$ mmoles/l.

to the influence of the cobalt complex. The rate of polymerization is characterized by a domain of independence for high values of i-Bu_2AlCl concentration. At lower values the rate v may be expressed as shown in eq. (2) (Fig. 3).

$$v = a[Al]^{1/2} - b \tag{2}$$

Throughout the whole studied interval of concentrations the molecular weight of the polymers is expressed by the relation

$$\bar{M}_v = K_{A1}[Al]^{-0.67} \tag{3}$$

where K_{A1} is a constant, probably under the given conditions only.

The above mentioned data have led to the following important conclusions.

In absence of water the soluble complex cobalt–aluminum catalyst does not bring about the formation of macromolecular products of butadiene. The water probably, stabilizes the polymerization active centers, favoring the increase of the polymeric chains to high molecular weights (of the order of 10^5). The mechanism of this phenomenon is, now, difficult to imagine. At the same time, in the polymerization system continuous degradation of the active catalytic centers takes place. This degradation probably occurs under the influence of water.

The predominance of one of the two factors (the degradation of the active catalytic centers and the stabilization of the polymeric chains) acting differently on the rate of the polymerization process determines the character of the curves (Fig. 1). At the same time it is found that the molecular weights of the obtained polymers increase continuously with increasing water concentration in the system.

References

1. Natta, G., *Chim. Ind. (Milan)*, **42**, 1207 (1960).
2. Dolgoplosk, B. A., et al., *Dokl. Akad. Nauk SSSR*, **135**, 847 (1960).
3. Longiave, C., R. Castelli, and G. F. Croce, *Chim. Ind. (Milan)*, **43**, 625 (1961).
4. Gippin, M., *Ind. Eng. Chem. Prod. Res. Devel.*, **1**, 32 (1962).
5. Zgonnik, V. N., B. A. Dolgoplosk, et al., *Dokl. Akad. Nauk SSSR*, **145**, 1285 (1962).
6. Zgonnik, V. N., B. A. Dolgoplosk, et al., *Vysokomol. Soedin.*, **4**, 1000 (1962).
7. Grechanovskiĭ, V. A., B. A. Dolgoplosk, et al., *Dokl. Akad. Nauk SSSR*, **144**, 792 (1962).
8. Childers, C. W., *J. Am. Chem. Soc.*, **85**, 229 (1963).
9. Sinn, H., H. Winter, and W. Tirpitz, *Makromol. Chem.*, **48**, 59 (1961).

Résumé

Les auteurs ont étudié la cinétique de préparation du polybutadiène-1,4-*cis* en présence du système catalytique formé de monochlorodiisobutylaluminium et du complexe alcoolique de chlorure de cobalt. Les expériences, conduites en solution benzénique homogène, à la température ambiante, mirent en évidence le rôle prépondérant joué par l'eau, en l'absence de laquelle le butadiène ne forme que des oligomères. Dans les conditions de travail adoptées, la vitesse de polymérisation du butadiène augmente avec l'accroissment de la concentration en composé de cobalt ou d'aluminium et varie de manière étrange avec la modification de la teneur en eau du système. La dépendance de la vitesse de polymérisation de la concentration en eau explique les difficultés concernant la reproductibilité des expériences. Le poids moléculaire des polymères obtenus augmente linéairement avec l'accroissement de la concentration en eau et diminue avec la diminution de concentration en composé de cobalt ou d'aluminium. On n'a pas observé une dépendance notable de la microstructure des polymères en fonction des conditions de travail.

Zusammenfassung

Die Kinetik der 1,4-*cis*-Polybutadienbildung in Gegenwart eines aus Monochlordi-isobutylaluminum und einem Kobaltchlorid-Alkoholkomplex zusammengesetzten Katalysators wurde untersucht. Die Versuche wurden in homogener Benzollösung bei Zimmertemperatur durchgeführt; dabei wurde die ausschlaggebende Rolle des Wassers, in dessen Abwesenheit aus Butadien Oligomere entstehen, hervorgehoben. Unter den gewählten Versuchsbedingungen wächst die Polymerisationsgeschwindigkeit des Butadiens mit der Konzentration der Co- bzw. Al-Verbindung. Die Geschwindigkeit zeigt eine ungewöhnliche Abhängigkeit von der Wasserkonzentration. Durch diese Abhängigkeit wird die Schwierigkeit, reproduzierbare Versuchsergebnisse zu erzielen, erklärt. Die Molekulargewichte der erhalten Polymeren nehmen mit der Wasserkonzentration zu und mit abnehmender Co- bzw. Al-Komplexkonzentration ab. Es wurde keine nennenswerte Abhängigkeit der Mikrostruktur der Polymeren von den Versuchsbedingungen beobachtet.

Influence of the Nature of the Initiator on the Bulk Polymerization of Methyl Methacrylate

S. R. RAFIKOV, G. P. GLADISHEV, N. F. KHASANOVA, and N. V. CHURBAKOVA, *Institute of Chemical Science, Academy of Sciences of the Kazakh S.S.R., Alma-Ata, Kazakh S.S.R., U.S.S.R.*

Synopsis

The kinetics of polymerization of MMA activated by ultraviolet irradiation at various temperatures and the polymerization of monomer with dicyclohexylperoxycarbonate have been studied. The activation energy of the polymerization with percarbonate is 14.9 kcal./mole, and that of polymerization with photooxidized monomer is 11.2 kcal./mole. The temperature at which ultraviolet-oxidation of MMA (0–40°C.) is carried out has no significant influence on the kinetics of polymerization of activated monomer. The gel effect in the case of the dicyclohexylperoxycarbonate-initiated polymerization of MMA is somewhat greater than that of monomer activated by photooxidation.

In a recent communication we have reported some results of studies of the polymerization of methyl methacrylate (MMA), activated by ionizing electrons[1] or ultraviolet[2] or visible[3] light in the presence of oxygen. The investigations of the polymerization of monomer activated in this manner show that the reaction proceeds at a good rate at low temperatures and that the kinetic curve is less steep than that in the polymerization of methyl methacrylate with benzoyl peroxide and some other initiators. The gel effect in the cases studied by us is insignificant but is quite significant at comparatively greater degrees of conversion.

It is known that peroxycarbonates are also capable of initiating polymerization at low temperatures.[4] It should be expected that the gel effect would be slight in the polymerization of MMA in this case as well as, in the case of polymerization by ultraviolet-initiated oxidation. This work is intended for comparison of the kinetics of the polymerization of MMA activated by ultraviolet irradiation at various temperatures in the presence of oxygen and the polymerization of monomer in the presence of dicyclohexylperoxycarbonate.

Monomer, thoroughly freed of stabilizer by vacuum distillation (at 80 mm.), was used for the experiments. The dicyclohexylperoxycarbonate was synthesized in accordance with the method described by Strain et al.[4]

The ultraviolet-initiated oxidation of MMA was carried out at various temperatures in a quartz cell.[2] The concentration of the peroxides in all

TABLE I

Oxidation of MMA under Irradiation by Ultraviolet Rays

Irradiation temperature, °C.	Irradiation time, min.	Peroxide concentration $\times 10^{-7}$, g.-eq./ml.
0	639	70
20	60	64
40	47	65
60	12	63
80	9	58

of the activated samples was maintained at approximately the same level by changing the time of oxidation (Table I).

Table I shows that the temperature has a great influence on the accumulation of peroxide during the irradiation. Approximate calculations made on the basis of reaction rates in the early stages show that the activation energy of the process of oxidation is 10 kcal./mole. This value agrees well with previous results.[2]

The analysis of the contents of peroxide was carried out in accordance with previously described methods. In all cases control runs were carried out, the results of which were considered in the calculations of the concentration of photoperoxides.

The kinetics of the polymerization of activated monomer has been studied by the dilatometric method with the use of mercury dilatometers. The
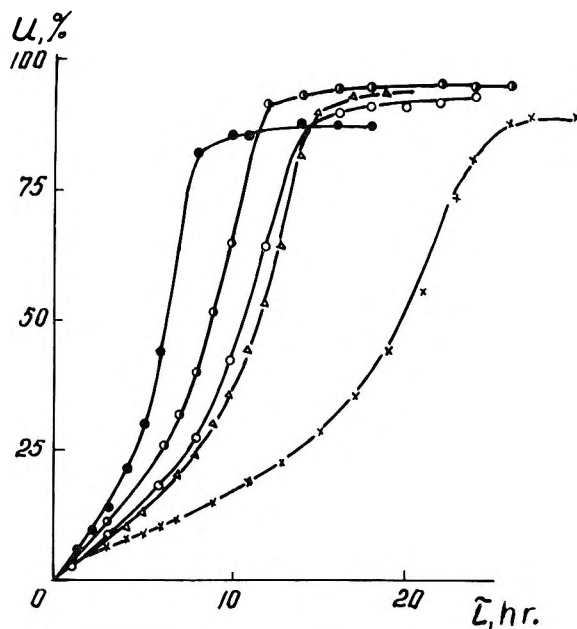
Fig. 1. Kinetics of polymerization at various temperatures of methyl methacrylate ultraviolet-activated at 80°C.: (●) 0°C.; (×) 20°C.; (O) 40°C.; (△) 60°C.; (◑) 80°C.
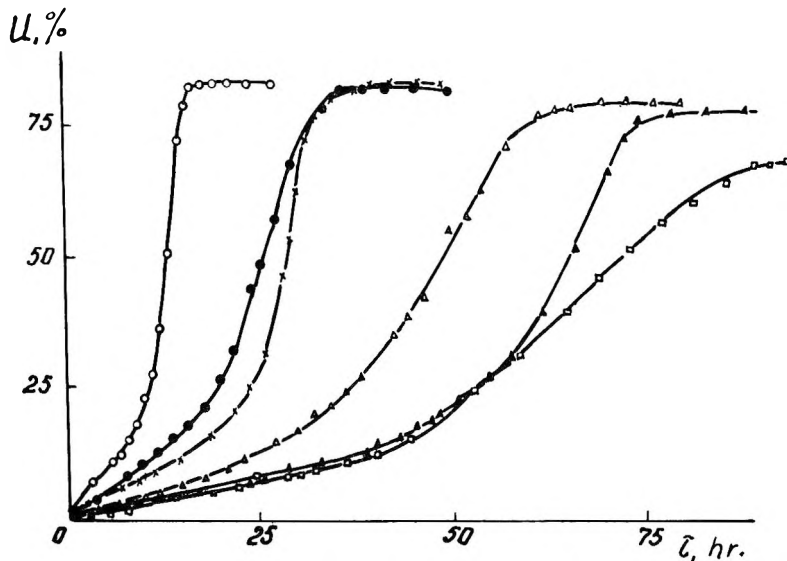
Fig. 2. Kinetics of polymerization of methyl methacrylate with dicyclohexylper-oxycarbonate as initiator: (O) 13.4 × 10^{-3}% initiator, 40°C.; (×) 13.4 × 10^{-3}% initiator, 30°C.; (▲) 13.4 × 10^{-3}% initiator, 20°C.; (●) 6.0 × 10^{-3}% initiator, 40°C.; (△) 6.0 × 10^{-3}% initiator, 30°C.; (□) 6.0 × 10^{-3}% initiator, 20°C.

dilatometers were placed in a water thermostat, the temperature of which was maintained constant to ±0.2°C.

Figures 1 and 2 show the kinetic curves of the polymerization of ultra-violet-activated monomer and polymerization initiated by percarbonate, respectively. These plots show that the curves in both cases are identical and do not differ in any way from those previously obtained in studies of the polymerization of ultraviolet-activated monomer.

Figures 3 and 4 show curves indicating the dependence of the relative rate of polymerization upon the reaction time (the results of one set of experiments). Figure 3 shows that the gel effect in the polymerization of ultraviolet-activated MMA at 60°C. is somewhat higher then that of the samples activated at other temperatures. It is probable that such a difference is due to the greater concentration of peroxides of MMA in the sample irradiated at 60°C. In samples irradiated at 80°C. the gel effect is less noticeable, probably, because of the accumulation of the products of the decomposition of the peroxides capable of terminating the chain. In all other cases (taking into consideration possible errors in the experiment) the relationship of the maximum rate of polymerization of the stage of autoacceleration to the initial rate is the same.

In most of the cases studied (Fig. 4) in the polymerization of MMA in the presence of dicyclohexylperoxycarbonate the gel effect is somewhat greater, and its value depends upon the concentration of the initiator. It could be assumed that the increase of the gel effect with increasing concentration of initiator was due to the change in the thermal conditions dur-
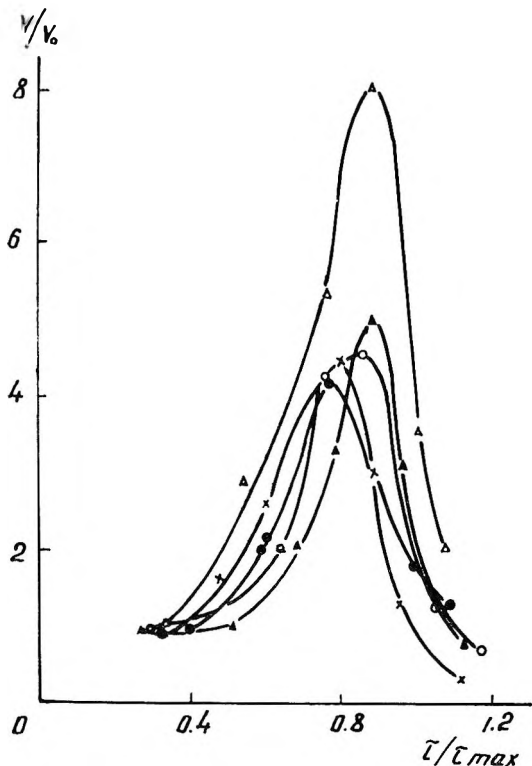
Fig. 3. Effect of temperature of activation on the kinetics of polymerization of methyl methacrylate at 20°C.: (●) 0°C.; (▲) 20°C.; (×) 40°C.; (△) 60°C.; (○) 80°C. V_0, initial rate of polymerization; V, rate of polymerization at time t; t_{max}, time, corresponding to abrupt slow-down of rate of reaction at conversion 70–80%.

ing the process. However, measurements in which the temperature was recorded to ±0.2°C. show that the polymerization in all cases continues without heating of the sample, the heat evolved as a result of the reaction being completely dissipated in the thermostatically controlled systems. It is possible that the relation of the magnitude of the gel effect to the concentration of percarbonate has to do primarily with the mechanism of the process of initiation.

Our data coincide with those obtained by other authors. Burnett and Duncan, for example, note that in the bulk photopolymerization of MMA the degree of conversion at which the autoacceleration begins, greatly depends on the rate of initiation. The larger the rate of polymerization, the higher the degree of conversion at which the autoacceleration begins.

Figure 4 shows that there is no direct connection between the gel effect data and the temperature (in the range of 20–40°C.) of polymerization when the polymerization of MMA is initiated with dicyclohexylperoxycarbonate. The kinetic curves of polymerization at 30°C. have a greater value for $(V/V_0)_{max}$. This phenomenon can be explained if we consider that the

correlation of the above mentioned values depends, besides the mechanism of the initiation process, on the mechanism of the chain termination. The latter is related to the viscosity of the medium and the temperature of polymerization.

It is our view that the late beginning of the autoaccelerative stage at increased concentrations of dicyclohexylperoxycarbonate has to do with the termination of the growing chains (in the range of degrees of conversion
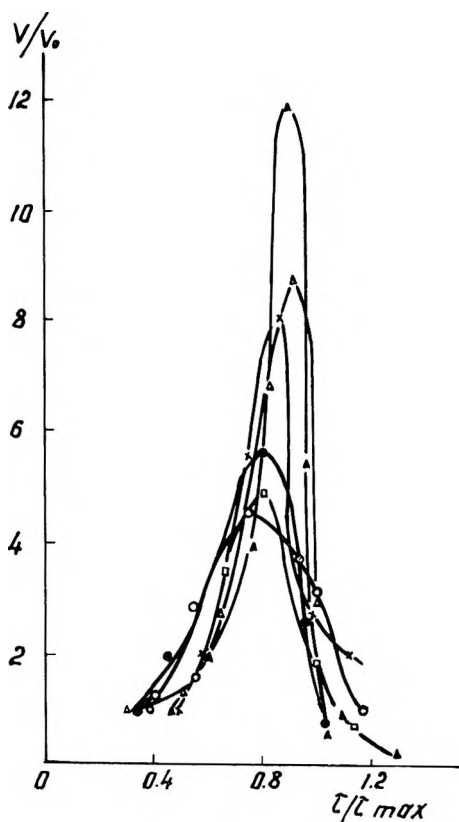
Fig. 4. Effect of conditions of reaction of kinetics of polymerization of methyl methacrylate with dicyclohexylperoxycarbonate as initiator: ($\times$) 13.4 $\times$ 10^{-3}% initiator, 40°C.; ($\blacktriangle$) 13.4 $\times$ 10^{-3}% initiator, 30°C.; ($\triangle$) 13.4 $\times$ 10^{-3}% initiator, 20°C.; ($\square$) 6.0 $\times$ 10^{-3}% initiator, 40°C.; ($\bullet$) 6.0 $\times$ 10^{-3}% initiator, 30°C.; (O) 6.0 $\times$ 10^{-3}% initiator, 20°C.

of 10–25%) as a result of interaction with primary radicals. This conclusion is proved by the analysis of the polymerization of MMA initiated with dimethylperoxycarbonate which is typical of the lack of dependence of the gel effect value on the initiator concentration.

The plot of V_0 versus $C^{1/2}$ shows that the law of proportionality of the initial rate of polymerization V_0 to the square root of the initiator concentration $C^{1/2}$ is quite applicable.

TABLE II
Comparison of the Polymerization of MMA
in the Presence of Various Initiators

Initiator	Mean $(V/V_0)_{max}$	Approximate point of noticeable acceleration of polymerization, % of conversion	Overall activation energy E, kcal./mole	Activation energy of initiation E_{in}, kcal./mole
Benzoyl peroxide	10–16	12	19.3	30
Dicyclohexyl-peroxycarbonate	5–8	14	14.9	20.2
Photoperoxides of MMA	4.8–4.7	21	11.2	12.6
Thermoperoxide of MMA	10	12	16	22

Table II shows the results of the analysis of MMA polymerization in the presence of various initiators.[1,2] These data show that the polymerizations of monomer activated by photooxidation as well as polymerization with percarbonate typically have a smaller gel effect, and the gel effect is observed at greater degrees of conversion than is the case of polymerization in the presence of benzoyl peroxide and the thermoperoxide of MMA. The polymerization of photooxidized monomer typically has the smallest gel effect and the smallest value for activation energy of the initiating reaction.

References

1. Tsetlin, B. L., V. A. Sergeev, S. R. Rafikov, V. V. Korshak, P. Y. Glazunov, and L. D. Bubis, *Dokl. Akad. Nauk SSSR*, **126**, 123 (1959).
2. Rafikov, S. R., and G. P. Gladishev, *Vysokomol. Soedin.*, **3**, 1034 (1961).
3. Gladishev, G. P., and S. R. Rafikov, *Vysokomol. Soedin.*, **3**, 1187 (1961); *ibid.*, **4**, 1345, 1356 (1962).
4. Strain, F., H. Rudoff, B. J. DeWitt, H. C. Stevens, and J. H. Langston, *J. Am. Chem. Soc.*, **72**, 1254 (1950).

Résumé

On a étudié la cinétique de polymérisation du méthacrylate de méthyle activée par irradiation aux rayons ultra-violets à des températures différentes et la cinétique de polymérisation de ce monomère avec le peroxydicarbonate de dicyclohexyle. L'énergie d'activation du processus de polymérisation par le percarbonate est égal à 14.9/kcal./mole et celle de la réaction avec le monomère photooxydé à 11.2/kcal./mole. On a trouvé que la température à laquelle on effectue l'oxydation du méthacrylate de méthyle par les rayons ultraviolets n'a pas d'influence marquée sur les courbes de polymérisation du monomère activé. Il est évident que "l'effet de gel" dans le cas de la polymérisation du

méthacrylate de méthyle par le peroxydicarbonate dicyclohexyle est un peu plus pro-
noncée que dans le cas du monomère activé par photooxydation.

Zusammenfassung

Die Kinetik der Polymerisation des durch Ultraviolettbestrahlung aktivierten MMA
bei verschiedenen Temperaturen und die Polymerisation des Monomeren mit Dizyklo-
hexylperoxydicarbonat wurden untersucht. Die Aktivierungsenergie für die Poly-
merisation mit Percarbonat beträgt 14,9 kcal/Mol und diejenige des Prozesses mit
photooxydiertem Monomeren ist 11,2 kcal/Mol. Es wurde festgestellt, dass die Tem-
peratur der UV-Oxydation von MMA (von 0° bis 40°C.) keinen merklichen Einfluss auf
die Polymerisationskurve des aktivierten Monomeren hat. Offenbar ist der Gel-Effekt
im Fall der Polymerisation von MMA mit Dizyklohexylperoxydicarbonat et was grösser
als beim durch Photooxydation aktivierten Monomeren.

Poly-1,3,4-oxadiazoles.
I. Polyphenylene-1,3,4-oxadiazoles

YOSHIO IWAKURA, KEIKICHI UNO, and SHIGEYOSHI HARA, *Department of Synthetic Chemistry, Faculty of Engineering, University of Tokyo, Tokyo, Japan*

Synopsis

Polyphenylene-1,3,4-oxadiazoles have been prepared from benzenedicarboxylic acids or their derivatives and hydrazine by solution polycondensation in fuming sulfuric acid or polyphosphoric acid. These polymers were characterized by good thermal stability, and the molecular weights attained were high enough for the products to exhibit fiber-or-film-forming properties. Concentrated sulfuric acid and polyphosphoric acid were the only solvents for these polymers.

INTRODUCTION

In recent years, many investigations have been carried out concerning thermally stable polymers with an aromatic repeating unit. We have already reported on the preparation of polyphenylenebenzimidazoles by solution polycondensation between 3,3′-diaminobenzidine tetrahydrochloride and benzenedicarboxylic acid or its derivatives in polyphosphoric acid (PPA).[1] The present paper describes a novel preparative method for polyphenylene-1,3,4-oxadiazoles.

Aromatic poly-1,3,4-oxadiazoles have previously been prepared by condensation between bistetrazoles and dicarboxylic acid chlorides[2] and by dehydration of polyhydrazides.[3] These polymers showed remarkable thermal and chemical stability.

2,5-Bis(*p*-aminophenyl)1,3,4-oxadiazole has been prepared by treating *p*-aminobenzoic acid with hydrazine sulfate in fuming sulfuric acid or polyphosphoric acid,[4] eq. (1)
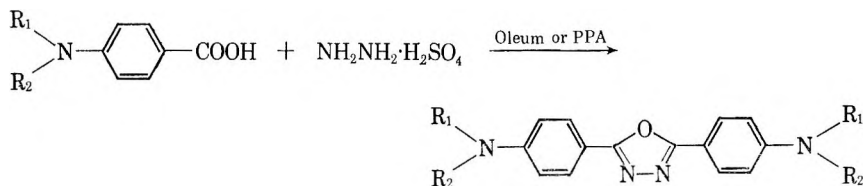
We have prepared polyphenylene-1,3,4-oxadiazoles of high molecular weight from benzenedicarboxylic acids or their simple derivatives and

hydrazine sulfate using fuming sulfuric acid or polyphosphoric acid which acted as solvent as well as condensing agent, eq. (2):
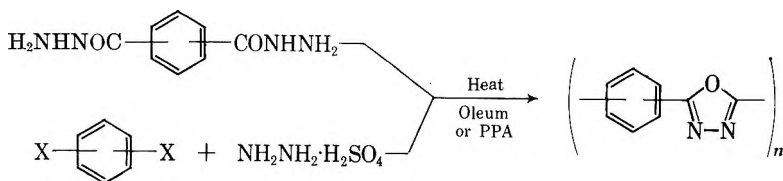
where X is —COOH, —CONH$_2$, or —CN.

RESULTS AND DISCUSSION

Tables I and II show the results of polycondensation. It can be seen from these data that fuming sulfuric acid is superior to polyphosphoric acid as the reaction medium. It was unnecessary to make hydrazine sulfate and dicarboxylic acid components equimolar in this reaction. So far as hydrazine was charged excessively, this reaction proceeded smoothly. In the cases of diamides or dinitriles the use of excess hydrazine was necessary to obtain polymers of high molecular weight. It was observed apparently that terephthalic acid and its derivatives reacted with hydrazine much faster than corresponding isophthalic acid derivatives.

The polymers were obtained in nearly quantitative yield in all cases. Poly-p-phenylene-1,3,4-oxadiazoles obtained here were yellowish brown, whereas poly-m-phenylene-1,3,4-oxadiazoles were almost colorless, but PIII-2, PIII-3, PIV-2, and PIV-4 were slightly reddish. It seems that the development of red color is due to the presence of small amount of impurities which comes from oxidation of hydrazine derivatives during the reaction. Poly-p-phenylene-1,3,4-oxadiazoles were tough and stiff resin, and could be fabricated to a film or fiber from the solution of concentrated sulfuric acid. On the other hand, poly-m-phenylene-1,3,4-oxadiazoles were brittle.

Infrared Spectra and Elemental Analyses

Evidence for the oxadiazole structure of the polymers prepared here was obtained from studies with model compounds and comparative infrared spectra. We prepared four such model compounds (M-1, M-2, M-3, and M-4), and compared their infrared spectra with those of the polymers. The infrared spectra are shown in Figure 1.

2,5-Diphenyl-1,3,4-oxadiazole (M-1)

N, N'-Dibenzoylhydrazine (M-2)

3,5−Diphenyl−4−amino−1,2,4−triazole (M−3)

3,5−Diphenyl−1,2,4−triazole (M−4)
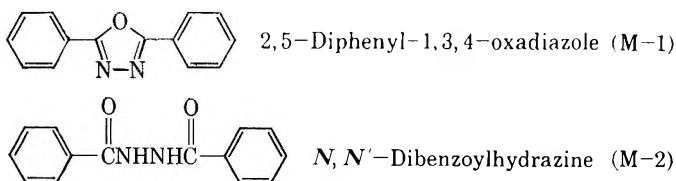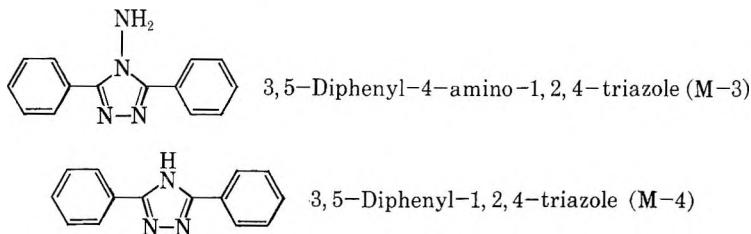
All the infrared spectra of the polymers prepared agreed with that of 2,5-diphenyl-1,3,4-oxadiazole. Moreover, it was observed that the infrared spectra of poly-m-phenylene-1,3,4-oxadiazole synthesized here gave good agreement with that of poly-m-phenylene-1,3,4-oxadiazole described by H. Frazer.[3] No absorption band characteristic of sulfonic acid was observed in the infrared spectra of the polymers prepared in fuming sulfuric acid.

Nitrogen contents of the polymers ranged from 18.81% to 19.57% excepting low molecular weight polymers such as PII-3 and PIV-4. Nitrogen content calculated for polyphenyleneoxadiazole is 19.44%.

These observations prove our polymers to be the expected polyphenylene-1,3,4-oxadiazoles.

Solubility

Polyphenylene-1,3,4-oxadiazoles were soluble only in concentrated sulfuric acid and polyphosphoric acid, producing stable solution. They were insoluble in any organic solvent, but swelled to some extent in such organic acids as formic acid, acetic acid, dichloroacetic acid, phenol, and m-cresol. This insolubility in organic solvents makes the fabrication of polyphenylene-1,3,4-oxadiazoles difficult.

Ultraviolet Absorption Spectra
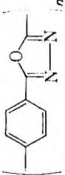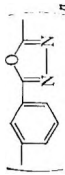
The ultraviolet spectral data of polyphenylene-1,3,4-oxadiazoles and a model compound in concentrated sulfuric acid are shown in Table III. Compared with the spectrum of 2,5-diphenyl-1,3,4-oxadiazole, a remarkable bathochromic shift was observed in the spectrum of poly-p-phenylene-1,3,4-oxadiazole, whereas no shift was observed in that of poly-m-phenylene-1,3,4-oxadiazole.

Crystallinity

The x-ray diffraction diagrams of polyphenylene-1,3,4-oxadiazoles shown in Figure 2 were obtained by the powder method with the use of nickel-filtered CuKα radiation.

The diagrams indicate that both poly-p-phenylene-1,3,4-oxadiazole and poly-m-phenylene-1,3,4-oxadiazole are crystalline, but the former has a higher degree of crystallinity because of its more symmetrical polymer structure.

TABLE I

Preparations of Polyphenylene-1,3,4-oxadiazoles in Fuming Sulfuric Acid

Polymer	No.	Dicarboxylic acid derivative	Wt. dicarboxylic acid, g.	Wt. hydrazine sulfate, g.	Wt. 30% oleum, g.	Reaction conditions		$[\eta]$, dl./g.[a]
						Temp., °C.	Time, hr.	
	PI-1	Terephthalic acid	8.3	6.5	125	85 125	3 1	3.7
	PI-2	Terephthaloyl di-hydrazide[b]	7.8	—	100	85	1.5	0.83
	PI-3	Terephthaloyl di-hydrazide dihy-drochloride[c]	1.4	—	15	85	1.5	2.5
	PI-4	Terephthalamide	1.6	1.6 (20% excess)	25	85 125	3 4	1.7
	PII-1	Isophthalic acid	8.3	6.5	125	125	3	2.2
	PII-2	Isophthaloyl dihydrazide	7.8	—	100	85 125	2 1	0.73
	PII-3	Isophthalamide	3.3	3.0 (20% excess)	50	85 125	3 3	0.1
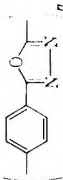
[a] Calculated from viscosities in 95% sulfuric acid at 30°C.

[b] Terephthaloyl dihydrazide used was washed repeatedly with hot ethanol. (Anal. Calc. for $C_8H_{10}O_2N_4$: N, 28.85%. Found: N, 26.12%.)

[c] Terephthaloyl dihydrazide dihydrochloride used was recrystallized from water. (Anal. Calc. for $C_8H_{12}O_2N_4Cl_2$: N, 20.97%, Found: N, 20.90%.)

TABLE II
Preparations of Polyphenylene-1,3,4-oxadiazoles in Polyphosphoric Acid

Polymer	No.	Dicarboxylic acid derivative	Wt. dicarboxylic acid, g.	Wt. hydrazine sulfate, g.	Wt 116% PPA, g.	Reaction conditions Temp., °C.	Time, hr.	η_{sp}/c, dl./g.[a]
(structure)	PIII-1	Terephthalic acid	3.3	3.1 (20% excess)	50	140 / 180	5 / 0.5	1.8
	PIII-2	Terephthaloyl dihydrazide[b]	4.0	—	50	135 / 180	6 / 2	0.4
	PIII-3	Terephthaloyl dihydrazide dihydrochloride[b]	1.4	—	15	140	3	0.85
	PIII-4	Terephthalamide	1.6	2.0 (50% excess)	25	170 / 140 / 170	3 / 3 / 11	1.15
	PIII-5	Terephthalonitrile	1.3	2.6 (100% excess)	25	140 / 170	3 / 13	1.6
(structure)	PIV-1	Isophthalic acid	3.3	3.1 (20% excess)	50	180	13	0.5
	PIV-2	Isophthaloyl dihydrazide	4.0	—	50	110 / 180	3 / 6	0.7
	PIV-3	Isophthalamide	1.6	2.0 (50% excess)	25	140 / 170	3 / 11	0.45
	PIV-4	Isophthalonitrile	1.3	2.6 (100% excess)	25	140 / 180	3 / 13	0.25

[a] Measured at a concentration of 0.2 g./100 ml. in 95% sulfuric acid at 30°C.
[b] See Table I.

Thermal Stability

Polyphenylene-1,3,4-oxadiazoles showed no melting point.   The thermal stability of the polyphenylene-1,3,4-oxadiazoles was determined by the thermogravimetric analysis; the curves are shown in Figure 3.   Only minor weight loss was observed below 450°C. in air, and an abrupt weight
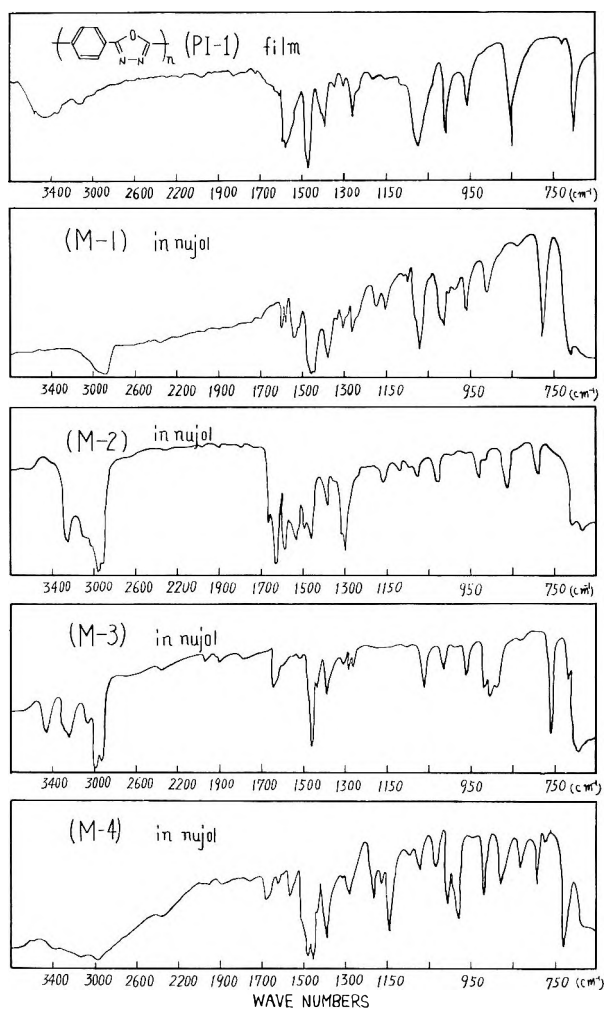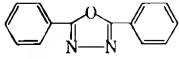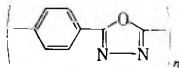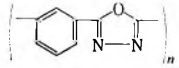
Fig. 1. Infrared spectra of the polymer and model compounds.

loss occurred above 450°C. in both poly-*p*-phenylene-1,3,4-oxadiazole and poly-*m*-phenylene-1,3,4-oxadiazole.   When a film of poly-*p*-phenylene-1,3,4-oxadiazole was heated at 450°C. for 2 hr. in air, it turned black and brittle, but the infrared spectrum remained almost unchanged.

TABLE III
Ultraviolet Spectral Data in Concentrated Sulfuric Acid

	λ_{max}, mμ	$E_{1\ cm.}^{1\%}$
(M-1)	301 247	1080 580
(PI-1)	367 352 270 (shoulder)	1240 1370
(PII-2)	301 228	1370 750
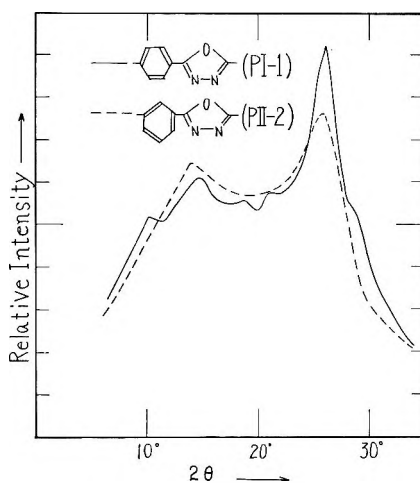
Fig. 2. X-ray diffraction pattern of polyphenylene-1,3,4-oxadiazoles with Ni-filtered CuKα radiation.

EXPERIMENTAL

Monomers

Hydrazine sulfate, isophthalic acid derivatives, and terephthalic acid derivatives were obtained as commercial reagents or prepared by usual methods.

Model Compounds

2,5-Diphenyl-1,3,4-oxadiazole. The procedure was that of the literature.[4] The compound was recrystallized from ethanol; m.p. 137.5–138°C. (lit.[5] m.p. 138°C.).

ANAL. Calcd. for $C_{14}H_{10}ON_2$: N, 12.56%. Found: N, 12.52%.
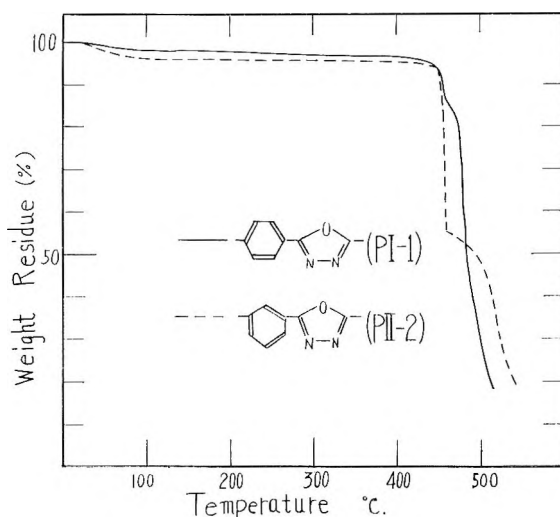
Fig. 3. Thermogravimetric analysis curves for polyphenylene-1,3,4-oxadiazoles in air.

N,N'-Dibenzoylhydrazine. This was prepared from benzoylhydrazine and benzoyl chloride, and was recrystallized from ethanol; m.p. 233–234°C. (lit.[6] m.p. 237–239°C.).

3,5-Diphenyl-4-amino-1,2,4-triazole. This compound was prepared by condensation of benzoylhydrazine or N,N'-dibenzoylhydrazine in the presence of excessive hydrazine.[7] It was recrystallized from ethanol; m.p. 265.5–266.5°C. (lit.[7] m.p. 263°C.).

ANAL. Calcd. for $C_{14}H_{12}N_4$: N, 23.72%. Found: N, 23.73%.

3,5-Diphenyl-1,2,4-triazole. This triazole was prepared by the reaction between 2,5-diphenyl-1,3,4-oxadiazole and formamide in an autoclave.[8] It was recrystallized from 70% ethanol; m.p. 193.5–194°C. (lit.[9] m.p. 192°C.).

Solution Polycondensation

Typical preparations of polyphenylene-1,3,4-oxadiazoles by solution polycondensation are mentioned below.

Preparation of Poly-p-phenylene-1,3,4-oxadiazole in Fuming Sulfuric Acid (PI-1). In a 100-ml. three-necked flask equipped with a sealed stirrer, air-condenser protected by a calcium chloride drying tube, and stopper was placed 125 g. of 30% SO_3 fuming sulfuric acid. Under a mechanical stirring, 3.5 g. of hydrazine sulfate was added gradually and into the resulting homogeneous solution was dissolved 8.3 g. of terephthalic acid. The mixture was heated at 85°C. for 3 hr. and then at 120°C. for 1 hr. It gradually became viscous as the polycondensation reaction proceeded. The polymer was isolated by pouring the cooled mixture into ice water, dipped in running water for three days to remove sulfuric acid, and dried in a vacuum oven heated at 70–80°C.

The polymer was obtained in a quantitative yield as a yellowish brown resin. The intrinsic viscosity of 3.7 dl./g. was calculated from viscosities measured in 95% sulfuric acid at 30°C.

ANAL. Calcd. for $C_8H_4ON_2$: C, 66.66%; H, 2.80%; N, 19.44%. Found: C, 64.88%; H, 2.80%; N, 19.57%.

Preparation of Poly-*p*-phenylene-1,3,4-oxadiazole in Polyphosphoric Acid (PIII-1).

In a 50-ml. three-necked flask equipped with a sealed stirrer, nitrogen inlet, and calcium chloride drying tube, was placed 50 g. of 116% polyphosphoric acid. In the acid was dissolved 3.1 g. of hydrazine sulfate and 3.3 g. of terephthalic acid at 140°C. under a thin stream of nitrogen. Heating was continued at 140°C. for 5 hr., and then at 180°C. for $^1/_2$ hr. The reaction mixture gradually became viscous and finally was enforced to discontinue stirring. The polymer was isolated by pouring the high viscous solution into water, washed with water by decantation and dipped in diluted Na_2CO_3 solution overnight. It was washed again thoroughly with water and dried in a vacuum oven heated at 70–80°C.

The polymer was obtained as a yellowish brown resin, in 2.8 g. yield. A 0.2 g./100 ml. solution of this polymer in 95% sulfuric acid at 30°C. showed η_{sp}/c of 1.8 dl./g.

Samples for Elemental Analysis and Thermal Stability Measurement

Samples were purified by extraction in boiling water for 5 hr. and dried in a vacuum oven at 80°C. overnight, then dried further at 222°C. for 30 min.

References

1. Iwakura, Y., K. Uno, and Y. Imai, *J. Polymer Sci.*, **A2**, 2605 (1964).
2. Abshire, C. J., and C. S. Marvel, *Makromol. Chem.*, **45/46**, 388 (1961).
3. Frazer, A. H., W. Sweeny, and F. T. Wallenberger, *J. Polymer Sci.*, **A2**, 1157 (1964).
4. Neugebauer, W., Japan Pat. 256,946 (1959).
5. Stollè, R., *J. Prakt. Chem.*, [2] **69**, 157 (1904).
6. Mohr, E., *J. Prakt. Chem.*, [2] **70**, 305 (1904).
7. Silberrad, O., *J. Chem. Soc.*, **77**, 1190 (1900).
8. Neugebauer, W., Japan Pat. 256,947 (1959).
9. Pinner, A., *Ann.*, **297**, 256 (1897).

Résumé

Le poly-1,3,4-oxadiazole a été préparé à partir des acides phényldicarboxyliques ou de leurs dérivés, et de l'hydrazine, par polycondensation en solution dans l'acide sulfurique fumant ou l'acide phosphorique. Ces polymères sont caractérisés par une bonne stabilité thermique, et les poids moléculaires atteints sont suffisamment élevés pour que ces polymères puissent former des fibres ou des films. L'acide sulfurique concentré et l'acide phosphorique sont les seuls solvants de ces polymères.

Zusammenfassung

Poly-1,3,4-oxadiazol wurde aus Benzoldicarbonsäuren oder ihren Derivaten und Hydrazin durch Lösungspolykondensation in rauchender Schwefelsäure oder Polyphosphorsäure dargestellt. Diese Polymeren waren durch gute thermische Stabilität ausgezeichnet, und die erreichten Molekulargewichte waren hoch genug, um faser- oder filmbildende Eigenschaften aufscheinen zu lassen. Konzentrierte Schwefelsäure und Polyphosphorsäure waren die einzigen Lösungsmittel für diese Polymeren.

Kinetics of the γ-Radiation-Induced Low Temperature Polymerization of Methyl Methacrylate

N. THORNTON LIPSCOMB and EDWIN C. WEBER, *Department of Chemistry, College of Arts and Sciences, University of Louisville, Louisville, Kentucky*

Synopsis

Studies have been made of the rates of γ-radiation-initiated polymerization of methyl methacrylate in bulk between the temperatures of −19 and −49°C. and at radiation intensities from 3.77 × 10⁵ to 1.35 × 10⁵ rad/hr. The activation energy over this temperature range was found to be 3.85 kcal./mole at 3.77 × 10⁵ rad/hr. The rate of the reaction was found to be proportional to the intensity to the 0.33 power at both −19°C. and −49°C. Molecular weight information showed that transfer to monomer was unimportant in the polymerization. Nuclear magnetic resonance studies showed that the amount of syndiotacticity in the polymer increases with decreasing temperature.

Introduction

Previous investigations of the kinetics of the γ-radiation-induced polymerization of pure methyl methacrylate have been made at temperatures of −18°C. to 70°C.[1-4] and radiation intensities up to 18,190 rad/min. Ballantine et al.[2] have reported an activation energy of 4.25 kcal./mole for this temperature range. Other workers have reported values of 4.0 kcal./mole[5] and 4.9 kcal./mole[6] using photochemical initiation.

The work reported here deals with the irradiation of liquid methyl methacrylate in the temperature range of −19 to −49°C. which has not been covered by previous investigations. Three different average intensities of γ-radiation were used: 3.77 × 10⁵ rad/hr., 2.04 × 10⁵ rad/hr., and 1.35 × 10⁵ rad/hr.

The series of reactions generally considered to cover the main routes available for liquid-phase, homogeneous, free-radical polymerization[3,7,8] applied to this reaction are shown in Table I. It is to be cautioned that no particular identity is assigned to the radicals, and that all the reactions will not necessarily be important in this specific instance. The conversion of monomer to polymer was held low so that the concentration of monomer was essentially static and may be incorporated into the constant.

Experimental

The irradiation facility used in these experiments is similar to that described previously,[9] and the ferrous ion dosimetry technique was described

TABLE I
Primary Reactions of Methyl Methacrylate Polymerization

Reaction	Equation	Rate expression
Primary initiation	$M + \gamma \rightarrow R\cdot$	$d[R\cdot]/dt = k_1 T$
Chain initiation	$R\cdot + M \rightarrow RM\cdot$	$-d[R\cdot]/dt = k_2[R\cdot][M]$
Propagation	$RM\cdot + M \rightarrow RM\cdot_{n+1}$	$-d[M]/dt = k_3[RM\cdot][M]$
Transfer	$RM_n\cdot + M \rightarrow RMH + M\cdot$	
	$RM_n\cdot + P \rightarrow RMH + P\cdot$	
Termination	$RM_n\cdot + RM_m\cdot \rightarrow RM_nM_mR$	$-d[RM\cdot]/dt = k_5[RM\cdot]^2$
	$RM_n\cdot + RM_m\cdot \rightarrow RM_nH + RM_{m-1}\!-\!CH\!=\!CH_2$	$-d[RM\cdot]/dt = k_5'[RM\cdot]^2$
	$RM_n\cdot + R\cdot \rightarrow RM_nR$	$-d[RM\cdot]/dt = k_5''[RM\cdot]$

by Weiss.[10,11] The methyl methacrylate was obtained from Matheson, Coleman and Bell Company.

After drying, the monomer was distilled under nitrogen.   Only the center cut was retained.   The sample was degassed four times in a scrupulously cleaned glass cell, then distilled into a second cell without the application of heat.   The first and second cells were connected in an evacuated isolated system and the first cell was allowed to warm to room temperature while the second was immersed in acetone–Dry Ice.   The degassing procedure was repeated twice more and the cell sealed under vacuum by collapsing the cell walls with a torch.   The cooling jacket, which contained the sample cell in the radiation chamber, was stainless steel and allowed cool methanol to be circulated in direct contact with the sample vial.   The methanol was pumped through cooling coils immersed in a temperature controlled methanol bath whose temperature was regulated by a thermostatically controlled pump which circulated methanol from another bath maintained at $-78°C$. by Dry Ice.   This system allowed accurately controlled temperature between $+10$ and $-50 \pm 0.5°C$.

Temperature, °C.	Average intensity, rad/hr.	Rate, %/hr.	Rate, mole/l./hr.
−19	377,000	3.05	0.309
−29	377,000	2.25	0.226
−39	377,000	1.60	0.153
−49	377,000	1.10	0.109
−19	204,000	2.50	0.253
−49	204,000	0.89	0.638
−19	135,000	2.13	0.216
−49	135,000	0.69	0.0680

The amount of polymer produced by irradiation was determined by precipitation in methanol and weighing.[12,13]   Table II is a tabulation of the average rates of polymerization as a function of temperature and radiation intensity.   Each value in this table was the result of a least-squares analysis of from three to eight individual runs of different duration.   All of these plots passed through the origin and no induction period was observed.

Nuclear magnetic resonance spectra were obtained by using a Varian Associates V-4302 dual purpose 60 Mcycle/sec. instrument in connection with a heated probe.   A 15% (w/v) solution of polymer in spectro grade chloroform was used and peak areas were approximated by triangulation. Final peak area reported is the average of several spectra.

Activation Energies

The activation energy for the series of polymerizations at 3.77×10^5 rad/hr. was found from an Arrhenius plot from rates of polymerization at four different temperatures (Fig. 1).   This value was calculated to be 3.85 kcal./mole.   The activation energies for the runs carried out at intensities of 2.04×10^5 and 1.35×10^5 rad/hr. were calculated less precisely from data for only two different temperatures, and were found to be 3.86 and 4.25 kcal./mole, respectively.   The latter value probably reflects experimental scatter rather than a variation of activation energy with intensity.
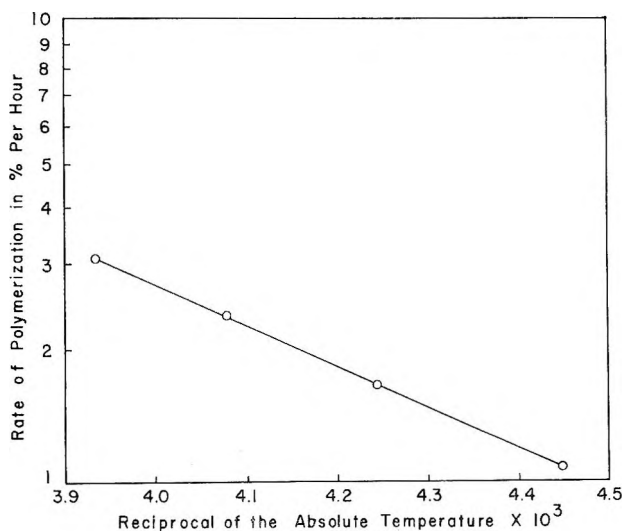
Fig. 1. Rate of polymerization as a function of temperature at 3.77×10^5 rad/hr.

Intensity Dependence

The general equation for the overall rate of polymerization is

$$\text{Rate} = kI^{\alpha}[\text{M}]^{\beta}$$

In the case of a bulk polymerization at low yield, the monomer concentration remains essentially constant to give:

$$\text{Rate} = k'I^{\alpha}$$

Thus, the slope of a plot of the logarithm of the rate versus the logarithm of intensity will yield α directly. The data at -19 and $-49°C$. yielded straight lines, both having a slope of 0.33.

The classic mechanism of a free-radical polymerization calls for an intensity dependence of 0.5, and this value has been reported for methyl methacrylate at lower intensities. Chapiro and Magat have shown, however, that the intensity dependence is equal to 0.5 only up to an intensity of about 0.42×10^4 rad/hr. At this point α starts to diminish toward zero, presumably because a significant amount of termination occurs by recombination of primary radicals. The intensity dependence of 0.33 found here supports the findings of Chapiro and Magat.

Molecular Weight

Examination of the molecular weight information listed in Table III shows that molecular weight increases with increasing temperature and

TABLE III
Molecular Weights of Polymers Obtained from Irradiation of
Liquid Methyl Methacrylate

Average intensity, rad/hr.	Temperature, °C.	Molecular weight
377,000	-49	2.0×10^5
135,000	-49	2.4×10^5
377,000	-19	3.4×10^5
204,000	-19	5.0×10^5

decreasing radiation intensity. An increase in molecular weight with increasing temperature indicates that the polymerization is not governed by a transfer reaction and the degree of polymerization adheres to the following expression:[14]

$$\text{DP} = Ke^{-E_a/RT}$$

The rate of propagation increases with temperature, leading to a greater degree of polymerization. The temperature effect on the termination step is small.

At higher intensity the rate of propagation remains the same but the increase in initiation provides a larger concentration of radicals which increase the probability of bimolecular termination. This, of course, causes a decrease in molecular weights. The general range of molecular weights reported here are in good agreement with the values reported earlier[2] at a slightly higher temperature.

NMR Spectra

Bovey and Tiers[15] have previously obtained NMR spectra of poly(methyl methacrylate) and have assigned τ values for the α-methyl peaks corresponding to different configurations. The peak at 8.78 was attributed by them to the isotactic configuration in which the α-methyl groups are flanked on both sides by units of the same configuration (i.e., *ddd* or *lll*). The peak at 9.09τ was attributed to the syndiotactic configuration of the forms *dld* or *ldl*. The α-methyl groups of the heterotactic configuration, *ldd*, *dll*, *ddl*, or *lld*, were assigned the peak at 8.95τ. The NMR data for polymers prepared in this work are shown in Table IV.

TABLE IV

Chemical Shift τ of the α-Methyl Peaks as a Function of Configuration and Irradiation Temperature for Polymers Produced in the Liquid State

Configuration	τ, p.p.m.				Literature values[a]
	$-19°C.$	$-29°C.$	$-39°$	$-49°C.$	
Isotactic	8.77	8.79	8.77	8.77	8.78
Heterotactic	8.94	8.96	8.97	8.92	8.95
Syndiotactic	9.07	9.11	9.08	9.12	9.09

[a] Data of Bovey and Tiers.[15]

Relative fraction of syndiotactic configuration as a function of irradiation temperature is shown in Table V. This relative fraction of the contribution of the syndiotactic configuration was calculated based on the total area of syndiotactic and heterotactic peaks. The isotactic peak was not used in this calculation because the area was essentially the same in all spectra and would not affect any trends. In addition, this peak was very small.

TABLE V

Relative Fraction of Syndiotactic Configuration as a Function of Irradiation Temperature

Temperature, °C.	Fraction syndiotactic
-19	0.77
-29	0.82
-39	0.85
-49	0.88

The relative amounts of syndiotacticity increases as the temperature of irradiation decreases. This same trend is noted by Bovey[16] for chemically initiated polymerization of methyl methacrylate. This is probably due to the fact that formation of the syndiotactic configuration requires 0.75

kcal./mole less energy than the formation of the heterotactic form.   This is attributed to steric hindrance.

The isotactic contribution is understandably small and it has been shown that isotactic placements are sterically almost impossible unless the polymer chain is in a helical configuration and the reacting monomer approaches from the direction corresponding to a continuation of the helix.

References

1. Ballantine, D., *J. Polymer Sci.*, **19**, 219 (1956).

2. Ballantine, D., B. Manowitz, A. Glines, P. Colombo, and S. Ballanca, P.R.O., Fissions Products Utilization, BNL-229 (1953).

3. Chapiro, A., and M. Magat, *Actions Chimiques et Biologiques des Radiation*, Vol. 3, Part II, Masson, Paris, 1955, p. 97.

4. Sebban-Danon, J., and A. Chapiro, *J. Chim. Phys.*, **54**, 776 (1957).

5. Mackay, H., and H. Melville, *Trans. Faraday Soc.*, **45**, 332 (1949).

6. Matheson, M., E. Auer, E. Bevilacqua, and E. Hart, *J. Am. Chem. Soc.*, **71**, 497 (1949).

7. Bouby, L., A. Chapiro, M. Magat, E. Migirdicyan, A. Provot-Bernas, L. Reinisch, and J. Sebbon, *Proceedings of the International Conference on Peaceful Uses of Atomic Energy*, Vol. 7, United Nations, New York, 1956, p. 526.

8. Charlesby, A., and M. G. Ormerod, *Proceedings of the International Symposium on Radiation-Induced Polymerization and Graft Copolymerization*, U.S. Atomic Energy Commission, Washington, D. C., TID-7634 1962, p. 199.

9. Burton, M., C. J. Hochanadel, and J. A. Ghormley, *Nucleonics*, **13**, 74 (1955).

10. Weiss, J., *Nucleonics*, **10**, 29 (1951).

11. Weiss, J., A. O. Allen, and H. A. Schwartz, *Proceedings of the International Conference on Peaceful Uses of Atomic Energy*, Vol. 14, United Nations, New York, 1956, p. 179.

12. Kleine, G. M., *Analytical Chemistry of Polymers*, Interscience, New York, Part I, 1962, p. 128.

13. Riddle, E. H., *Monomeric Acrylic Esters*, Reinhold, New York, 1954, p. 221.

14. Billmeyer, F. W., Jr., *Textbook of Polymer Chemistry*, Interscience, New York, 1959, p. 216.

15. Bovey, F. A., and G. V. D. Tiers, *J. Polymer Sci.*, **44**, 173 (1960).

16. Bovey, J. A., *J. Polymer Sci.*, **46**, 59 (1960).

Résumé

On a étudié la vitesse de la polymérisation en bloc du méthacrylate de méthyle, initiée par radiation-gamma entre $-19°$ et $-49°C$ et à des intensités de radiation allant de $3.77 \ 10^6$ rad/h jusqu'à $1.35 \ 10^5$ rad/h. L'énergie d'activation dans ce domaine de températures était de 3.85 kcal/mole à $3.77 \ 10^5$ rad/h. La vitesse de la réaction était proportionnelle à l'intensité à l'exposant 0.33 aussi bien à $-19°$ qu'à $-49°C$. Les mesures du poids moléculaire montrent que le transfert sur monomère est sans importance dans cette polymérisation. Des études de résonance magnétique nucléaire montrent que la syndiotacticité du polymère augmente avec une diminution de la température.

Zusammenfassung

Eine Untersuchung der Geschwindigkeit der durch Gammastrahlung initiierten Polymerisation von Methylmethacrylat in Substanz im Temperaturbereich von -19 bis $-49°C$ und bei Strahlungsintensitäten von $3,77.10^5$ rad/h bis $1,35.$ 10^5 rad/h wurd durchgeführt. Die Aktivierungsenergie ergab sich in diesem Temperaturbereich zu $3,85$ kcal/Mol bei $3,77à10^5$ rad/h. Die Reaktionsgeschwindigkeit war der Intensität zur $0,33$-Potenz sowohl bei $-19°C$ als auch bei $-49°$ proportional. Die Molekulargewichte zeigten, dass die Übertragung zum Monomeren bei der Polymerisation keine Bedeutung hatte. Kernmagnetische Resonanz untersuchungen zeigten, dass der Anteil an Syndiotaktizität im Polymeren mit fallender Temperatur zunimmt.

Study of Phenolic Resins by PMR Spectroscopy with Arsenic Trichloride as a Solvent

HERMAN A. SZYMANSKI and ALBERT BLUEMLE, *Canisius College, Buffalo, New York*

Synopsis

The PMR spectra of several phenolic resins and model compounds related to these resins are reported. Arsenic trichloride as a PMR solvent for the resins is suggested. The PMR spectra of a resin which is linked in the *ortho* position only is compared to that of a resin where both *ortho* and *para* linkages occur. It is shown that the completely *ortho*-linked resin gives a phenolic OH signal which does not shift when HCl gas is added, while it does shift if the resin has both *ortho* and *para* linkages. This observation is explained by assigning a strong intramolecular hydrogen bond to the *ortho*-linked resin. The behavior of the phenolic OH signal when HCl is added can therefore be used to distinguish between *ortho* and *ortho,para*-linked resins. A semiquantitative approach to obtaining average molecular weights is also presented. By integrating the PMR signals of various structural units of the resin it is possible to estimate the relative number and therefore the total number of units of this type in a molecule. The total number is a measure of the molecular weight. Spectral assignments are given for the various types of structural units present in the resins.

Introduction

Nuclear magnetic resonance spectroscopy has been used extensively in the study of the chemical shift parameters for numerous substituted phenols.[1] Both intramolecular and intermolecular bonding effects of the phenol OH proton have been investigated over a wide concentration and temperature range. However, the study of phenolic resins has thus far not been reported. The apparent lack of activity in this area appears to be due to the need of a suitable nonprotonated solvent. The conventional NMR solvents such as CCl_4, CS_2, $HCCl_3$, or $DCCl_3$ do not solubilize these materials. When the commonly known phenolic solvents, such as the low boiling alcohols and ketones are used, the spectrogram reveals only the solvent, the phenolic resonance peaks are not readily detectable. Szymanski[2] has previously utilized arsenic trichloride, a highly polar solvent, for both infrared and NMR studies. In this present work it was found that arsenic trichloride will dissolve both a heat-stable phenolic resin (novolac) and a heat-reactive resin (alkyl-substituted phenol). Other solvents, such as phosphorus trichloride or the completely halogenated acetone compounds, were found not to be adequate. Arsenic trichloride appears to be unique in its ability to be able to solubilize and disas-

sociate these hydrogen-bonded resins. It was found that arsenic trichloride has no noticeable degrading effect on the resins or model compounds. This was verified by running an infrared spectra of the resins in arsenic trichloride and comparing them to the spectra in inert solvents.

The heat- and acid-sensitive resins (resoles) cannot be studied in arsenic trichloride because of the liberation of hydrogen chloride from the solvent which in turn causes almost immediate resinification.

The commonly referred to "two-step" resins (novolac + curing agent) were studied to a limited extent. The spectra of the two-step resins are obtainable even though the curing agent, generally hexamethylenetetramine, forms complexes with the arsenic trichloride. The resites (thermoset resins) are not extractable in arsenic trichloride. Phenolic-impregnated glass and paper laminates were exposed to arsenic trichloride at reflux conditions for several days after which a spectrum was run on the extraction solvent. Apparently the phenolic laminates have excellent chemical resistance to the halide as none of the resin was leeched out.

We shall also discuss the use of NMR to study protonated modifiers as well as phenolic resins. The protonated modifiers could include alkyl- or aryl-substituted phenols or aldehydes, besides the conventionally used formaldehyde, and such additives as drying oil, etc. We further will assign the chemical shifts of nonequivalent nuclei in both the novolac and heat-reactive resins. The assignments of the novolac are based on the three isomers of dihydroxydiphenylmethanes, whereas the heat-reactive resin assignments are governed by model compounds of alkyl-substituted phenol dimers and alcohols. A series of *ortho*-linked compounds and novolacs were also evaluated. An explanation of the low field chemical shift of the OH proton in the *ortho*-linked materials will be explained in terms of intramolecular hydrogen bonding. A semiquantitative approach to average molecular weight determinations by NMR will also be briefly discussed.

Experimental

The nuclear magnetic resonance spectrometer employed was the high resolution Varian Associates A-60 spectrometer operating at 60 Mcycles/sec. The sample tubes were those supplied by the Varian Associates. The spectra were recorded at about 35 °C. (magnet gap temperature).

The arsenic trichloride used was a reagent grade product from Baker and Adamson Company. The use of redistilled or relatively dry solvent caused no change in resonance peaks other than the exchangeable OH proton. The resins themselves were mostly run at 10% concentration (by weight of the solvent). This low concentration was employed to reduce line broadening due to lack of molecular freedom. The model compounds were run at 10 and 30% concentrations (by weight of the solvent). Tetramethylsilane was used as the internal standard.

The resins evaluated were obtained thru the courtesy of Durez Plastics Division, Hooker Chemical Corporation and the model compounds were made available by the Central Research Laboratory of the Hooker Corpora-

tion. The model compounds' purity was verified by gas chromatography in some instances. The purity was >99.0% in the cases checked.

Results and Discussion

The building blocks for the heat stable novolac resins, are the p,p'-isomer, o,p'-isomer, and the o,o'-isomer of dihydroxydiphenylmethane. The typical novolac resins indicate that generally the commercially available products have an average molecular weight of about 500–600 with fractions ranging between a little over 200 to nearly 1300.[3] The ratio of the respective isomers and chain lengths is somewhat controllable by catalysts and manufacturing conditions. These manufacturing procedures are a well known art and will not be discussed here. Table I shows the chemical shifts for the respective isomers as well as those for various novolac resins. From a phenolic novolac (No. 6) one can expect three resonance signals, the CH_2, ring, and OH protons. The —CH_2— linkages of dihydroxydiphenylmethanes resolve into a broad singlet at approximately 3.81 ppm. The chemical shift is so slight that the individual isomers are not resolved from each other. As would be predicted, the —CH_2—
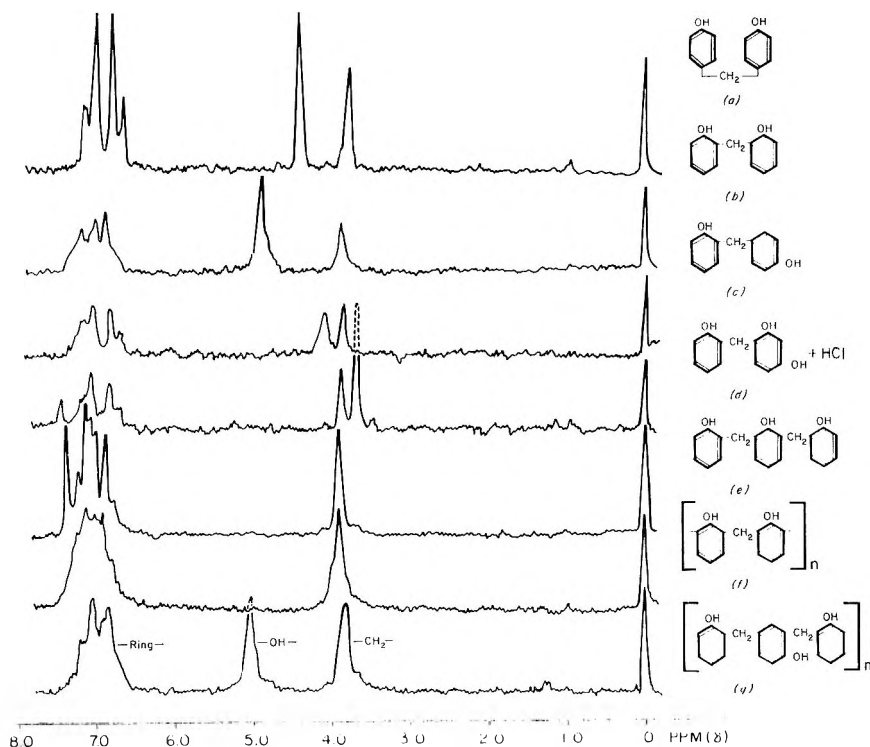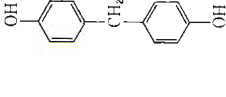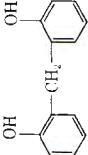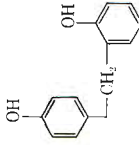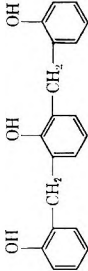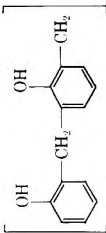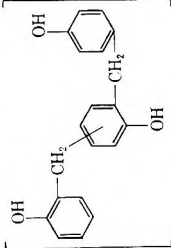
Fig. 1. PMR spectra of a number of model compounds and the *ortho*-linked resin formed from them. (*a*) *p-p'* isomer of dihydroxydiphenyl methane; (*b*) *o-o'* isomer of dihydroxydiphenyl methane; (*c*) *o-o'* isomer of dihydroxydiphenyl methane; (*d*) *o-o'* isomer of dihydroxydiphenyl methane; (*e*) phenol trimer (*ortho*-linked); novolac (*ortho*-linked); (*g*) novolac.

TABLE I

No.	Compound	Structural formula	Proton shifts for novolacs in arsenic trichloride ppm[a]		
			−OH	−CH$_2$−	Ring
1	p,p′-Dihydroxydiphenyl-methane		3.45	3.82	6.96 (A$_2$B$_2$ spectra)
2	o,o′-Dihydroxydiphenyl-methane		4.91	3.92	ca. 7.00
3	o,p′-Dihydroxydiphenyl methane		4.13	3.91	ca. 6.95

4	Phenol trimer (*ortho*-linked)		6.89	3.92	ca. 7.14
5	Novolac (*ortho*-linked)		about 7.3	3.92	ca. 7.08
6	Random novolac		5.16	3.81	ca. 6.94

^{a} Chemical shifts (δ) = $10^6(H - H_{ref}/H_{ref})$ are relative to tetramethylsilane as internal standard at 0.0 ppm.

protons of the p,p'-isomer of dihydroxydiphenylmethane (No. 1) are at higher field because they are in less of a paramagnetic environment. The spectrum is presented in Figure 1. The dihydroxydiphenyl-methanes may exist in different rotational configurations. The configuration will be dependent upon the degree of hydrogen bonding between the phenolic hydroxyl groups and also on steric factors.[4] If the two hydroxyl groups of an o,o-isomer are oriented so that there is intramolecular hydrogen bonding between them, the compound is referred to as being in the *cis* form. Our data (Table I) confirm the fact that the nonsterically hindered resins and model compounds are *ortho*-linked since the OH proton is shifted to lower field. Further, it is found that it is exceedingly more difficult to chemically shift these hydroxyl protons as the chain length increases.

In the case of the random novolac (greater steric hindrance and less hydrogen bonding) we were able to produce a chemical shift of the hydroxy proton to higher field strength by adding a minute amount of hydrogen chloride gas, while in the case of oriented *ortho*-linked compounds, the dimer and trimer hydroxy protons are very difficult to shift. For the oriented novolac resin (*ortho*-linked) we were unable to shift the hydroxy proton signal. The hydroxy proton remains superimposed beneath the ring proton signals.

It has been found[5] that the first hydroxy of a 2,2'-dihydroxydiphenyl-methane is hyperacid but that the second hydroxyl group shows little acidity. The model of this can be represented by structure I:
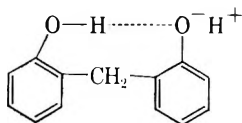
I

The acidity of the trimer, with the methylene in the *ortho* position, shows only one acidic proton. The remaining two are intramolecular hydrogen-bonded. In the case of the *ortho*-linked resin which has an average molecular weight of about 500–600, the spatial model would constitute about five phenolic nuclei. Four hydroxyl protons would be involved in intramolecular hydrogen bonding, while the remaining proton would be acidic in nature. This model would explain the PMR spectra we observe. We rule out a cyclic methylene derivative[6] of the five phenolic nuclei because of the reaction conditions.

Since the spectrum of a random novolac resolves into three resonant peaks and the *ortho*-linked novolac has two peaks, it is possible to distinguish between the two types of materials. Further, it appears that we have general method of determining the difference between an ordered and disordered resin by merely examining the position of the OH proton signal.

Resin novolac samples containing alkyl phenols as modifiers were also examined. These modifiers were chemically a part of the novolac. The alkyl protons were detectable provided the alkyl phenol's concentration

was above 10% of the total weight of the resin. Since the samples were run at 10% by weight of the solvent and the instrument is not sensitive below 1% levels, any small amount of modifier would not be detected. In particular, novolac resins modified with p-tert-butyl phenol and o-cresol show broad singlet peaks at 1.3 ppm and 2.14 ppm, respectively (Fig. 2). Since the nine protons in the tertiary butyl groups are equivalent, no spin-spin coupling would be expected, and the resonant signal should be a singlet. The three protons of the methyl groups also exhibit equivalence.

For the case in which the protonated modifier is unknown, there are published data concerning chemical shift and spin coupling.[7]

The heat-reactive resins, unlike the novolacs, contain several other functional groups. The ratio of the methylene protons (—CH$_2$—), ether protons (—CH$_2$OCH$_2$—), and methylol protons (—CH$_2$OH) are very dependent on variables such as catalyst, time, and ratio of reactants. By integrating the PMR signals of the spectra of these compounds it is possible to calculate the relative numbers of these structural groups in the resin.

It is known that hydrogen-bonded OH protons can show large chemical shifts.[8] Proton resonance studies of ortho-[9] and para-substituted[10] phenols are in agreement with our present findings. Dissociation of the hydrogen bonds causes a shift of the signal to higher fields. In their studies the shift was brought about by dilution effects. We have examined the shift of the hydroxy proton by dilution in arsenic trichloride and by using dry hydrogen chloride. Solvent effects of phenols have also been reported.[11] It has been shown that phenol in acetone has a low field signal which shift
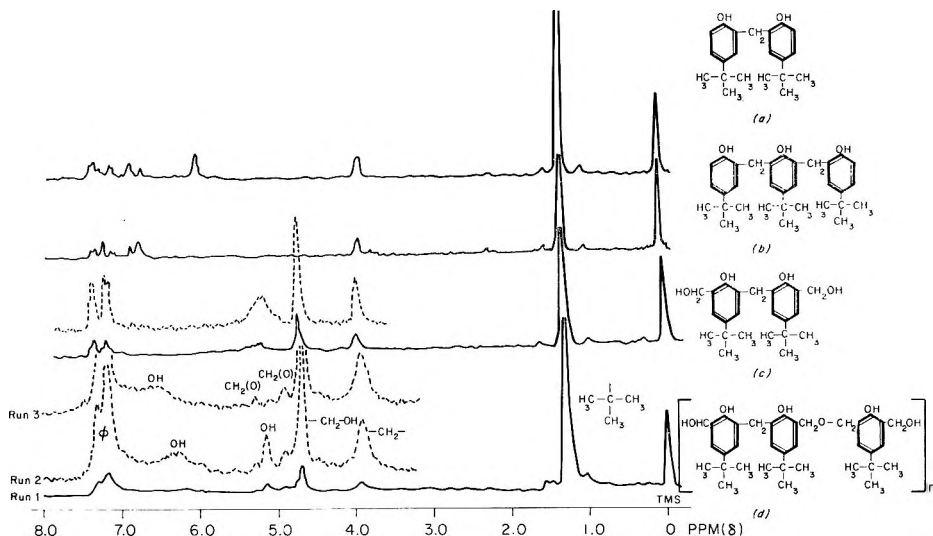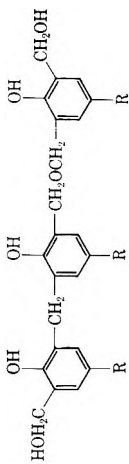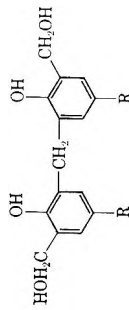
Fig. 2. PMR spectra of a number of model compounds and the p-tert-butyl phenol resin formed from them. Run 2 contained a small amount of HCl gas; Run 3 contained an appreciable amount of HCl gas. (a) p-t-butyl phenol dimer; (b) p-t-butyl phenol trimer; (c) p-t-butyl phenol dimer dialcohol; (d) p-t-butyl phenol heat reactive resin.

TABLE II

No.	Compound	Structural formula[a]		Proton shifts for heat-reactive resins in arsenic trichloride				
				-OH[b]	-CH₂-	-CH₂(0)	tert-Butyl protons	Ring
1	*p-tert*-Butyl phenol dimer	OH, OH, CH₂, R, R (structure)	No.	2	2	—	18	6
			Ratio	1	1	—	9	3
			Integrated signal height, cm.	1.15	1.0	—	8.95	3.0
			Chemical shift, δ, ppm.	6.0	3.92	—	1.28	ea. 7.0
2	*p-tert*-Butyl pheno trimer	OH, OH, OH, CH₂, CH₂, R, R, R (structure)	No.	3	4	—	27	8
			Ratio	1	1.33	—	9	2.66
			Integral signal height, cm.	1.3	1.3	—	8.5	2.7
			Chemical shift, δ, ppm.	6.65	3.9	—	1.27	ea. 7.0

3 p-tert-Butyl phenol dimer dialcohol

No.	4	2	4	18	4
Ratio	2	1	2	9	2
Integral signal height, cm.	1.14	0.7	1.12	6.3	1.13
Chemical shift, δ, ppm.	4.93	3.95	4.70	1.28	7.35 (A$_2$B$_2$ spectra)

4 p-tert-Butyl phenol heat-reactive resin[c]

No.	—	—	—	—	—
Ratio	—	—	—	—	—
Integral signal height, cm.	0.8	0.6	1.5	7.7	1.7
Chemical shift, δ, ppm.	6.3	3.94	4.70[d] 5.00[e]	1.28	7.3

a R represents the tert-butyl group.
b The OH signal would also include the water present in sample plus traces of water in the hydrophilic solvent.
c The resin contains ether, methylol methylene, tert-butyl, and hydroxyl protons.
d Methylene protons in methylol group.
e Methylene protons in ether group.

only when the molar concentration of the phenol falls below 60%. At this point further dilution with acetone causes a small shift to higher field. This chemical shift phenomena can be explained in terms of inter-molecular bonding of the carbonyl of acetone with the phenol OH. This bonding is greater than the association of the phenol molecules themselves until the concentration is lowered to approximately 60 mole-%.

The first model compound, and simplest product obtainable other than alkyl phenol itself, is the *ortho* dimer of *p-tert*-butyl phenol (Table II and Fig. 2). The *tert*-butyl protons, being equivalent, produce a sharp singlet at 1.28 ppm. The —CH₂— protons resonate at 3.92 ppm. The —CH₂— chemical shift is in good agreement with the methylene protons in the *ortho*-linked novolac (3.92 ppm.).

The *p-tert*-butyl trimer has the OH proton signal shifted to the lower field, as would be expected. It is much more difficult to produce the chemical shift in the trimer than in the dimer. In the *p-tert*-butyl phenol dimer dialcohol, the formation of *cis–trans* dimers (II) can occur along with intramolecular bonding of hydroxyl groups themselves as shown in structure III.

II

III
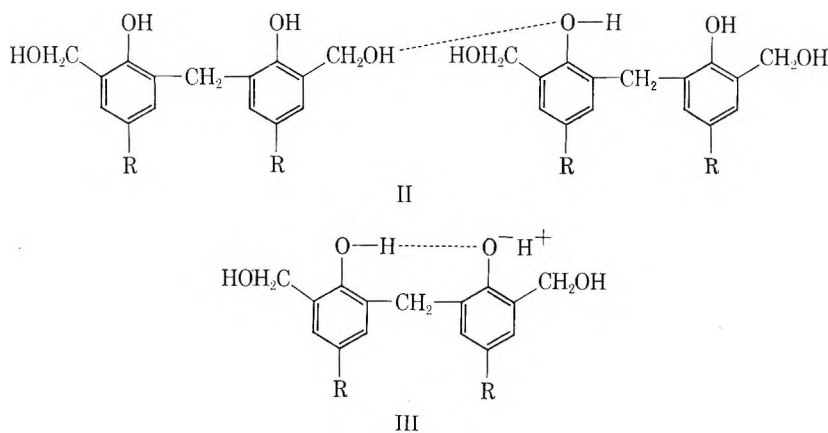
This type of *cis–trans* isomerism was originally interpreted on the basis of 2,6-substituted halogenated phenols. Equilibrium constants K_1 = *trans/cis* were calculated.[12] In the resin the hydrogen bonding effects result in a very broad signal at about 4.9 ppm. The methylene protons in the methylol groups show as a sharp singlet at 4.7 ppm. The ring protons are representative of an A_2B_2 spectra.

The resinous product which contains all of the functional groups of the formerly mentioned materials also contains ether linkages. The four protons (—CH₂—O—CH₂—) are located at about 5.0 ppm. In Figure 2, the addition of hydrogen chloride to the heat-reactive resin causes a low field chemical shift of the hydroxyl protons. The addition of hydrogen chloride results in a halomethylation of the phenol. The methylol OH groups are displaced in the electrophilic reaction. Since the methylol content of this *tert*-butyl derivative is about 10–11% of the total weight

of the resin, the average molecular weight would be in the range 550–600. The resin would consist essentially of trimers and tetramers. Knowing the methylol content, one could set up a quantitative ratio for the number of methylene protons versus methylol protons, or the ratio could also be extended to include the ether protons. Information of this nature can be of considerable value, for the performance of resin is very much dependent on the ratio and type of linkage obtained.

Semiquantitative investigation was conducted on the random novolac (Fig. 1). By the vapor pressure osmometer method (by use of a membrane osmometer designed by Mechrolab, Inc.), the molecular weight of the novolac resin averaged 518 (±5%). By comparing the relative intensities of ring protons versus the methylene protons, the molecular weight can be estimated if the following assumptions are made: (1) a novolac resin constitutes a structure with only three groups of nonequivalent nuclei; (2) any moisture present in the sample will be in proton exchange with the hydroxyl proton and will not interfere with calculations.

TABLE III

Chain length	Calculated mol. wt.	Ratio (—CH$_2$—) to ring	Ratios		
			11% conc. in AsCl$_3$	4.85% conc. in AsCl$_3$	2.83% conc. in AsCl$_3$
Dimer	200	1.0–4.0			
Trimer	306	1.0–2.75			
Tetramer	412	1.0–2.33			
Pentamer	518	1.0–2.12	1.0–2.30 ± 0.05[a]	1.0–2.16 ± 0.03[a]	1.0–2.11 ± 0.03[a]
Hexamer	624	1.0–2.00			
Heptamer	730	1.0–1.92			

[a] Standard deviation.

For the calculations, the resin signal was integrated a minimum of five times. Each step in the integral is a quantitative measurement of the number of protons beneath the area of the resonant signal. The five integrated heights are then averaged. If the resin constituted a dimer, the ratio of —CH$_2$— protons to ring protons would be 1:4. As the chain length is increased the ratio of —CH$_2$— protons to ring protons changes nonlinearly. In Table III are listed the ratios for various chain lengths.

At the lower concentrations, the molecular weight obtained is in good agreement with the osmotic method.

The studies of these resinous products by PMR shows that a wealth of information is obtainable. The data reported in this paper by no means has exploited the fullest potential of the instrument for many types of analyses. The use of arsenic trichloride as a solvent is especially promising and is being further investigated. A SbCl$_3$–AsCl$_3$ mixed solvent is also being examined and will be reported in a later publication.

References

1. Somers, B. G., and H. S. Gutowsky, *J. Am. Chem. Soc.*, **85**, 20, 3065 (1963).

2. Szymanski, H. A., paper presented at 7th Ottawa Symposium on Applied Spectroscopy, Ottawa, Ontario, Canada, September 1960.

3. Vanscheidt, A., *Ber.*, **69**, 1900 (1936).

4. Ambeland, J. C., and J. L. Binder, *J. Am. Chem. Soc.*, **75**, 946 (1953).

5. Sprengling, G. R., *J. Am. Chem. Soc.*, **76**, 1190 (1954).

6. Niederl, J. B., and J. S. McCoy, *J. Am. Chem. Soc.*, **65**, 629 (1943).

7. Chamberlain, N. F., *Anal. Chem.*, **31**, 56 (1959).

8. Allen, E. A., and L. W. Reeves, *J. Phys. Chem.*, **66**, 613 (1962).

9. Allen, E. A., and L. W. Reeves, *J. Phys. Chem.*, **67**, 591 (1963).

10. Patterson, W. G., and N. R. Typman, *Can. J. Chem.*, **40**, 2122 (1962).

11. Batdorf, R. L., Ph. D. thesis, Univ. of Minnesota, 1955.

12. Allen, E. A., and L. W. Reeves, *J. Phys. Chem.*, in press.

Résumé

On rapporte les spectres RMP de différentes résines phénoliques ainsi que de leurs composés modèles. On suggère l'emploi du trichlorure d'arsénique en tant que solvant RMP pour ces résines. Les spectres RMP d'une résine qui est liée seulement en position *ortho* sont comparés à ceux d'une résine où des liaisons *ortho* et *para* existent toutes deux. On montre que les résines liées en *ortho* donnent un signal phéenolique OH qui ne se déplace pas lorsqu'on ajoute HCl gazeux alors qu'ils glissent lorsque la résine a à la fois des liens *ortho* et *para*. Cette observation s'explique en admettant un puissant lien hydrogène intramoléculaire dans la résine liée en *ortho*. Le comportement du signal OH phénolique lorsqu'on ajoute de l'HCl permet de ce fait de distinguer entre résines liées en *ortho* et en *ortho-para*. On expose également une méthode semi-quantitative permettant de mesurer le poids moléculaire moyen. En intégrant les signaux RMP de diverses unités structurelles de la résine, on peut estimer le nombre relatif et de ce fait le nombre total d'unités de ce type dans la molécule. Le nombre total est une mesure du poids moléculaire. On donne les assignements spectraux des différents types d'unités structurelles présentes dans les résines.

Zusammenfassung

Die PMR-Spektren einiger Phenolharze und dazu in Beziehung stehender Modellverbindungen werden mitgeteilt. Arsentrichlorid wird als PMR-Lösungsmittel für die Harz vorgeschlagen. Das PMR-Spektrum eines nur in *ortho*-Stellung verknüpften Harzes wird mit demjenigen eines Harzes mit *ortho*- und *para*-Bindungen verglichen. Das vollständig *ortho*-verknüpfte Harz liefert ein Phenol-OH-Signal, das durch Zusatz von HCl-Gas nicht verschoben wird, während bei Anwesenheit von *ortho*- und *para*-Bindungen im Harz ein Verschiebung auftritt. Diese Beobachtung wird durch Annahme einer starken intramolekularen Wasserstoffbindung im *ortho*-verknüpften Harz erklärt. Das Verhalten des Phenol-OH-Signals bei Zusatz von HCl kann daher zur Unterscheidung zwischen *ortho*- und *para*-verknüpften Harzen herangezogen werden. Weiters wird eine halbquantitative Methode zur Ermittlung der Molekulargewichte angegeben. Durch Integration der PMR-Signale verschiedener Struktureinheiten des Harzes ist eine Bestimmung der relativen Anzahl und damit der Gesamtzahl der Einheiten dieses Typs in einem Molekül möglich. Die Gesamtzahl ist ein Mass für das Molekulargewicht. Eine spektrale Zuordnung der verschiedenen in den Harzen vorhandenen Struktureinheiten wird durchgeführt.

Radical Displacement in Allyl Ester Polymerization.
I.   Allyl Acetate; Evidence from Gas-Phase Kinetics

D. G. L. JAMES and G. E. TROUGHTON, *Department of Chemistry, University of British Columbia, Vancouver, British Columbia, Canada*

Synopsis

Photolysis of diethyl ketone in the presence of allyl acetate in the range 35–175°C. leads to the addition and dismutation reactions:

$$CH_3CH_2^{\cdot} + CH_2{=}CHCH_2OCOCH_3 \xrightarrow{k_7} CH_3CH_2CH_2\overset{\cdot}{C}HCH_2OCOCH_3$$

$$CH_3CH_2CH_2\overset{\cdot}{C}HCH_2OCOCH_3 \xrightarrow{k_8} C_5H_{10} + CO_2 + CH_3$$
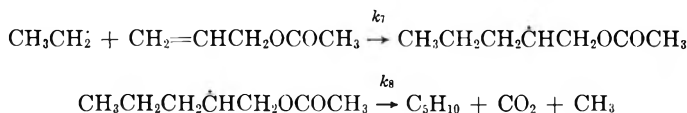
The proposed reaction scheme is supported by the values: $R(CO_2)/[R(C_5H_{10}) + R(C_4H_8)] = 1.02 \pm 0.03$, and $R(C_5H_{10})/[R(CH_4) + R(C_3H_8)] = 1.01 \pm 0.03$, and allows the evaluation of k_7 and k_8:

$$k_7/k_2^{1/2} = 10^{(-7.2 \pm 0.4)} \exp\{-7.7 \pm 0.6\}10^3/RT \quad (cm.^3/mol. \ sec.)^{1/2}$$

$$k_8 k_2^{1/2}/k_{7a} = 10^{(14.5 \pm 0.5)} \exp\{-15.8 \pm 1.0\}10^3/RT \ (mol./cm.^3 \ sec.)^{1/2}$$

where k_2 refers to: $2CH_3CH_2^{\cdot} \rightarrow C_4H_{10}$ and k_{7a} to: $CH_3CH_2^{\cdot} + \cdot C_5H_{10}OCOCH_3 \rightarrow C_7H_{15}OCOCH_3$. These results are discussed in relation to the radical displacement mechanism of effective chain transfer in the polymerization of allylic monomers.

Our knowledge of the nature of the chain transfer process in the radical polymerization of allyl esters has been reviewed recently by Gaylord, Katz, and Mark.[1]   In particular, the term "chain transfer" has been shown to cover a variety of reactions, which may be classed as "effective" if the rate constant (k_{ri}) for reinitiation by the radical formed in the transfer process is of a magnitude comparable with that of the rate constant (k_p) for propagation, or as "degradative" if k_{ri} is markedly less than k_p.   Gaylord[2] has reported the percentage of the total chain transfer which is effective at 80°C. for simple allyl esters:

acetate (24%) < propionate (43%) < trimethyl acetate (54%)

Effective chain transfer is clearly an important process in allyl ester polymerization at this temperature.

The accepted explanation for degradative transfer rests upon the low reactivity of an allylic radical formed in the process:

$$M_i^{\cdot} + CH_2{=}CHCH_2OCOR \rightarrow M_iH + [CH_2{\cdots}CH{\cdots}CHOCOR]^{\cdot}$$
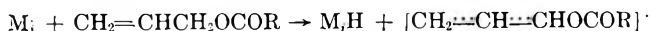
Gaylord and Eirich[3] have proposed that effective transfer among allyl esters may take the course:

$$M_i + CH_2{=}CHCH_2OCOR \rightarrow M_iCH_2CH{=}CH_2 + \dot{O}COR$$
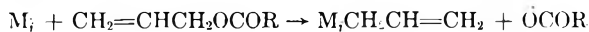
while Gaylord and Kujawa have interpreted the polymerization of 3-buten-2-yl propionate in this way.[4] Gaylord, Katz, and Mark[1] have reinvestigated this system and presented the first direct evidence for the radical displacement mechanism of effective chain transfer. They showed that carbon dioxide and ethane were evolved during the polymerization and that the quantities of each were consistent with their reaction scheme. We have found independent support for the radical displacement reaction in a study of free radical addition to allyl acetate in the gas phase.

Experimental

We are applying the methods of gas phase kinetics to a general study of the reactivity of unsaturated compounds as monomers in radical polymerization.[5-7] The photolysis of diethyl ketone generates the ethyl radical in the presence of the monomer vapor, and the rate constants of the consequent metathetical and addition reactions are measured over a range of temperature. The ethyl radical is chosen as the archetypal radical of all vinyl polymerization, but represents most closely the polyethylene radical. In this way the chain transfer and propagation reactions are simulated in a system for which polar effects are minimal, and the reactivity of a series of monomers can be related to a single standard attacking radical. It is as though ethylene had been used as a standard comonomer in kinetic studies of monomer reactivity in copolymerization, and the interpretation of the results had been freed from the effects of interactions between long molecules in the liquid phase. The validity of this method has been demonstrated in the case of allyl alcohol, where the results obtained accord with the behavior of this monomer in polymerization.[8] The experimental technique resembles that of an earlier study,[8] with certain improvements in the analysis of the products by gas chromatography.

Results

The ethyl radical is generated by the photolysis of diethyl ketone; it then reacts further according to the scheme:

$$CH_3CH_2COCH_2CH_3 + h\nu \rightarrow 2CH_3CH_2 + CO \tag{1}$$

$$2CH_3CH_2 \rightarrow C_4H_{10} \tag{2}$$

$$2CH_3CH_2 \rightarrow C_2H_6 + C_2H_4 \tag{3}$$

$$CH_3CH_2 + CH_3CH_2COCH_2CH_3 \rightarrow CH_3CH_3 + \dot{C}_2H_4COCH_2CH_3 \tag{4}$$

$$CH_3CH_2 + \dot{C}_2H_4COCH_2CH_3 \rightarrow C_4H_9COCH_2CH_3 \tag{4a}$$

$$CH_3CH_2 + CH_2{=}CHCH_2OCOCH_3 \rightarrow CH_3CH_4 + CH_2{=}CHCH_2OCOCH_2 \tag{5}$$

$$CH_3CH_2 + CH_2{=}CHCH_2OCOCH_2 \rightarrow CH_2{=}CHCH_2OCOC_3H_7 \tag{5a}$$

$$CH_3CH_2 + CH_2{=}CHCH_2OCOCH_3 \rightarrow CH_3CH_4 + CH_2{=}CH\dot{C}HOCOCH_3 \tag{6}$$

$$CH_3CH_2 + CH_2{=}CH\dot{C}HOCOCH_3 \rightarrow CH_2{=}CHCH(CH_2CH_3)OCOCH_3 \tag{6a}$$

$$CH_3CH_2 + CH_2{=}CHCH_2OCOCH_3 \rightarrow CH_3CH_2CH_2CHCH_2OCOCH_3 \quad (7)$$

$$CH_3CH_2 + CH_3CH_2CH_2CHCH_2OCOCH_3 \rightarrow$$

$$CH_3CH_2CH_2CH(CH_2CH_3)CH_2OCOCH_3 \quad (7a)$$

$$CH_3CH_2CH_2CHCH_2OCOCH_3 \rightarrow CH_3CH_2CH_2CH{=}CH_2 + CO_2 + CH_3 \quad (8)$$

The methyl radical formed in reaction (8) participates significantly in certain reactions analogous to those above, including:

$$CH_3 + CH_2CH_3 \rightarrow C_3H_8 \quad (2m)$$

$$CH_3 + CH_2CH_3 \rightarrow CH_4 + C_2H_4 \quad (3m)$$

and the methyl analogues of reactions (4), (5), (6), (7), and (8), e.g.,

$$CH_3 + CH_2{=}CHCH_2OCOCH_3 \rightarrow CH_3CH_2CHCH_2OCOCH_3 \quad (7m)$$

$$CH_3CH_2CHCH_2OCOCH_3 \rightarrow CH_3CH_2CH{=}CH_2 + CO_2 + CH_3 \quad (8m)$$
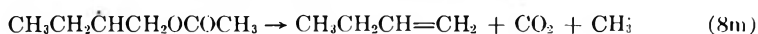
This reaction scheme is supported by the values:

$$R(CO_2)/[R(C_5H_{10}) + R(C_4H_8)] = 1.02 \pm 0.03$$

and

$$R(C_5H_{10})/[R(CH_4) + R(C_3H_8)] = 1.01 \pm 0.03$$

where $R(X)$ signifies the rate of formation of product X. Analysis of the results allows the evaluation of the rate constants:

$$k_7/k_2^{1/2} = 10^{(-7.2\pm0.4)} \exp\{-7.7 \pm 0.6\}10^3/RT \quad (cm.^3/mol.\ sec.)^{1/2}$$

and

$$k_8k_2^{1/2}/k_{7a} = 10^{(14.5\pm0.5)} \exp\{-15.8 \pm 1.0\}10^3/RT \quad (mol./cm.^5\ sec.)^{1/2}$$

limits of error are given at the 5% probability level in all cases.

A parallel study with $CH_2{=}CHCH_2OCOCD_3$ has confirmed these results. Figure 1 gives the Arrhenius plot for the decomposition of the allyl acetate adduct radical; open circles indicate results for the undeuterated acetate, and filled circles are used for the deuterated acetate.
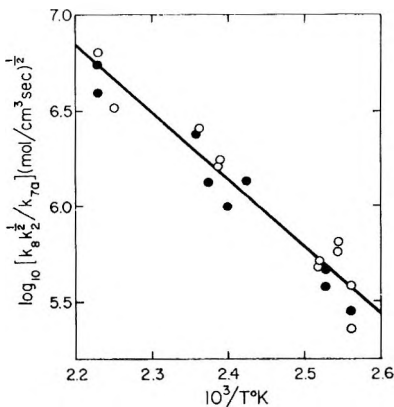
Fig. 1. Dismutation of the allyl acetate adduct radical: (O) $CH_2{=}CHCH_2OCOCH_3$ adduct; (●) $CH_2{=}CHCH_2OCOCD_3$ adduct.

Discussion

The energy of activation for the dismutation of the allyl acetate adduct radical is 16 ± 1 kcal./mole, and most probably measures the strength of the weak carbon–oxygen bond which must break to release the acetyloxy radical. This dismutation is detectable at 35°C., and at 110°C. the rate has increased sufficiently to allow precise measurement. The corresponding allyl alcohol radical adduct was found to be much more stable, and its dismutation was rarely detected below 145°C.[8] The greater instability of the allyl acetate adduct reflects the greater degree of stabilization possessed by the displaced acetyloxy radical, which would serve to lower the energy of activation for the process of dismutation.

Before we can apply the results of this study to the interpretation of the phenomena of allylic polymerization we have to decide to what extent the characteristic reactions of polymerization are represented in the gas-phase mechanism. Now in radical polymerization the process of chain transfer to monomer competes with the propagation process for the same reactant species, but fails to reproduce the chain center by simple addition. Turning to the gas-phase mechanism given above, and recalling that the ethyl radical simulates the polymer radical chain center, then it follows that the propagation process is represented by reaction (7), and effective transfer by the sequence of (7) followed by (8). Certainly the methyl radical formed in reaction (8) is as reactive as any other species present, so that this transfer may well be called effective. Degradative transfer is clearly represented by reaction (6), which forms an unreactive allylic radical. We may now discuss to what extent the results of gas-phase studies of allyl acetate and allyl alcohol parallel the behavior of these monomers in radical polymerization.

Allyl acetate and allyl alcohol are equally reactive toward the addition of the ethyl radical, as is clear on comparing the rate constant for allyl alcohol:[8]

$$k_1 k_2^{1/2} = 10^{(-7.2 \pm 0.2)} \exp\{-7.7 \pm 0.3\} 10^3/RT \; (\text{cm.}^3/\text{mol sec.})^{1/2}$$

with the almost identical value given above for allyl acetate. We may expect similar values for k_p for these monomers.

In contrast, allyl acetate and allyl alcohol differ strikingly in their response to the transfer reactions [represented by eqs. (5) and (6)]. Metathesis is rapid for allyl alcohol, with $(k_5 + k_6)/k_7 = 0.55$ at 60°C.; if this ratio gives a measure of k_f/k_p, the ratio of degradative transfer to propagation, then even telomerization would be very slow, as is indeed found. However for allyl acetate the sum of the rates of reactions (5) and (6) was too small to be detected, which means that $(k_5 + k_6)/k_7 < 0.1$, in harmony with the degree of polymerization of 13 observed for allyl acetate. It appears that the superior polymerizability of allyl acetate is due not to a more reactive double bond but rather to less reactive hydrogen atoms. This anomaly of an apparent difference in reactivity of the allylic hydrogen atoms of allyl acetate and allyl alcohol is remarkable; however the recent

work of Shannon and Harrison[9] indicates that much of the abstraction from allyl alcohol may occur at the hydroxylic hydrogen atom. The general problem of the abstraction of hydrogen from allylic compounds is being studied by the authors with the aid of deuterium tracer techniques.

References

1. Gaylord, N. G., M. Katz, and H. F. Mark, *J. Polymer Sci.*, **B2**, 151 (1964).
2. Gaylord, N. G., *J. Polymer Sci.*, **22**, 71 (1956).
3. Gaylord, N. G., and F. R. Eirich, *J. Am. Chem. Soc.*, **74**, 334 (1952).
4. Gaylord, N. G., and F. M. Kujawa, *J. Polymer Sci.*, **41** 495 (1959).
5. James, D. G. L., and E. W. R. Steacie, *Proc. Roy. Soc. (London)*, **A244**, 297 (1958).
6. James, D. G. L., and D. MacCallum, *Proc. Chem. Soc.*, **1961**, 259.
7. Brown, A. C. R., and D. G. L. James, *Proc. Chem. Soc.*, **1962**, 81.
8. Brown, A. C. R., and D. G. L. James, *Can. J. Chem.*, **40**, 796 (1962).
9. Shannon, T. W., and A. G. Harrison, *Can. J. Chem.*, **41**, 2455 (1963).

Résumé

La photolyse de la diéthylcétone en présence d'acétate d'allyle, dans le domaine de température compris entre 35° et 175°C., conduit aux réactions d'addition et de dismutation:

$$CH_3CH_2 + CH_2{=}CHCH_2OCOCH_3 \xrightarrow{k_7} CH_3CH_2CH_2\dot{C}HCH_2OCOCH_3$$

$$CH_3CH_2CH_2\dot{C}HCH_2OCOCH_2 \xrightarrow{k_8} C_5H_{10} + CO_2 + CH_3$$
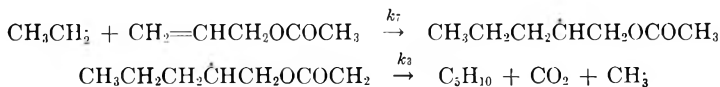
Les valeurs trouvées pour $R(CO_2)/[R(C_5H_{10}) + R(C_4H_8)] = 1.02 \pm 0.03$ et pour $R[C_5H_{10}]/[R(CH_4) + R(C_3H_8)] = 1.01 \pm 0.03$ supportent le schéma de réaction proposé et permettent d'évaluer k_7 et k_8:

$$k_7/k_2^{1/2} = 10^{(-7.2 \pm 0.4)} \exp(-7.7 \pm 0.6)10^3/RT \; (cm^3/mol.\,sec.)^{1/2}$$

$$k_8 k_2^{1/2}/k_7 a = 10^{(14.5 \pm 0.5)} \exp(-15.8 \pm 1.0)10^3/RT \; (mol./cm.^3\,sec.)^{1/2}$$

où k_2 caractérise la réaction $2CH_3CH_2 \rightarrow C_4H_{10}$ et k_{7a}: $CH_3CH_2 + C_5H_{10}OCOCH_3 \rightarrow C_7H_{15}OCOCH_3$. On discute ces résultats en les comparant au mécanisme de déplacement d'un radical lors du transfert de chaîne effectif en polymérisation allylique.

Zusammenfassung

Photolyse von Diäthylketon in Gegenwart von Allylacetat führt im Bereich von 35–175° zu folgender Additions- und Dismutierungsreaktion:

$$CH_3CH_2 + CH_2{=}CHCH_2OCOCH_3 \xrightarrow{k_7} CH_3CH_2CH_2\dot{C}HCH_2OCOCH_3$$

$$CH_3CH_2CH_2\dot{C}HCH_2OCOCH_3 \xrightarrow{k_8} C_5H_{10} + CO_2 + CH_3$$
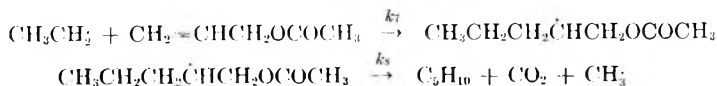
Das vorgeschlagene Reaktionsschema wird durch folgende Werte gestützt: $R(CO_2)/[R(C_5H_{10}) + R(C_4H_8)] = 1,02 \pm 0,03$ und $R(C_5H_{10})/R(CH_4) + R(C_3H_8) = 1,01 \pm 0,03$ und erlaubt die Ermittlung von k_7 und k_8:

$$k_7/k_2^{1/2} = 10^{(-7,2 \pm 0,4)} \exp\left(-7,7 \pm 0,6\right) 10^3/RT \, (\text{cm.}^3/\text{mol. sek})^{1/2}$$

$$k_8 k_2^{1/2}/k_{7a} = 10^{(14,5 \pm 0,5)} \exp\left(-15.8 \pm 1,0\right) 10^3/RT \, (\text{mol.}/\text{cm.}^3 \text{ sek})^{1/2}$$

wo k_2 sich auf $2CH_3CH_2 \rightarrow C_4H_{10}$ und k_{7a} auf $CH_3CH_2 + \dot{C}_5H_{10}OCOCH_3 \rightarrow C_7H_{15}OCOCH_3$ bezieht. Die Ergebnisse werden in Zusammengang mit dem Radikal-verschiebungsmechanismus der effektiven Kettenübertragung bei der Polymerisation von Allylmonomeren diskutiert.

Single Crystals Of Poly(ethylene Terephthalate)

YUHIKO YAMASHITA, *School of Engineering, Okayama University, Tsushima, Okayama, Japan*

Synopsis

Single crystals of poly(ethylene terephthalate) were prepared by evaporating the solvent slowly from dilute solution at crystallization temperature. The single crystals are parallelograms in shape and thicken by spiral growths with screw dislocations at their center. In the electron microscope they are seen to consist of platelets about 100 A. in thickness. Low-angle x-ray measurements on the film obtained by filtering the crystal suspension reveal a long spacing in good agreement with that calculated from shadow lengths. Electron and x-ray diffraction patterns show that the chain molecules are inclined at about 25–35° to the normal to the basal plane of the single crystals and sharply folded within the lamellae. Various morphological features and arrangement of the unit cell in the single crystal platelets are described and discussed.

INTRODUCTION

In 1957 Till,[1] Keller,[2] and Fischer[3] discovered independently that single crystals of polyethylene in the form of rhombic platelets were obtained by crystallization from dilute solutions. Since that time, the growth of single crystals from solutions and also from melts has been reported for a number of crystalline polymers. Poly(ethylene terephthalate) (PETP), however, has not been crystallized in the form of single crystals. We attempted to prepare single crystals of PETP from dilute solutions and succeeded by using suitable crystallization conditions.

The melting and glass transition temperature of PETP are quite high in comparison with other polyesters. PETP is of especial interest, since it is commercially available and can be easily quenched to a glasslike state. Spherulites of this polymer can be grown by annealing the glassy material at a temperature between the glass transition temperature and the melting point. No electron microscope studies of the morphology of these spherulites have been reported. The solid structure of PETP, however, has been studied in detail by means of x-ray,[4] infrared,[5] and other techniques.[6] Bunn et al.[7] determined the crystal structure of PETP and suggested that the high melting point of PETP was not due to the strong force between the molecular chain with polar groups but due to the high rigidity of the aromatic ring with its attached —COO— groups. According to their x-ray analysis, the unit cell which contains one chemical unit —COC$_6$H$_4$-CO·O(CH$_2$)$_2$O—, is triclinic with $a = 4.56$ A., $b = 5.94$ A., $c = 10.75$ A., $\alpha = 98.5°$, $\beta = 118°$, and $\gamma = 112°$.

In the investigations of single crystals of PETP we are interested in the following points: (a) whether the chain with high rigidity may be folded regularly; (b) whether single crystals with less symmetrical structure (triclinic crystal structure) may have any distinguishable features from those with more symmetrical structure. The present paper shows the results of our study on PETP single crystals by electron microscopy, electron diffraction, and low- and wide-angle x-ray diffraction.

EXPERIMENTAL AND RESULTS

Materials and Experimental Techniques

The material used in this study was unfractionated PETP with an average degree of polymerization of about 100. In order to find good solvents, we carried out a series of preliminary experiments. The polymer was dissolved in various hot solvents at concentrations ranging from 0.01 to 0.1% and was precipitated by cooling slowly. The cooling rate was 0.5°C./ hr. in the vicinity of the cloud point temperature of each solution. From a series of such experiments it was found that the best solvents were nitrobenzene, diphenyl ether and a diphenyl ether–phenol mixture. Under these crystallizations the polymer does not precipitate in the form of single crystals but in the form of spherulites at high concentrations or aggregations with the lamellar structure at lower concentrations. It was found, however, that single crystals are obtained by evaporating the solvent slowly from dilute solution at the crystallization temperature. Therefore the PETP crystals used in electron microscopic investigation were prepared, for instance, by placing drops of the hot solution in nitrobenzene at concentrations of about 0.01% on carbon-coated grids and evaporating the solvent in an air bath at 120°C. The specimens were shadowed with Ge and examined by direct transmission in a JEM 6A electron microscope. Selected area diffraction experiments were carried out with the same instrument. Calibration of the diffraction spots was made with the aid of a thin evaporated layer of aluminum on the same specimen. The film obtained by filtering the crystal suspension was used for the x-ray diffraction investigation. Wide-angle x-ray diffraction patterns were obtained in a flat film camera with the use of nickel-filtered $CuK\alpha$ radiation. Low-angle x-ray diffraction patterns were also obtained in with a Geigerflex (Rigaku Denki) instrument.

Morphology

It was found that the crystal habit is very strongly dependent upon the crystallization conditions, particularly upon the nature of solvents and the crystallization temperature. The electron micrograph in Figure 1 is representative of the spherulites obtained from dilute solution in diphenyl ether. This sheaflike structure is similar to that of nylon 610[8] and seems to be an incipient spherulite. The fibrillar units are flat ribbons, about
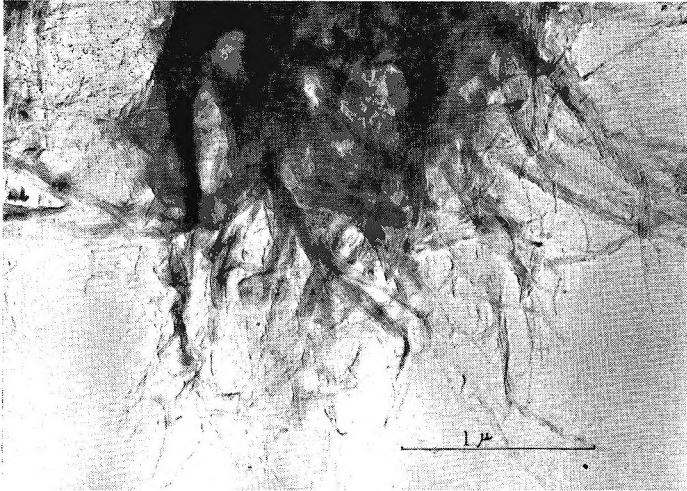
Fig. 1. Spherulites of PETP crystallized from dilute solution in diphenyl ether. The flat ribbons, about 100 A. thick, apparently are not single crystals, but may be some sort of helical aggregates of crystals.
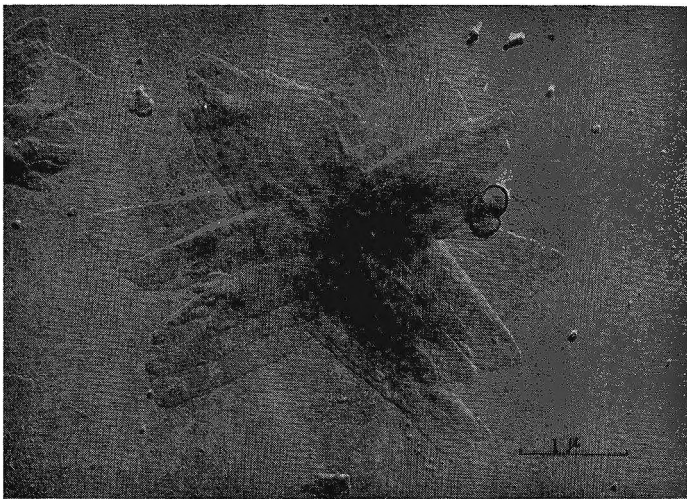
Fig. 2. Aggregates of single crystal lamellae associated with the central portion.   Single crystals may be parallelogram-shaped lamellae with the acute angle about 65°.

300 A. in width and 100 A. in thickness.   The electron micrographs in Figures 2–6 show the lamellar crystals of PETP.   These crystals do not always have a regular shape as in the case of many other polymers.   Under optimal conditions of crystallization temperature and concentration, single crystals may be parallelogram-shaped lamellae, as shown in Figure 2. The acute angle of the parallelogram is about 65°.   Crystals are often observed in the shape of spindlelike parallelograms with a smaller acute angle or slender plates as shown in Figures 3 and 4.   Lath-shaped lamellae, as shown in Figure 5, are twinned crystals which are similar to those ob-

Fig. 3. Spiral growth on a PETP crystal. The crystal shape is spindlelike
parallelograms.
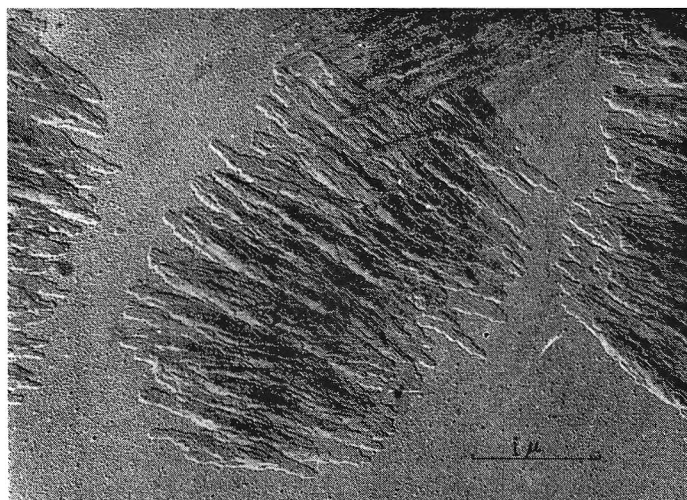
Fig. 4. Aggregates of slender-shaped crystals of PETP.

served in polyethylene. An increase in the concentration of the polymer
solution favors the growth of dendritic crystals or aggregated slender
crystals. Although the crystal shown in Figure 6 has a lozenge shape as
a whole, it seems to be a well developed dendrite. Figure 3 indicates that
thickening takes place by spiral growth similar to that reported for other
polymers. The thickness of these lamellae, estimated from the length
of the shadow, is about 100 A. Another morphological feature of the
crystals is the marked striations running parallel to the longer side of
the elongated parallelograms. These striations are quite similar to those
in single crystals of cellulose triacetate.[9]
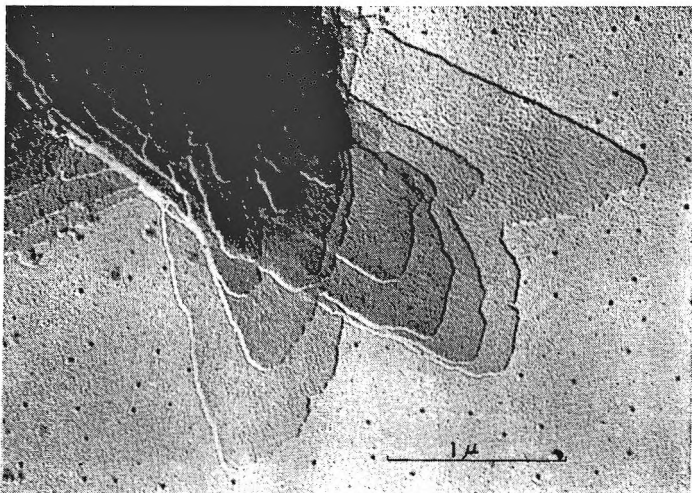
Fig. 5. Twinned crystals similar to those observed in polyethylene.
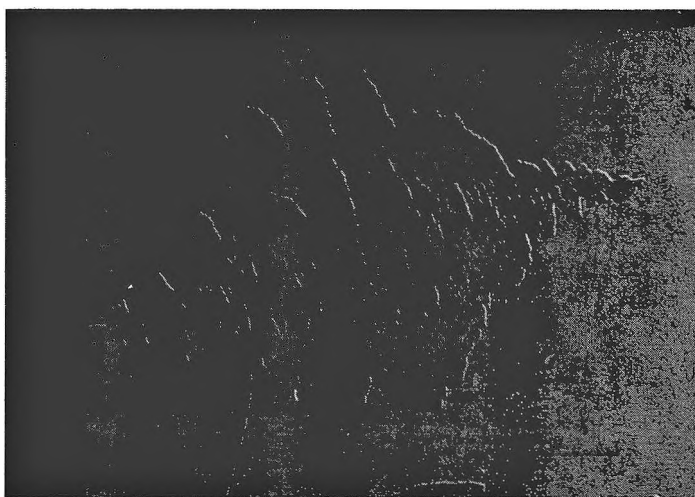
Fig. 6. Dendritic crystals of PETP. Although the crystal is lozenge-shaped as a whole, it seems to be a well developed dendrite.

Electron Diffraction and X-Ray Diffraction

Electron diffraction patterns are obtained only at very low beam currents. The diffraction power of the crystals is destroyed in a few seconds at normal beam intensities. A selected area electron diffraction pattern from a single crystal of PETP is shown in Figure 7. The spacings of the six observed reflections in Figure 7 correspond to those of the reflections from the (010), (020), ($\bar{1}$01), ($\bar{1}$11), ($\bar{1}$21), and ($\bar{1}$31) planes. The spacings and the intensities of such reflections agree with those of the x-ray reflections of PETP fibers. These planes are all represented by ($\bar{h}kl$) with $\bar{h} = l = 0, 1, k = 0, 1, 2, 3$. From these results, it is concluded that the
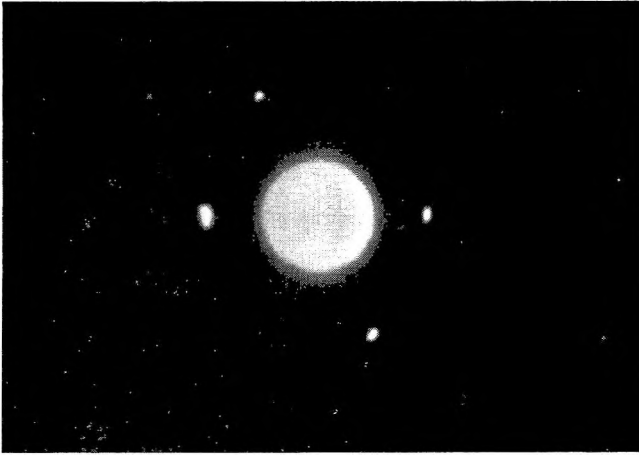
Fig. 7. Selected area electron diffraction pattern from a single crystal of PETP.

[101] direction of the unit cell corresponds to the direction of the normal to the basal plane of the single crystals[10] (the direction of the electron beam); that is, the chain molecules are not oriented perpendicular to the basal plane of the single crystals but inclined in the (010) plane of the single crystals. From exact calculations, this inclination was found to be about 25°. The correlation of the electron micrograph and the selected area electron diffraction pattern shows that the longer side of the parallelogram corresponds to the (010) plane and the shorter side to the (100) as shown schematically in Figure 8. The diffraction pattern from the (010) twinned crystal, as in Figure 9, is also obtained from the lath-shaped lamellae as
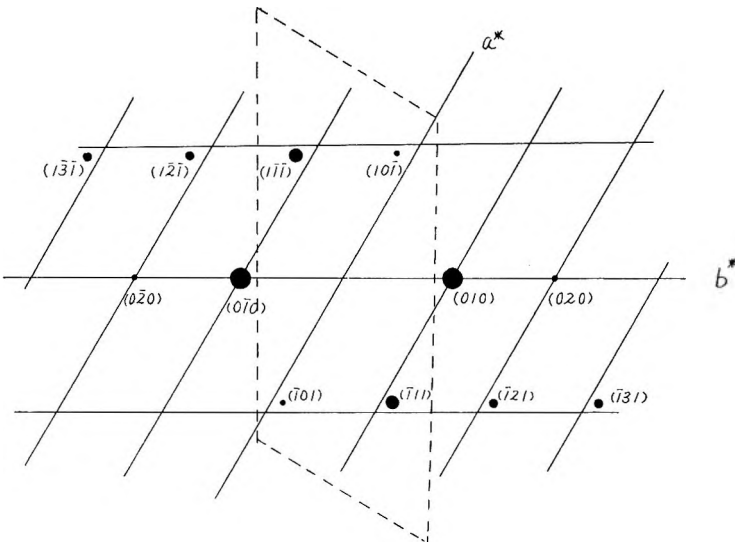
Fig. 8. Reflections and reciprocal lattice of a^*b^* planes. Dots show observed reflections; dotted lines show external form of a single crystal.
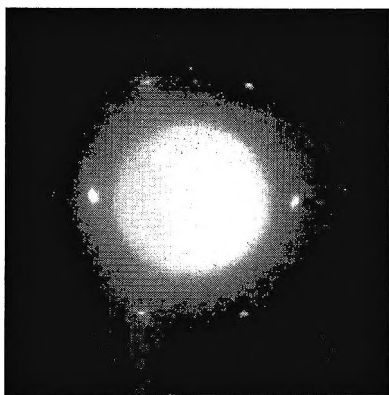
Fig. 9. Selected area electron diffraction pattern from the (010) twinned crystal. This pattern is also obtained from the lath-shaped lamellae as well as the more irregular lamellae.

well as the more irregular lamellae and the spindle-shaped lamellae. In these cases the longer direction of the lamella lies in the (010) plane. The diffraction pattern of the other twin type has not been obtained yet, but from the morphological observations, it is supposed that the (100) twinned crystal may also exist.

In order to obtain additional evidence on the orientation of the chain molecules in the single crystal platelets, a study of wide-angle x-ray diffraction was carried out. In this experiment the film obtained by filtering the crystal suspension carefully was used. The lamellar crystals in

a   b
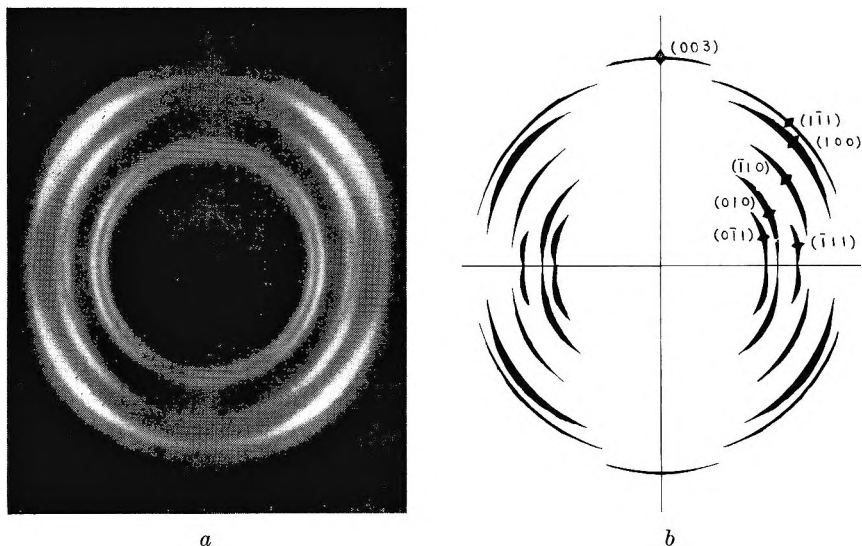
Fig. 10. (a) X-ray diffraction pattern of the film of precipitated lamellar crystals; x-ray parallel to the film surface. (b) Scale drawing of Fig. 10a. The points in the upper right-hand quadrant represent the calculated positions when the ab plane of the unit cell lies on the basal plane of single crystals which are parallel to the film surface.
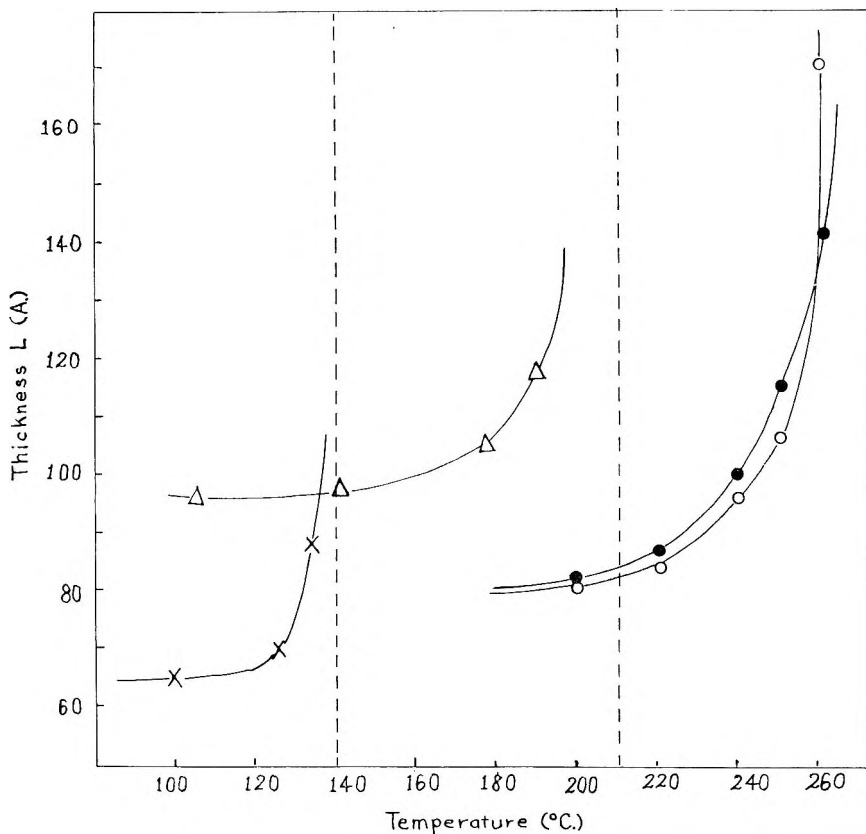
Fig. 11. Thickness of single crystals of PETP vs. crystallization temperature and annealing temperature: (O,●) annealed in air; (△) crystallized from diphenyl ether; (✕) crystallized from dimethyl phthalate.

this film lie with their basal planes parallel to the film surface. When the x-ray beam was oriented perpendicular to the film surface, the diffraction pattern showed continuous Debye-Scherrer rings. With the beam parallel to the film surface, which was oriented along the equator, the pattern showed preferential orientation as shown in Figure 10a and defined in the scale drawing of Figure 10b. All reflections of (hk0) planes do not always have their maximum on the equator. From these results, we shall conclude that the chain axis should be inclined normal direction cf the basal plane of lamellar crystals. This inclination was calculated to be about 35°, and the ab plane of the unit cell lies on the basal plane of the single crystals that is parallel to the film surface. This value of inclination does not differ so far from the value of 25° estimated from the selected area electron diffraction study of the single crystal, and this will be ciscussed later.

The low-angle x-ray diffraction patterns were obtained on the same specimen with the beam parallel to the film surface. The long spacing calculated

by assuming the Bragg equation is 106 A. for the sample prepared from the crystal suspension crystallized isothermally at 180°C. This value agrees with the thickness estimated from electron micrographs. The variation of the long spacing with the crystallization temperature or annealing temperature was also investigated. These results are shown in Figure 11. It was found that the lamella thickness depends not only on the crystallization temperature but also on the solvents. The thickness increases rapidly as the cloud point of each solvent is approached. Hirai et al.[11] reported that the thickness of lamellar crystals obtained from solution can be represented by the empirical equation

$$L = L_0 + A/(T_{cloud} - T) \tag{1}$$

where L is the thickness of the lamellar crystals, T is crystallization temperature, L_0 and A are calculated by using the data in Figure 11; these values are shown in Table I. The physical meaning of the constants L_0 and A has been previously discussed.[11]

TABLE I
Values of the Constants in Equation (1)

	L_0, A.	T_{cloud}, °C.	A, A.-deg.
Air	60	280	1650
Diphenyl ether	90	210	500
Dimethyl phthalate	60	140	190

Single Crystals of the Poly(ethylene Terephthalate) Oligomer

It was impressive that the characteristic habit of polyethylene single crystals was the same lozenge shape as that of n-paraffin crystals as seen

Fig. 12. Single crystals of poly(ethylene terephthalate) oligomer. The crystal shape is similar to that of PETP single crystals.

when single crystals of polyethylene were crystallized from dilute solution
in xylene the first time.   To examine the similarity of this oligomer analogy
for PETP single crystals, poly(ethylene terephthalate) oligomer was
crystallized from dilute solution in nitrobenzene.   Regular, parallelogram-
shaped single crystals were obtained, as shown in Figure 12.   The crystals
have spiral growth with screw dislocations at their center and twin growth
with the common (010) plane.   The selected area electron diffraction pattern
of a single crystal of poly(ethylene terephthalate) oligomer was almost the
same as that of PETP.   Since the elementary triclinic unit cells of oligomer
and polymer are identical, it seemed that the chain direction was also in-
clined at 25°.   However from the degree of polymerization it is concluded
that there is no folding within them.

DISCUSSION

In the preceding sections electron microscope, electron diffraction and
x-ray diffraction investigations have shown that PETP is crystallized by
evaporating the solvents from dilute solution as parallelogram-shaped
lamellae in which the molecular axis orients with an inclination of about
25–35° to the normal direction of basal plane.   In view of the lamellar
thickness and the average degree of polymerization, a given rigid molecule
must necessarily be folded in the platelet repeatedly.   The concept of
chain folding can be applied to single crystals of PETP as well as to those
of polymers with more symmetrical structure.   A study of a Stuart atomic
model indicates the possibility of folding within the (010) and (100) planes.
It is interesting to consider how the unit cells are arranged in the single
crystal platelets.   Based on the results of the electron diffraction pattern,
a possible mode of the unit cell packing can be visualized as shown sche-
matically in Figure 13.   As mentioned earlier, the long and short bounding
faces correspond to the (010) and (100) planes, respectively.   As these

(a)   (b)
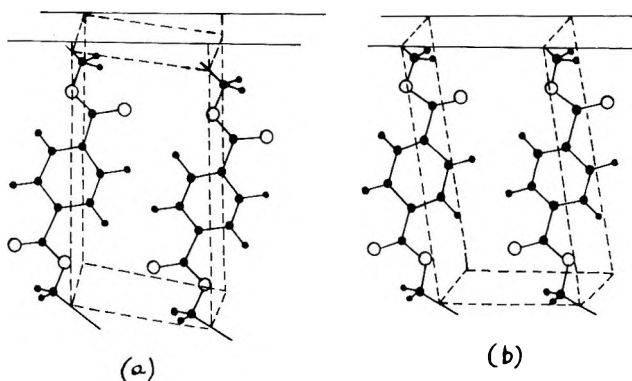
Fig. 13. Schematic representation of unit cell packing in a single crystal of PETP
based on: (a) electron diffraction pattern; (b) x-ray diffraction pattern. Heavy lines
represent lamellar surface; dotted lines show unit cell.

planes are both the growing faces, it is presumed that the chain molecules will fold along them. However, since the characteristic behaviors and the loop length of the folding in the (010) and (100) planes are considerably different, we shall presume that either of the two planes is a fold plane. The fracture of the PETP single crystals by means of ultrasonic vibrations is under investigation. Another puzzling problem of this packing is the departure of the (001) plane from the basal plane of the single crystal platelets. For this problem, we suppose that the observed reflections become possible by the molecular reorientation on drying. The striations running parallel to the (010) plane in the parallelogram-shaped lamellae seems to be the evidence of such reorientation. The reason for the reorientation is not understood at present. These striations are not a feature related to the chain folding since they are also observed in single crystals of the oligomer where no folding is presumed to exist. X-ray diffraction investigation on aggregates of the single crystals indicates that the (001) plane lies in the basal plane of the lamellae.[10] This packing is more reasonable for the single crystal platelets with the triclinic crystal structure.

Such phenomena seems to be true not only for the single crystals of PETP but also for any other polymers; it may be considered to be a general rule that in any single crystals of high polymers whose α or β of the unit cell is not 90°, the molecular chain axis is not normal but inclined to the basal plane (fold plane) by the angle between the c-axis and the ab plane. Experiments on this concept are now going on in our laboratory on single crystals of nylon 6, nylon 66, and poly(ethylene oxide).

References

1. Till, P. H., *J. Polymer Sci.*, **24**, 301 (1957).
2. Keller, A., *Phil. Mag.* [8], **2**, 171 (1957).
3. Fischer, E. W., *Z. Naturforsch.*, **12a**, 753 (1957).
4. Dalmage, W. J., and A. L. Geddes, *J. Polymer Sci.*, **31**, 499 (1958).
5. Tadokoro, H., K. Tatsuka, and S. Murahashi, *J. Polymer Sci.*, **59**, 413 (1962).
6. Keller, A., *J. Polymer Sci.*, **17**, 291 (1955).
7. Daubeny, R. De P., and C. W. Bunn, *Proc. Roy. Soc. (London)*, **A226**, 531 (1954).
8. Keller, A., *J. Polymer Sci.*, **36**, 361 (1959).
9. Manley, R. St. J., *J. Polymer Sci.*, **A1**, 1875 (1963).
10. Hirai, N., S. Fujita, K. Yamamoto, and Y. Yamashita, *Kobunshi Kagaku*, 21, 97 (1964).
11. Hirai, N., T. Tokumori, T. Katayama, S. Fujita, and Y. Yamashita, *Repts. Res. Lab. Surface Sci. Fac. Sci. Okayama Univ.*, **2**, No. 3, 91 (1963).

Résumé

On a préparé des monocristaux de téréphtalate de polyéthylène en évaporant lentement le solvant d'une solution diluée, à la température de cristallisation. Les monocristaux se présentent sous la forme de parallèlogrammes et s'épaississent par croissance en spirale avec dislocation de la vis vers le centre. Au microscope électronique, on peut voir qu'ils

sont constitués de feuillets d'une épaisseur de 100 A. Des mesures aux rayons-X aux
petits angles, effectuées sur le film obtenu par filtration de la suspension de cristaux,
révèlent un long intervalle en bon accord avec ce qu'on calcule à partir des longueurs des
taches. Les diagrammes de difraction des électrons et des rayons-X montrent que les
chaînes moléculaires sont inclinées à environ 25°–35° par rapport à la normale au plan
de base des monocristaux et qu'elles sont pliées étroitement entre les feuillets. Les dif-
férentes caractéristiques morphologiques et les dispositions des mailles dans les feuillets
de monocristaux sont décrites et discutées.

Zusammenfassung

Polyäthylenterephthalat-Einkristalle wurden durch langsame Verdampfung des
Lösungsmittels aus verdünnter Lösung bei der Kristallisationstemperatur dargestellt.
Einkristalle haben die Gestalt eines Parallelogramms, und die Dickenzunahme erfolgt
durch Spiralwachstum mit Schraubenversetzung im Zentrum. Im Elektronenmikroskop
zeigen sie einen Aufbau aus 100 A. dicken Plättchen. Röntgenkleinwinkel-Messungen
an dem durch Filtration der Kristallsuspension erhaltenen Film lassen eine Langperiode
erkennen, die gut mit der aus Schattenlängen berechneten übereinstimmt. Elektronen-
und Röntgenbeugungsdiagramme zeigen, dass die Kettenmoleküle um 25–35° gegen die
Normale auf die Basisebene der Einkristalle geneigt und innerhalb der Lamellen scharf
gefaltet sind. Verschiedene morphologische Züge und die Anordnung der Elementar-
zelle in den Einkristallplättchen werden beschrieben und diskutiert.

Synthesis of Trichain and Tetrachain Radial Polybutadienes

R. P. ZELINSKI and C. F. WOFFORD, *Research and Development Department, Phillips Petroleum Company, Bartlesville, Oklahoma*

Synopsis

Tri- and tetrachain radial polybutadienes have been synthesized by coupling very dilute solutions of linear polybutadienyllithium with stoichiometric amounts of methyltrichlorosilane or silicon tetrachloride. These polymers have three or four long chains (100–2000 carbon atoms) attached to a single atom.

I. INTRODUCTION

The effects of branching on visco-mechanical properties of polymers have not been widely recognized. Quantitative correlations have been illusive because the degree of branching could not be accurately predicted from the preparative methods or deduced from polymer analysis. Development of anionic polymerization has opened a route to the synthesis of long-chain, branched polymers of controlled structure and molecular weight. Branched polystyrenes from alkylation of polyhalides with polystyryl anions have already been reported.[1,2,3] The present study is concerned with the synthesis of tri- and tetrachain radial

Trichain radial   Tetrachain radial
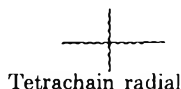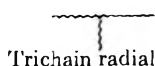
polybutadienes, polymers with three or four very long chains attached to a single atom.

II. EXPERIMENTAL

A. Reagents

Polymerization grade cyclohexane was dried by countercurrent scrubbing with nitrogen. Dry butadiene was obtained by flashing a special purity grade, scrubbing the gas with anhydrous ethylene glycol containing its sodium salt, and condensing it over Drierite. *n*-Butyllithium, purchased from Lithium Corporation of America as a concentrated heptane solution, was diluted to about 0.3*M* with dry cyclohexane and standardized with hydrochloric acid. Trimethylchlorosilane, dimethyldichlorosilane, methyl-

trichlorosilane, and silicon tetrachloride were pure grade materials obtained from Anderson Chemical Company and distilled under nitrogen. Center cuts were diluted with dry solvent and standardized by titration with alkali.

B. Polymerization

Polymerizations were conducted with 50 g. of butadiene in 500 ml. (390 g.) of cyclohexane in 26-oz. beverage bottles sealed with toluene-extracted, rubber gaskets under perforated metal caps. The bottles were charged with 200 ml. of dry solvent which was then purged with prepurified nitrogen admitted through a gas dispersion tube. They were capped, rinsed with 0.8 mmole of butyllithium added by syringe, and finally drained under nitrogen through a hypodermic needle.

Each polymerization series was charged from a single lot of reagents introduced into tared bottles by nitrogen pressure through hypodermic needles. The actual amounts of solvent and monomer were determined by weighing. Butyllithium was then added from a pressurized buret accurate to 0.01 ml., followed by prepurified nitrogen to raise the pressure to 25 psi. The bottle caps were further protected by inverted serum caps to keep them dry during later sampling, and then the bottles were tumbled in a water bath at 50°C.

The amount of impurity present in each lot of bottles, solvent, and monomer was estimated by determining the minimum amount (scavenger level) of butyllithium required to yield conversions of at least 90%. For this purpose, in consecutive bottles the amount of butyllithium was increased by small increments (0.025–0.05 mmole). One such increment was sufficient to raise conversion from 0–10% up to 90%. The scavenger level accounted for 0.15–0.35 mmoles of butyllithium (0.3–0.7 mmole/100 g. monomer). The polybutadienes obtained at the scavenger level were gel-free and had inherent viscosities of 5.0 or more.

Linear polybutadienes of lower viscosity were similarly prepared by initiation with amounts of butyllithium adjusted to compensate for the quantity of organolithium destroyed by impurities [eq. (1)]. Kinetic molecular weights[4] were predicted and preselected from eq. (2) which holds when all the effective butyllithium participates in initiation ($M_k \geq$ 20,000).[5]

$$RLi(\text{effective}) = RLi(\text{charged}) - RLi(\text{destroyed}) \qquad (1)$$

$$M_k = \text{Weight of butadiene/moles BuLi(effective)} \qquad (2)$$

Careful attention to detail resulted in excellent precision. Intrinsic viscosities ($[\eta] \leq 1.5$) of linear polybutadienes from a series of identically charged bottles were the same within experimental error. From series to series the deviation, after adjustment for differences in scavenger level, was usually only a little more.

Conversions were determined by evaporation and vacuum drying (at 60°C.) of known weights of the reaction solutions transferred by hypo-

dermic needle and syringe directly into tared pans containing some iso-propyl alcohol and an antioxidant, 2,2'-methylenebis(4-methyl-6-*tert*-butylphenol). This sample of the parent polybutadiene was used for intrinsic viscosity determination. Polybutadienes with molecular weights of 50,000 or less were washed in solution with very dilute hydrochloric acid and then with water. They were recovered by evaporation and vacuum drying at 60°C.

C. Reaction with Silicon Compounds

Within 7 hr. after initiation, weighed aliquots of the parent polybuta-dienyllithium solution were removed from each bottle of a series charged alike. Appropriate quantities of a silicon compound were added to the residues via hypodermic needle from an accurate buret. The quantities were so adjusted that in consecutive bottles the mole ratio of polymer-lithium to silicon compound increased in small increments from less than, to greater than, the theoretical optimum. The bottles were then tumbled at 50°C., conveniently overnight although 3 hr. was adequate. At the end

TABLE I
Typical Results for Reaction of Polybutadienyllithium with Silicon Chlorides

Silicon chloride	BuLi (effective), mmoles/50 g. butadiene	Mole ratio, PLi/silicon	$[\eta]$		Product ML-4 Mooney
			Parent	Product	
(CH₃)₃SiCl	—	0.5	1.35[a]	1.39[a]	—
(CH₃)₂SiCl₂	0.25[b]	1.2			56
		1.5			85
		1.8	1.97[b]	2.99[b]	103
		2.0			67
		2.5			61
CH₃SiCl₃	0.75	1.9		1.58	11
		2.4		1.69	42
		2.6		1.68	40
		2.8	0.99	1.71	51
		3.0	1.00	1.68	44
		3.2	1.00	1.63	40
		3.5		1.55	31
		4.2		1.52	25
		4.4		1.45	19
		9.7	0.99	1.17	4
SiCl₄	1.1	3.0		1.41	40
		3.5		1.51	50
		4.0		1.51	51
		4.3	0.84	1.61	52
		4.8	0.82	1.57	50
		5.0		1.57	47
		6.1		1.49	30

[a] Inherent viscosity.
[b] Silicon halide was introduced at 86% conversion. Viscosity-average molecular weights from eq. (4) were 175,000 for the parent and 331,000 for the product.

of this time an excess of butyllithium was added to destroy residual silicon–chlorine bonds followed shortly by isopropyl alcohol. The coupled polymers were recovered by coagulation or, if molecular weight was low, by washing with acid and water. All were vacuum-dried at 60°C. Typical results are listed in Table I.

D. Analyses

Inherent and intrinsic viscosities were measured in toluene at 25°C. and Mooney viscosities (ML-4) at 100°C. Fractionations were conducted by incremental addition of methanol to a 1% solution of polymer in toluene.[6] One fraction a day was collected. The per cent of *trans* and vinyl unsaturations were measured by infrared analysis according to a modification of a published method.[7]

E. Molecular Weights

Weight-average molecular weight $\bar{M}_w$ was measured by light scattering.[8] The polymerization procedure for estimating kinetic molecular weight (M_k) has already been described [eqs. (1) and (2)].
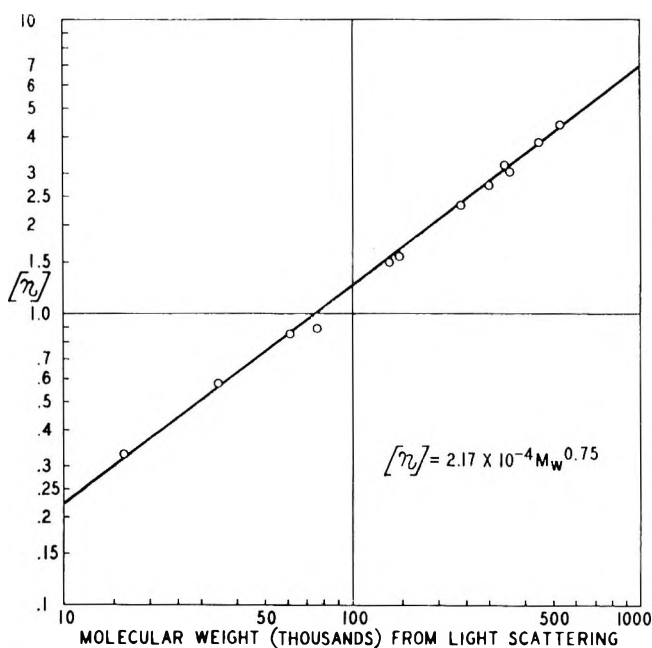
Fig. 1. Weight-average molecular weights $\bar{M}_w$ of linear, unfractionated polybutadienes.

A relationship of intrinsic viscosity to M_k [eq. (3)] was computed from 40 experimental points. Equation (4) shows a similar relationship derived from $\bar{M}_w$ (Fig. 1). Both apply to linear, unfractionated polybutadiene obtained by the described polymerization technique.

$$[\eta] = 7.76 \times 10^{-4} M_k^{0.65} \tag{3}$$

$$[\eta] = 2.17 \times 10^{-4} \overline{M}_w^{0.75} \tag{4}$$

III. RESULTS AND DISCUSSION

Preparation of polybutadiene with controlled, long-chain branching is basically a problem of organic synthesis with very dilute solutions (10^{-2} to 10^{-3} M) of very large alkenyllithiums (100–2000 carbon atoms). The first step is the preparation of the starting material, polybutadienyllithium, which is characterized through its hydrolysis product, polybutadiene. The second is a coupling reaction which must occur in high yield to synthesize directly as pure a product as possible.

Polymerization of butadiene in hydrocarbon solution by n-butyllithium forms essentially linear polybutadienyllithium with lithium on the allylic carbon at one end of the molecule. The reaction:

$$BuLi + nCH_2\!\!=\!\!CH\!-\!CH\!\!=\!\!CH_2 \rightarrow Bu\!-\!(CH_2\!-\!CH\!\!=\!\!CH\!-\!CH_2)_n\!-\!Li \tag{5}$$
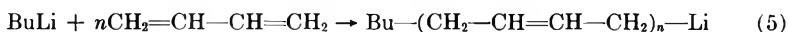
is quantitative and proceeds by consecutive stepwise addition, 92% of which is 1,4. For the purpose intended the presence of pendant vinyl groups (from 1,2 addition) on about every fourteenth carbon atom did not detract from the essential linearity of this alkenyllithium.

Chemical and kinetic evidence confirm this synthesis of polybutadienyllithium as a species with one lithium per molecule. Polymerization with a known amount of n-butyllithium and subsequent hydrolysis yields polybutadiene with a kinetic molecular weight[4] (M_k) which is predictable and in reasonable agreement with measured values. In the present work, reaction with a stoichiometric amount of dimethyldichlorosilane produced dipolybutadienyldimethylsilane in virtually quantitative yield [eq. (6)],

$$\begin{array}{c} CH_3 \\ | \\ 2PLi + (CH_3)_2SiCl_2 \rightarrow P\!-\!Si\!-\!P \\ | \\ CH_3 \end{array} \tag{6}$$
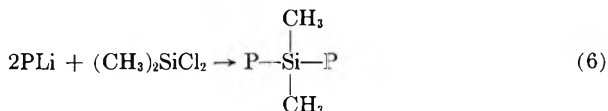
since the molecular weight of the product was almost double (190%) that of the starting polybutadienyllithium (Table I). Comparable results have been reported for coupling with bis(chloromethyl) ether.[9] Finally, the complete absence of gel (crosslinked product) from reaction with silicon tetrachloride argues against the presence of species with more than one lithium per molecule.

Kinetic evidence[5] is in agreement with these conclusions. Initiation is rapid, but not instantaneous. All the n-butyllithium is consumed if the quantity used is less than 5×10^{-3} moles/100 g. butadiene. Propagation is faster than initiation and occurs by consecutive stepwise addition without termination or transfer. Consequently, molecular weight distribution is quite limited. However, the experimental technique does not result in a monodisperse product ($\overline{M}_w/\overline{M}_n = 1.0$) in which all molecules are the same length. Reaction with impurities converts a small fraction of polybuta-
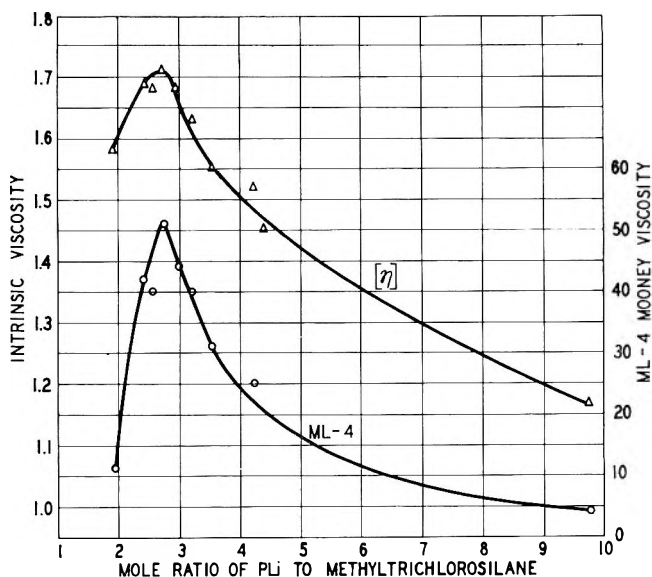
Fig. 2. Effect of varying methyltrichlorosilane with constant polybutadienyllithium $(M_k = 67,000)$.

dienyllithium to inert polybutadiene. The finite rate of initiation inherently results in a deviation from uniform size which is proportionately greater as molecular weight decreases. This is witnessed in the differences between the kinetic molecular weight M_k from catalyst charge [eqs. (1) and (2)], which should approximate number-average values $(\bar{M}_n)$, and the observed weight-average values $(\bar{M}_w)$ from light scattering. Equations (3) and (4) are convenient relations of intrinsic viscosity of unfractionated linear polybutadienes to the two kinds of molecular weights.

The conclusion that polybutadienyllithium is essentially linear, except for pendant vinyl groups, is based primarily on the rheological behavior of its hydrolysis product, polybutadiene, in comparison to the long-chain, branched polymers synthesized here.[10]

Reaction of polybutadienyllithium (PLi) with silicon halides should be analogous to those of simple compounds such as n-butyllithium. The only known reaction of alkyllithium with silicon halides is that of coupling.[11] In the present work with polyunsaturated chains, the possibility of cationic crosslinking was examined, but no indication of this was found. All reaction solutions and products were free of gel or fractions of unusually high molecular weight. Crosslinking during drying of recovered polymer can occur if polybutadienylchlorosilanes are present, but this was prevented by first converting them to polybutadienylbutylsilanes through treatment with excess n-butyllithium. The comparatively minute and stable butylmethylsilane moiety so formed is an integral part of the polymer and the site of the long-chain branching. This moiety itself does not alter polymer properties.

The principle difficulty in this synthesis of branched polymers is that of combining stoichiometric proportions of 10^{-2} to 10^{-4} moles of reactants so that the final product is substantially pure. Addition of different amounts of silicon halide to fixed amounts of polybutadienyllithium is a practical and effective solution. Polymer with the greatest molecular weight is obtained at actual stoichiometry and is readily identified by the fact that its solution or bulk viscosity is maximum (Table I and Fig. 2).

$$\tag{7}$$
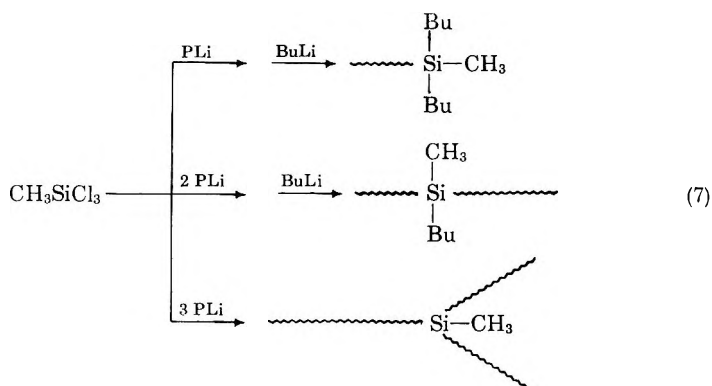
In practice such peak polymers are most readily detected by bulk viscosity, since viscous flow is profoundly altered by long-chain branching.

A number of trichain and tetrachain branched polybutadienes of different chain lengths were synthesized from polybutadienyllithium, methyltrichlorosilane and silicon tetrachloride (Figs. 3–5). In each case, the peak
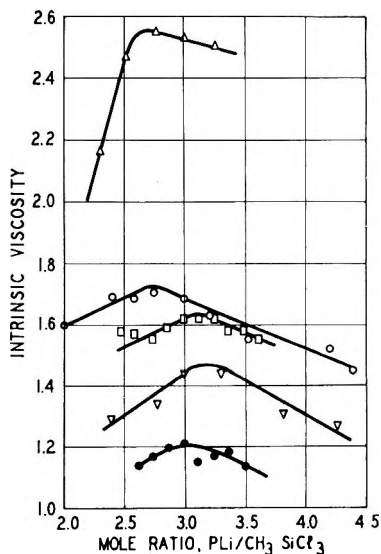
Fig. 3. Effect on intrinsic viscosity of varying the mole ratio of methyltrichlorosilane and polybutadienyllithium with molecular weights M_k of: ($\triangle$) 110,000; (O) 67,000; (☐) 48,000; (∇) 41,000; (●) 32,000.
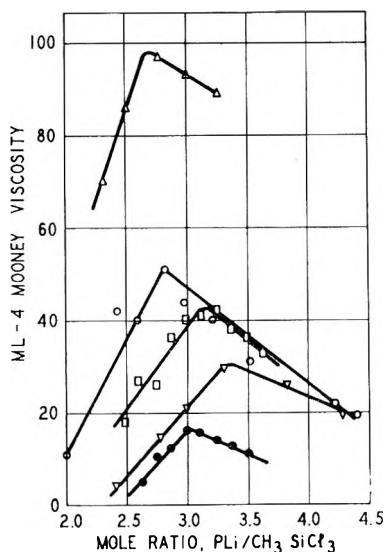
Fig. 4. Effect on ML-4 Mooney viscosity of varying the mole ratio of methyltrichloro-silane and polybutadienyllithium with molecular weights M_k of: ($\triangle$) 110,000; (O) 67,000; ($\square$) 48,000; (∇) 41,000; ($\bullet$) 32,000.
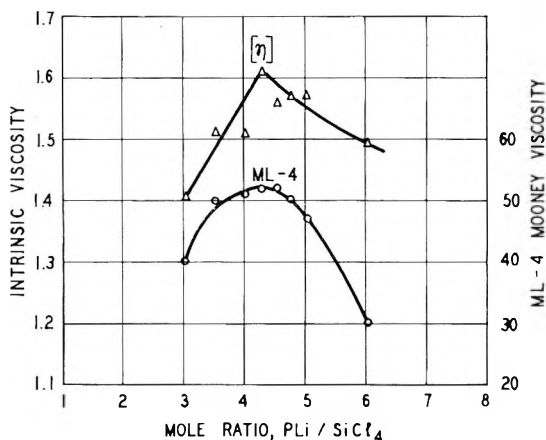
Fig. 5. Effect of varying silicon tetrachloride with constant polybutadienyllithium ($M_k = 45,000$).

polymer was obtained near the calculated stoichiometric ratio. Fractiona-tion established a high degree of homogeneity (Fig. 6). The principle impurity was of low molecular weight and probably represents linear poly-butadiene which resulted from destruction of polybutadienyllithium by impurities during its preparation and upon addition of the silicon halide. Gel and fractions of unusually high molecular weight were notably absent. Indeed, recombination of the major portions of each fractionation resulted in only a modest increase in intrinsic viscosity and little change in molecular weight (Table II).

TABLE II

Molecular Weights of Trichain and Tetrachain Radial Polybutadienes

	Unfractionated parent				Unfractionated branched					Fractionated branched			
$[\eta]_1$	$M_k \times 10^{-3}$	$\bar{M}_{vk} \times 10^{-3}$	$\bar{M}_{vw} \times 10^{-3}$	$[\eta]_b$	$M_k' \times 10^{-3}$	$\bar{M}_w \times 10^{-3}$	$\bar{M}_{vk}' \times 10^{-3}$	$\bar{M}_{rw}' \times 10^{-3}$	$[\eta]_b$	$\bar{M}_w \times 10^{-3}$	$\bar{M}_{vk}' \times 10^{-3}$	$\bar{M}_{vw}' \times 10^{-3}$
					Trichain								
1.56	110	122	138	2.55	330	—	316	307	2.62	333	329	318
0.99	67	62	75	1.71	201	184	171	180	1.78	172	182	190
0.91	48	53	67	1.62	144	—	158	167	1.72	170	172	182
0.83	41	45	60	1.44	123	141	131	144	1.56	148	148	160
0.68	32	34	46	1.15	96	—	93	106	1.21	116	100	114
0.43	16	17	25	0.74	48	—	47	59	—	—	—	—
					Tetrachain								
0.84	45	47	61	1.61	180	183	184	191	1.58	227	179	187
0.84	45	47	61	1.56	180	188	175	183	—	—	—	—
0.82	50	45	59	1.61	203	196	184	191	—	—	—	—
0.55	24	25	35	1.04	96	113	94	107	—	—	—	—
0.30	12	10	15	0.56	48	49	36	47	—	—	—	—

Three kinds of evidence confirm the successful synthesis of trichain and tetrachain radial polybutadienes. The actual optimum stoichiometry of coupling is close to the theoretical value. Rheological properties[12] of the products are strikingly different from those of linear polymers. And, finally, molecular weights calculated in several different ways are consistent and in good agreement with measured values.

Weight-average molecular weights $\bar{M}_w$ of the branched polymers were obtained by light scattering. They are in good agreement with the results (M_k') calculated for stoichiometric coupling of linear polybutadienyllithium for which kinetic molecular weights[4] M_k were estimated
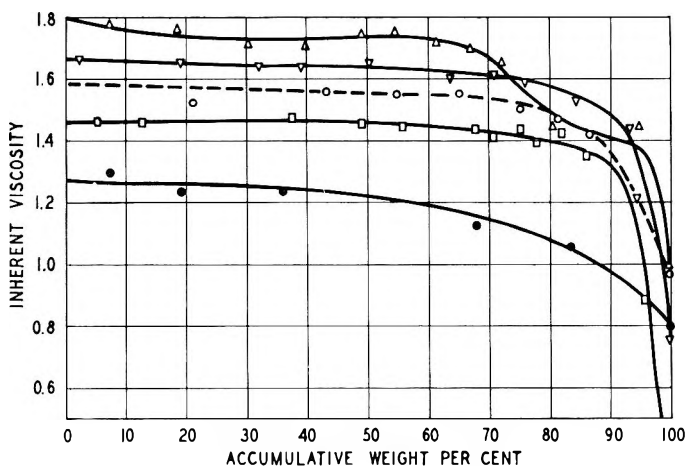
Fig. 6. Fractionation of (———) trichain and (- -) tetrachain radial polybutadienes with parent molecular weights M_k of: ($\triangle$) 110,000; (∇) 67,000; (O) 45,000; ($\square$) 41,000; ($\bullet$) 32,000.

from butyllithium charges. The agreement is excellent when intrinsic viscosities are used to calculate viscosity-average molecular weights of the linear parent $(\bar{M}_{vk})$ and the branched polymers $(\bar{M}_{vk}')$. The latter relation is readily obtained from the equation for linear, unfractionated polybutadiene after transformation into suitable expressions for branched polymers. This is done through the relation[13]

$$[\eta]_b / [\eta]_l = g^{1/2}$$

where g is obtained from

$$g = (3/p) - (2/p^2)$$

in which p is the number of branches.

Viscosity-average molecular weights $(\bar{M}_{vw}')$ for the branched polymers can also be calculated from intrinsic viscosity by similar transformations of eq. (4). They are consistent with the other values because coupling inherently decreases the differences between M_k and $\bar{M}_w$. Application

of these relations to polymers dissolved in good solvents appears to be justified by work reported for randomly branched polybutadienes.[14]

References

1. Morton, M., T. E. Helminiak, S. D. Gadkary, and F. Bueche, *J. Polymer Sci.*, **57**, 471 (1962).

2. Orofino, T. A., and F. Wenger, *J. Phys. Chem.*, **67**, 566 (1963).

3. Yen, S.-P. S., paper presented at 145th Meeting, American Chemical Society, New York, September 1963.

4. Morton, M., E. E. Bostick, and R. Livigni, *Rubber Plastics Age*, **42**, 397 (1961).

5. Hsieh, H. L., *J. Polymer Sci.*, **A3**, 163 (1965).

6. Flory, P. J., *Principles of Polymer Chemistry*, Cornell Univ. Press, Ithaca, N. Y., 1953, p. 339.

7. Silas, R. S., J. Yates, and V. Thornton, *Anal. Chem.*, **31**, 529 (1959).

8. Stacy, C. J., and R. L. Arnett, *J. Polymer Sci.*, **A2**, 197(1964).

9. Zelinski, R. P., and H. L. Hsieh, U. S. Pat. 3,078,254 (Feb. 19, 1963).

10. Kraus, G., and J. T. Gruver, *J. Polymer Sci.*, in press.

11. Wittenberg, D., and H. Gilman, *Quart. Rev.*, **13**, 116 (1959).

12. Kraus, G., and J. T. Gruver, *J. Polymer Sci.*, **A3**, 105 (1965).

13. Zimm, B. H., and R. W. Kilb, *J. Polymer Sci.*, **37**, 19 (1959).

14. Poddubnyĭ, I. Ya., and E. G. Erenburg, *Vysokomol. Soedin.*, **2**, 1625 (1960); *Rubber Chem. Technol.*, **34**, 975 (1961).

Résumé

On a synthétisé des polybutadienes ramifiés à trois et quatre chaînes latérales en couplant des solutions très diluées de polybutadiényllithium linéaire avec des quantités stoéchiométriques de méthyltrichlorosilane ou de tétrachlorure de silicium. Ces polymeres possèdent trois ou quatre longues chaînes (100 à 2000 atomes de carbone) fixées sur un seul atome.

Zusammenfassung

Radiale Tri- und Tetrakettenpolybutadiene wurden durch Kupplung sehr verdünnter Lösungen von linearem Polybutadienyllithium mit stöchiometrischen Mengen von Methyltrichlorsilan oder Siliziumtetrachlorid synthetisiert. Diese Polymere besitzen drei oder vier lange Ketten (100–2000 Kohlenstoff-atome), die an einem Atom befestigt sind.

Rheological Properties of Multichain Polybutadienes

GERARD KRAUS and J. T. GRUVER, *Research and Development Department, Phillips Petroleum Company, Bartlesville, Oklahoma*

Synopsis

The introduction of one or two long chain branches into a polybutadiene molecule to form trichain or tetrachain molecules, respectively, leads to profound changes in rheological behavior. At low molecular weights the Newtonian (zero shear) viscosity is decreased relative to a linear polymer of the same molecular weight. At molecular weights exceeding 60,000 (trichain) or 100,000 (tetrachain), the Newtonian viscosity rises rapidly above the corresponding value for a linear polybutadiene. However, non-Newtonian behavior of the branched polymers becomes more pronounced the higher the molecular weight, so that at moderate to high shear rates the viscosity of the branched polymers is uniformly lower than that of linear polymers of identical molecular weight.

I. INTRODUCTION

The flow properties of polybutadienes obtained by n-butyllithium initiation have been the subject of an earlier report.[1] Relative to most polymer systems described in the literature, these elastomers were shown to exhibit Newtonian flow to a surprisingly high degree. This apparently unusual behavior was ascribed to the extreme narrowness of the molecular weight distribution and freedom from long chain branching in these polymers. In the present work we have examined the effect of long-chain branching on the rheological properties of polybutadiene.

It is possible to prepare branched polymers of controlled structure by terminating n-butyllithium-initiated polymer with a polyfunctional reagent, e.g., methyltrichlorosilane. The result is a multichain "star-shaped" polymer. Some measurements of the bulk viscosity of multichain polymers have already been reported in the literature. Schaefgen and Flory[2] worked with multichain poly-ϵ-caprolactams and observed little effect of branching on the bulk viscosity except for octachain polymers. In the latter case the branched polymers had lower viscosity than linear polymers of the same molecular weight. Charlesby[3] reported on polydimethylsiloxanes branched by irradiation and also observed a lowering of the bulk viscosity for branched polymer. Recently Fox and Allen[4] have described results of studies made with multichain polystyrenes. In their paper they indicate that multichain molecules with 3, 4, and 8 branches have progressively lower bulk viscosities than the corresponding linear polymer, and the viscosities obey the well-known 3.4 power law in weight-average molecular weight.

Theoretical treatments by F. Bueche[5] and Ham[6] have also predicted a lowering of the Newtonian viscosity due to branching. On the other hand, a recent study by Berry[7] on branched poly(vinyl acetates) has shown that sufficiently long branches can lead to increases in the melt viscosity.

It will be shown that the effect of long-chain branching on the rheological properties of polybutadiene appears to depend primarily on the relation of the branch length to the entanglement spacing molecular weight. Thus, we shall demonstrate that at low molecular weights the viscosity of a multichain polybutadiene is less than that of a linear polybutadiene of equal molecular weight, in agreement with the work quoted above. On the other hand as the molecular weight increases to the point where each branch contains several entanglements, the reverse becomes true. Along with this effect the flow becomes strongly non-Newtonian.

II. EXPERIMENTAL

A. Polymers

The multichain polybutadienes used in these experiments were prepared by R. P. Zelinski and C. F. Wofford. Their synthesis is described in detail in the accompanying paper.[8]

B. Viscosity Measurements

Three methods were used in the determination of viscosity. For liquid polymers (<2,000 poise) an Ostwald-Cannon-Fenske viscometer was used. All other polymers were investigated with a capillary extrusion rheometer and several rubbers in excess of 100,000 molecular weight by the tensile creep technique. The capillary extrusion rheometry is described in more detail in an earlier paper.[1] To obtain the lowest shear rates reported here capillaries with L/R ratios of 100 were used; most of the data at higher shear rates were obtained with $L/R \approx 18$.

The creep measurements were carried out as follows. The polymers were dissolved in benzene and cast on pools of mercury. The resulting films were approximately 0.5 mm. thick. Creep samples (0.317 cm. in width) were died out from these films. Gage marks were placed on the samples after which they were clamped in a holder and placed in glass tubes sealed in a thermostated water bath. The small weights attached to the other end of the sample rested on pistonlike supports. The support was pulled out rapidly to start the test. The creep was followed with a cathetometer reading to 0.005 cm. Elongations were kept below 10% to avoid serious complications due to change in cross section.

Methods of calculation have been described previously.[1] All capillary extrusion measurements were corrected for entrance effect and maximum shear rate at the wall as described by Philippoff and Gaskins.[9] Viscosities from creep data were calculated by the permanent set method:[10]

$$\eta = t/3[J(t) - J'(\infty)] = Sl_0t/3\Delta l \tag{1}$$

where $J(t)$ is the tensile compliance at time t, $J'(\infty)$ the recovered elastic compliance, S the tensile stress, l_0 the original length of the specimen, and Δl the permanent set.

III. CHARACTERIZATION OF MULTICHAIN POLYBUTADIENES

A potential difficulty in the synthesis of multichain polymers by the present method is the possibility of halogen–metal interchange. This would lead to molecules of differing functionality.[11] As Zelinski and Wofford[8] point out, this complication did not occur here. Their results also show the yield of multichain polymer at optimum stoichiometry to be in the vicinity of 90%. Accordingly, no attempt was made to isolate the multichain polymer in pure form for the rheological measurements.
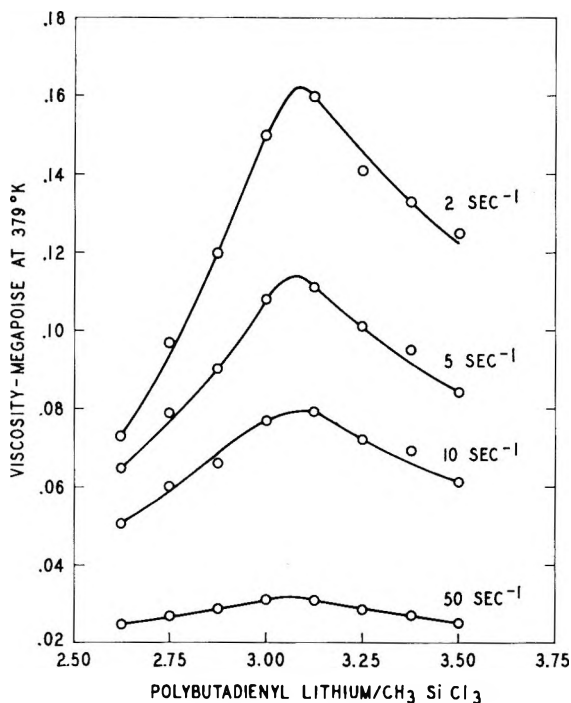
Fig. 1. Determination of optimum coupling ratio for polymer D.

It was felt that, with an unsaturated polymer, the possibility of degradation during fractionation might lead to more serious complications than a relatively small amount of the uncoupled species.

To establish the optimum coupling ratio the bulk viscosity itself was used as the criterion. Figure 1 shows a typical set of plots of bulk viscosity at several rates of shear versus coupling stoichiometry for a trichain polymer. In this and all other sample series investigated the maximum in viscosity occurred between 2.7 and 3.3 coupling ratio for trichain

TABLE I
Molecular Weight Data

Polymer	Coupling ratio	Parent polymer			[η]	Coupled polymer $M_w/1000$			
		[η]	$M_w/1000$	$M_n/1000$		Intrinsic viscosity	Light scattering	Sedim. velocity	Calc.[a]
Trichain polymers									
A	2.77	1.56	138	110	2.55	303	333[b]	365	358
B	2.77	0.99	75	67	1.73	180	184	205	209
C	3.30	0.83	60	41	1.47	144	141, 148[b]	155	142
D	3.13	0.64	42	33	1.19	109	116[b]	110	108
E	3.13	0.43	15	17.4	0.74	58	--	63	60
F	3.25	0.20	8.9	5.0[e]	0.34	20.6	--	--	20[d]
G	3.25	0.12	4.5	2.3	0.20	10.1	--	--	9.1
Tetrachain polymers									
H	3.8	0.82	59	50	1.61	182	196	178	209
J	3.8	0.595	38	24	1.04	105	113	102	110
K	3.8	0.30	15.3	12.8	0.56	45	49	53	54
L	3.8	0.19	8.4	6.7[e]	0.39	27.6	29.0	33.5	28.5
M	4.2	0.11	4.0	2.3	0.22	12.9	10.6	--	10.9

[a] For stoichiometric coupling.
[b] On fractionated sample (main fraction).
[c] 5400 by ebulliometry.
[d] $M_n = 15,000$ by ebulliometry.
[e] 6100 by ebulliometry.

polymers, i.e., near the theoretical value of 3.0. For tetrachain polymers the maximum occurred between 3.8 and 4.2. Ultracentrifuge sedimentation velocity experiments on the peak viscosity members of each series showed the presence of a single boundary, thus failing to detect or resolve the presence of uncoupled or dichain polymers. Fractionation of some of the polymers in a Baker-Williams column[13] led to recovery of about 90% of the total weight of the sample as the appropriate multichain species.[8] These considerations suggest that halogen–metal exchange did not seriously interfere with the preparation of multichain polymer in high yield. Further confirmation for this is shown in Table I listing molecular weight data prior to and after coupling.

The weight-average molecular weight prior to coupling was found from the intrinsic viscosity in toluene (25°C.) by using a correlation with light-scattering molecular weights:*

$$[\eta] = 2.17 \times 10^{-4}\bar{M}_w^{0.75} \tag{2}$$

The number-average molecular weight was found by calculation from the initiator level after correction for n-butyllithium destroyed by impurities and unreacted initiator remaining after the polymerization is complete. The correction was determined separately for each experiment. For the coupled polymer several molecular weight estimates are given. The sedimentation velocity molecular weight was calculated from the sedimentation coefficient in n-heptane by using a correlation developed for linear polymer:

$$s = 4.53 \times 10^{-15} \bar{M}_w^{0.428} \tag{3}$$

i.e., any possible effects of long-chain branching on the sedimentation coefficient were neglected, a procedure which may not be entirely justified. The viscometric value was obtained by correcting the intrinsic viscosity by the Zimm and Kilb[14] relation:

$$[\eta]_b/[\eta]_l = g^{1/2} \tag{4}$$

where $[\eta]_b$ and $[\eta]_l$ are the intrinsic viscosities of the branched and unbranched molecules, respectively, and

$$g = (3/p) - (2/p^2) \tag{5}$$

For trichain polymers, $p = 3$ and $g = {}^7/_9$; similarly, for tetrachain polymers $g = {}^5/_8$. Equation (2) was then applied to the corrected intrinsic viscosity. It should be noted that eq. (4) applies theoretically only to a theta solvent. However, it has been shown that its validity is not seriously impaired even in good solvents.[12,16] Four of the trichain and all of the tetrachain polymers were checked by light scattering. Finally, the calculated $\bar{M}_w$ in Table I were obtained from the molecular weight

* Reference 1 lists an equation with slightly different parameters. The present formula represents a revision resulting from additional determinations.

data on the uncoupled rubbers, taking into account the sharpening of the molecular weight distribution due to random coupling (see Appendix). The generally good agreement between the various estimates is further evidence for the high content of multichain molecules in the coupled polymers.

IV. RESULTS OF RHEOLOGICAL MEASUREMENTS

Table II lists the capillary extrusion rheometer data obtained. A summary of all Newtonian viscosities is shown in Table III.

Figure 2 shows a typical tensile creep curve. The dashed line connects the final experimental point on the creep curve with the measured recoverable compliance plotted at $t = 0$; the slope of this line is therefore equal to $(1/3\eta)$. For all trichain polymers of $\bar{M}_w \leq 180,000$ the behavior was as shown in Figure 2; i.e., steady state was either attained or approached quite closely in the duration of the experiment. Above this molecular weight, the creep tended to become increasingly nonlinear, giving rise to smaller viscosities as the tensile stress was increased. In other words, these creep viscosities appear to be non-Newtonian. A summary of the creep data is shown in Table IV. For the highest molecular weight trichain polymer, A, recovery was in excess of 95%, leading to very high and poorly defined viscosity values. The extreme nonlinearity in the creep compliance of this polymer is illustrated in Figure 3. It almost appears as if the polymer were crosslinked, but this is not the case, the rubber being completely soluble in benzene. This behavior
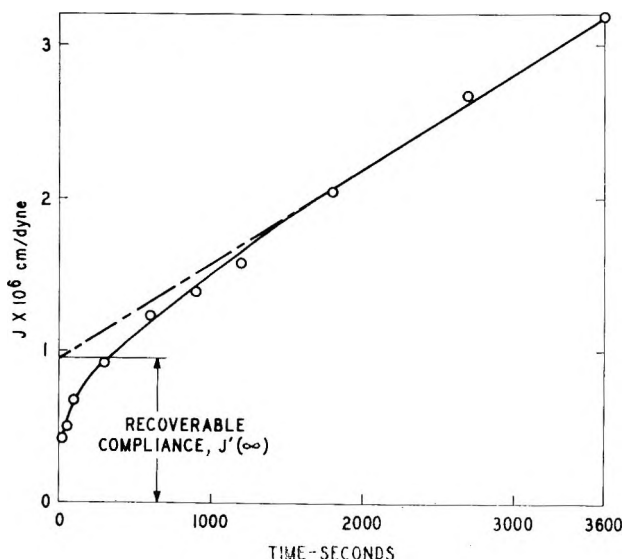
Fig. 2. Typical creep curve for trichain polybutadiene at 25°C. (polymer B, tensile stress = 17,200 dynes/cm.²).

TABLE II. Capillary Viscometer Data

Polymer	Temp., °K.	$f \times 10^{-6}$, dynes/cm.^{2}	$\dot{s}$, sec.$^{-1}$
A	379	0.44	0.021
		0.57	0.051
		0.66	0.15
		0.84	0.21
		1.12[a]	0.48
		1.28	0.64
		1.51	1.01
		1.63	1.15
		1.80	1.56
		1.92	1.77
		2.17	2.56
		2.22	2.56
		2.36	3.13
		2.54	3.68
B	379	0.0198	0.0011
		0.039	0.0021
		0.062	0.0039
		0.112	0.0086
		0.17	0.0162
		0.225	0.025
		0.28	0.042
		0.34	0.066
		0.39	0.098
		0.50	0.37
		0.67	0.71
		0.87	1.72
		0.99	2.46
		1.17[a]	3.84
		1.29	4.60
		1.48	7.43
		1.68	9.55
		1.82	12.8
		1.96	14.6
		2.20	19.7
		2.29	23.0
		2.43	27.5
C	299	0.34	0.054
		0.65	0.187
		0.99[a]	0.54
		1.18	0.89
		1.33	1.17
		1.52	1.71
		1.67	2.10
		1.86	2.83
		2.01	2.87
		2.20	4.32
		2.34	5.05
		2.53	6.53
		2.69	7.99
		2.91	9.64
C	379	0.017	0.014
		0.041	0.033
		0.63	0.051
		0.130	0.096
		0.170	0.167

TABLE II (*continued*)

Polymer	Temp., °K.	$f \times 10^{-6}$, dynes/cm.^{2}	$\dot{s}$, sec.$^{-1}$
C	379	0.22	0.25
		0.28	0.36
		0.33	0.53
		0.34	0.62
		0.40	0.76
		0.50	1.37
		0.72	3.00
		0.88	5.13
		1.01	6.86
		1.19[a]	10.3
		1.33	13.8
		1.60	22.6
		1.71	25.2
		1.92	35.2
		2.07	40.9
		2.22	51.7
		2.36	59.8
D	299	0.33	0.13
		0.53	0.32
		0.65	0.52
		0.82	0.83
		1.00[a]	1.50
		1.17	2.23
		1.33	3.21
		1.52	4.58
		1.65	5.56
		1.83	7.53
		2.01	10.1
		2.19	13.1
		2.36	16.1
		2.50	19.1
		2.68	23.2
		2.87	29.9
D	379	0.17	0.90
		0.36	2.45
		0.52	4.24
		0.68	7.59
		0.87	10.8
		1.02	17.1
		1.25	27.7
		1.39	40.9
		1.58[a]	56.9
		1.73	72.4
		1.91	95.5
		2.08	119
E	299	0.085	1.28
		0.194	3.05
		0.36	6.29
		0.54	10.7
		0.72	15.6
		1.07	27.6
		1.23	38.6
		1.42	44.6
		1.60	57.7
		1.75	72.2

TABLE II (*continued*)

Polymer	Temp., °K.	$f \times 10^{-6}$, dynes/cm.^{2}	$\mathring{s}$, sec.$^{-1}$
E	379	0.088	23.8
		0.18	32.1
		0.27	64.0
		0.34	91.2
		0.52	143
		0.63	159
		0.70	200
		0.88	287
H	379	0.0155	0.0022
		0.032	0.0028
		0.045	0.0054
		0.088	0.0083
		0.134	0.0152
		0.181	0.024
		0.214	0.037
		0.30	0.071
		0.33	0.105
		0.52	0.34
		0.70	1.01
		0.83	1.81
		0.90	2.46
		1.08	4.23
		1.42[a]	9.45
		1.76	17.9
		2.07	28.6
		2.45	44.8
		2.74	61.0
		3.13	89.7
J	379	0.0111	0.225
		0.0223	0.45
		0.0317	0.61
		0.0449	0.88
		0.090	1.74
		0.096	1.86
		0.13	2.64
		0.214	4.41
		0.215	3.84
		0.31	7.03
		0.39	7.79
		0.57	15.3
		0.77	26.4
		0.94	55.0
		1.12	59.8
		1.48	114
		1.86[a]	187
		2.20	283
K	379	0.106	122
		0.215	286
		0.42	542
		0.57	737
		0.81	1140
		0.96	1440
		1.18	1920
		1.58	3010
		2.00	4560

[a] First appearance of extrudate roughness.

TABLE III
Newtonian Viscosities

Polymer	p	$\bar{M}_w/1000$[a]	Temp., °K.	Viscosity, poise
A	3	303	379	—[b]
B	3	180	379	1.84×10^7
C	3	144	379	1.24×10^6
D	3	109	379	2.2×10^5
			299	2.7×10^6
E	3	58	379	4.7×10^3
			299	6.4×10^4
F	3	20.6	379	59.3
G	3	10.1	379	5.5
			299	61.2
H	4	182	379	1.1×10^7
J	4	105	379	5.0×10^4
K	4	45	379	7.0×10^2
L	4	27.6	379	95.0
M	4	12.9	379	5.9

[a] Intrinsic viscosity.
[b] Non-Newtonian over entire range of shear rates investigated.

TABLE IV
Viscosities from Tensile Creep (25°C.)

Polymer	$\bar{M}_w$[a]	Tensile stress, dynes/cm.[2]	Viscosity, Mpoise
A	303,000	13,000	330,000 (?)
		211,000	29,000 (?)
B	180,000	17,000	540
		32,000	620
		71,000	340
		211,000	416
C	144,000	5,500	30.4
		8,400	31.0
		13,000	31.0
		52,000	28.4
D	109,000	2,400	7.8
		6,000	5.9
		6,500	6.3

[a] Intrinsic viscosity.

appears to be characteristic of high molecular weight branched polymers. Further evidence of this will be given in a subsequent report.

Figure 4 is a composite plot of the data on trichain polymers (Table II) with the rheological curves at 299°K. shifted to 379°K. by use of appropriate shift factors. The values of these shift factors are given in Table V. This compares to a mean shift factor of about 11 for linear polybutadienes between these temperatures.[1] Evidently the introduction of long chain
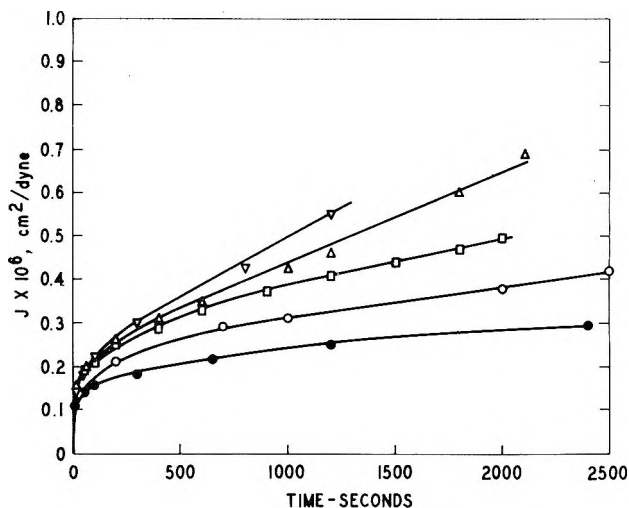
Fig. 3. Creep of trichain polybutadiene A at 26°C. at various stresses: (∇) 5.5 × 10^{5} dynes/cm.[2]; ($\triangle$) 4.7 × 10^{5} dynes/cm.[2]; ($\square$) 4.0 × 10^{5} dynes/cm.[2]; ($\bigcirc$) 2.0 × 10^{5} dynes/cm.[2]; ($\bullet$) 1.6 × 10^{5} dynes/cm.[2].

TABLE V

Polymer	$\bar{M}_w{}^a$	a^b
C	144,000	11.5
D	109,000	12.5
E	58,000	13.5
G	10,100	11.1
	Mean	12.15

[a] Intrinsic viscosity.
[b] $a = \eta_{299}/\eta_{379}$

branching has little, if any, effect on the activation energy for flow. Figure 5 is a similar plot of the data on tetrachain polybutadienes (at 379°K.).

Finally, in Figure 6 the zero shear Newtonian viscosities are plotted against $\bar{M}_w$ and compared to the corresponding curve for the linear polymers.[1]

V. DISCUSSION

Figure 6 shows clearly that, whereas the linear polymers follow the usual behavior, i.e., a 3.4th power dependence with $\bar{M}_w$ above a certain critical molecular weight, the multichain polybutadienes do not. It has been reported that with multichain poly-ϵ-caprolactams[2] and multichain polystyrenes,[4] the melt viscosity of a branched polymer is decreased relative to a linear polymer of the same $\bar{M}_w$. In the present work this is found only when $\bar{M}_w < 60,000$ for the trichain polymers or $\bar{M}_w < 100,000$ for the tetrachain species.
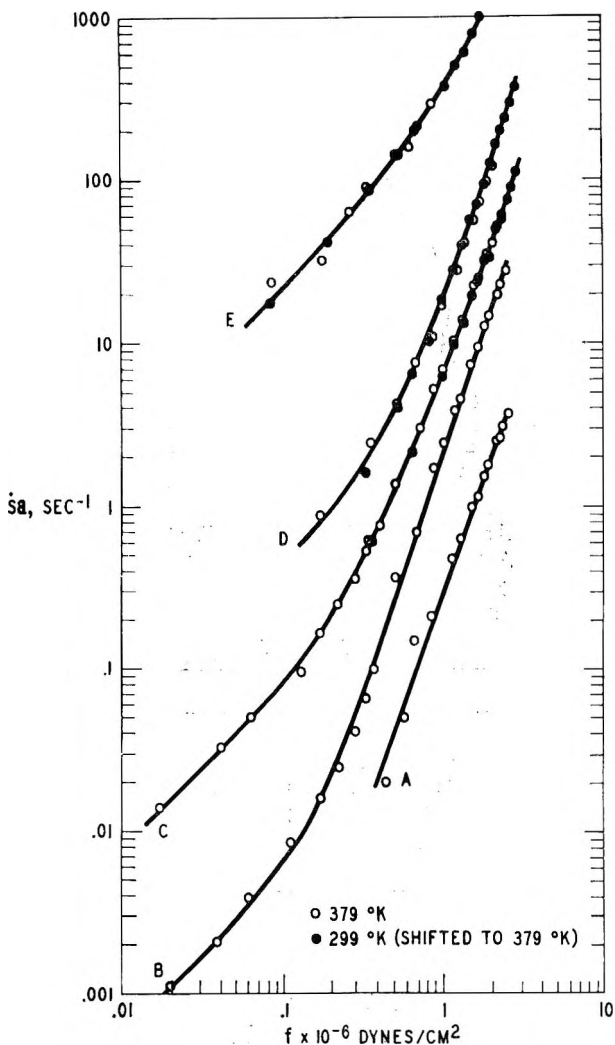
Fig. 4. Rheological curves for trichain polybutadienes: (○) 379°K.; (●) 299°K. (shifted to 379°K.).

Above these molecular weights the slope of the curves increases rapidly, with the viscosity of the multichain molecules eventually becoming several orders of magnitude greater than that of the linear polymers. We propose the following explanation for this behavior. At low molecular weights, when the branches of the multichain polymers are not much longer than the entanglement spacing molecular weight M_e (about 5,600 for n-butyl-lithium-initiated polybutadiene),* flow occurs with little coupling between molecules. The principal factor governing viscosity is then the

* In this paper as well as in the previous one,[1] we have followed Markovitz, Fox, and Ferry[16] in identifying the break in the viscosity–molecular weight curve directly with the molecular weight between entanglements.
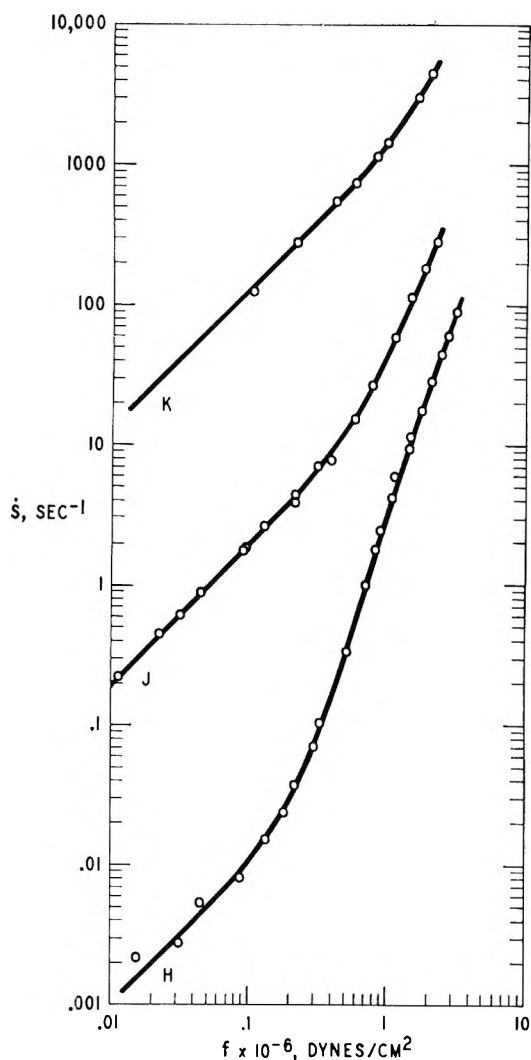
Fig. 5.   Rheological curves for tetrachain polybutadienes (379°K.).

size of the polymer coil, which is smaller for the branched molecules. Ultimately, however, entanglements of branches belonging to different molecules appear to lead to extensive coupling as the branch length is increased. Such entanglement coupling occurs also in purely linear polymers, but in the branched polymer the branch point assumes the role of a permanent constraint, incapable of slippage during flow under low shear stresses. This constraint eventually outweighs the coil dimension effect and the viscosity becomes larger than that of the linear polymer. The crossover point appears to be related to M_e. In the present system it occurs when the branch length is roughly $3M_e$ for trichain and $4M_e$ for the tetrachain polymer. If the same were true in polystyrene, where
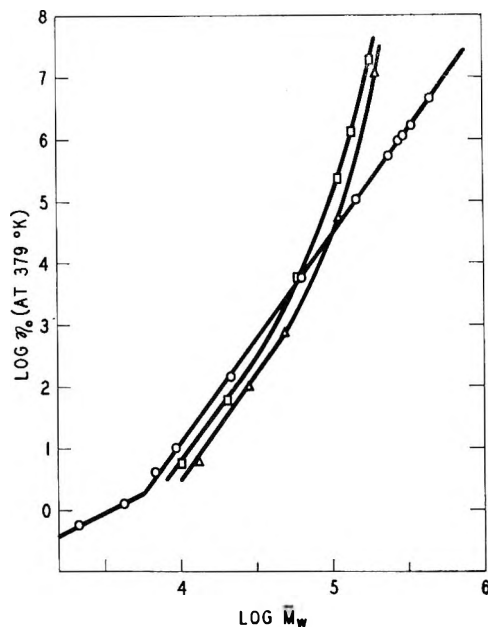
Fig. 6. Dependence of Newtonian viscosity on molecular weight: (O) linear; (□) trichain; (△) tetrachain.

$M_e \cong 38,000$, the crossover would occur above 350,000 molecular weight, which is outside the range studied by Fox and Allen.[4]

It is of interest to note that below 50,000 molecular weight our data are in reasonably good agreement with the theory of Bueche.[5] This is apparent from a comparison of the ratios η_b/η_l with $g^{3.4}$ (Table VI).

TABLE VI

p	g	$g^{3.4}$	η_b/η_l
1 or 2	1.000	1.00	1.00
3	0.778	0.43	0.46
4	0.625	0.20	0.22

That the behavior of the high molecular weight branched polybutadienes—though at variance with the Bueche and Ham theories—is real and is not caused by structural imperfections can be established from the following. Dilution with linear polymer due to incomplete coupling may alter somewhat the quantitative relationships at zero shear but cannot produce an increase in viscosity as is apparent from Figure 1, nor can it produce a crossover in the viscosity–molecular weight relation. Likewise, several facts may be quoted against the possibility of uncontrolled crosslinking.

(a) All polymers, linear or branched, were gel-free and filtered freely through the Millipore filters used to clarify the solutions for light scattering measurements.

(b) None gave unreasonably high molecular weights by light scattering.

(c) When viscosity measurements were taken at ascending and descending shear rates in the capillary rheometer, the results were found to coincide. Crosslinking in the rheometer invariably results in a discrepancy in ascending and descending sets of data.

(d) Measurements taken at room temperature (Table III), in which the polymer was never heated were entirely consistent with the data taken at 379°K.
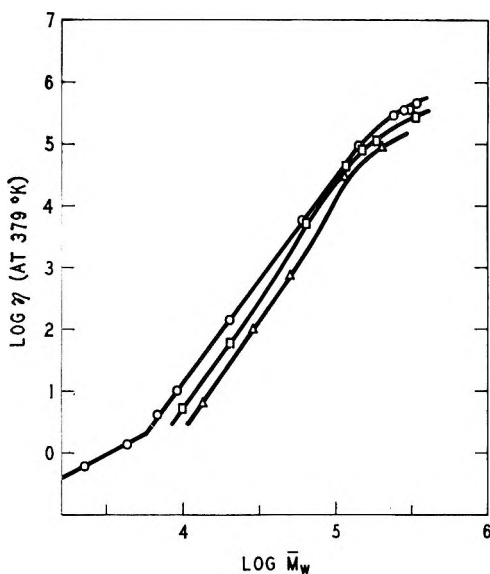
Fig. 7. Viscosity vs. molecular weight at shear rate 20 sec.$^{-1}$: (O) linear; (□) trichain; (△) tetrachain.

Comparison of the entire flow curves for linear and multichain polybutadienes reveals that the branched polymers deviate far more from Newtonian behavior than do the linear polymers. Figure 7 shows η versus $\bar{M}_w$ at $\dot{s} = 20$ sec.$^{-1}$, the data for linear polymers being taken from the previous paper.[1] At this shear rate the curves for the multichain polymers lie entirely below that representing the linear polymers. It has been proposed by Porter and Johnson[17] that the importance of polymer entanglements becomes less with increasing shear and that the limiting high shear viscosities should increase with molecular weight in a manner similar to unentangled molecules. In the limit of high shear rate both the linear and multichain polymers would then exhibit viscosities roughly proportional to the first power of molecular weight with the branched polymers lying below the linear ones. The behavior observed at $\dot{s} = 20$

sec.$^{-1}$ might be expected of a stage intermediate in the approach to the high shear viscosity regime.

Comparison of the zero-shear viscosities from capillary extrusion data and creep—after the appropriate temperature shift—reveals a discrepancy of the order of a factor of 2 in the direction of higher viscosity from the creep data. This is generally not observed in linear polybutadienes.[1] We ascribe this behavior to a small increase in molecular weight due to cross-linking in the preparation of the creep samples. According to Figure 6, the slope of the logarithmic viscosity–molecular weight relationship for trichain polymers above $\bar{M}_w = 100,000$ is of the order of 9. An 8% increase in molecular weight would suffice to produce the effect observed.

We, finally, wish to comment further on the unusual behavior of polymer A. Its extremely high viscosity and nonlinear creep are not unlike the behavior of high molecular weight polysiloxanes reported by Plazek, Dannhauser, and Ferry.[18] These results indicate that in polymers of high molecular weight, coil–coil interactions are much greater than those normally seen in polymers of moderate molecular weights where the classical η–$M^{3.4}$ relationship applies and that this behavior may be accentuated by branching.

APPENDIX

Narrowing of Molecular Weight Distribution Due to Coupling

Let $f_n(M)$ be the number distribution function of molecular weights. The number-average, and weight-average molecular weights will be

$$\bar{M}_n = \left[\int_0^\infty f_n(M) M \, dM \right] / \left[\int_0^\infty f_n(M) \, dM \right] \tag{6}$$

and

$$\bar{M}_w = \left[\int_0^\infty f_n(M) M^2 \, dM \right] / \left[\int_0^\infty f_n(M) M \, dM \right] \tag{7}$$

Making use of the definition of the variance of the distribution, σ_n^2, it is easily shown that

$$\sigma_n^2 = \bar{M}_n(\bar{M}_w - \bar{M}_n) \tag{8}$$

regardless of the particular form of $f_n(M)$.

If the molecules are coupled x at a time, the variance of the numbers distribution of the coupled polymer will be

$$\sigma_n^2 = x\sigma_n^2 \tag{9}$$

and the mean

$$\bar{M}_n' = x\bar{M}_n \tag{10}$$

Since eq. (8) also holds in the primed (coupled) distribution

$$x\bar{M}_n(\bar{M}_w - \bar{M}_n) = \bar{M}_n'(\bar{M}_w' - \bar{M}_n'), \tag{11}$$

from which

$$\bar{M}_w' = \bar{M}_w + (x - 1)\bar{M}_n \tag{12}$$

and

$$\bar{M}_w'/\bar{M}_n' = \bar{M}_w/\bar{M}_n + (x - 1)/x \tag{13}$$

References

1. Gruver, J. T., and G. Kraus, *J. Polymer Sci.*, **A2,** 797 (1964).
2. Schaefgen, J. R., and P. J. Flory, *J. Am. Chem. Soc.*, **70,** 2709 (1948).
3. Charlesby, A. J., *J. Polymer Sci.*, **17,** 379 (1955).
4. Fox, T. G, and V. R. Allen, paper presented to Division of Polymer Chemistry, 141st Meeting, American Chemical Society, Washington, D. C., March 1962.
5. Bueche, F., *J. Chem. Phys.*, **40,** 484 (1964).
6. Ham, J. S., *J. Chem. Phys.*, **26,** 625 (1957).
7. Berry, G. C., Ph.D. Dissertation, Univ. of Michigan, 1961.
8. Zelinski, R. P., and C. F. Wofford, *J. Polymer Sci.*, **A3,** 93 (1965).
9. Philippoff, W., and F. H. Gaskins, *Trans. Soc. Rheol.*, **2,** 263 (1958).
10. Bueche, F., *J. Appl. Phys.*, **26,** 738 (1955).
11. Wenger, F., and S.-P.S. Yen, paper presented to Division of Polymer Chemistry, 141st Meeting, American Chemical Society, Washington, D. C., March 1962.
12. Morton, M., T. E. Helminiak, S. D. Gadkary, and F. Bueche, *J. Polymer Sci.*, **57,** 471 (1962).
13. Baker, C. A., and R. J. P. Williams, *J. Chem. Soc.*, **1956,** 2352.
14. Zimm, B. H., and R. W. Kilb, *J. Polymer Sci.*, **37,** 19 (1959).
15. Mayerhoff, G., *Fortschr. Hochpolymer. Forsch.*, **3,** 59 (1961).
16. Markovitz, H., T. G Fox, and J. D. Ferry, *J. Phys. Chem.*, **66,** 1567 (1962).
17. Porter, R. S., and J. F. Johnson, *SPE Trans.*, **3,** 18 (1963).
18. Plazek, D. J., W. Dannhauser, and J. D. Ferry, *J. Colloid Sci.*, **16,** 101 (1961).

Résumé

L'introduction d'une ou deux camifications à longue chaîne dans une molécule de polybutadiene, pour former des molécules à trois ou quatre chaînes respectivement, provoque des changements importants dans le comportement rhéologique. Pour des faibles poids moléculaires, la viscosité Newtonienne (cisaillement zéro) est diminuée comparativement aux polymeres linéaires de même poids moléculaire. Pour des poids moléculaires, supérieurs a 60.000 (trois chaînes) la viscosité Newtonienne augmente rapidement pour dépasser la valeur correspondante d'un polybutadiene linéaire. Néanmoins, plus le poids moléculaire augmente, plus le comportement non-Newtonien des polymères ramifiés devient prononcé, de sorte que, pour des vitesses de cisaillement modérées et élevées, la viscosité des polymères ramifiés est uniformement plus faible que celle des polymeres linéaires d'un poids moléculaire identique.

Zusammenfassung

Die Einführung einer oder zweier langer Kettenverzweigungen in ein Polybutadien-molekül unter Bildung drei- bzw. vierkettiger Moleküle führt zu tiefgreifenden Änderungen im rjeologischen Verhalten. Bei niedrigen Moleukulargewichten wurde die New-

tonsche (Scherung Null) Viskosität relativ zu einem linearen Polymeren vom gleichen Molekulargewicht herabgesetzt. Bei Molekulargewichten oberhalb 60.000 (dreikettig) oder 100.000 (vierkettig) steigt die Newtonsche Viskosität rasch über den entsprechenden Wert für ein lineares Polybutadien an. Hingegen tritt das nicht-Newtonsche Verhalten der verzweigten Polymeren bei hohem Molekulargewicht stark hervor, sodass bei mässigen bis hohen Schergeschwindigkeiten die Viskosität des verzweigten Polymeren einheitlich niedriger als diejenige linearer Polymerer mit identischen Molekulargewichten ist.

Stereospecific Polymerization of 2-Substituted 1,3-Butadienes. II. Stereospecific Polymers of 2-*n*-Propyl-1,3-Butadiene

W. MARCONI, A. MAZZEI, S. CUCINELLA, M. CESARI, and E. PAULUZZI, *SNAM-Laboratori Riuniti Studi e Ricerche, San Donato, Milano, Italy*

Synopsis

The stereospecific polymerization of 2-*n*-propyl-1,3-butadiene with aluminum alkyls or aluminum hydride and different transition metal salts was investigated. The behavior of this monomer with respect to the various catalysts employed is similar to that of isoprene. With the AlEt₃–TiCl₄ and AlHCl₂·(C₂H₅)₂O–TiCl₄ systems, rubbery polymers are obtained whose infrared spectra are consistent with the 1,4-*cis* structure. With the AlEt₃–Ti(*i*-C₃H₇O)₄ catalyst, a low molecular weight polymer with a prevailing 3,4 structure is obtained. The AlEt₃–VCl₃ system gives a crystalline product melting at 42°C. The identity period has been determined, and two possible chain conformations are proposed.

INTRODUCTION

Stereospecific polymerization of 2-*tert*-butyl-1,3-butadiene and its crystalline 1,4-*cis* polymers have been previously reported.[1]

In the field of polymerization of 2-alkyl-substituted diolefins with stereospecific catalysts, we have extended our research to the polymers of 2-*n*-propyl-1,3-butadiene.

It is well known that it is possible to obtain a polymer of butadiene and isoprene with a predominantly 1,4-*cis*,[2–4] 1,4-*trans*,[5] and 1,2 [6,7] (or 3,4) structure by using stereospecific catalysts prepared from aluminum alkyls or aluminum hydrides and different transition metal salts.

Similar behavior, with respect to the various catalysts employed, is shown by 2-*n*-propylbutadiene. It is thus possible to obtain elastic, rubbery polymers with a prevailing 1,4-*cis* structure, amorphous low molecular weight polymers with a 3,4 configuration, and 1,4-*trans* crystalline polymers.

EXPERIMENTAL

Materials

The monomer was prepared by catalytic ethynylation in liquid ammonia of *n*-propyl methyl ketone, followed by selective hydrogenation on Pd/

$CaCO_3$ and dehydration over alumina. The product was distilled through a fractionating column and the portion boiling at 91 to 94 °C. collected. The monomer was 99.5% pure according to chromatographic analysis and was distilled on Na–K alloy at reduced pressure just before use.

$TiCl_4$ was a commercial product used without further purification. $Al(C_2H_5)_3$ was produced by Ethyl Co. (purity about 97%). Aluminum chlorohydride was prepared according to the literature.[8] Reagent-grade benzene and n-heptane were used as solvents; they were purified and distilled over sodium in a nitrogen atmosphere before use.

Polymerization

The polymerizations were carried out in screw-cap bottles as previously described.[1] The catalyst was prepared in the presence of monomer with addition of reagents in the order: solvent, transition metal compound, monomer, and aluminum compound. The polymer was precipitated with methanol–HCl in the presence of an antioxidant and purified by dissolving in benzene and precipitating with methanol.

Polymer Characterization

X-ray diffraction patterns were obtained with a Philips diffractometer equipped with proportional counter.

Infrared spectra of the polymer as carbon disulfide solutions or films obtained by slow evaporation of the solvent were obtained with a Perkin-Elmer 21 spectrometer.

The intrinsic viscosity $[\eta]$ was determined in toluene at 30 °C. in a Ubbelhode suspended-level viscometer.

RESULTS AND DISCUSSION

Some results of our polymerization tests are reported in Table I.

By means of the catalytic system $Al(C_2H_5)_3$–$TiCl_4$ or $AlHCl_2 \cdot O(C_2H_5)_2$–$TiCl_4$ (runs 1 and 2) it is possible to obtain an elastic amorphous polymer whose infrared spectrum, shown in Figure $1A$, is very similar to that of a 1,4-cis-polyisoprene.

As in the cis-polyisoprene, a very strong band at 11.9 μ, due to the C—H out-of-plane vibration,[9] is present. The relative intensity of the CH_2 and CH_3 deformation bands at about 7 μ is in the ratio expected for a higher content of CH_2 with respect to CH_3.

The 8.83 μ band, which we shall discuss later, is attributed to a 1,4-cis configuration. The presence of the vinylidene C—H deformation band at 11.23 μ and of the C=C stretching band at 6.08 μ (the latter partially overlapped by the C=C stretching band of 6.02 μ due to the internal double bond) are evidence of a certain amount of 3,4 configuration.

Further evidences of the 3,4 configuration content are given by the comparison with the spectrum in Figure $1B$ of the poly-2-n-propylbutadiene obtained with the $Al(C_2H_5)_3$–$Ti(O-i-C_3H_7)_4$ catalyst system (runs 5 and 6).

TABLE I

Polymerization of 2-n-Propyl-1,3-Butadiene[a]

No.	Solvent		Catalyst		Cocatalyst		Mole ratio	Temp., °C.	Time, hr.	Yield, g.
	Type	Vol., ml.	Type	Amt., mole $\times 10^3$	Type	Amt., mole $\times 10^3$	$\dfrac{\text{cocatalyst}}{\text{catalyst}}$			
1	Benzene	60	TiCl$_4$	0.455	AlEt$_3$	0.455	1	5	16	2[b]
2	Benzene	30	TiCl$_4$	0.6	AlHCl$_2$·OEt$_2$	0.975	1.6	13	16	4.5
3	n-Heptane	25	VCl$_3$	1.26	AlEt$_3$	4.4	3.5	15	46	1.5
4	n-Heptane	25	VCl$_3$	0.63	AlEt$_3$	2.2	3.5	15	88	1
5	n-Heptane	25	Ti(O-i-C$_3$H$_7$)$_4$	1.2	AlEt$_3$	6.24	5	20	88	3.5
6	n-Heptane	25	Ti(O-i-C$_3$H$_7$)$_4$	0.6	AlEt$_4$	3.12	5	20	88	low

[a] Monomer 10 ml.
[b] $[\eta] = 1.71$.
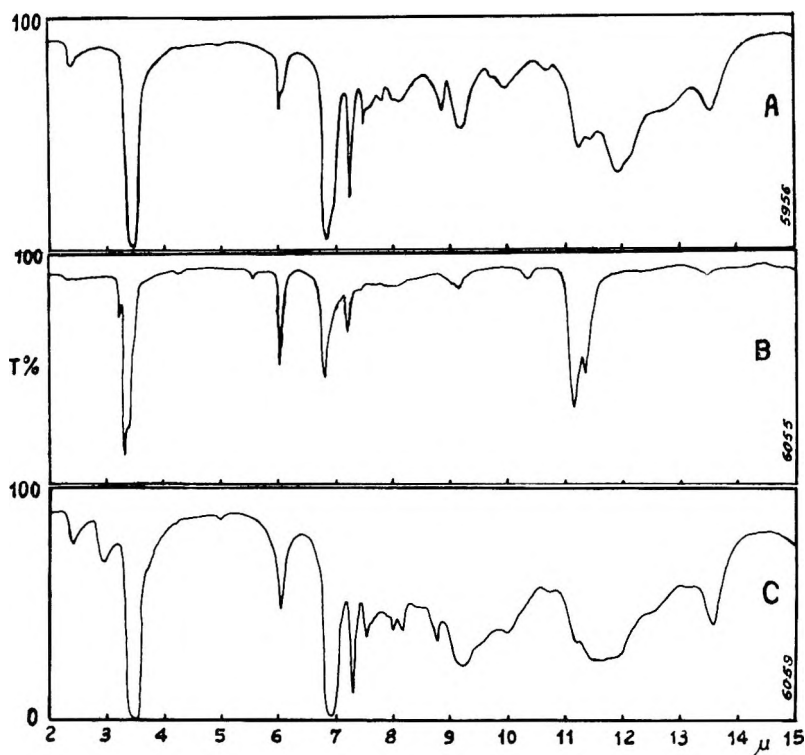
Fig. 1. Infrared spectra of poly-2-*n*-propyl-1,3-butadienes: (*A*) 1,4-*cis*; (*B*) 3,4;
(*C*) 1,4-*trans*.

It should be pointed out that this catalyst system yields polyisoprene essentially in the 3,4 configuration.[10]

In the spectrum of Figure 1*B*, the 3,4 configuration is identified beyond any doubt from the 6.08 and 11.23 μ bands and from the C—H stretching band at 3.25 μ. The assignment of the 11.45 μ band is not equally certain. Saunders and Smith[11] assigned the 11.49 μ band in polyisoprene to a CH_3 wagging, while Binder[9] has classified it as a crystallinity band. On the other hand, if these bands are generated by the same motion, we exclude the crystalline origin of these bands because our polymer is a high viscosity liquid.

Polymerization of 2-*n*-propyl-butadiene with $Al(C_2H_5)$–VCl_3 yielded a solid, crystalline polymer which is very difficult to purify (runs 3 and 4). The infrared spectrum of this polymer is shown in Figure 1*C*. The 8.73 μ band is attributed to a 1,4-*trans* configuration. We find this reasonable if we consider that in polyisoprene the analytical band for the 1,4-*trans* appears at 8.68 μ while for the 1,4-*cis* the same band is seen at 8.85 μ.

Further a band at 8.78 μ has been found in 1,4-*cis*-poly-2-*tert*-butyl-butadiene.[1] On this basis we attribute primarily a 1,4-*trans* configuration to the polymer prepared with $Al(C_2H_5)_3$–VCl_3, as a source of the band at 8.73 μ. On the other hand, the 1,4-*cis* configuration can be assumed for
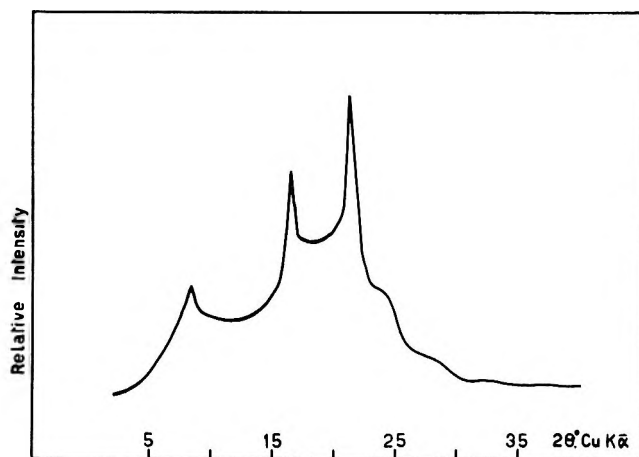
Fig. 2. X-ray diffractometer pattern of the 1,4-*trans* form of the poly-2-*n*-propyl-1,3-butadiene.

the polymer prepared with $AlEt_3$–$TiCl_4$ or $AlHCl_2 \cdot O(C_2H_5)_2$–$TiCl_4$, on the basis of the band at higher wavelength (8.83 μ).

The assignment of the 8.68 and 8.85 μ bands in polyisoprene is doubtful. Saunders and Smith[11] attributed the 8.85 μ band to a CH_2 wagging, Sutherland and Jones[12] to a CH_3 in plane deformation. Binder[9] confirmed that the 8.68 and 8.85 μ bands are due to a C—CH_3 vibration of the $C(CH_3)$=CH group.

The absence of a methyl group directly bonded to an unsaturated carbon in both poly-2-*n*-propylbutadiene and poly-2-*tert*-butylbutadiene led us to think that these bands, if their origin is the same, cannot be related to a CH_3 vibration.

Examination of the *trans* polymer by an x-ray diffraction technique shows that it is partially crystalline. Its diffractometer pattern, shown in Figure 2, presents three sharp reflections. The melting point is about 42°C. The fiber spectrum gives an identity period along the fiber axis of 9.2 ± 0.1 A. The equatorial layer may be interpreted on the basis of a rectangular net with the following axis: $a' = 10.95$ A. and $b' = 6.65$ A. By assuming four monomeric units per unit cell, a density of $d_c = 0.95$ is calculated, in good agreement with the observed density $d_0 = 0.92$.

The experimental value of the identity period is consistent with a chain built up by a succession of two monomeric units, both characterized by a *trans* configuration of the double bond. In fact, all models of 1,4-*cis* polymers of 1,3-butadiene theoretically predicted and experimentally found, have values of the identity period ranging from 8.1 (as the poly-1,4-*cis*-isoprene[13,14] to 8.6 A. (as the poly-1,4-*cis*-butadiene[15]); the only way of lengthening such a period would be improbable alterations of bond length and bond rotational angles.

On the contrary, for the *trans* configuration, two chain models are proposed by Bunn for α and γ gutta-percha[14] with a period very close to that

found for the poly-n-propylbutadiene.   These models may be defined by
internal rotational angles of the single bonds as shown in Table II.

TABLE II

	σ_1	σ_2	n_3	σ_4	σ_5
Model I	120°	240°	180°	240°	120°
Model II	120°	120°	180°	240°	240°

The σ angles are referred to the single bonds as shown in Figure 3: for
instance, σ_2 is the angle between the planes P (2,3,4) and P (3,4,5).   The
identity period is for both models 9.2–9.4 A., depending on the angles near
the double bond (120°–125°).
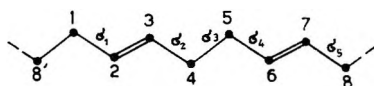
Fig. 3. Segment of a chain of the 1,4-$trans$-polybutadiene stretched in a plane.   In-
ternal rotational angles of the single bonds, σ_i, are indicated for two consecutive mono-
meric units.

In Figure 4 the two possible models of chain for the poly-2-n-propyl-
butadiene are presented;   the side groups being placed in accord with the
principle of the maximum displacement of the single bonds.   The di-
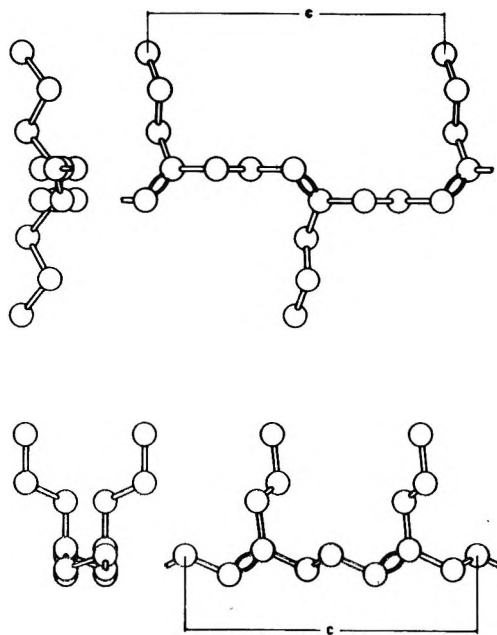
Fig. 4. Chain models for the 1,4-$trans$ poly-n-propyl-1,3-butadiene in agreement with
experimental identity period: (top) model I; (bottom) model II.

mensions of the section of the unit cell indicates that model II is the more probable.

References

1. Marconi, W., A. Mazzei, S. Cucinella and M. Cesari, *J. Polymer Sci.*, **A3**, 123 (1965).

2. Saltman, W. M., W. E. Gibbs, and J. Lal, *J. Am. Chem. Soc.*, **80**, 5615 (1958).

3. Marconi, W., A. Mazzei, S. Cucinella, and M. De Maldé, *Makromol. Chem.*, **71**, 118 (1964); *ibid.*, **71**, 134 (1964).

4. Phillips Petroleum Co., Belgian Pat. 551,851 (Oct. 17, 1956).

5. Natta, G., L. Porri, P. Corradini, and D. Morero, *Chim. Ind. (Milan)*, **40**, 362 (1958).

6. Natta, G., L. Porri, G. Zanini, and A. Palvarini, *Chim. Ind. (Milan)*, **41**, 1163 (1959).

7. Mazzei, A., S. Cucinella, W. Marconi, and M. De Maldé, *Chim. Ind. (Milan)*, **45**, 528 (1963).

8. Wiberg, E., et al., *Rev. Acad. Cienc. Exact. Fis. Quim. Nat. Zaragoza*, **9**, 91 (1954).

9. Binder, J. L., *J. Polymer Sci.*, **A1**, 37 (1963).

10. Montecatini, Belgian Pat. 549,554 (July 14, 1956).

11. Saunders, R. A., and D. C. Smith, *J. Appl. Phys.*, **20**, 953 (1949).

12. Sutherland, G. B. B. M., and A. V. Jones, *Discussions Faraday Soc.*, **9**, 281 (1950).

13. Nyburg, S. C., *Acta Cryst.*, **7**, 385 (1964).

14. Bunn, C. W., *Proc. Roy. Soc. (London)*, **A180**, 40 (1942).

15. Natta, G., and P. Corradini, *Nuovo Cimento Suppl.*, **15**, 111 (1960).

Résumé

On a étudié la polymérisation stéréospécifique du 2-n-propyle-1,3-butadiène avec des alcoyles aluminium ou l'hydrure d'aluminium et différents sels de métaux de transition. Le comportement de ce monomère avec les différents catalyseurs employés est semblable à celui de l'isoprène. Les systèmes AlEt₃–TiCl₄ et AlHCl₂·(C₂H₅)₂O–TiCl₄ donnent des polymères caoutchouteux, dont les spectres infra-rouges révèlent une structure 1,4-*cis*. Au moyen du catalyseur AlEt₃–Ti(*i*C₃H₇O)₄ on obtient un polymère de bas poids moléculaire possédant une structure prédominante 3,4. Le système AlEt₃–VCl₃ donne un polymère cristallin qui fond à 42°C. La période d'identité est déterminée et deux conformations possibles de chaîne sont proposées.

Zusammenfassung

Die stereospezifische Polymerisation von 2-n-Propyl-1,3-butadien mit Aluminium-alkylen oder Aluminiumhydrid in verschiedenen Übergangsmetallsalzen wurde untersucht. Das Verhalten dieses Monomeren ähnelt in bezug auf die verschiedenen verwendeten Katalysatoren demjenigen von Isopren. Mit AlEt₃–TiCl₄ und AlHCl₂·(C₂H₅)₂O–TiCl₄-Systemen werden kautschukartige Polymere erhalten, deren Infrarot-spektren der 1,4-*cis*-Struktur entsprechen. Mit dem AlEt₃–Ti(*i*C₃H₇O₄)-Katalysator wird ein niedrigmolekulares Polymeres mit vorwiegender 3,4-Struktur erhaten. Das AlEt₃–VCl₃-System liefert ein kristallines, bei 42°C. schmelzendes Produkt. Die Identitätsperiode wurde bestimmt, und zwei mögliche Kettenkonformationen werden vorgeschlagen.

Phase Equilibria of Polymer–Solvent Systems at High Pressures Near Their Critical Loci. II. Polyethylene–Ethylene

PAUL EHRLICH,* *Plastics Division Research Laboratory, Monsanto Company, Springfield, Massachusetts*

Synopsis

The system polyethylene–ethylene exhibits the same type of phase behavior as that described earlier for polyethylene–*n*-alkane systems well above the boiling points, or above the critical points of the solvents. In this case, the solvent is always above its critical temperature in the region investigated, and one has here another case of infinite polymer-gas miscibility. The critical locus was determined, from its intersection with the crystallization surface at about 115 to 200°C., and the three-dimensional phase model in (P, T, composition) space is visualized.

Introduction

A new type of polymer–solvent equilibrium occurring in the neighborhood of the critical temperature of the solvent and at high pressures was described recently, and was illustrated with data for polyethylene with *n*-alkane solvents of low molecular weights.[1] At sufficiently high pressures, polymer and solvent showed infinite mutual solubility, even in cases where the solvent was above its critical temperature, and hence a gas. The binary systems therefore exhibited critical points, lying on a fluid–liquid critical locus which encompassed a wide temperature range at a pressure which, in general, varied only slowly. This pressure was termed an upper critical solution pressure (UCSP) and represents what has sometimes been called a plait point.[2]

Polyethylene–ethylene is a system of the same type. It deserves special consideration because of its commercial importance and because it permits extension of the earlier results from paraffinic to olefinic solvents. Here the solvent (ethylene) is above its critical temperature in the entire region of appreciable or infinite mutual solubility. It is therefore legitimate to refer to a gas–liquid critical locus and to infinite miscibility of polymer and gas.[3] Although one is dealing here entirely with vapor–liquid equilibria, the terms "solvent" and "solute" will be retained for ethylene

131

and polyethylene, respectively, to emphasize the analogy with the systems studied earlier[1] and with polymer solutions of the familiar type.

Experimental Method

The equipment and method of experimentation were as described earlier.[1] The work was performed with Fractions 1 and 5 of a high pressure (non-linear) polyethylene also described. They were obtained in the same rough solvent–nonsolvent fractionation. Hence crosslinked, or highly branched, material was eliminated from consideration at the start. Fraction 1, which was allowed to represent the behavior of a high molecular weight Fraction, was the less soluble portion obtained by a refractionation of Fraction 2, used in the earlier study.[1] The intrinsic viscosities of Fractions 1 and 21 were within experimental error, and their phase behavior with ethylene was only marginally different. The whole polymer was a
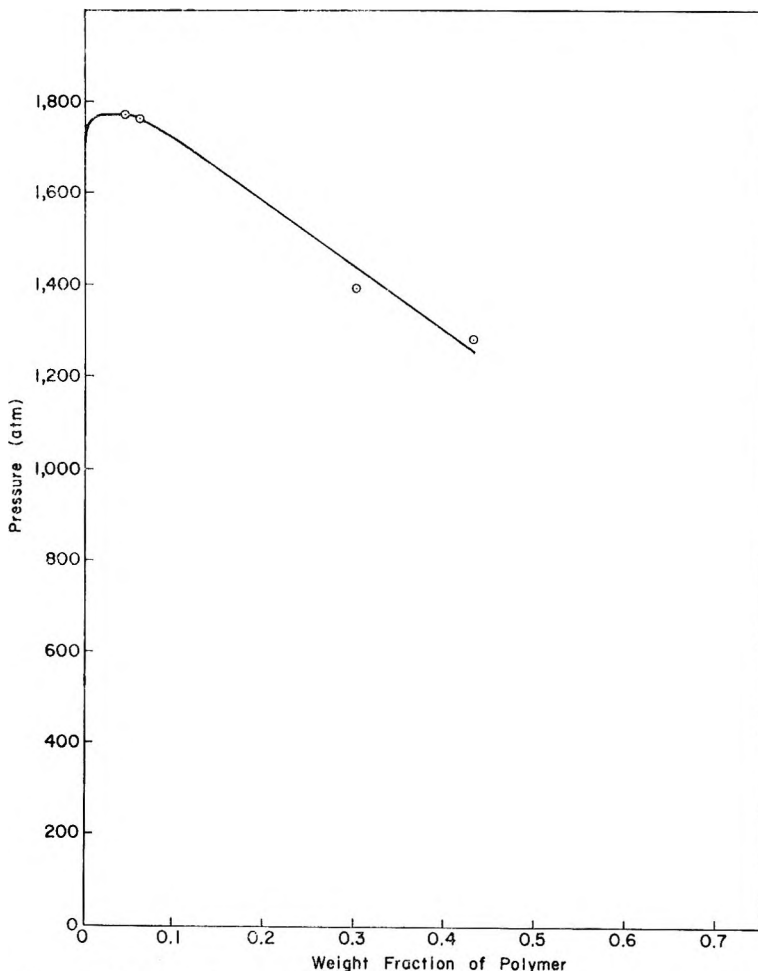
Fig. 1. 130°C. Isotherm for polyethylene with ethylene (whole polymer).

high pressure polyethylene of intrinsic viscosity 0.70 (g./100 cc.)$^{-1}$ and $\bar{M}_v$ 28,000. The linear polyethylene was a high molecular weight fraction of Marlex 50, Type 40, (Phillips Petroleum Company), of intrinsic viscosity 2.3 (g./100 cc.)$^{-1}$ and $\bar{M}_v$ 100,000.

Results and Discussion

Figure 1 shows an isotherm at 130°C. for the whole polymer, showing the upper dew point line and part of the bubble point line with the UCSP of 1760 atm. at their intersection. Although data much below the critical
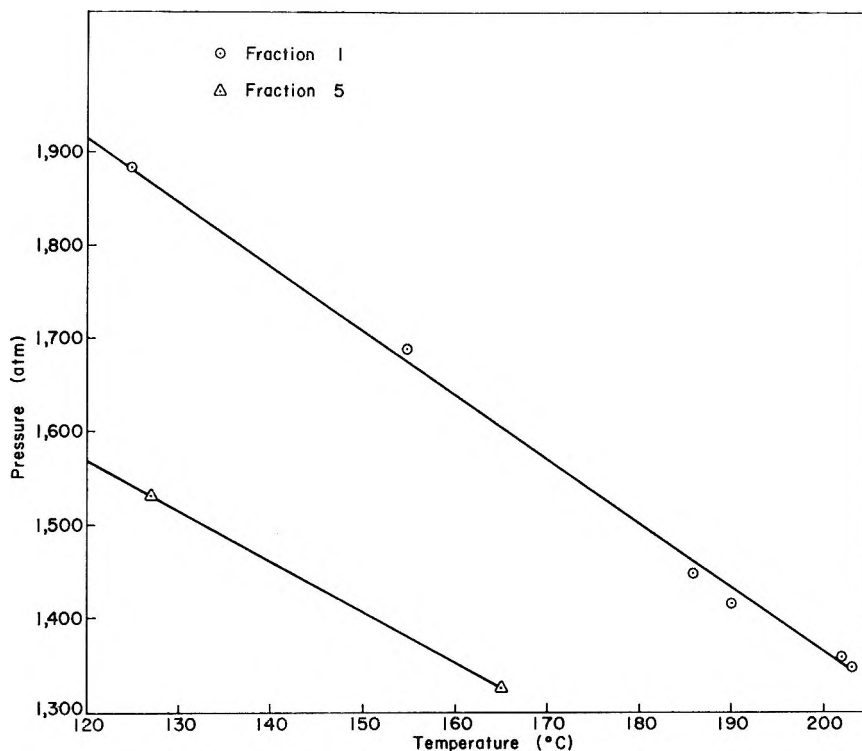
Fig. 2. Critical locus for two polyethylene fractions with ethylene.

polymer concentration (roughly 5 wt.-% polymer) were not taken, the upper dew point curve is known to be nearly flat to extremely low polymer concentrations in the system polyethylene–n-propane, and this is assumed to be true also here. This region is sometimes referred to as one of retrograde condensation of the first kind.[2] Here liquid separates upon reducing the pressure. The highest polymer concentration to which the bubble point line can be traced by means of the method employed is limited by the viscosity of the system. The critical polymer concentration appears to be somewhat higher at 200°C., but this shift could not be demonstrated to exceed the experimental error.
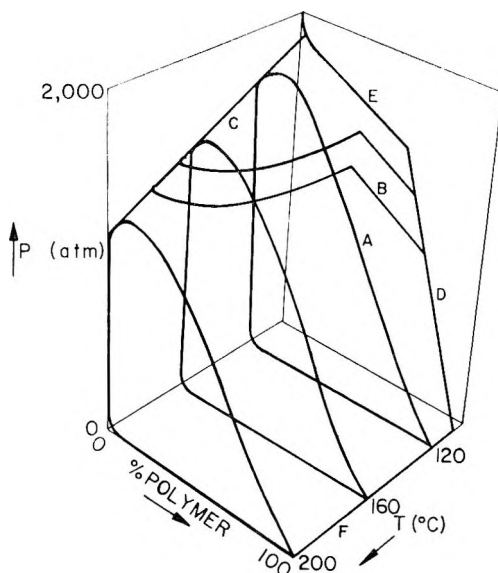
Fig. 3. Three-dimensional (P, T, composition) model for polyethylene–ethylene:
(A) isotherm; (B) isobar; (C) critical locus; (D) melting point of pure polymer as
f(P); (E) melting point as f(diluent); (F) vapor pressure of pure polymer as f(T).

Figure 2 shows the critical locus for Fractions 1 and 5. This is the
projection of all critical points onto the P, T plane. This locus was
determined from its intersection with the crystallization surface (at about
115°C. and 1900 atm. for Fraction 1) to 200°C. The locus therefore does
not end in a lower critical endpoint,[4] and is a straight line with slope
$(dP/dT)_c$ which is negative throughout the entire region, suggesting
positive heats and entropies of mixing.[1] The points for the high molecular
weight fraction of linear polyethylene lie on the locus for Fraction 1, indicat-
ing that the small amount of branching in the high pressure polymer
(1.7%)[1] has no effect on critical liquid–gas mixing. The crystallization
surface is, however, intersected at a higher temperature, reflecting the
higher melting point of linear polyethylene. It had been found with
n-alkane solvents that the highest pressure on the critical locus lies near the
critical temperature of the solvent, thus giving this locus a negative slope
beyond this temperature, and the system polyethylene–ethylene evidently
provides no exception to this rule.*

The approximate magnitude of the UCSP of polyethylene–n-alkane
systems has been rationalized by means of modified lattice and regular
solutions concepts,[1] although it was recognized that the use of lattice
theories is not justified in the region of a fluid–liquid critical locus. Rough
estimates of the UCSP for polyethylene–ethylene can again be made by

---

* Gilchrist has recently reported on the solubility of polyethylene in ethylene under
similar conditions.[5] His data on bubble point pressures near the UCSP at 200°C. agree
closely with the UCSP reported here, and no major discrepancies between any of the
other data cited in the two studies were apparent.

means of the Hildebrand–Scatchard solubility parameter considered as a free energy. The UCSP at 130°C. then occurs at a solubility parameter for ethylene of 6.4 and at a reduced density of 2.3. The former value is somewhat higher than, the latter closely similar to, that for ethane.

Figure 3 represents a schematic diagram of the phase model in three-dimensional (P, T, composition) space between the crystallization surface and 200°C. for the whole polymer. Several isotherms and the critical locus, which is drawn to scale, are shown. The upper dew point curves and the bubble point curves at fairly high solvent concentrations have already been discussed. These are the only regions for which experimental information has been obtained. The lower dew point curves must start at the vapor pressure of the polymer and follow closely the pressure, and then the composition axis. The bubble point curves, which give the solubility of ethylene in the polymer melt, may show a point of inflection. This would appear to follow from an analysis of gas solubility at high pressures based on regular solution theory[6] when combined with Flory–Huggins entropies, and from Lundberg's[7] data of the solubility of gases in polymer melts at high pressures, both of which suggest that at low gas solubility the bubble point line lies below the hypothetical straight line connecting the experimental region with the vapor pressure of the pure polymer. The isobars at pressures less than the maximum on the critical locus are clearly of the same type as those for a crystalline polymer in the presence of a poor solvent,[8] and show an upper critical solution temperature.

It may be in order to re-emphasize the main distinguishing characteristics of a polymer–solvent, liquid–fluid, critical locus. These are its extension over a wide temperature range at a pressure much greater than the critical pressure of the solvent, and the very small shift in critical concentration which remains low over this entire temperature range.

References

1. Ehrlich, P., and J. J. Kurpen, *J. Polymer Sci.*, **A1**, 3217 (1963).

2. Rowlinson, J. S., *Liquids and Liquid Mixtures*, Academic Press, New York, and Butterworths, London, Chaps. 5 and 6.

3. Ehrlich, P., and E. B. Graham, *J. Polymer Sci.*, **45**, 246 (1960).

4. Freeman, P. I., and J. S. Rowlinson, *Polymer*, **1**, 20 (1960).

5. Gilchrist, A., paper presented at Faraday Society Informal Discussion on "Solubility of High Polymers," Battersea College of Technology, London, March 25, 1964.

6. Prausnitz, J. M., *AIChE J.*, **4**, 269 (1958).

7. Lundberg, J. L., M. B. Wilk, and M. J. Huyett, *J. Polymer Sci.*, **57**, 275 (1962).

8. Richards, R. B., *Trans. Faraday Soc.*, **42**, 10 (1946).

Résumé

Le système polyéthlyène–éthylène présente le même type de comportement de phase que celui décrit antérieurement pour les systèmes polyéthyléne–*n*-alklane au-dessus des point d'ébullition ou au-dessus des points critiques des solvants. Dans ce cas-ci, le

solvant est toujours au-desus de sa température critique dans la région étudiée et on est en présence ici d'un autre cas de miscibilité infinie polymère-gaz.   Le point critique a été déterminé à partir de son intersection avec la surface de cristallisation à des températures de 115°C à 200°C, et on a représenté la modèle de phase dans un système à 3 dimensions (P, T, composition).

Zusammenfassung

Das System Polyäthylen–Athylen zeigt den gleichen Typ von Phasenverhalten, wie er früher für Polyäthylen–n-Alkansysteme weit oberhalb des Siedepunktes oder oberhalb des kritischen Punktes der Lösungsmittel beschrieben wurde.   Im vorliegenden Fall befindet sich das Lösungsmittel im untersuchten Bereich immer oberhalb seiner kritischen Temperatur, und es besteht hier ein weiterer Fall von unbegrenzter Polymer-Gasmischbarkeit. Der kritische Ort wurde aus seinem Schnitt mit der Kristallisationsoberfläche bei etwa 115°C. bis 200°C. bestimmt und das dreidimensionale Phasenmodell im (P, T, Zusammensetzungs)-Raum dargestellt.

Experiments with a Synthetic Polyampholyte

J. P. ALLISON* and C. S. MARVEL, *Department of Chemistry, University of Arizona, Tucson, Arizona*

Synopsis

The synthesis of the polyampholyte of regular structure first devised by Marvel and DeTommaso has been improved. Viscometric studies have given some evidence of contractile properties. Low molecular weight of the polyampholyte has prevented the formation of strong fibers.

SYNTHETIC STUDIES

In attempting to repeat the synthesis of the regular polyampholyte of structure I which was described by Marvel

$$+S—S+CH_2+_3CH+CH_2+_2CH+CH_2+_3+_n$$

$$\overset{|}{NH_2} \qquad \overset{|}{CO_2H}$$

$$I$$
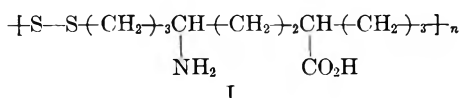
and DeTommaso,[1] some difficulty was encountered in converting the ethyl hydrogen 2,5-diallyladipate to the corresponding urethan ester. Originally this was accomplished via the acid chloride, amide, and Hofmann reaction.[2] In the present work the Curtius reaction was used on the acid chloride ester (II) and the yield of 4-carbethoxy-7-aminocarboethoxydeca-1,9-diene (III) was 85% of the theory. This intermediate was converted

$$CH_2=CH—CH_2—CH—(CH_2)_2—CH—CH_2—CH=CH_2 \xrightarrow[\text{C}_2\text{H}_5\text{OH}]{\text{NaN}_3}$$

$$\overset{|}{COCl} \qquad \overset{|}{CO_2C_2H_5}$$

$$II$$

$$CH_2=CH—CH_2—CH—(CH_2)_2—CH—CH_2—CH=CH_2$$

$$\overset{|}{NHCO_2C_2H_5} \quad \overset{|}{CO_2C_2H_5}$$

$$III$$
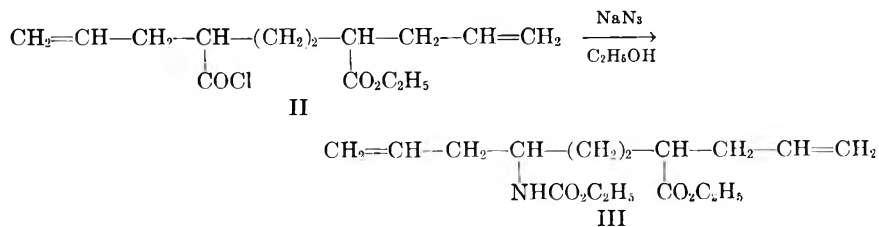
to 3,6-bis-(3-mercaptopropyl)-piperid-2-one as previously described.[1] Better results were obtained in the purification of the dimercaptan via the lead salt when this salt was decomposed with hydrogen sulfide in cold ether (0°C.) containing 20% of ethanol.

The polymerization to the polydisulfide was carried out essentially as before, except that oxygen was introduced to the reaction flask through a sintered glass disk set in the base of a round-bottomed flask, and vigorous stirring was maintained during the oxidation step. The polymers were isolated by pouring the oxidation mixture into an equivolume mixture of methanol and water and then reprecipitating from an equivolume mixture of chloroform and acetic acid by pouring into cold methanol in a Waring Blendor.

Hydrolyzing the piperidone to give the amino acid salt has been successful when carried out with hydrochloric acid dissolved in formic or acetic acid. The polyampholyte was recovered from the salt by dissolving the salt in water and adjusting the pH to about 3.5 at which point the solution became turbid. Adding more alkali resulted in precipitation of a pale brown coagulated lump of rubbery polyampholyte. After washing out all of the inorganic salts and drying this became a hard brown material. It was insoluble in dimethyl sulfoxide, dimethylformamide, dimethylacetamide, acetylacetone, dimethylaminoethanol, benzene, chlorobenzene, pyridine, quinoline, methylorthoformate, diglyme, N-methylpyrrolidone, 1,1,2,2-tetrachloroethane, isopropanol, acetone, phenol, dioxane, tetrahydrofuran, and water. It did dissolve in aqueous alkali or acid except in the pH range of 3.5–10.5.

It was also found that dialysis of a dilute water solution of the salt would yield a coagulated polyampholyte which could be freeze-dried to give good yields of product.

EXPERIMENTAL

4-Carboethoxy-7-aminocarbethoxydeca-1,9-diene

Ethyl 2,5-diallyladipoyl chloride (106.2 g., 0.39 mole) was dissolved in dry acetone (1 liter) and the solution cooled to 0°C. Sodium azide (Eastman Organic Chemicals, practical grade) (28.0 g., 0.43 mole) was dissolved in hot water (80 ml.) and added immediately to the cold acetone solution. After being shaken vigorously for 30 min., the turbid liquid containing precipitated sodium chloride was poured into ice cold water (5 liters). The azide which separated as an oil was extracted with benzene (3 × 200 ml.). After drying over anhydrous calcium chloride, it was filtered into a 1-liter, round-bottomed flask containing anhydrous ethanol (120 ml.). Very gentle heat was applied until the evolution of nitrogen had almost stopped; then the mixture was refluxed for 1 hr. The product was recovered by fractional distillation under reduced pressure. The yield was 98.4 g. (0.33 mole, 85% theoretical), b.p. 129°C./0.4 mm. Hg.

3,6-Bis(3-mercaptopropyl)piperidone

The ethyl ester was converted to the piperidone and this in turn to 3,6-bis(3-mercaptopropyl)piperidone diacetate as described before.[1] Hydrol-

ysis of the acetate was carried out as before but the purification through the lead salt was improved by adding a small amount of ethanol to the ether used to suspend the lead salt.

Polymerizations

Polymerizations were carried out in vigorously stirred suspension at 60°C. by bubbling in a rapid current of oxygen for 9–19 days. The charges, conditions and yields, and viscosities are reported in Table I.

TABLE I
Oxidative Polymerization of 3,6-Bis(3-mercaptopropyl)piperidone

Polymer no.	Dimercaptan, g.	Potassium laurate, g.	Potassium hydroxide, g.	Selenium dioxide, mg.	Water, ml.	Time, days	Yield, g.	η_{inh} (30°C.)[a]
1	5.0	2.24	4.46	28	100	9	—	0.10
2	10.0	4.5	9.0	40	130	9	2.3	0.25
3	3.2	1.43	2.86	25	40	10	3.4[b]	0.46
4	8.0	3.6	7.2	25	100	13	5.9	0.88
5	11.9[c]	9.0	17.4	40	250	18	2.85	0.965

[a] Determined in a mixture of equal volumes of acetic acid and chloroform as solvent.

[b] Contained some selenium dioxide which was removed before viscosity was determined on remainder of polymer.

[c] Monomer purity was not 100%.

Hydrolysis of Piperidone Derivative to Polyampholyte Hydrochloride

No. 3i. Polymer 3 (1.0 g.) was dissolved in equivolume formic acid–chloroform (40 ml.). After the apparatus was flushed with nitrogen, concentrated hydrochloric acid (40 ml.) was added, which resulted in polymer precipitation. The mixture was maintained at 85°C. for 45 hr. About half the polymer had redissolved by this time to give a yellow solution. Formic acid (10 ml.) and hydrochloric acid (15 ml.) were added and the mixture maintained at 90°C. for a further 24 hr. The cold, murky solution was filtered and the filtrate evaporated to dryness. An aqueous solution of the residue was boiled with decolorizing charcoal prior to filtration and freeze-drying. Polyampholyte hydrochloride was recovered as a shiny, black-green solid. The yield was 0.73 g. (73% of theory). Inherent viscosity was 0.026 (0.0749 g. in 25 ml. of water).*

No. 3ii. Polymer 3 (1.0 g.) was suspended in anhydrous formic acid (30 ml.). After the flask was flushed with nitrogen, hydrochloric acid (50 ml.) was added and the mixture heated at 100°C. for 24 hr. The salt was recovered in the usual manner. The yield was 0.76 g. (76% of theory). Inherent viscosity was 0.11 (0.0698 g. in 25 ml. water).

* $\eta_{inh}^{30°C.} = 2.303 \log (t_2/t_1)/c$.

No. 4i.   Polymer 4 (1.0 g.) was suspended in a mixture of anhydrous formic acid (20 ml.) and concentrated hydrochloric acid (50 ml.).   A few crystals of an antioxidant (du Pont No. 29) were added.   After the apparatus was flushed with nitrogen, the mixture was heated at 105°C. for 30 hr.   The polymer coagulated and assumed a pale brown color. As it dissolved the solution became yellow.   Formic acid (15 ml.) was added after 20 hr. to immerse polymer which had coagulated on the flask surface above the liquid level.

The yellow solution was evaporated to dryness in a stream of nitrogen and redissolved in distilled water.   The brown solution was freeze-dried. A pale brown solid was the result.

The yield was 0.65 g. (65% of theory), $\eta_{inh}(H_2O)$, = 0.13 (9) (0.081 g./25 ml.).

No. 4iii.   Polymer 4 (1.0 g.) was suspended in a mixture of anhydrous formic acid (20 ml.) and concentrated hydrochloric acid (50 ml.).   A few crystals of an antioxidant (du Pont No. 29) were added, and the apparatus was flushed with nitrogen prior to heating at 105°C. for 30 hr. in a current of nitrogen.   An addition of formic acid (10 ml.) was made after 20 hr. heating.

On diluting the solution with water, a brown polymer separated.   The solution was evaporated to dryness.   The brown polymer dissolved on heating.

The yield was 0.73 g. (73% of theory), $\eta_{inh(H_2O)}$ = 0.48 (7) (0.076 g./25 ml.).

It was noticed, as in previous instances, that a very dilute aqueous solution of polyampholyte hydrochloride exhibited marked turbidity.

No. 4iv.   Polymer 4 (1.0 g.) suspended in concentrated formic acid (20 ml.) and concentrated hydrochloric acid (50 ml.) after flushing with nitrogen and addition of a trace of antioxidant (du Pont No. 29), the mixture was heated at 105°C. for 44 hr.   After evaporating to dryness, the residue was dissolved in water and the green, fluorescing solution freeze-dried.

The yield was 0.68 g. (68% of theory), $\eta_{inh(H_2O)}$ = 0.16 (1) (0.065 g./25 ml.).

No. 4v.   Polymer 4 (1.0 g.) was dissolved in hot formic acid (25 ml.) in the presence of an antioxidant (du Pont No. 29) and in a stream of nitrogen.   Concentrated hydrochloric acid (50 ml.) was then added to the cold solution and the mixture heated at 105°C. for 30 hr.   The solution was evaporated to dryness, the residue dissolved in distilled water and the solution freeze-dried.

The yield was 0.67 g. (67% of theory), $\eta_{inh(H_2O)}$ = 0.64 (4) (0.071 g./25 ml.).

Preparation of Free Polyampholyte

A typical isolation of the free amino acid from the hydrochloride is the following.

Polyampholyte hydrochloride 3ii (0.639 g.) was dissolved in distilled water and treated with $0.441M$ potassium hydroxide solution 0.00227 mole). The mixture was allowed to stand overnight. The mixture was freeze-dried and partial powdered and the residue was treated 3 times with distilled water before a final drying *in vacuo*. The yield of free amino acid was 0.487 g. (88% of theory). In similar experiments 0.417 g. of polyampholyte hydrochloride 4iii gave 0.3 g. of free amino acid.

Copolymerization of 3,6-Bis(3-mercaptopropyl)piperid-2-one and *n*-Hexane 1,6-dithiol

The apparatus for oxidation-emulsion polymerization first described by Marvel, Bonsignore, and Banerjee[3] was modified for this preparation. A slow stream of oxygen was admitted to the polymerization mixture through a sintered glass disc set in the base of a 1-liter, round-bottomed flask equipped with a condenser, mechanical stirrer, and thermometer. The apparatus was heated by immersion in an oil bath.

3,6-Bis(3-mercaptopropyl)piperid-2-one (6.8 g., 0.028 mole) and freshly distilled *n*-hexane-1,6-dithiol (Aldrich Chemical Co.) (5.8 g., 0.039 mole) were stirred into a solution of potassium laurate (5.65 g.) and potassium hydroxide (11.3 g.) in distilled water (158 ml.). Selenium dioxide (0.1 g.) was added as a catalyst. Oxygen was bubbled through the hot (75°C.), vigorously stirred mixture at the rate of 80 bubbles/min. The duration of the polymerization was 14 days. Dow Corning Antifoam A was added periodically. Almost all the polymer had coagulated by this time. After precipitation into acidified (HCl), aqueous methanol (50:50) and filtration, the polymer was dissolved in chloroform–acetic acid containing an excess of the former, and reprecipitated into 80% aqueous methanol using a Waring Blendor. The polymer which coagulated into a single lump of rubbery solid, was washed with methanol and dried *in vacuo*.

The yield was 6.1 g. (48% of theory); $\eta_{inh} = 0.69$ (chloroform–acetic acid, 50-15 by volume). Anal.: N, found 1.94%; this corresponds to a mole fraction of 0.24 for the piperidone unit.

The infrared spectrum of the copolymer showed absorption bands characteristic of the piperidone unit.

POLYMER PROPERTIES

Discussion

This particular polyampholyte was chosen for synthesis since it was felt that the principal interaction between the acidic and basic group would occur between the pairs in a chain rather than between chains (Fig. 1). If the chains are fully extended the maximum contraction that could occur with the formation of an induced salt would be approximately 7%.

Viscometric Studies

The viscosities of the initial polymers were measured in equivolume mixtures of glacial acetic acid and chloroform by means of a Cannon-Fenske viscometer at 30°C. The maximum inherent viscosity recorded was 0.88. The viscosities of samples of polyampholyte hydrochloride were determined in water, formic acid, and methanesulfonic acid. The maximum inherent viscosity here was 0.64, but values varied over a wide range, even for compounds prepared from the same sample of the original polymer.
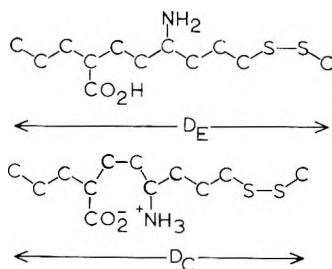
Figure 1.

A graph of (η_{sp}/C) against C gives divergent results for the three solvents (see Fig. 2). The behavior in methanesulfonic acid is reminiscent of that of polyelectrolytes.

Viscosity readings were taken at different pH values. The insolubility of polyampholyte in water in the pH range of 3–10.5 curtailed this approach, and the measurements did not show significant changes.
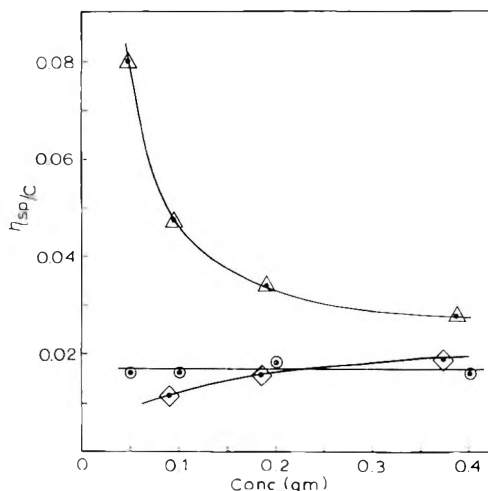
Fig. 2. Effect of various solvents on the viscosity of polyampholyte hydrochloride: ($\triangle$) methanesulfonic acid; ($\diamondsuit$) water; ($\odot$) formic acid.

Infrared Spectra

Infrared spectra were taken in a variety of media, smears in chloroform of the initial polymer being quite satisfactory. However, the general insolubility in organic solvents of the polyampholyte necessitated the employment of potassium bromide in disk form.

The spectra of the compounds investigated show in the main only qualitative differences, i.e., depressed amine or carboxyl absorption depending upon the nature of the salt. A comparison of the spectra of polyampholyte and initial polymer shows two distinct compounds. The carbonyl absorption at 1670 cm.$^{-1}$ in the latter is diminished in intensity and shifted to 1640 cm.$^{-1}$ in the former. Amine absorption at 1400–1500 cm.$^{-1}$ for the polylactam was also shifted slightly to a lower frequency in the instances of polyampholyte.

Contractile Properties in Linear Polyampholytes

To demonstrate that mechanical energy might be attained by the effect of pH on the polymer, it was necessary first to fabricate the polyampholyte into a suitable form such as a fiber. The fabrication of satisfactory fibers is dependent largely upon the molecular weight of the polymer, and the samples of polyampholyte prepared so far have been quite unsuitable for this purpose. Precipitation of an aqueous solution of polyampholyte hydrochloride into a concentrated solution of sodium acetate seemed to offer a possible method of fiber production, but the dry material was extremely brittle.

After acid hydrolysis of a sample of the initial polymer, a thin film of partially hydrolyzed material remained stretched across the interior of the flask. After decanting away the solution containing polyampholyte hydrochloride washing out the flask with water produced an immediate contraction in this diaphragm, presumably due to hydrolysis of the amine hydrochloride and subsequent interaction of the amine and carboxyl functions.

Some fibers of pre-polyampholyte were prepared from a sample of copolymer of 3,6-bis(3-mercaptopropyl)piperid-2-one and n-hexane-1,6-dithiol, $\eta_{inh} = 0.69$. The lactam functions were to be destroyed by cold, concentrated hydrochloric acid. Unfortunately, the fibers were too fragile for tests.

Since a fiber could not be obtained, it was decided to perform an experiment which might magnify this effect. A solution of homopolymer in 1,1,2,2-tetrachloroethane was allowed to evaporate slowly on a mercury surface. This resulted in a rather brittle film. Another rather poor sample of polymer was cast into a plate using heat treatment. Both specimens were imbedded in blocks of paraffin wax so that only one surface was exposed to acid hydrolysis. These were then immersed in concentrated hydrochloric acid at room temperature for 30 days. The by now soft and flexible specimens were removed from their wax frames and immersed in

distilled water. The hydrolyzed surface of each polymer whitened within 1 min., indicating some change in character, and a concavity formed simultaneously due to the attractive forces between the amine and carboxyl groups produced by this process. Another sample of polymer confirmed this first observation. Reversal of the effect by adding acid or alkali was not tried.

This experiment illustrates a combination of intramolecular and intermolecular forces. A total separation of the two effects seems unlikely.

References

1. Marvel, C. S., and G. L. DeTommaso, *J. Org. Chem.*, **25**, 2207 (1960).
2. Marvel, C. S., and W. W. Moyer, Jr., *J. Am. Chem. Soc.*, **79**, 4990 (1957).
3. Marvel, C. S., P. V. Bonsignore, and S. Banerjee, *J. Org. Chem.*, **25**, 237 (1960).

Résumé

La synthèse du polyampholyte de structure régulière, trouvé pour la première fois par Marvel et DeTommaso, a été perfectionnée. Des études viscosimétriques ont mis en évidence les propriétés de contraction. Le faible poids moléculaire du polyampholyte a empêché la formation de fibres résistantes.

Zusammenfassung

Die zuerst von Marvel und DeTommaso angegebene Synthese eines Polyampholyten mit regulärer Struktur wurde verbessert. Viskosimetrische Untersucungen lieferten einige Hinweise auf kontraktive Eigenschaften. Das niedrige Molekulargewicht des Polyampholyten verhinderte die Bildung fester Fasern.

Polymerization of N-Methyl-β-Propiolactam with Ionic Catalysts

TSUTOMU KAGIYA, HIROSHI KISHIMOTO, SHIZUO NARISAWA, and KENICHI FUKUI, *Faculty of Engineering, Kyoto University, Kyoto, Japan*

Synopsis

The polymerization of N-methyl-β-propiolactam with various ionic catalysts in bulk was carried out at 140–190°C. Organic compounds containing a carboxyl group have a high catalytic activity for the polymerization and gave crystalline polymer melting at 180–225°C. No polymer of N-methyl-β-propiolactam was formed at 140°C., but the polymerization of N-methylacrylamide took place. The polymer of N-methylacrylamide was amorphous and its infrared spectrum was quite different from that of poly-N-methyl-β-propiolactam. The infrared spectrum of poly-N-methyl-β-propiolactam showed a major absorption peak characteristic of a polyamide structure. On the basis of the infrared spectrum of an equimolar mixture of monomer and catalyst heated at 130°C., a mechanism was proposed.

INTRODUCTION

In recent years, it has been found that the polymer of β-alanine[1–4] can be obtained either by the hydrogen migration polymerization of acrylamide or by the polymerization of 2-azetidinone (β-propiolactam) with various kinds of alkali catalysts.[5] Hall[6] proposed a mechanism for the polymerization of various lactams with alkali catalysts, and suggested that the polymerization of N-alkyl lactams did not take place by the use of alkali catalysts.

In this paper, the polymerization of N-methyl-β-propiolactam with various kinds of cationic and anionic catalysts was studied. The result added some new experimental facts to the mechanism for lactam polymerizations with ionic catalysts and to some physical properties of the polymer obtained.

EXPERIMENTAL

The method for preparing N-methyl-β-propiolactam was essentially the same as that described by Holley.[7] The monomer (b.p. 68.8–68.9°C./18 mm. Hg; n_D^{25} 1.4529) was obtained according to eq. (1) in very low yield (5.43%).

$$CH_3NHCH_2CH_2CO_2C_2H_5 \xrightarrow{C_2H_5MgBr} CH_3NCH_2CH_2CO_2C_2H_5$$

$$\underset{MgBr}{\big|}$$

$$\xrightarrow{H_2O} \begin{array}{c} CH_2\!\!-\!\!C\!\!=\!\!O \\ | \qquad | \\ CH_2\!\!-\!\!N\!\!-\!\!CH_3 \end{array} \quad (1)$$
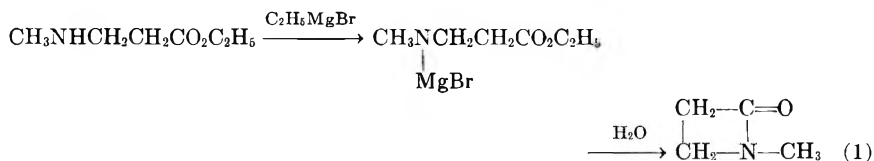
As is shown in Figure 1, the infrared spectrum of the monomer displayed a major absorption peak at 1732 cm.$^{-1}$ which is assigned to the carbonyl band of lactam.
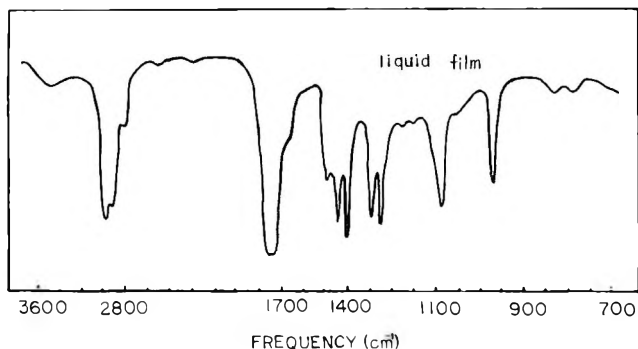
Fig. 1. Infrared spectrum of N-methyl-β-propiolactam.

A 0.5–0.6 g. portion of the monomer and a definite amount of catalyst (5 wt.-% based on monomer) were placed into a glass ampule (6 ml.) in nitrogen, and the reaction vessel was heated to the reaction temperature. After 4–30 hr., the polymer produced was isolated from the mixture, washed with acetone and dried *in vacuo* at 50°C. The viscosity of the polymer was determined at 35°C. in 98% sulfuric acid in an Ostwald viscometer. The melting point of polymer was visually determined in the air in an electric heater. X-ray diffractions were obtained with a powder camera in a Rigakudenki x-ray diffraction apparatus (Model D-3F) by the use of standard techniques. The infrared spectra were determined with a Nippon Bunko Ltd. (Model DS-301) spectrophotometer on KBr pellets.

RESULTS AND DISCUSSION

Polymerization of N-Methyl-β-Propiolactam with Various Ionic Catalysts

Table I gives the polymer yield at the temperatures of 190°C. and 140°C. in the absence of catalyst, and at 140°C. with various catalysts. The polymer yield was very low at 140°C., and but a small amount of polymer was obtained even at 190°C. in the absence of catalyst, while a considerable amount of polymer was formed at 140°C. in the presence of benzoic acid, N-methyl-β-alanine, or β-alanine as catalysts.

These results indicate that organic compounds containing a carboxyl group had a catalytic activity for the polymerization of N-methyl-β-

TABLE I

Bulk Polymerization of *N*-Methyl-β-Propiolactam with Various Ionic Catalysts

Catalyst[a]	Temp., °C.	Reaction time, hr.	Polymer yield, wt.-%	Intrinsic viscosity	M.p., °C.
None	190	4	30.8	0.055	199–202
None	140	4	0	—	—
None	140	30	1.42	—	224.5
HCl	140	16	17.0	0.119	198–202
H_2O	140	30	1.82	—	223–224
C_6H_5COOH	140	5.5	48.0	0.341	207
C_6H_5COOH	140	9.0	85.2	0.134	210
$H_2NCH_2CH_2COOH$	140	13	50.1	0.130	197.5
$CH_3NHCH_2CH_2COOH$	140	7	49.7	0.084	203
Betain	140	30	4.16	—	>235
$CH_3NHCH_2CH_2COOC_2H_5$	140	32	1.36	—	221–222
$C_6H_5NHCH_3$	140	31	1.93	—	225
$(C_2H_5)_2NH$	140	30	1.80	—	218
$C_6H_5COOH-(C_2H_5)_2NH$[b]	140	4	27.9	0.133	234

[a] The amount of catalyst employed was 5 wt.-% based on monomer.

[b] Equimolar mixture of benzoic acid and diethylamine.

propiolactam. β-Alanine and *N*-methyl-β-alanine having two functional groups, that is, amino and carboxyl, also had catalytic activity for the polymerization. In order to elucidate the role of carboxyl and amino groups in the catalytic action, ethyl β-methylaminopropionate, diethyl-amine and monomethylaniline were tested, but no polymer was obtained. Hence, it is not the amino group but the carboxyl group that is actually effective for the polymerization.

Physical Properties of the Polymer

As is shown in Figure 2, the infrared spectrum of poly-*N*-methyl-β-propiolactam showed a characteristic absorption peak attributed to the tertiary amide group at 1630 cm.$^{-1}$. The infrared spectra of the two poly-
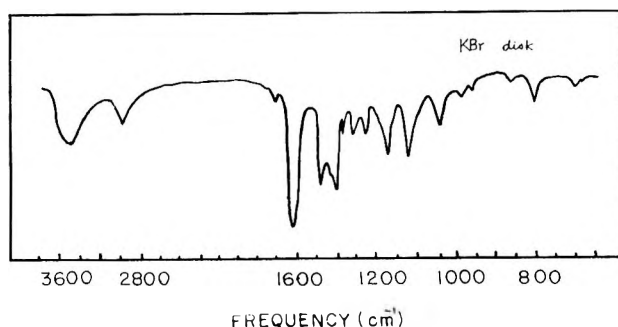
Fig. 2. Infrared spectrum of poly-*N*-methyl-β-propiolactam obtained with benzoic acid catalyst.
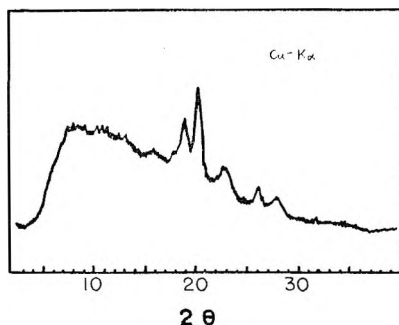
Fig. 3. X-ray diagram of poly-N-methyl-β-propiolactam obtained with benzoic acid catalyst.

mers which were obtained in the presence of benzoic acid and in the absence of catalyst were identical.

The x-ray diagram of poly-N-methyl-β-propiolactam obtained with benzoic acid catalyst is shown in Figure 3. From this, it is clear that the poly-N-methyl-β-propiolactam formed is crystalline.

This polymer melts at 198–225°C. in air and was soluble in hot water and in glacial acetic acid and partially soluble in methanol; the polymer obtained in the absence of catalyst was soluble in methanol.

Polymerization of N-Methylacrylamide

In order to study the possibility of hydrogen migration polymerization of N-methyl-β-propiolactam through N-methylacrylamide structure, [eq. (2)] the polymerization of

$$\begin{array}{c} CH_2\!-\!C\!=\!O \\ |\qquad | \\ CH_2\!-\!N\!-\!CH_3 \end{array} \rightarrow CH_2\!\!=\!\!CHCONHCH_3 \rightarrow -(CH_2CH)_n\!- \\ \underset{\underset{NHCH_3}{|}}{\overset{|}{CO}}$$

(2)
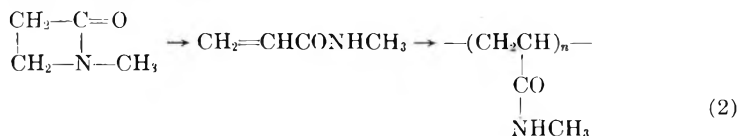
N-methylacrylamide and the comparison of the polymer structure with that of the poly-N-methyl-β-propiolactam were carried out.

As shown in Table II, N-methylacrylamide was polymerized at 140°C., at which no polymer of N-methyl-β-propiolactam was obtained in the absence of catalyst. Figure 4 shows the infrared spectrum of poly-N-methylacrylamide, which displays the characteristic absorption peaks

TABLE II
Bulk Polymerization of N-Methylacrylamide in the Absence of Catalyst

Temp., °C.	Reaction time, hr.	Polymer yield, wt.-%	Intrinsic viscosity	M.p., °C.
190	4	43.9	0.308	262–270
140	4	11.6	—	286–288
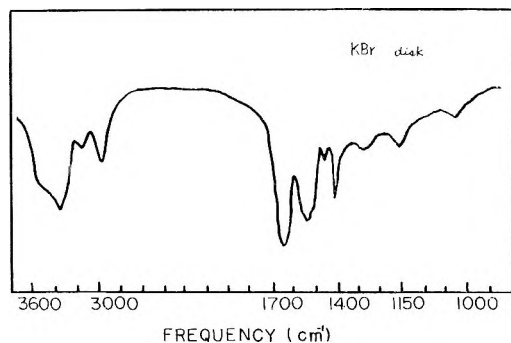
Fig. 4. Infrared spectrum of poly-N-methylacrylamide.

at 1655 and 1560 cm.$^{-1}$ attributable to secondary amide group. This is a feature which is quite different from the spectrum of poly-N-methyl-β-propiolactam indicated in Figure 2.

The x-ray diagram of the polymer of N-methylacrylamide shows that it is amorphous and different in structure from poly-N-methyl-β-propiolactam. The polymer of N-methylacrylamide was soluble in dimethylformamide, while the polymer of N-methyl-β-propiolactam was insoluble. The melting point of the former was higher than that of the latter.

Mechanism of the Polymerization of N-Methyl-β-Propiolactam

One of the possible mechanisms of polymerization may be as shown in eq. (3).

$$\begin{array}{c} CH_2\text{---}C\text{=}O \\ | \quad\quad | \\ CH_2\text{---}N\text{---}CH_3 \end{array} \rightarrow CH_2\text{=}CHCONHCH_3 \rightarrow \text{---}(CH_2CH_2CO\overset{\displaystyle CH_3}{\overset{|}{N}})_n\text{---} \qquad (3)$$
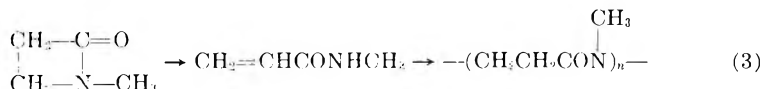
It is clear, however, that this mechanism based on hydrogen migration is in conflict with the above experimental results. Another mechanism may be proposed, in which the monomer is first hydrolyzed and the resulting amino acid condenses in the manner shown in eqs. (4) and (5).

$$\begin{array}{c} CH_2\text{---}C\text{---}O \\ | \quad\quad | \\ CH_2\text{---}N\text{---}CH_3 \end{array} \xrightarrow{\;\;H_2O\;\;} HOOCCH_2CH_2NHCH_3 \qquad (4)$$

$$n(HOOCCH_2CH_2NHCH_3) \rightarrow \text{---}(\overset{\displaystyle O}{\overset{\|}{C}}CH_2CH_2\overset{\displaystyle CH_3}{\overset{|}{N}})_n\text{---} + n\;H_2O \qquad (5)$$

Since no polymer was obtained when N-methyl-β-alanine was heated at 190°C. for 4 hr., at which a considerable amount of polymer was obtained from N-methyl-β-propiolactam, the condensation mechanism is also not agreeable.

The infrared spectrum of an equimolar mixture of N-methyl-β-propiolactam and benzoic acid heated at 130°C. is shown in Figure 5. The spectra showed major absorption peaks at 1610 and 1410 cm.$^{-1}$, which are
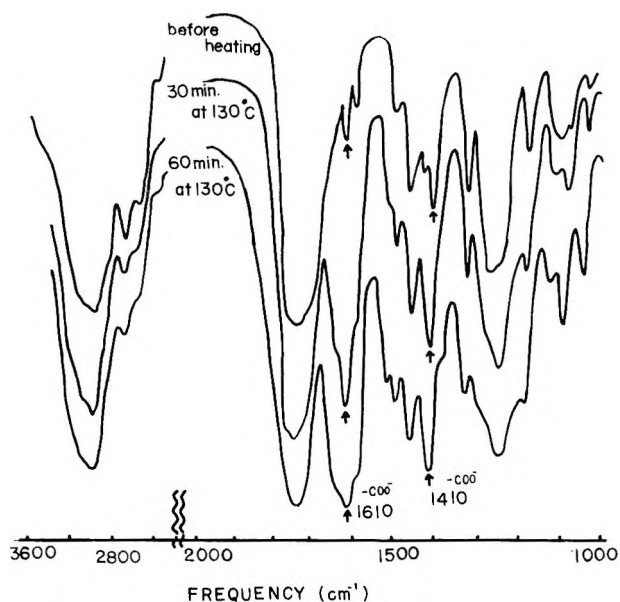
Fig. 5. Infrared spectrum of an equimolar mixture of N-methyl-β-propiolactam and benzoic acid heated at 130°C.

characteristic bands assigned to carboxylate anion.   It was found that the intensity of these absorption peaks increased rapidly with the time of heating.   These results demonstrate that a carboxylate anion has been formed as an intermediate.   Hydrolysis of N-alkyl-β-propiolactams with aqueous alkali or acid yields β-alanine, as has been reported by Holley.[7] The evidence thus reported supports the suggestion that the N-methyl-β-propiolactam is hydrolyzed with a trace of water in the presence of carboxylic acid catalysts.   Since no absorption peak in the range of anhydride band was observed, as shown in Figure 5, the structure of the polymer end may be carboxylic acid.

According to these results, a mechanism for the polymerization of N-methyl-β-propiolactam may be proposed as shown in eqs. (6)–(9):

Initiation:

$$R\!-\!\underset{\underset{O}{\|}}{C}\!-\!OH \;+\; \underset{\underset{CH_2\!-\!N\!-\!CH_3}{|}}{\overset{CH_2\!-\!C\!=\!O}{|}} \;+\; H_2O \;\rightarrow\; \underset{\underset{\underset{CH_3}{|}}{\overset{\oplus}{N}H_2}}{\overset{\overset{O}{\|}}{\underset{\overset{|}{CH_2}}{\overset{CH_2\!-\!C\!-\!OH}{}}}} \;\; \overset{\ominus}{O}\!-\!\underset{\underset{O}{\|}}{C}\!-\!R \tag{6}$$

Propagation:

$$\underset{H\;\;H}{\overset{\overset{CH_3}{\overset{|}{\underset{}{}}}}{\cdots\!\!\cdots\!-\!\overset{\oplus}{N}}}\;\; \overset{\ominus}{O}\!-\!\underset{\underset{O}{\|}}{C}\!-\!R \;\rightleftarrows\; \underset{H}{\overset{\overset{CH_3}{|}}{\cdots\!\!\cdots\!-\!N:}} \;+\; R\!-\!\underset{\underset{O}{\|}}{C}\!-\!OH \tag{7}$$

$$(8)$$

In the propagation reaction, a proton transfer from the growing chain end to the monomer takes place, with formation of an ion pair of protonated lactam cation and carboxylate anion, accompanied by the attack of the nitrogen lone pair of the chain end on the carbonyl carbon of the protonated monomer.

References

1. Breslow, D. S., G. E. Hulse, and A. S. Metlack, *J. Am. Chem. Soc.*, **79**, 3760 (1957).
2. Ogata, N., *Bull. Chem. Soc. Japan*, **33**, 906 (1960).
3. Ogata, N., *Makromol. Chem.*, **40**, 55 (1960).
4. Ogata, N., *J. Polymer Sci.*, **46**, 271 (1960).
5. Graf, R., G. Lohaus, K. Börner, E. Schmidt, and H. Bestian, *Angew. Chem.*, **74**, 523 (1962).
6. Hall, H. K., Jr., *J. Am. Chem. Soc.*, **80**, 6404 (1958).
7. Holley, R. W., and A. D. Holley, *J. Am. Chem. Soc.*, **71**, 2124 (1949).

Résumé

On a effectué à 140–190°C la polymérisation en bloc de la *N*-méthyl-β-propiolactame avec différents catalyseurs ioniques. Les composés organiques contenant un groupement carboxyle possèdent une activité catalytique élevée pour la polymérisation et fournissent un polymère cristallin fondant vers 180–225°C. On n'obtient pas de polymère de la *N*-méthyl-β-propiolactame à 140°C., température à laquelle a lieu la polymérisation du *N*-méthylacrylamide. Le polymère formé a partir de *N*-méthyl-acrylamide est amorphe et son spectre infrarouge est tout à fait différent de celui de la poly(*N*-méthyl-β-propiolactame) qui présente un pic d'absorption principal, caractéristique d'une structure polyamide. On propose un mécanisme sur la base des spectres infrarouges d'un mélange équimolaire de monomère et de catalyseurs chauffé a 130°C.

Zusammenfassung

Die Polymerisation von *N*-Methyl-β-propiolactam mit verschiedenen ionischen Katalysatoren wurde in Substanz bie 140–190°C ausgeführt. Organische Verbindungen mit Carboxylgruppen besitzen eine hohe katalytische Aktivität für die Polymerisation und liefert ein kristallines bei 180–225°C. schmelzendes Polymeres. Kein Polymeres von *N*-Methyl-β-propiolactan wurde bei 140°C. erhalten, bei welcher Temperatur die

Polymerisation von N-Methylacrylamid stattfand. Das Polymere von N-Methylacrylamid war amorph und sein Infrarotspektrum war vollständig von dem des Poly-(N-methyl-β-propiolactan) verschieden. Das Infrarotspektrum von Poly(N-methyl-β-propiolactan) zeigte ein für eine Polyamidstruktur charakteristisches Hauptmaximum. Auf Grundlage des Infrarotspektrums der äquimolaren auf 130°C. erhitzten Mischung von Monomerem und Katalysator wurde ein Mechanismus vorgeschlagen.

Kinetics of Polymerization of Butadiene, Isoprene, and Styrene with Alkyllithiums. Part I. Rate of Polymerization

HENRY L. HSIEH, *Research and Development Department, Phillips Petroleum Company, Bartlesville, Oklahoma*

Synopsis

The kinetics were determined for the polymerization of butadiene, isoprene, and styrene with n-, sec-, and tert-BuLi in hydrocarbon solvents. Polymerization has the mechanism of a homogeneous, "intermittent" stepwise addition reaction with no true termination reaction. In cyclohexane, n-hexane or toluene at 5–50°C. there is no chain transfer. When n-BuLi was used, the rate of polymerization was a combined rate of initiation and propagation. It was proportional to $[M]^2$ and dependent on $[n\text{-BuLi}]$ at low initiator concentration and almost independent at high concentration. The limits are established and discussed. The rate constants calculated for the monomers were in the order styrene > isoprene ≫ butadiene. For the solvents the order was toluene ≫ cyclohexane > n-hexane.

I. INTRODUCTION

Although the kinetics of the anionic polymerization of styrene[1-3] and isoprene[4,5,7-10] have been reported, the polymerization of butadiene has received very little attention. In this investigation, butadiene was extensively studied and direct comparisons were made among these monomers.

In the published kinetic studies, rate of polymerization had been most thoroughly examined.[1,2,4,8,10] However, there are considerable and significant disagreements among the results obtained by different investigators. Part of the difficulty is because rate of polymerization includes rates of initiation and propagation.

The total objective of this work is, of course, the elucidation of the mechanisms of polymerization initiated with alkyllithium.

II. EXPERIMENTAL

A. Materials

The solvents employed, petroleum-derived toluene and Phillips' pure grade cyclohexane were carefully dried by countercurrent scrubbing with prepurified nitrogen followed by passage over activated alumina. Phillips' special purity butadiene was distilled through sodium dissolved in ethylene

glycol before it was condensed and transferred into bottles containing Drierite. Phillips' polymerization grade isoprene was refluxed over sodium wire in a nitrogen atmosphere for about three hours and distilled into bottles. Styrene, polymerization grade, was vacuum-distilled. All monomers were stored in a deep freeze. The n-BuLi in heptane and sec-BuLi and $tert$-BuLi in pentane were obtained from Lithium Corporation of America as approximately $2M$ solutions.

B. Polymerization Procedure

Polymerizations were conducted in new, 32-oz. bottles which were cleaned and air-dried at 60°C. Solvent was first added to each bottle under a nitrogen blanket through a specially constructed and calibrated solvent charging apparatus. The charging apparatus was directly connected to the storage tank which was in turn connected to the solvent-drying apparatus. After the solvent was introduced, prepurified nitrogen was dispersed through a fritted glass tube and purged through the solvent at the rate of 3 l./min. for 10 min. in an effort to remove residual amounts of moisture and air. The bottles were capped with toluene-extracted, self-sealing rubber gaskets and perforated metal caps having three holes. This technique gave very reproducible results. Monomer was added directly to the solvent from a calibrated monomer dispenser. The mixture was brought to the desired reaction temperature by tumbling the bottles in a constant temperature bath. Then the initiator solution was added from a calibrated syringe. The bottles were tumbled in the constant temperature bath for the necessary time. To prevent any possible leakage into the bottle cap in the bath, 25–40 psi of prepurified nitrogen pressure, depending on the reaction temperature, was introduced into the bottle after all the reagents were added. In addition, a rubber serium cap was tightly fitted over the metal cap and neck. For rate studies, the bottle, cap and gasket, solvent, monomer, and initiator solution were weighed after each step. Polymer solution was transferred to a tared aluminum dish containing isopropyl alcohol via a syringe valve and needle. The amount was measured by weighing the bottle before and after sampling. The sample was evaporated in a hot-air oven and then finally dried in a vacuum oven to obtain conversion.

Small amounts of impurities present in the polymerization systems were not removed. The amount of alkyllithium destroyed by the impurities was called the scavenger level and was predetermined for each monomer-solvent combination. The scavenger level varied from 0.2×10^{-3} to 0.4×10^{-3} mole/l. The alkyllithium concentration reported is the effective level, namely the difference between the actually charged level and the scavenger level.

III. RESULTS

Butadiene, isoprene, and styrene in cyclohexane were readily polymerized with BuLi initiators. For n-BuLi, approximations of the well-known,
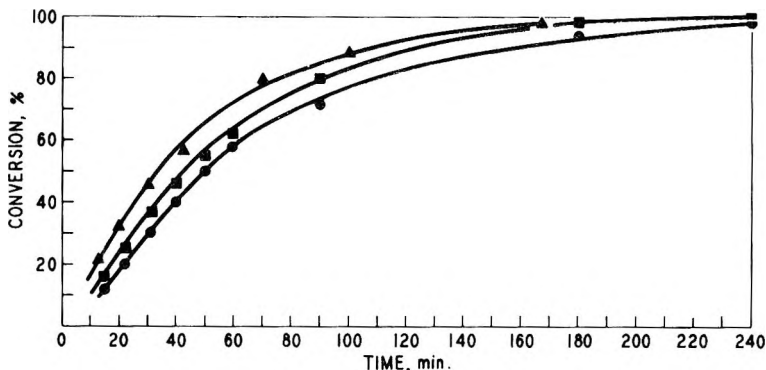
Fig. 1. Polymerization of butadiene (1.4 mole/l.) in cyclohexane at 50°C. with BuL (0.32 × 10⁻³ mole/l.): (●) n-BuLi; (▲) sec-BuLi; (■) tert-BuLi.
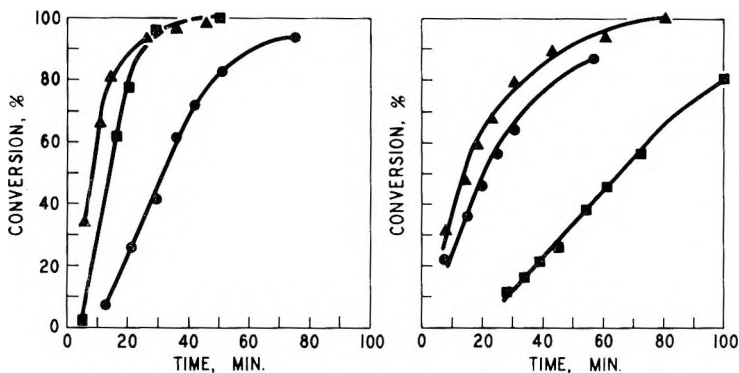
Fig. 2 (left). Polymerization of isoprene (1.1 mole/l.) in cyclohexane at 50°C. with BuLi (0.74 × 10⁻³ mole/l.): (●) n-BuLi; (▲) sec-BuLi; (■) tert-BuLi.
Fig. 3 (right). Polymerization of styrene (0.8 mole/l.) in cyclohexane at 50°C. with BuLi (0.24 × 10⁻³ mole/l.): (●) n-BuLi; (▲) sec-BuLi; (■) tert-BuLi.

S-shaped conversion curves were obtained. At very low conversions, they do not go through the origin. However, the rate of polymerization of any one of the three monomers was dependent on the type of the BuLi used. In the case of butadiene, as shown in Figure 1, the rate of polymerization was highest with sec-BuLi and lowest with n-BuLi. Qualitatively, Figure 2 illustrates that this was also true with isoprene. For styrene, however, the rate of polymerization was lowest with tert-BuLi, as shown in Figure 3. Furthermore, the rate curves obtained by means of sec-BuLi, particularly with butadiene or styrene, were straight lines from origin to about 50% conversion.

These rate studies were examined and compared in another manner. Figures 4 and 5 are attempts to fit the data to first-order rate plots. As can be readily seen for all the three monomers, only those initiated with sec-BuLi followed the first-order relationship closely throughout the range.

Rates of polymerization of butadiene, isoprene, and styrene in cyclohexane, n-hexane, and toluene were determined from the linear portion
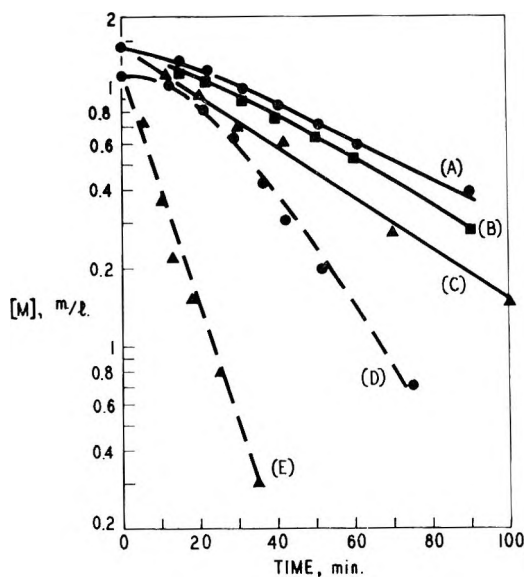
Fig. 4. Monomer concentration vs. time in cyclohexane at 50°C.: (A) butadiene with n-BuLi; (B) butadiene with tert-BuLi; (C) butadiene with sec-BuLi; (D) isoprene with n-BuLi; (E) isoprene with sec-BuLi.
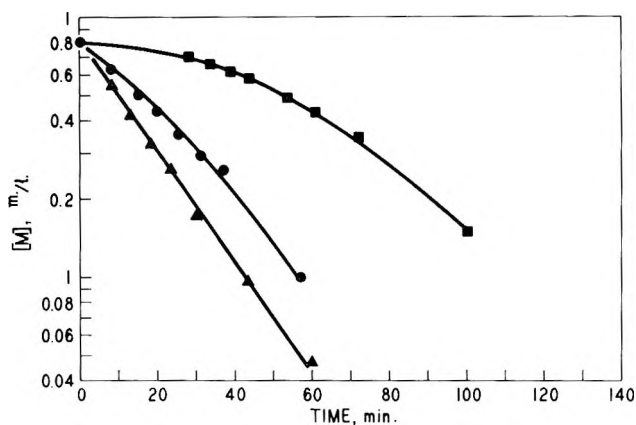
Fig. 5. Monomer concentration vs. time of styrene polymerization in cyclohexane at 50°C.: (●) n-BuLi; (▲) sec-BuLi; (■) tert-BuLi.

of the S-shaped conversion curves. It is evident from Figures 6–10 that at high initiator concentration the rates of polymerization were almost constant over a wide range of n-BuLi concentrations. This is in agreement with the data of O'Driscoll and Tobolsky[1] and Welch[2] on styrene and Kortkov[10] and Spirin[4] on isoprene.

The relationship between rate of polymerization and initial monomer concentration [M], was also examined. The results are shown in Figure
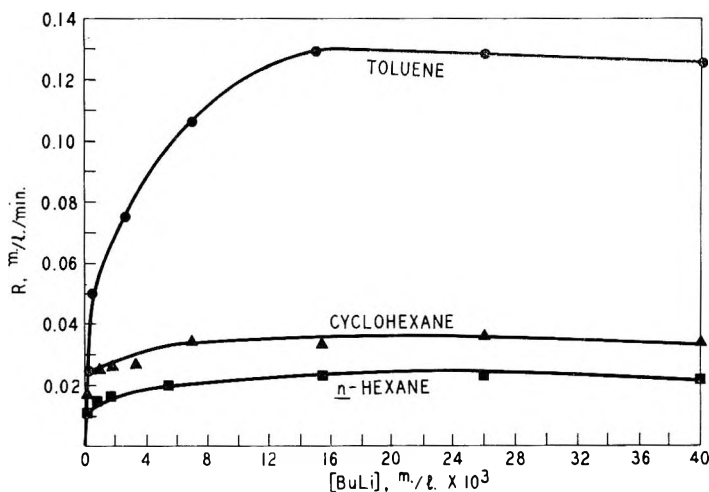
Fig. 6. Rate of polymerization of butadiene (1.7 mole/l.) at 50°C.
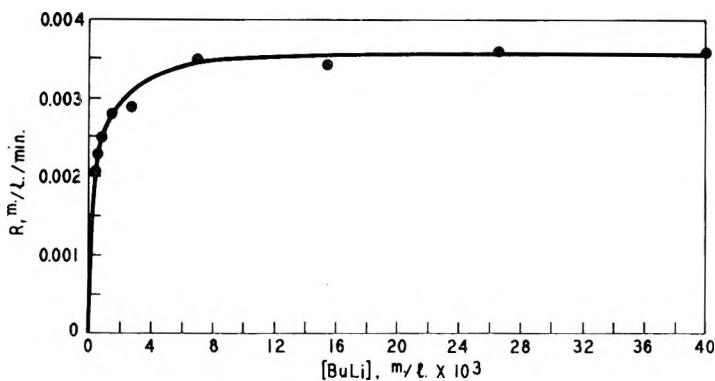
Fig. 7. Rate of polymerization of butadiene (1.7 mole/l.) in cyclohexane at 30°C.

11.   Rate of polymerization was proportional to the square of the initial monomer concentration as reported earlier for styrene[1] and isoprene.[10]

IV. DISCUSSION

In general two basic reaction mechanisms, namely a chain catalytic reaction[10] or stepwise addition[1-3,7,11-13] had been considered for BuLi-initiated polymerizations. The S-shaped conversion curves obtained from n-BuLi were interpreted by Korotkov[10] as evidence for an induction period followed by polymerization as a case of chain catalysis. Our results obtained with sec-BuLi proved that polymerization of butadiene or styrene does not follow the S-shaped curve, although this type of curve is obtained with n-BuLi. Indeed, the time delay is due to the slow reaction of alkyllithium and monomer. In other words the nature of the lithium compound affects kinetics, a fact that has not been recognized. It is
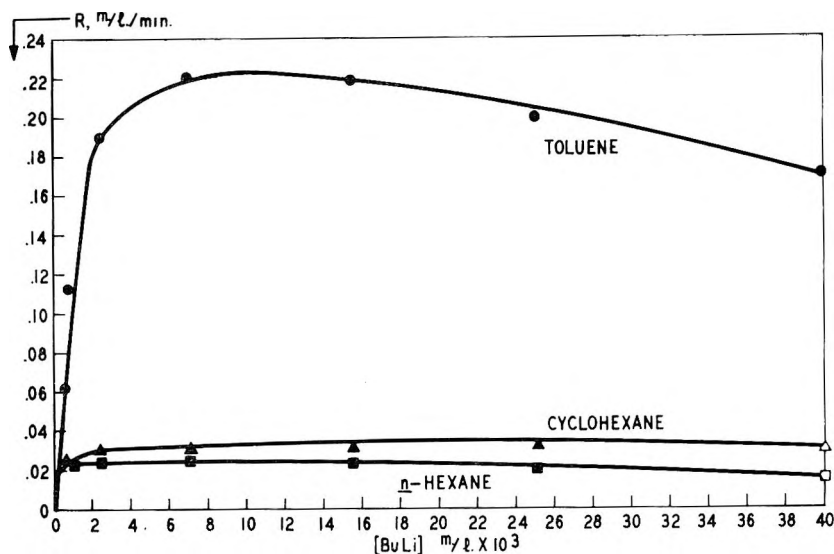
Fig. 8. Rate of polymerization of isoprene (1.3 mole/l.) at 50°C.
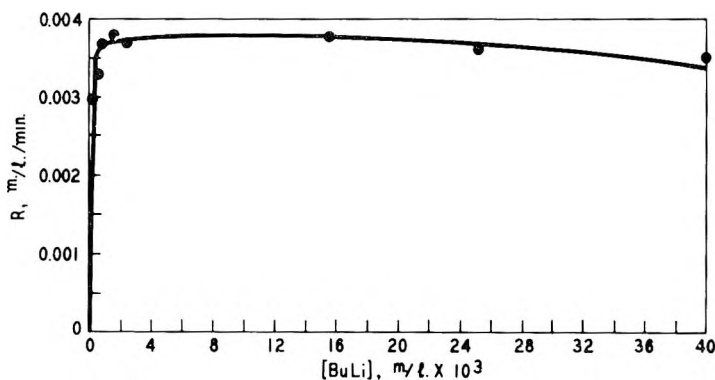
Fig. 9. Rate of polymerization of isoprene (1.3 mole/l.) in cyclohexane at 30°C.

generally accepted that polymerization with alkyllithium is a homo-
geneous, stepwise reaction with no true termination reaction. In most
hydrocarbon solvents at normal temperature, there is no chain transfer.
In the present work nothing was found to contradict these beliefs.

The rate of polymerization R of butadiene, isoprene, and styrene with
n-BuLi is dependent on temperature and type of solvent, increasing ap-
proximately fourfold per 10°C. temperature increase. This is true since
rates of both initiation and propagation increase. Rate of polymerization
is highest in toluene and lowest in n-hexane. In cyclohexane it is slightly
higher than in n-hexane. It is interesting to note that regardless of the
monomer, temperature, or initiator level, conversions shortly after addition
of initiator are higher in n-hexane than in cyclohexane. The conversion
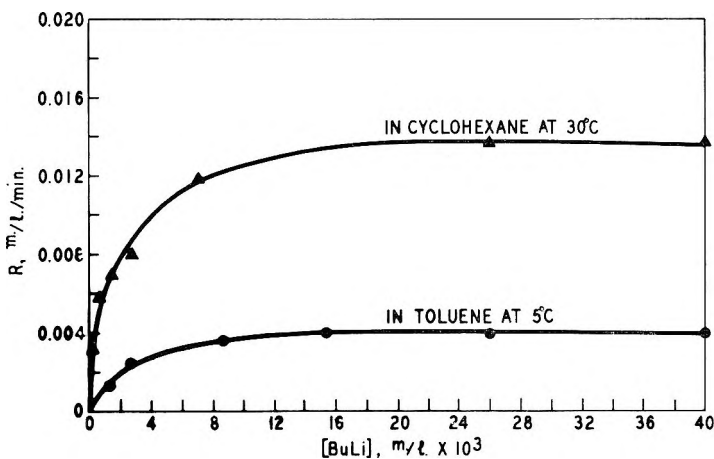
Fig. 10. Rate of polymerization of styrene (1.0 mole/l.).
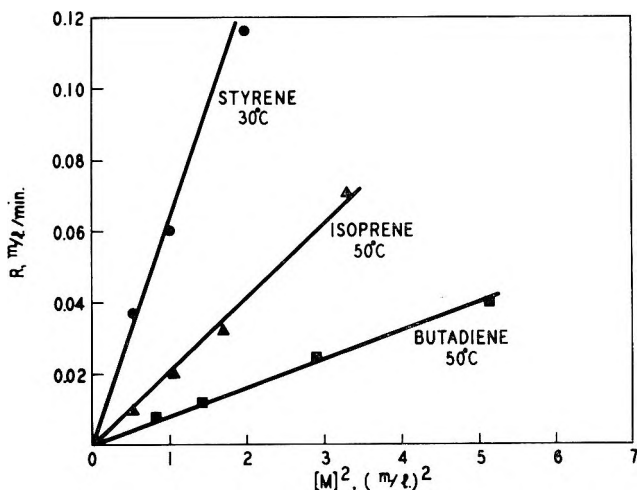
Fig. 11. Rate of polymerization in cyclohexane vs. $[M]^2$.

curves cross over at 8–15% conversion. This suggests that the rate of initiation is higher and rate of propagation is lower in n-hexane than in cyclohexane.

The rate of polymerization is proportional to $[M]^2$. This is in agreement with the facts that both rates of initiation and propagation are proportional to monomer concentration. Chromatographic analyses of hydrolyzed mixtures at various conversions showed clearly that both initiation and propagation occurred simultaneously during the linear portion of the rate curves (Part II).[14] Therefore, there is no doubt that rate of polymerization R is a combined study of rate of initiation R_i and rate of propagation R_p when n-BuLi was used.

As reported by other workers, rate of polymerization is dependent on [n-BuLi] at low concentration and almost independent at high concentration. In fact, in some instances,[4] the rate is even reduced when [n-BuLi] becomes very high (Figs. 6 and 8).

The association of alkyllithium in hydrocarbon solvent is well known.[15-21] The association number has been reported as 4 for tert-BuLi,[20] an equilibrium between 4 and 6 for EtLi[19] and mostly as 2 for alkyllithium.[17] Presumably, it depends to a certain extent on concentration and solvent. It is generally assumed that only the unassociated polymer-Li propagates. The polymer-Li can associate either with BuLi or polymer-Li to form temporary inactive associated aggregates. Unfortunately, the exact nature of these associations is not known.

TABLE I
Polymerization Rate Constants
$R = K[M]^2$

	K, l./mole/min.			
	Cyclohexane, 30°C.	Cyclohexane, 50°C.	Hexane, 50°C.	Toluene, 50°C.
Butadiene	0.0012[a]	0.0114[b]	0.0076[a]	0.0443[c]
Isoprene	0.0022[b]	0.0189[b]	0.0148[b]	0.118[d]
Styrene	0.0131[e]	—	—	—

[a] [n-BuLi] > 0.004 mole/l.
[b] [n-BuLi] > 0.001 mole/l.
[c] [n-BuLi] > 0.010 mole/l.
[d] [n-BuLi] = 0.002–0.04 mole/l.
[e] [n-BuLi] > 0.007 mole/l.

At low n-BuLi concentrations, the rate of polymerization is proportional to monomer and initiator concentrations. Although the dependence of rate on n-BuLi concentration was clearly demonstrated, because of impurities, studies could not be conducted at extremely low concentrations to establish quantitative relationship.

At high concentrations of n-BuLi, $R = K[M]^2$. The rate constants were calculated as shown in Table I.

The minimum concentration at which the rate is independent of [n-BuLi] seems directly related to rate of initiation of the particular system. The higher the rate of initiation of a particular system, the higher is the minimum. For example, the lower limit is the highest for styrene and lowest for isoprene among the three monomers. The lower limit is higher in toluene than in cyclohexane or n-hexane.

References

1. O'Driscoll, K. F., and A. V. Tobolsky, *J. Polymer Sci.*, **35,** 259 (1959).

2. Welch, F. J., *J. Am. Chem. Soc.*, **81,** 1345 (1959).

3. Worsfold, D. J., and A. Bywater, *Can. J. Chem.*, **38,** 1891 (1960).

4. Spirin, Yu. L., A. R. Gantmakher, and S. S. Medvedev, *J. Polymer Sci.*, **53,** 233 (1961).

5. Morton, M., E. E. Bostick, and R. Livigni, *Rubber Plastics Age*, **42,** 397 (1961).

6. Morton, M., A. A. Rembaum, and J. L. Hall, *J. Polymer Sci.*, **A1,** 461 (1963).

7. Morton, M., L. J. Fetters, and E. E. Bostick, *J. Polymer Sci.*, **C1,** 311 (1963).

8. Lundborg, C., and H. Sinn, *Makromol. Chem.*, **41,** 242 (1960).

9. Morton, M., E. E. Bostick, and R. G. Clarke, *J. Polymer Sci.*, **A1,** 475 (1963).

10. Korotkov, A. A., N. N. Chesnokova, and L. B. Trukhmanova, *Vysokomol. Soedin.*, **1,** 46 (1959).

11. Hsieh, H. L., Thesis, Princeton University, 1957.

12. Kropachev, V. A., B. A. Dolgoplosk, and H. I. Vikoloev, *Dokl. Akad. Nauk SSSR*, **115,** 737 (1957).

13. Ziegler, K., et al., *Ann.*, **511,** 13, 45, 64 (1934).

14. Hsieh, H. L., *J. Polymer Sci.*, **A3,** 163 (1965).

15. Warhurst, E., *Discussions Faraday Soc.*, **2,** 239 (1947).

16. Rogers, M. T., and T. L. Brown *J. Phys. Chem.*, **61,** 366 (1957).

17. Wittig, G., paper presented to International Congress of Pure and Applied Chemistry, 16th Congress, Paris, July 1957.

18. Coates, G. E., *Organo-Metallic Compounds*, Methuen, London, 1956, p. 7.

19. Brown, T. L., and M. T. Rogers, *J. Am. Chem. Soc.*, **79,** 1858 (1957).

20. West, R., and W. Glaze, *J. Am. Chem. Soc.*, **83,** 3580 (1961).

21. Weiner, M., G. Vogel, and R. West, *Inorg. Chem.*, **1,** 654 (1962).

Résumé

On a déterminé les cinétiques de polymérisation du butadiène, de l'isoprène et du styrène avec le *n*, *sec*- et *tert*-BuLi dans des solvants hydrocarbonés. Le mécanisme est une réaction homogène d'addition "intermittent," par étapes sans réaction de terminaison véritable. Il n'y a pas de transfert de chaîne dans le cyclohexane, le *n*-hexane ou le toluène à 5–50°C. Quand on emploie le n-BuLi, la vitesse de polymérisation est une combinaison d'une vitesse d'initiation et de propagation. Elle est proportionnelle à $(M)^2$ et dépend e (*n*-BuLi) à faible concentration en initiateur; par contre elle en est indépendante à concentration élevée. On en définit et discute les limites. L'ordre des constantes de vitesses calculées pour les monomeres sont: styrène > isoprene >> butadiène. Pour les solvents l'ordre est: toluène >> cyclohexane > *n*-hexane.

Zusammenfassung

Die Kinetik der Polymerisation von Butadien, Isopren und Styrol mit *n*-, *sek*- und *tert*-BuLi in Kohlenwasserstofflösung wurde untersucht. Der Polymerisationsmechanismus entspricht einer homogenen "intermittierenden" schrittweisen Additionsreaktion ohne wahre Abbruchreaktion. In Zyklohexan, *n*-Hexan oder Toluol bei 5–50°C. tritt keine Kettenübertragung auf. Mit *n*-BuLi war die Polymerisationsgeschwin digkeit eine Kombination von Start und Wachstumgeschwindigkeit. Sie war zu $[M]^2$ proportional und von [*n*-BuLi] bei niedriger Starterkonzentration abhängig, bei hoher Konzentration aber fast unabhängig. Die Grenzen werden bestimmt und diskutiert. Die für die Monomeren berechneten Geschwindigkeitskonstanten lagen in der Reihenfolge Styrol > Isopren >> Butadien. Bei den Lösungsmitteln war die Reihenfolge Toluol >> Zyklohexan > *n*-Hexan.

Kinetics of Polymerization of Butadiene, Isoprene, and Styrene with Alkyllithiums. Part II.   Rate of Initiation

HENRY L. HSIEH, *Research and Development Department, Phillips Petroleum Company, Bartlesville, Oklahoma*

Synopsis

By gas chromatographic analysis of the hydrolyzed polymerization solutions, the per cent of BuLi unreacted was measured at various conversions.   The effects of BuLi concentration, the structure of the butyl group, and the solvent type were studied.   The rates of initiation (R_i) for butadiene, isoprene, and styrene were determined.   For dienes, the order was *sec*-BuLi > *i*-PrLi > *tert*-BuLi > *i*-BuLi > *n*-BuLi.   For styrene, it was *sec*-BuLi > *i*-PrLi > *i*-BuLi > *n*-BuLi > *tert*-BuLi.   With *n*-BuLi, the order was styrene > butadiene > isoprene.   For any particular monomer–initiator combination, the order was toluene ≫ *n*-hexane > cyclohexane.   The results obtained here proved that $R_i = k_i$ [RLi] [M] for all three monomers.

I. INTRODUCTION

In anionic polymerization, rate of initiation, in spite of its great importance, has been least studied by other investigators.   In fact, only the reaction rate of *n*-BuLi with styrene has been reported.   Worsfold and Bywater[1] studied this photometrically.   Because of the high extinction coefficient of both styrene and styryl anion, this technique was useful only for limited concentration ranges.   In the present study, by employing gas chromatographic analysis it was possible to follow the initiation reaction for wide ranges of concentrations of alkyllithiums with styrene as well as diene monomers.

The organic moiety of the alkyllithium initiators has no effect on the microstructure[2–6] of the polydiene formed.   It was extremely interesting to study the effect of the organic moiety of the alkyllithium compounds on the rate of initiation, a study made possible by the chromatographic technique.   This undoubtedly will add knowledge to the nature of initiation reactions.

II. EXPERIMENTAL

The solvents used and *n*-BuLi, *sec*-BuLi and *tert*-BuLi were discussed in Part I.[7]   Isopropyllithium (*i*-PrLi) and isobutyllithium (*i*-BuLi) in pentane were also obtained from Lithium Corporation of America.
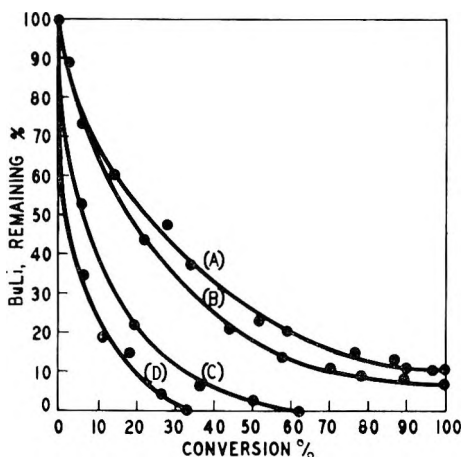
Fig. 1. Relationships between BuLi remaining and conversion of polymerization of butadiene (1.7 mole/l.) in cyclohexane at 50°C. at various initial n-BuLi concentrations: (A) 26×10^{-3} mole/l.; (B) 8.7×10^{-3} mole/l.; (C) 2.6×10^{-3} mole/l.; (D) 0.9×10^{-3} mole/l.
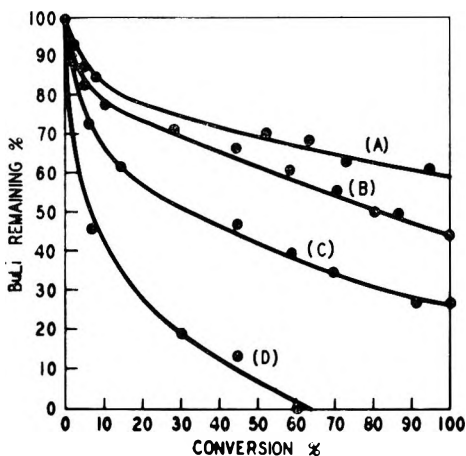
Fig. 2. Relationship between BuLi remaining and conversion of polymerization of isoprene (1.3 mole/l.) in cyclohexane at 50°C. at various n-BuLi concentrations: (A) 26×10^{-3} mole/l.; (B) 8.7×10^{-3} mole/l.; (C) 2.6×10^{-3} mole/l.; (D) 0.9×10^{-3} mole/l.

For rate of initiation studies, 12-oz. bottles were used. At the desired time, deionized water was added to terminate polymerization and hydrolyze residual active BuLi molecules. The butane content of each bottle was then determined by gas chromatography. The solution was finally evaporated to dryness to obtain conversion. The chromatographic procedure for direct analysis is essentially as follows:

A 20-ft. column containing 20 wt.-% 1,2,3-triscyanoethoxypropane on Chromosorb was used. The column was operated at 50°C. and a helium
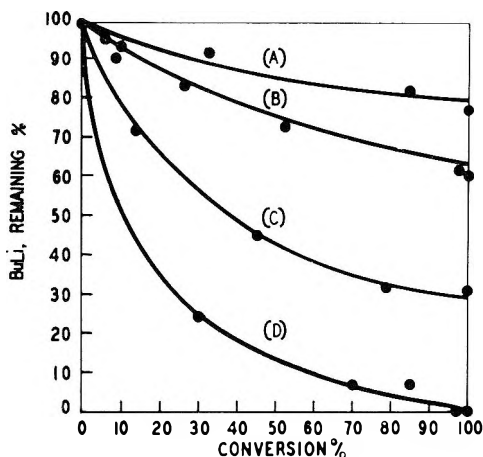
Fig. 3. Relationship between BuLi remaining and conversion of polymerization of styrene (1.0 mole/l.) in cyclohexane at 50°C. at various n-BuLi concentrations: (A) 26×10^{-3} mole/l.; (B) 8.7×10^{-3} mole/l.; (C) 2.6×10^{-3} mole/l.; (D) 0.9×10^{-3} mole/l.
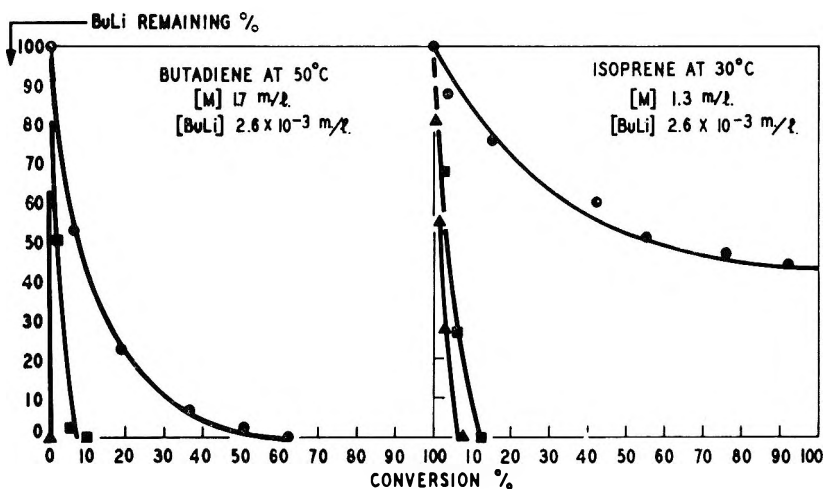
Fig. 4. Effect of BuLi structure on rate of initiation in cyclohexane: ($\bullet$) n-BuLi; ($\blacksquare$) $tert$-BuLi; ($\blacktriangle$) sec-BuLi.

flow rate of 55 cc./min. The sample was injected via a chilled microliter syringe. If 0.5 mmole or less of butane was present, a sample size of 40 μl. was used; for greater concentrations, 20 μl. was sufficient. Butane could be detected in concentrations as low as 0.05 mmole/200 g. of polymer solution or approximately 20 ppm of solution. The peak height of the butane was measured and compared with a known concentration of n-butane in a synthetic blend.

However, it was found that more accurate and reproducible results can be obtained by using an internal reference standard. For n-butane analy-
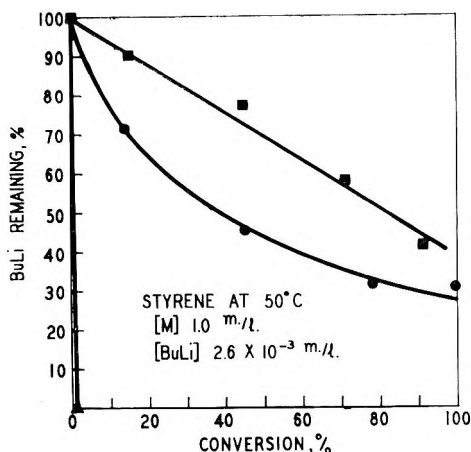
Fig. 5. Effect of BuLi structure on rate of initiation in cyclohexane: (●) n-BuLi; (■) tert-BuLi; (▲) sec-BuLi.
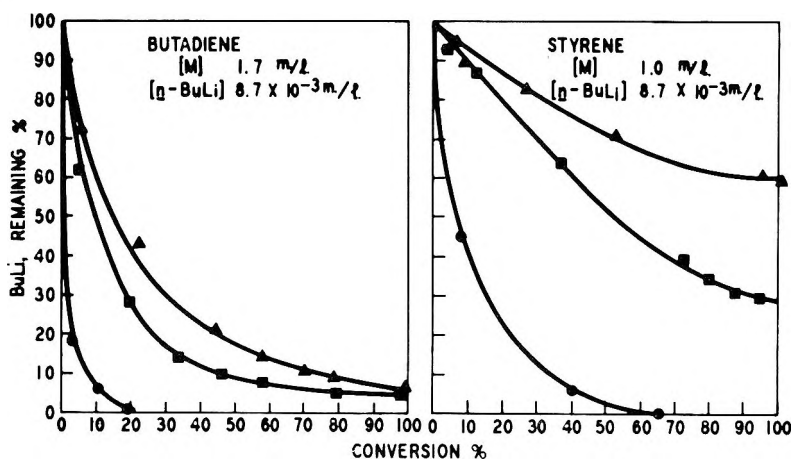
Fig. 6. Effect of solvent on rate of initiation at 50°C.: (▲) cyclohexane; (■) n-hexane; (●) toluene.

sis, isobutane was used as internal standard and vice versa. For propane analysis, propylene was used. The technique is described below.

A known amount of the reference gas is injected into the bottle during the preparation of the sample. After the hydrolysis, a liquid sample was introduced into a 20-ft. hexamethylphosphonamide column operated at room temperature and 25 psig helium carrier gas pressure. Corrections were made for the difference in thermal conductivity of the gases. The amount of the gas analyzed was calculated by the following relationship:

$$X_D = L_D/L_B \, A + G_D \, [1 - P_B^{\circ}/_D^{\circ}P]$$

where A is the number of millimoles of standard reference material (B) added, P_B° is the vapor pressure of pure B at temperature of the test, P_D° is
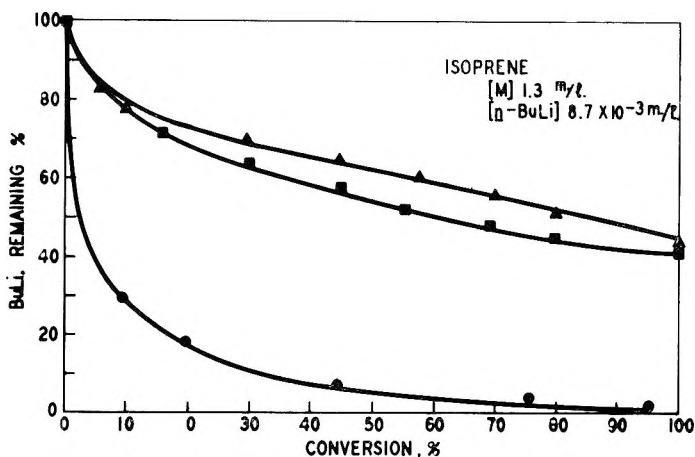
Fig. 7. Effect of solvent on rate of initiation at 50°C.: (▲) cyclohexane; (■) n-hexane; (●) toluene.
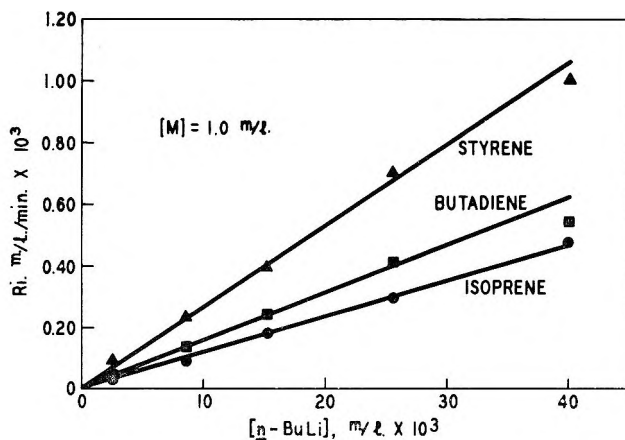
Fig. 8. Rate of initiation in cyclohexane at 50°C. vs. n-BuLi concentration.

the vapor pressure of pure D at temperature of the test, G_D is the amount of component D in the vapor, L_D is the amount of component D in the liquid, and L_B is the amount of component B in the liquid.

The term, $G_D[1 - (P°_B/P°_D)]$, is very small compared to X_D and, therefore, it was neglected in actual calculations.

III. RESULTS

By gas chromatographic analysis of the hydrolyzed polymerization solutions at different reaction times, the per cent of BuLi unreacted was measured at various conversions. The effect of BuLi concentration is shown in Figures 1–3, and that of the structure of the butyl group in Figures 4 and 5. The effect of solvent type is illustrated in Figures 6 and 7.
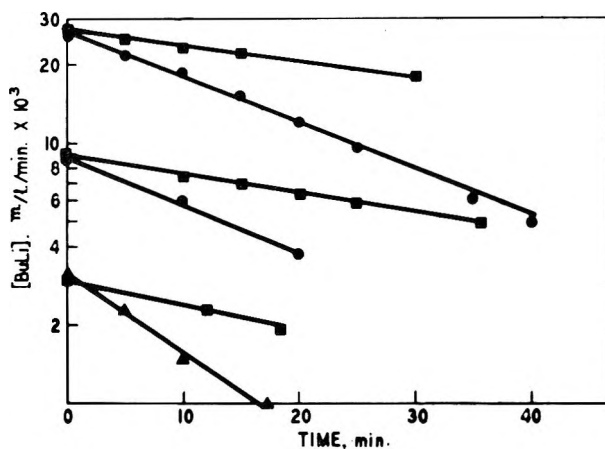
Fig. 9. BuLi concentration vs. time for polymerization in cyclohexane at 50°C.: (●) butadiene (1.7 mole/l.); (■) isoprene (1.3 mole/l.); (▲) styrene (1.0 mole/l.).

The rate of initiation, measured from the initial reaction rate of BuLi and monomer, was easily calculated from the butane analyses. These rates, listed in Tables I and II, demonstrate the solvent and BuLi structure effects for butadiene, isoprene, and styrene.

TABLE I

Effect of Butyllithium Structure on Rate of Initiation in Cyclohexane
[n-BuLi], 2.6×10^{-3} mole/l.

Monomer	[M], mole/l.	Temp., °C.	R_i, mole/l./min. $\times 10^3$			
			n-BuLi	sec-BuLi	$tert$-BuLi	i-BuLi
Butadiene	1.7	50	0.08	4.0	0.7	—
		30	0.02	0.8	0.13	—
Isoprene	1.3	50	0.05	1.5	0.9	0.12
		30	0.01	0.3	0.2	—
Styrene	1.0	50	0.09	5.2	0.04	0.19
		30	0.02	1.2	—	—

TABLE II

Effect of Solvent on Rate of Initiation at 50°C.

Monomer	[M], mole/l.	[n-BuLi], mole/l. $\times 10^3$	R_i, mole/l./min. $\times 10^3$		
			Toluene	Cyclohexane	Hexane
Butadiene	1.7	2.6	2.4	0.08	0.12
		8.7	7.1	0.23	0.33
Isoprene	1.3	2.6	1.6	0.05	0.07
		8.7	4.4	0.12	0.18
Styrene	1.0	2.6	2.3	0.09	0.13
		8.7	7.2	0.24	0.30
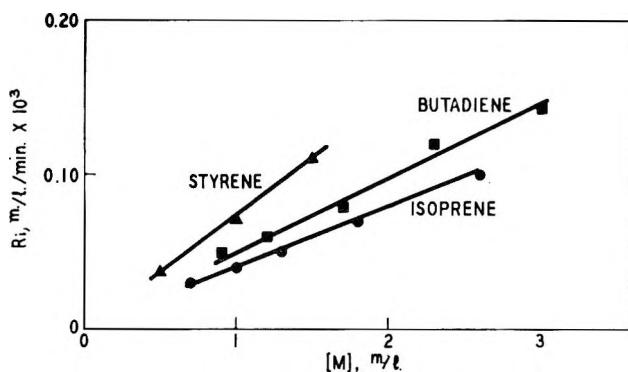
Fig. 10. Rate of initiation in cyclohexane at 50°C. with n-BuLi vs. monomer concentration.
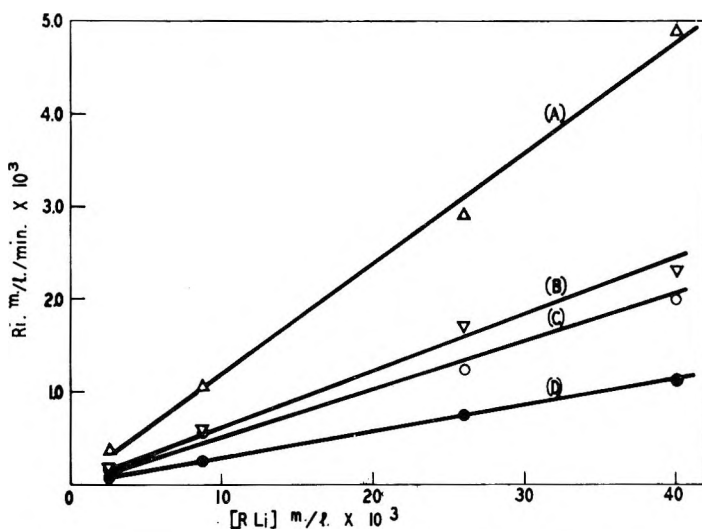
Fig. 11. Rate of initiation vs. [RLi]: (A) styrene (1.0 mole/l.) with i-PrLi at 30°C.; (B) styrene (1.0 mole/l.) with i-BuLi at 50°C.; (C) butadiene (1.0 mole/l.) with i-PrLi at 30°C.; (D) isoprene (1.0 mole/l.) with i-BuLi at 50°C.

The rates of initiation for the three monomers with n-BuLi in cyclohexane at 50°C. were examined for a range of n-BuLi concentrations.   At least in the range of 3×10^{-2} to $4 \times 10^{-3}M$, the initial rate of initiation for styrene and dienes was proportional to initial [BuLi] as shown in Figure 8.   First-order kinetic behavior with respect to [BuLi] at any time is shown in Figure 9, a semilogarithmic plot of [BuLi] versus time.   Since the propagation step rapidly consumed the monomer, a first-order plot of this nature holds only up to fairly low conversions (below 30%).

The rate of initiation was also first-order in monomer concentration. This is illustrated in Figure 10.

Rate of initiation with i-PrLi and i-BuLi was also examined.   The first-order relationship was again demonstrated (Figure 11).

TABLE III
Initiation Rate Constants
$R_i = k_i [\text{BuLi}] [\text{M}]$

| | k_i (n-BuLi at 50°C.)[a] | | | k_i (cyclohexane at 50°C.)[a] | | | |
	Cyclohexane	n-Hexane	Toluene	n-BuLi	sec-BuLi	$tert$-BuLi	i-BuLi
Butadiene	0.015 ± 0.002	0.024 ± 0.003	0.51 ± 0.03	0.015	0.90	0.16	—
Isoprene	0.012 ± 0.002	0.018 ± 0.003	0.43 ± 0.03	0.012	0.44	0.27	0.035
Styrene	0.028 ± 0.002	0.042 ± 0.008	0.85 ± 0.03	0.028	2.0	0.015	0.061

[a] $k_i = 1./\text{mole}/\text{min}.$

IV. DISCUSSION

The curves of conversion versus unreacted BuLi for the three monomers at various BuLi concentrations clearly demonstrated that rate of polymerization R is indeed a study of combined rates of propagation, and initiation (see Part I).[7]   It also showed that at higher concentrations, proportionally, less BuLi was consumed.   At the same concentration the most unreacted BuLi was found with styrene or isoprene and least with butadiene.   This is in agreement with the results that for rate of propagation, the order is styrene > isoprene ≫ butadiene (see Part III);[8] for rate of initiation the order is styrene > butadiene > isoprene.

One of the interesting findings is the fact that *tert*-BuLi is a very active initiator with dienes but a relatively inactive initiator with styrene.   If rate of dissociation of the alkyllithium alone controls the rate of initiation, then the rates should be about the same for dienes and styrene.   From the data obtained here, it seems the rate of initiation is determined by the reaction between a particular combination of alkyllithium and monomer. For diene monomers, the order of decreasing activity is *sec*-BuLi > *i*-PrLi > *tert*-BuLi > *i*-BuLi > *n*-BuLi.   For styrene, the order is the same, except that *tert*-BuLi is the slowest.   It may be speculated that this is controlled by the anion stability of the initiator as well as steric factors.

The study of solvent effect indicated that rate of initiation is highest in toluene and lowest in cyclohexane.   From examination of the rate of polymerization[7] it was predicted that the rate of initiation would be faster in n-hexane than in cyclohexane as discussed earlier.

The results obtained here showed that $R_i = k_i[\mathrm{RLi}][\mathrm{M}]$.   The first-order relationship between rate of initiation and [RLi] does not agree with the data reported for styrene by Worsfold and Bywater.   The origin of this discrepancy is not clear.   These authors found the rate to be low order (between $1/_3$ and $1/_7$) from which they assumed that n-BuLi is a hexamer in hydrocarbon solvent.   The first-order kinetics do not necessarily indicate that the initiator molecules are not associated at the concentrations studied. They do suggest that the initiation rate is independent of association number of a particular alkyllithium.

The rate constant k_i for the three monomers in cyclohexane, n-hexane, and toluene as well as k_i for the three monomers with n-, *sec*-, *i*-, and *tert*-BuLi were calculated to demonstrate the relative rates.   These constants are shown in Table III.

References

1. Worsfold, D. J., and A. Bywater, *Can. J. Chem.*, **38,** 1891 (1960).
2. Hsieh, H., D. J. Kelley, and A. V. Tobolsky, *J. Polymer Sci.*, **26,** 240 (1957).
3. Morita, H., and A. V. Tobolsky, *J. Am. Chem. Soc.*, **79,** 5853 (1957).
4. Tobolsky, A. V., and C. E. Rogers, *J. Polymer Sci.*, **40,** 73 (1959).
5. Stearns, R. S., and L. E. Forman, *J. Polymer Sci.*, **41,** 381 (1959).

6. Kuntz, I., and A. Gerber, *J. Polymer Sci.*, **43,** 299 (1960).

7. Hsieh, H. L., *J. Polymer Sci.*, **A3,** 153 (1965).

8. Hsieh, H. L., *J. Polymer Sci.*, **A3,** 173 (1965).

Résumé

On a mesuré, a divers taux de conversion, par chromatographie en phase gazeuse, le pourcentage de BuLi qui n'a pas régi apres hydrolyse des polymeres en solution.   On a étudié l'influence de la concentration en BuLi, ainsi que l'influence de la structure du groupement butyle et le type de solvant.   On a déterminé les vitesses d'initiation (R_i) pour les butadiene, l'isoprène et le styrène.   Pour les diènes, l'ordre est *sec*-BuLi > *iso*-BuLi > *tert*-BuLi > *iso*-BuLi > *n*-BuLi.   Pour le styrene il est *sec*-BuLi > *iso*-PrLi > *iso*-BuLi > *n*-BuLi > *tert*-BuLi.   Pour le *n*-BuLi l'ordre est styrene > butadiene > isoprène.   Pour chaque combinaison monomère–initiateur l'ordre est toluene >> *n*-hexane > cyclohexane.   Les résultats obtenus montrent que $R_i = k_i$ (RLi)(M) pour chacun des trois monomères.

Zusammenfassung

Durch gaschromatographische Analyse der hydrolysierten Polymerisationslösungen wurde der Prozentgehalt an nicht reagiertem BuLi bei verschiedenem Umsatz gemessen. Der Einfluss der BuLi-Konzentration, der Struktur der Butylgruppe und des Lösungs-mitteltyps wurde untersucht.   Die Startgeschwindigkeit (R_i) wurde für Butadien, Iso-pren und Styrol bestimmt.   Bei den Dienen war die Reihenfolge *sek*-BuLi > *i*-PrLi > *tert*-BuLi > *i*-BuLi > *n*-BuLi.   Bei Styrol war sie *sek*-BuLi > *i*-PrLi > *i*-BuLi > *n*-BuLi > *tert*-BuLi.   Mit *n*-BuLi war die Reihenfolge Styrol > Butadien > Isopren.   Für jede Monomer–Starterkombination war die Reihenfolge Toluol >> *n*-Hexan > Zyklo-hexan.   Die hier erhaltenen Ergebnisse zeigen, dass bei allen drei Monomeren $R_i = k_i$ [RLi][M] ist.

Kinetics of Polymerization of Butadiene, Isoprene, and Styrene with Alkyllithiums.
Part III.   Rate of Propagation

HENRY L. HSIEH, *Research and Development Department, Phillips Petroleum Company, Bartlesville, Oklahoma*

Synopsis

Initial propagation rates R_p for butadiene, isoprene, and styrene were obtained by using *sec*-BuLi as the initiator.   With this alkyllithium, initiation was so very rapid that propagation alone was easily studied.   In the case of diene monomers at $[RLi] > 10^{-2}M$ and for styrene, $R_p = k_p [RLi]^{1/2}[M]$.   Here no unreacted BuLi is present to associate with polymer-Li.   However, polymer-Li association can occur to temporarily inactivate the propagating anion.   A mechanism was proposed and the kinetic equations were derived.   When [RLi] was 10^{-4} to $10^{-2}M$, $R_p = k_p[RLi]^{1/3}[M]$ for both dienes, but not for styrene.   Some propagation rate constants were calculated.   The order of rate of propagation for three monomers was styrene > isoprene > butadiene.

I. INTRODUCTION

In the anionic polymerization system, the rate of propagation has received little attention, mainly due to the difficulty of separately studying rate of propagation and rate of initiation.   Morton and his co-workers[1] used "seeded" initiators to obtain rate of propagation values.   Worsfold and Bywater[2] also obtained values for the propagation rate of styrene by following the reaction photometrically using the known absorption bands of styrene and the absorption band of the polystyryl anion.   This enabled study of the propagation step after measurements indicated that initiation was complete.   However, this often required the introduction of additional styrene.   For an extensive comparison of the three common monomers, development of a new approach was indicated.   In the present work the propagation step was kinetically isolated by use of an anionic initiator having an extremely rapid rate of initiation.

II. EXPERIMENTAL

The materials used and the polymerization technique were extensively discussed in Part I.[3]   "Seeded" initiator was prepared by adding 3 moles butadiene or isoprene in three increments to a 0.3M *sec*-BuLi solution at 70°C.

III. RESULTS

Initial propagation rates for butadiene, isoprene, and styrene were obtained by using sec-BuLi as the initiator.   With this alkyllithium initiation was so very rapid that propagation alone was easily studied.   For styrene and butadiene, no measurable amount of alkyllithium remained in the mixture at conversions more than 1 or 2%, even at a very high (62 × 10⁻³ mole/l.) initiator level.   For isoprene, the initiation reaction was generally completed before 4–10% conversions.[4]   Therefore, the calculations of rate propagation for isoprene were based on approximately 10–30% conversions.
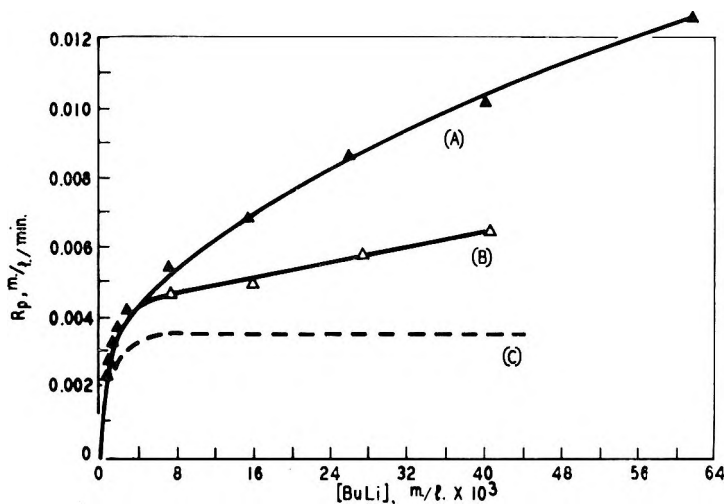
Fig. 1. Rate of propagation of butadiene (1.7 mole/l.) in cyclohexane at 30°C.; (*A*) initiated with *sec*-BuLi or seeded (*sec*-BuLi) initiator; (*B*) initiated with incompletely seeded (*n*-BuLi) initiator; (*C*) initiated with *n*-BuLi (see Part I[3]).
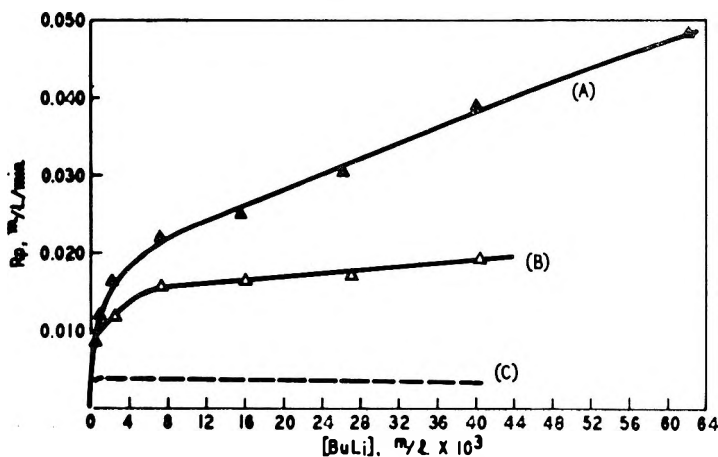
Fig. 2. Rate of propagation of isoprene (1.3 mole/l.) in cyclohexane at 30°C.: (*A*) initiated with *sec*-BuLi or seeded (*sec*-BuLi) initiator; (*B*) initiated with incompletely seeded (*n*-BuLi) initiator; (*C*) initiated with *n*-BuLi (see Part I[3]).
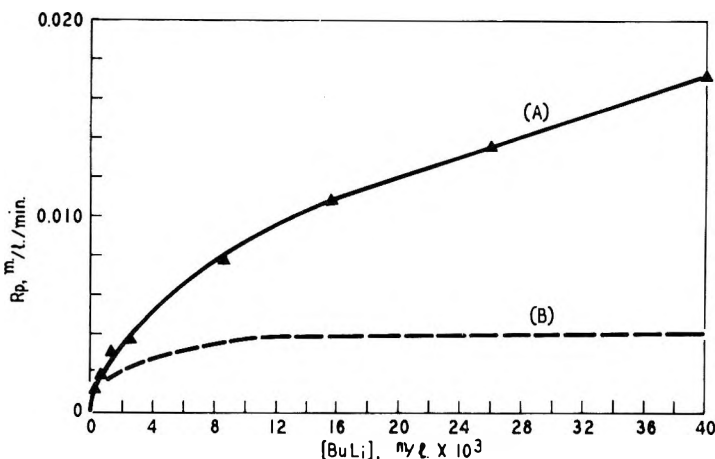
Fig. 3. Rate of propagation of styrene (1.0 mole/l.) in toluene at 5°C.: (A) initiated with sec-BuLi; (B) initiated with n-BuLi (see Part I[3]).
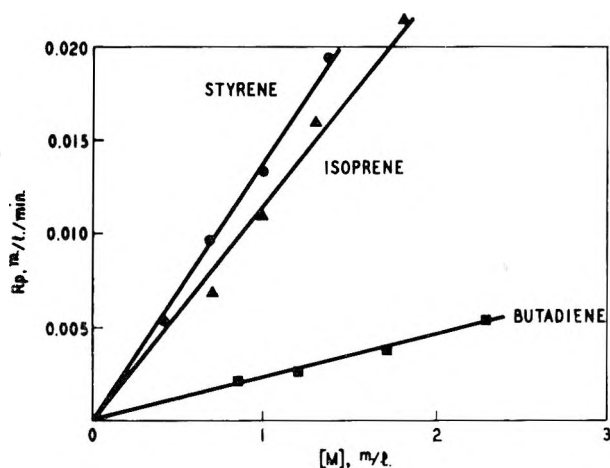
Fig. 4. Rate of propagation in cyclohexane at 30°C. vs. monomer concentration.

Seeded initiators were also employed to check the results obtained from sec-BuLi. At first, n-BuLi was used for the seeded experiments. Approximately 1 mole of butadiene (the monomer with the lowest ratio of propagation to initiation rates) was added incrementally to 0.1 mole of BuLi in 250 ml. cyclohexane at 70 and 100°C. However, chromatographic analysis of the hydrolyzed products proved that about 30% of the n-BuLi remained unreacted. The rates obtained at 30 and 50°C. from this initiator were, in every case, higher than those from unseeded n-BuLi, but lower than rates obtained with unseeded sec-BuLi. Furthermore, the analysis showed that during polymerization an initiation reaction from the unseeded n-BuLi was occurring. Indeed, the propagation and initiation steps were not completely separated. It was concluded that the complete
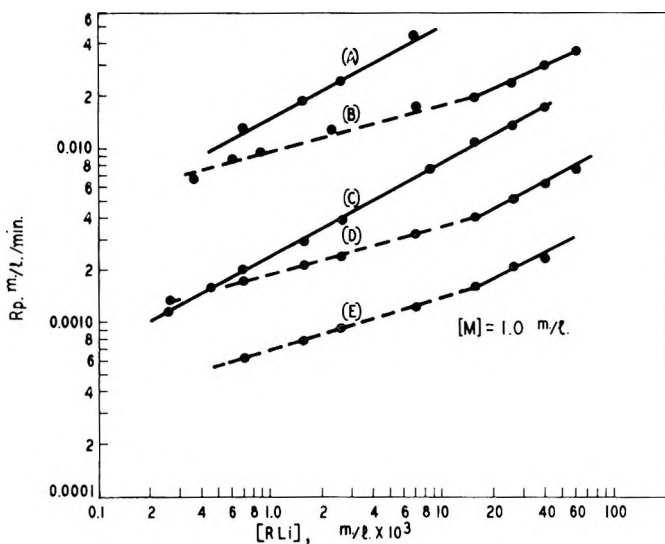
Fig. 5. Rate of propagation vs. [RLi]: (*A*) styrene in cyclohexane at 30°C.; (*B*) isoprene in cyclohexane at 30°C.; (*C*) styrene in toluene at 5°C.; (*D*) butadiene in cyclohexane at 30°C.; (*E*) isoprene in toluene at 5°C.
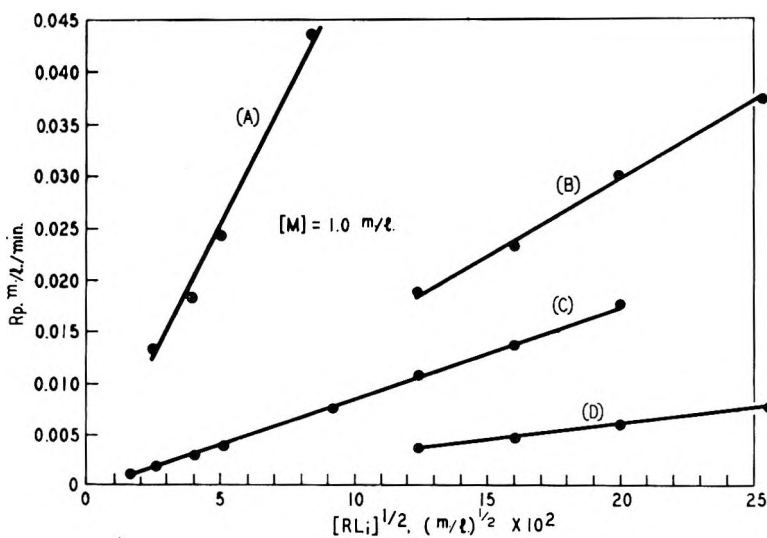
Fig. 6. Rate of propagation vs. $[RLi]^{1/2}$: (*A*) styrene in cyclohexane at 30°C.; (*B*) isoprene in cyclohexane at 30°C.; (*C*) styrene in toluene at 5°C.; (*D*) butadiene in cyclohexane at 30°C.

seeding of *n*-BuLi was rather difficult. However, the preparation of seeded initiator from *sec*-BuLi could be carried out conveniently and with certainty. Hydrolysis and chromatographic analysis of the seeded initiators proved that all the *sec*-BuLi had reacted. The polymerization results were identical, within experimental error, to those obtained from
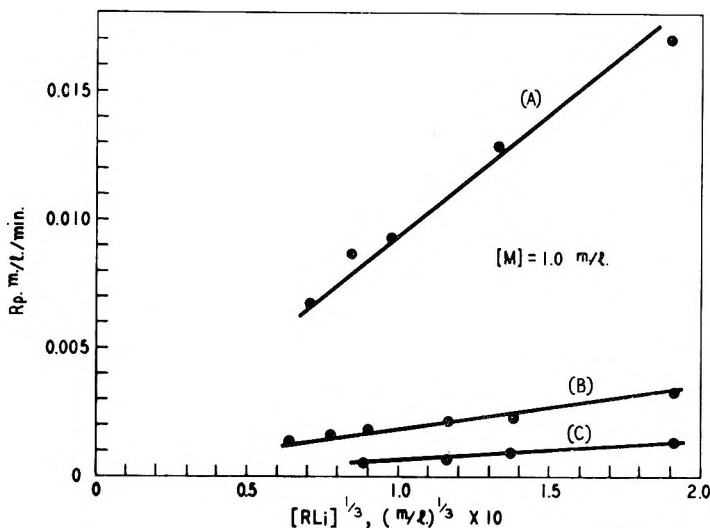
Fig. 7. Rate of propagation vs. $[RLi]^{1/3}$: (A) isoprene in cyclohexane at 30°C.; (B) butadiene in cyclohexane at 30°C.; (C) isoprene in toluene at 5°C.

sec-BuLi directly.   Figures 1–3 show the difference between rate of polymerization obtained from n-BuLi (Part I)[3] and rate of propagation from sec-BuLi and also that rate of propagation was dependent on initiator level.

The relationship between initial rate of propagation and initial monomer concentration [M] was examined.   Figure 4 showed that the rate of propagation was directly proportional to monomer concentration.   Similar conclusions have been reported in the literature.[1,2,5]

The rate of propagation has been reported as proportional to $[RLi]^{1/2}$ for styrene[1,2] as well as for diene monomers.[1]   Another investigator[5] measured only the rate in the later stages of polymerization and showed that the propagation step was almost independent of initiator concentration above 0.02 mole/l. of n-BuLi.   These results at high initiator levels were presumably depressed by the presence of unreacted n-BuLi (the incompleteness of separating initiation from the propagation steps).   In still another study,[6] the overall rate was reported to be proportional to $[RLi]^{1/n}$, with n values of 6 at $10^{-2}M$ and 3 at $10^{-5}M$.

The initial propagation rates and RLi concentrations from our investigation are plotted logarithmically in Figure 5.   Two distinct slopes were observed.   One showed the initial rate was proportional to $[RLi]^{1/2}$ for styrene at $[RLi] > 10^{-4}M$ and for butadiene and isoprene at $[RLi] > 10^{-2}M$. The other slope demonstrated that the initial rate was proportional to $[RLi]^{1/3}$ for dienes at $[RLi]$ between 10^{-4} and $10^{-2}M$.   These two proportionalities are also shown in Figures 6 and 7.

It is interesting to observe that a proportionality of between $^1/_5$ and $^1/_6$ was obtained for diene monomers when the incompletely seeded n-BuLi was used.   This, of course, does not represent a true relationship between

R_p and [RLi], since the initiation reaction was not completely separated from propagation reaction.

IV. DISCUSSION

In the case of diene monomers at [RLi] $>10^{-2}M$ and styrene, $R_p = k_p[\text{RLi}]^{1/2}[\text{M}]$. Here no unreacted BuLi is present to associate with polymer-Li. However, polymer-Li association can occur to temporarily inactivate the propagating anion. The propagation reaction is

$$\text{P*} + \text{M} \xrightarrow{k_2} \text{P'*} \tag{1}$$

and the association reaction is

$$\text{P*} + \text{P*} \underset{k_{-3}}{\overset{k_3}{\rightleftharpoons}} \text{P·P} \tag{2}$$
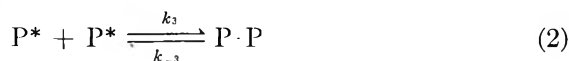
where P* and P'* are unassociated, active polymer-Li, M is monomer, and P·P is associated polymers. Here k_2 is the propagation rate constant, and k_3 and k_{-3} are forward and reverse reaction constants for the association reaction. From eq. (2),

$$k_3/k_{-3} = [\text{P·P}]/[\text{P*}]^2 = K_3 \tag{3}$$

$$[\text{P·P}] = K_3[\text{P*}]^2 \tag{4}$$

The initial BuLi concentration is n_0

$$n_0 = [\text{P*}] + 2[\text{P·P}] \tag{5}$$

and then,

$$[\text{P*}] = n_0 - 2[\text{P·P}] \tag{6}$$

From eqs. (4) and (6)

$$[\text{P*}] = n_0 - 2K_3[\text{P*}]^2 \tag{7}$$

$$[\text{P*}] = (1/4K_3)[(1 + 8K_3n_0)^{1/2} - 1] \tag{8}$$

The rate of propagation R_p is

$$-dM/dt = k_2 [\text{P*}][\text{M}] \tag{9}$$

From eqs. (8) and (9)

$$R_p = (k_2/4K_3)[\text{M}][(1 + 8K_3n_0)^{1/2} - 1] \tag{10}$$

This is the general expression for the rate of propagation. However, at relatively high initial BuLi concentration (n_0), the term $8K_3n_0$ is large, and eq. (10) can be expressed as

$$R_p = (k_2/4K_3)[\text{M}](8K_3n_0)^{1/2} \tag{11}$$

$$= k_2/(2K_3)^{1/2}[\text{M}]n_0^{1/2}$$

At extremely low n_0, $8K_3n_0$ is small.   One can express the rate equation by applying the mathematical approximation of $(1 + A)^m = 1 + mA$.   Therefore,

$$R_p = (k_2/4K_3)[\text{M}](4K_3n_0) = k_2[\text{M}]n_0 \tag{12}$$

The kinetic equations predict a square root relationship at high RLi concentration and first-order at very low RLi concentration.   The association of polymer molecules to form a dimer had been suggested by Morton[1] based on intrinsic viscosity determinations of terminated and unterminated polymer solutions.   The reason for observed relationship of R_p to $[\text{RLi}]^{1/3}$ for both dienes at [RLi] between 10^{-4} and $10^{-2}M$ is not understood.   An assumption of formation of trimer, instead of dimer, can be made here. However, this is not in agreement with Morton's work,[1] which showed that polydienes as well as polystyrene have association numbers of $n = 2$. Furthermore, it is difficult to visualize the formation of dimer at higher concentration and trimer at lower concentration.   Nevertheless, our relationship was shown with both dienes with either sec-BuLi or seeded initiator, in cyclohexane or toluene and at both 30 and 5°C.   Lundborg and Sinn[6] reported earlier that the overall rate of polymerization is proportional to $[\text{RLi}]^{1/3}$ at [RLi] of $10^{-5}M$.   The exact meaning of overall rate is not clear, but the expression is in agreement with our data.   The discrepancy between this and Morton's results requires further investigation.

TABLE I

Rate of Propagation Constants

| Solvent | Temp., °C. | Monomer | | | | Styrene, $k_p{}^a$ |
| | | Butadiene | | Isoprene | | |
		$k_p{}^a$	$k_p{}'^b$	$k_p{}^a$	$k_p{}'^b$	
Cyclohexane	30	0.033	0.020	0.155	0.096	0.494
Toluene	5	—	—	0.012	0.0067	0.080

[a] $R_p = k_p[\text{RLi}]^{1/2}[\text{M}]$; [RLi] $> 10^{-2}$ mole/l. for dienes and $>10^{-4}$ mole/l. for styrene.
[b] $R_p = k_p'[\text{RLi}]^{1/3}[\text{M}]$; [RLi] $> 10^{-4}$ mole/l. but $< 10^{-2}$ mole/l. for dienes.

Some propagation rate constants were calculated as shown in Table I to demonstrate the relative rates for different monomers and in different solvents.

References

1. Morton, M., et al., J. Polymer Sci., 61, 311 (1963).
2. Worsford, D. J., and A. Bywater, Can. J. Chem., 38, 1891 (1960).
3. Hsieh, H. L., J. Polymer Sci., A3, 153 (1965).
4. Hsieh, H. L., J. Polymer Sci., A3, 163 (1965).
5. Welch, F. J., J. Am. Chem. Soc., 81, 1345 (1959).
6. Lundborg, G., and H. Sinn, Makromol. Chem., 41, 242 (1960).

Résumé

On a obtenu des vitesses initiales de propagation (R_p) pour le butadiène, l'isoprène et le styrène, avec le sec-BuLi comme initiateur. Avec cet alcoyl-lithium l'initiation a lieu si rapidement qu'on a étudié uniquement la propagation. Dans le cas des monomeres diéniques pour (RLi) > 10^{-2} mol et pour le styrène, $R_p = k_p[\text{RLi}]^{1/2}[\text{M}]$. Dan, ce cas il n'y a pas de BuLi qui n'a pas réagi, et s'associerait au lithium du polymère. Toutefois l'association avec le lithium du polymère peut se faire en désactivant provisoirement l'anion propagateur. On propose un mécanisme et on en déduit les équations cinétiques. Quand (RLi) est 10^{-4} à 10^{-2} molaire, $R_p = k_p[\text{RLi}]^{1/8}[\text{M}]$ pour les deux diènes mais pas pour le styrène. On a calculé quelques constantes de vitesse de propagation. L'ordre de la vitesse de propagation pour les trois monomères est styrène > isoprène > butadiène.

Zusammenfassung

Anfangswachstumsgeschwindigkeiten (R_p) wurden für Butadien, Isopren und Styros mit sek-BuLi als Starter erhalten. Mit diesem Alkyllithium war der Start so schnell dass das Wachstum allein leicht untersucht werden konnte. Im Fall der Diene bei [RLi] > 10^{-2} Molar und von Styrol, $R_p = k_p[\text{RLi}]^{1/2}[\text{M}]$. Hier ist kein unreagiertes BuLi vorhanden, das mit Polymer-Li assoziieren könnte. Es kann jedoch Polymer-Li-Assoziation auftreten und temporär das wachsende Anion inaktivieren. Ein Mechanismus wurde vorgeschlagen und die kinetischen Gleichungen abgeletit. Wenn [RLi] zwischen 10^{-4} und 10^{-2} Molar liegt, gilt für beide Diene, nicht aber für Styrol $R_p = k_p[\text{RLi}]^{1/3}[\text{M}]$. Einige Wachstumsgeschwindigkeitskonstanten wurden berechnet. Die Reihenfolge der Wachstumsgeschwindigkeit für die drei Monomeren war Styrol > Isopren > Butadien.

Microstructures of Polydienes Prepared from Alkyllithium

HENRY L. HSIEH, *Research and Development Department, Phillips Petroleum Company, Bartlesville, Oklahoma*

Synopsis

The stereochemistry of polymerization of isoprene and butadiene by means of alkyllithium initiators was examined. The stereochemistry of polybutadiene and polyisoprene responded to the same variables in anionic polymerization. Microstructure of both polymers is sensitive to initiator level, solvent type, and polymerization temperature, but is independent of monomer concentration, conversion and initiator structure. The heat activation energy leading to 1,2 addition is greater than that leading to *trans*-1,4 addition (1200 cal./mole). The exact pictorial sequence leading to stereospecific polymerization of dienes by means of alkyllithium is still not clear. However, it seems to involve the orientation of the incoming monomer units by association and passage through a transition complex in which all bonds are largely covalent in character and within which polymerization occurs.

I. INTRODUCTION

The polymerization of isoprene by means of alkyllithium initiators has been studied extensively. Hsieh and Tobolsky reported that high-*cis* polyisoprene could be prepared with alkyllithium in heptane or benzene.[1] Polymers prepared in ethers showed a change in stereochemistry toward increased isopropenyl (3,4 addition product), vinyl (1,2 addition product), and *trans* unsaturations.[2] The microstructure was found to be independent of the organic moiety of the initiator.[3] The effects of the alkyllithium structure, solvent type, temperature, initiator level, conversion and complexing agents on the polymer stereochemistry were further investigated by others.[4-6]

Ziegler reported the polymerization of butadiene with BuLi,[7] and an Australian patent was granted to Foster in this area.[8] However, examination of the stereochemistry of polymerization of butadiene by means of alkyllithium received very little attention. Kuntz and Gerber described the effect of polymerization variables on the polymer microstructure.[9] Considerable differences were observed between their work with polybutadiene and that of others with polyisoprene. This report attempts to clarify some of the discrepancies reported in literature and provide new information leading to better understanding of the stereochemistry of anionic polymerization of dienes.

II. EXPERIMENTAL

A. Materials

The solvents employed, petroleum-derived toluene, reagent grade benzene, pure grade n-pentane and n-heptane, and polymerization grade cyclohexane were dried by countercurrent scrubbing with prepurified nitrogen followed by passage over activated alumina. Phillips' special purity butadiene was distilled through sodium dissolved in ethylene glycol before it was condensed and transferred into bottles containing Drierite. Phillips' polymerization grade isoprene was refluxed over sodium wire in a nitrogen atmosphere for about 3 hr. and distilled into bottles. Both monomers were stored in a deepfreeze. The n-BuLi in heptane and sec-BuLi, $tert$-BuLi and isopropyllithium in pentane were obtained from Lithium Corporation of America as approximately $2M$ solutions. Allyllithium in heptane was obtained from Orgmet.

B. Polymerization Procedure

Polymerizations were carried out in new beverage bottles which were cleaned and air-dried at 60°C. Solvent was first added to each bottle under a nitrogen blanket through a specially constructed and calibrated solvent charging apparatus. After the solvent was introduced, prepurified nitrogen was dispersed through a fritted glass tube and purged through the solvent at the rate of 3 l./min. for 10 min. in an effort to remove residual amounts of moisture and air. The bottles were capped with toluene-extracted, self-sealing rubber gaskets and perforated metal caps having three holes. Monomer was added directly to the solvent from a calibrated monomer dispenser. The solution was brought to desired reaction temperature by tumbling the bottles in a constant temperature bath. Then the initiator solution was added from a calibrated syringe. The bottles were tumbled in the constant temperature bath for the necessary time. To prevent any possible leakage into the bottle cap in the bath, 25 psi of prepurified nitrogen pressure was introduced into the bottle after all the reagents were added. For high temperature studies, (higher than 70°C.) polymerization was carried out in a modified 1-liter Paar reactor. Polymers were recovered by coagulation with isopropyl alcohol and dried in a vacuum oven. 2,2'-Methylene bis(4-methyl-6-$tert$-butylphenol) (3 wt.-%) was added as anti-oxidant to the polymer solution before coagulation.

C. Analyses

The microstructures of the polymers were determined by infrared spectroscopy. Spectra of all samples were obtained with either Perkin-Elmer Model 21 or an Infracord Instrument equipped with sodium chloride prisms. Samples were examined as 2.5% solutions of polymer in carbon disulfide between potassium bromide plates of conventional, sealed absorption cells.

For polybutadiene, the procedure developed by Silas, Yates, and Thornton[10] was employed. However, *cis* unsaturation was not actually determined. The estimated values were obtained by assuming the polymer had 100% unsaturation. For polyisoprene, *cis* and isopropenyl unsaturations were measured at 8.86 and 11.25μ respectively. Calibration was accomplished by using purified, deproteinized natural rubber, assumed to have 99% *cis* unsaturation, and 2-methyl-1-hexene as standards; the *trans* unsaturations were estimated.

Inherent viscosity was determined in toluene at 25°C. No gel was observed in the samples.

III. RESULTS

The microstructure of polybutadiene and polyisoprene was again demonstrated to be independent of the organic moiety of the alkyllithium initiator. The experimental results are shown in Tables I and II. The data also showed the dependence of the polymer microstructure on the solvent type, and molecular weight of the polymer and, therefore, the initial initiator concentration.

The relationship between the microstructure of the polymer and the initial initiator concentration (basically, the molecular weight of the polymer at quantitative conversion) was further examined under identical and controlled conditions. The results are shown in Tables III and IV. Figures 1 and 2 show the general relationship between configurations of polybutadiene and polyisoprene prepared with different alkyllithium

TABLE I

Effect of the Structure of Alkyllithium on Microstructure of Polybutadiene Prepared at 50°C.

Solvent	RLi	Inherent viscosity	Configuration, %		
			trans	*cis*	Vinyl
Cyclohexane	*n*-BuLi	6.26	36.8	58.0	5.2
	tert-BuLi	6.10	35.8	57.8	6.4
	n-BuLi	2.92	48.9	44.2	6.9
	tert-BuLi	2.55	49.5	43.6	6.9
	tert-BuLi	1.84	48.7	44.7	6.6
	Allyl Li	1.70	49.1	44.1	6.8
	n-BuLi	1.30	54.3	38.7	7.0
	tert-BuLi	1.29	52.3	40.7	7.0
	i-PrLi	1.34	51.7	41.3	7.0
	Allyl Li	1.15	52.7	39.9	7.4
	i-PrLi	0.83	53.6	39.2	7.2
	tert-BuLi	0.65	54.6	38.3	7.1
	n-BuLi	0.54	54.0	38.7	7.3
	n-BuLi	0.34	54.9	37.8	7.3
	tert-BuLi	0.34	54.7	38.0	7.3
Toluene	*n*-BuLi	1.80	51.1	38.7	10.2
	sec-BuLi	1.31	51.1	38.6	10.3

TABLE II

Effect of the Structure of Alkyllithium on Microstructure of Polyisoprene Prepared at 50°C.

Solvent	RLi	Inherent viscosity	Configuration, %			
			cis	trans	Isopropenyl	Vinyl
Cyclohexane	n-BuLi	6.06	84.2	10.2	5.6	0
	sec-BuLi	6.13	84.2	11.5	4.3	0
	n-BuLi	2.96	76.6	16.6	6.8	0
	tert-BuLi	2.48	76.6	16.8	6.6	0
	n-BuLi	1.54	75.0	17.9	7.1	0
	tert-BuLi	1.42	76.6	15.6	7.8	0
	i-PrLi	0.86	70.4	22.1	7.5	0
	i-PrLi	0.48	68.9	23.3	7.8	0
	n-BuLi	0.37	70.4	21.8	7.8	0
	tert-BuLi	0.31	68.9	23.3	7.8	0
Toluene	n-BuLi	1.17	64.3	26.0	9.7	0
	sec-BuLi	1.10	67.4	25.9	9.7	0

TABLE III

Effect of Butyllithium Level on Microstructure of Polybutadiene Prepared in Cyclohexane at 50°C.

[n-BuLi], mmoles/100 g. monomer	Inherent viscosity[a]	Configuration, %		
		trans	cis	Vinyl
0.10	7.92	34.1	60.8	5.1
0.15	6.15	39.3	54.3	5.4
0.20	3.95	44.1	50.0	5.9
0.30	2.93	45.5	48.5	6.0
0.40	2.40	48.7	45.1	6.2
0.50	2.16	48.5	45.1	6.4
0.60	2.06	51.5	41.8	6.7
2.7	0.78	53.1	40.3	6.6
39.7	0.19	52.6	40.1	7.3

[a] 100% conversion.

TABLE IV

Effect of Butyllithium Concentration on Microstructure of Polyisoprene Prepared in Cyclohexane at 50°C.

[n-BuLi], mmoles/100 g. monomer	Inherent viscosity[a]	Configuration, %			
		cis	trans	Isopropenyl	Vinyl
<0.1	6.06	84.2	10.1	5.7	0
0.4	2.12	70.0	23.0	7.0	0
1.4	1.00	67.4	25.3	7.3	0
4.4	0.49	67.4	25.1	7.5	0
39.4	0.19	61.3	30.8	7.9	0

[a] 100% conversion.
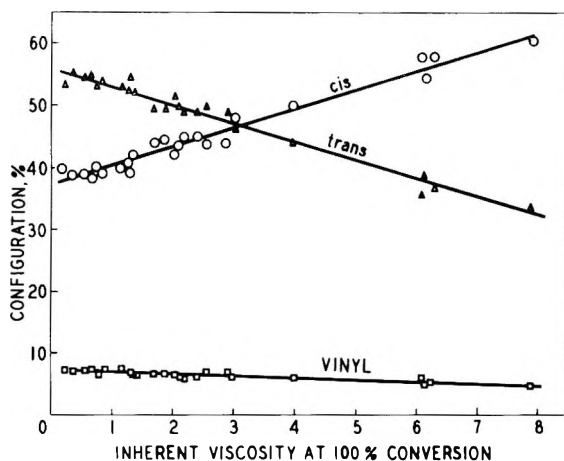
Fig. 1. Microstructure of polybutadiene initiated with alkyllithium in cyclohexane at 50°C.
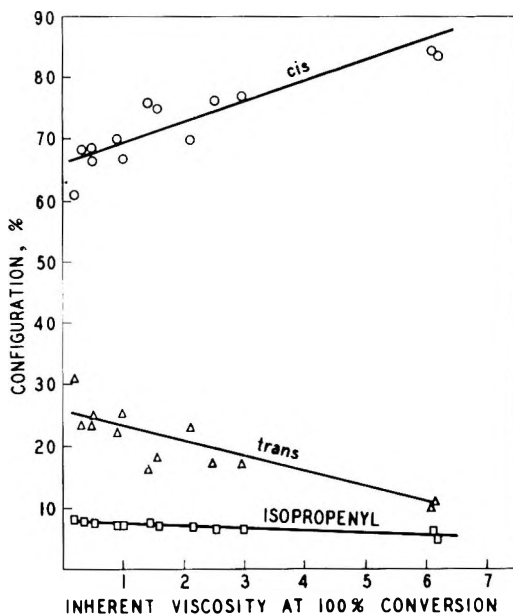
Fig. 2. Microstructure of polyisoprene initiated with alkyllithium in cyclohexane at 50°C.

initiators and the inherent viscosity of the polymers at quantitative conversion.

Polymer microstructure as a function of conversion is shown in Figure 3. For both polybutadiene and polyisoprene it is independent of conversion within experimental error.

The results obtained by using different nonpolar solvents, are shown in Table V. Use of aromatic solvents, particularly toluene, increased the
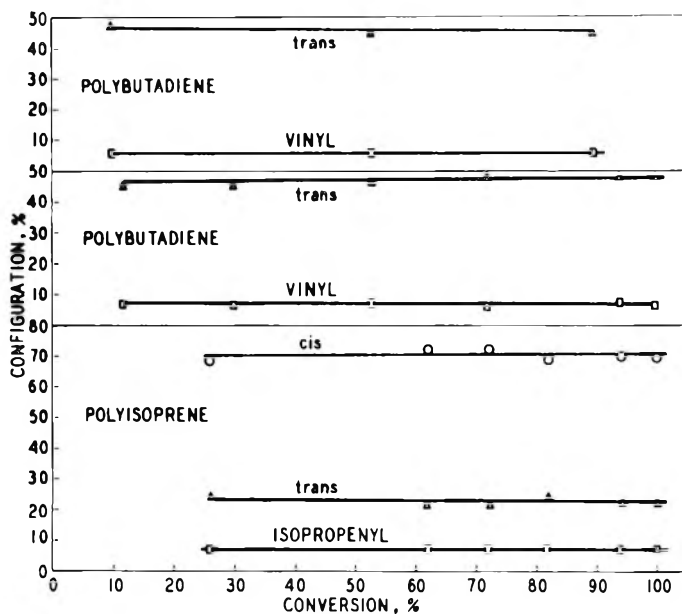
Fig. 3. Microstructure of polymer vs. conversion.

vinyl unsaturation of the polybutadiene. Similar results were also observed for polyisoprene.

Table VI shows the results at constant [M]/[BuLi] and variable solvent levels (monomer concentrations). A fourfold increase of solvent level did not alter the microstructure of the polybutadiene.

TABLE V

Effect of Nonpolar Solvent on Microstructure of Polybutadiene Prepared at 50°C.

Solvent	Inherent viscosity	Configuration, %		
		trans	cis	Vinyl
Toluene	1.66	51.5	37.4	11.1
Benzene	1.34	52.9	37.2	9.9
Cyclohexane	1.43	53.8	38.9	7.3
n-Heptane	1.60	54.7	38.3	7.0
n-Pentane	1.07	53.3	39.4	7.3

TABLE VI

Effect of Solvent Level on Microstructure of Polybutadiene Prepared at 50°C.
[n-BuLi] = 0.6 mmole/100 g. monomers)

Cyclohexane, g./100 g. monomer	Cyclohexane, Inherent viscosity	Configuration, %		
		trans	cis	Vinyl
1560	2.22	49.5	44.2	6.3
780	2.12	50.5	43.1	6.4
390	2.46	50.1	43.2	6.7
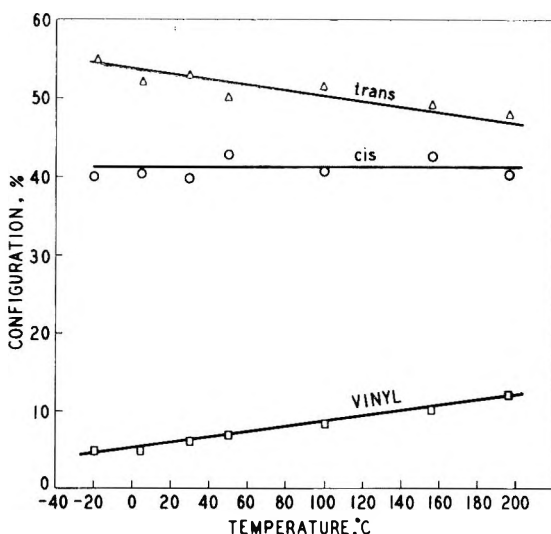
Fig. 4. Effect of temperature of polybutadiene prepared in cyclohexane.

The effect of polymerization temperature on microstructure of poly-butadiene in cyclohexane at constant BuLi concentration is shown in Figure 4. As in the case of polyisoprene,[6] the microstructure of poly-butadiene is dependent on polymerization temperature.

IV. DISCUSSION

Polymerization of isoprene in nonpolar solvent by alkyllithium resulted largely in *cis* unsaturation (70–90%), and polymerization of butadiene resulted in a large amount of *cis* unsaturation (40–60%) and *trans* un-saturation (35–55%). Nevertheless, in both instances, the *cis* unsaturation decreased and vinyl (or isopropenyl) and especially *trans* unsaturation in-creased with the increase of initiator level. Stearns and Forman[6] have suggested that the association of initiator, RLi, and polydienyllithium, $R(M)_n Li$, interfered with the formation of a cyclic activated complex in much the same manner as ethers and the net-result is to lead to *trans* unsaturation and 3,4 addition product. However, it has been shown[11] that for diene monomers, the initiation with *sec*-BuLi, *i*-PrLi, and *tert*-BuLi is extremely rapid and that all the initiator, even at very high levels, is completely consumed at a very early stage of the polymerization. Yet, the polymer microstructure changed with very small changes of the initiator level in these systems. Furthermore, by use of these initiators which in most instances were completely consumed at less than 5–10% conversion, the same microstructure resulted as those in polymers initiated with *n*-BuLi at concentrations which are not completely used up at the end of polymerization.[11] Furthermore, at *n*-BuLi levels of 0.1 and 0.4 mmoles/ 100 g. of butadiene, no unreacted BuLi remained in the system after about 10% conversion.[11] Examination of data in Table III showed the *cis*
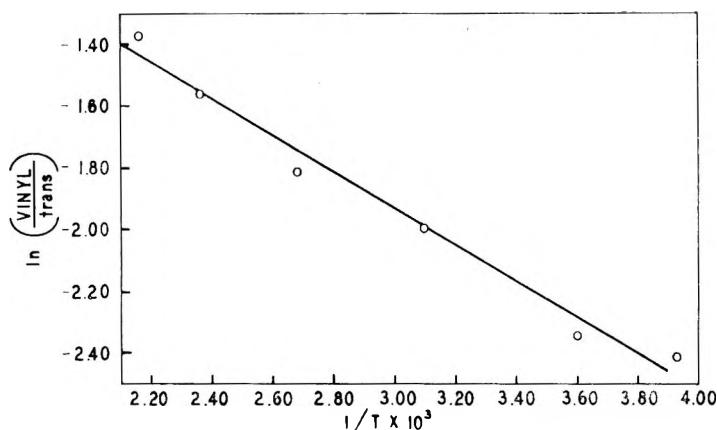
Fig. 5. Effect of temperature on stereochemistry of polybutadiene.

unsaturation of polybutadiene changed from 61% to 45%. Therefore, the suggestion that association of initiator and active polymer chain-end interfered with stereospecificity of polymerization is not consistent with experimental facts.

Raman spectroscopy has indicated that isoprene monomer contains 85% *cis* isomer at 50°C. and that the calculated energy difference between the *cis* and *trans* resonance isomers is 900 cal./mole.[12] For butadiene, it was estimated that the equilibrium mixture contains less than 4% *cis* isomer at room temperature[13] and that the energy difference between the more stable *trans* and the *cis* isomer is about 2000 cal./mole.[14] The preparation of *cis*-polyisoprene, therefore, could be explained as due to a *cis* coordination complex of the monomer in the *cis* configuration with the C-Li bond of the growing polymer.[6] By applying the same reasoning, one would expect the formation of high-*trans* polybutadiene from alkyllithium initiation. The inability of this system to prepare high-*trans* polybutadiene indicated that the energetic differences, indeed, do not influence the polymer microstructure. Kuntz and Gerber have postulated that the steric requirements and energy of both the *cis* and *trans* configurations of butadiene are not very different. In effect, the polymer C-Li bond must convert molecules in the *trans* configuration in solution into *cis* molecules in the coordination complex.[9]

The effect of polymerization temperature on the stereochemistry can be expressed by an Arrhenius-type equation as shown in Figure 5. It is calculated that the overall heat activation energy leading to 1,2 addition is greater than that leading to *trans*-1,4 addition ($\Delta H_t - \Delta H_v = -1200$ cal./mole). It is also found that entropy of activation is greater for 1,2 addition than *trans*-1,4 addition ($\Delta S_t - \Delta S_v = -0.4$ e. u.).

The data presented here demonstrated that the stereochemistry of polybutadiene and polyisoprene responded to the same variables in anionic polymerization. The microstructure of both polymers is sensitive to initiator level, solvent type, and polymerization temperature, but is in-

dependent of monomer concentration, conversion, and initiator structure. This is contrary to the results reported that the *cis* unsaturation of polyisoprene decreased as conversion was increased[6] and that the microstructure of polybutadiene is independent of temperature and initiator level.[9] The exact pictorial sequence leading to stereospecific polymerization of dienes by means of alkyllithium is still not clear. However, it is generally agreed[5,6,9] that it involves the orientation of the incoming monomer units by association and passage through a transition complex in which all bonds are largely covalent in character and within which polymerization occurs.

References

1. Hsieh, H., and A. V. Tobolsky, *J. Polymer Sci.*, **25**, 245 (1957).
2. Hsieh, H., D. J. Kelley, and A. V. Tobolsky, *J. Polymer Sci.*, **26**, 240 (1957).
3. Hsieh, H. L., Thesis, Princeton University, 1957.
4. Morita, H., and A. V. Tobolsky, *J. Am. Chem. Soc.*, **79**, 5853 (1957).
5. Tobolsky, A. V., and C. E. Rogers, *J. Polymer Sci.*, **40**, 73 (1959).
6. Stearns, R. S., and L. E. Forman, *J. Polymer Sci.*, **41**, 381 (1959).
7. Ziegler, K., and L. Jakob, *Ann. Chem. Liebigs*, **511**, 45 (1934).
8. Foster, F. C. (Firestone Tire and Rubber Company), Australian Pat. 222,373 (October 29, 1959).
9. Kuntz, I., and A. Gerber, *J. Polymer Sci.*, **42**, 299 (1960).
10. Silas, R. S., J. Yates, and V. Thornton. *Anal. Chem.*, **31**, 529 (1959).
11. Hsieh, H. L., *J. Polymer Sci.*, **A3**, 163 (1965).
12. Nikitin, V. N., and T. V. Yakovleva, *Zhur. Fiz. Khim.*, **28**, 696 (1954);
13. Richards, C. M., and J. R. Nielsen, *J. Opt. Soc. Am.*, **40**, 438 (1950).
14. Aston, J. G., G. Szosz, and H. W. Woodley, *J. Chem. Phys.*, **14**, 67 (1946).

Résumé

On a étudié la stéréochimie de la polymérisation de l'isoprène et du butadiène au moyen d'alcoyl-lithium comme initiateur. La stéréochimie du polybutadiène et du polyisoprène répond aux mêmes variables en polymérisation anionique. La microstructure des deux polymères est sensible a la quantité d'initiateur, au type de solvant et à la température de polymérisation, mais est indépendante de la concentration en monomère, du degré de conversion et de la structure de l'initiateur. L'énergie d'activation conduisant à l'addtion-1,2 est plus grande que celle conduisant à la *trans*-addition-1,4 (1200 cal/mole). L'image exacte des séquences conduisant à la polymérisation stéréospécifique des diènes au moyen d'alcoyl-lithium n'est pas encore éclaircie, cependant il semble qu'il y ait une orientation des unités de monomères par association et passage au travers d'un complexe transitoire dans lequel tous les liens sont largement covalents et par lequel la polymérisation se poursuit.

Zusammenfassung

Die Stereochemie der Polymerisation von Isopren und Butadien bei Alkyllithium-Start wurde untersucht. Die Stereochemie von Polybutadien und Polyisopren hängt von den gleichen Variablen bei der anionischen Polymerisation ab. Die Mikrostruktur beider Polymern spricht auf die Startermenge, den Lösungsmitteltyp und die Polymerisationstemperatur an, ist aber unabhängig von Monomerkonzentration, Umsatz und Starterstruktur. Die Aktivierungsenergie für die 1,2-Addition ist grösser als diejenige für die *trans*-1,4-Addition (1200 cal./Mol). Die genaue Folge der Ereignisse, die zur stereo-

spezifischen Polymerisation von Dienen in Alkyllithium führt, ist noch nicht klar. Es scheint jedoch eine Orientierung der herantretenden Monomereinheiten durch Assoziation und Bildung eines Ubergangkomplexes stattzufinden, in welchem alle Bindungen grösstenteils covalenten Charakter besitzen und innerhalb welchem die Polymerisation abläuft.

Molecular Weight and Molecular Weight Distribution of Polymers Prepared from Butyllithiums

HENRY L. HSIEH, *Research and Development Department, Phillips Petroleum Company, Bartlesville, Oklahoma*

Synopsis

The calculated kinetic molecular weight M_k was compared with experimentally determined viscosity molecular weight M_v of polybutadiene, polyisoprene, and polystyrene initiated with *n*-BuLi, *sec*-BuLi, and *tert*-BuLi. The discrepancy between M_k and M_v depends on the ratio of rates of initiation R_i and propagation R_p, which in turn depends on initiator structure and monomer. In the alkyllithium-initiated polymerization system, M_k based on the [RLi] consumed rather than charged, is almost equal to the actual molecular weight. The ratio of R_i and R_p also affects the molecular weight distribution. The order of monodispersity for polydienes is *sec*-BuLi $\cong$ *tert*-BuLi > *n*-BuLi. For styrene, it is *sec*-BuLi $\gg$ *n*-BuLi $\gg$ *tert*-BuLi. The fractionation data are in perfect agreement with the predictions of the kinetic data. The ideal conditions for the preparation of monodispersed polymer by means of anionic polymerization are also discussed.

I. INTRODUCTION

It has been generally accepted[1-8] that polymerization of diene and styrene monomers with alkyllithium is a stepwise addition reaction with no true termination reaction. In most hydrocarbon solvents at normal temperatures, there is no chain transfer. In theory, then, the polymer thus formed should have a molecular weight equal to 100/[RLi], where [RLi] is the number of moles of RLi/100 g. of monomer. The polymer should also be monodispersed.

Our kinetic data[8] showed that the rate of initiation R_i depends on the monomer and the structure of alkyllithium. In this investigation, an attempt was made to show the close relationships between the ratio of rates of initiation and propagation (R_i/R_p) and molecular weight of polymer as well as molecular weight distribution.

II. EXPERIMENTAL

A. Materials and Polymerization Procedure

The materials used and the polymerization technique are described extensively elsewhere.[8] Small amounts of impurities present in the polymerization systems were not removed. The amount of alkyllithium destroyed by the impurities was called the scavenger level and was predetermined for each monomer-solvent combination. The scavenger level

varied from 0.2×10^{-3} to 0.4×10^{-3} mole/l. The alkyllithium level used to calculate the kinetic molecular weight is the effective level, namely the difference between the charged and the scavenger levels.

B. Viscosity Measurements

The solution viscosity of the polymers was determined in toluene at 25°C. in the usual manner. Viscosity molecular weight M_v was calculated from intrinsic viscosity by the relation:

$$[\eta] = kM_v^a$$

where, for butadiene,[9] $k = 2.17 \times 10^{-4}$, $a = 0.75$; for isoprene,[10] $k = 5.02 \times 10^{-4}$, $a = 0.67$; and for styrene,[11] $k = 1.7 \times 10^{-4}$, $a = 0.69$.

C. Fractionations

The column method of fractionation of polymers utilizes both a solvent gradient and a temperature gradient. Each of these gradients used individually would perform a single-phase extraction of the sample, but used together they constitute a multiphase extraction.

The column used was a 100 cm. long, 4 cm. diameter glass column fitted at the lower end with a Teflon metering valve. The column was enclosed in an insulating jacket to maintain a temperature gradient along the column varying from 44°C. at the top to 24°C. at the bottom. The column was packed with 0.1 mm. glass microbeads which had been acid-washed and dried prior to use. The solvent gradient was provided by a stainless steel reservoir system containing mixtures of isopropyl alcohol and toluene. A nitrogen atmosphere was maintained in the reservoir system. The fractions were collected in an automatic fraction collector.

A 1-g. polymer sample was dissolved in a mixture of isopropyl alcohol and toluene in which it was barely completely soluble at 65°C. This polymer solution at 65°C. was charged into the column which had been preheated to about the same temperature. The column was then allowed to cool to room temperature over an 8-hr. period. This allowed the polymer to slowly precipitate onto the beads in reverse order of molecular weight to that at which it will be removed. The column was then heated to the operating temperatures (44–24°C.) and allowed to equilibrate. The mixing reservoir which contained the same ratio of isopropyl alcohol and toluene as that from which the sample was precipitated was attached to the top of the column. A siphon was established between the mixing reservoir and the solvent reservoir which contained pure toluene. Both reservoirs contained antioxidant.

The Teflon metering valve at the bottom of the column was adjusted to a flow rate of about 20 ml./hr. Progress of the fractionation was followed by determining the solid content of a 5 ml. aliquot of each fraction. The fractions were combined in such a manner that the combined fractions each contained about 5% of the total polymer.

III. RESULTS

A. Molecular Weight

The linear relationships between log η (where η is inherent viscosity) and log [BuLi], over a wide range of [BuLi], for three polymers are shown in
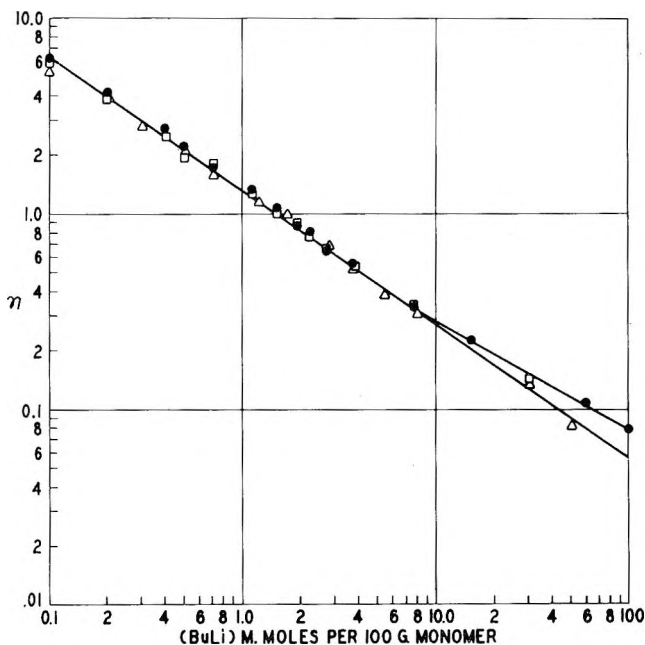
Fig. 1. Inherent viscosity and initiator level relationship for polybutadiene: ($\bullet$) n-BuLi; ($\triangle$) sec-BuLi; ($\square$) $tert$-BuLi.

TABLE I

Kinetic Molecular Weight M_k versus Viscosity-Average Molecular Weight M_v for Polybutadiene, Polyisoprene, and Polystyrene

$M_k \times 10^{-3}$	$M_v \times 10^{-3}$					
	Polybutadiene	Polyisoprene		Polystyrene		
	n-, sec-, and $tert$-BuLi	n-BuLi	sec- and $tert$-BuLi	n-BuLi	sec-BuLi	$tert$-BuLi
500	—	—	—	490	470	580
200	210	220	195	250	196	315
100	110	126	97	140	98	190
50	54	67	49	75	50	125
25	29	—	—	44	26	69
20	—	33	19	—	—	—
10	12	19	10	21	12	41
5	—	11	5	—	—	—
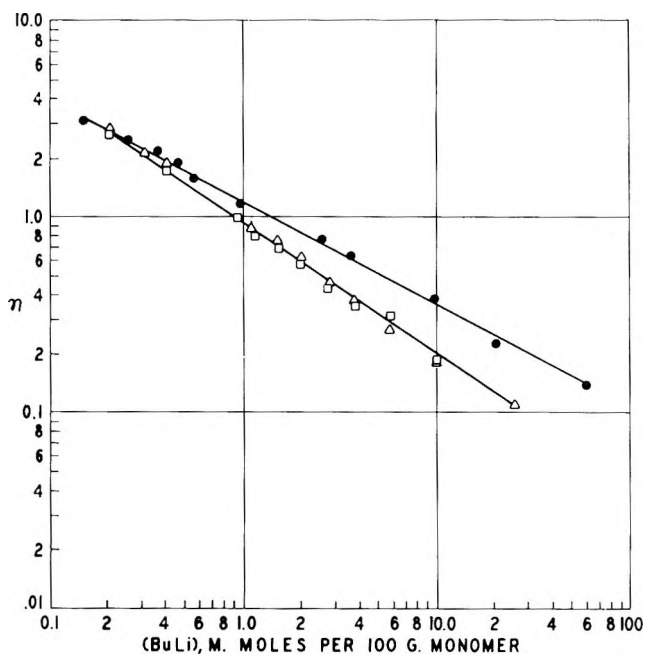
Fig. 2. Inherent viscosity and initiator level relationship for polyisoprene: (●) n-BuLi (△) sec-BuLi; (□) tert-BuLi.
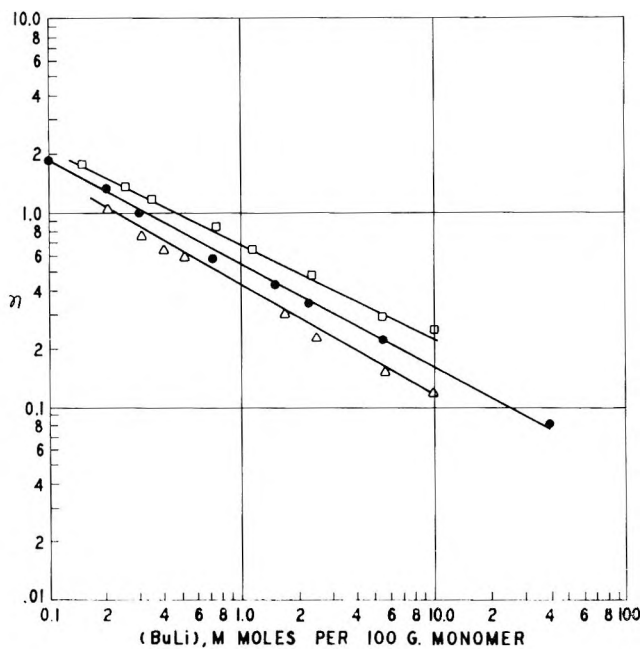
Fig. 3. Inherent viscosity and initiator level relationship for polystyrene: (●) n-BuLi; (△) sec-BuLi; (□) tert-BuLi.

Figures 1–3. In the case of polybutadiene, only one line can be drawn through all the points (up to [BuLi] = 10 mmole/100 g. monomer). Two and three lines are drawn for polyisoprene and polystyrene, respectively.

Table I shows the comparison of calculated kinetic molecular weight and viscosity molecular weight for three polymers initiated with n-BuLi, sec-BuLi, and tert-BuLi.

It can be readily seen that for polybutadiene, no appreciable difference in molecular weight was observed with three butyllithiums. Only at extremely high initiator level (10 mmole/100 g. butadiene or higher), could a slight increase in molecular weight be detected with n-BuLi. Furthermore, the viscosity molecular weights were in fairly good agreement with kinetic molecular weight. For polyisoprene, samples initiated with n-BuLi gave consistently higher molecular weight than those initiated with sec-BuLi and tert-BuLi. Considerable discrepancy between viscosity molecular weight and kinetic molecular weight, particularly in the lower range, was observed with n-BuLi. For polystyrene, samples initiated with tert-BuLi gave highest molecular weight and sec-BuLi gave the lowest. The discrepancy between the kinetic and viscosity molecular weights was quite substantial with n-BuLi and even more so with tert-BuLi. In all the cases, again, the lower the molecular weight, the greater was the discrepancy.

B. Molecular Weight Distribution

Fractionation results are shown in Figures 4–6. A polybutadiene prepared in emulsion is included for comparison. In general, two distinct characteristics of these alkyllithium-initiated polymers are apparent—the extremely narrow molecular weight distribution and the rapid cut-off on the high molecular weight end.

IV. DISCUSSION

Kinetic studies[8] demonstrated clearly that the effective alkyllithium level does not necessarily represent the actual amount of alkyllithium reacted. They also showed that at higher concentrations, proportionally, less alkyllithium was consumed. At the same n-BuLi concentration the most unreacted BuLi was found with styrene or isoprene and least with butadiene.

For butadiene and isoprene, initiation with sec-BuLi and tert-BuLi was very rapid and no unreacted BuLi could be detected at the end of polymerization. With n-BuLi a small amount of unreacted BuLi was found at very high initial BuLi concentration (6–7 mmole/100 g. monomer or higher) for butadiene. Unreacted n-BuLi was found even at concentrations of 2–3 mmoles/100 g. monomer for isoprene. For example, in a polymerization containing 10 mmoles n-BuLi/100 g. isoprene, only about 50% of the BuLi was consumed at the end of polymerization.[8] Therefore the molecular weight is double the value calculated using effective initiator level. This is indeed the case (Table I).
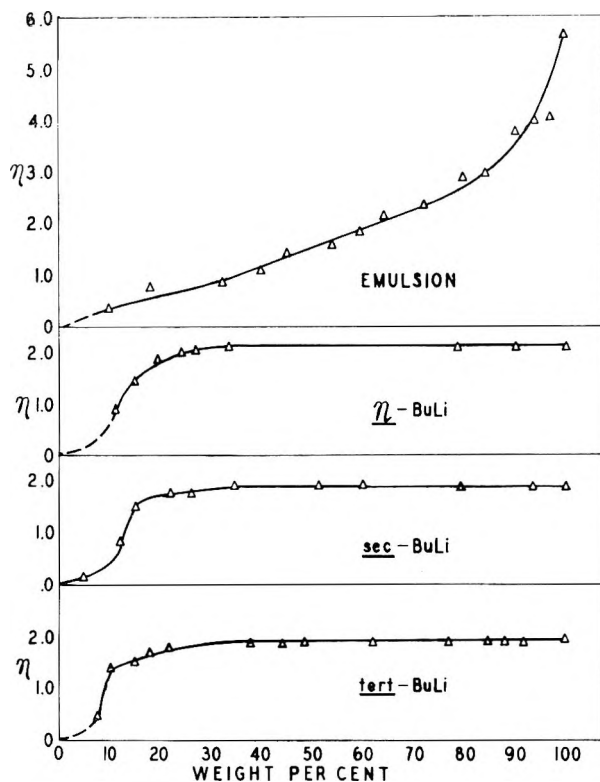
Fig. 4. Fractionation of polybutadiene.

For styrene,[8] tert-BuLi is the slowest initiator and sec-BuLi is the fastest. sec-BuLi is the only one of the three that is completely reacted at the end of polymerization. With n-BuLi, a trace of the unreacted initiator could be found at initial concentration as low as 1 mmole/100 g. styrene. This again is in perfect agreement with the data shown in Table I as well as Figure 3.

It can be stated that in the alkyllithium-initiated polymerization system, M_k based on the [RLi] consumed is almost equal to the actual molecular weight. The use of gas chromatography[8] to determine the unreacted BuLi at the end of polymerization should provide the true initiator level.

In addition to the kinetic molecular weight, the ratio of R_t and R_p should effect the molecular weight distribution. Present work clearly dem-

TABLE II
Effect of Alkyllithium Structure on Molecular Weight Distribution

Polymer	Order of decrease in monodispersity
Polybutadiene	sec-BuLi $\cong$ tert-BuLi > n-BuLi
Polyisoprene	sec-BuLi $\cong$ tert-BuLi $\gg$ n-BuLi
Polystyrene	sec-BuLi $\gg$ n-BuLi $\gg$ tert-BuLi
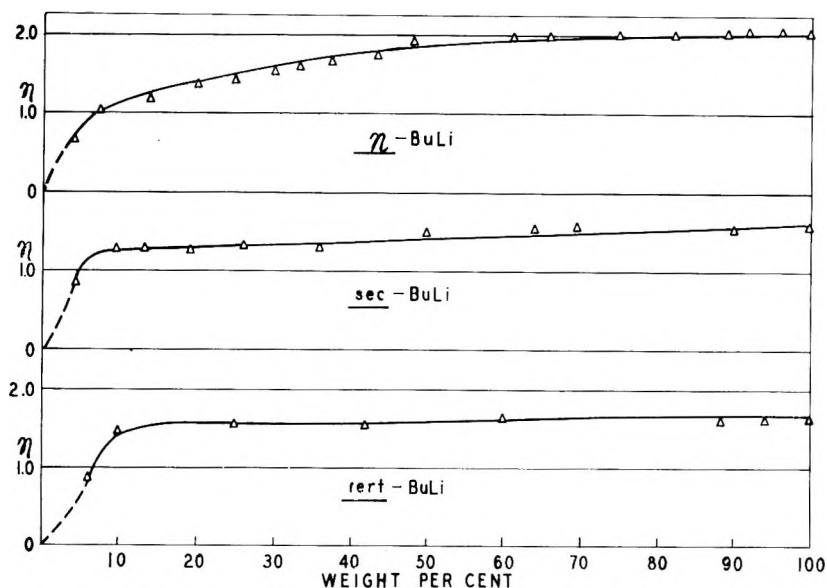
Fig. 5. Fractionation of polyisoprene.
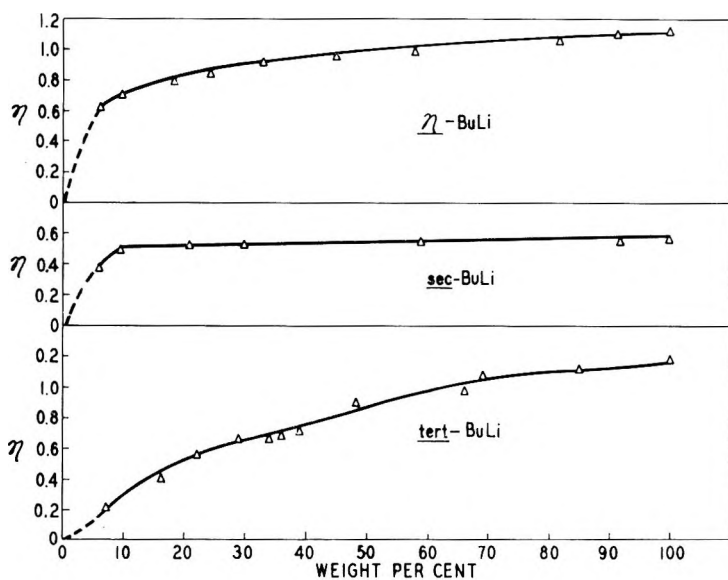
Fig. 6. Fractionation of polystyrene.

onstrated this. The fractionation data shown in Figures 4–6 can be summarized as shown in Table II.

This is in agreement with the predictions of the kinetic data.[8] It is concluded that polymer with extremely narrow molecular weight distribution can be easily prepared by using alkyllithium initiators and selecting a combination of solvent and alkyllithium which gives highest R_i/R_p.

It should be noted that cyclohexane used in this investigation is one of the least desired solvents for preparing monodispersed polymer. The R_i/R_p ratio is much higher in toluene than in cyclohexane.[8] The selection of cyclohexane here is to dramatize the effect, particularly with experiments concerning kinetic molecular weight.

References

1. O'Driscoll, K. F., and A. V. Tobolsky, *J. Polymer Sci.*, **35**, 259 (1959).
2. Welch, F. J., *J. Am. Chem. Soc.*, **81**, 1345 (1959).
3. Worsfold, D. J., and A. Bywater, *Can. J. Chem.*, **38**, 1891 (1960).
4. Morton, M., E. E. Bostick, and R. Livigni, *Rubber Plastics Age*, **42**, 397 (1961).
5. Morton, M., A. A. Rembaum, and J. L. Hall, *J. Polymer Sci.*, **A1**, 461 (1963).
6. Morton, M., E. E. Bostick, and R. G. Clarke, *J. Polymer Sci.*, **A1**, 475 (1963).
7. Morton, M., L. J. Fetters, and E. E. Bostick, *J. Polymer Sci.*, **C1**, 311 (1963).
8. Hsieh, H. L., *J. Polymer Sci.*, **A3**, 163 (1965).
9. Gregg, R. Q., private communication.
10. Carter, W. C., R. L. Scott, and M. Magat, *J. Am. Chem. Soc.*, **68**, 1480 (1946).
11. Outer, P., C. I. Carr, and B. Zimm, *J. Chem. Phys.*, **18**, 830 (1950).

Résumé

Le poids moléculaire cinétique calculé M_k a été comparé avec le poids moléculaire déterminé expérimentalement par viscosimétrie M_v du polybutadiène, du polyisoprène et du polystyrène, initiés par le *n*-BuLi, *sec*-BuLi et *tert*-BuLi. La différence entre M_k et M_v dépend du rapport des vitesses d'initiation R_i et de propagation R_p, qui eux-mêmes dépendent de la structure de l'initiateur et du monomère. Dans le système de polymérisation initié par des alcoyllithiens, M_k, basé sur [RLi] consommé plutôt qu'engagé, est généralement égal au poids moléculaire réel. Le rapport de R_i et R_p affecte aussi la distribution du poids moléculaire. L'ordre de la monodispersité pour les polydiènes est le suivant: *sec*-BuLi $\cong$ *tert*-BuLi $>$ *n*-BuLi. Pour le styrène, il est: *sec*-BuLi $\gg$ *n*-BuLi $\gg$ *tert*-BuLi. Les données de fractionnements sont en parfait accord avec les prédictions des données cinétiques. Les conditions idéales pour la préparation de polymère monodispersé par polymérisation ionique sont également discutées.

Zusammenfassung

Das berechnete kinetische Molekulargewicht M_k wurde für *n*-BuLi, *sek*-BuLi-und *tert*-BuLi-gestartetes Polybutadien, Polyisopren und Polystyrol mit dem experimentell bestimmten Molekulargewicht M_v verglichen. Die Diskrepanz zwischen M_k, und M_v hängt vom Verhältnis der Startgeschwindigkeit R_i und Wachstumsgeschwindigkeit R_p ab, welche ihrerseits von der Starterstruktur und dem Monomeren bestimmt sind. Beim Alkyllithium-gestarteten Polymerisationssystem ist das aus dem verbrauchten [RLi] und nicht aus dem angewendeten, berechnete, M_k nahezu gleich dem tatsächlichen Molekulargewicht. Das Verhältnis von R_i zu R_p beeinfluss auch die Molekulargewichtsverteilung. Die Reihenfolge der Monodispersität für Polydiene ist *sek*-BuLi $\cong$ *tert*-BuLi $>$ *n*-BuLi. Bei Styrol ist sie *sek*-BuLi $\gg$ *n*-BuLi $\gg$ *tert*-BuLi. Die Fraktionierungsdaten stimmen völlig mit den Folgerungen aus den kinetischen Daten überein. Schliesslich werden die idealen Bedingungen für die Darstellung monodisperser Polymerer durch anionische Polymerisation diskutiert.

Studies of the Reduction of Titanates and Alkoxytitanium(IV) Chlorides by Alkylaluminum Chlorides

PATRICIA H. MOYER, *The B. F. Goodrich Research Center, Brecksville, Ohio*

Synopsis

Replacement of up to two of the chloride ligands on titanium tetrachloride with isopropoxy or butoxy groups results in an increase in the rate of reduction by alkylaluminum chlorides. The final product is still a titanium(III) compound. A decrease in rate results from replacement of more than two of the chloride ligands by alkoxy, or of the chloride ligands on aluminum by alkoxy. Exchange of alkoxy between titanium and aluminum occurs concurrently with reduction. These observations are explained in terms of the relative ease of replacement of a ligand on titanium by alkyl and the relative stability of the alkyltitanium compounds formed.

INTRODUCTION

Replacement of some of the chloride ligands by alkoxy in the catalyst $RAlCl_2–TiCl_4–TiCl_3$[1] caused an increase in the maximum rate of polymerization of ethylene (Fig. 1). The higher the maximum rate, the more rapidly the rate decreased after the maximum. Wesslau[1] had indicated that a narrowing of the molecular weight distribution resulted from such a replacement, and that the effect was produced by replacement of chloride on aluminum as well as on titanium. Accordingly, we were prompted to examine the reactions between alkylaluminum compounds and mixtures of titanium tetrachloride with titanates. The points investigated included the effect on ease of titanium(IV) reduction when chloride on titanium or aluminum is replaced by alkoxy, the distribution of titanium and aluminum between the precipitated and soluble products from the reaction, and the distribution of alkoxy between aluminum and titanium.

RESULTS

Mixing solutions of titanium tetrachloride and a titanate in quantities stoichiometric for a given mixed titanium(IV) salt probably resulted in very rapid formation of that salt. Mixed salts of this type are well known[2,3] and show no particular tendency to disproportionate. A considerable amount of heat was evolved during mixing of the solutions. No effort
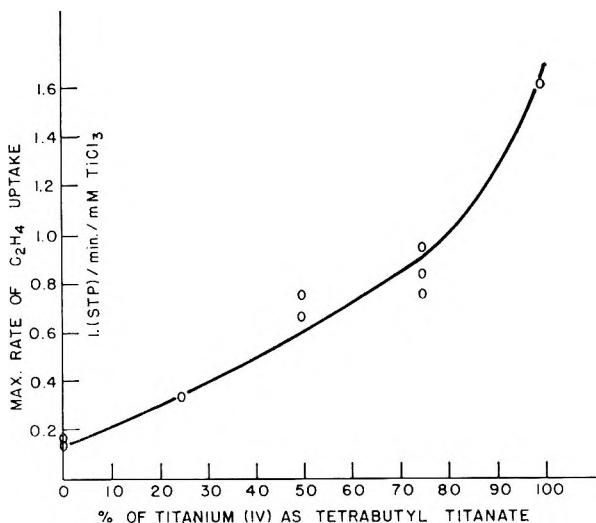
Fig. 1. Effect on polymerization of ethylene of replacing titanium tetrachloride with tetrabutyl titanate. Catalyst: 3.2 mmole/l. EtAlCl₂, 3.2 mmole/l. TiCl₃, 0.80 mmole/l. titanium(IV). Solvent: saturated C₉ hydrocarbon mixture (625 ml.). Temperature: 70°C.
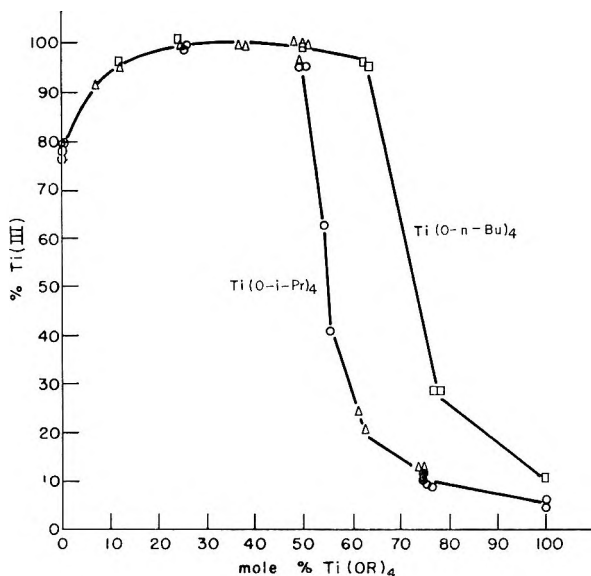
Fig. 2. Effect on amount of Ti(III) produced of replacing titanium tetrachloride with tetraisopropyl or tetra-n-butyl titanate: (□) TiCl₄ and Ti(O-n-Bu)₄ mixed 10–20 min. before Et₂AlCl added; (O) TiCl₄ and Ti(O-i-Pr)₄ mixed 10–20 min. before Et₂AlCl added; (△) TiCl₄ and Ti(O-i-Pr)₄ mixed 70 min. before Et₂AlCl added; (●) TiCl₄ and Ti-(O-i-Pr)₄ mixed 23 hr. before Et₂AlCl added. [Ti] ≅ 0.1 mg.-atom/g. of reaction mixture, [Al]/[Ti] ≅ 1.5, solvent = hydrogenated propylene trimer, temperature approx. 25°C., time of reduction 33 min.
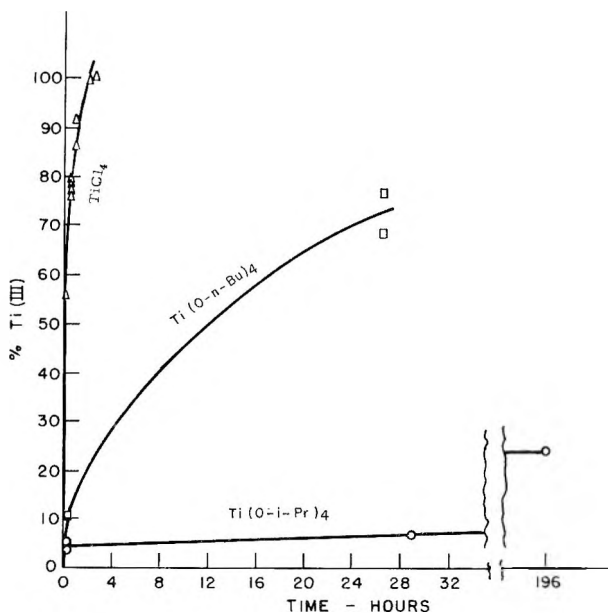
Fig. 3. Effect of alkyl group in tetraalkyl titanate on rate of its reduction by diethylaluminum chloride. [Ti] $\cong$ 0.1 mg.-atom/g. of reaction mixture, [Al]/[Ti] $\cong$ 1.5, solvent = hydrogenated propylene trimer, temperature approx. 25°C.

was made to isolate the compounds, but in one instance, during preparation of a solution intended to contain 0.66 mg.-atom of titanium/g., half of which derived from tetraisopropyl titanate, a white crystalline solid deposited. It and a second crop, together accounting for 80% of the titanium charged, each had the correct analysis for diisopropoxytitanium dichloride, reported to be a white solid by Jennings, Wardlaw, and Way.[2]

Mixing nonstoichiometric quantities probably gave a mixture of the two salts whose compositions were closest to that of the overall mixture. Henceforth, however, all compositions will be referred to simply as mixtures.

Treatment of mixtures containing 0–100% titanate with 1.5 molar equivalents of diethylaluminum chloride gave the results shown in Figure 2. The reactions were conducted at room temperature for 33 min. at a titanium concentration of 0.1 mg.-atom/g. of solution. Although pure tetraisopropyl and tetrabutyl titanates were reduced much more slowly than titanium tetrachloride (see also Fig. 3), mixtures containing up to 50% of either titanate were reduced more rapidly. In mixtures containing 25–50% titanate, all the titanium was reduced to the (III) state. Titrations according to the method of Martin and Stedefeder[4] applied to mixtures containing 50% tetraisopropyl titanate showed no titanium(II), however. Similarly, no titanium(II) had been found upon reduction of titanium tetrachloride by alkylaluminum chlorides.[5,6] No discernible effect resulted from changes in the time elapsed between mixing the ti-

TABLE I

Composition of Products from Reaction of Diethylaluminum
Chloride with Dialkoxytitanium Dichloride[a]

	Run 1	Run 2	Run 3	Run 4
Reaction time, hr.	$2^2/_3$	$2^2/_3$	18	18
Alkoxy	i-PrO	n-BuO	i-PrO	n-BuO
Found in filtrate:				
Al, % of total	—	—	67.1	73.1
Ti, % of total	—	—	0.00	0.00
Ti, % of total as Ti(III)	69.8	90.6	—	—
[Cl]/[Al]	—	—	0.85	0.73
[Cl]/[Al] expected in filtrate had no				
exchange occurred	—	—	1.67	1.67
OR which exchanged to aluminum, %[b]	—	—	61	69
Found in solid:				
Al, % of total	—	—	11.9	3.14
Ti, % of total	—	—	—	—
Ti, % of total as Ti(III)	29.8	8.04	96.6	80.9
[Cl]/[Ti]	—	—	2.61	2.71
[Al]/[Ti]	—	—	0.19	0.058
Recovery, %				
Al	—	—	95[c]	100[d]
Ti	99.6	98.6	97[c]	81[d]
Cl	—	—	100[c]	—

[a] $[Al]/[Ti] = 1.5$; % titanium as titanate = 50–51; $[Ti] = 0.1$ mg.-atom/g. of reaction mixture; temperature = $\sim 25°C$.; solvent, runs 1 and 2 = hydrogenated propylene trimer; solvent, runs 3 and 4 = hexane.

[b] This figure = $\{(\text{expected } [Cl]/[Al]) - (\text{found } [Cl]/[Al])\}/\{\text{original } [OR]/[Al]\}$, or $\{1.67 - (\text{found } [Cl]/[Al])\}/1.33$.

[c] Including amounts found in each of four washes.

[d] Including amounts found in first two washes. A third wash was not analyzed.

tanium tetrachloride with titanate and adding the diethylaluminum chloride. The amount of titanium(III) produced declined more steeply for tetraisopropyl titanate than for tetrabutyl titanate as the per cent titanate rose beyond 50%. This paralleled the slower rate of reduction of tetraisopropyl titanate.

Titanium(III) remained in solution (or perhaps in colloidal suspension) long after reduction of mixtures containing 50% titanate was complete. Thus, after $2^2/_3$ hr. of reaction, the ratio of titanium(III) in the precipitate to that in the filtrate was 70/30 from the mixture containing tetraisopropyl and 8/92 from the mixture containing tetrabutyl titanate.*

* The amounts of titanium(III) found in the solid and supernatant liquid from reduction of tetrabutyl titanate added up to 99% of the amount of titanium charged. This rules out the possibility that titanium(II) was present in the precipitate, with enough dissolved titanium(IV) to make three the average valence state of the titanium. This is because the method used to destroy alkyl-metal bonds in this instance, adding ethanol at 0°C., would have resulted in oxidation of any titanium(II) in the solid to titanium (III). The amounts of titanium(III) then could not total to 100%.

TABLE II
Dependence of Rate of Reduction on Initial Distribution of Substituents[a]

Al compd. used	Titanium as titanate, %	Al/Ti	Time of reaction, min.	Ti(III) formed, %
Case I				
Et_2AlCl	0	1.48–1.54	33	76–80[b]
Et_2AlCl	25	1.51	33	99
Et_2AlCl	25	1.48	33	99
$Et_{2.02}AlCl_{0.33}(O\text{-}n\text{-}Bu)_{0.65}$	0	1.53	33	92
$Et_{2.02}AlCl_{0.33}(O\text{-}n\text{-}Bu)_{0.65}$	0	1.53	33	93
Case II				
$Et_{1.5}AlCl_{1.5}$	0	1.15	180	72
$Et_{1.5}AlCl_{1.5}$	0	1.16	180	71
$Et_{1.5}AlCl_{1.5}$	15	1.21	180	57
$Et_{1.5}AlCl_{1.5}$	15	1.21	180	57
$Et_{1.5}AlCl (O\text{-}n\text{-}Bu)_{0.5}$	0	1.17	180	38
$Et_{1.5}AlCl (O\text{-}n\text{-}Bu)_{0.5}$	0	1.17	180	37

[a] [Ti] = 0.1 mg.-atom/g. of reaction mixture; temperature = ~25°C.
[b] Eight runs.

The filtrates were deeply colored.   After 18 hr., virtually all the titanium (III) had precipitated in both cases, and the filtrates were colorless.   Reduction was accompanied by exchange of alkoxy groups from titanium to aluminum.   Migration to aluminum was the fate of 61% of the isopropoxy groups from tetraisopropyl titanate and 69% of the butoxy groups from tetrabutyl titanate.   The findings on distribution of titanium, aluminum, alkoxy, and chloride are summarized in Table I.

Less titanium(III) was formed in mixtures in which butoxy was bound initially to aluminum than in corresponding mixtures in which it was bound initially to titanium.   This is shown in Table II, which gives the amounts of titanium(III) formed in a given time in two sets of experiments.   Within each set, the compositions of the mixtures were identical with respect to numbers of titanium, aluminum, and chloride atoms, and ethyl and butoxy groups, and differed only as to the metal atom to which the butoxy groups were attached.   The results of parallel experiments on mixtures containing no alkoxy groups are also shown.   In case I, in which the R/Al ratio was 2.0 and the Al/Ti ratio 1.5, less titanium (III) was formed in the all-chloride system than in the mixtures containing alkoxy groups.   In case II, in which the R/Al ratio was 1.5 and the Al/Ti ratio 1.2, more titanium(III) was formed in the all-chloride system.

DISCUSSION

The mode of reduction of titanates and mixed titanium salts by alkylaluminum chlorides is probably similar to that of titanium tetrachloride, which is first alkylated.[7]

$$(R_2AlCl)_2 + 2 TiCl_4 \; \rightleftharpoons \; (RAlCl_2)_2 + 2 RTiCl_3 \qquad (1)$$
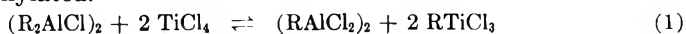
That this is an equilibrium reaction was established for the methyl series.[8,9] As indicated, alkylaluminum chlorides are dimeric.[10] The second step is the decomposition of the alkyltitanium trichloride to give hydrocarbons and titanium trichloride. In aliphatic solvents this proceeds via a path in which no free radicals are produced.[7,11]

$$2RTiCl_3 \rightarrow 2\ TiCl_3 + alkane + alkene \qquad (2)$$
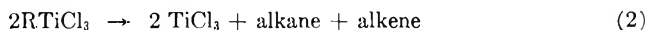
Two factors would combine to make reduction of titanates extremely slow. Alkoxy would bear a smaller partial negative charge than chloride (as calculated according to the method of Sanderson[12]) and would therefore shift equilibrium (1) to the left. In addition, alkyltitanium trialkylate would be more stable than alkyltitanium trichloride, because a larger negative charge would reside on the alkyl. This follows from Herman and Nelson's[13] finding that the stability of alkyltitanium compounds increases as the electronegativity of the alkyl groups increases. The stability factor is the more important, as indicated by the sharp drop in the rate of reduction when the titanate content of a mixture is raised from 50 to 75%. The lesser but real influence of the first step is manifested in the further drop in rate as the titanate content is raised from 75 to 100%. The fact that the rate of reduction is lowered more by isopropoxy than by butoxy substitution shows the part played by steric hindrance.

More study would be required for a complete understanding, particularly of the accelerated reductions. Clearly, however, limited substitution of alkoxy on titanium accelerates reduction, while on aluminum it retards reduction. Exchange of alkoxys between the two certainly occurs, and can have a decisive influence. Thus the results given in Table II point to the conclusion that the preferred site for alkoxy attachment is titanium in case I, and aluminum in case II. The rate of exchange toward the favored site must be of a magnitude comparable to the rate of reduction. If it were much faster, the rate of reduction would be the same whether alkoxy were bound to aluminum or titanium originally. If it were much slower, the rate of reduction would always increase on going from a mixture having alkoxy on aluminum initially, to one having no alkoxy, and finally to one having alkoxy on titanium initially. Further exchange could occur after reduction, however, since the equilibrium distribution could depend on the valence state of titanium as well as on the quantities of the various substances present. In cases where prior to reduction, the preferred site of alkoxy is titanium, the remaining chloride ligands would bear a higher partial negative charge[12] than the chloride of titanium tetrachloride. Equilibrium (1) would shift to the right. This would account for at least part of the acceleration which occurs in such cases.

The results observed in the polymerization of ethylene can be understood in the light of these findings. Substitution of butoxy for chloride ligands shifted equilibrium (1) to the right. This increased the rate of polymerization by increasing the concentration of alkylated titanium

species, presumed to constitute the active catalyst.[4,11,14-16] The increased concentration of alkyltitanium compounds also accelerated reaction (2), however, causing the observed drop in rate of polymerization, which was the more rapid, the higher the maximum had been.

EXPERIMENTAL

Materials

Hydrogenated propylene trimer and hexane were purified by treatment with Linde 5A molecular sieves.

Triethylaluminum and diethylaluminum chloride from Ethyl Corp. were used as received. Ethylaluminum sesquichloride was prepared by Dr. L. C. Kreider of these laboratories, by reaction of aluminum with ethyl chloride. Solutions of $(C_2H_5)_{1.5}AlCl(O-n-Bu)_{0.5}$ and $(C_2H_5)_{2.02}AlCl_{0.33}(O-n-Bu)_{0.65}$ were prepared from appropriate quantities of diethylaluminum chloride solutions in the first instance, and from triethylaluminum, diethylaluminum chloride, and n-butanol solutions in the second instance. The n-butanol was Eastman Kodak White Label, flash-distilled from calcium hydride.

Fisher purified titanium tetrachloride was distilled from copper turnings, b.p. 132°C. Tetraisopropyl titanate from du Pont, b.p. 88°C./2 mm., and tetrabutyl titanate from Anderson Chemical Company, b.p. 145/147°C./0.36 mm., were distilled.

Reduction Experiments—Measurement of Titanium Valence State

All operations were performed under nitrogen of high purity. The solvent, titanium compound(s), and alkylaluminum compound were added to the reaction flask by means of syringes, the exact amounts being determined by weight. The alkylaluminum compound was added with stirring. After the designated reaction time, the reaction flask was plunged into a cold bath. For all but two of the reductions of titanium tetrachloride, and for four of the reductions of mixtures containing 50% tetraisopropyl titanate, the temperature of this bath was −70°C. At this temperature ethanol reacts with alkylmetal bonds but does not oxidize titanium(II) to titanium (III).[4] Hence had any titanium(II) been present it would have been detected in the subsequent titration, but in no case was it found. For the remaining reductions, the quench bath was held at 0°C. After 5 min., ethanol of the same temperature as the bath was added to destroy alkylmetal bonds. Excess $0.1N$ ferric chloride in ethanol was then added, and the ferrous ion titrated with ceric ammonium sulfate, either potentiometrically or with barium diphenylamine sulfonate as indicator.

To determine the distribution of titanium between the precipitate and filtrate, the reduction was conducted in an assembly of the type shown in Figure 4. After $2^2/_3$ hr., the supernatant liquid was filtered into the bottom flask. The two parts of the apparatus were then separated under

nitrogen cover, and the amount of titanium(III) in each was determined according to the method outlined above, a −70°C. quench being used for the experiment involving tetraisopropyl titanate and a 0°C. quench for that involving tetrabutyl titanate.

The experiments on distribution of alkoxy were conducted in a similar manner, with hexane as solvent. After the initial filtration, the solids were washed repeatedly with hexane. The filtrate, the washings, and the dried solid were than analyzed for aluminum, titanium, and chloride. For combined aluminum and titanium, a method developed in these laboratories[17]
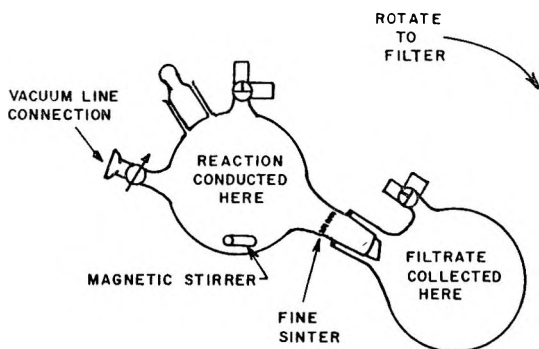
Fig. 4. Flask for work-up of reduction products.

was used. The metal ions were complexed with an excess of 1,2-cyclohexanediamine-tetraacetic acid and the excess complexing agent back-titrated with zinc with the use of dithizone as an indicator. Whichever element was present in lesser amount was then determined colorimetrically.[18] Halogens were determined by stoichiometric titration with silver nitrate.

Preparation of Diisopropoxytitanium Dichloride

Hexane (52.6 g.), tetraisopropyl titanate (5.8 g., 0.02 mole), and titanium tetrachloride (3.9 g., 0.02 mole) were added in that order to the top part of the assembly shown in Figure 4. Heat was evolved, and crystals started forming immediately. After the mixture has stood overnight, the first crop (1.72 g.) was collected. The filtrate, after several days in the freezer, gave a second crop (6.15 g.).

ANAL. Calc. for $Ti(O-i-Pr)_2Cl_2$: Cl, 31.2%; Ti, 21.1%. Found (first crop): Cl, 29.4%; Ti, 20.4%. Found (second crop): Cl, 29.8%; Ti, 20.3%.

References

1. Wesslau, H., *Makromol. Chem.*, **26,** 102 (1958).
2. Jennings, J. S., W. Wardlaw, and W. J. R. Way, *J. Chem. Soc.*, **1936,** 637.
3. Adrianov, K. A., V. V. Astakhin, and I. V. Sukhanova, *Zh. Obshch. Khim.*, **31,** 232 (1961).
4. Martin, H., and J. Stedefeder, *Ann. Chem.*, **618,** 17 (1958).
5. Boldyreva, I. I., B. A. Dolgoplosk, and V. A. Krol, *Vysokomolekul. Soedin.*, **1,** 900 (1959).
6. Van Helden, R., A. F. Bickel, and E. C. Kooyman, *Tetrahedron Letters*, **1959,** No. 12, 18.
7. Beermann, C., and H. Bestian, *Angew. Chem.*, **71,** 618 (1959).
8. Groenewege, M. P., *Z. Physik. Chem. (Frankfurt)*, **18,** 147 (1958).
9. Gray, A. P., A. B. Callear, and F. H. C. Edgecombe, *Can. J. Chem.*, **41,** 1502 (1963).
10. Coates, G. E., *Organometallic Compounds*, Wiley, New York, 1956, p. 82.
11. DeVries, Hn., *Rev. Trav. Chim.*, **80,** 866 (1961).
12. Sanderson, R. T., *J. Chem. Educ.*, **32,** 140 (1955).
13. Herman, D. F., and W. K. Nelson, *J. Am. Chem. Soc.*, **75,** 3877 (1953).
14. Roha, M., L. C. Kreider, M. R. Frederick, and W. L. Beears, *J. Polymer Sci.*, **38,** 51 (1959).
15. Chien, J. C. W., *J. Am. Chem. Soc.*, **81,** 86 (1959).
16. Long, W. P., and D. S. Breslow, *J. Am. Chem. Soc.*, **82,** 1953 (1960).
17. Tyler, W. P., private communication.
18. Sandell, E. B., *Chemical Analysis, Vol. III. Colorimetric Determination of Traces of Metals*, 2nd Ed., Interscience, New York, 1950, pp. 152–153, 576.

Résumé

Le remplacement, au maximum, de deux atomes de chlore dans le tétrachlorure de titane par des groupements oxy-isopropyles ou oxy-butyliques provoque une augmentation de la vitesse de réduction par les chlorures d'alcoyl-aluminium. Le produit final reste toujours un composé du titane III. Une diminution de la vitesse est due au remplacement de plus de deux atomes de chlore par un oxy-alcoyle, ou de tous les chlores liés à l'aluminium par des groupements oxy-alcoyles. L'échange de l'oxy-alcoyle entre le titane et l'aluminium a lieu concomittament à la réduction. Ces observations sont expliquées par la facilité relative à remplacer un liant du titane par un groupement alcoyle et par la stabilité relative des produits alcoyl-titanes obtenus.

Zusammenfassung

Der Ersatz von bis zu zwei Chloridliganden in Titantetrachlorid durch Isopropoxy oder Butoxygruppen führt zu einer Zunahme der Reduktionsgeschwindigkeit durch Alkylaluminiumchloride. Das Endprodukt ist immer eine Titan-(III)-Verbindung. Eine Herabsetzung der Geschwindigkeit wird durch Ersatz von mehr als zwei der Chloridliganden durch Alkoxy oder der Chloridliganden am Aluminium durch Alkoxy bewirkt. Austausch von Alkoxy zwischen Titan und Aluminium tritt gleichzeitig mit der Reduktion auf. Diese Beobachtungen werden anhand der relativen Leichtigkeit des Ersatzes eines Liganden an Titan durch Alkyl und der relativen Beständigkeit der gebildeten Alkyl-Titanverbindungen erklärt.

Reactions of Titanium Tetrachloride (Tetraiodide, Dichlorodiiodide) with Alkylaluminum Compounds

PATRICIA H. MOYER, *The B. F. Goodrich Research Center, Brecksville, Ohio*

Synopsis

Titanium tetraiodide and titanium dichlorodiiodide are reduced by triisobutylaluminum or diisobutylaluminum iodide to form products analogous to those obtained with titanium tetrachloride. In the reaction products, the preferred site for iodide ligands is titanium, that for chloride ligands, aluminum.

INTRODUCTION

The reactions which occur on admixture of titanium tetrachloride with various alkylaluminum compounds have been studied by numerous investigators. Such broad interest was aroused by the fact that these mixtures form Ziegler catalysts, which can catalyze the polymerization of ethylene to linear polyethylene, olefins to stereoregular polyolefins, or dienes to polydienes, also of stereoregular structure.[1] The corresponding reactions of titanium tetraiodide have been little studied. The behavior of this substance was of interest to us, since it can replace titanium tetrachloride, partially or completely, in Ziegler systems for polymerization of dienes, giving somewhat modified results.[2] Accordingly, a study was undertaken of the reactions of alkylaluminum compounds with titanium tetraiodide and titanium dichlorodiiodide. The results were compared with those for titanium tetrachloride, previously reported or obtained in this work.

RESULTS AND DISCUSSION

Reaction of titanium tetrachloride, dichlorodiiodide, or tetraiodide with alkylaluminum compounds leads to the formation of insoluble solids containing nearly all the titanium in a reduced form. The reduced species obtained at an R_3Al/Ti ratio of one is mainly the trihalide in all three cases[3-6] (Fig. 2, Table I). The overall reaction may be summarized

$$R_3Al + TiX_4 \rightarrow R_2AlX + TiX_3 + [R] \qquad (1)$$
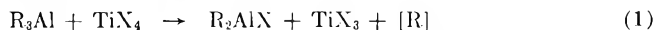
The X/Al ratio found in the filtrates is close to unity[5,6] (Fig. 1, runs 14 and 15 of Table I), and the X/Ti ratio found in the insoluble products is close to three[3-6] (Fig. 2, Runs 14 and 15 of Table I), as would be expected
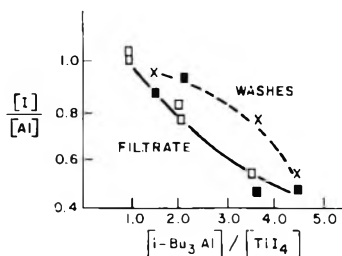
Fig. 1. Composition of filtrate and washes from reaction of i-Bu$_3$Al with TiI$_4$: (□)
[I]/[Al] in filtrate after 2 hr. of reaction; (■) [I]/[Al] in filtrate after 18 hr. of reaction;
(×) [I]/[Al] in combined first three washes, where reaction time was 18 hr. [Ti] =
0.02 mg.-atom/g., room temperature.
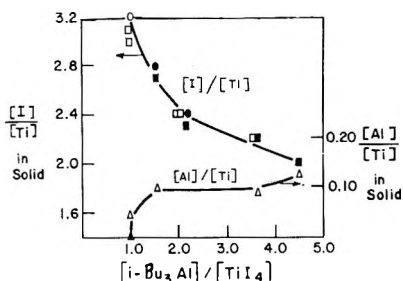
Fig. 2. Composition of solid from reaction of i-Bu$_3$Al with TiI$_4$: (○) [I]/[Ti] in solid
after 2 hr. of reaction; (□) calcd. [I]/[Ti] in solid (based on composition of filtrate) after
2 hr. of reaction; (●) [I]/[Ti] in solid after 18 hr. of reaction. (■) calcd. [I]/[Ti] in
solid (based on composition of filtrate) after 18 hr. of reaction; (△) [Al]/[Ti] in solid
(results at $[i$-Bu$_3$Al]/[TiI$_4$] = 1.0 were obtained after 2 hr. of reaction, others after 18
hr.); [Ti] = 0.02 mg.-atom/g., room temperature.

from eq. (1).   Valence state determinations verify that the titanium species
derived from titanium tetrachloride is in the trivalent state,[7−9] although
one author reported half of it to be tetravalent.[10]   These results indicate
that titanium (III) is not reduced by dialkylaluminum halide.

As the R$_3$Al/Ti ratio is raised, reaction of all three substances proceeds
further[3−6,8] (Fig. 2, Tables I and II).   This is indicated by a progressive
decrease of the X/Ti ratios in the insoluble products.   Unreacted tri-
isobutylaluminum remains after reaction of titanium tetraiodide, as shown
by I/Al ratios below one in the filtrates (Fig. 2).   In the reaction of
titanium tetrachloride, the Cl/Ti ratio in the solid drops below two as the
R$_3$Al/Ti ratio in the reactants is raised above three,[4,5,11] but I/Ti ratios
below two are not observed in the reaction of titanium tetraiodide (Fig. 2).
This difference may not be significant, because reactions of titanium tetra-
iodide must be conducted at concentrations lower than those used in the
reported studies on titanium tetrachloride owing to the insolubility of the
tetraiodide.   When comparable conditions are used, reactions of titanium
tetrachloride (runs 17 and 18, Table II) and titanium tetraiodide (Figs. 1
and 2) are more alike, with reduction and/or alkylation of titanium tetra-

TABLE I

Halogen Distribution in the Products from Reaction of Alkylaluminum Compounds with Titanium Dichlorodiiodide

| Conditions[a] | | | | | | Filtrate | | Products — Solid | | | | |
Run no.	Reaction time, hr.	Initial [Ti], mg.-atom/g.	[Cl]/[total X] in TiCl₂I₂	Alkyl aluminum	Initial [Al]/[Ti]	[Cl]/[total X]	[total X]/[Al]	[Cl]/[total X] Found	[Cl]/[total X] Calcd.[b]	[total X]/[Ti] Found	[total X]/[Ti] Calcd.[b]	[Al]/[Ti]
10	2	0.078	0.52	i-Bu₃Al	2.0	0.91	0.99	—	0.15	—	2.1	—
11	2	0.078	0.52	i-Bu₃Al	2.0	0.91	0.95	—	0.17	—	2.1	—
12	18	0.10	0.50	i-Bu₃Al	2.0	0.89	1.00	—	0.11	—	2.1	—
13	18	0.10	0.50	i-Bu₃Al	2.0	0.91	1.00	0.17	0.08	2.2	2.0	0.081
14	2½	0.093	0.52	i-Bu₃Al	0.93	0.81	0.97[c]	0.40	0.39	3.1	3.0	0.00
15	2½	0.093	0.52	i-Bu₃Al	0.93	0.84	1.05[c]	0.39	0.39	2.9	3.0	0.02
16	18	0.076	0.50	i-Bu₂AlI	1.5	0.73	1.6[c,d] 1.6[e] 2.2[f]	0.04	0.01	3.0	3.1	0.01

[a] Solvent: benzene; reaction temperature: ~25°C.

[b] Runs 10–15, washes were not analyzed. Chloride, total halogen, and titanium expected in the solid were calculated by subtracting the amount found in the supernatant liquid from the amount charged. The weight of the supernatant liquid was taken as the weight of the total reaction mixture after the first filtration minus the weight of the dry solid.

[c] Contained up to 10% of the total titanium charged, presumably as titanium(IV). The [total X]/[Al] ratios are corrected in accordance with this assumption. The remaining filtrates contained less than 1% of the total titanium charged.

[d] Run 16, washes were analyzed. Chloride, total halogen, and titanium expected in the solid were calculated by subtracting the amounts found in the filtrate and first two washes from the amount charged.

[e] First wash.

[f] Second wash. Contained 1.8% of the total aluminum charged.

TABLE II
Composition of Products from Reaction of
Triisobutylaluminum and Titanium Tetrachloride

			Conditions[a]			Products			
								Solid	
Run no.	Reaction time, hr.	Solvent	Initial [Ti], mg.-atom/ g.	Initial [Al] [Ti]	Filtrate [Cl]/[Al]		[Cl]/[Ti] Found	[Cl]/[Ti] Calcd.	[Al] [Ti]
17	2	Benzene	0.021	2.0	0.83		2.4	2.4[b]	0.13
18	18	Benzene	0.019	2.0	1.03		2.4	2.2[c]	0.16
19	18	Benzene	0.10	2.0	1.04		2.3	2.2[c]	0.16
20	2	Hexane	0.11	2.0	1.00 1.00[d]		2.2	2.2[b]	0.15
21	2	Hexane	0.11	2.0	1.01 1.01[e]		2.1	2.2[b]	0.19
22	16	Hexane	0.11	2.0	1.00 1.02[f]		—	2.2[b]	0.22

[a] Reaction temperature: ~25°C.

[b] Chloride expected in the solid was calculated by subtracting the amount found in he filtrate and washes from the amount charged. The solid in Run 17 was washed four times, but the combined washes contained virtually no aluminum, titanium, or chloride.

[c] See Table I, note b.

[d] Combined first three washes. Fourth wash contained <0.03% of the aluminum charged.

[e] All six washes combined.

[f] Both washes combined.

chloride proceeding perhaps slightly further than that of titanium tetra-iodide over the longer reaction period of 18 hr. When titanium tetra-chloride and titanium dichlorodiiodide are reacted under comparable conditions (compare run 19 of Table II with runs 12 and 13 of Table I), they also give similar products, i.e., little unreacted triisobutylaluminum in the filtrates (X/Al ratios close to one), and X/Ti ratios slightly greater than two in the solids.

It is further observed, as the R_3Al/Ti ratio is raised, that the solids retain significant quantities of aluminum[4,5,11] (Fig. 2, Tables I and II). Only Saltman[3] has obtained solids virtually devoid of aluminum from reaction of titanium tetrachloride at high R_3Al/Ti ratios. His solids were extensively aged, and were retained by a medium sinter,[3] while the solids obtained in this work were retained only by a fine sinter; hence differences in particle size may account for the disagreement among various reports[4,5,11] on the amount of aluminum in solids prepared under similar conditions.

Runs 20–22 of Table II are included to show that the nature of the products from titanium tetrachloride does not depend on whether the solvent is aliphatic or aromatic.

In the products from reaction of titanium dichlorodiiodide (Table I), the filtrates contain chiefly alkylaluminum chlorides, while the solids retain

most of the iodide originally charged. This suggests that titanium is the preferred site of attachment for iodide. Confirming this is the fact that when diisobutylaluminum iodide is used (run 16), exchange of iodide from aluminum to titanium occurs, giving titanium triiodide as the main titanium species in the product. A similar observation was made by Havinga and Tan,[12] who found that in the reduction of titanium tetrachloride by diethylaluminum bromide at Al/Ti ratios from one to six, the amount of bromide bound to titanium in the products is greater than that to be expected from a statistical redistribution. The preferred site of attachment for the more highly polarizable (larger)[13a] ligand is thus the larger[13b] metallic ion.

EXPERIMENTAL

Materials

Benzene and heptane were distilled from the blue sodium–benzophenone complex. Hexane was sieved through Linde 4A molecular sieves, and in some cases was also distilled from the sodium–benzophenone complex.

Ethyl Corporation triisobutylaluminum was used as received. Diisobutylaluminum iodide was prepared by Dr. L. C. Kreider of these laboratories, by equilibration of triisobutylaluminum with aluminum triiodide.

Fisher purified titanium tetrachloride was distilled from copper turnings, b.p. 132°C. Titanium tetraiodide from Matheson, Stauffer, or A. D. Mackay was used as received. The halogen/titanium ratio in the solutions containing titanium tetraiodide or titanium dichlorodiiodide was checked by analysis and found to be 4.0 ± 0.1 except in the titanium tetraiodide solution used in runs 1 and 3, in which it was 4.3 ± 0.1. In these runs, allowance was made for the excess iodide in checking halogen material balances.

Reduction Experiments

All operations were performed under high-purity nitrogen. Benzene was chosen as solvent for most of these experiments as a matter of necessity,
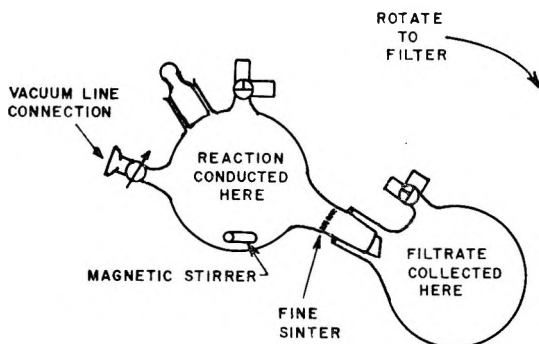
Fig. 3. Flask for work-up of reduction products.

because of the extremely limited solubility of titanium tetraiodide in aliphatic solvents. Washings were performed with hexane or heptane, however, because benzene tended to peptize the solids, causing them to clog the filter. The reactions were conducted in an assembly of the type

TABLE III
Comparison of Calculated and Found Values for Aluminum
Concentration in the Filtrate

Conditions					Results		
			[Ti], mg.-atom/g. reaction mixture	Reaction time, hr.	[Al] in filtrate, mg.-atom/g		
Run no.	[i-Bu$_3$Al] / [Ti]	Ti Compound			Found	Calcd. (method A)[a]	Calcd. (method B)[b]
1	4.5	TiI$_4$	0.015	18	0.076	0.072	0.072
3	3.7	TiI$_4$	0.022	18	0.091	0.084	0.085
6	2.2	TiI$_4$	0.019	18	0.036	0.042	—
7	1.6	TiI$_4$	0.020	18	0.038	0.038	0.038
8	1.0	TiI$_4$	0.019	2	0.021	0.023	—
9	1.0	TiI$_4$	0.019	2	0.020	0.021	—
13	2.0	TiCl$_2$I$_2$	0.10	18	0.21	0.20	—
14	0.93	TiCl$_2$I$_2$	0.093	2^1/$_2$	0.090	0.092	—
15	0.93	TiCl$_2$I$_2$	0.093	2^1/$_2$	0.090	0.092	—
16	1.5[c]	TiCl$_2$I$_2$	0.076	18	0.15	0.125	0.126
17	2.0	TiCl$_4$	0.021	2	0.060	0.065	0.067
18	2.0	TiCl$_1$	0.019	18	0.035	0.036	—
19	2.0	TiCl$_4$	0.10	18	0.19	0.19	—
20	2.0	TiCl$_4$	0.11	2	0.22	0.22	0.22
21	2.0	TiCl$_4$	0.11	2	0.29	0.28	0.29
22	2.0	TiCl$_4$	0.11	16	0.22	0.21	0.22

[a] Expected [Al] in the filtrate was calculated by subtracting the amount found in the solid from the amount charged, and dividing by the weight of the supernatant liquid. The weight of the supernatant liquid was taken as the weight of the total reaction mixture after the first filtration minus the weight of the dry solid. This calculation would be in error f an appreciable amount of alkylaluminum, adsorbed in the solid at the time the filtrate was removed, was subsequently washed out. Agreement between values calculated by method A and method B was good, indicating that such error was small.

[b] Expected [Al] in the filtrate was calculated by subtracting the combined amounts found in the solid and washes 'rom the amount charged, and dividing by the weight of the filtrate.

[c] Aluminum compound = diisobutylaluminum iodide.

shown in Figure 3. The solvent, titanium compound(s), and alkylaluminum compound were added to the flask by means of syringes, the exact amounts being determined by weight. The mixture was stirred for 1–2 hr., allowed to settle for the remainder of the specified time of reaction, and filtered. The solids in runs 6, 8, 9, 13, 18, 19, and 22 were then washed twice, all others at least three times. After removal of the last wash, the solids were either reslurried in benzene or dried under vacuum.

Analyses

For combined aluminum and titanium, a method developed in these laboratories[14] was used. The metal ions were complexed with an excess of 1,2-cyclohexanediaminetetraacetic acid and the excess complexing agent back-titrated with zinc, dithizone being used as an indicator. Whichever element was present in lesser amount was then determined colorimetrically.[15] Halogens were determined by titration with silver nitrate. Agreement between calculated and found halogen/Ti ratios in the solids is within 5% in most cases, 10% at worst (Fig. 1, Tables I and II). As shown in Table III, agreement between calculated and found aluminum concentration in the filtrate is also within 5% in most cases, although the average difference is slightly greater for the runs at low concentrations ([Ti] = 0.02 mg.-atom/g. of reaction mixture). Runs 6 and 16 are exceptional, in that they showed 15% differences between the calculated and found values. In Run 6, the washes were not analyzed, so that the difference conceivably could have arisen because an exceptionally large amount of aluminum, adsorbed on the solid at the time the filtrate was removed, had later been removed in the washes. This is unlikely, however, because in runs 1, 3, and 7, the combined washes contained only 0.6, 0.97, and 1.3% of the total charged aluminum, respectively. The found I/Al ratio in this run (filled square above the line marked "filtrate" in Fig. 1) is therefore believed to be too high. In Run 16, the filtrate, washes, and solid were analyzed, and the recoveries of iodide, chloride, titanium, and aluminum were 95, 104, 100, and 115%, respectively. The found aluminum concentration in the filtrate is thus believed to be too high, and therefore the halogen/Al ratio given for the filtrate in Table I is based on the found total halogen, and expected total aluminum.

References

1. Gaylord, N. G., and H. F. Mark, *Linear and Stereoregular Addition Polymers*, Interscience, New York, 1959.

2. Moyer, P. H., and M. H. Lehr, *J. Polymer Sci.*, **A3**, 217 (1965).

3. Saltman, W. M., W. E. Gibbs, and J. Lal, *J. Am. Chem. Soc.*, **80**, 5615 (1958).

4. Natta, G., L. Porri, A. Mazzei, and D. Morero, *Chim. Ind. (Milan)*, **41**, 398 (1959).

5. Cooper, M. L., and J. B. Rose, *J. Chem. Soc.*, **1959**, 795.

6. Tepenitsyna, E. P., M I. Farberov, A. M. Kutin, and G. S. Levskaya, *Vysokomolekul. Soedin.*, **1**, 1148 (1959).

7. Friedlander, H. N., and K. Oita, *Ind. Eng. Chem.*, **49**, 1885 (1957).

8. Martin, H., and J. Stedefeder, *Ann. Chem.*, **618**, 17 (1958).

9. Beermann, C., and H. Bestian, *Angew. Chem.*, **71**, 618 (1959).

10. Jones, M. H., U. Martius, and M. P. Thorne, *Can. J. Chem.*, **38**, 2303 (1960).

11. Simon, A., and G. Ghymes, *J. Polymer Sci.*, **53,** 327 (1961).

12. Havinga, R., and Y. Y. Tan, *Rec. Trav. Chim.*, **79,** 56 (1960).

13. Pauling, L., *The Nature of the Chemical Bond*, 3rd Ed., Cornell Univ. Press, Ithaca, N. Y., 1960, (a) pp. 514, 608; (b) p. 518.

14. Tyler, W. P., private communication.

15. Sandell, E. B., *Chemical Analysis, Vol. III. Colorimetric Determination of Traces of Metals*, 2nd Ed., Interscience, New York, 1950, pp. 152–53, 576.

Résumé

Le tétraiodure de titane et le dichlorodiiodure de titane sont reduits par le triisobutyl aluminium ou l'iodure de diisobutyl aluminium, pour obtenir des produits analogues à ceux obtenus par le tétrachlorure de titane. Dans les produits de réaction, l'iode est préférentiellement lié au titane et le chlore à l'aluminium.

Zusammenfassung

Titantetrajodid und Titandichlordijodid werden durch Triisobutylaluminium oder Diisobutylaluminium Jodid unter Bildung von zu dem mit Titantetrachlorid erhaltenen analogen Produkten reduziert. In den Reaktionsprodukten ist der bevorzugte Ort für Jodidliganden das Titan, für Chloridliganden das Aluminium.

Studies of the Polymerization of Butadiene by Titanium(IV) Compounds with Alkylaluminums

PATRICIA H. MOYER and MARVIN H. LEHR, *The B. F. Goodrich Research Center, Brecksville, Ohio*

Synopsis

Catalysts for the polymerization of butadiene consisting of an alkylaluminum compound with a titanium(IV) compound show variations in reactivity with Al/Ti ratio. The ratio at which maximum reactivity is obtained increases as the electronegativity of the ligands bound to titanium decreases. This is observed on replacement of the chloride ligands of titanium tetrachloride by either iodide or isopropoxy ligands. Catalysts prepared from titanium dichlorodiiodide or titanium chlorotriiodide behave like those from titanium tetraiodide, as would be expected from the previous observation that titanium is the preferred site of attachment for iodide in the reduction products of mixed salts. The *cis* content of the polymers obtained with the iodide-containing salts can be 90% or more, but decreases with increasing titanium concentration, whereas the structure of polymers obtained with titanium tetrachloride is independent of catalyst concentration. Polymerization is not induced by either the soluble alkylaluminum compounds or the insoluble reduced titanium iodides which are produced by the reaction of triisobutylaluminum with titanium tetraiodide. The insoluble material can be activated by triisobutylaluminum or, less readily, by diisobutylaluminum iodide.

INTRODUCTION

Soon after Ziegler[1] announced his discovery of catalysts for the polymerization of ethylene consisting of an alkylmetal and a titanium compound, it was shown that these catalysts also can be used to prepare 1,4-polydienes.[2] Polyisoprene prepared with titanium tetrachloride as the titanium compound is very high in *cis* content,[2] polybutadiene somewhat less so (see text),[3,4] although a fraction very high in *cis* can be isolated.[3] To obtain polybutadiene of higher overall *cis* content, the use of titanium tetraiodide,[5] mixtures of titanium tetrachloride and titanium tetraiodide,[6–8] or mixtures of titanium tetrachloride with iodine or an iodide compound[9–12] has been suggested. We report here a study of the behavior of iodide-containing systems in butadiene polymerization.

RESULTS

Figures 1–4 summarize the effects of variations in catalyst ratio and concentration, and of the iodide content of the titanium salt, on polybutadiene yield, structure, and dilute solution viscosity.
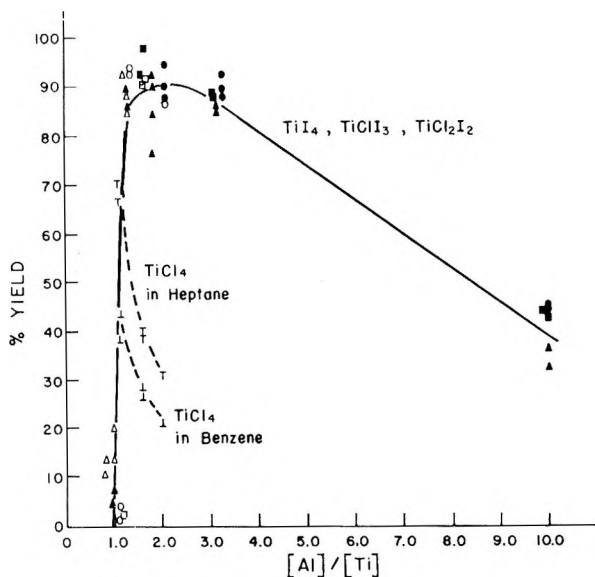
Fig. 1. Conversion to polybutadiene as a function of catalyst ratio (cocatalyst i-Bu$_3$Al; except for TiCl$_4$, polymerization solvent benzene, 4 hr., 30°C, [monomer] = 12 wt.-%); (●) TiI$_4$, [Ti] = 6 mg.-atom/100 g. monomer; (O) TiI$_4$, [Ti] = 10 mg.-atom/100 g.; (■) TiClI$_3$, [Ti] = 6 mg.-atom/100 g.; (□) TiClI$_3$, [Ti] = 10 mg.-atom/100 g.; (▲) TiCl$_2$I$_2$, [Ti] = 6 mg.-atom/100 g.; (△) TiCl$_2$I$_2$, [Ti] = 14.5 mg.-atom/100 g.; (⊤) TiCl$_4$, [Ti] = 6 mg.-atom/100 g. (heptane, 2.5 hr., 30°C., [monomer] = 20 wt.-%); (⊥) TiCl$_4$, [Ti] = 3 mg.-atom/100 g. (benzene, 3 hr., 30°C., [monomer] = 12 wt.-%).
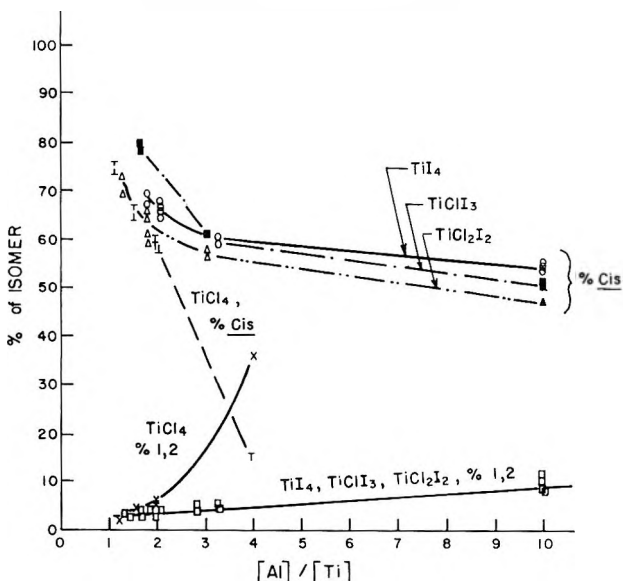
Fig. 2. Polymer structure as a function of catalyst ratio (cocatalyst i-Bu$_3$Al; except for TiCl$_4$, polymerization solvent benzene, 4 hr., 30°C., [Ti] = 6 mg.-atom/100 g. monomer; [monomer] = 12 wt.-%): (O) TiI$_4$; (■) TiClI$_3$; (△) TiCl$_2$I$_2$; (⊤) TiCl$_4$ (heptane, 2.5-21 hr.; 30°C.; [Ti] = 6 mg.-atom/100 g., [monomer] = 20 wt.-%); (⊥) TiCl$_4$ (benzene, 3 hr., 30°C., [Ti] = 3 mg.-atom/100 g., [monomer] = 12 wt.-%).
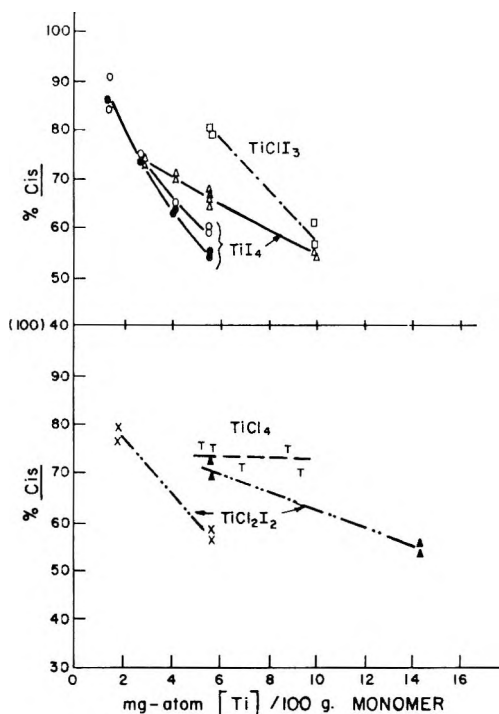
Fig. 3. Polymer structure as a function of catalyst concentration (cocatalyst i-Bu$_3$Al; except for TiCl$_4$, polymerization solvent benzene, 4 hr., 30°C., [monomer] = 12 wt.-%): (●) TiI$_4$, [Al]/[Ti] = 10; (O) TiI$_4$, [Al]/[Ti] = 3.3; (△) TiI$_4$, [Al]/[Ti] = 2.1; (□) TiClI$_3$, [Al]/[Ti] = 1.7; (×) TiCl$_2$I$_2$, [Al]/[Ti] = 3.1; (▲) TiCl$_2$I$_2$, [Al]/[Ti] = 1.3; (⊥) TiCl$_4$, [Al]/[Ti] = 1.2 (heptane, 2.5–6.5 hr., 30°C., [monomer] = 20 wt.-%).
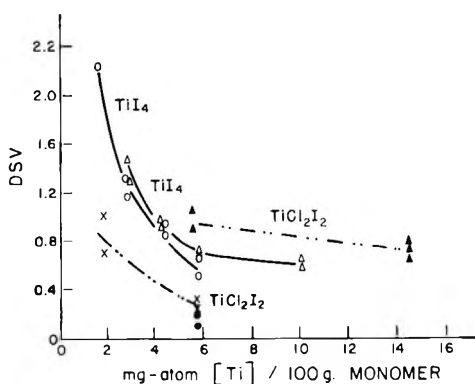
Fig. 4. Dilute solution viscosity (DSV) of polybutadiene as a function of catalyst concentration (cocatalyst i-Bu$_3$Al; benzene, 4 hr., 30°C., [monomer] = 12 wt.-%): (●) TiI$_4$, [Al]/[Ti] = 10; (O) TiI$_4$, [Al]/[Ti] = 3.3; (△) TiI$_4$, [Al]/[Ti] = 2.1; (×) TiCl$_2$I$_2$, [Al]/[Ti] = 3.1; (▲) TiCl$_2$I$_2$, [Al]/[Ti] = 1.3.

TABLE I

Attempted Polymerization of Butadiene with Filtrate or Solid from the Reaction of i-Bu$_3$Al with TiI$_4$ as Catalyst[a]

Run no.	Catalyst Filtrate (f) or solid (s)[b]	$\dfrac{[\text{Al}]^c}{[\text{Ti}]}$	$\dfrac{[\text{I}]^d}{[\text{Ti}]}$	[Al], mg.-atom/100 g. monomer As i-Bu$_3$Al	As i-Bu$_2$AlI	[Ti], mg.-atom/ 100 g. monomer	Time, hr.	Results Yield, %	cis content, %
1	2f	3.6	—	11	13	≦0.02	17	9.3	91
2,3[e]	4f	2.1	—	1.9	6.8	0.00	4, 27	0	—
4,5[e]	6f	2.2	—	0.6–1.9	6.8	0.00	5	0	—
6,7[e]	9f	1.0	—	0	3.8	≦0.01	5	0	—
8,9[e]	2s	3.6	2.2	<0.7		7	17	0	—
10	6s	2.2	2.3–2.4	<0.4		4	17	0	—
11	9s	1.0	3.1–3.2	<0.4		4	5	0	—

[a] Solvent: benzene; polymerization temperature: 30°C.; [monomer]: 12 wt.-%.
[b] Numbers given are run numbers of the catalyst preparations. See Experimental part.
[c] Ratio at which reaction between i-Bu$_3$Al and TiI$_4$ was conducted.
[d] Ratio in solid, where used. First number (or single number) indicates ratio calculated from the amount of iodide displaced to the filtrate. Second number is ratio found in solid. The solids were dispensed as slurries.
[e] Duplicate runs.

TABLE II

Polymerization of Butadiene with Solids from Reaction of i-Bu$_3$Al with TiI$_4$, plus Further i-Bu$_3$Al and/or Corresponding Filtrate as Catalyst[a]

Run no.	Catalyst			Polymerization conditions					Results		
	Filtrate (f) or solid (s)[b]	$\frac{[Al]}{[Ti]}$[c]	$\frac{[I]}{[Ti]}$[d]	[Al], mg.-atom/ 100 g. monomer As i-Bu$_3$Al	As i-Bu$_2$AlI	[Ti], mg.-atom/ 100 g. monomer	$\frac{[Al]}{[Ti]}$	Time, hr.	Yield, %	cis content, %	DSV[g]
12	3s	3.7	2.2	28	<1.4	14	2	17	80	70	0.532
13	2s	3.6	2.2	5.6	<0.7	7	0.7	17	98	93	—
14	3s	3.7	2.2	14	<0.7	7	2	17	87	91	1.48
15	3s	3.7	2.2	14	<0.7	7	2	17	94	89	1.28
16	3s	3.7	2.2	28	<0.7	7	4	17	55	83	1.21
17	3s	3.7	2.2	28	<0.7	7	4	17	66	80	1.01
18	2f + 2s[e]	3.6	2.2	6.3	7.2	4	3.5	17	100	82	—
19	2f + 2s[e]	3.6	2.2	6.3	7.2	4	3.5	17	98	82	—
20	6s	2.2	2.3–2.4	11[f]	<0.4	4	3	1	51	88	1.45
21	9s	1.0	3.1–3.2	11[f]	≤0.4	4	3	1	94	71	0.723
22	9f + 6s	1.0, 2.2	2.3–2.4	5.5[f]	1.9	2	4	1	90	87	1.07
23	9f + 9s	1.0	3.1–3.2	5.5[f]	1.9	2	4	1	88	81	1.24

[a] Solvent: benzene; polymerization temperature: 30°C.; [monomer]: 12 wt.-%.
[b] Numbers given are run numbers of the catalyst preparations.
[c] Ratio at which reaction between i-Bu$_3$Al and TiI$_4$ was conducted.
[d] Ratio in solid, where used. First number (or single number) indicates ratio calculated from the amount of iodide displaced to the filtrate. Second number is the ratio found in the solid. The solids were dispensed as slurries.
[e] All the alkylaluminum used in these runs was in the filtrate (2f) added.
[f] Added after a reaction period of 4 hr. at 30°C. had produced no polymer.
[g] DSV is dilute solution viscosity.
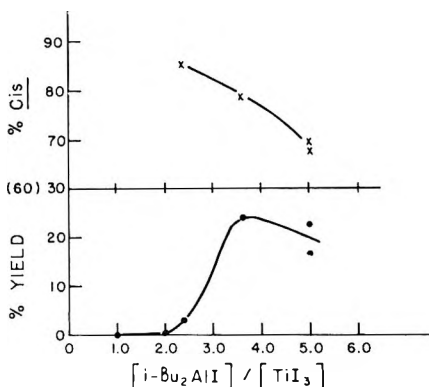
Fig. 5. Conversion to polybutadiene in 22 hr. at 30°C. and *cis* content as a function of catalyst ratio. Solvent benzene, monomer = 12 wt.-%, [Ti] = 13 mg.-atom/100 g. monomer.

Polymerizations in the presence of catalysts containing titanium tetraiodide, titanium chlorotriiodide, or titanium dichlorodiiodide all showed a similar dependence of yield on Al/Ti ratio, characterized by maximum yields at Al/Ti ratios ranging from 1.5 to 3.0. Catalysts containing titanium tetrachloride exhibit maximum activity at Al/Ti ratios of 1.0–1.2.[3]

The 1,2-content of all polymers prepared with catalysts containing iodide was low and changed very little with ratio. The 1,2-content of the polymers prepared with titanium tetrachloride, though low at ratios of two and below, rose rapidly as the ratio was increased above two. The *cis* content increased with decreasing titanium concentration or Al/Ti ratio when the titanium salt was the tetraiodide, the chlorotriiodide or the dichlorodiiodide. When the titanium salt was the tetrachloride, the *cis* content varied little with titanium concentration and rose with decreasing Al/Ti ratio in the range studied.

The dilute solution viscosities decreased with increasing titanium concentration, Al/Ti ratio, and chloride content of the titanium salt. Since in most cases structural changes were occurring as well, the changes in dilute solution viscosity cannot be assumed to be directly related to molecular weight changes.

Polymerization of butadiene was not induced by either the soluble (chiefly alkylaluminum compounds[13]) or the insoluble (chiefly reduced and/or alkylated titanium iodides[13]) products of reaction between triisobutylaluminum and titanium tetraiodide, as shown in Table I. However, triisobutylaluminum, added independently or as a part of a filtrate, activated the insoluble material, regardless of the I/Ti ratio in it, over a range of Al/Ti ratios from 0.8 to 4 (Table II). Diisobutylaluminum iodide was a poorer activator, as shown by the following experiments. Slurries containing equimolar quantities of diisobutylaluminum iodide and titanium triiodide were prepared by aging triisobutylaluminum and titanium

TABLE III

Polymerization of Butadiene by i-Bu$_3$Al–i-Bu$_2$AlX–TiX$_4$ Mixtures[a]

$\dfrac{[i\text{-Bu}_3\text{Al}]}{[\text{Ti}]}$	[Ti], mg.-atom/ 100 g. monomer	(i-C$_4$H$_9$)$_3$Al–(i-C$_4$H$_9$)$_2$AlI–TiCl$_4$				(i-C$_4$H$_9$)$_3$Al–(i-C$_4$H$_9$)$_2$AlCl–TiI$_4$			
		Initial [i-Bu$_2$AlI], mmole/100 g. monomer	Conversion, %[b]	cis content, %[b]	1,2 content, %[b]	Initial [i-Bu$_2$AlCl], mmole/100 g. monomer	Conversion, %[b]	cis content, %[b]	1,2 content, %[b]
4.8	5.0	20	85	62	5	—	—	—	—
4.0	5.7	None	22	12	38	None	80–85[c]	55–60[c]	5[c]
4.8	10	40	78	47	6	40	80	42	6
2.0	5.0	20	90	57	4	20	97	59	4
2.0	5.7	None	32	57	7	None	90	67	4
2.0	10	40	88	45	3	40	92	43	4
2.0	10	—	—	—	—	None	87	55	4
1.0	10	40	98	65	3	40	0	—	—

[a] Solvent: benzene; [monomer]: 12 wt.-%; 4 hr.; 30°C.; [I]/[Cl]: 1.0, where both are present.

[b] All values are average of two runs.

[c] Interpolated, using TiI$_4$ curve shown in Figure 2.
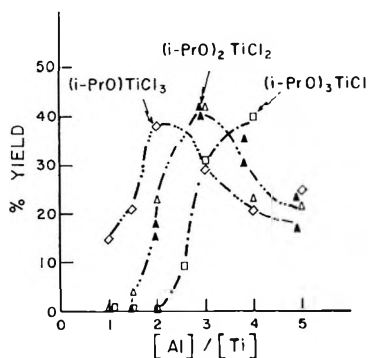
Fig. 6. Conversion to polybutadiene in 21 hr. at 30°C. ([monomer] = 20 wt.-%): (□) (i-PrO)$_3$TiCl, [Ti] = 19 mg.-atom/100 g. monomer, cocatalyst i-Bu$_2$AlH, solvent heptane; (△) (i-PrO)$_2$TiCl$_2$, [Ti] = 19 mg.-atom/100 g., cocatalyst i-Bu$_2$AlH, solvent heptane; (▲) (i-PrO)$_2$TiCl$_2$, [Ti] = 10 mg.-atom/100 g., cocatalyst i-Bu$_3$Al, solvent benzene; (◇) (i-PrO)TiCl$_3$, [Ti] = 19 mg.-atom/100 g., cocatalyst i-Bu$_2$AlH, solvent heptane.

tetraiodide together at a ratio of unity, and butadiene and various amounts of diisobutylaluminum iodide then were added. Yields were poor even at an i-Bu$_2$AlI/TiI$_3$ ratio of five (Fig. 5). The *cis* content dropped as the Al/Ti ratio was increased, and the polymers were translucent and slightly waxy, in contrast to the rubbery materials obtained with triisobutylaluminum.

In these experiments with separated catalysts, the yield dropped when the i-Bu$_3$Al/Ti ratio was raised as high as 4.0 (runs 16 and 17 of Table II). The *cis* content decreased with increasing titanium concentration, I/Ti ratio in the solid, and Al/Ti ratio.

The experiments shown in Table III indicate that under some conditions the relative rates of polymerization and halide exchange between titanium and aluminum are such that in mixtures containing equimolar quantities of chloride and iodide, it makes no difference which halide is initially bound to titanium. Thus at i-Bu$_3$Al/Ti ratios of 4.8 and 2.0, the mixtures i-Bu$_3$Al–i-Bu$_2$AlI–TiCl$_4$ and i-Bu$_3$Al–i-Bu$_2$AlCl–TiI$_4$ both behaved like a mixture of triisobutylaluminum with titanium tetraiodide. Yields were similar, the *cis* content decreased with increasing catalyst concentration, as with titanium tetraiodide catalysts, and the slightly lower *cis* content presumably was due to the presence of the additional diisobutylaluminum halide. At an i-Bu$_3$Al/Ti ratio of 1.0, however, each mixture behaved like the corresponding one having no diisobutylaluminum halide present.

Figure 6 shows related experiments in an analogous mixed system. With triisobutylaluminum or diisobutylaluminum hydride and isopropoxytitanium trichloride, diisopropoxytitanium dichloride or triisopropoxytitanium chloride, the Al/Ti ratio at which maximum activity was attained increased as the number of chloride ligands on titanium was decreased.

DISCUSSION

In all these systems, the components necessary for catalytic activity are (1) triisobutylaluminum or diisobutylaluminum halide and (2) a reduced titanium compound. The need for both is clear from the following. The solids formed by reduction of titanium tetrachloride are active catalysts only in the presence of an alkylaluminum compound, either adsorbed during the preparation of the solid or added subsequently.[3,14] Similarly, we have found that the solids formed from the reduction of titanium tetraiodide are inactive until combined with triisobutylaluminum or diisobutylaluminum iodide (Tables I and II, Fig. 5).

The participation of a titanium(IV) compound as a cocatalyst is virtually ruled out, because it has been shown (1) that titanium tetrachloride is rapidly reduced to titanium trichloride by trialkylaluminum,[15-18] and (2) that titanium tetrahalides with two or more iodide ligands afford inactive catalyst systems at an Al/Ti ratio of unity (Fig. 1), the ratio among those tried at which titanium(IV) compounds would be most likely to exist.

Butadiene can be polymerized by diethylaluminum chloride with titanium trichloride[19] or by diisobutylaluminum iodide with titanium triiodide (prepared by reaction of triisobutylaluminum with titanium tetraiodide; Fig. 5). These observations establish the cocatalytic activity of both trihalides, because the trichloride is not reduced by diethylaluminum chloride,[19-21] and the triiodide is not reduced by diisobutylaluminum iodide.[13] Whether titanium(II) halides can function as cocatalysts is not known, because no examples exist in which authentic titanium dichloride or a solid known to contain no titanium(III) has shown cocatalytic activity with an alkylmetal for polymerization of dienes.

It has been demonstrated that in the Ziegler-type polymerizations of ethylene and propylene, propagation occurs by the insertion of monomer at a carbon-metal bond.[22-24] Several authors[3,14,25,27] have extended this mechanism to diene polymerizations. The site of insertion is thought to be a carbon–aluminum bond by some,[14,25,27] a carbon–titanium bond by others.[3,26] Our results are consistent either with the latter view or with the view that both titanium and aluminum are required to form a catalyst site. This follows from the findings that behavior typical of catalysts in which only iodide ligands are present is obtained with catalysts containing both chloride and iodide (Figs. 1–4, Table III), and that titanium is the preferred site for attachment of iodide.[13] This preference is so pronounced that the product of reduction of titanium dichlorodiiodide by diisobutylaluminum iodide at an Al/Ti ratio of 1.5 is 99% titanium triiodide.[13] The results obtained in polymerizations in which i-Bu$_3$Al–i-Bu$_2$AlX–TiX$_4$ mixtures were used as catalysts (Table III) suggest that at i-Bu$_3$Al/Ti ratios of 2.0 and 4.8, replacement of chloride on titanium by iodide precedes polymerization, while at a ratio of unity in the mixtures containing titanium tetrachloride, this replacement is slower than reduction and polymerization.

The observation that a higher Al/Ti ratio is required for maximum activity in the iodide-containing catalyst systems than in the triisobutyl-aluminum-titanium tetrachloride system can be accounted for in terms of equilibria (1) and (2). In the iodide-containing catalyst systems the position of equilibrium (1) may be shifted more to the left than the corresponding equilibrium (2) for the chloride systems.

$$R_3Al(R_2AlX) + TiI_3(TiClI_2) \rightleftharpoons R_2AlX(RAlX_2) + RTiI_2 \qquad (1)$$

$$R_3Al(R_2AlCl) + TiCl_3 \rightleftharpoons R_2AlCl(RAlCl_2) + RTiCl_2 \qquad (2)$$
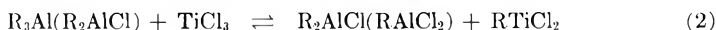
This would be expected for titanium triiodide, because iodide would bear a smaller partial negative charge than chloride,[28] and would thus be less easily displaced. With titanium chlorodiiodide, the need for a high Al/Ti ratio may be accounted for by the statistically smaller chance of attack of the single chloride ligand. The hypothesis that the activity of these catalysts depends on the position of equilibrium (1) is supported by the fact that a higher aluminum/titanium ratio was required with the poorer alkylating agent, diisobutylaluminum iodide.

The results obtained with alkoxytitanium(IV) chlorides can be rationalized similarly. A greater variation in the optimum Al/Ti ratio is observed because the difference between the polarities of chloride and alkoxy is greater than that between chloride and iodide.[28] As the number of alkoxy ligands on titanium increases, the position of equilibrium (3)

$$R_3Al + i\text{-PrOTiCl}_2[(i\text{-PrO})_2\text{TiCl}, (i\text{-PrO})_3\text{Ti}] \rightleftharpoons$$
$$R_2AlY + RTi(O\text{-}i\text{-Pr})Cl[RTi(O\text{-}i\text{-Pr})_2] \quad (3)$$
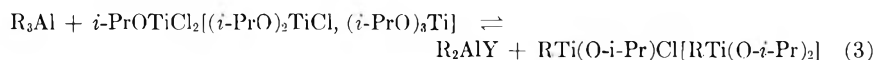
shifts to the left; hence an increase is observed in the ratio required for maximum activity. It should be noted that while the thermodynamic, alkylation hypothesis discussed above is consistent with our observations, its validity has not been confirmed.

The decrease in activity which occurs as the amount of trialkylaluminum is raised beyond the optimum is probably caused by reduction of the titanium compounds to inactive species and/or displacement of monomer from catalyst sites by alkylaluminum.

The polymer structure obtained in these polymerizations depends on a complex of interrelated factors. Further work is required before a comprehensive interpretation can be offered. For example, it is not known whether the *trans* units that form in the presence of diisobutyl-aluminum iodide are copolymerized with the *cis* and 1,2 units in the polymer, or homopolymerized. Both possibilities merit consideration, because both have been realized by Natta[3] using catalysts derived from titanium tetrachloride.

EXPERIMENTAL

Materials

Benzene was distilled from the blue sodium–benzophenone complex. Phillips "special purity" butadiene was distilled through calcium hydride.

Ethyl Corporation triisobutylaluminum was used as received. Diisobutylaluminum chloride and diisobutylaluminum iodide were prepared by Dr. L. C. Kreider of these laboratories, by equilibration of triisobutylaluminum with the appropriate aluminum halide.

Fisher purified titanium tetrachloride was distilled from copper turnings, b.p. 132°C. Titanium tetraiodide from Matheson, Stauffer, or A. D. Mackay was used as received.

The solutions of titanium tetraiodide and of the mixed iodide–chloride salts were analyzed for halide and titanium according to the method described previously.[13] The halogen/titanium ratios were between 4.0 and 4.3 in all cases. Allowance was made for any excess halide present, assuming that it would be converted to diisobutylaluminum halide, in computing i-Bu$_3$Al/Ti ratios. The correction was small, however, and omitting it would not have caused much change in the appearance of the plots.

Polymerizations

All manipulations were performed under prepurified nitrogen which passed through phosphorus pentoxide before use. The polymerizations were conducted in tubes sealed with crown caps. The order of addition of reagents was benzene, alkylaluminum solution, then titanium tetrahalide solution and butadiene or vice versa. Butadiene was added last

TABLE IV

Composition of the Filtrates and Solids Used as Catalysts for the Polymerization of Butadiene

Run no.[a]	[Al]/[Ti][b]	Filtrate (f) [I]/[Al]	Solid (s) [I]/[Ti]	
			Found	Calcd.
2	3.6	0.53	—	2.2
3	3.7	0.47	—	2.2
4	2.1	0.77	—	2.4
6	2.2	0.93	2.4	2.3
9	1.0	1.03	3.2	3.1

[a] Run no. in the previous paper.[13]

[b] Ratio at which catalyst was prepared.

in the experiments shown in Table III. It was added 18 hr. after mixing of the triisobutylaluminum and titanium tetraiodide in the runs shown in Figure 5, and the i-Bu$_2$AlI/TiI$_3$ ratio was computed assuming that all the triisobutylaluminum was converted to diisobutylaluminum iodide during the aging period.

The preparation and analysis of the separated solids was described previously.[13] Benzene and whatever filtrate and/or slurry was to be used were combined, and then butadiene was added. Where additional alkyl-

aluminum was used, this followed the butadiene. Table IV gives data on the composition of the filtrates and solids.

The tubes were rotated in a 30°C. bath for the designated time, quenched with a 20/80 methanol–benzene mixture, and isolated by precipitation with methanol. Infrared structural analyses were performed according to a method similar to that of Silas, Yates, and Thornton.[29] Dilute solution viscosities were determined in toluene at 0.4 g. /100 ml.

References

1. Ziegler, K., E. Holzcamp, H. Breil, and H. Martin, *Angew. Chem.*, **67**, 426 (1955).
2. Belg. Pat. 543,292, to Goodrich-Gulf Chemicals Co. (December 2, 1955).
3. Natta, G., L. Porri, A. Mazzei, and D. Morero, *Chim. Ind. (Milan)*, **41**, 398 (1959).
4. Gaylord, N. G., T. K. Kwei, and H. F. Mark, *J. Polymer Sci.*, **42**, 417 (1960).
5. Belg. Pat. 551,851, to Phillips Petroleum Co. (October 17, 1956).
6. Belg. Pat. 610,400, to Polymer Corp., Ltd. (November 16, 1961).
7. Belg. Pat. 612,732, to Farbenfabrike-Bayer A. G. (January 17, 1962).
8. Brit. Pat. 865,337, to Phillips Petroleum Co. (April 12, 1961).
9. Belg. Pat. 612,539, to Lab. Riunite Studi e Richerche S. p. H. (January 11, 1962).
10. Belg. Pat. 616,725, to Laboratori (April 20, 1962).
11. Brit Pat. 910,216, to Phillips Petroleum Co. (June 6, 1961).
12. Zelinski, R. P., and D. R. Smith, U. S. Pat. 3,050,513, to Phillips Petroleum Co. (August 21, 1962).
13. Moyer, P. H., *J. Polymer Sci.*, **A3**, 209 (1965).
14. Saltman, W. M., *J. Polymer Sci.*, **A1**, 373 (1963).
15. Martin, H., and J. Stedefeder, *Ann. Chem.*, **618**, 17 (1958).
16. Beermann, C., and H. Bestian, *Angew. Chem.*, **71**, 618 (1959).
17. Posamantir, A. G., A. A. Korotkov, and I. S. Lishanskiĭ, *Vysokomolekul. Socdin.*, **1**, 1207 (1959).
18. Tepenitsyna, E. P., M. I. Farberov, A. M. Kutin, and G. S. Levskaya, *Vysokomolekul. Soedin.*, **1**, 1148 (1959).
19. Natta, G., L. Porri, and L. Fiore, *Gazz. Chim. Ital.*, **89**, 761 (1959).
20. Simon, A., and G. Ghymes, *J. Polymer Sci.*, **53**, 327 (1961).
21. Boldyreva, I. I., B. A. Dolgoplosk, and V. A. Krol, *Vysokomolekul. Soedin.*, **1**, 900 (1959).
22. Chien, J. C. W., *J. Am. Chem. Soc.*, **81**, 86 (1959).
23. Feldman, C. F., and E. Perry, *J. Polymer Sci.*, **46**, 217 (1960).
24. Natta, G., G. Pajaro, I. Pasquon, and V. Stellacci, *Atti Accad. Nazl. Lincei, Rend. Classe Sci. Fis. Mat. Nat.*, **24**, 479 (1958).
25. Uelzmann, H., *J. Polymer Sci.*, **32**, 457 (1958).
26. Roha, M. E., *Fortschr. Hochpolymer. Forsch.*, **1**, 512 (1960).
27. Bresler, S. E., M. I. Mosevitzskiĭ, I. Ya. Poddubnyĭ, and Shi Guan-i, *J. Polymer Sci.*, **52**, 317 (1961).
28. R. J. Sanderson, *J. Chem. Educ.*, **32**, 140 (1955).
29. Silas, R. S., J. Yates, and V. Thornton, *Anal. Chem.*, **31**, 529 (1959).

Résumé

Les catalyseurs pour la polymérisation du butadiène, constitués d'un composé alcoyl-aluminium avec un composé du Ti(IV), présentaient des changements de réactivité suivant le rapport Al/Ti.   Le rapport pour lequel on obtient la plus grande réactivité augmente quand l'électronégativité des ligands du titane diminue.   On observe cela quand on remplace le chlore du tétrachlorure de titanium par l'iode ou le groupe oxyiso-propyle.   Les catalyseurs préparés à partir du dichlorodiiodure de titane ou du chloro-triodure de titane se comportent comme ceux à partir de tétraiodure, comm prévu aux dépens des observations antérieures, à savoir que le titane est le site préféré pour la fixation de l'iodure dans les produits de réduction des sels mixtes.   La teneur en com-posé *cis* dans les polymères obtenus avec les sels contenant de l'iodure peut atteindre 90% ou plus, mais diminue lorsque la concentration en titane augmente, tandis que la structure des polymères obtenus avec le tétrachlorure de titane est indépendante de la concentration en catalyseur.   La polymérisation n'est pas initiée par les composés alcoyl-aluminum solubles ou par les iodures de titane réduits insolubles qui sont produits dans lar éaction de triisobutylaluminium avec le tétraiodure de titane.   Le produit in-soluble peut être activé par le triisobutylaluminium ou, moins rapidement, par l'iodure de diisobutylaluminium.

Zusammenfassung

Katalysatoren für die Butadienpolymerisation, die aus einer Alkylaluminiumver-bindung und einer Titan-(IV)-Verbindung bestehen, zeigen eine Abhängigkeit der Reaktivität vom Verhältnis Al/Ti.   Das Verhältnis mit der maximalen Reaktivität nimmt mit fallender Elektronegativität der an Titan gebundenen Liganden zu.   Das wird beim Ersatz der Chloridliganden von Titantetrachlorid sowohl durch Jodid als auch Isopropoxyliganden beobachtet.   Aus Titandichlordiiodid oder Titanchlortrijodid dargestellte Katalysatoren verhalten sich wie diejenigen aus Titantetrajodid, was nach der früheren Beobachtung, dass Titan der bevorzugte Ort für Jod in den Reduktions-produkten von gemischten Salzen ist, zu erwarten ist.   Der *cis*-Gehalt der mit Jodid enthalten den Salzen erhaltenen Polymeren kann 90% oder mehr betragen, nimmt aber mit steigender Titankonzentration ab, während die Struktur der mit Titantetrachlorid erhaltenen Polymeren von der Katalysatorkonzentration unabhängig ist.   Weder durch die löslichen Alkylaluminiumverbindungen noch durch die unlöslichen reduzierten Titanjodide, die bei der Reaktion von Triisobutylaluminium mit Titantetrajodid entste-hen, wird Polymerisation angeregt.   Das unlösliche Material kann durch Triisobutylalu-minium oder, weniger leicht, durch Diisobutylaluminiumjodid aktiviert werden.

Polymerization of Butadiene by *n*-Butyllithium– Titanium Tetrachloride (Tetraiodide) Catalysts

MARVIN H. LEHR and PATRICIA H. MOYER, *The B. F. Goodrich Research Center, Brecksville, Ohio*

Synopsis

The structure of polybutadiene obtained with a *n*-BuLi- TiX$_4$ (X = Cl, I) catalyst depends on the Li/Ti ratio. At Li/Ti < 2.5 the result is similar to that with (*i*-Bu)$_3$Al–TiX$_4$, predominantly, *cis*-1,4-polybutadiene. On the other hand, in the range Li/Ti = 3–4, the chloride catalyst produces largely 1,2-polybutadiene, and at Li/Ti = 3 it is unaffected by ether in contrast to other ratios investigated. At Li/Ti $\geq$ 5 in both halide systems, the structure is essentially a mixture of isomers characteristic of the *n*-BuLi catalyst alone.

INTRODUCTION

The catalyst systems prepared from *n*-BuLi and TiCl$_4$ show variable activity depending on the Li/Ti ratio. This behavior has been explained in terms of complexes between metal alkyl and titanium halide. We report here data on butadiene polymerizations which indicate more specifically the nature of the complexes.

RESULTS AND EXPERIMENTAL

The results are summarized in Figures 1 and 2 and in Table I. The solvent was dried by distilling from Na–benzophenone and stored under N$_2$. The *n*-BuLi was used as received from the Lithium Corp. Concentration was determined by the Gilman method. Fisher's TiCl$_4$ was used after distilling from Cu turnings. Titanium tetraiodide was used as received from Stauffer; the I/Ti ratio analyzed 4.3. Phillips special purity butadiene was distilled through CaH$_2$. Baker analyzed anhydrous ether was taken without further drying.

The reagents were charged to heavy-walled tubes equipped with caps containing self-sealing rubber gaskets. The rubber was previously extracted to remove soluble impurities. The order of charging was; solvent, *n*-BuLi, TiX$_4$, Et$_2$O; the tubes were then capped and monomer finally added. The tubes, syringes, and needles were dried in an oven at 125°C. and cooled under prepurified N$_2$, dried with P$_2$O$_5$. All charging operations were under N$_2$.
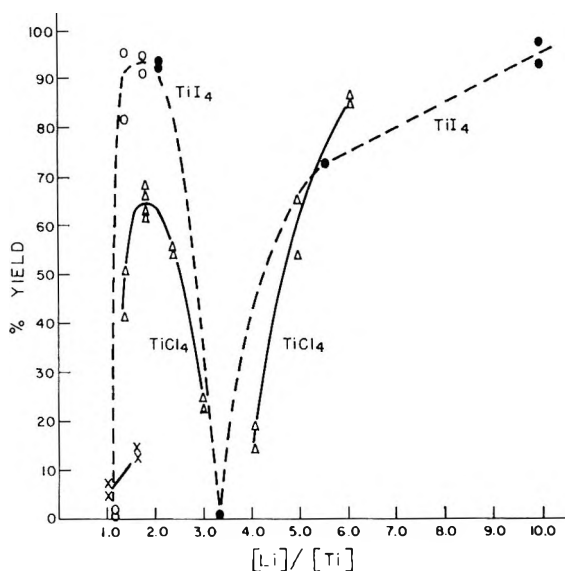
Fig. 1. Yield of polybutadiene as a function of catalyst ratio: (△) 11 mmole TiCl₄ /100 g. monomer, polymerization time 21 hr.; (×) 11 mmole TiCl₄/100 g., polymerization time 2 hr.; (●) 5.7 mmole TiI₄/100 g., polymerization time 4 hr.; (○) 10 mmole TiI₄/100 g., polymerization time 4 hr.; (○) 10 mmole TiI₄/100 g., polymerization time 4 hr. Solvent benzene (20 ml.), temperature 30°C., cocatalyst n-butyllithium.
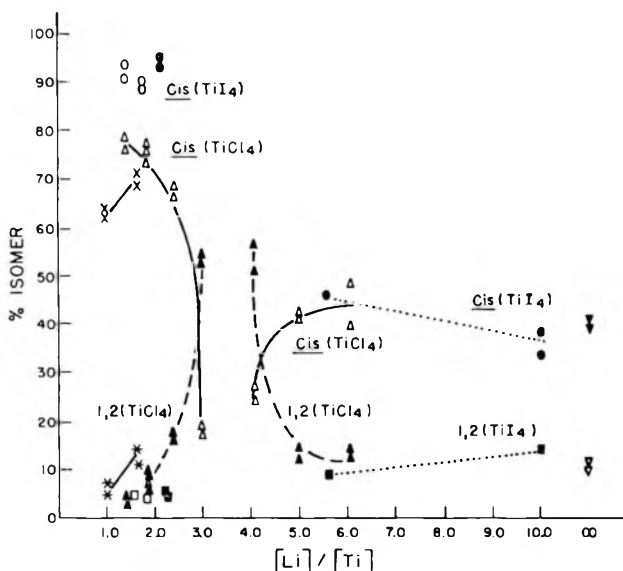
Fig. 2. Structure of polybutadiene as a function of catalyst ratio: (○, □) 10 mmole TiI₄/100 g. monomer; (●, ■) 5.7 mmole TiI₄/100 g.; (×, *) 11 mmole TiCl₄/100 g. (2 hr.); (△, ▲) 11 mmole TiCl₄/100 g. (21 hr.); (▽, ▼) 1.2–1.6 mmole n-C₄H₉Li/100 g. (17 hr., 30°C., 25 ml. benzene). Conditions as in Fig. 1.

TABLE I
Polymerization of Butadiene with n-BuLi–TiCl$_4$–Et$_2$O at 30°C.[a]

Run	[Li]/[Ti]	Yield, %	cis content, %	trans content, %	1, 2 content, %
1	1.4	1	—	—	—
2	1.4	0	—	—	—
3	2.0	10	20	10.5	69.5
4	2.0	8	27	8	64.5
5	3.0	16	15	26.5	58.5
6	3.0	21	10	25	65
7	5.0	88	26	38.5	36
8	5.0	92	25.5	38	36
9	∞	97	26	38	36
10	∞	98	25	38	37

[a] Conditions: Benzene, 20 ml.; butadiene, 4.5 g.; TiCl$_4$–0.48 mmole as 0.48M solution; n-BuLi as 0.69M solution or as 0.50M solution (runs 9 and 10); Et$_2$O/Li = 4; time = 21 hr.

The tubes were contained in safety jackets and rotated in a 30°C. bath. The reactions were quenched with an alcohol–benzene mixture and the polymers recovered by precipitation with excess methanol. Drying was under vacuum at 50°C.

Infrared spectra were run on films cast from benzene solutions. The calculations were similar to those reported elsewhere.[1]

DISCUSSION

It has been shown that n-BuLi does not completely reduce TiCl$_4$, the extent of reduction depending on order of addition of reagents, Li/Ti ratio, and concentration.[2–5] Maximum reduction occurs at Li/Ti = 1.5–2.0.[3,5] At these ratios, where as much as 55% Ti(III) is found, the rate of ethylene polymerization also exhibits a maximum.[3,6,7] On either side the extent of reduction drops rapidly, as does the rate of polymerization, until at Li/Ti > 4 the titanium is practically all in the (IV) state.[3,5,6] The Ti(IV) compound evidently is not free TiCl$_4$, because in titrating n-BuLi with TiCl$_4$, Evans and Owen[8] found that the yellow color of free TiCl$_4$ does not appear until Li/Ti ∼ 1.1. They also observed that by adding HCl to destroy metal alkyl at Li/Ti = 1.2–2.0 the color can be generated. In other experiments they showed, as had others earlier,[3] that free n-BuLi exists only at Li/Ti > 3.4.

To account for the incomplete reduction of titanium tetrahalide and the absence of free metal alkyl, several explanations have been suggested, either complex formation[3,4] according to eq. (1)

$$TiCl_4 + nRLi \rightarrow TiCl_4 \cdot (RLi)_n \tag{1}$$

or alkylation,[3,6] for example[6]

$$TiCl_4 + nRLi \rightarrow R_nTiCl_{4-n} + nLiCl \tag{2}$$
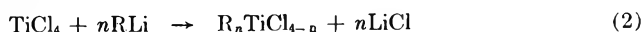
where alkylation might proceed until all chloride ligands are replaced. It is generally agreed[3,4,8] that reduction to Ti (III) occurs, analogous to that effected by R_3Al, and gives $TiCl_3$ [eq. 3] as indicated by x-ray analysis.[4] Further

$$TiCl_4 + RLi \rightarrow TiCl_3 + LiCl + [R] \tag{3}$$

complexing or alkylation of $TiCl_3$ has been suggested.[3,4,8]

In our studies of the butadiene polymerization we observed that at Li/Ti = 1.0–2.5 the n-BuLi–TiX_4 (X = Cl,I) catalyst systems (Figs. 1 and 2) are strikingly similar to the $(i$-Bu$)_3Al$–TiX_4 (X = Cl,I) catalyst systems[9] at approximately the same catalyst ratios. For example, in both iodide systems, Al–Ti and Li–Ti, high (> 90%) cis-1,4-polybutadiene is formed, while in both chloride systems, the cis content of the polymer and the yield reach a maximum at approximately the same catalyst ratio. These similarities suggest that the Li–Ti system at Li/Ti = 1.0–2.5 can be partly described by reactions four and five which are similar to those advanced

$$TiCl_3 + RLi \rightarrow TiCl_3 \cdot RLi \tag{4a}$$

$$TiCl_3 + RLi \rightarrow RTiCl_2 + LiCl \tag{4b}$$

$$TiCl_3 \cdot RLi + RLi \rightarrow TiCl_3 \cdot (RLi)_2 \tag{5a}$$

$$RTiCl_2 + RLi \rightarrow R_2TiCl + LiCl \tag{5b}$$
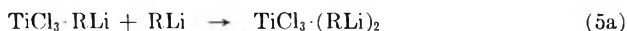
for the Al–Ti system.[10–12] The ratio at which a maximum in yield is obtained, Li/Ti $\sim$ 2 (Figure 1), is within the range (1.5–2.0) at which maximum reduction of $TiCl_4$ to Ti(III) is found.[3,5] The hypothesis that at these ratios the main catalyst species is formed according to reaction 4 accommodates this observation and is supported by previous findings that $TiCl_3$[12,13] or TiI_3[9] acts as a cocatalyst with alkylaluminum compounds in butadiene polymerizations. As in the Al–Ti systems, the Li–Ti systems at Li/Ti > 2 exhibit a rapid decline in yield. Since Ti(III) is still present[3,5] at Li/Ti = 3, additional complexing or alkylation by metal alkyl to remove the active sites which produce predominantly cis polymer is indicated [eq. (5)]. It is apparent (Figure 2) that further reaction with metal alkyl leads also to formation of a different catalyst producing predominantly 1,2-polybutadiene at Li/Ti = 3–4. Finally, at higher ratios, Li/Ti $\geqslant$ 5, we obtained polymer characteristic of that formed by n-BuLi alone (Fig. 2) in agreement with other data which show the presence of free n-BuLi under these conditions.[3,5,6]

Additional insight into the nature of the n-BuLi–$TiCl_4$ catalyst system was obtained by addition of ether at various ratios (Table I). At Li/Ti = 1.4 no polymer forms in the presence of ether, thus indicating that the cis catalyst [eq. (4)] is either complexed or destroyed. However, at Li/Ti = 2.0, polymer is obtained in the presence of ether, but it is predominantly 1,2-polybutadiene. This indicates that here again the cis catalyst is either complexed or destroyed, and that an additional cat-

alyst species is present which produces 1,2-polybutadiene. At Li/Ti = 3.0, unlike other ratios studied, the catalyst is insensitive to ether, the yield and structure of the polymer being essentially the same in both cases (see Figs. 1 and 2 and Table I). The same catalyst is evidently also present at Li/Ti = 4.0 because yield and structure are similar to those at Li/Ti = 3.0. It is suggested that this catalyst species is $TiCl_3 \cdot (LiR)_2$, or some alkylated equivalent thereof, formed according to reaction (5).

Finally at higher ratios, Li/Ti $\geqslant$ 5, the ether results are the same as those without $TiCl_4$ (runs 7–10), thus providing further evidence for the existence of free n-BuLi.

In this work we have determined to some degree the operational limits of reactions (4) and (5). We find that reaction (4) is important at least as low as Li/Ti = 1.0, but no higher than Li/Ti = 2.5, and that reaction (5) is principally operative at Li/Ti = 2–4. These conclusions are consistent with the reduction data which show reaction (3) to be significant over the range Li/Ti = 1–4.[5]

References

1. Silas, R. S., J. Yates, and V. Thornton, *Anal. Chem.*, **31**, 529 (1959).
2. Korotkov, A. A., and I. L. Artamonova, *Vysokomolekul. Soedinen.*, **4**, 10 (1961).
3. Friedlander, H. N., and K. Oita, *Ind. Eng. Chem.*, **49**, 1885 (1957).
4. Jones, M. H., A. Martius, and M. P. Thorne, *Can. J. Chem.*, **38**, 2303 (1960).
5. Heller, J., D. O. Tieszen, and D. B. Parkinson, *J. Polymer Sci.*, **A1**, 125 (1963).
6. Ludlum, D. B., A. W. Anderson and C. E. Ashby, *J. Am. Chem. Soc.*, **80**, 1380 (1958).
7. Frankel, M., J. Rabani, and A. Zilkha, *J. Polymer Sci.*, **28**, 387 (1958).
8. Evans, A. G., and G. O. T. Owen, *J. Chem. Soc.*, **1961**, 1733.
9. Moyer, P. H., and M. H. Lehr, *J. Polymer Sci.*, **A3**, 217 (1965).
10. Malatesta, A., *Can. J. Chem.*, **37**, 1176 (1959).
11. Saltman, W. M., W. E. Gibbs, and J. Lal, *J. Am. Chem. Soc.*, **80**, 5615 (1958).
12. Bresler, S. E., M. I. Mosevitskiĭ, I. Ya. Poddubnyĭ, and Shi Guan-i, *Vysokomolekul. Soedinen.*, **3**, 1591 (1961).
13. Natta, G., L. Porri, and L. Fiore, *Gazz. Chim. Ital.*, **89**, 761 (1959).

Résumé

La structure du polybutadiène obtenue avec un catalyseur n-BuLi–TiX₄ (X = Cl, I) dépend du rapport Li/Ti. Pour un rapport Li/Ti < 2.5 le résultat est semblable à celui obtenue avec (i-Bu)₃Al–TiX₄ avec prédominance de cis-1,4-polybutadiène. D'autre part, pour un rapport Li/Ti = 3–4 le catalyseur chloré donne surtout du 1,2-polybutadiène et pour un rapport égal à 3 il n'est pas affecté par l'éther contrairement aux autres rapports envisagés. Pour Li/Ti $\geq$ 5, dans les deux systèmes halogénés, la structure consiste essentiellement en un mélange d'isomères, caractéristique du catalyseur n-BuLi seul.

Zusammenfassung

Die Struktur des mit einem n-BuLi–TiX$_4$-(X = Cl, J)-Katalysators erhaltenen Polybutadiens hängt vom Verhältnis Li/Ti ab. Bei Li/Ti < 2,5 entsteht, ähnlich wie mit (i-Bu)$_3$Al-TiX$_4$, vorwiegend cis-1,4-Polybutadien. Andrerseits erzeugt der Chloridkatalysator im Bereich Li/Ti = 3–4 zum Grossteil 1,2-Polybutadien, und bei Li/Ti = 3 wird es im Gegensatz zu den anderen untersuchten Verhältnissen durch Äther nicht beeinflusst. Bei Li/Ti ≥ 5 ist bei beiden Halidsystemen die Struktur im wesentlichen eine für den n-BuLi-Katalysator allein charakteristischen Mischung der Isomeren.

Viscosities of Concentrated Polymer Solutions

NORIO NISHIMURA, *Faculty of Science, Okayama University, Okayama, Japan*

Synopsis

A general relationship between the viscosity and the concentration of polymer solutions has been derived for relatively low concentration regions by means of the method which was proposed by Brinkman. The relationship was extended so as to be applicable for extremely concentrated solutions by allowing for the volume shrinkage of polymers. With increasing concentration, the apparent volume which a polymer in solution occupies above some critical volume fraction ϕ_c, is assumed to be given by $\Omega = s v_0 \phi^{-\beta}$, where s is the swelling factor at $\phi = 1$ and β is a constant which measures a reluctance against the intermolecular permeation; v_0 and ϕ are the net volume of the polymer molecule and the volume fraction of the polymer, respectively. The dependence of η on ϕ is given by the equation $d \log \eta / d\phi = C/\phi^\gamma (1 - \phi)$, where C and γ are constants to be determined empirically. In order to test the validity of the equation, our experimental and some other available data were used. Although neither temperature nor molecular weight factor is involved in this equation, it accounts well for the dependence of the viscosity on the concentration of polymers over a wide range of concentration, and fairly satisfactory agreement was found between theory and experiment.

1. INTRODUCTION

Progress in both theoretical and experimental work on the viscosity characteristics of extremely dilute polymer solutions has led us naturally to the elucidation of problems of the viscosities of concentrated polymer solutions, because the flow properties of these concentrated solutions involve many important problems. Up to now, some theories concerning the relationships between the viscosity of concentrated polymer solutions and the bulk viscosity of molten polymers on the one hand, and their molecular weight, temperature, and concentration on the other hand, have been proposed. In developing these theories, some authors[1,2] have attributed the enormous increase in the viscosity with increasing concentration to the formation of intermolecular linkages between polymers, and have adopted a working model of entangled polymer molecules, whereas Fujita et al.[3] have introduced the concept of free volume into the problem, instead of directly considering the interchain entanglement effect. Another way of approaching the problem was proposed by Brinkman.[4] He derived an equation which relates the viscosity of emulsions to their concentration at higher levels of concentration, on the basis of a theory for infinite dilution.

An analogous but modified treatment is worked out here in order to inter-pret the dependence of viscosity on concentration over a wide range and re-sults are compared with some of the available data.

2. EXPERIMENTAL

Since we are interested in accelerated bulk polymerizations,[5] monomeric styrene was chosen as the solvent. The method of purification of com-mercial styrene and benzene has been described elsewhere.[5] Polystyrene (Dow 666) was not subjected to further purification. In order to avoid polymerization, purified hydroquinone was saturated in styrene monomer. An appropriate amount of polystyrene was dissolved into the styrene monomer. After the viscosity of the solution had been measured, the poly-mer was precipitated in ice–methanol, and the polymer concentration was determined by means of the gravimetric method.

In order to make sure that the degree of polymerization does not change during the period of the viscosity measurements, the recovered polystyrene was again dissolved in benzene and the intrinsic viscosities were determined in an Ostwald type viscometer. The number-average degree of polymer-ization was determined by eq. (1):[6]

$$\bar{P}_n = 1770 \; [\eta]^{1.40} \tag{1}$$

The densities of the polymer solutions of various concentrations at var-ious temperatures were estimated from a diagram showing the relationship between weight concentration and density. The densities of the polymer and monomer reported by Matheson et al.[7] were used.

The viscosity of the polystyrene solutions of the concentrations ranging from 0 to 6% was measured by a capillary viscometer of an Ostwald type which has a capillary radius of 0.0306 cm. and capillary length 10 cm. The Reynolds number was calculated to be 115 at 50°C. for styrene monomer. For the calculation of viscosity, the general practice is to determine a rela-tive viscosity with respect to a liquid of known viscosity. Since the exact viscosities of water at 30, 40, and 50°C. are known to be 0.797, 0.653, and 0.548 cpoise, respectively, the apparent viscosities of the polymer solutions were calculated by using these values and the densities of water and of the solutions. The correction term due to kinetic energy loss could be neglected.

For more concentrated solutions (6–46 wt.-%), a rotating viscometer (Tokyo Keiki Co., BL type) was used. The viscometer is equipped with several kinds of rotors which can be used in turn and which can be rotated at velocities of 60, 30, 12, and 6 rpm; it is designed for measuring the vis-cosity of a liquid which is of infinite spread. (In this case no correction for wall effect is necessary.) However, due to experimental limitations, the solution was charged in a cylindrical flask, 500 ml. in volume and 7.5 cm. in diameter. The axis of the rotor was set to coincide with the midline of the cylinder and the rotor was driven to rotate by a synchronous motor

with a uniform angular velocity, and the apparent viscosities were read off.

For solutions of concentrations ranging from 25 to 50%, the falling ball method was applied. Six kinds of steel balls (kindly supplied by the Japan Miniature Ball Bearing Co.) having diameters of 0.15 (0.1498), 0.12 (0.1198), 0.10 (0.0997), 0.08 (0.0797), 0.06 (0.0604), and 0.04 (0.0394) cm., were used; the values in parentheses here were obtained experimentally from the density and the weight of the balls.

About 15 ml. of the polymer solution was charged in a precision test tube 20 cm. in length and 1.43 cm. in diameter. The ball was made to drop along the center line of the tube and after a terminal velocity was attained, the falling velocity was measured by following the moving ball with a travelling microscope. Stokes' law applies, strictly speaking, only when a liquid is of infinite spread. However, sufficiently accurate viscosity values for our present purpose could be obtained by using Faxen's equation:

$$\eta = (gd^2/18v)(\rho_s - \rho)[1 - 2.104(d/D) + 2.09(d/D)^3] \qquad (2)$$

where g denotes the acceleration of gravity, v the velocity of the falling ball, ρ_s and ρ the densities of the ball and the solution, respectively, and d and D the diameters of the ball and the cylinder in which the solution is charged, respectively. The higher correction terms could reasonably be overlooked. The Reynolds number for the falling ball method must be much smaller than unity. It was found that this condition is satisfied in the present experiment.

Fractionations of the polystyrene were made according to the method reported in the previous paper,[5] and from the integral weight distribution curve, the weight-average degree of polymerization was calculated.

3. VISCOSITY OF POLYMER SOLUTIONS AS A FUNCTION OF THE VOLUME FRACTION OF POLYMERS

It is well known that the intrinsic viscosity of polymer solutions $[\eta]$ is related to the molecular weight of the polymer M by the empirical eq. (3):

$$[\eta] = KM^\alpha \qquad (3)$$

where K and α are constants and are nearly independent of temperature. Theoretical approaches toward eq. (3) have successfully revealed the hydrodynamic behavior of polymers in extremely dilute solutions. For a polymer solution of extremely low concentration, eq. (3) may be written in the form

$$\eta = \eta_0 (1 + K'nM^{\alpha+1}) \qquad (4)$$

where η and η_0 are the viscosity of the solution containing n polymer molecules per cubic centimeter and that of the solvent, respectively, and K' is a proportionality constant. For some concentrated solutions, however, eq.

(4) has been invalidated by experimental results, and many empirical equations have been proposed.

In order to treat the viscosity of concentrated solutions, hydrodynamic interactions between polymers must be taken into account. But we encounter some mathematical difficulties if we take these factors into account in a direct way.

Although the assumption made by Brinkman is far from rigorous, just because it avoids the direct calculation of the effect of hydrodynamic interactions between polymers, it seems practical to apply his method in order to understand the essential features of the dependence of viscosity on the concentration of polymers.

On the basis of the Einstein equation, he has derived equations which relate the viscosity of suspensions to the volume fraction. He suggested that his method might be applicable in all cases if an equation for infinite dilution were known. A similar procedure, therefore, was carried out here as follows. If we add one polymer having net volume v_0* to a solvent of volume V, then from eq. (4), we get

$$\eta = \eta_0 [1 + K'M^{\alpha+1}/(V + v_0)] \tag{5}$$

the volume additivity being assumed. According to Brinkman, eq. (5) would be valid for the process that one polymer molecule is added to the solvent of volume V containing p polymer molecules. These polymer molecules are assumed to have the same molecular weight. In this case, we have only to replace η by $\eta + \Delta\eta$ and η_0 by η, thus we have

$$\eta + \Delta\eta = \eta [1 + K'M^{\alpha+1}/(V + v_0)] \tag{6}$$

Since the volume fraction of the polymer ϕ is given by $\phi = pv_0/V$ eq. (6) can be expressed in the form of the difference equation, eq. (7):

$$\eta + \Delta\eta = \eta [1 + (K'/v_0)M^{\alpha+1} \Delta\phi/(1 - \phi)] \tag{7}$$

Integrating eq. (7) from $\eta = \eta_0$ to η and $\phi = 0$ to ϕ, one obtains

$$\ln \eta = \ln \eta_0 - (K'/v_0)M^{\alpha+1}\ln (1 - \phi) \tag{8}$$

It is to be noted that the procedure just developed involves taking into account the interactions between a specified polymer and the remaining system composed of solvent and polymers.

In order to interpret the characteristic behavior of viscosity in the region of high concentration and molten state, the concept of intermolecular entanglements has been introduced.[1,2,8] The entanglement would result in the connection of polymer molecules in a cluster and hence the same effect of increasing molecular weight. Hirai has introduced the entanglement

* v_0 is the volume formally defined as the weight of a polymer divided by the bulk density, and hence it must not be confused with the apparent encompassed volume occupied by the polymer in bulk.

effect into the Staudinger-type equation [essentially the same as eq. (4)] and explained the dependence of η on the concentration and the molecular weight of polymers. However, if we started from eq. (8), and allowed for a particular effect due to the entanglement, the viscosity of the solution at higher levels of concentration would be much greater than that expected from eq. (8). As we shall show later, the reverse is true, and the viscosity of polymer solutions usually increases far less rapidly than would be expected from eq. (8).

This fact has led us to the following consideration. As we add polymer molecules successively to the solution, the sum of the apparent volumes occupied by the polymers would reach the volume of the system V at some critical concentration or the volume fraction ϕ_c. Rough calculation indicates us that a solution containing a few per cent vinyl polymer having 10^3 monomer units corresponds to this concentration.

The concept that the compression of coiling molecules in good solvents at finite concentration occurs has been introduced by Simha et al.[9-11] They investigated the solution viscosities of flexible polymers in the range of concentration where the pervaded volumes of the polymer coils begin to overlap, and evaluated the dependence of the molecular dimensions of the coils on concentration in the vicinity of the concentration of incipient overlap. In fact, intra- and intermolecular interactions must be taken into account for the rigorous calculation of the compression effects. However, the effect of the concentration on the encompassed volume could be interpreted in the following manner: above the critical concentration, two limiting cases can be considered.

Case I. If we add more polymers to the solution, the swollen polymers are forced to reduce their apparent volume, like sponges crowded in a box, by mutual mechanical contact, but they can not come into neighboring molecules. This model is the same as that adopted by Kuhn[12] and Cerf,[13] in that the molecule is completely impermeable but differs in that it is not an elastic incompressible sphere. It is easily seen in this case that the encompassed volume Ω is inversely proportional to the first power of ϕ, i.e., Ω is expressed approximately as

$$\Omega \cong v_0/\phi.$$

Case II. Polymer molecules are permeable to each other and can enter into any neighboring coils as if they were not affected by any force or limitation. In such a case of perfect permeation, Ω must be independent of ϕ. Hence we may write $\Omega = s_0 v_0$, where s_0 is the swelling factor of the polymer in extreme dilution.

The usual case may be between these two limiting cases and Ω may be written in the form

$$\Omega = s v_0 \phi^{-\beta} \qquad \begin{array}{l} 0 \leqslant \beta \leqslant 1 \\ 1 \leqslant s \leqslant s_0 \end{array} \qquad (9)$$

where s and β are constants which should be independent of ϕ. Case I corresponds to $s = 1$, $\beta = 1$ and case II to $s = s_0$ and $\beta = 0$. It is noted that s is the swelling factor at $\phi = 1$.

Equation (8) has been derived on the tacit assumption that the encompassed volumes of the coiling polymers have maintained their original volumes up to ϕ. However, if Ω is forced to reduce with increasing concentration in accordance with eq. (9), eq. (8) would no longer be valid. Although eq. (3) and the following equations do not involve the molecular volume explicitly, the theories from which eq. (3) has been derived are based on the calculations of the spatial extension of the atomic groups of polymers and the hydrodynamic interactions between these groups. Kuhn[12] pointed out that the molecular volume Ω of a randomly coiled molecule should be proportional to the volume of a sphere whose radius is equal to the average square end-to-end distance. The latter should be proportional to $M^{3/2}$ for the ideal case where any kind of interactions do not exist and the distributions of the atomic groups are of the Gaussian type. In general, however, Ω may or may not be a simple function of M depending on various factors such as solvent–polymer combinations. As an approximation, if Ω is assumed to be proportional to some powers of M above ϕ_c, eq. (7), together with eq. (9), may be written in the differential form:

$$d\ln\eta/d\phi = C/[\phi^\gamma(1 - \phi)] \tag{10}$$

in which γ and C are constants to be determined empirically. It is noted that eq. (10) should be taken to be a semiempirical expression, since it involves theoretically indefinable parameters. If eq. (10) is valid for a sufficiently wide range of concentration, it can be integrated to the form:

$$\ln\eta = \ln\eta_c + C[F(\phi) - F(\phi_c)] \tag{11}$$

where η_c is the viscosity at $\phi = \phi_c$. The function $F(\phi)$ is expressed explicitly in closed forms when γ takes a whole number or a simple fraction; for instance,

$$F(\phi) = -\ln(1 - \phi)$$

when
$$\gamma = 0 \tag{12}$$

$$F(\phi) = \ln\phi/(1 - \phi)$$

when

$$\gamma = 1 \tag{13}$$

$$F(\phi) = \ln(1 + \phi^{1/2})/(1 - \phi^{1/2})$$

when

$$\gamma = {}^1/_2 \tag{14}$$

$$F(\phi) = \ln(1 + \phi^{1/3} + \phi^{2/3})^{1/2}/(1 - \phi^{1/3})$$

$$\pm \sqrt{3}\,\tan^{-1}[2({}^1/_2 + \phi^{1/3})/\sqrt{3}] \tag{15}$$

where the radical $\pm\sqrt{3}$ is positive for $\gamma = 2/3$ and negative for $\gamma = 1/3$. Incidentally, the function $F(\phi)$ has the characteristic that for both extremely low and high values of ϕ, $F(\phi)$ increases sharply with increasing ϕ. At a moderate value of ϕ, $F(\phi)$ increases almost linearly. In the next section we shall apply these equations to some of the available data.

4. COMPARISON WITH EXPERIMENTAL RESULTS

a. Polystyrene–Styrene

Viscosity data at various temperatures and concentrations are given in Table I. Data for samples 1–7 were obtained by a capillary method. Capillary viscometry is applicable only to Newtonian liquids for which there is strict proportionality between the shearing stress and the rate of shear. However, the shearing stress at the wall of a capillary was calculated to be about 1.7 dyne/cm.^{2} for our present experimental condition. Hence the apparent viscosity values were approximated to be those at zero shearing stress.

TABLE I

Viscosities of Solution of Polystyrene in Styrene as a Function of Temperature and Concentration

| No. | u_2 | log η, poises | | | | | Q, kcal./ mole | $\bar{P}_n$ |
		20°C.	30°C.	40°C.	50°C.	60°C.		
1	0.0000		−2.175	−2.231	−2.282		2.29	
2	0.00474		−2.025	−2.085	−2.141		2.63	
3	0.00789		−1.936	−1.996	−2.054		2.63	
4	0.01315		−1.796	−1.860	−1.932		3.20	
5	0.02188		−1.595	−1.660	−1.721		2.75	
6	0.03638		−1.319	−1.389	−1.452		2.97	
7	0.06040		−0.943	−1.028	−1.096		3.09	
8	0.06150	−0.839	−0.896	−0.963	−0.863[a]	−0.932[b]	2.63	1424
9	0.09410	−0.500	−0.561	−0.622	−0.666	−0.735	2.57	1417
10	0.1302	−0.121	−0.204	−0.277	−0.347	−0.406	3.11	1422
11	0.1675	0.292	0.215	0.140	0.076	0.013	3.09	1433
12	0.1809	0.400	0.322	0.253	0.185	0.127	3.09	1410
13	0.2065	0.666	0.580	0.502	0.441	0.375	3.20	1406
14	0.2173	0.771	0.687	0.612	0.415[c]	0.471	3.20	1406
15	0.3193	1.691	1.597	1.498	1.430		3.68	1461
16	0.3262		1.535	1.420	1.318	1.228	4.94	1410
17	0.4559		2.734	2.561	2.417	2.279	6.96	1410
18	0.2634		1.109	1.008	0.908	0.816	4.44	1429
19	0.3044		1.493	1.371	1.266	1.174	4.85	1442
20	0.4094		2.426	2.266	2.128	2.005	6.68	1452
21	0.4457		2.693	2.520	2.368	2.226	7.05	1424
22	0.5075		3.561	3.318	3.087	2.915	9.43	1442

[a] At 25°C.

[b] At 35°C.

[c] At 70°C.

A rotating viscometer was used for more concentrated solutions and the data for samples 8–17 were thus obtained. The rotation speed was fixed at 60, 30, 12, and 6 rpm. The rate of shear at the wall of the rotor correspondingly changes from about 14.6 to 1.3 sec.$^{-1}$ However, no dependence of the apparent viscosity on the rate of shear was detected, and so average values are tabulated.

Viscosity data for samples 18–22 were obtained by means of the falling ball method. Apparent viscosity values calculated directly from the Stokes equation have increased systematically with the increase in the diameter of
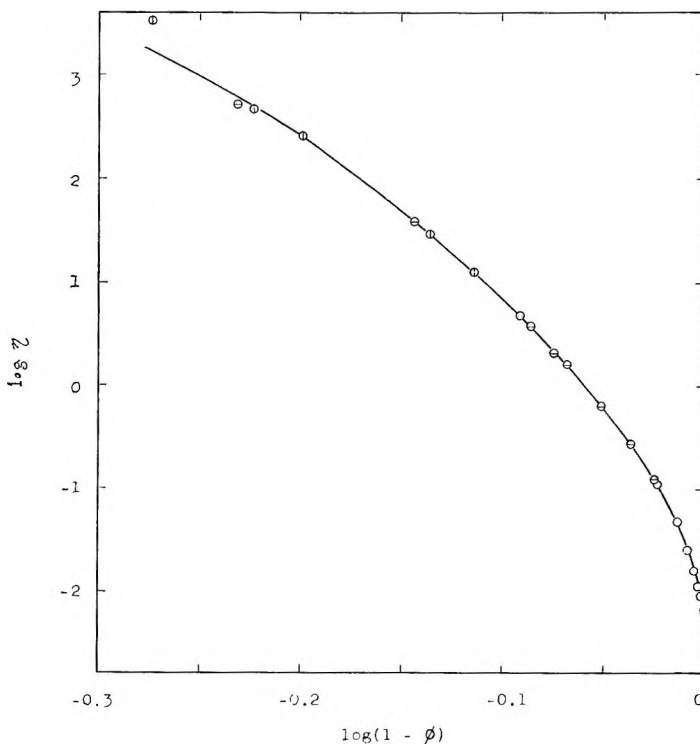
Fig. 1. Plot of log η vs. log($1 - \phi$) at 30°C. for polystyrene–styrene system, according to eq. (8): (O) capillary method; (⊖) rotating method; (⊕) falling ball method.

the falling balls. However, the viscosity values, when multiplied by Faxen's correction term, did not deviate more than 1% from the mean value, and thus the mean values are listed.

The number-average degrees of polymerization for the recovered polystyrene are also listed in Table I together with the heat of activation for flow. It may be noted that the degree of polymerization did not change during the period of the viscosity measurement.

Equation (8) tells us that a plot of log η against log $(1 - \phi)$ should give a straight line up to moderate concentration. As seen in Figure 1, however, the slope decreases rapidly with increasing concentration. The de-

crease in the slope may be attributed to the decrease in the molecular volume of the polymer Ω.

In order to estimate the approximate values of s_0 and Ω at infinite dilution, the net volume v_0 must properly be estimated. For a polydisperse system, v_0 must be replaced by $\bar{v}_0$, the average volume of a polymer, which has the same effect on the volume fraction. The volume fraction for this system can be defined as

$$\phi = \Sigma p_i v_i / V = (p/V)(m\bar{P}_n/d_p) \tag{16}$$

where p_i denotes the number of polymers of net volume v_i, $p = \Sigma p_i$, m the weight of the monomer unit, $\bar{P}_n$ the number-average degree of polymerization, and d_p the density of the polymer. Hence it may be reasonable to replace v_0 by $\bar{v}_0$, which can be defined as $\bar{v}_0 = m\bar{P}_n/d_p$. As seen in Table I, the value of $\bar{P}_n$ is 1400. The average volume, therefore, should be about 2.4×10^{-19} cc./molecule. If we replace the polymer coil by a sphere whose swelling factor is s_0, $K'M^{\alpha+1}/v_0$ in eq. (8) may be set equal to $2.5s_0$. Since the tangent of the curve at $\phi = 0$ in Figure 1 is about 80, $s_0 \cong 30$, and hence $\Omega = 7 \times 10^{-18}$ cc./molecule. This value of Ω at $\phi \cong 0$ is approximately the same as the volume of the sphere whose radius is equal to the average square end-to-end distance, calculation of the latter having been made on the assumption that the distribution of the atomic groups is Gaussian. The critical concentration expressed in volume fraction, ϕ_c is given by $\phi_c \cong v_0/\Omega = 1/s_0$ and therefore it may be about 0.03. These calculations, however, imply considerable arbitrariness and so, not much can be said about the absolute magnitude of Ω, s_0, and ϕ_c.

The distribution of the molecular weight was incidentally examined by fractionation, and the data are listed in Table II.

TABLE II
Fractionation of Polystyrene Dow 666

Fraction no.	Weight, g.	%	DP
Unfractionated	10.000		1426
1	0.893	9.27	3140
2	1.277	13.25	2920
3	0.908	9.42	2100
4	0.964	10.00	1908
5	0.175	1.81	1575
6	1.599	16.59	1295
7	0.383	3.97	1161
8	1.195	12.39	816
9	0.341	3.54	776
10	1.906	19.77	344

As an approximation, the degrees of polymerization were calculated by using eq. (1). On the basis of the data in Table II, the integral weight distribution curve was drawn and the curve was divided into ten fractions
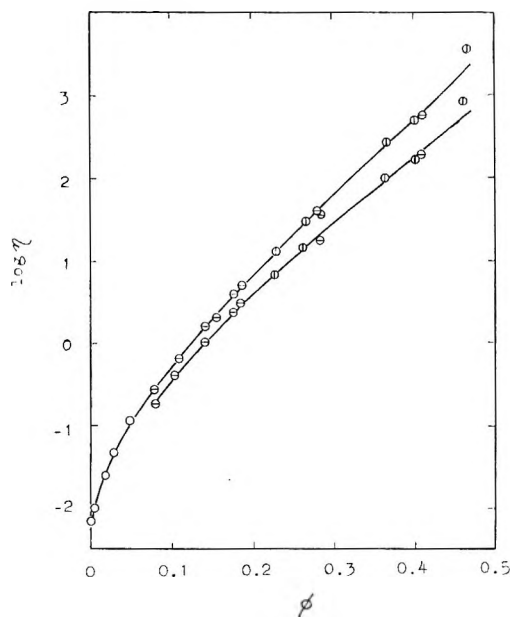
Fig. 2. Bulk viscosity of polystyrene in styrene as a function of the volume fraction ϕ. Symbols as shown in Fig. 1.
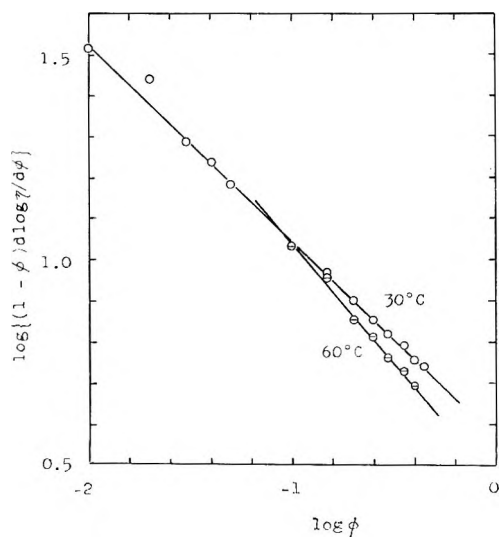
Fig. 3. Plots of log $[(1 - \phi)d\log\eta/d\phi]$ against log ϕ for polystyrene in styrene at 30 and 60°C. according to eq. (10).

of equal weight having the degree of polymerization P_i for the ith fraction. By using eqs. (17) and (18)[14]

$$\bar{P}_w = 0.1 \sum_{i=1}^{10} P_i \tag{17}$$

$$\bar{P}_n = 10 / \sum_{i=1}^{10} (1/P_i) \tag{18}$$

the weight-average and number-average degrees of polymerization were calculated to be $\bar{P}_w = 1600$ and $\bar{P}_n = 1000$, respectively. The value of $\bar{P}_n$ calculated is too small compared with that of unfractionated polymer. This discrepancy is probably due to an experimental error in fractionation and the uncertainty in drawing the distribution curve.
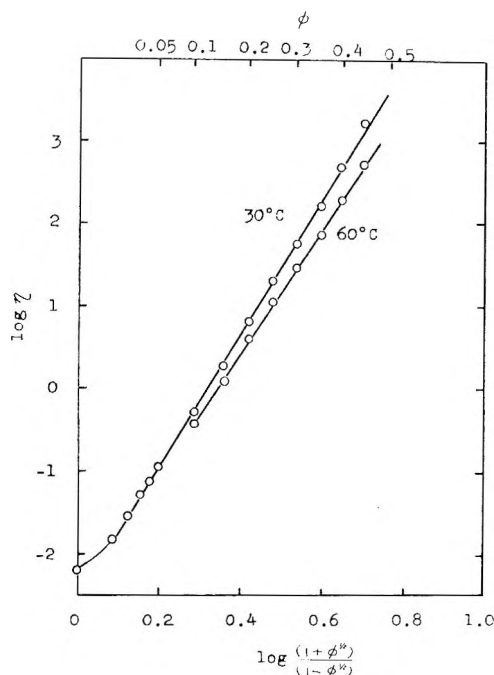
Fig. 4. Relationship between log η and $F(\phi)$ for polystyrene in styrene according to eq. (11).

We are now in the stage of examining eqs. (10) and (11). As was stated in Section 3, the shrinkage in the hydrodynamic volume of the polymer has now been taken into account. The values of log η at 30° and 60°C. are plotted in Figure 2 against the volume fraction of polystyrene. From the slope at any ϕ, $d\log \eta/d\phi$ can be obtained. Figure 3 shows the plots of log $[(1 - \phi)d\log \eta/d\phi]$ versus log ϕ. It is noted that the slope denoting γ is virtually constant over the entire range of ϕ except when ϕ is very near zero, in which case eq. (10) becomes invalid. The constancy of the value γ makes us possible to integrate eq. (10). In order to simplify the calculation, γ is set equal to 0.5 and as seen in Figure 4, log η is plotted against $F(\phi)$ in accordance with eq. (14). It may be seen that the linearity is fairly satisfactory.

b. Poly(methyl Methacrylate)–Diethyl Phthalate

Bueche[15] reported the viscosity data of the system poly(methyl methacrylate)–diethyl phthalate over a wide range in concentration and temperature. The weight fractions of the polymer which he gave in his table
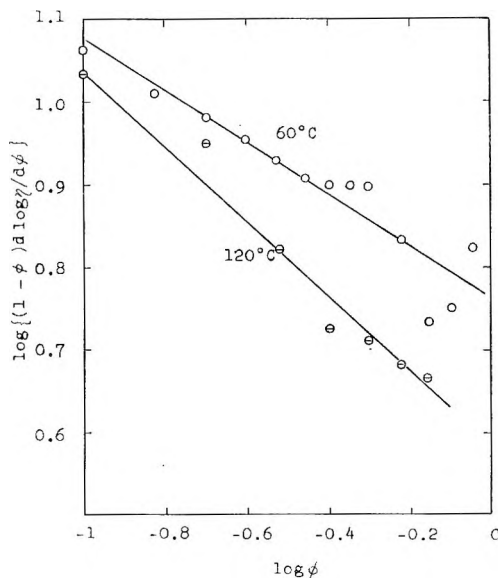
Fig. 5. Plots of log $[(1 - \phi)d\log\eta/d\phi]$ vs. log ϕ for poly(methyl methacrylate)–diethyl phthalate: (O) 60°C.; (⊖) 120°C. Data of Bueche.[15]

were converted to the volume fractions using the densities 1.085 (60°C.) and 1.030 (120°C.) for diethyl phthalate and 1.175 (60°C.) and 1.159 (120°C.) for the polymer.

In Figure 5, log $[(1 - \phi) d\log\eta/d\phi]$ is plotted against log ϕ in accordance with eq. (10), the values $d\log \eta/d\phi$ being estimated from the curve log η versus ϕ. In spite of the fact that there is some uncertainty in estimating the tangents of the log η versus ϕ curve and hence these values seem to be considerably scattered, it is likely that they can be represented by a straight line for each temperature. The values of γ are 0.32 and 0.46 at 60 and 120°C., respectively. If log η is plotted against $F(\phi)$, according to eq. (11), one obtains Figure 6, where γ is set equal to $^1/_3$ for 60°C. and $^1/_2$ for 120°C., respectively, for simplifying calculation. As seen in Figure 6, the data fall on a straight line for each temperature over an entire range of concentration except for the highest concentration regions near $\phi = 1$.

c. Polystyrene–Diethylbenzene

The bulk viscosity of the system polystyrene–diethylbenzene was reported by Bueche[16] over the concentration range of 8–80 wt.-% and the temperature range of 30–130°C. The weight per cent given in his table

was converted to the volume fraction by using the densities 0.85 (35°C.) and 0.82 (70°C.) for diethylbenzene and 1.07 (35°C.) and 1.05 (70°C.) for polystyrene.   The relationship given by eq. (10) is shown in Figure 7.   It is noted that there is a considerable deviation from linearity.   For both
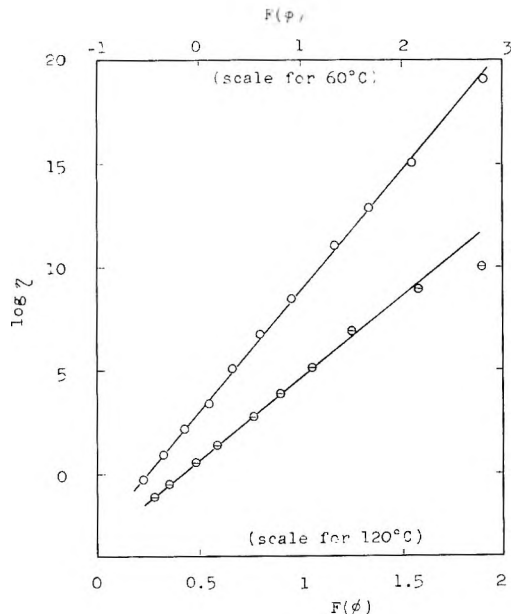
Fig. 6. Plots of log η vs. $F(\phi)$ for poly(methyl methacrylate)–diethyl phthalate: (O) 60°C.; (Ə) 120°C. $F(\phi)$ for 60°C. is given by eq. (15) and $F(\phi)$ for 120°C. by eq. (14).   Data of Bueche.[15]
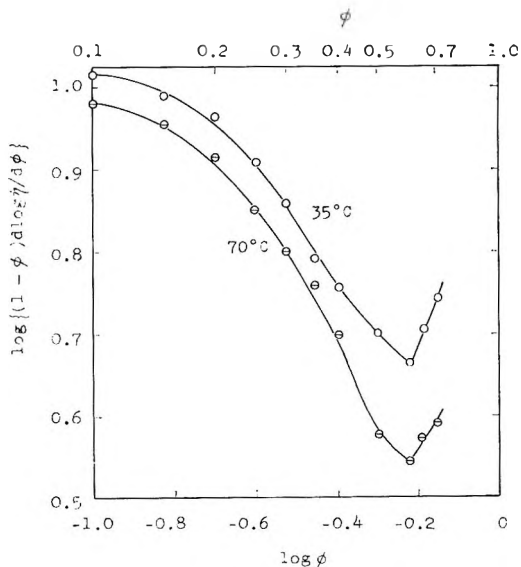
Fig. 7. Plots of log $[(1 - \phi)d\log\eta/d\phi]$ vs. log ϕ for polystyrene–diethylbenzene.   Data of Bueche.[16]

lines, the slope and hence the value of γ increases steadily and changes its sign at about $\phi = 0.6$. The negative value of γ can not be explained simply by what we have mentioned.

d. Cellulose Tributyrate–1,2,3-Trichloropropane

Landel et al.[17] have reported the viscosity data for fractionated cellulose tributyrate in 1,2,3-trichloropropane. Figure 8 represents the relationship given by eq. (10) for three different molecular weights. The densities of the polymer and the plasticizer were taken to be the same for simplicity and the weight fractions given in their table were equated to the corresponding volume fractions. It seems that the value of γ remains constant but C depends on the molecular weight.
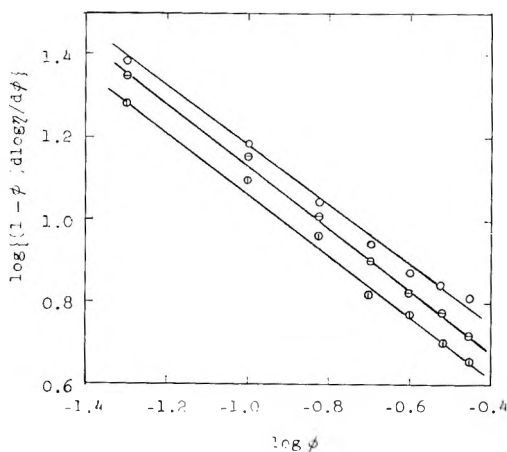
Fig. 8. Plots of log $[(1 - \phi)d\log\eta/d\phi]$ vs. log ϕ for cellulose tributyrate in trichloropropane at 25°C.: (O) $\bar{M}_w = 22.2 \times 10^4$; (⊖) $\bar{M}_w = 13.4 \times 10^4$; (⊕) $\bar{M}_w = 5.5 \times 10^4$. Data of Landel et al.[17]

e. Polyisobutylene–Xylene

Viscosities of polyisobutylene in xylene were given by Johnson et al.[18] The weight fractions were converted to the corresponding volume fractions and the same plot was made as shown in Figure 9. Although the concentration is limited to a rather narrow region, a good straight line with a slope of 0.95 was obtained. The other curve in Figure 9 represents the relationship between log η and log $\phi/(1 - \phi)$, γ being approximated to unity.

5. DISCUSSION

Several examples shown above have been given to test the equations we derived. There are some other available data for which eq. (10) and hence eq. (11) can be applied well. However, concentrations seemed in too narrow ranges to test the validity of eq. (10). Even in the case where γ shows no constancy, the characteristic dependence of the viscosity of
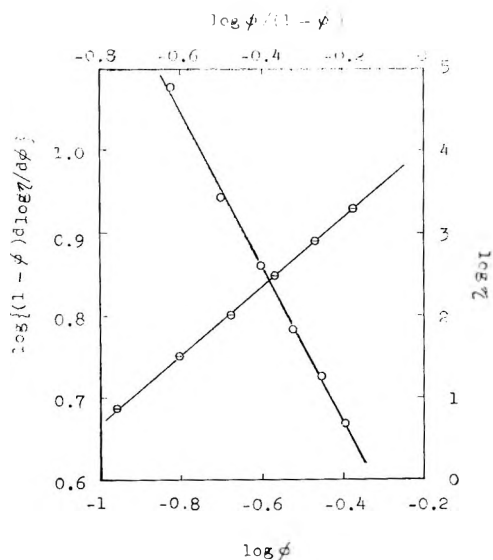
Fig. 9. Dependence of viscosity on the volume fraction for polyisobutylene in xylene at 25°C.: (O) plot according to eq. (10); (⊖) plot according to eq. (11). Data of Johnson et al.[18]

polymer solutions on concentration seems to be well represented, at least qualitatively, by the function $F(\phi)$.

In Table III, numerical values for C and γ are listed together with pertinent data.

As stated in Section 3, the factor s is a measure of the apparent volume which one polymer would occupy in an unplasticized state. The lower

TABLE III
Values of the Constants C and γ for Various Polymer Solutions

Polymer[a]	Solvent[b]	$M_w \times 10^{-4}$	Temp., °C.	C_w, %	C	γ	Ref.
PS	S	16	30	0 – 51	8.5	0.48	This work
PS	S	16	60	9.4– 51	6.8	0.56	This work
PMMA	DP	6.3	60	8.8–100	13	0.32	15
PMMA	DP	6.3	120	8.8–100	9.0	0.46	15
PS	DB	72	35	8.9– 80	7.8[c]	0.65[c]	16
PS	DB	72	70	8.9– 80	3.8[c]	1.0[c]	16
CT	TCP	22.2	25	0.5– 36	6.8	0.71	17
CT	TCP	13.4	25	1.1– 36	5.8	0.74	17
CT	TCP	5.5	25	0.7– 31	5.0	0.73	17
PIB	X	32	25	13 – 40	4.5	0.95	18

[a] PS, polystyrene; PMMA, poly(methyl methacrylate); CT, cellulose tributyrate; PIB, polyisobutylene.

[b] S, styrene; DP, diethyl phthalate; DB, diethylbenzene; TCP, trichloropropane; X, xylene.

[c] Values at $\phi = 0.4$.

limit of the swelling factor is equal to unity and its upper limit may be 50 at most for vinyl polymers consisting of 10^4 monomer units at infinite dilution. Therefore the value of s cannot exceed s_0 and it should be in the vicinity of unity. As suggested earlier; if swollen polymer coils could be replaced by sphere, the constants C and γ could be set $C \cong 2.5s$ $(1 \leqslant s \leqslant s_0)$ and $\gamma \cong \beta$ $(0 \leqslant \beta \leqslant 1)$, respectively. It may be seen in Table III, that C and γ are taking permissible numerical values. Also, it seems that C decreases with decreasing molecular weight and/or with increasing temperature.

It is hard to give γ a clear physical concept, but it must be some kind of measure of the reluctance of a polymer to permeate into neighboring polymers. It is known that in the usual case, the apparent viscosity of polymer solutions becomes more susceptible to the rate of shear when the temperature is lowered, and vice versa.[19] This fact suggests that the micro-Brownian motions of segments, which depend much on temperature, have a close connection with the interactions between molecules and hence to the permeability or reluctance of polymers.

In deriving expressions for the viscosity of concentrated polymer solutions, only the effects of volume fraction have been taken into account explicitly and any loose ends have been tucked into the constants C and γ. Therefore, in these equations, η is not expressed in terms of an explicit function of temperature or of the molecular weight of polymers. How these factors embody themselves has been left for future investigation. Viscosities in the vicinity of ϕ_c may follow.

References

1. Hirai, N., *J. Polymer Sci.*, **39**, 435 (1959); *ibid.*, **40**, 255 (1959).
2. Kawai, T., *J. Chem. Soc. Japan*, **79**, 1334 (1958).
3. Fujita, H., and A. Kishimoto, *J. Chem. Phys.*, **34**, 393 (1961).
4. Brinkman, H. C., *J. Chem. Phys.*, **20**, 571 (1952).
5. Nishimura, N., *Bull. Chem. Soc. Japan*, **34**, 1158 (1961).
6. Johnson, D. H., and A. V. Tobolsky, *J. Am. Chem. Soc.*, **74**, 938 (1952).
7. Matheson, M. S., E. E. Auer, E. B. Bevilacqua, and E. T. Hart, *J. Am. Chem. Soc.*, **73**, 1700 (1951).
8. Bueche, F., *J. Chem. Phys.*, **20**, 1959 (1952); *ibid.*, **25**, 599 (1956).
9. Weissberg, S. G., R. Simha, and S. Rothman, *J. Res. Natl. Bur. Std.*, **47**, 298 (1951).
10. Simha, R., and J. L. Zakin, *J. Chem. Phys.*, **33**, 1791 (1960).
11. Simha, R., and J. L. Zakin, *J. Colloid Sci.*, **17**, 270 (1962).
12. Kuhn, W., *Kolloid-Z.*, **68**, 2 (1934).
13. Cerf, R., *J. Chem. Phys.*, **20**, 395 (1952).
14. Schulz, G. V., *Z. Elektrochem.*, **60**, 199 (1956).
15. Bueche, F., *J. Appl. Phys.*, **26**, 738 (1955).
16. Bueche, F., *J. Appl. Phys.*, **24**, 423 (1953).
17. Landel, R. F., J. W. Berge, and J. D. Ferry, *J. Colloid Sci.*, **12**, 400 (1957).
18. Johnson, M. F., W. W. Evans, I. Jordan, and J. D. Ferry, *J. Colloid Sci.*, **7**, 498 (1952).
19. Maeda, H., T. Kawai, and U. Sato, *J. Chem. Soc. Japan*, **80**, 243 (1959).

Résumé

On a obtenu une relation générale entre la viscosité et la concentration des solutions polymériques pour des régions de concentration assez basses par la méthode proposée par Brinkman. On a étendu l'applicabilité de cette relation aux solutions très concentrées en tenant compte de la diminution de volume des polymères. Lorsqu'on augmentait la concentration, le volume apparent, qu le polymère en solution occupe au-dessus d'une fraction de volume critique ϕ_c, est donné par $\Omega = sv_0\phi^{-\beta}$, où s est le facteur de gonflement pour $\phi = 1$ et β est une constante qui mesure une répulsion vis-à-vis de la perméation intermoléculaire; v_0 et ϕ sont le volume absolu de la molécule de polymere et la fraction de volume du polymère respectivement. La relation entre η et ϕ est donnée par l'équation $d \log \eta/d\phi = C/\phi^{\gamma}(1 - \phi)$, où C et γ sont des constantes déterminées empiriquement. Pour controler la validité de cette relation on a employé nos valeurs expérimentales et certaines valeurs données par la littérature. Quoique ni la température, ni le poids moléculaire n'interviennent dans cette équation, elle tient bien compte de la relation entre la viscosité et la concentration des polymeres sur un large domaine de concentrations. Les expériences confirment assez bien la théorie proposée.

Zusammenfassung

Eine allgemeine Beziehung zwischen der Viskosität und der Konzentration von Polymerlösungen wurde mit der von Brinkman vorgeschlagenen Methode für Bereiche verhältnismässig niedriger Konzentration abgeleitet. Durch Berücksichtigung der Volumschrumpfung der Polymeren wurde die Beziehung für eine Anwendung auf extrem konzentrierte Lösungen erweitert. Es wird angenommen, dass mit steigender Konzentration das scheinbare Volumen, welches ein Polymeres in Lösung oberhalb eines gewissen kritischen Volumbruches ϕ_c einnimmt, durch $\Omega = sv_0\phi^{-\beta}$ gegeben ist, wo s der Quellungsfaktor bei $\phi = 1$ und β eine Konstante, welche den Widerstand gegen intermolekulare Permeation misst, ist; v_0 und ϕ sind das Nettovolumen der Polymermoleküle bzw. der Volumsbruch des Polymeren. Die Abhängigkeit von η von ϕ ist durch die Gleichung $d \log\eta/d\phi = C/\phi^{\gamma}(1 - \phi)$ gegeben, wo C und γ empirisch zu bestimmende Konstanten sind. Zur Überprüfung der Gültigkeit der Gleichung wurden die eigenen Versuchsergebnisse und einige andere vorhandene Daten benützt. Obwohl weder die Temperatur noch ein Molekulargewichtsfaktor in dieser Gleichung auftritt, kann sie die Abhängigkeit der Viskosität von der Polymerkonzentration in einem weiten Konzentrationsbereich darstellen, und es besteht eine ziemlich befriedigende Übereinstimmung von Theorie und Experiment.

Electron Spin Resonance Spectra of Poly(methyl Methacrylate) Irradiated at 77°K.

YOSHIOKI HAJIMOTO, *Matsushita Research Institute Tokyo, Inc., Ikuta, Kawasaki-shi, Kanagawa, Japan*, NAOYUKI TAMURA,* *Japanese Association for Radiation Research on Polymers, Komagome-Kamifujimae, Bunkyo-ku, Tokyo, Japan*, and SHIGEHARU OKAMOTO, *Faculty of Applied Physics, Waseda University, Shinjuku-ku, Tokyo, Japan*

Synopsis

It is shown that there exists a difference in the electron spin resonance spectrum of poly(methyl methacrylate) irradiated with electrons and observed at 77°K. and that at room temperature. One of the radicals trapped at 77°K. is probably ·COOCH₃, which gives the spectrum of a single line, and the others giving triplet and quartet are perhaps ·CHO and ·CH₃, the splitting of which are 132 gauss and 23 gauss, respectively. With the elevation of the annealing temperature the unstable radicals recombine or convert to the stable radicals; near room temperature they are completely replaced by the stable radical which gives the nine-line spectrum.

INTRODUCTION

Many workers[1-3] have obtained the ESR spectrum of irradiated poly-(methyl methacrylate) (PMMA). Ovenall[3] found that the ESR spectrum of PMMA irradiated and observed at 77°K. consists of five lines. When the sample is allowed to warm up to 300°K., a nine-line spectrum is observed which is identical with that for a sample irradiated at room temperature. However the types and behaviors of free radicals in the lower temperature region have not yet been demonstrated.

We undertook the present study to obtain further knowledge of the radicals formed in PMMA, especially of their behavior in the lower temperature ranges.

EXPERIMENTAL

Materials

Two kinds of samples were used: a commercial sample (sample A) and a laboratory prepared one (sample B). Sample A is in the form of chip made by Mitsubishi Rayon Company Ltd. The sample B was prepared

by the following procedures. Methyl methacrylate was polymerized by using benzoyl peroxide initiator. The products were dissolved in toluene containing hydroquinone inhibitor, and then the polymers were precipitated by pouring into methanol. The PMMA was washed with additional methanol, and the solvent was decanted. The polymers were dried under 2 mm. Hg pressure at 80°C. for 24 hr. The sample obtained was a powder.

Method

The samples were degassed and sealed in 4 mm. outer diameter glass tubes under high vacuum and then irradiated. Irradiation was carried out with electrons from a Van de Graaff accelerator made by Mitsubishi Electric Company Ltd. at a dose rate of 5×10^6 rad/min.

ESR measurements were made at a frequency of 9.3 Gcycles/sec. with a 3A type spectrometer of Japan Electron Optics Laboratory Company Ltd. Field modulation of 80 cycles/sec. was used and the microwave power entering the cavity was attenuated to about 0.9 mw. to minimize saturation effect.

RESULTS AND DISCUSSION

The spectra obtained from samples A and B irradiated and observed at room temperature are shown in Figure 1. The spectral shape of sample
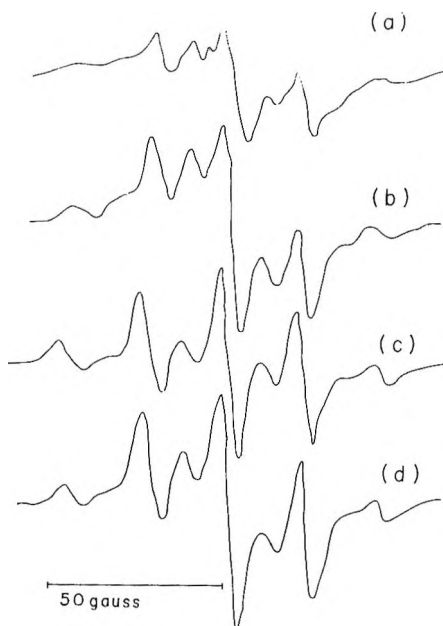
Fig. 1. ESR spectra of PMMA irradiated and observed at room temperature: (a) sample B (freed from monomers) irradiated to 0.43 Mrad; (b) sample B irradiated to 27 Mrad; (c) sample A (commercial PMMA) irradiated to 0.43 Mrad; (d) sample A irradiated to 30 Mrad.

A is almost the same as those obtained by other workers.[2,4] The spectral shape of sample B, however, is sharper than that of very pure PMMA obtained by Unger et al.[4] Though the main reason for this difference is probably the residue of some extent of monomers in our samples, one of the other reasons may be the microwave power used. The spectrum of sample B is rather more diffuse than that of sample A. The nine-line spectrum has been attributed to the radical

$$-CH_2-\overset{\overset{\displaystyle CH_3}{|}}{\underset{\underset{\displaystyle COOCH_3}{|}}{C}}\cdot$$
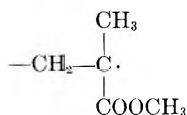
However Unger et al.[4] concluded that the spectrum is produced only when excess monomer is present.

Samples A and B irradiated and observed at 77°K. give the spectra shown in Figure 2. The spectrum 2a of sample A consists of a diffuse seven-line spectrum with the overall splitting of about 120 gauss and interline splitting of 21.6 gauss excepting the splitting between the center line and the next lines, which apparently resembles the spectrum obtained from irradiated MMA monomer.[6] With increase of dosage the spectrum increases in intensity. The spectral shape, however, does not change much, except that the increase of the center line is more obvious than that of the other lines.

The spectra of sample B (Figs. 2b, 2c) are more complicated in shape; the intensity of the center line increases and the spectral shape approaches that of sample A with the increase of dosage. This result suggests the
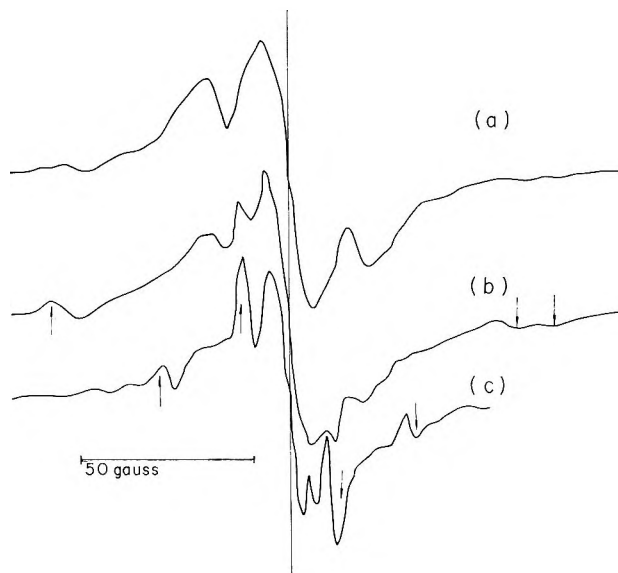
Fig. 2. ESR spectra of PMMA irradiated and observed at 77°K.: (a) sample A (commercial PMMA) irradiated to 30 Mrad; (b) sample B (freed from monomers) irradiated to 30 Mrad; (c) sample B irradiated to 3 Mrad.
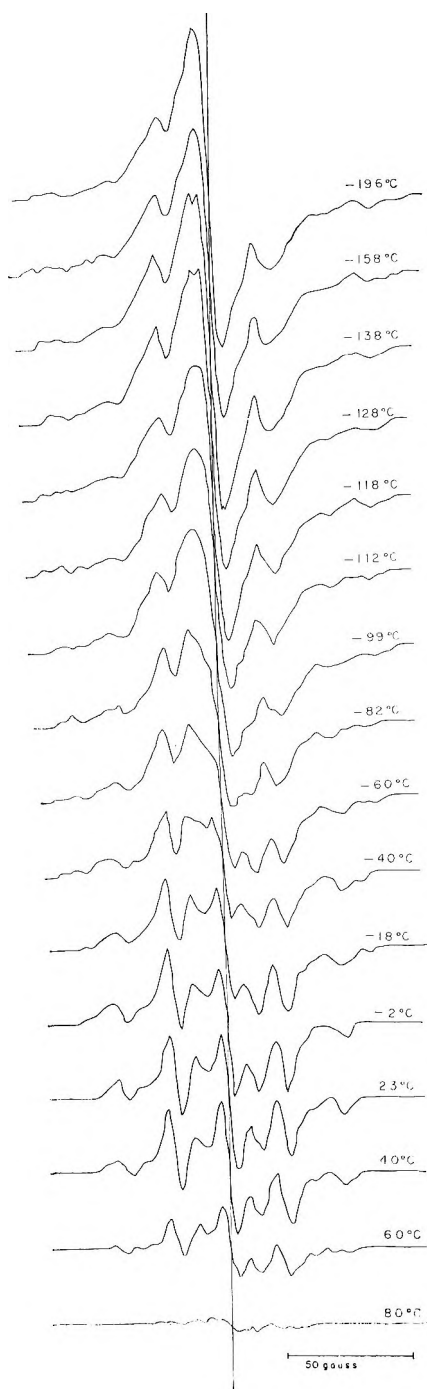
Fig. 3. Change and decay of ESR spectrum of PMMA (sample A) irradiated to 100 Mrad at 77°K. with heat treatment.   Sample was heated for 4 min. at each temperature; ESR was measured at 77°K.
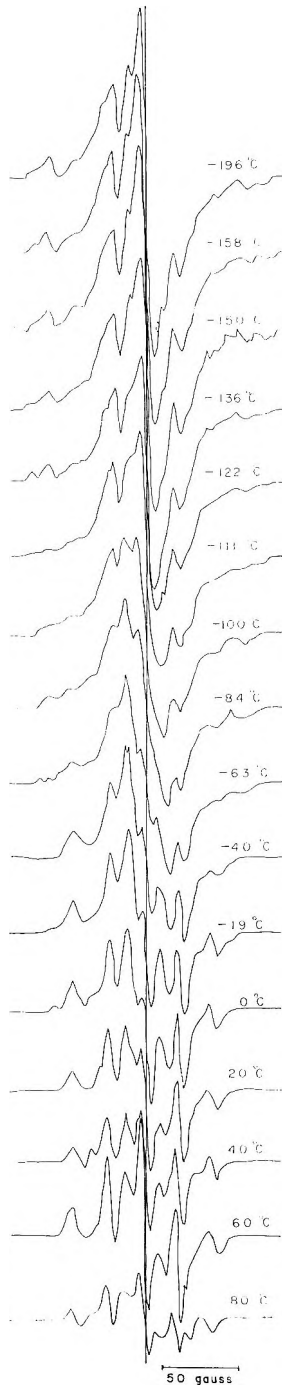
Fig. 4. Change and decay of ESR spectrum of PMMA (sample B) irradiated to 5 Mrad at 77°K. with heat treatment. Sample was heated for 4 min. at each temperature; ESR was measured at 77°K.
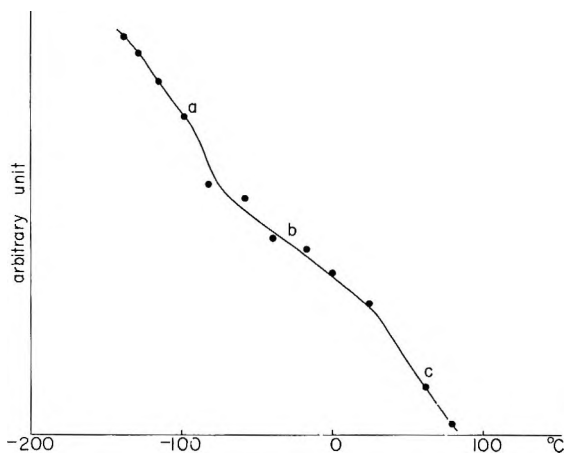
Fig. 5. Relative intensity of ESR spectrum of PMMA (sample A) irradiated to 100 Mrad at 77°K. as a function of annealing temperature. Sample was heated for 4 min. at each temperature; ESR was measured at 77°K.

spectral variation with dosage is caused by the increase of included monomer. Moreover the outermost peaks and inner four peaks (arrow) of the hyperfine structure coincide with those of methanol irradiated and measured at 77°K.,[9,10] suggesting the existence of the radicals ·CHO and ·CH₃. Their splittings are 132 gauss and 23 gauss, respectively.

With increasing annealing temperature, these spectra were observed to vary both in shape and in intensity. The variations of the spectra are shown in Figures 3 and 4; in each case the sample was warmed to each temperature for 4 min. and cooled back to 77°K. for measurement. With an increase in temperature the sharp line at the center position decays first and the nine-line spectrum becomes visible near room temperature, which suggests the existence of some other kinds of radicals at 77°K.

Figure 5 shows the variation of the spectral intensity of sample A with annealing temperature. The curve can be divided into three parts, suggesting that there are more than three kinds of radicals. The spectra for the radicals disappearing at these decay regions are shown in Figure 6; these were obtained by subtracting the spectra observed at the higher temperature from those at the lower in each decay region.

The spectrum obtained in the first decay region is shown in Figure 6a, which consists of the overlapping curves of a single line and a diffuse quartet. The singlet is probably attributable to the radical ·COOCH₃. The outermost peaks of the diffuse quartet are attributed to the ·CHO radical, but the others are not identified. The existence of a single line was found also by Ovenall[3] with γ-irradiated poly(methacrylic acid), where the single line was ascribed to the radical ·COOH.

The spectrum obtained in the second decay region is shown in Figure 6b, which is apparently a double sextet. The third spectrum is shown in Figure 6c, which consists of nine lines and is undoubtedly due to the
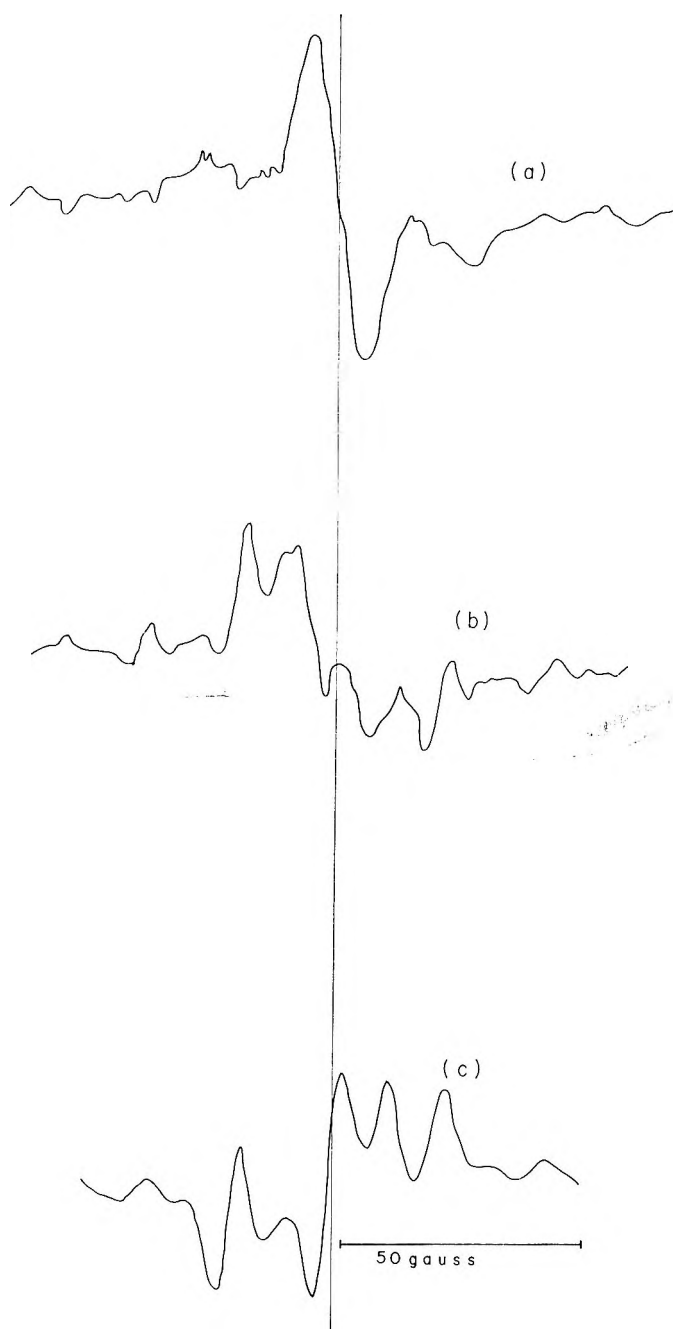
Fig. 6. ESR spectra of PMMA (sample A) disappearing between (a) −150 and −100°C.; (b) −84 and 0°C.; (c) 40 and 80°C.

radical $-CH_2-\overset{\cdot}{C}(CH_3)-COOCH_3$. Comparing the spectral shape of spectrum 6*b* with that of 6*c*, it is found that the minimum positions of the spectrum 6*c* are exactly in agreement with the maximum positions of spectrum 6*b*. This fact suggests that the radical $-CH_2-\overset{\cdot}{C}(CH_3)-COOCH_3$ was produced in the second decay region, where some of the initial radicals decay by recombination or some other mechanism and the others are converted to the propagating radicals when monomers are present in the sample. A similar result was obtained with the sample B, but the intensity of the ratio of the singlet to the diffuse quartet is larger than that in the case of sample A. This result is consistent with the fact that sample B contains less monomer than sample A.

The shape of the nine-line spectrum apparently does not change during the decay above room temperature, suggesting that the nine-line spectrum is produced from only one type of radical. This result agrees with Symons'[7] conclusion, contrary to Piette's[8] postulate. Above the glass transition temperature the spectrum completely decays.

Conclusions

The electron spin resonance in poly(methyl methacrylate) irradiated with electrons at 77°K. has been studied. With a commercial PMMA sample the spectrum observed at 77°K. without intermediate warming consists of seven diffuse lines. With the samples freed from monomers the spectra have the same overall splitting as for the commercial samples, but are more complicated in shape and vary with the irradiation dose. It was found by heat-treating procedures that there are three decay regions of radicals in PMMA irradiated at 77°K. Below room temperature the existence of three kinds of spectra are found. One radical decaying in the lower temperature ranges is probably $\cdot COOCH_3$, and the others are supposed to be $\cdot CHO, \cdot CH_3$. The stable radical $-CH_2-\overset{\cdot}{C}(CH_3)-COOCH_3$ was found to be produced partly also by the radical conversion when monomers are present in the sample.

References

1. Ingram, D. J., M. C. R. Symons, and M. G. Townsend, *Trans. Faraday Soc.*, **54**, 409 (1958).

2. Abraham, R. J., H. W. Meville, D. W. Ovenall, and D. H. Whiffen, *Trans. Faraday Soc.*, **54**, 1133 (1958).

3. Ovenall, W., *J. Polymer Sci.*, **41**, 199 (1959).

4. Unger, I. S., W. B. Gager, and R. I. Leininger, *J. Polymer Sci.*, **44**, 295 (1960).

5. Ohnishi, S., Y. Ikeda, S. Sugimoto, and I. Nitta, *J. Polymer Sci.*, **38**, 451 (1959).

6. Marx, R., and M. R. Bensasson, *J. Chim. Phys.*, **57**, 673 (1960).

7. Symons, M. C. R., *J. Chem. Soc.*, **1963**, 1186.

8. Piette, L. H., *NMR and EPR Spectroscopy*, Pergamon Press, Oxford, 1960, p. 218.

9. Sullivan, P. J., and W. S. Koski, *J. Am. Chem. Soc.*, **85**, 384 (1962).

10. Adrian, F. J. E. L. Cochean, and V. A. Bowers, *J. Chem. Phys.*, **36**, 1166 (1962).

Résumé

On montre la différence qui existe entre les spectres de spin électronique du poly-méthacrylate de méthyle irradié par électrons et observés a 77°K ainsi qu'a température ordinaire. Un des radicaux piégés a 77°K est probablement ·COOCH₃ qui apparaît spectralement sous forme d'un pic simple, les autres donnant un triplet et un quartet sont peut-être ·CHO et ·CH₃, les livages spin-spin étant respectivement de 132 et 23 gauss. Par élévation de la température ambiante, les radicaux instables se recombinent ou se convertissent en radicaux stables et aux approches de la température ordinaire, ils sont totalement remplacés par des radicaux stables donnant le spectre a 9 raies.

Zusammenfassung

Es wird gezeigt, dass ein Unterschied zwischen dem Elektronenspinresonanzspektrum von bei 77°K bestrahltem und untersuchtem Polymethylmethacrylat und demjenigen bei Raumtemperatur besteht. Eines der bei 77°K eingeschlossenen Radikale ist wahrscheinlich ·COOCH₃, welches ein einliniges Spektrum liefert, und die anderen, die ein Triplett und Quartett besitzen, sind vielleicht ·CHO und ·CH₃, deren Aufspaltung 132 und 23 Gauss beträgt. Bei Erhöhung der Temperungstemperatur rekombinieren die instabilen Radikale oder wandeln sich in stabile Radikale um, und in der Nähe der Raumtemperatur werden sie vollständig durch das stabile Radikal mit dem Neunlinienspektrum ersetzt.

Copolymerization of Styrene and *p*-Divinylbenzene. Initial Rates and Gel Points

BAYARD T. STOREY, *Rohm & Haas Company, Research Laboratories, Philadelphia, Pennsylvania*

Synopsis

Initial rates of polymerization were measured at 70.0 and 89.7°C. for styrene, *p*-divinylbenzene, and mixtures of the two monomers initiated with 1% benzoyl peroxide. The rates relative to styrene increased linearly with mole fraction of *p*-divinylbenzene; the latter monomer polymerized faster than styrene by a factor of 2.50 at 70.0°C. and 3.54 at 89.7°C. Times to gelation were also measured for those samples containing *p*-divinylbenzene, and from these times the corresponding fractional conversion at the gel point was calculated. The conversion at the gel point passed through a minimum with increasing content of *p*-divinylbenzene. The gelation behavior is explained by concurrent interchain crosslinking to give a network and intrachain crosslinking to give microgels which accumulate to give macrogel, the latter process being dominant at all but low concentrations of *p*-divinylbenzene. The higher the content of crosslinker, the less swollen the microgels, and the greater the conversion required to give gelation by this process. The linear increase in rate with increasing *p*-divinylbenzene content was also explained by intrachain crosslinking: growing polymer radicals which undergo this process have a reduced rate of termination. The factor by which the termination rate constant is reduced with increasing divinylbenzene content is the same factor as that by which the conversion required to give gelation by accumulation of microgels is increased.

INTRODUCTION

The copolymerization of divinylbenzene with styrene was first carried out by Staudinger[1] in order to demonstrate that crosslinking caused by the divinyl monomer would make the polystyrene insoluble in all solvents. In recent years, the insoluble gels obtained from copolymerization of these two monomers have become important as backbones for synthetic ion exchange resins. The properties of the finished copolymers have been studied,[2] but the copolymerization process itself has been virtually ignored. There is a practical reason for this: commercial divinylbenzene is a complex mixture containing both *meta* and *para* isomers of divinylbenzene as well as other related hydrocarbons, and its composition is not a variable easily controlled in polymerization studies. This work was undertaken to remedy the lack of information on the rates and gel points of polymerizing styrene–divinylbenzene mixtures. The problems associated with commercial divinylbenzene were avoided by using pure *p*-divinylbenzene, which can be separated from the commercial mixture by a bromination–debromination sequence.

The Problem of Gelation

When a monovinyl monomer is copolymerized with a divinyl monomer, the reaction mass will usually gel at a conversion characteristic of the monomers and the reaction conditions. The transition from fluid to gel is that point at which a gas bubble or glass ball moving gently through the polymerizing mixture suddenly becomes immobilized. In other words, it is that point at which the mixture appears to develop a very small but finite yield stress. The actual measurement made is that of time to gelation; coupled with the known rate of polymerization, the fraction of monomer converted to polymer at the gel point can be calculated.

Gelation is taken to mean the formation of a three-dimensional polymer network in the polymerizing mixture, the implication being that such a network is required for the development of the observed yield stress. The usual method of observing the gel point—subjecting the reaction mass to low shear stress by a slowly moving probe—will show a gel point not only with a three-dimensional network but also with a polymer of high enough molecular weight to immobilize the probe by high viscosity alone. The latter "gel point" can be easily avoided by running the polymerization so as to give short chain lengths; the transition to gel also becomes much sharper under these conditions. (For these reasons, a relatively high initiator concentration of 1 wt.-% was used in this study.) There is a third method by which gelation may occur: the accumulation of microgels. This form of gelation was elegantly demonstrated by Shashoua and Beaman,[3] who prepared special microgels by emulsion polymerization and with them gelled a swelling solvent for the polymers at a definite volume fraction of microgel.

Flory's equation[4] relating the gel point to the amount of crosslinker and chain length of the uncrosslinked polymer states that:

$$\alpha_g = (\bar{Y}_w X_D)^{-1} \tag{1}$$

where α_g is fractional conversion at the gel point, X_D is the fraction of double bonds belonging to the divinyl monomer in the mixture, and $\bar{Y}_w$ is the weight-average degree of polymerization of the "backbone chain." In practice, $\bar{Y}_w$ is taken to be the weight-average degree of polymerization of the homopolymer from the monovinyl monomer polymerized under the same conditions. Equation (1) presupposes that the following conditions are met: first, the vinyl groups in the system are of equal reactivity; second, the pendent vinyl group of a singly reacted divinyl monomer is consumed only in interchain polymerization. Walling[5] showed that eq. (1) held for vinyl acetate–divinyl adipate and methyl methacrylate–ethylene dimethacrylate, i.e., systems with vinyl groups of equal reactivity, at low crosslinker levels. At higher crosslinker levels, eq. (1) predicts the gel point at conversions that are much too low. The most reasonable explanation for the deviation is that crosslinks are wasted by intrachain polymerization.[4,6] Considerable evidence for this wastage has been put forward by Loshaek and Fox[7] and Hwa and Fox[8] in the methacrylate–dimethacrylate system.

Reactivity Ratios for Styrene and p-Divinylbenzene

The styrene–p-divinylbenzene system appeared to be a good candidate to study the effect of intrachain polymerization on gelation. The position of the two vinyl groups of the crosslinker *para* to each other prevents the formation of small rings by cyclopolymerization; intrachain polymerization should occur by a true "back-biting" reaction to give large, strain-free rings. If back-biting is prevalent in this system, it should be prevalent in most vinyl–divinyl systems. The extent of intrachain reaction can be inferred by comparing the observed gel-point with that predicted by the Flory equation. For the comparison to be valid, the relative reactivities of the vinyl groups of the styrene and p-divinylbenzene must be essentially equal to one. The reactivity ratios of styrene and the isomeric divinylbenzenes were determined by Wiley, who used styrene labeled with C^{14} to get the composition of the copolymer formed. He obtained $r_1 = 0.92$, $r_2 = 1.00$ for styrene (M_1)–o-divinylbenzene (M_2) mixtures,[9] which give soluble polymer by cyclopolymerization, and $r_1 = 0.65$, $r_2 = 0.60$ with m-divinylbenzene[10] as M_2, the r_2 values referring to one of the double bonds of the divinylbenzene. A set of values for r_1 and r_2 which were constant with changing monomer composition were not obtained with p-divinylbenzene; the variability was attributed to concurrent polymerization of pendent vinyl groups, which would be equivalent to a three-component system.[10] An estimate made from runs of lower divinylbenzene content gave the improbable values of $r_1 = 0.14$ and $r_2 = 0.5$.[9] There is no apparent reason why a vinyl group *para* to the reacting vinyl group should have such a profound influence on the latter's reactivity, while the same group *ortho* to the reacting group shows none.

The relative reactivity of one vinyl group of p-divinylbenzene may be estimated by making use of Walling's observation that the reactivities of substituted styryl radicals towards styrene and of styryl radicals towards substituted styrenes follow the Hammett σ–ρ relation.[11] The σ value for the p-vinyl group was found in these laboratories to be -0.05 by comparison of the pK_a of p-vinylbenzoic acid in 50% ethanol, which is 5.80,[12] with that of benzoic acid in the same solvent, which is 5.73.[13] Walling found ρ for these radical reactions to be only 0.5;[11] therefore the relative reactivities of the vinyl groups of styrene and p-divinylbenzene can be taken as equal to one within experimental error. This result is in accord with the values of r_1 and r_2 obtained for o-divinylbenzene, as expected. In view of this accord and of the large uncertainty in the values determined directly, the r_1 and r_2 values for the styrene–p-divinylbenzene system are taken as equal to one in this paper.

The correct equation defining instantaneous copolymer composition for the vinyl–divinyl case was shown by Wiley[10] to be:

$$m_2/m_1 = 2M_2(2r_2M_2 + M_1)/M_1(r_1M_1 + 2M_2) \qquad (2)$$

where m_2 and m_1 refer to divinyl and monovinyl units in the polymer and

M_2 and M_1 are the molar concentrations of divinyl and monovinyl mono-
mer, respectively. For $r_1 = r_2 = 1$, the equation simplifies to

$$m_2/m_1 = 2M_2/M_1 \tag{3}$$

and the mole fraction of divinyl units in the polymer is just equal to the
fraction of vinyl groups belonging to the divinyl monomer, or X_D.

$$m_2/(m_1 + m_2) = 2M_2/(M_1 + 2M_2) = X_D \tag{4}$$

The fraction X_D can also be expressed in terms of mole fraction of divinyl
monomer, n:

$$X_D = 2n/(n + 1) \tag{5}$$

EXPERIMENTAL

Materials

Styrene was either Koppers Company or Dow material. It was distilled
prior to use in a series of runs and stored under prepurified nitrogen in the
refrigerator. In a few cases, the monomer was redistilled on a spinning
band column just before use in a kinetic run; no difference in rate of poly-
merization was observed. Analysis of the distilled and redistilled samples
showed that 0.3% ethylbenzene was present and no other impurities.

p-Divinylbenzene was isolated from Koppers divinylbenzene concentrate,
which contained 55–60% divinylbenzene with a ratio of *meta* to *para* isomer
of about 2.5, by bromination to the crystalline tetrabromide.[14] A 170-g.
portion of concentrate was combined with 500 ml. of carbon tetrachloride,
to which was added 320 g. (110 ml.) of bromine over the course of 1 hr., with
stirring and cooling to keep the temperature at 20–25°C. The bromine
color was discharged immediately at first, then more slowly, until the color
persisted for about 15 min. Then 10-ml. portions of concentrate were
added at 15 min. intervals until the bromine color disappeared; two por-
tions usually sufficed. Crystals began to form during the late stages of
bromine addition. The mixture was cooled to 0°C. and stirred for 1 hr.;
the mass of crystals which had formed was filtered with suction and sucked
as dry as possible. The yield of crude tetrabromide was 90–125 g. After
four recrystallizations from benzene, 50–70 g. of product melting at 163°C.
was obtained; further recrystallization did not raise the melting point. p-
Divinylbenzene tetrabromide [p-bis(1,2-dibromoethyl)benzene] with a
melting point of 163°C. was needed to get p-divinylbenzene of the desired
purity. The debromination was carried out by dissolving 58.2 g. (0.129
mole) of tetrabromide and 0.5 g. of p-methoxyphenol in 300 ml. of dioxane
and 26 ml. of water, heating to 85°C., and then adding 18.9 g. (0.29 mole)
of zinc dust during 15 min. at such a rate as to keep the reaction temper-
ature at 95°C. The reaction mixture was held at 95°C. for an additional
5 min., cooled with an ice bath to 20°C., and then filtered to remove excess
zinc. A 500-ml. portion of ethylene dichloride was added to the filtrate
which was then washed with five 250-ml. portions of water to remove zinc
bromide and dioxane. The organic layer was dried with anhydrous sodium

sulfate and the bulk of the ethylene dichloride removed under reduced pressure with a water pump.   Distillation of the residue under vacuum through a spinning band column yielded a product with boiling point 40–43°C./0.7 mm., melting point 25–26°C.   Analysis by vapor-phase chromatography showed only 0.2–0.5% *p*-ethylvinylbenzene, and no other impurities.   Yields were about 60% of theory.   The capillary boiling tube must be open to the air during the vacuum distillation to allow trace amounts of oxygen to enter; otherwise the monomer polymerizes in the still pot.

Benzyl peroxide was recrystallized from chloroform by precipitation with methanol.

Density Determinations

The densities of the monomer mixtures were measured in 5 ml. pycnometers; results are shown in Table I.   A trace of *tert*-butylcatechol was added to inhibit polymerization.

The density measurements on the monomers were reproducible to ± 0.0003 g./cm.^{3} The densities of the polymers were also taken in pycnometers, using inhibited styrene or xylene as solvent or swelling liquid.   The polymers were cured for 16 hr. at 125°C.; samples cured under vacuum had the same density as those cured in air.   The densities were not reproducible with all samples; however, the values were independent of divinylbenzene content and all clustered about the value of polystyrene swollen in monomer at the same temperature.   At 70.1°C., the value was 1.051 g./cm.,^{3} in agreement with Matheson's result;[15] at 89.7°C., it was 1.041 g./cm.^{3}.   These density values for polymer and monomer were used to compute the volume shrinkage in passing from monomer to polymer for the different mixtures. The insensitivity of polymer density to divinylbenzene content implies that the volume shrinkages resulting from the polymerization of divinylbenzene and of styrene are about the same, which is reasonable because the volume change results from the collapse of separate monomer molecules into a polymer chain.   The volume shrinkage contributed by a pendent vinyl group on the chain should be negligible.

TABLE I
Densities of Mixtures of Styrene and *p*-Divinylbenzene

DVB, %	Density, g./cm.^{3}	
	70.1°C.	89.7°C.
0	0.8624	0.8455
4	0.8626	0.8456
10	0.8631	0.8471
20	0.8650	0.8493
35	0.8729	0.8560
50	0.8820	0.8606
65	0.8837	0.8656
75	0.8878	0.8695
100	0.8957	0.8763

Polymerization Rates

Initial rates of polymerization for the styrene–divinylbenzene mixtures were determined by measuring the volume shrinkage of the reacting mixture as a function of time by means of a recording dilatometer developed in these laboratories.   A diagram of the dilatometer in the upright position is shown in Figure 1.   The device works as follows: as the monomer, which is trapped in the reaction bulb by the mercury, shrinks in volume during polymerization, the level of the mercury column in the precision bore tubing drops in direct proportion.   A metal probe follows the mercury level by means of a special motor which drives the probe into the mercury, thereby closing the circuit through the platinum wire shown in the figure.   Closing the circuit causes the motor to reverse, which removes the probe from the mercury, thereby opening the circuit.   The latter action starts the probe anew towards the mercury.   This on-off drive keeps the probe just at the surface of the mercury.   The probe is connected to a linear potentiometer, which is in turn connected to a recorder.   The recorder trace gives the lin-
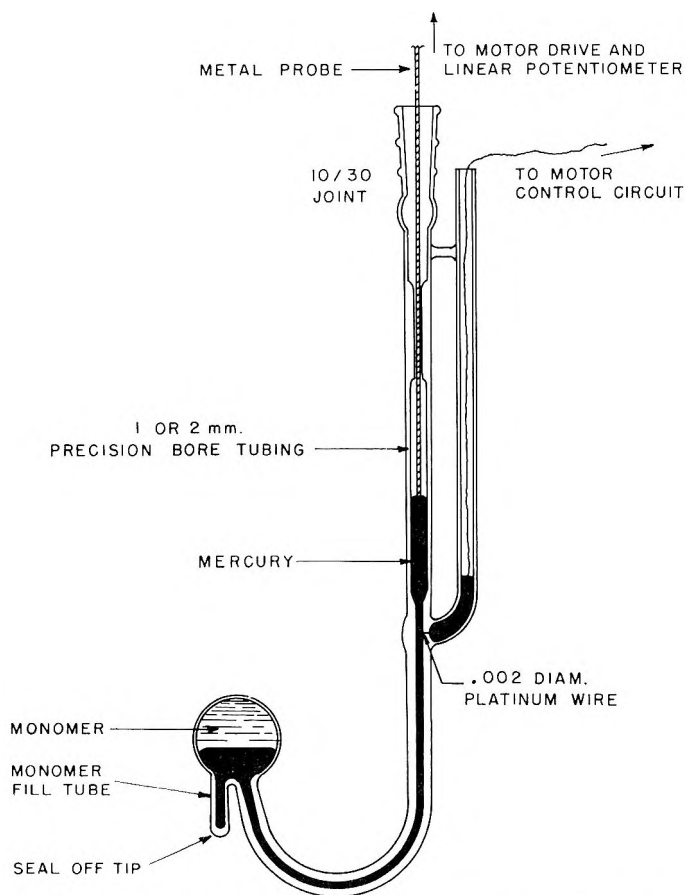
Fig. 1. Recording dilatometer for determining rates of polymerization.

ear travel of the probe as a function of time; since the cross section of the precision bore tube is known and constant, the volume shrinkage as a function of time is easily calculated. The volume shrinkage is assumed to be linear in conversion, and the rate of conversion can be calculated directly. In practice, the polymerization is taken to low enough conversion—6% or less— that the recorder trace is a straight line whose slope can be measured accurately. In one set of runs, the potentiometer was changed to let the trace follow the runs to high conversion.

The dilatometer assembly shown in Figure 1 was prepared as follows. The empty dilatometer tube was hung on a balance so that the monomer bulb and precision bore section hung downward. The monomer mixture was weighted into the bulb through the monomer fill tube whose tip was then sealed off. The dilatometer tube, still upside down to keep the monomer in the bulb, was attached to a vacuum line by means of the standard taper joint. The monomer was alternately frozen and thawed three times under vacuum to remove dissolved gases; helium was admitted after each thaw to sweep out the released gases. The monomer was frozen for the final time, the dilatometer tube put under full vacuum, and mercury allowed to flow into the evacuated tube to confine the monomer. The tube was then put in the upright position and removed from the vacuum line. Excess mercury was removed from the tube with a syringe and a small amount placed in the side arm to provide contact between the platinum wire embedded in the tube and the wire leading to the drive motor.

The kinetic run was started by immersing the dilatometer tube in a constant temperature bath held at ±0.02°C. so that the mercury surface was well below the bath surface. The mercury rose in the dilatometer barrel until thermal equilibrium had been achieved; the time to equilibrium was usually less than 1 min. The probe was set at the mercury surface and the run allowed to proceed to the desired conversion.

The use of narrow-bore dilatometer tubes, small dilatometer bulbs, and monomer samples about 100 mg. in size ensured that thermal equilibrium was reached rapidly and that the heat of polymerization did not change the sample temperature. The latter point was checked in some runs by changing the sample size by a factor of two with no effect on the rate.

Gel Point Determinations

The gel point tube is shown in Figure 2. The monomer chamber was filled about three-quarters full with monomer. The monomer mixture was degassed by three freeze-thaw cycles under vacuum, after which the tube was filled with helium. A melting point capillary tube containing isooctane colored red was inserted quickly into the tube, as shown, and the tube was tightly stoppered. Upon immersion of the gel point tube in the constant temperature bath, the red isooctane rose in its capillary until thermal equilibrium had been reached, which usually took less than 1 min. The rate measurements had shown that, with the degassed, uninhibited monomer mixtures used here, induction periods were negligible; zero time was there-
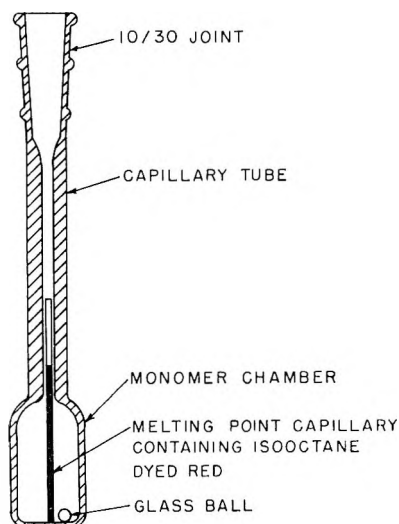
Fig. 2. Gel point tube for determining time to gelation.

fore taken at thermal equilibrium. The vibration of the motor stirring the constant temperature bath caused the little glass ball to spin in the bottom of the gel point tube. The point at which the ball stopped spinning was taken as the gel point; the endpoint was usually sharp, except at very low levels of divinylbenzene. The determination of zero time was more difficult and one of the main sources of error; the end of the thermal expansion of the isooctane was a little hard to judge, and there always remained the possibility of a significant induction period caused by an unknown impurity. The gel points were calculated from the gel times and initial rates; first-order disappearance of monomers was assumed for this region of conversion.

Calculation of Weight-Average Degree of Polymerization, $\bar{Y}_w$

The value of $\bar{Y}_w$ for uncrosslinked polystyrene in this system was calculated from the number-average degree of polymerization, which in turn was calculated from eq. (16):[4b]

$$(\bar{Y}_n)^{-1} = C_M + \{(k_t/k_p^2)R_p/[M]^2\} + (C_I[I]/[M]) \qquad (6)$$

In this equation, C_M is the chain transfer constant for monomer, R_p is the overall rate of polymerization, $[M]$ is the monomer concentration, C_I is the chain transfer constant for the initiator, and $[I]$ is the initiator concentration. At 60°C., $C_M = 0.60 \times 10^{-4}$ and $C_I = 0.055$.[16] The temperature dependence of these constants is not known; it was estimated as follows: The value of C_M for styrene is nearly equal to that for ethylbenzene;[4c] the two molecules have structures similar enough that one can reasonably assume that their chain transfer constants will have the same temperature dependence. This assumption gives the estimated values of C_M: 0.75×10^{-4} at 70.0°C. and 1.16×10^{-4} at 89.7°C. Benzoyl peroxide, the initiator, has a transfer constant only six times that of CCl_4 in the

styrene system.[4c] For lack of a better estimate, C_I is assumed to have the same temperature dependence in the styrene system as does CCl_4. This assumption yields the estimated values of C_I: 0.069 at 70.0°C. and 0.096 at 89.7°C. Using the values for the rate of polymerization of styrene with 1% benzoyl peroxide determined in this study and the estimated values listed above, one obtains $\bar{Y}_n = 400$ at 70.0°C. and $\bar{Y}_n = 229$ at 89.7°C. Polystyrene radicals combine when they react,[17] in which case $\bar{Y}_w = 1.5$ $\bar{Y}_n$. Hence at 70.0°C., $\bar{Y}_w = 600$ and at 89.7°C., $\bar{Y}_w = 344$. These values correspond to molecular weights of 62,400 at 70.0°C. and 35,800 at 89.7°C. The viscosity-average molecular of two polystyrene samples polymerized with 1% benzoyl peroxide at the two temperatures, and isolated by methanol precipitation at 16% conversion, was 70,000 at 70.0°C. and 34,600 at 89.7°C. The agreement is satisfactory, considering the approximations made in the calculation and the inevitable loss of low molecular weight polymer in the isolation step. The calculated values of $\bar{Y}_w$ are used in this paper in calculations with the Flory gel point equation.

RESULTS

Rates of Polymerization

The overall first-order rate constants for polymerization with 1% benzoyl peroxide of styrene–p-divinylbenzene mixtures ranging in composition from straight styrene to straight divinylbenzene are reported in Table II. These values obtain from the start of polymerization to the gel point and, at low crosslinker levels to a little beyond the gel point. The initial rate constants relative to that for styrene at the same temperature increase linearly with mole fraction of divinylbenzene, as shown in Figure 3. The increase for p-divinylbenzene over styrene at both temperatures studied is

TABLE II

Overall First-Order Rate Constants K for the Polymerization
of Styrene–p-Divinylbenzene Mixtures Initiated with 1% Benzoyl Peroxide[a]

p-DVB		K, min.$^{-1} \times 10^3$	
Wt.-%	Mole fraction	Temp. = 70.1°C., $[Bz_2O_2] = 0.0356M$	Temp. = 89.7°C., $[Bz_2O_2] = 0.0349M$
0	0	1.34 ± 0.00	6.9 ± 0.3
4	0.032	1.42 ± 0.04	7.8 ± 0.0
10	0.082	1.48 ± 0.02	8.9 ± 0.2
20	0.167	1.62 ± 0.02	9.5 ± 0.4
35	0.301	1.90 ± 0.01	12.5 ± 0.1
50	0.445	2.33 ± 0.04	14.9 ± 0.2
65	0.598	2.69 ± 0.03	16.7 ± 0.3
75	0.706	2.85 ± 0.01	18.7 ± 0.5
900	1.00	3.25 ± 0.07	25.0 ± 0.5

[a] K defined by the equation: $-d[M]/dt = K[M]$, where $[M]$ is the concentration of monomer. Values of K are averages from two or three runs; precision limits are standard deviations.
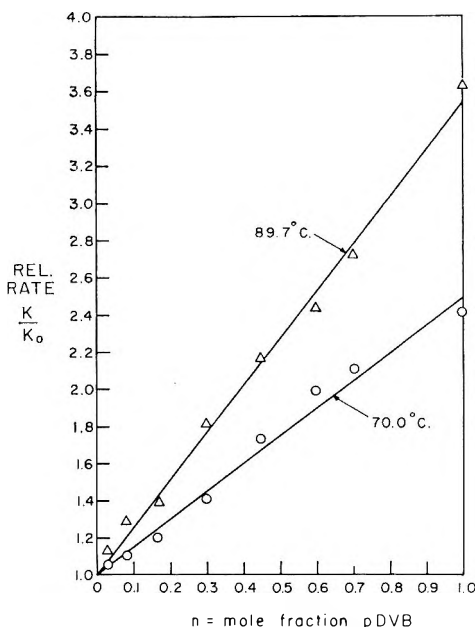
Fig. 3. Rate relative to styrene of the polymerization of styrene–p–divinylbenzene mixtures.

greater than the factor of two expected on a statistical basis for the divinyl over the monovinyl monomer; at 70.0°C. the factor is 2.50, at 89.7°C. it is 3.54.

The overall constant K is a composite; in terms of more familiar constants,

$$K = (\bar{k}_d[I])^{1/2}k_t^{-1/2}k_p \tag{7}$$

where $[I]$ is the initiator concentration, k_d is the rate constant for decomposition of initiator to free radicals, k_p is the rate constant for polymer radical propagation, and k_t is the rate constant for polymer radical termination. The value of k_d for benzoyl peroxide in toluene solution was measured at different temperatures by Bawn and Mellish[17] using diphenyl picryl hydrazyl to trap the radicals generated; the value of $k_p/k_t^{1/2}$ was obtained at different temperatures by Matheson.[15]   From their results, the value of K for styrene is calculated to be 1.35×10^{-3} min.$^{-1}$ at 70°C. and 6.6×10^{-3} min.$^{-1}$ at 90°C., in good agreement with the results of this work.   The calculation assumes that the efficiency of initiation is unity, which was found to be the case at 60°C.[16]

After the gel point, the polymerization rates increase, the increase being greater at the higher divinylbenzene content.   The shape of the conversion curves obtained from the dilatometric measurement is shown in Figure 4 for 4, 10, and 20% divinylbenzene at 70.0°C.; a similar set of curves is obtained at 89.7°C.   The reproducibility of the polymerization curves after the gel point was fairly satisfactory up to 20% divinylbenzene; at higher
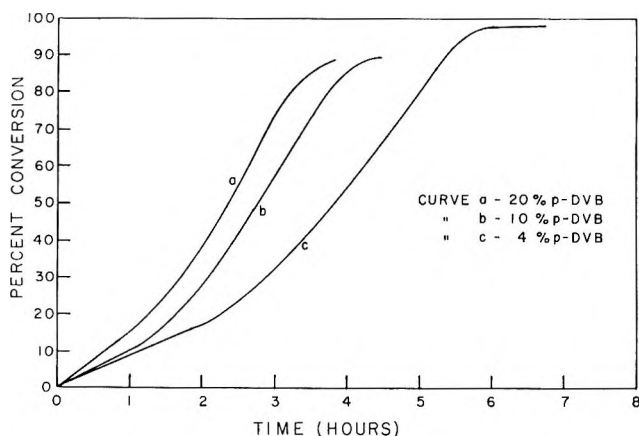
Fig. 4. Per cent conversion as a function of time for mixtures of styrene and (*a*) 20%
p-DVB, (*b*) 10% *p*-DVB, and (*c*) 4% *p*-DVB; 70.0°C.

crosslinker contents only the initial rates were reproducible.   The shape
of the curves is that to be expected for systems which, as polymerization
proceeds show progressively reduced termination rates due to reduced rate
of polymer radical diffusion.[18]   Gelled systems of this type would be just
the ones expected to slow down radical termination by trapping polymer
radicals in the gel.

TABLE III
Conversions at the Gel Point for Polymerizing Mixtures of
Styrene–*p*-Divinylbenzene Initiated with 1% Benzoyl Peroxide

p-DVB		Temp. = 70.1°C., [Bz$_2$O$_2$] = 0.0356M		Temp. = 89.7°C., [Bz$_2$O$_2$] = 0.0349M	
Wt.-%	Mole fraction	Gel time, min.[a]	Conversion at gel point, %	Gel time, min.[a]	Conversion at gel point, %
0.5[b]	0.004	131 ± 2	16.1	73 ± 3	39.5
1.0[b]	0.008	112 ± 4	14.1	40.5 ± 0.9	24.5
2.5[b]	0.020	57.4 ± 2.0	7.6	17.1 ± 0.4	11.3
4	0.032	54.5 ± 0.4	7.4	12.45 ± 0.01	9.2
10	0.082	36.4 ± 0.5	5.2	7.65 ± 0.06	6.5
20	0.167	28.3 ± 0.1	4.5	5.80 ± 0.22	5.4
35	0.301	24.0 ± 0.3	4.5	4.83 ± 0.03	5.8
50	0.445	19.8 ± 0.6	4.5	4.23 ± 0.01	6.1
65	0.598	19.4 ± 0.5	5.1	3.84 ± 0.04	6.2
75	0.706	18.1 ± 0.4	5.0	3.49 ± 0.06	6.3
100	1.00	15.4 ± 0.6	4.9	2.62 ± 0.16	6.3

[a] Gel times are averages from two or three runs.   Precision limits are standard deviations.

[b] Initial rates for these *p*-DVB concentrations calculated from straight lines in Figure 3.

Gel Points

Times to gelation and conversions at the gel point are presented in Table III for the various styrene–divinylbenzene mixtures. The gel points show a minimum around 20% divinylbenzene and actually increase with increasing crosslinker content beyond this point. This system, therefore, is also one which shows marked deviation from the Flory equation. The hypothesis that this deviation is probably due to intrachain crosslinking to form microgels is supported by the increasing sharpness of the gel point with increasing crosslinker. At high divinylbenzene contents, the mixture remains very fluid right up to gelation, at which point it sets up very suddenly. The same sort of sudden transition to macrogel was observed by Shashoua and Beaman[3] in their microgel experiments. At lower divinylbenzene contents, the mixture becomes quite viscous, and the transition to gel is less sudden. This was particularly true of the runs made with 0.5, 1.0, and 2.5% divinylbenzene, and the gel points determined at these levels are less reliable than those obtained at 4% divinylbenzene and higher.

DISCUSSION

The results of the gel point determination on polymerizing mixtures of styrene and p-divinylbenzene imply that intrachain crosslinking to produce microgels is an important reaction even at low crosslinker levels and is the dominant reaction at moderate to high levels. It seems a reasonable hypothesis that the increase in initial polymerization rate with increasing divinylbenzene content is also a consequence of this same reaction. A reaction scheme is proposed below which relates both the gel point and the polymerization rate to the same intrachain crosslinking reaction.

Dependence of the Gel Point on p-Divinylbenzene Content

Two mechanisms appear to be operating in this system to produce gelation. One is the conventional buildup of a three-dimensional network by interchain crosslinking. The other is accumulation of sufficient intramolecularly crosslinked microgels to cause macrogelation. A simple gel point equation expressing this idea can be written for vinyl–divinyl monomer polymerizations, based on the following postulates. (a) all double bonds in the system are of equal reactivity; (b) gelation occurs by both interchain crosslinking and by accumulation of microgels, the effects being strictly additive; (c) the volume of a microgel decreases as the crosslinker content increases by a factor $(1 + \epsilon X_D)^{-1}$, where ϵ is a constant.

The first postulate is common to all gel point equations of this type and avoids the mathematical difficulties resulting from the introduction of monomer reactivity ratios. The postulate appears to be valid for the styrene–p-divinylbenzene system. The second postulate is made to simplify the mathematics and is admittedly arbitrary. Its physical basis derives from the fact that interchain crosslinking and microgel accumulation should give quite different gel structures which can exist side by side

without interference. The great difference in viscosity and sedimentation behavior in solvents of microgels and linear polymers supports this picture.[3] The third postulate states that the volume of a microgel is inversely proportional to the number of divinylbenzene units incorporated in the basic chain, which in turn is presumed to control the number of intrachain links in each microgel. The greater the number of these links, the more tightly crosslinked is the microgel, and hence the smaller is its swollen volume.

The contribution to gelation from interchain crosslinking is given directly by the Flory equation:

$$\alpha_i = (Y_w X_D)^{-1} \tag{1a}$$

where α_i is now the fraction of monomer converted to chains with no internal crosslinks at the gel point. If the volume of a microgel containing but one internal crosslink at nearly zero crosslinker concentration is taken as V_0, then the average volume V of a microgel with a divinylbenzene content corresponding to X_D is:

$$V = V_0(1 + \epsilon X_D)^{-1} \tag{8}$$

The contribution to gelation by microgel accumulation, α_M, is expressed by:

$$\alpha_m = \alpha_{m_0}(1 + \epsilon X_D) \tag{9}$$

where α_{m_0} is the fractional conversion at the gel point corresponding to V_0 if gelation were solely due to accumulation of swollen microgels with volume V_0. The sum of α_i and α_m then gives the actual gel point for the system:

$$\alpha_g = (\bar{Y}_w X_D)^{-1} + \alpha_{m_0}(1 + \epsilon X_D) \tag{10}$$

Qualitatively, eq. (10) is of the type which should give the observed gel point minimum. A quantitative test of the equation will be deferred until after discussion of the polymerization rate.

Dependence of Polymerization Rate on Divinylbenzene Content

A relatively simple reaction scheme, applicable at low conversions, may be written which makes provision for intramolecular crosssslinking if the postulates made for the gel point equation are assumed to hold and, in addition, if the following postulates are also admitted. (a) The termination rate constant k_{t_g} for the reaction of two microgel radicals is less than the termination constant k_{t_0} for two open chain radicals. Further, the rate constant is less because of the smaller effective volume of the two microgel radicals, and the second-order rate constant k_{t_g} is related to k_{t_0} by the relation:

$$k_{t_g} = k_{t_0} (1 + \epsilon X_D)^{-2} \tag{11}$$

(b) The cross-termination constant k_{t_c} for the reaction of an open chain radical with a microgel radical is equal to the geometric mean of k_{t_0} and k_{t_g}:

$$k_{t_c} = (k_{t_0} k_{t_g})^{1/2} \tag{12}$$

(c) The intrachain reaction is proportional to the mole fraction of divinylbenzene units in the chain, is first-order in open chain radicals, and does not depend on molecular weight if the chain is indeed of polymeric dimensions.

The justification for the first postulate is that microgel radicals have a much reduced effective volume which decreases their rate of reaction with each other. The further assumption that this reduction in volume is proportional to $(1 + \epsilon X_D)^{-1}$ is the same one made for reduction in microgel volume and is admittedly arbitrary. Since two such radicals must react to give the termination reaction, the rate constant k_{t_g} should be inversely proportional to $(1 + \epsilon X_D)^{-2}$. The second postulate is again arbitrary and is made to simplify the mathematics. It is physically reasonable since the radicals are chemically the same, but differ only in their physical shape. The third postulate rests on the idea that, once a chain has grown to sufficient length, the back-biting reaction depends on the concentration of pendent vinyl groups in the vicinity of the growing chain end rather than on the total number of such groups along the chain.

In the set of reactions, eqs. (13)–(23), written for a fixed divinylbenzene concentration, the symbol p· is used for an open chain polymer radical and g· for a microgel radical. The symbols S, D, and I stand for styrene, divinylbenzene, and initiator, respectively. It must be emphasized that these reactions are meant to describe the polymerization process only at low conversion and that the rate expressions derived from them are valid only in this region.

$$I \xrightarrow{k_d} 2R \cdot \tag{13}$$

$$R \cdot + S \xrightarrow{k_a} p \cdot \tag{14}$$

$$R \cdot + D \xrightarrow{2k_a} p \cdot \tag{15}$$

$$p \cdot + S \xrightarrow{k_p} p \cdot \tag{16}$$

$$p \cdot + D \xrightarrow{2k_p} p \cdot \tag{17}$$

$$p \cdot \xrightarrow{k_x'} g \cdot \qquad k_x' = k_x(X_D) \tag{18}$$

$$g \cdot + S \xrightarrow{k_p} g \cdot \tag{19}$$

$$g \cdot + D \xrightarrow{2k_p} g \cdot \tag{20}$$

$$p \cdot + p \cdot \xrightarrow{k_{t0}} polymer \tag{21}$$

$$p \cdot + g \cdot \xrightarrow{k_{tc}} polymer \qquad k_{tc} = (k_{t0}k_{tg})^{1/2} \tag{22}$$

$$g \cdot + g \cdot \xrightarrow{k_{tg}} polymer \qquad k_{tg} = k_{t0}(1 + \epsilon X_D)^{-2} \tag{23}$$
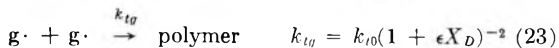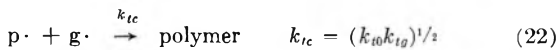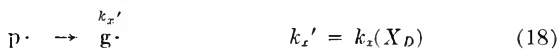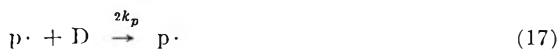
The rate equation for the disappearance of styrene and divinylbenzene based on the reaction scheme is the following:

$$d([S] + [D]) = k_p([S] + 2[D]) ([p \cdot] + [g \cdot]) \tag{24}$$

If the concentrations of all radicals in the system are assumed as usual to be small and invariant with time, the concentration of polymer radicals is given by the expression:

$$[p\cdot] + [g\cdot] = A(k_d[I]/k_{t_0})^{1/2} \tag{25}$$

where

$$A = \left\{\frac{k_d^{1/2}[I]^{1/2} + k_x(X_D)/k_{t_g}^{1/2}}{k_d^{1/2}[I]^{1/2} + k_x(X_D)/k_{t_0}^{1/2}}\right\} \tag{26}$$

Substituting eqs. (25) and (26) into eq. (24), one obtains the rate equation:

$$-d([S] + [D])/dt = (k_d[I]/k_{t_0})^{1/2}k_pA([S] + 2[D]) \tag{27}$$

Equation (16) can be modified slightly to make it correspond to the usual form of the rate equation for polymerization:

$$-d([S] + [D])/dt = k_d[I]/k_{t_0})^{1/2}k_pA(1 + n)([S] + [D]) \tag{28}$$

where n is the mole fraction of divinylbenzene in the mixture. The overall first-order rate constant K is then expressed by:

$$K = (k_d[I]/k_{t_0})^{1/2}k_pA(1 + n) \tag{29}$$

With no divinylbenzene present, $n = 0$, $X_D = 0$, and $A = 1$, in which case K is just the overall first-order constant for styrene, K_0. The overall rate constant at any divinylbenzene content is then

$$K = K_0 A(1 + n) \tag{30}$$

and the product A $(1 + n)$ equal to K/K_0 must, according to Figure 3, be linear in n with a slope greater than one.

The quantity A, defined by equation (26), is a complex ratio which is a function of initiator concentration and of the parameter X_D. As written, the expression for A is too complicated to be useful in correlating polymerization rates. However, if intrachain crosslinking dominates in this system to the extent implied by the gel point observations, then the ratios $k_x(X_D)/k_{t_g}^{1/2}$ and $k_x(X_D)/k_{t_0}^{1/2}$ should be significantly greater than $k_d^{1/2}[I]^{1/2}$, even at low divinylbenzene levels. The expression for A then simplifies to

$$A\ k_{t_0}^{1/2}/k_{t_g}^{1/2} = (1 + \epsilon X_D) \tag{31}$$

by combination with eq. (11). The expression for K/K_0 then becomes

$$K/K_0 = A(1 + n) = 1 + (1 + 2\epsilon)n \tag{32}$$

by using the relation between X_D and the mole fraction n. This relation fits the requirements of linearity and slope imposed by Figure 3; from the plot, the value of ϵ at 70°C. is 0.25 and that at 89.7°C. is 0.77.

Correlation of Polymerization Rates and Gel Point

The model discussed in the preceding paragraphs for styrene–*p*-divinylbenzene polymerization yields two equations which share the common

parameter ϵ. The slope of the lines in Figure 1 allows ϵ to be calculated from eq. (32) at the two temperatures studied. The gel point equation eq. (1) contains another quantity α_{m_0}, whose value is unknown, but which should be independent of divinylbenzene content. With values for ϵ available, the value of α_{m_0} may be calculated from the observed gel points at the different divinylbenzene levels by means of the equation

$$\alpha_{m_0} = [\alpha_g - (\bar{Y}_w X_D)^{-1}]/(1 + \epsilon X_D) \tag{33}$$

which is just eq. (10) suitably rearranged. Values of α_{m_0} are shown in Table IV; they are independent not only of crosslinker content, but also of polymerization temperature. The average value of α_{m_0} corresponds to a volume fraction of polymer of about 0.033. According to the original definition of α_{m_0}, this volume fraction is the minimum required for any assemblage of microgels to cause gelation, since it is the volume fraction occupied by microgels with but one internal crosslink. These hypothetical microgels would have a volume swelling ratio of about 30 from dry polymer to fully swollen state. The gel point equation for bulk polymerization of styrene–p–divinylbenzene systems can then be written

$$\alpha_g = (\bar{Y}_w X_D)^{-1} + 0.038 (1 + \epsilon X_D) \tag{34}$$

The equation has the advantage that there is no crosslinking efficiency factor attached to the Flory term, and that it contains only one undefined parameter, ϵ, which can be obtained from the rate of polymerization. The fact that the term ϵ does tie together the gel point and polymerization rate supports the mechanism of extensive intrachain crosslinking in this system.

TABLE IV
Values of α_{m_0} Calculated from Equation (23)

p-DVB, %	X_D	Temp. = 70.0°C., $\bar{Y}_w = 600$, $\epsilon = 0.25$			Temp. = 89.7°C., $\bar{Y}_w = 344$, $\epsilon = 0.77$		
		α_g	$(\bar{Y}_w X_D)^{-1}$	α_{m_0}	α_g	$(Y_w X_D)^{-1}$	α_{m_0}
0.5	0.008	0.162[a]	0.208	−0.046[b]	0.395	0.362	0.032
1.0	0.016	0.141	0.104	0.037	0.245[c]	0.182	0.063[b]
2.5	0.039	0.076	0.043	0.033	0.113	0.075	0.037
4.0	0.062	0.074	0.027	0.046	0.092	0.047	0.043
10	0.115	0.052	0.011	0.039	0.065	0.019	0.040
20	0.287	0.045	0.006	0.036	0.054	0.010	0.036
35	0.461	0.045	0.004	0.037	0.058	0.006	0.039
50	0.616	0.045	0.003	0.037	0.061	0.005	0.038
65	0.750	0.051	0.002	0.041	0.062	0.004	0.036
75	0.828	0.050	0.002	0.040	0.063	0.004	0.036
100	1.00	0.049	0.002	0.039	0.063	0.003	0.034
			Avg.	0.038		Avg.	0.037

[a] Value apparently too low, probably because of high viscosity prior to actual gel point.

[b] Value not used in computing average.

[c] Value apparently too high, possibly because of impurity causing induction period.

The quantity α_{m_0} in eq. (10) should increase if a diluent is added to the system, because a greater conversion of monomer to polymer must take place to produce the volume fraction of microgels required for macrogelation.   It should, in fact, be possible to select a solvent–monomer system that will not gel, regardless of the crosslinker content of the monomer component.   Zimm[19] has demonstrated this by polymerizing a styrene–20% divinylbenzene mixture in carbon tetrachloride to high conversion without gelation.   The soluble polymers isolated from that series of experiments behaved like microgels in that they had unusually low viscosity for the molecular weight measured by light scattering.   This is further evidence for microgel formation in the styrene–divinylbenzene system.

References

1. Staudinger, H., and W. Heuer, *Ber.*, **67**, 1164 (1934).

2. Ueberreiter, K., and G. Kanig, *J. Chem. Phys.*, **18**, 399 (1950);   K. Ueberreiter and E. Otto-Laupenmühlen, *Kolloid-Z.*, **133**, 26 (1953);   K. Kawata, *J. Polymer Sci.*, **19**, 359 (1956).

3. Shashoua, V. E., and R. G. Beaman, *J. Polymer Sci.*, **33**, 101 (1958).

4. Flory, P. J., *Principles of Polymer Chemistry*, Cornell Univ. Press, Ithaca, N. Y., 1953, (a) pp. 391–392;   (b) p. 138;   (c) p. 143.

5. Walling, C., *J. Am. Chem. Soc.*, **67**, 441 (1945).

6. Minnema, L., and A. J. Staverman, *J. Polymer Sci.*, **29**, 281 (1958).

7. Loshaek, S., and T. G Fox, *J. Am. Chem. Soc.*, **75**, 3544 (1953).

8. Hwa, J. C. H., and T. G Fox, paper presented at 131st Meeting American Chemical Society, Miami, April 9, 1957;   *Abstracts of Papers*, p. 145.

9. Wiley, R. H., and B. Davis, *J. Polymer Sci.*, **31**, 463 (1963).

10. Wiley, R. H., and E. E. Sale, *J. Polymer Sci.*, **42**, 491 (1960).

11. Walling, C., *Free Radicals in Solution*, Wiley, New York, 1957, pp. 135–140.

12. McCallum, K., unpublished results.

13. Roberts, J. D., E. A. McElhill, and R. Armstrong, *J. Am. Chem. Soc.*, **71**, 2923 (1949).

14. Lyman, W. R., procedure developed in these laboratories.

15. Matheson, M. S., E. E. Auer, E. B. Bevilacqua, and E. J. Hart, *J. Am. Chem. Soc.*, **73**, 1700 (1951).

16. Mayo, F. R., R. A. Gregg, and M. S. Matheson, *J. Am. Chem. Soc.*, **73**, 1691 (1951).

17. Bawn, C. E., and S. Mellish, *Trans. Faraday Soc.*, **47**, 1216 (1951).

18. Trommsdorf, E., H. Kölde, and P. Langally, *Makromol. Chem.*, **1**, 169 (1948); G. V. Schulz and G. Habor h, *ibid.*, **1**, 106 (1948).

19. Zimm, B. H., F. P. Price, and J. B. Bianchi, *J. Phys. Chem.*, **62**, 979 (1958).

Résumé

Les vitesses initiales de polymérisation du styrène, du p-divinylbenzène et du mélange des deux monomères, initiés avec le peroxyde de benzoyle à 1% ont été mesurées à 70°C et à 89,7°C.   Les vitesses relatives du styrène augmentent linéairement avec la fraction molaire du p-divinylbenzène;   ce dernier monomère polymérise plus vite que le styrène et ceci avec un facteur de 2,5 à 70°C et de 3,54 à 89,7°C.   Les temps de formation de gels ont été également mesurés pour ces échantillons contenant du p-divinylbenzène, et à partir de ces temps on a calculé la conversion partielle correspondant au point de

gélification. La conversion au point de gélification passe par un minimum en augmentant la teneur en *p*-divinylbenzène. Le phénomène de gélification est expliqué par le pontage entre les chaînes polymériques pour donner un réseau et par le pontage dans la chaîne même pour donner des microgels qui s'accumulent pour former un macrogel, ce dernier phénomène étant dominant pour toutes que les faibles concentrations en *p*-divinylbenzène. Au plus il y a d'agent de ramification au moins les microgels sont gonflés, et au plus une plus grande conversion est nécessaire pour former un gel par ce processus. L'augmentation linéaire de la vitesse avec une teneur croissante en *p*-divinylbenzène est également expliquée par pontage dans la chaîne: des radicaux polymériques en croissance, qui subissent ce processus, ont une vitesse de terminaison réduite. Le facteur par lequel la constante de vitesse de terminaison est réduite avec une augmentation de la teneur en divinylbenzène, est identique à celui par lequel la conversion nécessaire pour former un gel par accumulation de microgels est augmentée.

Zusammenfassung

Die Anfangsgeschwindigkeit der Polymerisation bei 70,0°C und 89,7°C wurde für Styrol, *p*-Divinylbenzol und Mischungen der beiden Monomeren mit Start 1% Benzoylperoxyd gemessen. Bezogen auf Styrol nahm die Geschwindigkeit linear mit dem Molenbruch an *p*-Divinylbenzol zu; letzteres Monomeres polymerisierte bei 70,0°C um einen Faktor 2,50 rascher als Styrol, bei 89,7°C um einen Faktor 3,54. Für die *p*-Divinylbenzol-enthaltenden Proben wurde auch die Gelbildungsdauer gemessen, und aus diesen Zeiten wurde der entsprechende Umsatz beim Gelpunkt berechnet. Der Umsatz beim Gelpunkt ging mit zunehmendem Gehalt an *p*-Divinylbenzol durch ein Minimum. Das Gelbildungsverhalten wird durch gleichzeitige Zwischenkettenvernetzung unter Bildung eines Netzwerkes und Intrakettenvernetzung unter Bildung eines Mikrogels, das sich zu einem Makrogel akkumuliert, erklärt; letzterer Vorgang ist bei allen ausser niedrigen *p*-Divinylbenzolkonzentrationen vorherrschend. Je höher der Gehalt an Vernetzung, umso weniger gequollen sind die Mikrogele und umso grösser ist der für eine Gelbildung durch diesen Vorgang erforderliche Umsatz. Auch die lineare Geschwindigkeitszunahme mit steigendem *p*-Divinylbenzolgehalt wurde durch Intrakettenvernetzung erklärt: Wachsende Polymerradikale, bei denen dieser Vorgang auftritt, besitzen eine herabgesetzte Abbruchgeschwindigkeit. Der Faktor, um welchen die Abbruchsgeschwindigkeitskonstante mit wachsendem *p*-Divinylbezolgehalt herabgesetzt wird, ist der gleiche, um welchen der zur Gelbildung durch Akkumulation von Mikrogelen erforderliche Umsatz erhöht wird.

Kinetics of Polymerization of Styrene Initiated by Substituted Peroxides.   II. Decomposition Rate Constants and Efficiencies*

K. F. O'DRISCOLL and P. J. WHITE, *Department of Chemistry, Villanova University, Villanova, Pennsylvania*

Synopsis

The following bis-substituted benzoyl peroxides were used as initiators for the polymerization of bulk styrene monomer at 90°C.: p-methoxy-, p-methyl-, p-chloro-, m-bromo-, 3,4-dichloro-, p-cyano-, and p-nitro-; in addition, unsubstituted benzoyl peroxide was also studied. From the observed rates of polymerization the rate constants for the unimolecular decomposition and for the radical-induced decomposition of the peroxides were obtained, as well as the efficiency of initiation of polymerization. It was observed that substituents more electron-withdrawing than p-chloro did not change the unimolecular rate constant. Conversely, substituents less electron-releasing than p-chloro had little effect on the efficiency of initiation. The induced decomposition rate constant gave a simple linear Hammett plot with positive slope.

INTRODUCTION

In free radical-initiated vinyl polymerization, radicals produced from the homolytic scission of benzoyl peroxide at the peroxide linkage may either combine with a monomer molecule, generating a new radical and starting a polymer chain, or they may lose carbon dioxide to become phenyl radicals. The phenyl radicals may start polymer chains or may combine with other radicals to give biphenyl or phenyl benzoate, neither of which are capable of initiation at normal conditions. Thus, there may be associated with the initiator both a homolytic decomposition rate constant k_d, and an efficiency, f, which describes the fraction of the radicals which are successful in starting chains.

The expression given as eq. (1) may be derived for the rate of polymerization by use of the steady-state assumptions often used in free-radical processes:

$$-d[M]/dt = k_p(fk_d[Cat]/k_t)^{1/2}[M] \qquad (1)$$

where [M] = monomer concentration, [Cat] = initiator concentration, k_d = initiator dissociation rate constant, k_p = propagation rate constant,

k_t = termination rate constant, and f = fraction of radicals produced from the initiator which are successful in starting polymer chains.

An examination of this equation shows that a study of kinetics at very low conversions ([M] and [Cat] equal to starting concentrations) yields fk_d as an inseparable product. This of course requires an external knowledge of k_d such as would be found by thiosulfate titration of undecomposed peroxide to allow calculation of efficiency in polymerization.

The only scheme allowing determination of f and k_d from the same polymerization experiments to date is that of "dead end" polymerization presented by Tobolsky, Rogers, and Brickman.[1] They have investigated 2,2'-azobisisobutyronitrile (AIBN) as an initiator by this technique and have obtained good agreement with values determined by other methods in separate experiments for k_d. However, as we pointed out previously,[2] the treatment is inapplicable at the high thermal conversions associated with the long times and high temperatures necessary to apply the treatment to benzoyl peroxides. At any rate, application of the treatment to benzoyl peroxides would be questionable, since first-order initiator decomposition is assumed. Nozaki and Bartlett[3] have shown that an induced decomposition is a factor in decomposition of benzoyl peroxide and that kinetics of the following type are produced:

$$-d[\text{Cat}]/dt = k_d[\text{Cat}] + k_i[\text{Cat}]^n \tag{2}$$

where k_i is the rate constant for the radical-induced decomposition and n varies somewhat with solvent but usually equals 1.5. Styrene was included among the solvents in their study, but the viscous state of the reaction mix made analysis difficult. It is noteworthy that Tobolsky's work was done on AIBN which apparently does not undergo an induced decomposition.

Obviously k_d could be determined from titration experiments without interference from induced decomposition if the radicals could be trapped as soon as they were formed. Swain, Stockmayer, and Clarke[4] and Blomquist and Buselli[5] have made such studies on several substituted benzoyl peroxides. The former employed dioxane $0.2M$ in 3,4-dichlorostyrene and the latter acetophenone as solvents. The results of the two studies agreed fairly well and were shown to have some connection with Hammett functions. These values, however, could not be used in polymerization experiments to calculate f if induced decomposition were taking place, since use of k_d alone would not completely describe the disappearance of initiator.

The study reported here was thus undertaken for two general purposes: (a) to determine rate constants for both homolytic and induced decomposition and to determine the efficiency of homolytically produced radicals all in a polymerizing system, and (b) by varying ring substituents on the benzoyl peroxides, to study electronic effects on the above parameters. To do this, a new kinetic scheme was evolved and is discussed below.

In bulk polymerization of styrene by free radical initiation the following reactions are assumed to take place at the rates shown in eqs. (3)–(6).

A. Peroxide Decomposition and Initiation:

$$Cat \xrightarrow{k_d} 2R\cdot$$

$$R\cdot + M \rightarrow M\cdot$$

$$d[M\cdot]/dt = 2fk_d[Cat] \qquad (3)$$
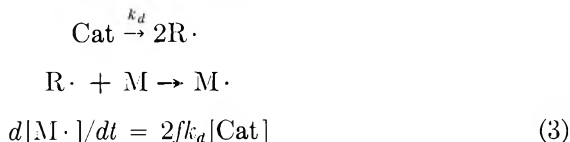
where Cat = peroxide, $R\cdot$ = radicals homolytically produced from the peroxide, M = monomer, f = fraction of total $R\cdot$'s which initiate polymer chains, and $M\cdot$ = growing polymer chain.

B. Chain Propagation:

$$M\cdot + M \xrightarrow{k_p} M\cdot$$

$$-d[M]/dt = k_p[M\cdot][M] \qquad (4)$$
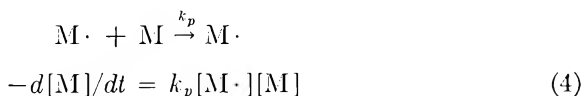
The assumption is made that all growing chains have the same activity regardless of length.

C. Termination:

$$M\cdot + M\cdot \xrightarrow{k_t} P$$
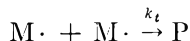
where P = dead polymer

$$-d[M\cdot]/dt = 2k_t[M\cdot]^2 \qquad (5)$$

D. Induced Decomposition:

$$M\cdot + Cat \xrightarrow{k_x} P + R\cdot$$

$$-d[Cat]/dt = k_x[Cat][M\cdot] \qquad (6)$$
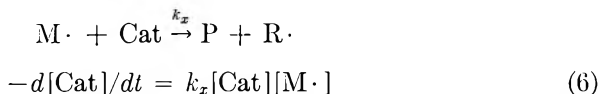
This is seen to correspond to a catalyst transfer. It is assumed that each $R\cdot$ produced by chain transfer is successful in starting a new chain. The assumption seems reasonable since the $R\cdot$ would have to find another $R\cdot$ or $M\cdot$ to engage in a reaction leading to inefficiency. This seems unlikely in comparison to reaction A, where both radicals are in the same cage and can react to inert products after one or both lose carbon dioxide. Two other reactions—transfer to monomer and chain termination by initiator radicals—are possible but are ignored here. The rate constant for transfer to the monomer is shown by Baysal and Tobolsky[6] to be several orders of magnitude less than k_p. Bamford, Jenkins, and Johnston[7] very elegantly show that at low initiator and high monomer concentrations termination by primary radicals is negligible.

For the four reactions given, and assuming a steady-state radical concentration:

$$2fk_d[Cat] + k_x[Cat][M\cdot] = 2k_t[M\cdot]^2 + k_x[Cat][M\cdot] \qquad (7)$$

$$[M\cdot] = (fk_d[Cat]/k_t)^{1/2} \qquad (8)$$

A differential equation for the disappearance of catalyst may also be written:

$$-d[\text{Cat}]/dt = k_d[\text{Cat}] + k_x[\text{Cat}][\text{M} \cdot] \qquad (9)$$

Equation (9) may be integrated after substitution for $[\text{M} \cdot]$ from eq. (8). This result combined with eq. (4) readily yields:

$$(R_p/[\text{M}]_0)(R_p/[\text{M}])_t = e^{k_d t} + (e^{k_d t} - 1) \, (k_i/k_d) \, [\text{Cat}]_0^{1/2} \qquad (10)$$

where $k_i \equiv k_x f k_d^{1/2}/k_t$.

For several runs in which $[\text{Cat}]_0^{1/2}$ is varied, values for $(R_p/[\text{M}])_0/(R_p/[\text{M}])_t$ may be taken at specific times and plotted against $[\text{Cat}]_0^{1/2}$. A straight line represented by eq. (10) should result, allowing calculation of k_d and k_i from the intercept and slope. The efficiency, f, may then be calculated from the value of $\ln (R_p/[\text{M}])$ extrapolated to time zero.

It will be noted that constant volume is tacitly assumed in the above kinetics. This, of course, is not the case. However, since volume change is less than 2% in this work it is felt that the effects on concentration are negligible.

With the exception of the negligible primary radical termination, the processes leading to inefficient use of homolytically produced radicals involve loss of carbon dioxide from one or both of the radicals. That is, simple recombination of the aroyloxy radicals does not involve loss of initiator; however, production of substituted aryl aroyloates or biaryls does. Assuming that the radicals operate in a cage, of an initiator molecule, the reaction may be written as in eq. (11):

$$
\begin{array}{c}
[\text{Cat}]_{\text{cage}} \\
k_d \downarrow \\
[\text{R} \cdot + \text{R} \cdot]_{\text{cage}} \\
\swarrow^{k_f} \qquad\qquad \searrow^{k_v} \\
2\text{I} \cdot \xleftarrow{k_f} [\text{R} \cdot + \text{B} \cdot]_{\text{cage}} + \text{CO}_2 \\
+M \downarrow k_m \qquad\qquad \downarrow k_c \\
\text{M} \cdot \qquad\qquad\quad \text{RB}
\end{array}
\qquad (11)
$$
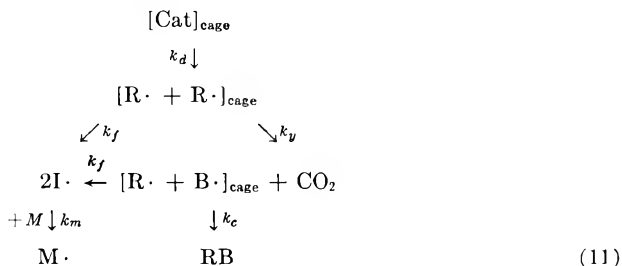
The new rate constants are associated with reactions as follows: k_f = diffusion of radicals from the cage; k_v = loss of carbon dioxide from an aroyloxy radical; k_c = combination of aroyloxy and aroyl radicals in a cage to dead initiator; k_m = addition of monomer. The possibility of both radicals in a single cage losing carbon dioxide before combination or initiation is ignored. The quantities in a cage are treated as single entities which undergo first-order reactions.

The balances shown in eqs. (12)–(15) may be drawn on a steady-state assumption, where brackets and the subscript c denote a cage condition:

$$d[\text{R} \cdot + \text{R} \cdot]_c/d_t = k_d[\text{Cat}]_c - k_f[\text{R} \cdot + \text{R} \cdot]_c = 0 \qquad (12)$$

$$d[\text{R} \cdot + \text{B} \cdot]_c/d_t = k_v[\text{R} \cdot + \text{R} \cdot]_c -$$
$$k_c[\text{R} \cdot + \text{B} \cdot]_c - k_f[\text{R} \cdot + \text{B} \cdot]_c = 0 \qquad (13)$$

$$d[I \cdot]/d_t = 2k_f[R \cdot + R \cdot]_c +$$

$$[R \cdot + B \cdot]_c - k_m[I \cdot][M] = 0 \quad (14)$$

$$f = 2k_f \frac{k_d[\text{Cat}]_c}{k_f + k_y} + \frac{k_y k_d[\text{Cat}]_c}{(k_f + k_y)(k_f + k_c)} \Big/ 2k_d[\text{Cat}]_c \quad (15)$$

Assuming k_c to be much larger than k_y or k_f, and rearranging yields:

$$k_y/k_f = (1 - f)/f \quad (16)$$

If it is assumed that k_f is constant for the various substituted radicals, it is realized that such a quantity will drop out of Hammett calculations. We may therefore write:

$$\log [(k_y) \text{ subs.}/(k_y) \text{ unsubs.}] = \rho\sigma =$$

$$\log \left\{ [(1 - f)/f]_{\text{subs.}}/[(1 - f)/f]_{\text{unsubs.}} \right\} \quad (17)$$

It should be strongly emphasized that the efficiency as defined here is not connected at all with initiator wastage by chain transfer to catalyst. Efficiency deals only with the fate of homolytically produced initiator fragments. Another commonly used definition of efficiency is that portion of the initiator consumption which successfully starts chains. The latter value must of course be equal to or less than that defined in this work.

To allow kinetic measurements over a reasonable time span while using low initiator concentrations, 90°C. was chosen as an operating temperature. At this level, thermal polymerization of styrene is appreciable (about 1%/hr.) and should be recognized. Observed data may be corrected for thermal initiation by the eq. (18)[2,8]

$$R_{p,\text{Cat}} = {R^2}_{p,\text{total}} - {R^2}_{p,\text{thermal}}{}^{1/2} \quad (18)$$

where $R_{p,\text{thermal}}$ is the rate of polymerization which would be observed thermally at the same conditions of temperature and monomer concentration at which $R_{p,\text{total}}$ was measured. It is understood that in the derivation leading to eq. (10) R_p is equal to $R_{p,\text{Cat}}$.

EXPERIMENTAL

Dilatometers were constructed with a 15-cm. measuring section of 3.175 ± 0.005 mm. precision bore tubing. This was topped with a section of 10 mm. tubing for filling and sealing. The bulb section on the bottom was constructed of 16 mm. tubing in lengths which produced total volumes of about 12, 25, and 40 ml. The various sized dilatometers were employed to keep the rates of level change in the same range as initiator and initiator concentration were changed.

Level readings were made with a cathetometer capable of a vernier reading of 0.005 cm. All runs were made at 90°C. in a constant temperature bath with an observed variation of about ±0.02–0.03°C.

Styrene was freshly distilled at 10 mm. Hg pressure of nitrogen and center fraction was taken. Peroxides were weighed and dissolved in styrene and the desired amounts added volumetrically to dilatometers. After making up to a predetermined volume with freshly distilled styrene the dilatometers were degassed five times, sealed under a vacuum, and held in liquid nitrogen until use.

At the end of each run, the tube was quenched in ice water and the contents sucked into a filtering flask. The tube was washed with three 5-ml. aliquots of chloroform, and the washings were added to the flask. This material was then slowly added, with vigorous hand stirring, to a twenty to thirtyfold excess of methanol. After aging at least overnight, the precipitate was filtered in sintered glass filters of medium porosity, dried overnight at 70–80°C. and 20–25 in. of vacuum and weighed to constant weight. In two runs, the filtrate was also evaporated to dryness under vacuum and weighed. The low molecular weight polymers recovered amounted to only about 1% of the precipitated polymer and were therefore ignored.

The dilatometric method employed required knowledge of a shrinkage factor, i.e., the fractional volume reduction for complete polymerization. This was first calculated from the polymer and monomer density data of Patnode and Scheiber[9] as a shrinkage of 0.182 ml./ml. of styrene polymerized. As data accumulated, this was compared to a value of 0.200 calculated from the observed volume change and weight of precipitate polymer. As a check on this latter value, known weights of dry polymer and styrene were added to a dilatometer tube and their resultant volume measured at 90°C. With a known styrene density at 90°C. (0.8415 g./ml.) and the assumption of volume additivity, polymer density at 90°C. was calculated as 1.0485 g./ml. This compared to values of 1.0293 g./ml. for Patnode and Scheiber[9] and 1.0406 g./ml. for Matheson, Auer, Bevilacqua, and Hart[10] and produced a shrinkage factor of 0.1974. The
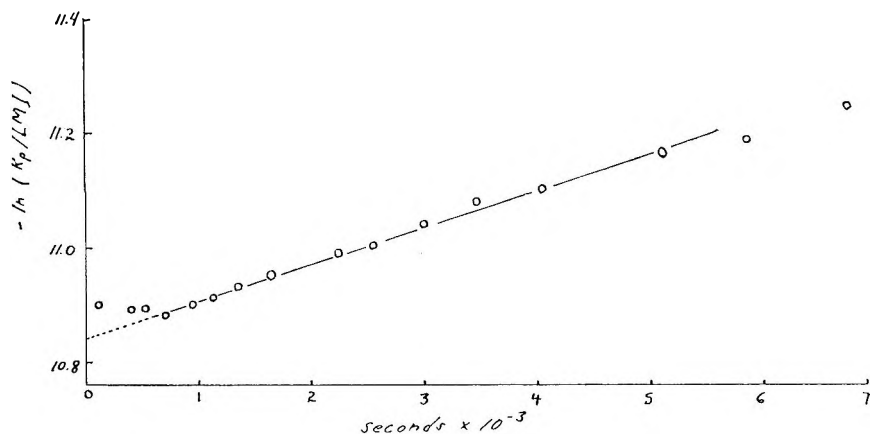
Fig. 1. Initial polymerization of styrene at 90°C. with 7.10×10^{-4} mole/l. benzoyl peroxide.

agreement with the above average value prompted use of 0.200 for all calculations.

Benzoyl peroxide was purchased from Eastman. p-Chlorobenzoyl peroxide was purchased as a 50% paste in dibutyl phthalate (removed by methanol) from Lucidol Division of Wallace and Tiernan. All other peroxides were synthesized from the parent acid chloride by the method first used by Price and Krebs.[11] All peroxides were purified by recrystallization. Recrystallization solvents were the same as those tabulated by Swain et. al.,[4] except that toluene was substituted for benzene in those cases in which benzene was the sole solvent. 3,4-Dichlorobenzoyl peroxide was recrystallized from toluene.

For all synthesized peroxides other than p-cyano and p-methyl, purchased acid chlorides were available. For these two materials it was necessary to synthesize the acid chloride from the acid reaction with thionyl chloride. The method is described by Vogel[12] and was followed, except that additional excess thionyl chloride was used and was stripped off under vacuum. p-Cyanobenzoyl chloride distilled at 128°C./7 mm. Hg and p-methylbenzoyl chloride at 104°C./9 mm. Hg.

Although yields were not measured, it was quantatively obvious that improved yields of peroxides with electron-withdrawing substituents were obtained if reaction time was shortened. Therefore, p-nitro, p-cyano-, 3,4-dichloro-, and 3,5-dinitrobenzoyl peroxides were reacted no more than 5 minutes. Others were reacted about 30 min.

Decomposition points and elemental analyses for the peroxides demonstrated that all the peroxides were of quite good purity.

RESULTS

It was recognized early in the work that meaningful data had to be obtained before the diffusion control of the termination reaction caused a
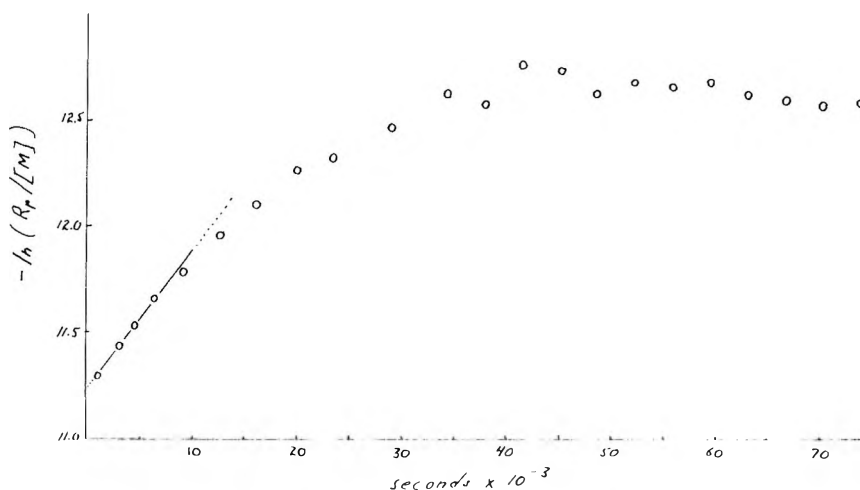
Fig. 2. Polymerization of styrene at 90°C. with 3.26 × 10⁻⁴ mole/l. benzoyl peroxide.
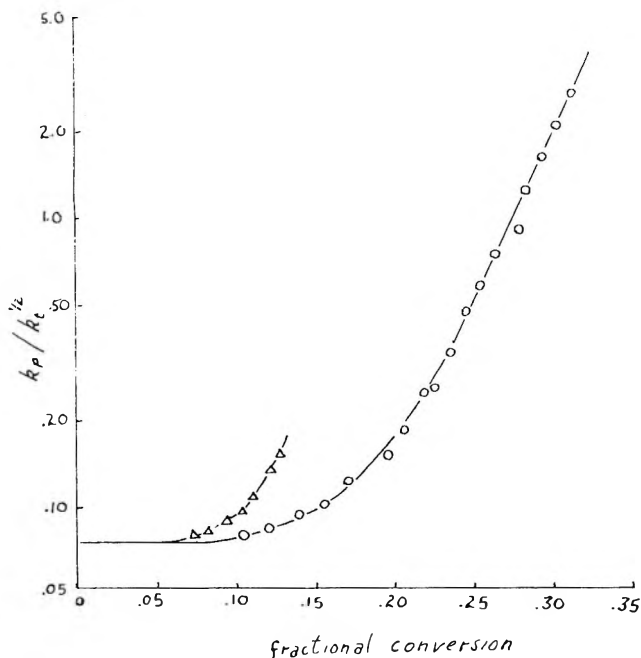
Fig. 3. Diffusion control of termination in polymerization of styrene at 90°C.: (O) with 3.26 × 10⁻⁴ mole/l. benzoyl peroxide; (△) with 2.61 × 10⁻⁴ mole/l. p-methoxybenzoyl peroxide.

TABLE I

Average Values of Decomposition Rate Constants and Efficiencies For Bis-Substituted Benzoyl Peroxides at 90°C. in Styrene

Substituent	Number of runs	$k_d \times 10^4$, sec.$^{-1}$ Observed	$k_d \times 10^4$, sec.$^{-1}$ Literature	f	$k_t \times 10^3$, (l./mol./sec.)$^{1/2}$
p-Methoxy	5	3.29 ± 0.2	3.92[a] 5.20[b]	0.80	<0.2[c]
p-Methyl	3	1.93 ± 0.1	2.05[a] 1.98[b]	0.73	<0.2[c]
None	6	1.33 ± 0.1	1.41[a] 1.44[b]	0.72	<0.2[c]
p-Chloro	5	0.94 ± 0.1	1.21[a] 1.28[b]	0.77	1.23 ± 0.3
m-Bromo	6	1.00 ± 0.1	0.81[a]	0.47	0.88 ± 0.3
3,4-Dichloro	9	1.11 ± 0.2	— —	0.36	1.16 ± 0.5
p-Cyano	4	0.97 ± 0.1	0.68[a] 0.81[b]	0.34	1.25 ± 0.3
p-Nitro	4	0.87 ± 0.3	1.45[b]	0.27	10.9 ± 1.0

[a] Data of Swain et al.[4]

[b] Data of Blomquist and Buselli.[5]

[c] Lower limit of measurement.

change in the termination rate constant k_t, since this number is employed in the calculation of the efficiency f.   Although it is usual to associate such effects with high conversions, North[13] has shown that diffusion-caused changes can be observed from the very beginning in the polymerization of
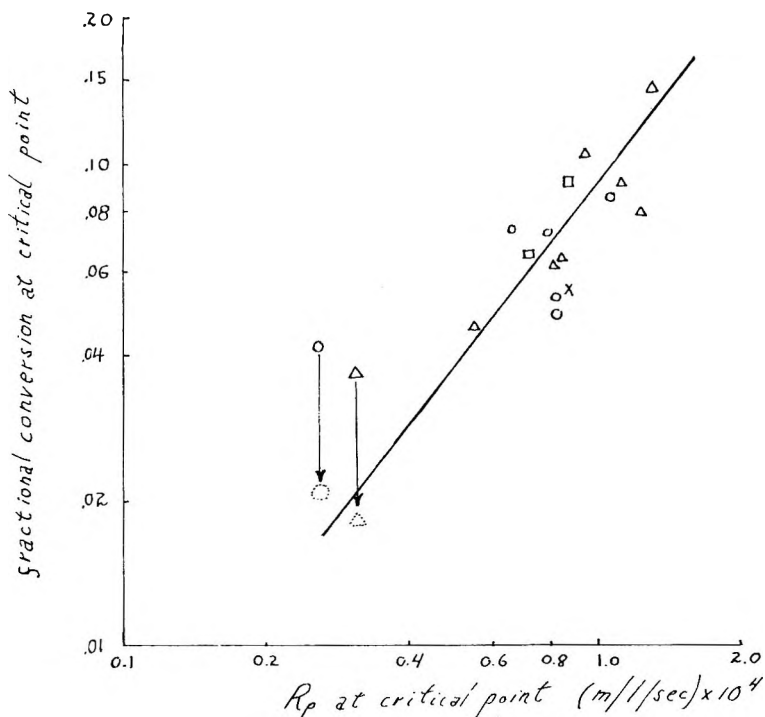
Fig. 4. Effect of rate of polymerization styrene at 90°C. on conversion at which diffusion control becomes apparent: (O) benzoyl peroxide; (Δ) p-methoxybenzoyl peroxide; dotted symbols corrected for monomer concentration.
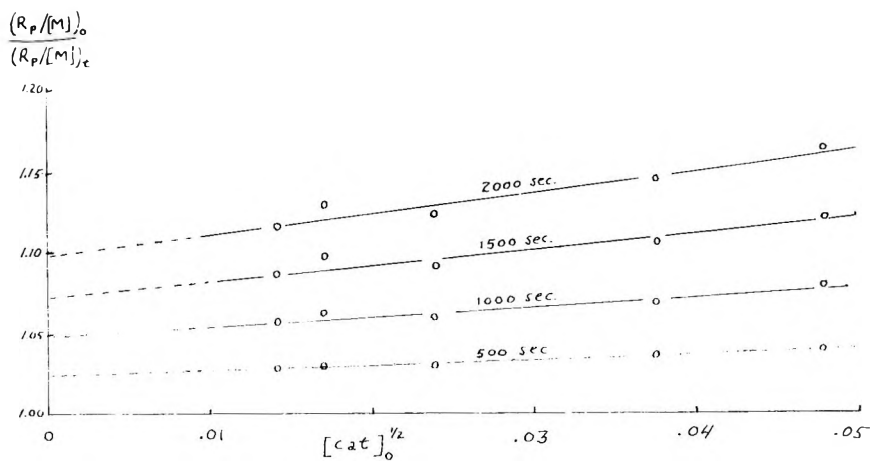
Fig. 5. Plot of eq. (10) for p-chlorobenzoyl peroxide in styrene at 90°C.

methyl methacrylate. It was shown above that plots of $\ln(R_p/[M])$ versus time ought to be linear at low time. Using those initiators which are later shown to be free from any appreciable induced decomposition, we
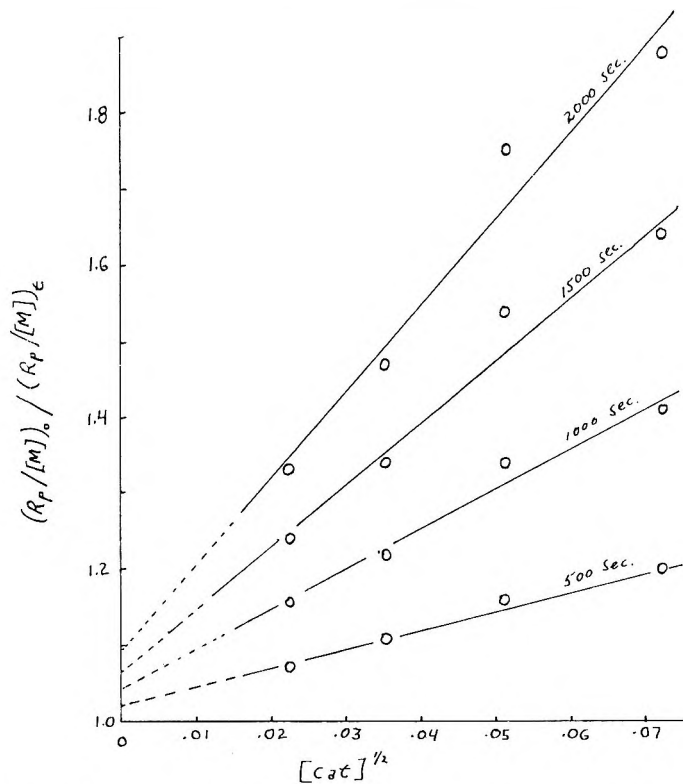
Fig. 6. Plot of eq. (10) for *p*-nitro benzoyl peroxide in styrene at 90°C.
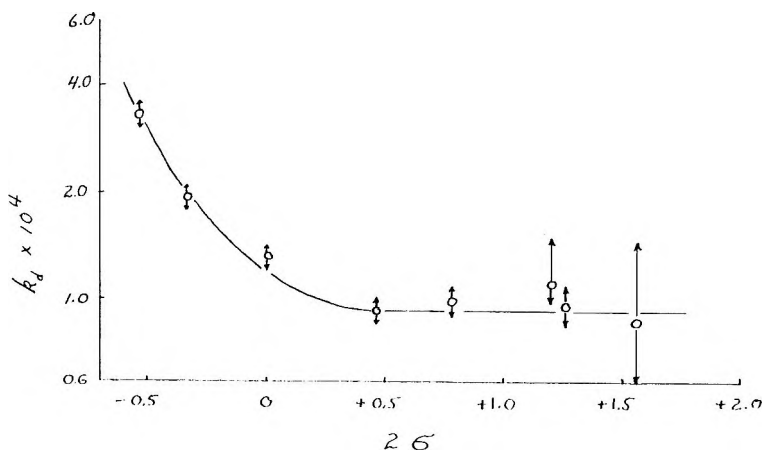
Fig. 7. Hammett plot of decomposition rate constants for symmetrically substituted benzoyl peroxides at 90°C.
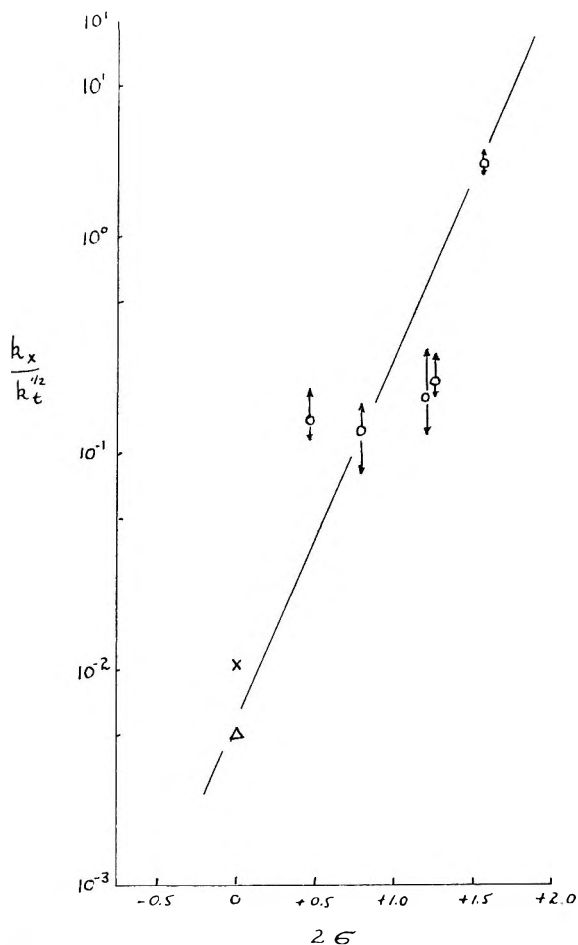
Fig. 8. Hammett plot of induced decomposition rate constants for symmetrically substituted benzoyl peroxides at 90°C.

can calculate f and k_d from the initial low-conversion straight lines as in Figure 1. Any curvature in the plot, such as in Figure 2, is then attributed to changes in k_t, and from it we can calculate the value of the ratio $k_p/k_t^{1/2}$ at various conversions. A plot of this ratio for two typical runs is shown in Figure 3. If the conversion where the change in k_t becomes apparent is plotted versus the concurrent rate of polymerization, Figure 4 is obtained. All data were obtained in bulk styrene except the lowest two points in Figure 4, which were obtained in 50% benzene solution. The two points are adjusted accordingly. All data reported below were obtained under conditions corresponding to the area below and to the right of the line in Figure 4, and are therefore free of any effect of changes in viscosity of the reaction.

For initiators that do show induced decomposition, values of f and k_d might be obtained from low conversion portion of plots such as Figure 1
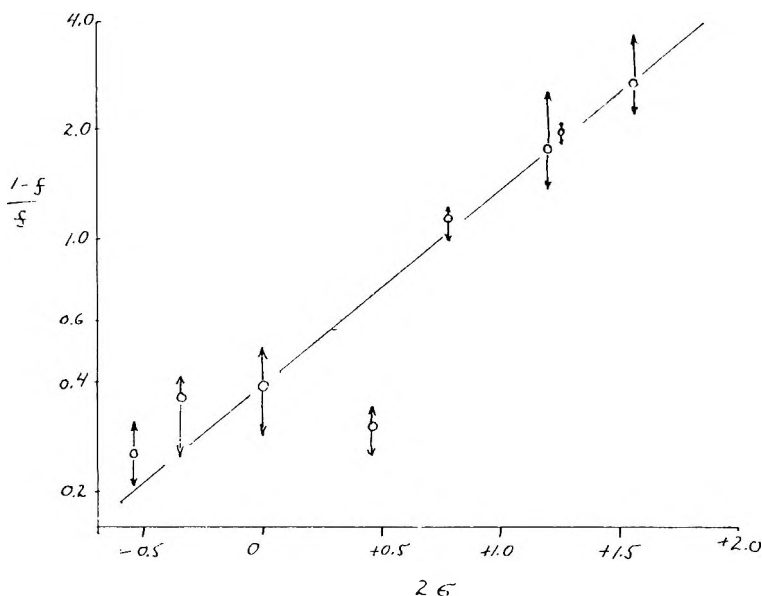
Fig. 9. Hammett plot of efficiency data according to eq. (16) for symmetrically substituted benzoyl peroxides at 90°C.

or 2. However, k_i can also be obtained if, instead, eq. (10) is plotted at specific times for various initiator concentrations as described earlier. Plots for two extreme examples are shown in Figures 5 and 6.

A summary of the values of the derived rate constants k_d, k_i, and f is given in Table I. Hammett plots are shown in Figures 7, 8, and 9 of k_d, k_x (calculated from k_i) and the function $(1 - f)/f$.

DISCUSSION OF RESULTS

A. Homolytic Decomposition Rate Constant k_d

From the plot of k_d versus 2σ (Fig. 7), it must be held that the homolytic decomposition rate constants do not follow simple Hammett behavior. Hammett values are those collected by Jaffe.[14] Swain et al.[4] hinted at the same type of behavior by pointing out that the decomposition could be considered as resulting from mutual repulsion of negative charges at the O-O bond. They suggested that the charges on the peroxide oxygen atoms were linear functions of Hammett σ constants and that the rate constants obeyed the relation:

$$\log k_d = \text{constant} + \beta(\sigma_m - \sigma_1)(\sigma_m - \sigma_2)$$

Where σ_m is the Hammett constant for a hypothetical substituent which would reduce one of these charges to zero.

Swain also points out that if stability of the radicals resulting from dissociation could play a part in determining k_d, a minimum would be
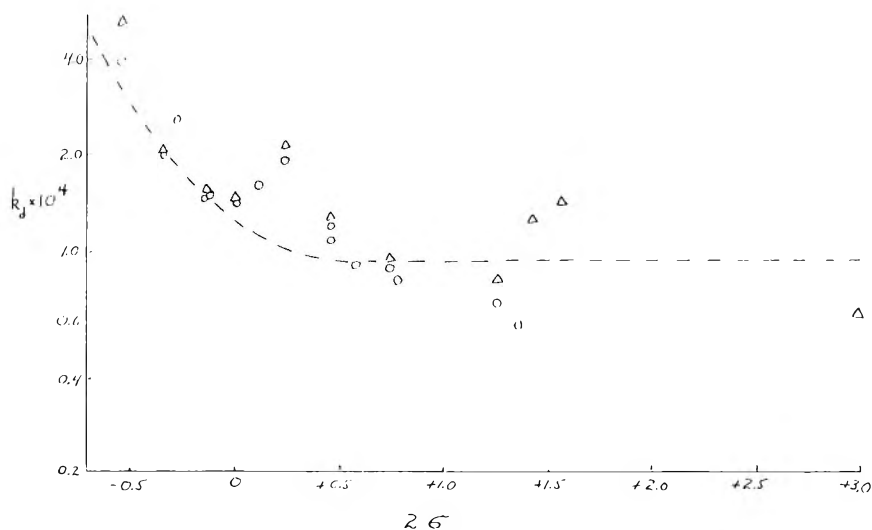
Fig. 10. Hammett plot of literature data for k_d at 90°C.: (- -) from Fig. 7 of this work; (O) data of Swain et al.;[4] (△) data of Blomquist and Buselli.[5]
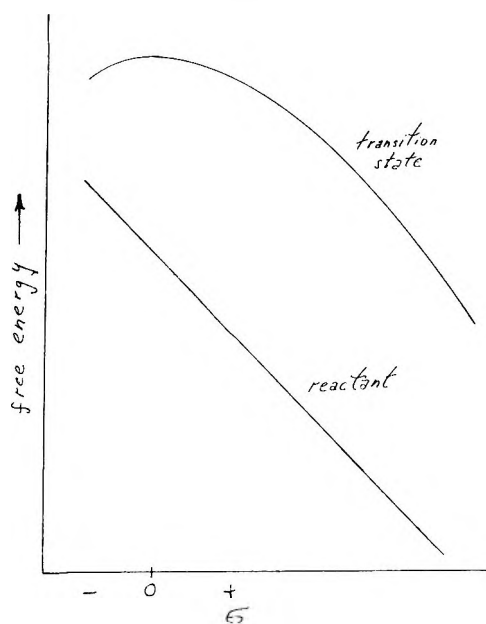
Fig. 11. Schematic of free energy dependencies on Hammett σ.

expected in the Hammett plot, since either $+ \sigma$ or $- \sigma$ substituents stabilize triphenylmethyl radicals in dissociation from hexaphenylethane,[15] as well as benzoate radicals from substituted benzoyl peroxides.[16] Since Swain et al. do not find a minimum in the Hammett plot, they conclude that radical stability is not a critical factor in determining k_d. Blomquist and

Buselli[5] did find a minimum in their Hammett plot, but it occurs at about $2\sigma = +0.8$ rather than at $\sigma = 0.0$ as would be expected if radical stability were a controlling factor. As a matter of interest, Figure 10 plots the data of both Swain et al.[4] and Blomquist and Buselli[5] along with the line derived for this study in Figure 7. An activation energy of 30 kcal./mole was used to extrapolate to 90°C. It is noted from Figure 10 that—considering solvent differences—the data agree fairly well, but interpretation is the point of disagreement.

We believe that both electrostatic repulsion at the O–O bond and radical stability determine k_d. Referring to Figure 11, we show a schematic plot of free energy of the reactant as a function of 2σ. At some large positive value of 2σ the charge on the peroxidic oxygen atoms would probably reverse sign with higher values contributing to a higher free energy through plus–plus repulsion as Swain suggests.[4] If the transition state is assumed to be quite similar to the products (radicals), which are stabilized by any substituent, we may also plot free energy of the transition state versus 2σ as shown in Figure 11. The free energy of activation, $\Delta F\ddagger$, is then the difference between the two curves. If, as shown, the two curves are approximately parallel in the positive σ region studied, $\Delta F\ddagger$ and k_d should become constant.

B. Induced Decomposition Rate Constant, k_i

The values of the rate constant k_x for chain transfer to catalyst, derived from this study are not sufficient to determine whether or not k_x follows a simple Hammett function, since k_i values could not be determined for substituents below p-Cl in σ value. However, the data of Nozaki and Bartlett[3] may be extrapolated to a value of $k_x/k_t^{1/2} = 1.07 \times 10^{-2}$ (l./mole/sec.)$^{1/2}$ with their activation energy of 25,230 cal./mole. Also, Baysal and Tobolsky[6] present a value of k_x/k_p at 60°C. By use of the relation

$$k_t = k_x(fk_d/k_i)^{1/2}$$

and activation energies of 33,300,[3] 25,230,[3] 2370,[10] and 7760[10] cal./mole for k_d, k_i, k_t, and k_p, respectively, an activation energy of 2 kcal./mole is calculated for k_x/k_p. Extrapolating Baysal and Tobolsky's value to 90°C. with this activation energy and multiplying[17] by $k_p/k_t^{1/2} = 7.45 \times 10^{-2}$ gives $k_x/k_t^{1/2} = 5 \times 10^{-3}$ (mole/l./sec.)$^{1/2}$.

These values are included in Figure 8, where it is seen that a case may be made for k_x obeying Hammett rules. Certainly, it seems likely that attack by a radical should be enhanced by removal of electron density from the area linking the two rings. Referring to change in 2σ, a reaction parameter ρ of $+1.72$ is calculated.

C. Initiator Efficiency, f

As derived earlier in the section dealing with theory, there is reason to expect that $\ln[(1-f)/f]$ might be a function of Hammett σ values. In-

deed, Figure 9 shows that (with the exception of p-chloro) a quite good plot is found. Alternately, using reasoning analogous to that in Figure 11, a case can be made for a constant value of ln $[(1 - f)/f]$ for 2σ values less than that of p-chloro and a steeper line for more positive 2σ values.

Little is available in the literature to aid a choice there. Bevington and Lewis[18] and Bevington, Toole, and Trossarelli[19] indicate the anisoyloxy radical to be more stable toward loss of carbon dioxide than is the benzoyloxy radical. The work was done by using C^{14}-labeled initiators (either in the ring or in the carbonyl carbon) and examining the polymer for radioactivity and molecular weight. Bevington has published a great deal of such work, and there are also articles by Dannley and Essig.[20] In general, the indication of finite chain transfer constants for the various benzoyl peroxides throws a question on interpretation of such work. The appearance of a benzoyloxy residue in the polymer does not indicate whether it was placed there by initiation or transfer. This is especially true of Dannley and Essig's work, in which high concentrations of initiators such as p-nitrobenzoyl peroxide were used.

In the work of Bevington and Lewis quoted above, however, it was shown that end groups in p-methoxybenzoyl peroxide-initiated polymers contained

O=C—O— to a greater degree than those in benzoyl peroxide-initiated polymers. Since this result is contrary to that which would be expected for chain transfer to catalyst, it seems logical to believe that anisoyl per-
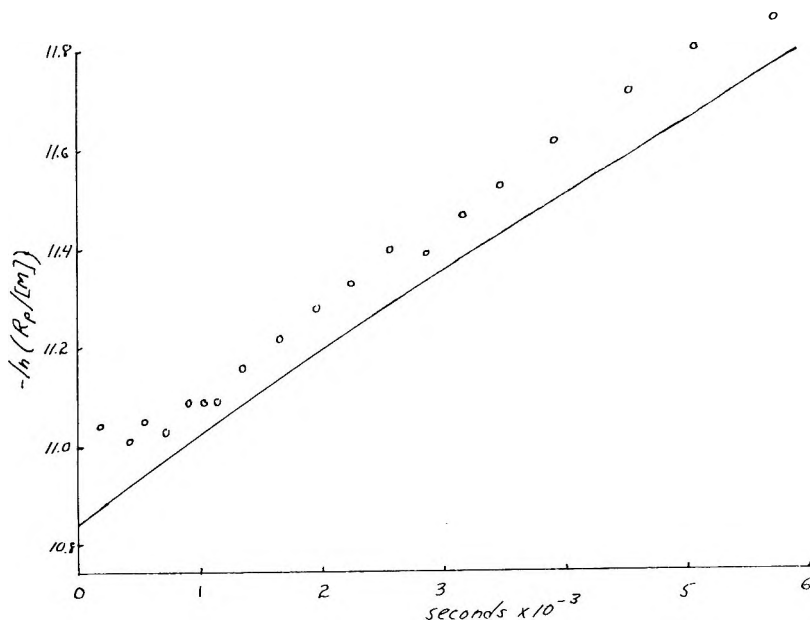
Fig. 12. Polymerization of styrene at 90°C. with a mixture of 1.46×10^{-4} mole/l. p-methoxy-benzoyl peroxide and 1.34×10^{-3} mole/l. p-nitro-benzoyl peroxide: (———) predicted; (O) observed.

oxide does have a higher efficiency than benzoyl peroxide. With this small outside aid, a single straight line is favored in Figure 9. Again referring to a change in 2σ, a ρ of $+0.54$ is calculated.

D. Prediction of Polymerization Rates

As a sort of "cumulative" test for the constants derived and the principles involved in this work, a FORTRAN program was written for an IBM 1620 to predict ln $(R_p/[M])$ as a function of time for a bulk styrene polymerization involving simultaneous use of two different initiators. Constant volume was assumed. Two runs (essentially duplicates) were made and calculated just as were all other runs. p-Nitro and p-methoxybenzoyl peroxides, the most divergent initiators available, were used in a ratio of concentration of approximately ten to one. The predicted and actual results of one of these runs corrected for thermal rate are shown in Figure 12. Agreement is good in slope but varies somewhat in level. The variation shown in level is equivalent to that which would be associated with about 10% change in the product of fk_d, well within the total experimental error of the various measurements. Any synergistic decomposition behavior between the two peroxides must be small or nonexistent.

References

1. Tobolsky, A. V., C. E. Rogers, and R. D. Brickman, *J. Am. Chem. Soc.*, **82**, 1277 (1960).

2. O'Driscoll, K. F., and P. J. White, *J. Polymer Sci.*, **B1**, 597 (1963).

3. Nozaki, K., and P. D. Bartlett, *J. Am. Chem. Soc.*, **68**, 1686 (1946).

4. C. G. Swain, W. H. Stockmayer, and J. T. Clarke, *J. Am. Chem. Soc.*, **72**, 5426 (1950).

5. Blomquist, A. T., and A. J. Buselli, *J. Am. Chem. Soc.*, **73**, 3883 (1951).

6. Baysal, B., and A. V. Tobolsky, *J. Polymer Sci.*, **8**, 529 (1952).

7. Bamford, C. H., A. D. Jenkins, and R. Johnston, *Trans. Faraday Soc.*, **55**, 1451 (1959).

8. Haward, R. N., and W. Simpson, *Trans. Faraday Soc.*, **47**, 212 (1951).

9. Patnode, W., and W. J. Scheiber, *J. Am. Chem. Soc.*, **61**, 3449 (1939).

10. Matheson, M. S., E. E. Auer, E. B. Bevilacqua, and E. S. Hart, *J. Am. Chem. Soc.*, **73**, 1700 (1951).

11. Price, C. C., and E. Krebs, *Org. Synthesis*, **23**, 65 (1943).

12. Vogel, A. I., *A Textbook of Practical Organic Chemistry*, 3rd Ed., Longmans, London (1961).

13. North, A., and G. Reed, *Trans. Faraday Soc.*, **57**, 859 (1961).

14. Jaffe, H. H., *Chem. Rev.*, **53**, 191 (1953).

15. Marvel, C. S., J. F. Kaplan, and C. M. Himer, *J. Am. Chem. Soc.*, **63**, 1892 (1941).

16. Wieland, H., and G. Rasuwajew, *Ann.*, **480**, 157 (1930).

17. Tobolsky, A. V., and J. Offenbach, *J. Polymer Sci.*, **16**, 311 (1955).

18. Bevington, J. C., and T. D. Lewis, *Trans. Faraday Soc.*, **54**, 1340 (1958).

19. Bevington, J. C., J. Toole, and L. Tosssarelli, *Trans. Faraday Soc.*, **54**, 863 (1958).

20. Dannley, R. L., and H. J. Essig, *J. Polymer Sci.*, **42**, 129 (1960).

Résumé

On a employé les peroxydes de benzoyle bisubstitués suivants, comme initiateurs de polymérisation du styrène en bloc à 90°C, le *p*-méthoxy, le *p*-méthyle, le peroxyde non-substitué, le *p*-chloro, le *m*-bromo, le 3,4-dichloro, le *p*-cyano et le *p*-nitro. On a obtenu, à partir des vitesses de polymérisation observées, les constantes de vitesse pour la décomposition unimoléculaire et les constantes de vitesse de décomposition induite des peroxydes par des radicaux ainsi que l'efficacité d'initiation de la polymérisation. On a observé que des substituants plus électro-capteurs que le *p*-chlore ne changent pas la constante de vitesse monomoléculaire. Au contraire, les substituants moins électro-donneurs que le *p*-chloro ont un faible effet sur l'efficacité d'initiation. La constante de vitesse de décomposition induite donne une relation d'Hammett simple et linéaire avec une pente positive.

Zusammenfassung

Die folgenden bis-substituierten Benzoylperoxyde wurden als Starter für die Polymerisation von Styrol in Substanz bei 90°C benützt: *p*-Methoxy-, *p*-Methyl-, unsubstituiertes, *p*-Chlor-, *m*-Brom-, 3,4-Dichlor-, *p*-Cyan- und *p*-Nitroperoxyd. Aus der beobachteten Polymerisationsgeschwindigkeit wurden die Geschwindigkeitskonstanten für die monomolekulare Zersetzung und für die radikalinduzierte Zersetzung des Peroxyds sowie auch die Starterausbeute für die Polymerisation erhalten. Stärker elektronenentziehende Substituenten als *p*-Chlor veränderten die monomolekulare Geschwindigkeitskonstante nicht. Umgekehrt hatten weniger elektronen-liefernde Substituenten als *p*-Chlor wenig Einfluss auf die Starterausbeute. Die Geschwindigkeitskonstante der induzierten Zersetzung ergab ein einfaches lineares Hammett-Diagramm mit positiver Neigung.

Rheo-optical Properties of Polymers.   VII.
On Time-Dependent Infrared Absorbance in Polymer Films

D. G. LeGRAND, *General Electric Research Laboratory, Schenectady, New York*

Synopsis

A theory is developed to show the use of infrared spectroscopy in the study of response of polymers to dynamic mechanical stress or strain.   Preliminary experimental results are presented.

Introduction

It is well known that polymer molecules are oriented when deformed by uniaxial extension.   It has been shown that the stress required to obtain this orientation is proportional to the change in the configurational entropy of all the molecular chains in the system and that subsequent relaxation of the stress at constant length for viscoelastic materials takes place by a diffusional relaxation of the configurations of the molecules.   Various optical techniques have been used to study these relaxation phenomena.[1,2] Most of these techniques are limited to measuring the average motion of very large cavities, e.g., birefringence of molecular chains.   In this note, we propose the use of infrared absorbency as a tool capable of measuring either the motion of very small parts of the molecular chains, for example, the orientational relaxation of —CH₂ groups in various polymers or structural isomerization changes, for example, helical to random coil configuration in polypropylene.   Some of these types of measurements have been carried out under static conditions.[3,4]

The theory proposed combines Mooney's theory of viscoelasticity with the theory proposed by Marrinan for infrared absorbency of rubberlike materials and complements Read's theory of dynamic birefringence.[5–7]

Theory: Linear Viscoelastic Polymer

Marrinan has shown that for a single chain, stretched along the external coordinate OX′ axis, that the absorption parallel to the stretching direction is given by

$$i_{OX'} = KZ \left\{ \left[\frac{1}{3} + \frac{2}{5} \left(\frac{h}{Za} \right)^2 \right] \pi_{11} + \left[\frac{2}{3} - \frac{2}{5} \left(\frac{h}{Za} \right)^2 \left(\frac{\pi_{22} + \pi_{33}}{2} \right) \right] \right\} \quad (1)$$

$$i_{OY'} = i_{OZ'} = KZ \left\{ \left[\frac{1}{3} - \frac{1}{5} \left(\frac{h}{Za} \right)^2 \right] \pi_{11} \right.$$

$$\left. + \left[\frac{2}{3} + \frac{1}{5} \left(\frac{h}{Za} \right)^2 \left(\frac{\pi_{22} + \pi_{33}}{2} \right) \right] \right\} \quad (2)$$

where K is a constant for a given vibration, Z is the number of links in a chain, a is the length of a link, h is the distance between the ends of a single chain, and the link is characterized by an absorption tensor π, whose components π_{ij} are referred to the $OX_1X_2X_3$ coordinate system where OX_1 lies along the link direction.

For a system containing N chains/unit volume stretched along the OX axis an amount λx, where λx is equal to the ratio of the extended length divided by the initial length, Marrinan obtains for radiation parallel to the extension axis

$$I_{OX} = KN \left[\frac{Z}{3} (\pi_{11} + \pi_{22} + \pi_{33}) + \frac{2}{15} \left(\pi_{11} - \frac{\pi_{22} + \pi_{33}}{2} \right) \left(\alpha_x^2 - \frac{1}{\alpha_x} \right) \right]$$

$$(3)$$

and

$$I_{OY} = I_{OZ} = KN \left[\frac{Z}{3} (\pi_{11} + \pi_{22} + \pi_{33}) \right.$$

$$\left. - \frac{1}{15} \left(\pi_{11} - \frac{\pi_{22} + \pi_{33}}{2} \right) \left(\alpha_x^2 - \frac{1}{\alpha_x} \right) \right] \quad (4)$$

In Mooney's theory, each polymer chain is arbitrarily divided into ν submolecules, long enough so that its end-to-end distance obeys Gaussian statistics and the motion of the polymer chains is described (with the aid of the normal coordinate method of analysis) as a sum of cooperative movements at the ends of the submolecule. For a system in which the configurations are not at equilibrium, relaxation to the equilibrium state will take place at rates dependent upon the mobility and length of the links involved. Following Read's usage of Mooney's theory of stress relaxation, it may be shown that eqs. (3) and (4) change to

$$I_{OX}(t) = KN \left[\frac{Z}{3} (\pi_{11} + \pi_{22} + \pi_{33}) \right.$$

$$\left. + \frac{2}{15} \left(\pi_{11} - \frac{\pi_{22} + \pi_{33}}{2} \right) \sum_{n=1}^{\nu} (B_{xn}^2 - B_{yn}^2) \right] \quad (5)$$

and $I_{OY}(t) = I_{OZ}(t)$

$$= KN \left[\frac{Z}{3} (\pi_{11} + \pi_{22} + \pi_{33}) \right.$$

$$\left. - \frac{1}{15} \left(\pi_{11} - \frac{\pi_{22} + \pi_{33}}{2} \right) \sum_{n=1}^{\nu} (B_x^2 - B_y^2) \right] \quad (6)$$

where B_{xn} and B_{yn} represent the time-dependent deformation along the normal coordinates.* From Mooney's theory it is found that

$$B_{xn}{}^2 - B_{yn}{}^2 = [\alpha_x{}^2 - (1/\alpha_x)]e^{-t/\tau_n} \tag{7}$$

where the relaxation time, τ_n, which characterizes the diffusion rate of the nth mode, is equal to $(4bD_n)^{-1}$. For ν chains,

$$\sum_{n=1}^{\nu} (B_x{}^2 - B_{yn}{}^2) = [\alpha_x{}^2 - (1/\alpha_x)] \sum_{n=1}^{\nu} e^{-t/\tau_n} \tag{8}$$

Thus, eqs. (5) and (6) give then

$$I_{\mathrm{OX}}(t) = KN\left[\frac{Z}{3}(\pi_{11} + \pi_{22} + \pi_{33})\right.$$

$$\left. + \frac{2}{15}\left(\pi_{11} - \frac{\pi_{22} + \pi_{33}}{2}\right)\left(\alpha_x{}^2 + \frac{1}{\alpha_x}\right)\sum_{n=1}^{\nu} e^{-t/\tau_n}\right] \tag{9}$$

and

$$I_{\mathrm{OY}}(t) = I_{\mathrm{OZ}}(t)$$

$$= KN\left[\frac{Z}{3}(\pi_{11} + \pi_{22} + \pi_{33}) - \frac{1}{15}\left(\pi_{11} - \frac{\pi_{22} + \pi_{33}}{2}\right)\left(\alpha_x{}^2 - \frac{1}{\alpha_x}\right)\right.$$

$$\left. \times \sum_{n=1}^{\nu} e^{-t/\tau_n}\right] \tag{10}$$

while for unpolarized radiation, we obtain

$$I_{u_n}(t) = \frac{1}{2}[I_{\mathrm{OX}}(t) + I_{\mathrm{OY}}(t)]$$

$$= \frac{KN}{2}\left[\frac{2}{3}Z(\pi_{11} + \pi_{22} + \pi_{33}) + \frac{1}{15}\right.$$

$$\left. \times \left(\pi_{11} - \frac{\pi_{22} + \pi_{33}}{2}\right)\left(\alpha_x{}^2 - \frac{1}{\alpha_x}\right)\sum_{n=1}^{\nu} e^{-t/\tau_n}\right] \tag{11}$$

The dichroic ratio is

$$D = I_{\mathrm{OY}}(t)/I_{\mathrm{OZ}}(t)$$

$$= \frac{\left[Z(\pi_{11} + \pi_{22} + \pi_{33}) + \frac{2}{5}\left(\pi_{11} - \frac{\pi_{22} + \pi_{33}}{2}\right)\left(\alpha_x{}^2 - \frac{1}{\alpha_x}\right)\sum_{n=1}^{\nu} e^{-t/\tau_n}\right]}{\left[Z(\pi_{11} + \pi_{22} + \pi_{33}) - \frac{1}{5}\left(\pi_{11} - \frac{\pi_{22} + \pi_{33}}{2}\right)\left(\alpha_x{}^2 - \frac{1}{\alpha_x}\right)\sum_{n=1}^{\nu} e^{-t/\tau_n}\right]}$$

$$\cong 1 + \frac{3}{5}\left[\frac{\left(\pi_{11} - \frac{\pi_{22} + \pi_{33}}{2}\right)\left(\alpha_x{}^2 - \frac{1}{\alpha_x}\right)\sum_{n=1}^{\nu} e^{-t/\tau_n}}{Z(\pi_{11} + \pi_{22} + \pi_{33})}\right] \tag{12}$$

* See Mooney[5] for further details.

where higher terms are negligible if α is not too large or n too small.[10]
Mooney's equation for stress relaxation is

$$\sigma = N_c kT \left(\alpha_x{}^2 - \frac{1}{\alpha_x}\right) \sum_{n=1}^{\nu} e^{-t/\tau_n} \tag{13}$$

where N_c is the number of chains per cubic centimeter, k is Boltzmann's
constant, T is the absolute temperature, and σ the stress. The ratio of eq.
(12) to eq. (13) gives

$$\frac{D-1}{\sigma} \cong \frac{3}{5} \frac{M_0 z}{\rho N_0 kT} \left[\frac{\pi_{11} - \left(\dfrac{\pi_{22} + \pi_{33}}{2}\right)}{\pi_{11} + \pi_{22} + \pi_{33}} \right] \tag{14}$$

where z is the number of monomers per segment. If α is the angle which
each transition moment p makes with each link direction, then the compo-
nents of the absorption tensor, π_{ii} will be given as

$$\pi_{11} = np^2\cos^2\alpha \tag{15}$$

where n is the number of repeat units/link and

$$\pi_{22} + \pi_{33} = np^2\sin^2\alpha \tag{16}$$

Therefore eq. (14) may be rewritten as

$$\frac{D-1}{\sigma} \cong \frac{3}{5} \frac{M_0 z}{\rho N_0 kT} \left[\cos^2\alpha - \frac{\sin^2\alpha}{2} \right] \tag{17}$$

For $\alpha = 90°$,

$$(D-1)/\sigma \cong 3M_0 z/10\rho N_0 kT \tag{18}$$

while for $\alpha = 0°$,

$$(D-1)/\sigma \cong 3M_0 z/5\rho N_0 kT \tag{19}$$

Thus, this ratio is not only time-independent, but provides a technique
for measuring the size of the relaxing segment.

Semicrystalline Polymers

For semicrystalline polymers, characteristic bands in the infrared as-
sociated with crystalline material are observed. Using polarized or un-
polarized radiation, it is possible to detect changes in orientation of these
crystalline bands, which occur as a result of deformation.[8,9] For poly-
ethylene, Stein has shown that for uniaxial deformation

$$A_{c_{720}(OX)} = K_c \cos^2\beta \tag{20}$$

and

$$A_{c_{730}(OX)} = K_c \cos^2\alpha \tag{21}$$

where K_c is a proportionality constant, and α and β are angles characterizing the angles between the stretching direction and the a and b axis of the unit cell, respectively.[10] Following the theory proposed by LeGrand[11] for dynamic birefringence of semicrystalline polymers, i.e.,

$$\overline{\cos^2\alpha} = Qe^{-t/\tau_a} \tag{22}$$

where τ_a is the relaxation time for rotation of crystals about the b and c axis while

$$\overline{\cos^2\beta} = Pe^{-t/\tau_b} \tag{23}$$

and τ_b is the relaxation time about the a and c axis, i.e.,

$$1/\tau_a = (1/\tau_b) + (1/\tau_c) \tag{24}$$

and

$$1/\tau_b = (1/\tau_a) + (1/\tau_c) \tag{25}$$

Thus,

$$A_{c_{720}(\text{OX})} = K_cQe^{-t/\tau_a} \tag{26}$$

while

$$A_{c_{730}(\text{OX})} = K_cPe^{-t/\tau_b} \tag{27}$$

Similarly, for perpendicular radiation,

$$A_{c_{720}}\perp = (K_c/2)\overline{\sin^2\alpha} = (K_c/2)(1 - Qe^{-t/\tau_a}) \tag{28}$$

$$A_{c_{730}}\perp = (K_c/2)\overline{\sin^2\beta} = (K_c/2)(1 - Pe^{-t/\tau_a}) \tag{29}$$

The dichroic ratios of these two bands are then

$$D_\perp = A_{c_{720}}||/A_{c_{720}}\perp = [Qe^{-t/\tau_a}/(1 - Qe^{-t/\tau_a})] \tag{30}$$

and

$$D_\perp = A_{c_{730}}||/A_{c_{730}}\perp = 2[P_e^{-t/\tau_b}/(1 - Pe^{-t/\tau_b})] \tag{31}$$

Thus, from such measurements, an independent measurement of the mobility of the crystalline material can be obtained.

Preliminary Experiments

A major difficulty in the use of infrared dichroism is the limited sensitivity at low degrees of orientation. Stein has suggested an alternate technique for increasing the sensitivity 100-fold for static measurements.[13] Our system is similar to Stein's wherein the difference between modulated signals is measured. The technique is as follows. A double-beam spectrometer is used with a vertical polarizer in one beam and a horizontal polarizer is employed in the second beam; the sample is stretched in the two beams by using a long enough sample. The difference output of the two beams is measured.
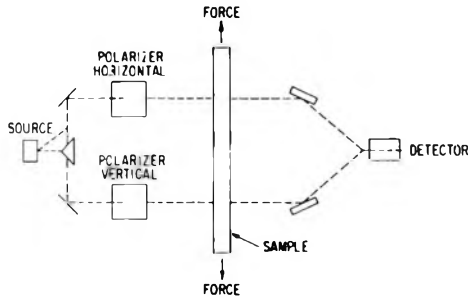
Fig. 1. Experimental setup.
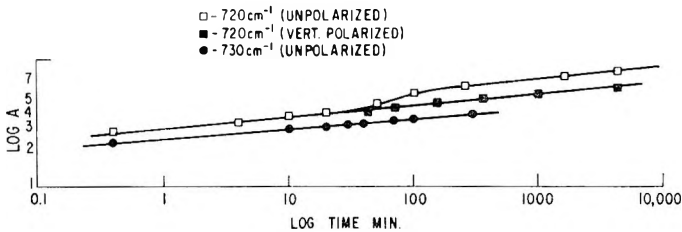
Fig. 2. Strain and infrared absorbance during creep for polyethylene.
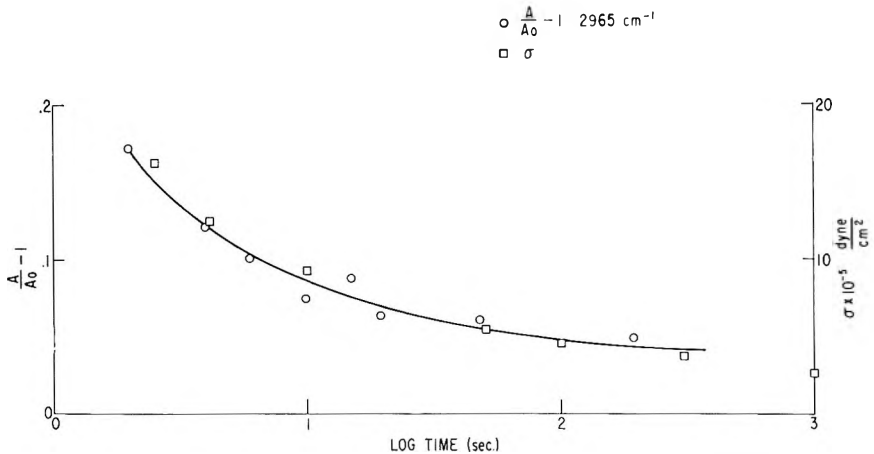
Fig. 3. Stress and infrared absorbance during relaxation for a phenyl methyl silicone polymer.

The system employed is shown in Figure 1. Under static conditions, the difference output is nulled by using the normal chopping signal of 13 cycles/sec., which is standard to most spectrometers. However, under dynamic conditions, this chopper is removed and replaced by the straining frequency. This technique is currently being put into operation.

In order to show other types of experiments which can be performed, we present preliminary data obtained in creep for polyethylene and in relaxation for a phenyl methyl silicone polymer in Figures 2 and 3.

The data in Figure 2 shows that the mechanism of orientation of the crystals occurs by a rotation about the a and b axes and the rate of rotations are not the same. In fact, rotation about the a axis occurs more rapidly than about the b axis, which supports previous data obtained from static measurements.[14]

The data for the phenyl methyl silicone includes data for stress relaxation as well as changes in absorbance. The similarity between infrared and stress relaxation data in Figure 3 is encouraging, since it suggests that this technique can be used to measure the size of the relaxing segment and as predicted from theory.

A more detailed report of this work will be presented later.

References

1. LeGrand, D. G., and P. F. Erhardt, *Trans. Soc. Rheol.*, **6,** 301 (1962).
2. LeGrand, D. G., and W. R. Haaf, *J. Polymer Sci.*, **C5**, 153 (1964).
3. Tobin, R. C., and M. J. Carrano, *J. Polymer Sci.*, **24,** 93 (1957).
4. Schmidtt, P. G., *J. Polymer Sci.*, **A1,** 1271, 2317 (1963).
5. Mooney, M., *J. Polymer Sci.*, **34,** 599 (1959).
6. Marrinan, H. J., *J. Polymer Sci.*, **39,** 461 (1960).
7. Read, B. E., *Polymer*, **3,** 143 (1962).
8. Caroti, G., and J. H. Dunesbury, *J. Polymer Sci.*, **22,** 399 (1956).
9. Dulmage, W. J., and A. L. Geddes, *J. Polymer Sci.*, **31,** 499 (1958).
10. Stein, R. S., *J. Polymer Sci.*, **31,** 327 (1958).
11. LeGrand, D. G., *J. Polymer Sci.*, in press.
12. Stein, R. S., *J. Polymer Sci.*, **28,** 83 (1958).
13. Stein, R. S., ONR Tech. Rept. #25, Cont. Nonr. 2151(00), Project NR 356–378, Aug. 27, 1960.
14. Hoshino, S., J. Powers, D. G. LeGrand, H. Kawai, and R. S. Stein, *J. Polymer Sci.*, **58,** 185 (1962).

Résumé

On a développé une théorie qui permet l'utilisation de la spectroscopie infra-rouge pour l'étude des propriétés mécaniques dynamiques des polymères On présente des résultats préliminaires.

Zusammenfassung

Eine Theorie wird entwickelt, die die Brauchbarkeit der Infrarotspektroskopie zur Untersuchung des Verhaltens von Polymeren unter dynamisch-mechanischer Spannung oder Verformung zeigt. Vorläufige Versuchsergebnisse werden vorgelegt.

An Infrared Structural Study of Fluorocarbon Polymers

HORACE F. WHITE,* *M. W. Kellogg Company, Jersey City, New Jersey*

Synopsis

The 3μ infrared spectra of copolymers of ethylene and 1,1-difluoroethylene with chlorotrifluoroethylene have been investigated. By applying "dilute solution" techniques, models for head-to-head and head-to-tail polymers have been prepared and spectrally characterized. The model spectra have been used to explain the polymerization of homopolymers and copolymers of halogenated ethylenes.

Introduction

The infrared spectra of copolymers of 1,1-difluoroethylene and chlorotrifluoroethylene exhibit only two peaks in the carbon–hydrogen stretching region over a wide range of copolymer compositions. The spectra of simple liquid hydrocarbons and polyethylene, on the other hand, consist of numerous bands in this region,[1,2] consistent with the complex vibrations occurring in these systems. The simple spectrum of each of the various copolymers investigated is explained as resulting from the two stretching motions[3] of the methylene group of isolated (noninteracting) 1,1-difluoroethylene units within the polymer chain, and the purpose of this study is to determine the particular orientation, if selective, of pairs of 1,1-difluoroethylene units in a copolymer chain of 1,1-difluoroethylene with chlorotrifluoroethylene.

Experimental

Investigations of the carbon–hydrogen fundamental stretching region of the various polymeric systems were made on a model 21 Perkin-Elmer spectrophotometer fitted with a rock salt prism. The spectra of these polymers also were investigated on a Perkin-Elmer model 112 spectrophotometer fitted with a calcium fluoride prism; no additional bands were found under higher resolution, thus confirming the lower resolution work.

The polymers were investigated as transparent films that ranged in thickness from 2 to 65 mils (thousandths of an inch). Polymeric films were prepared by pressing polymeric powder at 260°C. at a positive press pressure of approximately 20,000 psi for 3 min. The press was then released and the pressing immersed in water cooled to between 0–15°C. Pressing

temperature might vary slightly from polymer to polymer. In general
the films so produced showed no selective rotation to polarized light and
might be considered of random orientation.

Results and Discussion

Copolymerization of two monomers offers the possibility of producing
random or block copolymers; when one comonomer is present in consider-
ably lower concentrations than the other, however, the resulting copolymer
will be a random copolymer, if the reacting monomers polymerize at corre-
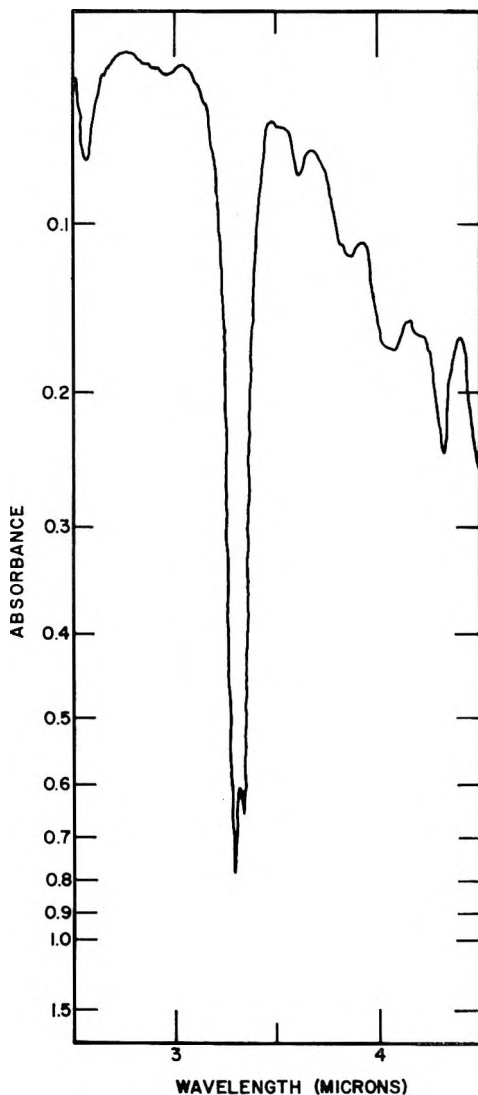
Fig. 1. Spectrum of 1,1-difluoroethylene in tetrafluoroethylene.
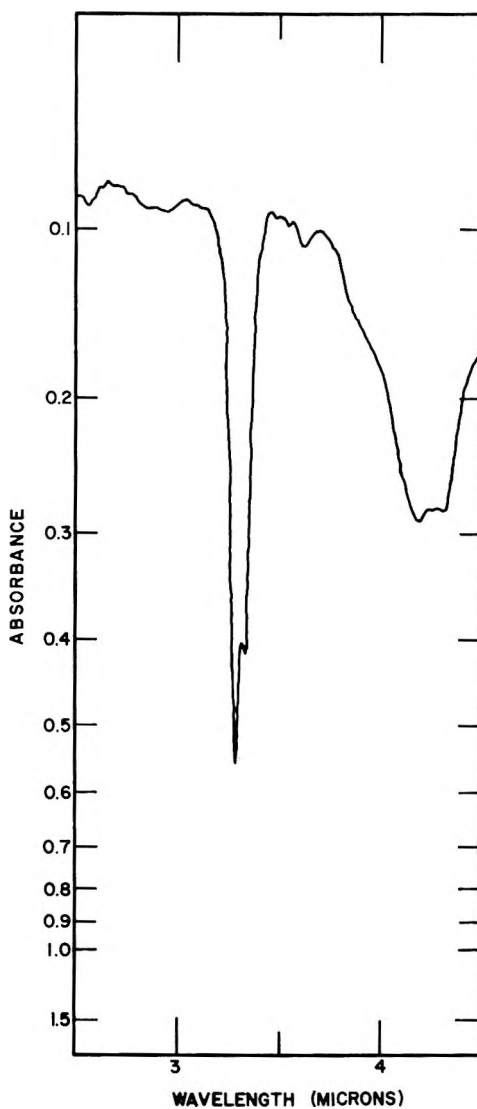
Fig. 2. Spectrum of 1-chloro-1-fluoroethylene in tetrafluoroethylene.

sponding polymerization rates. Because 1,1-difluoroethylene and chloro-trifluoroethylene have been found to have similar polymerization rates,[4] low concentrations of 1,1-difluoroethylene in the monomer mixture most probably will produce random copolymers. Two 1,1-difluoroethylene molecules can enter the polymer chain at adjacent positions in any one of three orientations, and Table I illustrates the various pair orientations of adjacent 1,1-difluoroethylene groups in the polymer chain. For this particular discussion the number of orientations is effectively reduced by one if the CF_2 group of 1,1-difluoroethylene affects the infrared spectrum of the CH_2

TABLE I
1,1-Difluoroethylene Molecule Pair Orientations[a]

Orientation	Type	Wavelength, μ
X—CH$_2$—CF$_2$—CH$_2$—CF$_2$—X	I	3.32, 3.36
X—CH$_2$—CF$_2$—CF$_2$—CH$_2$—X	II	3.32, 3.36
X—CF$_2$—CH$_2$—CH$_2$—CF$_2$—X	III	3.36, 3.48

[a] X is either —CF$_2$— or —CFCl—.
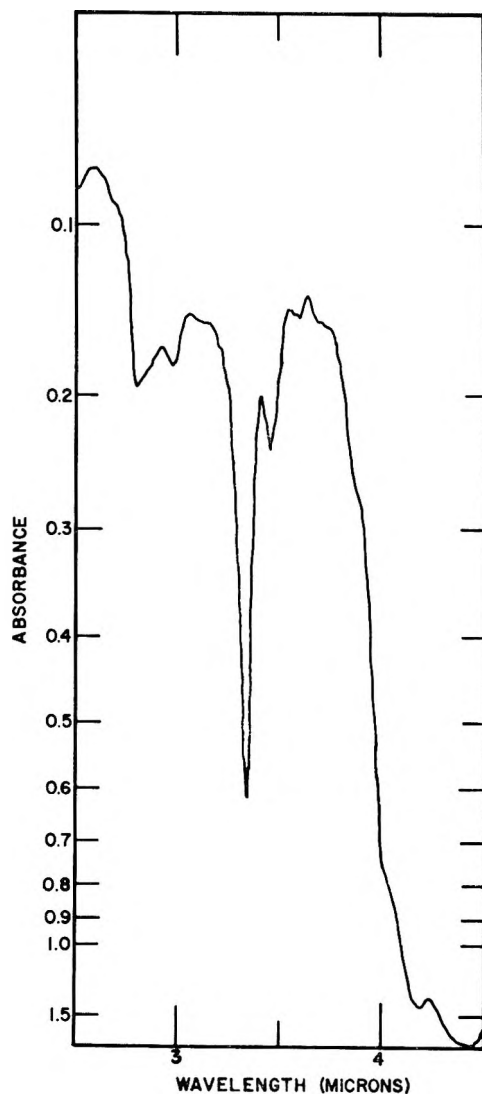
Fig. 3. Spectrum of 2.3% ethylene in chlorotrifluoroethylene.
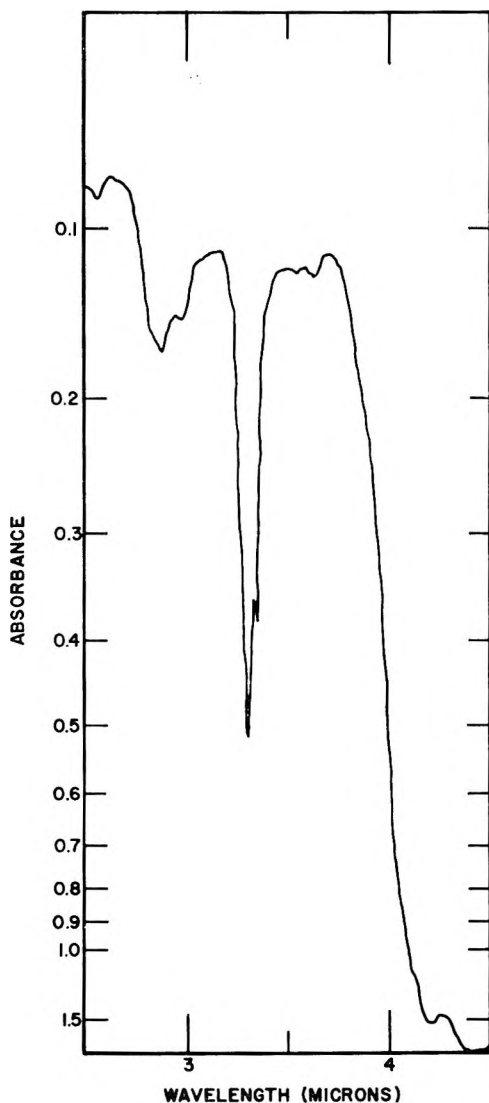
Fig. 4. Spectrum of 4% 1,1-difluoroethylene in chlorotrifluoroethylene.

group in a fashion analogous to the effect of the chlorotrifluoroethylene groups on the CH_2 group frequencies and if the $CFCl$ and CF_2 groups produce similar interactions with the CH_2 group.

In fact, the $3-\mu$ region of copolymers of 1,1-difluoroethylene and tetrafluoroethylene (Fig. 1) and 1-chloro-1-fluoroethylene and tetrafluoroethylene (Fig. 2) indicate that to a first approximation the perturbation to the —CH_2— group fundamental vibrations by the —$CFCl$— group is equivalent to the perturbation by the —CF_2— groups. To a first approximation, then, the spectra at 3μ of orientations I and II above are identical.

Studies of mixed crystals[5,6] have shown that the unperturbed molecular vibration frequency is most nearly observed when the molecular concentration approaches zero. This type of argument is extended to molec-
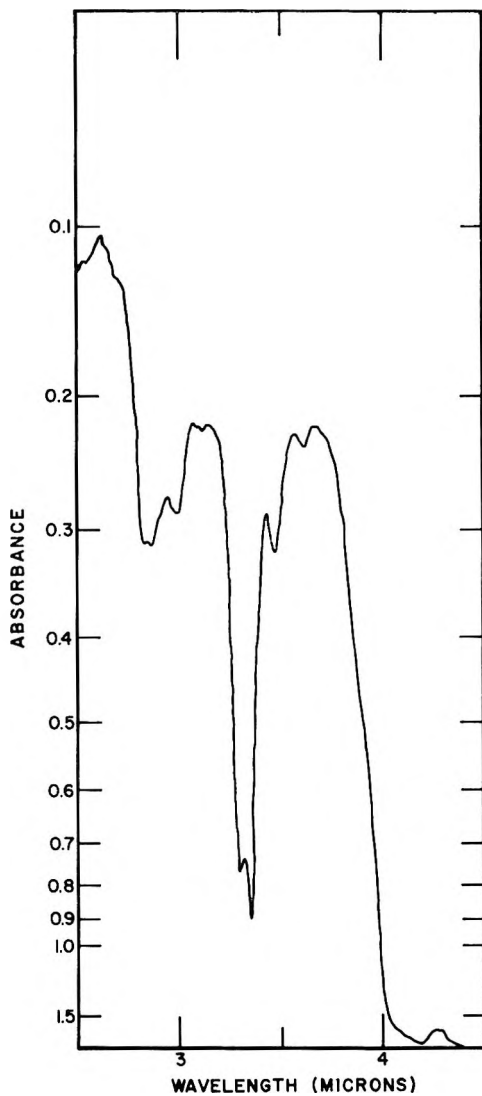
Fig. 5. Instrumental resultant spectrum of orientations, type I and III.

ular groups of polymeric materials derived from halogenated ethylenes. A dilute solution model for the type III orientation was prepared by copolymerizing ethylene and chlorotrifluoroethylene at very low concentrations of ethylene. It was hoped that by keeping the ethylene concentration low only isolated ethylene molecules would result in the polymer, and

the spectrum of an isolated unit of linear polyethylene would arise yielding the typical "in phase" and "out-of-phase" hydrogen vibrations at 3.42 and 3.50 μ.[7] In the polymers produced, bands near these wavelengths were found even down to the 0.7 mole-% ethylene composition level. It is felt that these materials represent the type III orientation in which a single —CH_2— group has one —CH_2— group nearest neighbor. The spectrum of the 2.3 mole-% ethylene in chlorotrifluoroethylene is given in Figure 3 as typical of this structure.

Varying concentration of 1,1-difluoroethylene in chlorotrifluoroethylene produced a carbon–hydrogen spectrum differing from that of ethylene in chlorotrifluoroethylene but invariant in the composition range 0.5–7.0 mole-% 1,1-difluoroethylene in chlorotrifluoroethylene. The spectrum of the 4 mole-% 1,1-difluoroethylene copolymer is given in Figure 4 as typical of the type I orientation which represents a single —CH_2— group in the polymer chain with no —CH_2— group nearest neighbors. Figure 5 shows the instrumental resultant spectrum formed by superimposing two copolymer films—typical orientations type I and III—at the spectrometer slit. Table I also lists the hydrogen–carbon frequencies of the type I and III orientations.

From this study and an investigation of the spectra, it can be concluded that this polymerization produced material of orientation type I (head-to-tail) or type II when the following systems are polymerized: 1,1-difluoroethylene and 1-chloro-1-fluoroethylene as homopolymers, and copolymers of 1,1-difluoroethylene with chlorotrifluoroethylene and 1,1-difluoroethylene with tetrafluoroethylene. Essentially no type III (head-to-head) polymerization is found.

The structural data presented could be greatly refined by using modern NMR techniques and data analysis similar to those used by Wilson[8] on poly(vinylidene fluoride).

References

1. Sheppard, N., and D. M. Simpson, *Quart. Rev.*, **7**, 19 (1953).

2. Rugg, F. M., J. J. Smith, and L. H. Wartman, *Ann. N. Y. Acad. Sci.*, **57**, 398 (1953).

3. Bellamy, L. J., *The Infra-Red Spectra of Complex Molecules*, Methuen, London, 1958; Wiley, New York; p. 15.

4. Bolstad, A. N., private communication.

5. Hrostowski, H. J., and G. C. Pimentel, *J. Chem. Phys.*, **19**, 661 (1952).

6. Heibert, G. L., and D. F. Hornig, *J. Chem. Phys.*, **20**, 918 (1953).

7. Fox, J. J., and A. E. Martin, *Proc. Roy. Soc. (London)*, **A175**, 208 (1940).

8. Wilson, C. W., III, *J. Polymer Sci.*, **A1**, 1305 (1963).

Résumé

On a étudié les spectres infra-rouges à 3μ de copolymères d'éthylène et de 1,1-difluoroéthylène avec le chlorotrifluoroéthylène. En appliquant les techniques des "solutions diluées," on a préparé les modèles pour des polymères "tête-à-tête" et "tête-à-queu," et on les a caractérisés spectrographiquement. Ces spectres modèles sont employés pour expliquer la polymérisation de homopolymères et de copolymères d'éthylènes halogénés.

Zusammenfassung

Die Infrarotspektren von Kopolymeren von Äthylen und 1,1-Difluoräthylen mit Chlortrifluoräthylen wurden im Drei-Mikron-Wellenlängenbereich untersucht. Mit dem "Verdünnte-Lösung"-Verfahren wurden Modelle für die "Kopf-Kopf"- und "Kopf-Schwanz"-Polymeren dargestellt und spektrometrisch charakterisiert. Die Modellspektren wurden zur Erklärung der Polymerisation von Homopolymeren und Kopolymeren und Kopolymeren von halogenierten Äthylenen verwendet.

Crystal Structure of the γ-Form of Nylon 6*

H. ARIMOTO, M. ISHIBASHI, and M. HIRAI, *Research Institute, Nippon Rayon Company, Ltd., Uji, Kyoto, Japan,* and Y. CHATANI,† *Department of Polymer Science, Faculty of Science, Osaka University, Nakanoshima, Osaka, Japan*

Synopsis

The crystal structure of the γ-form of nylon 6 (polycaproamide) obtained by the iodine treatment of the α-form of nylon 6 has been determined by x-ray diffraction. The unit cell contains four repeating units [—CH₂—₅CONH—] and is monoclinic with $a = 9.33$ A., $b = 16.88$ A. (fiber axis), $c = 4.78$ A., $\beta = 121°$. The space group is $P2_1/a$. There is considerable deviation from the planar configuration in the amide group of the chain. The plane of the CH₂ chain zigzag lies nearly parallel to the (001) plane. The crystal is composed of the pleated sheets of the parallel chains joined by hydrogen bond between the adjacent chains. The chain directions are opposite in alternating sheets. The hydrogen-bond length is 2.83 A., a reasonable figure for an NH···O chains joined by a hydrogen bond between the adjacent chains. The direction of the hydrogen bond makes an angle of 12° with the (100) plane, and the C=O and NH bonds are nearly colinear. The amide groups lie at the same level in the cell.

INTRODUCTION

The crystal structures of nylon 6 (polycaproamide) have been studied by several authors.[1–6] The usual α-form of nylon 6 is easily converted into a new crystal form when treated with an aqueous iodine–potassium iodide solution and with an aqueous sodium thiosulfate solution.[7–9]

Kinoshita[9] has shown that ordinary polyamides with odd numbers of CH₂ groups exhibit a new crystal form which has a somewhat similar configuration to the pleated-sheet structure proposed by Corey and Pauling[10] for the structure of polypeptide. This new crystal form of polyamides inclusive of the iodine-treated nylon 6 was named the γ-form by Kinoshita.[9] He has determined the crystal structure of nylon 77 (polyheptamethylene pimelamide) as an example of the γ-form[11] and he has suggested that the crystal repeating unit is twice the monomeric unit and the space group is $P2_1$ for the γ-form of polyamides from ω-amino acids with odd numbers of CH₂ groups.[9]

One of the authors[12] has previously shown that the amide plane is distorted from the plane of the zigzag CH₂ chain and on the basis of infrared

---

† Present address: Department of Chemistry, Duke University, Durham, North Carolina.

measurements proposed a model of the γ-form of nylon 6. The present paper concerns the x-ray analysis of the crystal structure of the γ-form of nylon 6.

EXPERIMENTAL

Materials

Samples were prepared as follows. A uniaxially oriented specimen was prepared from an extruded and quenched nylon 6 bristle (about 3.6 mm. in diameter) by drawing to 3.5 times and annealing at 135°C. A doubly oriented specimen was obtained from uniaxially oriented specimen by rolling at 130°C. and annealing at 135°C., the direction of rolling being the same as that of drawing. These specimens were treated with 1.23 N iodine–potassium iodide aqueous solution for a week. The absorbed iodine was removed by sodium thiosulfate.

X-Ray Measurements

X-ray diffraction patterns of the specimens were obtained with use of nickel-filtered CuK$_\alpha$ radiation. Flat-plate and cylindrical cameras were used. Figures 1 and 2 show x-ray photographs of the untreated (the α-form) and the iodine-treated (the γ-form) specimens, respectively.

Intensities were estimated visually by using standard intensity scales. A Weissenberg camera was used for measuring the reflection intensities of planes normal to the fiber axis. The doubly oriented specimen was not suitable for intensity measurement but was useful in confirming the unit cell. Lorentz and polarization corrections were made. Corrections for spot shape were made by measuring areas of the spots.
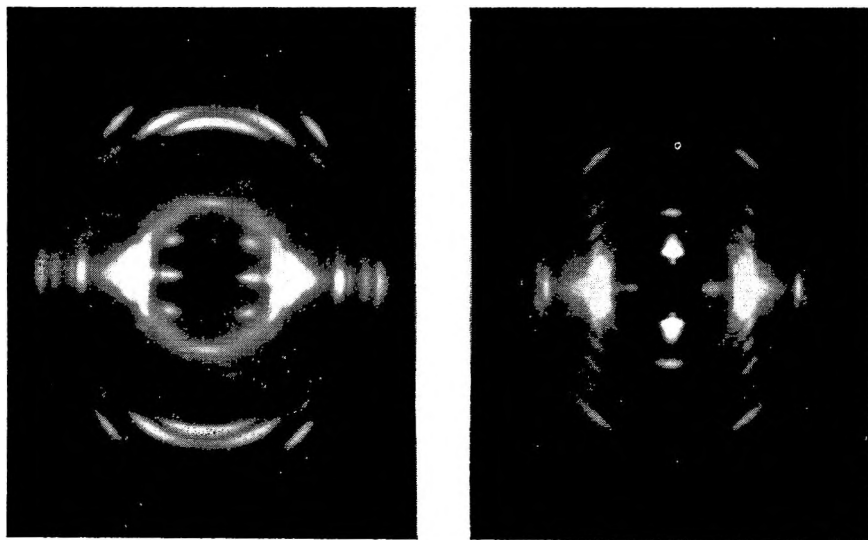
Fig. 1 (left). X-ray diffraction photograph of the α-form of nylon 6.
Fig. 2 (right). X-ray diffraction photograph of the γ-form of nylon 6.

The identity period was determined from an oscillation photograph taken with the fiber axis horizontal.

The lateral dimensions of the unit cell were obtained from photographs of the uniaxially oriented and the doubly oriented specimens.

DETERMINATION OF UNIT CELL AND STRUCTURE

The x-ray diffraction pattern of the doubly oriented γ-form specimen of nylon 6 taken with the beam parallel to the direction of drawing and the corresponding reciprocal lattice net are illustrated in Figure 3.

The unit cell is monoclinic with four $|$ $+CH_2+_5CONH|$ repeating units. The unit cell dimensions are: $a = 9.33$ A., $b = 16.88$ A. (fiber axis), $c = 4.78$ A., $\beta = 121°$.

The assumption of four repeating units per unit cell leads to a calculated density of 1.17 g./cc., which seems reasonable compared with the measured density (by the flotation method) of 1.14 g./cc.

There was no systematic absence on the photographs of the uniaxially or the doubly oriented specimen for the (hkl) reflections with no zero index. The reflections $(0k0)$ for k odd are absent. The space group may be therefore $P2_1$, $P2_1/m$, or $P2_1/a$. The presence of the twofold screw axis is expected in view of the geometry of the polymer chain. The form of the chain having a mirror plane perpendicular to the chain axis should not be allowed as a possible configuration, therefore the space group is limited to be either $P2_1$ or $P2_1/a$. The $(1k1)$ reflections are apparently recognized, although the intensities of the spots for $k = 3, 5, 7$ are very weak. The photograph taken with crystal-monochromatized CuK$_\alpha$ radiation reveals that the appearance of the $(11\bar{1})$ reflection, which is located near the strongest equatorial spot, is not due to the diffraction of white radiation in the
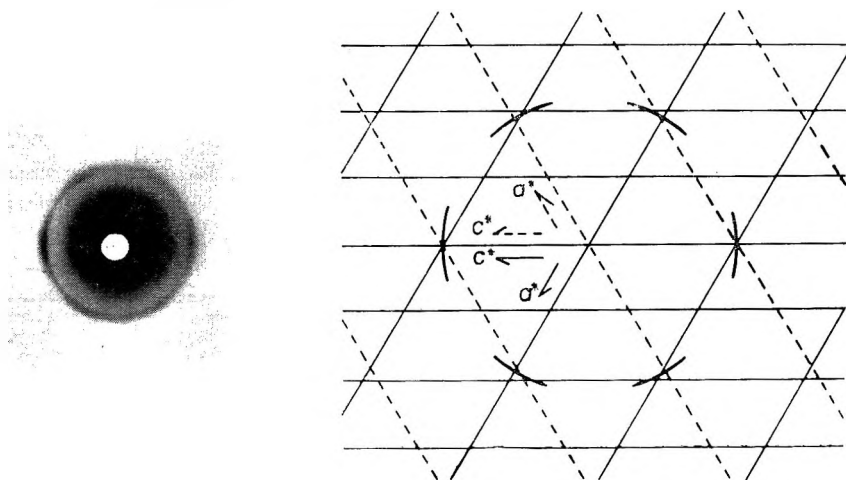
Fig. 3. Flat-plate x-ray diffraction photograph of the doubly oriented γ-form specimen of nylon 6 taken with the beam parallel to the direction of drawing and the corresponding reciprocal lattice net.
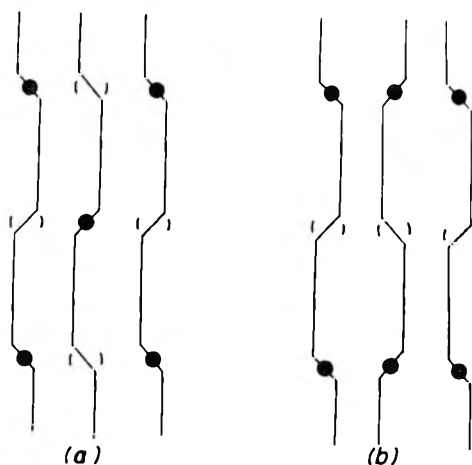
Fig. 4. Stacking of pleated hydrogen-bonded molecular sheets in (a) model I and (b) model II. The filled circles (●) denote a forward array of oxygen atoms; the parentheses ( ) denotes a backward array of oxygen atoms.

x-ray beams. Moreover, it is observed that the intensity ratio of the (111) reflection to the other is constant in every photograph, and that the strongest $\binom{0\ 0\ 2}{2\ 0\ 2}$ reflection in the α-form does not appear anywhere. In addition to these results, Ōta, Yoshizaki, and Nagai[13] have recently shown by a tilt method that the (111) reflection is not the equatorial but a layer reflection. These results confirm that the (111) reflection really originates from the γ-form of nylon 6. The presence of the $(1\bar{k}1)$ reflections shows the space group to be $P2_1/a$.

The crystal structure which has the space group $P2_1/a$ was confirmed by the intensity calculation. Based on the space group $P2_1/a$, the structure is fully described by a determination of the atomic coordinates of one asymmetric unit, half the chain repeat.

The intensity calculation was made with the use of trial-and-error method. First, structure factors of the (h0l) reflections were calculated. The identity period 16.88 A. for the γ-form suggests that the polymer chain is distorted from the fully extended zigzag chain for the α-form. From the polarized microinfrared measurement on doubly oriented specimens of the γ-form of nylon 6, it was found that the plane of the amide group is preferentially twisted in a direction roughly perpendicular to the rolled plane, but the plane of the CH_2 zigzag chain is almost parallel to the rolled plane in the γ-form.[12] Hence, the calculation was carried out by changing an angle between the CH_2 zigzag plane and the (100) plane, and an angle of the rotation around of the C—C′ and C—N single bond in the C—C′ONH—C group. Standard bond angles and bond distances were used. The angles which gave the best result were found to be 60° for the angle between the CH_2 zigzag plane and (100) plane, and to be 67° for the angle of rotation around of the C—C′ and C—N single bond in the C—C′ONH—C group from the *trans* position of the next bond taken as an origin of reference.

Structure factor calculation was carried out by using the atomic scatter-
ing of C, O, and N for all reflections except for the (0k0) reflections.   For
the (0k0) reflections, the atomic scattering of C, O, N, and H was used in the
calculation.   The values of the atomic scattering factors are those of Berg-
huis et al.[14] for C, N, and O, and that of McWeeny[15] for H.

Second, the determination of y parameters for each atom was made from
the (0k0) intensity calculation.   When the oxygen atom is located at $y =$
-0.016 (model I) or $y = 0.234$ (model II), a satisfactory agreement between
observed and calculated intensities is obtained for the (0k0).   Models I
and II correspond with the structures shown in Figures 4a and 4b, respec-
tively.   On the basis of comparison with observed and calculated intensities
of the (hkl) reflections, model I was accepted.

Introduction of an asymmetric temperature factor led to a good agree-
ment between observed and calculated intensities.   The anisotropy of the
thermal factor used in the final intensity calculations is expressed by

$$\exp - \frac{1}{4} \left\{ B_\perp [(h^2/a^2) + (l^2/c^2) + (2hl/ac) \cos \beta] + B_\parallel (k^2/b^2) \right\}$$

where $B_\perp$ and $B_\parallel$ are, respectively, the thermal factors in the directions
perpendicular and parallel to the b axis (fiber axis).   The appropriate
thermal factors were found to be $B_\perp = 7$ A.^{2} and $B_\parallel = 2$ A.^{2} The atomic

TABLE I
Atomic Coordinates

Atom	X/a	Y/b	Z/c
C_1	$+0.290$	$+0.169$	$+0.116$
C_2	$+0.390$	$+0.097$	$+0.108$
N	$+0.306$	$+0.022$	$+0.114$
O	$+0.236$	-0.016	-0.394
C_3	$+0.236$	-0.029	-0.138
C_4	$+0.153$	-0.103	-0.105
C_5	$+0.236$	-0.181	-0.109
C_6	$+0.134$	-0.251	-0.105

TABLE II
Interatomic Distances and Bond Angles[a]

Atoms	Interatomic distance, A.	Angle	Magnitude
C_1—C_2	1.53	$\angle C_1C_2N$	$110°$
C_2—N	1.50	$\angle C_2NC_3$	$124°$
N—C_3	1.34	$\angle NC_3O$	$119°$
C_3—O	1.24	$\angle NC_3C_4$	$118°$
C_3—C_4	1.52	$\angle C_3C_4C_5$	$115°$
C_4—C_5	1.53	$\angle C_4C_5C_6$	$111°$
C_5—C_6	1.52	$\angle C_5C_6C_1'$	$112°$
C_6—C_1'	1.54	$\angle C_6C_1'C_2'$	$115°$

[a] Hydrogen-bonded distance 2.83 A.

TABLE III
Comparison of Observed and Calculated Intensities (Arbitrary Scale)

hkl	$I_{obs.}$	$I_{calc.}$		hkl	$I_{obs.}$	$I_{calc.}$	
001			176	041			2
20$\bar{1}$	690	690	227	24$\bar{1}$	26	26	0
200			287	240			24
20$\bar{2}$	41	37					
002	10	7	2	15$\bar{1}$	4	4	
40$\bar{2}$			5	051			6
20$\bar{3}$			1	25$\bar{1}$	18	12	0
40$\bar{3}$			5	250			6
202			2	061			1
401	10	10	2	26$\bar{1}$	40	38	0
60$\bar{1}$			0	260			37
60$\bar{2}$			0	16$\bar{2}$			0
11$\bar{1}$	20	25		36$\bar{2}$	10	9	1
011			59	46$\bar{1}$			7
21$\bar{1}$	120	126	2	261			1
210			65	460	8	9	
11$\bar{2}$			3	071			4
31$\bar{2}$	14	23	1	27$\bar{1}$	25	34	28
41$\bar{1}$			2	270			2
211			17				
012	10	13	13	020	86	87	
41$\bar{2}$			0	040	35	33	
021			5	060	15	12	
22$\bar{1}$	30	35	1	080	6	6	
220			29	0100	4	3	
13$\bar{1}$	8	7		0120	4	3	
031			17	0140	6	5	
23$\bar{1}$	20	26	0				
230			9				
13$\bar{2}$			3				
33$\bar{2}$	6	8	2				
43$\bar{1}$			0				
231			3				

coordinates are presented in Table I. Interatomic distances and bond angles in the final intensity calculation are given in Table II.

The observed and calculated intensities of the reflections are given in Table III. The intensity calculation was performed over a wide range of index but only the reflections where an intensity is measured are listed in Table III.

The factor

$$R' = \frac{\Sigma |I_{obs.} - I_{calc.}|}{\Sigma I_{obs.}}$$

for these reflections has the value 0.167. Note that R' is based on the whole calculated intensities and not on structure factors.

DISCUSSION

Holmes, Bunn, and Smith[6] have shown that the structure of the α-form of nylon 6 is composed of the sheets of fully extended planar chains joined by the hydrogen bonds between the antiparallel chains. Figures 5a and 5b are given to facilitate the chain directions in the hydrogen-bonded sheets of the α-form and of the γ-form of nylon 6. As shown in Figure 5b, the γ-form crystal is composed of sheets of parallel chains joined by hydrogen bonds between the adjacent chains. The chain directions are opposite in alternating sheets. The reversible α–γ transition of nylon 6 suggests that the antiparallel chains pass through the cell of the γ-form. A doubly oriented specimen of the α-form of nylon 6 could be converted into a doubly oriented specimen of the γ-form by iodine treatment. This result also supports the above suggestion.
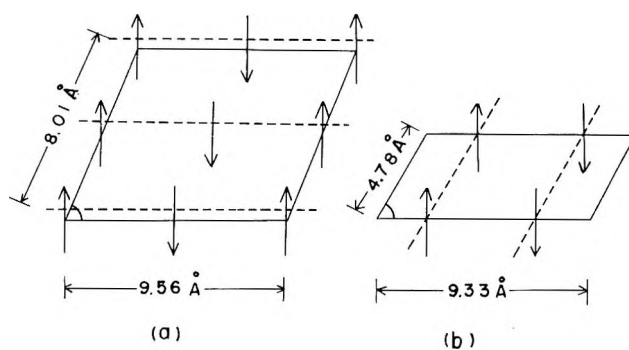
Fig. 5. The chain directions in the unit cell of (a) the α-form of nylon 6 and (b) the γ-form of nylon 6.
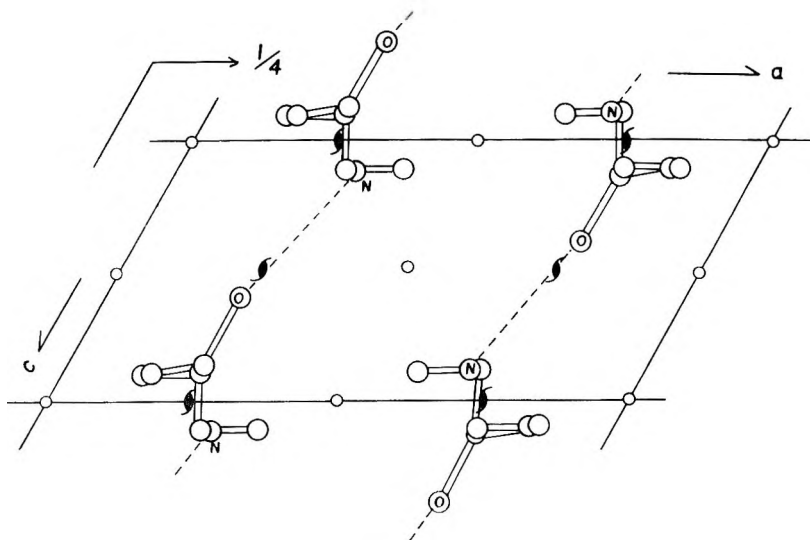
Fig. 6. Arrangement of the γ-form of nylon 6 molecules in the b-projection. The lower half of the chains was omitted.
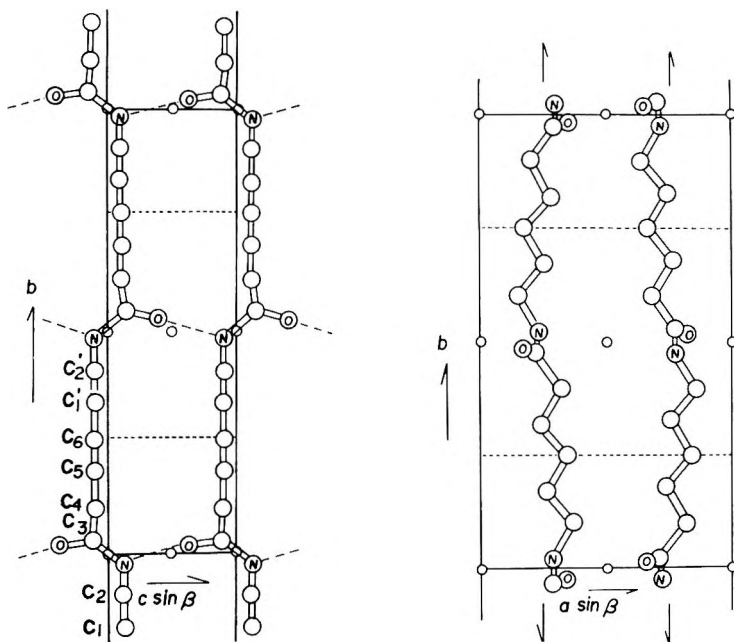
Fig. 7 (left). Arrangement of the γ-form of nylon 6 molecules in the a-projection.
Fig. 8 (right). Arrangement of the γ-form of nylon 6 molecules in the c-projection.

Figures 6–8 all represent the structure of the γ-form of nylon 6. The plane of the CH_2 zigzag chain lies nearly parallel to the (00$1$) plane.

The hydrogen-bond length is 2.83 A., a reasonable figure for an NH....O bond. It makes angle of 12° with the ($1$00) plane, and the C=O and N–H bonds are nearly colinear. Adjacent molecules in the direction of the a axis are spaced at 4.66 A., which is satisfactory with the Van der Waal's contact radii of chain atoms. The amide groups lie at the same level in the cell. Hence, the hydrogen-bonded sheets pack together in such a way that charged groups are gathered at the same level.

In the crystal of the α-form the hydrogen-bonded sheets pack together with (3/14) b staggered shear to give a uniform distribution of the charged group.[6] How the dipole–dipole repulsive force is cancelled in the structure of the γ-form of nylon 6 is an open question. This is also still a question in the structure of the γ-form of nylon 77.[11] It is probable that the pleated sheet structure makes possible such a packing of sheets.

It is a common feature in the crystals of the γ-form of polyamides that the angle of the internal rotation of the amide group is roughly 60° from the position of the fully extended planar position and that the pleated sheet structure is formed to maintain complete hydrogen bonding between adjacent molecules.

The pseudo-hexagonal structures in nylon 6 have been studied by many workers. One of these was the mesomorphous structure such as that obtained by rapid cooling from a melt or by high-speed melt spinning of nylon

6 proposed by Sandeman and Keller,[16] Tsuruta, Arimoto, and Ishibashi,[8] and Ziabicki.[17] This structure is easily converted into the usual α-form by annealing. Another structure, the γ-form, is stable against annealing and can be converted to the usual α-form only by treatments such as melting, drawing, or phenol treatment which destroy the hydrogen bonds. Usually nylon 6 is obtained in the α-form, but nylon 8 exhibits a crystal structure similar to that of the γ-form of nylon 6.[9,18,19] The γ-form of nylon 8 is converted into the α-form by drawing.[19] These phenomena suggest that the choice of the crystal form (the α- or the γ-form) in the even polyamides depends on the chain repeat length and that the polyamides with the longer repeat unit have the greater tendency to assume the γ-form. This tendency probably relates to the reduction of stress or steric hindrance caused by the rotation of the amide group around the C—CO and C—NH single bonds to form a hydrogen bond between the adjacent parallel chains instead of the adjacent antiparallel chains. Because every chain has statistically an equal chance to meet a parallel adjacent chain and an antiparallel one, if conditions are favorable for the formation of the hydrogen bond between the parallel chains, it would be expected that nylon 6 crystallize in the γ-form.

After completion of the present study, two papers concerning the crystal structure of the γ-form of nylon 6 obtained by iodine treatment have been published. Vogelsong[20] has proposed another unit cell with one molecule passing through it. However the existence of the $(1\bar{k}1)$ spots mentioned in the present study leads to a unit cell with two molecules passing through it. The reversible α–γ transition of nylon 6 cannot be explained in terms of a structure which has the unit cell with only one chain passing through it.

Bradbury and Elliot[21] have reported results of infrared measurements of the γ-form of nylon 6. Their data support strongly the conclusion in the present study. They have also proposed in their additional note that the structure has a body-centered orthorhombic symmetry and that the packing of chain molecules is closely similar to the structure in the present study. The unit cell in the present study could almost be translated to their cell. However, in the present study it was not found from the x-ray pattern that there is so good symmetry as to assume an orthorhombic cell.

References

1. Brill, R., Z. Physik. Chem., B53, 61 (1943).
2. Broser, V. W., K. Goldstein, and H. E. Krüger, Kolloid Z., 106, 187 (1944).
3. Wallner, L. G., Monatsh. Chem., 79, 279 (1948).
4. Kordes, E., F. Günther, L. Büchs, and W. Göttner, Kolloid Z., 119, 23 (1950).
5. Okada, A., and K. Fuchino, Kobunshi Kagaku, 7, 122 (1950).
6. Holmes, D. R., C. W. Bunn, and D. J. Smith, J. Polymer Sci., 17, 159 (1955).
7. Ueda, S., and T. Kimura, Kobunshi Kagaku, 15, 234 (1958).
8. Tsuruta, M., H. Arimoto, and M. Ishibashi, Kobunshi Kagaku, 15, 619 (1958).

9. Kinoshita, Y., *Makromol. Chem.*, **33**, 1 (1959).

10. Corey, R. B., and L. Pauling, *Proc. Roy. Soc. (London)*, **B141**, 10 (1953).

11. Kinoshita, Y., *Makromol. Chem.*, **33**, 21 (1959).

12. Arimoto, H., *J. Polymer Sci.*, **A2**, 2283 (1964).

13. Ōta, T., O. Yoshizaki, and E. Nagai, paper presented at the 11th Annual Meeting of the Society Polymer Science, Japan, May 1962.

14. Berghuis, J., J. M. Haanappel, M. Potters, B. O. Loopstra, C. H. MacGillavry, and A. L. Veenendall, *Acta Cryst.*, **8**, 478 (1955).

15. McWeeny, R., *Acta Cryst.*, **4**, 513 (1951).

16. Sandeman, I., and A. Keller, *J. Polymer Sci.*, **19**, 401 (1956).

17. Ziabicki, A., *Kolloid-Z.*, **167**, 132 (1960).

18. Slichter, W. P., *J. Polymer Sci.*, **36**, 259 (1959).

19. Vogelsong, D. C., and E. M. Pearce, *J. Polymer Sci.*, **45**, 546 (1960).

20. Vogelsong, D. C., *J. Polymer Sci.*, **A1**, 1055 (1963).

21. Bradbury, E. M., and A. Elliot, *Polymer*, **4**, 47 (1963).

Résumé

On a déterminé la structure cristalline de la forme gamma du nylon 6 (polycaproamide) obtenue par traitement à l'iode de la forme alpha du nylon 6 par diffraction aux rayons-X. L'unité cellulaire contient quatre unités unités de répitition $[+CH_2+_5CONH—]$ et est monoclinique avec $a = 9.33$ A., $b = 16.22$ A. (axe de la fibre), $c = 4.78$ A., $\beta = 121°$. Le groupe spatial est $P2_1/a$. Il y a une déviation considérable de la configuration planaire dans le groupe amide de la chaîne. Le plan de la chaîne CH_2 en zig-zag se trouve presque parallèle au plan (001). Le cristal est composé de plaques de chaînes parallèles jointes par des liens hydrogènes entre chaînes adjacentes. Les directions des chaînes sont opposées en feuilles alternantes. La longueur du lien hydrogène est 2.83 Å, une valeur raisonable pour une chaîne $NH\cdots O$ joint par des liens hydrogènes entre les chaînes adjacentes. La direction des liens hydrogène fait un angle de 12° avec le plan (100) et les liens $C=O$ et NH sont environ colinéaires. Les groupes amides se trouvent au même niveau dans la cellule.

Zusammenfassung

Die Kristallstruktur der durch Jodbehandlung der α-Form von Nylon-6 (Polycapronamid) hergestellte γ-Form von Nylon-6 wurde mittels Röntgenbeugung untersucht. Die Elementarzelle enthält vier wiederkehrende Einheiten $[+CH_2+_5CONH—]$, ist monoklin mit $a = 9,33$ A., $b = 16,88$ A. (Faserachse), $c = 4,77$ A., und $\beta = 121°$ und gehört der Raumgruppe $P2_1/a$ an. In der Amidgruppe der Kette treten merkliche Abweichungen von der planaren Konfiguration auf. Die Ebene der CH_2-Zickzackkette ist zur (001)-Ebene und zur Faserachse fast parallel. Der Kristall besteht aus gefalteten Schichten, die aus durch Wasserstoffbindungen zwischen benachbarten Ketten verbundenen parallelen Ketten aufgebaut sind. In aufeinanderfolgenden Schichten liegen die Ketten in entgegengesetzter Richtung. Die Länge der Wasserstoffbindung ist 2,83 A. Dieser Wert ist für durch Wasserstoffbindungen zwischen benachbarten Ketten verbundene $NH\cdots O$-Ketten plausibel. Die Richtung der Wasserstoffbindung schliesst mit der (100)-Ebene enein Winkel von 12° ein und die $C=O$— und NH-Bindungen sind fast kolinear. Die Amidgruppen liegen in der Zelle auf gleichem Niveau.

Investigation of Polyacetaldehyde Structure by High Resolution Nuclear Magnetic Resonance*

MURRAY GOODMAN and JOHANNES BRANDRUP, *Polymer Research Institute, Polytechnic Institute of Brooklyn, Brooklyn, New York, and Chemstrand Research Center, Durham, North Carolina*

Synopsis

We examined the configurations of cationically produced amorphous polyacetaldehyde by high resolution NMR spectroscopy at high temperature in such solvents as dimethylformamide and aniline. Our results show that the polymer backbone is composed of heterotactic and isotactic triad sequences, the former predominating over the latter. Using a 60 Mcycle instrument with or without spin decoupling, we were unable to detect any syndiotactic triad sequences. In addition, the 60 Mcycle NMR spectrum of poly-α-deuteroacetaldehyde shows the presence of only the same two stereochemical triads as above. However, examination of polyacetaldehyde with a 100-Mcycle instrument indicated that a small shoulder exists on the low field side of the heterotactic peak which is probably caused by a small syndiotactic triad content. We used these findings to propose a mechanism for the cationic polymerization of acetaldehyde. We suggest that acetaldehyde may exist in a dimeric form under polymerization conditions leading to a preferred incorporation of mesodimeric units into the propagating chain. Model compound studies involving α,α'-dimethoxyethyl ether are consistent with this postulate.

INTRODUCTION

The structure and polymerization of acetaldehyde has attracted considerable interest in recent years since Vogl,[3] Natta,[4] and Furukawa[5] prepared crystalline polyacetaldehyde using anionic catalysts at low temperature. Amorphous polyacetaldehyde, known since 1936,[6] can be prepared by use of a large variety of catalysts[7] assumed to be mostly cationic.[3]

According to x-ray determinations,[8] the crystalline modification possesses an isotactic configuration of its chain substituents. The structure of the amorphous polyacetaldehyde has not been determined with certainty. Two structural postulates have been advanced. Amorphous polyacetaldehyde has been considered to be atactic,[9] built up from random placements of syndiotactic, heterotactic, and isotactic units; or, more recently a syndiotactic configuration was also suggested.[10] Infrared determinations[5] and x-ray[11] diffraction analyses have failed to give a definitive answer

---

* A preliminary report of this work has appeared.[1] Independent of our work, Dr. O. Vogl, R. S. Sudol, and E. G. Brame of E. I. du Pont de Nemours & Company carried out a stereochemical study on polyacetaldehyde. We wish to acknowledge the many rewarding discussions with them on this subject.[2]

to this question. We applied high resolution nuclear magnetic resonance (NMR) for the elucidation of the structure of this polymer. This method has been favored in recent years for the determination of the configuration of polymers[12] and has given valuable results unobtainable by methods known before for many polymers. As we stated in a preliminary publication,[1] NMR is an appropriate tool for this polymer, because the acetal linkages in the main chain prevent spin–spin splitting of the signals generally found in vinyl polymers because of the continuous arrangement of hydrogen atoms in their main chain. Application of this new technique does, in fact, give valuable information on the structure of amorphous polyacetaldehyde.

RESULTS AND DISCUSSION

Simple low molecular weight acetals of acetaldehyde yield a doublet for the methyl group and a quadruplet for the single hydrogen attached to the carbon atom according to simple splitting rules. A similar spectrum is

TABLE I

NMR Spectra of Amorphous Polyacetaldehyde Prepared with Different Catalysts

Polymeriza-tion Catalyst	NMR conditions		Position of doublets		
	Solvent	Temp., °C.	Hetero-tactic(H)	Isotactic (I)	Intensity ratio H/I
TiCl₄	Aniline	145	8.61	8.67	2.85
γ-rays[a]	Aniline	150	—	—	2.14
BF₃/molecular sieves	Chlorobenzene	130	8.61	8.67	1.75
BF₃/Florisil	Chlorobenzene	130	—	—	2.03
	DMF	170	8.71	8.74	2.13
AlCl₃	Chlorobenzene	130	8.59	8.66	2.21
H₃PO₄	Chlorobenzene	130	8.56	8.64	1.90
H₃PO₄/Florisil	Chlorobenzene	130	—	—	1.95
”	Diphenyloxide	160	8.52	8.60	
”	DMF	130	8.66	8.69	1.95
”	Aniline	150	8.58	8.66	2.21
”	Aniline[b]	149	—	—	1.90
”	Aniline[c]	150	—	—	2.18
H₃PO₄/Florisil[d]	Aniline	150	8.59	8.67	1.01
	Average for aromatic solvents[e]		8.58	8.66	
			$\Delta\delta = 4.8$ cycle/sec.)		
	Average for aliphatic solvents[e]		8.69	8.72	
			($\Delta\delta = 1.8$ cycle/sec.)		

[a] Polymerized at −196°

[b] Double resonance experiments.[1]

[c] Deuterated polyacetaldehyde.

[d] Polymerized with ether as solvent.

[e] See Brandrup and Goodman.[1]
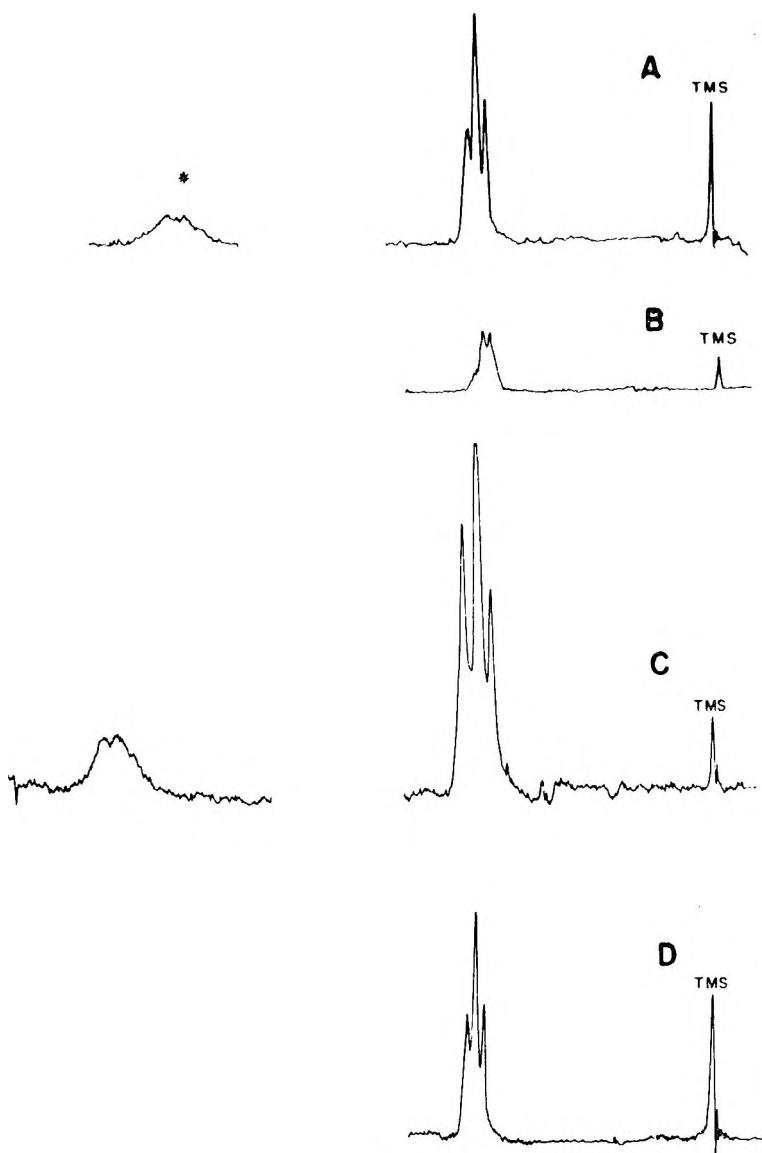
Fig. 1. NMR spectra (60 Mcycle) of polyacetaldehyde prepared under different conditions: (A) prepared with 0.1% H_3PO_4 in ether (30% monomer) at $-80°C.$; (B) prepared with 0.5% $Zn(C_2H_5)_2$ at $-80°C.$; (C) Prepared with γ-rays at $-196°C.$; (D) Prepared with $Al/Zn(C_2H_5)_2$ according to Furukawa.[16] Spectra taken in aniline at $150°C.$

expected for polyacetaldehyde—a high molecular weight polyacetal. The exact placement of the peaks in the magnetic field (their chemical shift) is dependent on more than the nearest neighboring protons. Therefore, different shifts for different configurational placements are expected. Since there are three possibilities for placement of three methyl groups—iso-

| Polymerization Catalyst | NMR conditions | | Position of Doublets | | Intensity ratio H/I |
	Solvent	Temp., °C.	Hetero-tactic(H)	Iso-tactic(I)	
Al/Zn(C$_2$H$_5$)$_2$[a]	Aniline	150	8.58	8.66	1.30
AlCl(C$_2$H$_5$)$_2$					
Methanol extract	DMF	151	8.71	8.74	2.23
DMF extract	DMF	152	8.69	8.73	1.50
Al(i-C$_4$H$_9$)$_3$					
Acetone extract	DMF	150	8.66	8.69	2.13
DMF extract	DMF	148	8.69	8.73	1.56
Zn(C$_2$H$_5$)$_2$					
Acetone extract	Aniline	135	8.56	8.64	1.94
Residue	Aniline	150		8.68	

[a] Catalyst prepared according to Hiroyasu et al.[16]

tactic, heterotactic, syndiotactic—three doublets at different positions should be observed. NMR spectra (60 Mcycle) for polyacetaldehyde obtained under different conditions are shown in Figure 1. At low field, an unresolved multiplet for the backbone hydrogen is observed (5.1–5.4 τ values) which occasionally splits into several peaks, most clearly into a quintet, if the measurements were carried out in aliphatic solvents such as dimethylformamide or 1,2,3,-trichloropropane.[1] The poor resolution of this peak can be attributed to the fact that a hydrogen atom attached directly to the backbone of the polymer is stiffer than a pendant side group. Therefore, the peak broadens considerable.

More information is obtained from the signal of the methyl group observed at higher field (8.5–8.75 τ values). A triplet is obtained instead of the doublet observed in simple low molecular weight acetals. The appearance of these peaks and their shift are independent of temperature and the kind of aromatic solvent used, as seen in Tables I and II. We reported data obtained in aliphatic solvents in our previous communication.[1] The similarity of all these spectra excludes the possibility that different conformations of the polymer chains contribute to the spectrum. Therefore, this triplet has its origin clearly in the different configurations of the monomer units in the polymer chain.

A triplet can be explained only by the overlapping of two doublets. The missing third doublet may mean that two configurations experience nearly the same magnetic environment and therefore have shift values smaller than the limit of resolution of these spectra. It also may mean that one doublet is missing, indicating the absence of one configuration in the polymer.

Polymerization of Deuterated Acetaldehyde

We undertook the polymerizations of α-deuterated acetaldehyde to differentiate between these two alternatives. The substitution of hydrogen
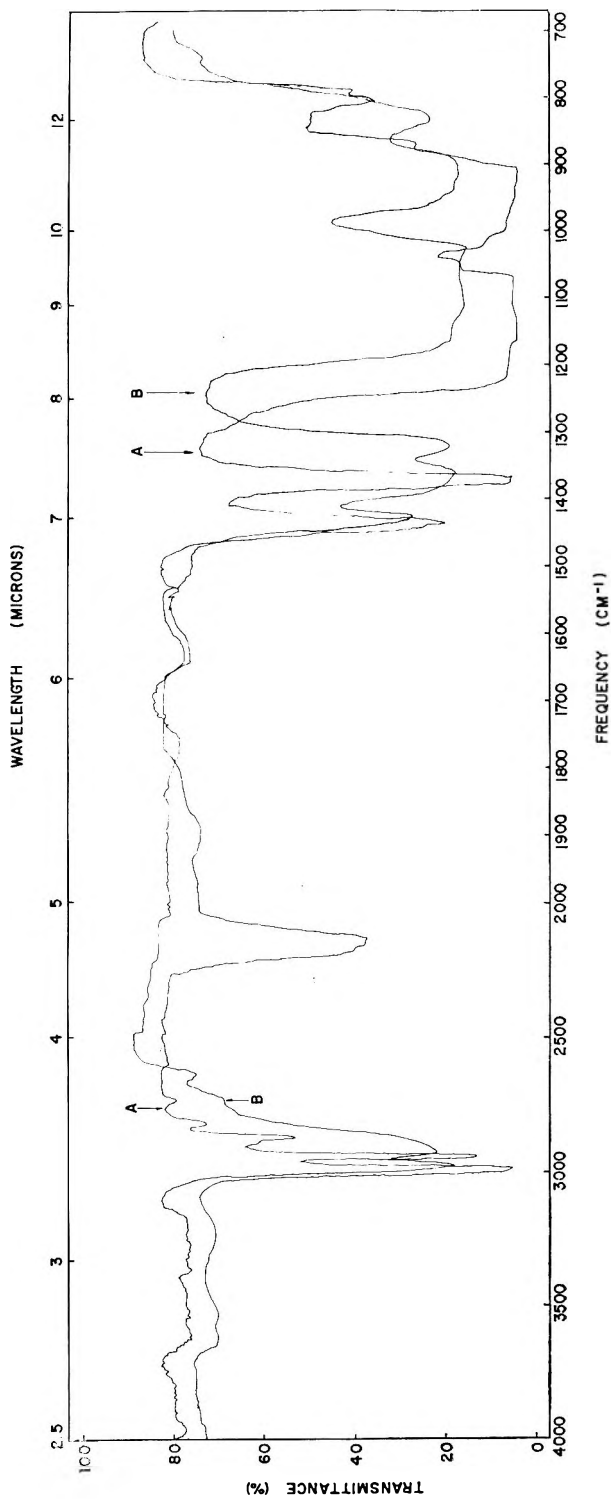
Fig. 2. Infrared spectra of (A) α-deuterated polyacetaldehyde (film cast from methanol) and (B) polyacetaldehyde.
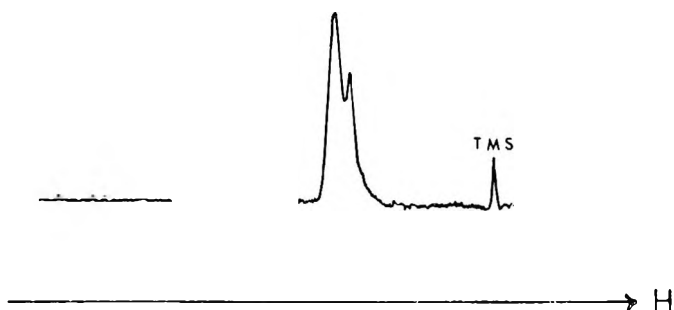
Fig. 3. NMR spectrum (60 Mcycle) of α-deuterated polyacetaldehyde in aniline at 150°C.

by deuterium in the α-position removes any spin–spin splitting, and the methyl groups should show a singlet instead of the doublet. Three stereochemical placements should yield three singlets. Acetaldehyde deuterated in the α-position was polymerized at −80°C. with H_3PO_4 supported on Florisil as catalyst. The polymer obtained remained deuterated according to the infrared spectrum (Fig. 2). The C—D stretching band is seen at 2120 cm.$^{-1}$. Therefore no major deuterium exchange occurred during the polymerization and isolation of the polymer. The polymer was dissolved in aniline and the 60 Mcycle spectrum was obtained at 150°C. The spectrum (Fig. 3) shows two singlets of differing intensity which correspond in shift value and intensity ratio to the triplet observed in regular polymers. Unfortunately, the resolution of these peaks was not as good as in the case of regular polyacetaldehyde because of second-order coupling between deuterium and hydrogen of the methyl group.

These experiments are in agreement with the result of the double resonance experiment described in our prevous report[1] and tend to confirm the second alternative, that only two of the three configurations exist. The exclusion of one configuration in the polymer results in a stereoblock structure of the polymer as we previously suggested.[1]

100 Mcycle NMR Spectra

According to recent experiments, this explanation of the structure of the polymer must be modified. Fortunately, we were able to obtain a 100-Mcycle spectrum of polyacetaldehyde in aniline at 145°C.* (Fig. 4). This spectrum resembles closely the spectrum at 60 Mcycles except for the low field side of the triplet at high field. This side is considerably broader with the slight indication of a shoulder. This shoulder may belong to the third doublet not observed in the other spectra. Even in this spectrum, the configuration giving rise to this doublet experiences apparently nearly the same magnetic environment as one of the other doublet placements and therefore the shift difference is not sufficiently large to permit complete

Fig. 4. NMR spectrum (100 Mcycle) of polyacetaldehyde in aniline at 145°C. Peak on left arbitrarily increased in size.
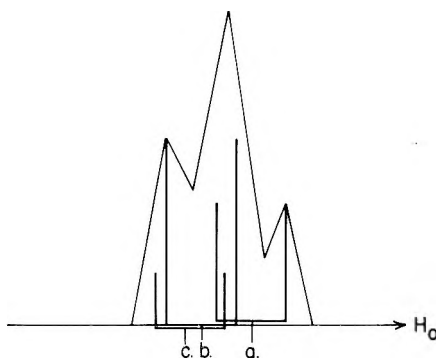
Fig. 5. Interpretation of the high field triplet observed for polyacetaldehyde in aniline at 150°C. (60 Mcycle spectrum).

resolution of this peak. Any quantitative determination of this peak is impossible at this time.

The triplet observed in a 60 Mcycle spectrum can now be interpreted by the arrangement of three doublets shown in Figure 5.

Assignment of the Peaks

The next step in our analysis of the NMR spectra of polyacetaldehyde involves the assignment of the three doublets to their corresponding configurations. With polyacetaldehyde NMR does not provide an absolute determination of the configuration as in the case of poly(methyl methacrylate).[12] Most probably, the doublet at higher field must derive from an isotactic configuration. This is supported by the following considerations:

(a) Paraldehyde and metaldehyde show only one quadruplet and one doublet whose position is given in Table III. Previous determinations of their structure by electron diffraction and x-ray[13] have shown that all methyl groups are aligned equatorially to the ring. This equatorial posi-

TABLE III
NMR Spectra of Model Compounds for Polyacetaldehyde

Compound	Center of quadruplet for —C—H	Center of doublet for —C—CH₃	Coupling constant J, cycle/sec.
Dimethylacetal[a]	5.59	8.84	4.8
α,α'di-methoxyethyl ether[b]	5.23	8.74	4.8
Paraldehyde[a]			
all-*cis*	5.12 (5.08[c])	8.75 (8.74[c])	4.8
cis-trans-cis[c]	4.72	8.61	5.0
cis-cis-trans[c]	4.79	8.76	5.8
Metaldehyde[d]	5.52	8.75	4.8

[a] Measured in chlorobenzene at 130°C.

[b] Measured in dimethylformamide at 125°C.

[c] Values were kindly submitted by Dr. J. L. Jungnickel, Shell Development Company.[15]

[d] Measured in aniline at 150°C.

tion of the methyl groups will place them in isotactic positions after hypothetical opening of the ring. The position of the doublets in these ring compounds is at somewhat higher field than observed in the polymer.

(b) Recently, a second configuration of paraldehyde has been found[14] which is not contained in commercial paraldehyde. The NMR spectrum of this isomer has been obtained[15] and the position of its doublets is at lower field, as seen in Table III. The configuration of its methyl groups would be *cis-trans-cis* (syndiotactic) and *cis-cis-trans* (heterotactic).*

(c) In a single experiment, we succeeded in obtaining a spectrum of a crystalline polyacetaldehyde (Fig. 1). Polyacetaldehyde prepared with diethyl zinc as catalyst at −80°C. could be separated by extraction with acetone into an amorphous and a crystalline part. The amorphous polymer showed the usual triplet comparable to other polymers (Table II). The insoluble crystalline residue was slurried in aniline and heated to 130°C. Partial solution resulted, and a poorly resolved spectrum was obtained which showed two peaks of nearly equal size whose shift corresponded to the high field section of the triplet.

(d) The stereoblock polymer prepared according to the procedure of Furukawa[16] showed an intensity increase of the right peak (Fig. 1D). This polymer supposedly contains longer blocks of isotactic configurations.

(e) Successive extraction of crystalline polyacetaldehyde with better and better solvents yields different fractions with increasing isotactic content. The high field doublet correspondingly increases in intensity, as seen in Table II. Once the isotactic placements are assigned, the remaining peaks can be treated in a straightforward manner. The heterotactic configuration should experience an intermediate magnetic field between isotactic and syndiotactic configuration in analogy to other polymers.

* We wish to thank Dr. J. L. Jungnickel of the Shell Development Laboratories, Emeryville, California, for calling our attention to these results.

Therefore, we assign the doublet b in Figure 5 to the heterotactic configuration and doublet c to the syndiotactic configuration.

Polymerization Mechanism

Two peculiarities of these spectra have to be mentioned. First of all, it is very surprising to find that the isotactic placements are more frequent at this low temperature than the syndiotactic placements. Generally, uncomplexed polymerization via free growing active ends produces increasingly syndiotactic polymers with decreasing temperature. Second of all, the intensity ratio of these three doublets does not seem to obey simple Bernoullian statistics which are applicable for any free growing chain, free radical or cationic, uninfluenced by penultimate unit effects or complexation of the growing end as described by Bovey.[12]

Deviation from the intensity ratios derived from these statistics denotes that in our case additional influences have to be considered. Exact calculations cannot be obtained at this time because of insufficient resolution of the third small doublet. However, rough calculations indicate that the syndiotactic configuration exists less in these polymers than expected from a random statistical treatment.

The preponderance of heterotactic and isotactic placements can best be explained by the assumption of stereoblocks composed of two or multiples of two monomer units of identical stereochemical configuration (DDLLDDDDLL). (In our preliminary report[1] we indicated that groups of similar configurational units might involve three monomer residues. This hypothesis was proposed because of the presence of some paraldehyde. We now believe that the dimer propagating unit fits our data much better.)

A structure of this type could be obtained by assuming an association of the monomeric acetaldehyde into dimers prior to polymerization. Random placements of these dimer units would yield a structure with only heterotactic and isotactic configurations. Participation of small amounts
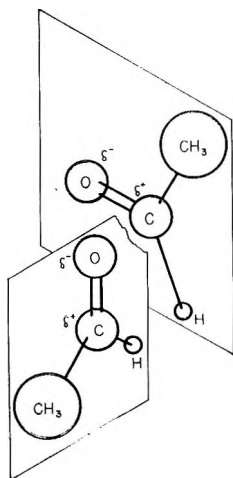
Fig. 6. Structure of the associate between two acetaldehyde molecules (similar to Schneider[17]).

of monomeric acetaldehyde in a free growing uncomplexed polymerization may yield the small amount of syndiotactic triads observed (see next section).

We can support this assumption by the following experimental details.

a. Randomness of Polymerization. Initiation of the polymerization with different catalysts can demonstrate whether complexation of the growing end is involved. Different free radical systems yield the same polymer structure under any set of conditions independent of the origin of the radical. Similar considerations should apply for a polymerization via freely growing cations.

Table I shows some of the results obtained. The ratio H/I is used because the 60 Mcycle spectrum does not resolve the third doublet.

Within the experimental error, all polymerizations yield the same ratio H/I, even with the use of different catalysts. This clearly demonstrates that major portions of the polymer are produced in a polymerization via free growing uncomplexed cations.

b. Association of Acetaldehydes. The association of acetaldehyde has already been described.[17] According to these results no hydrogen bonding of the single α-hydrogen is involved, and, therefore, the polar carbonyl groups associate alone. A dipole strength of 2.49 Debye units[18] seems to be a sufficient driving force for this complex formation.

Acetaldehyde apparently primarily dimerizes, as has been calculated from the second virial coefficient.[19] The structure of these associates might be as explained by Schneider and Bernstein[17] (Fig. 6). The construction of Fisher-Herzfelder models shows that the closest overlap of two carbonyl functions places the methyl group as far apart as possible.

The concerted reaction of these dimers with the free growing ultimate end will always add two monomeric units of identical stereo configuration.

Inversion of the configuration of the ultimate carbon before addition of the dimer will produce syndiotactic units as seen in the scheme of eqs. (1) and (2).

$$\text{DD}\!-\!\begin{cases}\rightarrow\text{DDDD}\\[1em]\rightarrow\text{DDLL}\end{cases} \qquad\qquad (1)$$

<div align="center">normal end</div>

$$\text{DL}\!-\!\begin{cases}\rightarrow\text{DLDD}\\[1em]\rightarrow\text{DLLL}\end{cases} \qquad\qquad (2)$$

<div align="center">inverted end</div>

Since the NMR technique yields the configuration of three monomeric units (triads), this scheme explains the appearance of predominant heterotactic and isotactic placements in the spectrum of polyacetaldehyde.

Model Compound Studies

The feasibility of such dimerization process was also suggested by the results obtained with α,α'-dimethoxyethyl ether, a dimer model for poly-

acetaldehyde (Table III)   The spectrum of this dimer showed only one doublet,[20] indicating only one configuration.   The synthesis of this compound goes through many cationic intermediates and should lead to both isomeric forms, *racemic* and *meso*.   The gas chromatographic analysis in a temperature programmed capillary column with ca. 60,000 theoretical plates likewise indicated the presence of only one configuration.   We similarly propose that the acetaldehyde has reacted in a dimeric form with hydrogen chloride yielding only *meso* α,α'-dichloroethyl ether (see experimental section) which after substitution with sodium methoxide yields *meso* α,α'-dimethoxyethyl ether.

The assumption of the participation of dimeric acetaldehyde in an otherwise free growing polymerization yielding a polymer with predominantly heterotactic and isotactic configurations explains many experimental observations.

(*1*) The similarity of the infrared spectra of amorphous and crystalline polyacetaldehyde is surprising, since most other polymers show significant differences.   As we see now, amorphous and crystalline polyacetaldehyde are basically similar.   The lack of crystallinity is explained by the much shorter sequence length of isotactic placements in the amorphous polymer. The average sequence length for two different polymers was calculated by adopting the mathematical treatment of Johnson[21] (Fig. 7).   Less than 8% of the polymer contains sequences which are longer than 10 units (Fig. 8).   Between 10 and 20 monomeric units are assumed to be necessary for crystallization.[22]

(*2*) The cyclization of acetaldehyde to paraldehyde, the cyclic trimer, at room temperature and to metaldehyde, the cyclic tetramer, at low temperature is also explained by this scheme.   At low temperature, two dimers react, yielding the tetramer.   At room temperature, sufficient amounts of unassociated acetaldehyde exist in order to react with the dimer or other unassociated species yielding the trimer.

(*3*) Finally, it is interesting to note that the polymer prepared in the
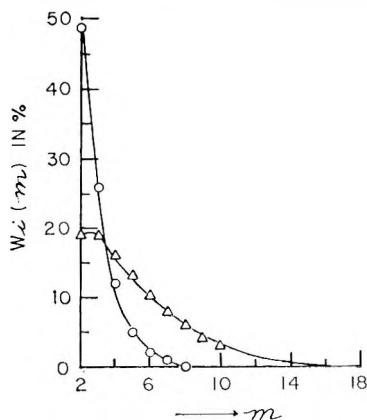
Fig. 7. Weight fraction of isotactic sequences with length *m* as a function of m: (O) polyacetaldehyde prepared with Florisil at $-80°C$.; ($\triangle$) polyacetaldehyde prepared in ether with H_3PO_4 at $-80°C$.
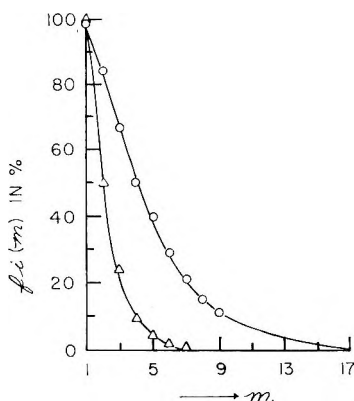
Fig. 8. Weight fraction of isotactic sequences greater than m: ($\triangle$) polyacetaldehyde prepared with Florisil at $-80°C$.; (O) polyacetaldehyde prepared in ether with H_3PO_4 at $-80°C$.

solid state at $-196°C$. shows a similar structure (Fig. 1). Letort and Richard[10] polymerized acetaldehyde in the solid state and obtained a rubbery amorphous polymer similar to the polymer prepared under different conditions in the liquid state. They concluded by means of a geometric analysis of the polymerization process that the amorphous polymer should have a syndiotactic configuration. The fact that even this polymer shows a triplet in the 60 Mcycle spectrum completely excludes this possibility.

According to our results, the structure of amorphous polyacetaldehyde is best explained by the existence of mainly stereoblocks of configurations such as DDLLLLDDLL which are formed according to a mechanism described above.

EXPERIMENTAL

Polymerization of Acetaldehyde

Commercial paraldehyde (Metro Industries) was stored over calcium hydride and distilled from triisobutyl aluminum shortly before use in order to remove any trace of water. Paraldehyde treated accordingly was slowly decomposed with anhydrous copper sulfate into acetaldehyde which was immediately distilled into a flask containing the catalyst at $-80°C$. The acetaldehyde was precooled to at least $-50°C$. before contact with the catalyst. The catalyst concentration was in the range of 0.1–0.5%. Molecular sieves and Florisil earth were dried for 24 hr. at 500°C. before use. The polymerization flask was stored for a week at $-80°C$. At this time 40–60% of the acetaldehyde had polymerized. The polymer was dissolved in acetone or methanol, filtered, precipitated in water, and after two reprecipitations dissolved in benzene and freeze-dried at high vacuum. Paraldehyde formed during the polymerization as a side product was completely removed in this manner. NMR spectra were taken immediately afterwards. Commercially available materials were used as catalysts without purification; solvents were purified and dried according to standard procedures.

α-Deuterated acetaldehyde was obtained from Merck, Canada, distilled through a column filled with molecular sieves, and polymerized with H_3PO_4 supported on Florisil at $-80°C$. The isolation and purification corresponded to the treatment given for other polymers above.

Preparation of Model Compounds

Dimethylacetal was prepared according to Croxall.[23] Metaldehyde was obtained by treating acetaldehyde with a trace of H_2SO_4 at $-40°C$. The dimer of polyacetaldehyde, α,α'-methoxyethyl ether was prepared by allowing acetaldehyde to react with excess anhydrous hydrogen chloride at $-10°C$. The resulting α,α'-dichloroethyl ether was treated with sodium methoxide according to Laatsch.[24] The α,α'-dimethoxyethyl ether with a boiling point of $126-127°C$. was obtained in 70% yield. The structure was confirmed by molecular weight determinations, infrared, and NMR measurements.

Nuclear Magnetic Resonance Measurements

Spectra were obtained with a Varian HR 60 NMR spectrometer (unless otherwise specified). A 6% solution of the polymers was prepared in various solvents and investigated up to 200°C., the upper temperature limit of the spectrometer. Serious experimental difficulties arose because of the thermal instability of the polymer. A stabilizer composed of Ultramid IC (BASF, Ludwigshafen, Germany) and β-naphthylamine,[25] together with 2,4-dinitrobenzene, gave a stability sufficient to permit experiments to be conducted at temperatures of 150–180°C. (ca. 30 min.). The shift of the peaks is given in τ values.[26]

References

1. Brandrup, J., and M. Goodman, *J. Polymer Sci.*, **B2**, 123 (1964).
2. Brame, F. G., Jr., R. S. Sudol, and O. Vogl, *J. Polymer Sci.*, **A2**, 5337 (1964).
3. Vogl, O., *J. Polymer Sci.*, **46**, 261 (1960).
4. Natta, G., G. Massanti, P. Corradini, and J. W. Bassi, *Makromol. Chem.*, **37**, 156 (1960).
5. Furukawa, J., T. Saegusa, A. Fujii, A. Kawawaski, H. Imai, and Y. Fujii, *Makromol. Chem.*, **37**, 149 (1960); *ibid.*, **44/46**, 398 (1961).
6. Travers, M. W., *Trans. Faraday Soc.*, **32**, 243 (1936); M. Letort Hebd, *Seances Acad. Sci.*, **202**, 767 (1936).
7. Letort, M., *Compt. Rend.*, **240**, 86 (1955); *ibid.*, **241**, 651,1765 (1955); J. N. Koral and B. W. Song, *J. Polymer Sci.*, **54**, S34 (1961); J. Furukawa, T. Saegusa, T. Tsurata, H. Fujii, and T. Tatano, *J. Polymer Sci.*, **36**, 546 (1959).
8. Natta, G., P. Corradini, and J. W. Bassi, *J. Polymer Sci.*, **51**, 505 (1961).
9. Furukawa, J., T. Saegusa, T. Tsurata, H. Fujii, A. Kawasaki, and T. Tatano, *Makromol. Chem.*, **33**, 32 (1959).
10. Letort, M., and A. J. Richard, *J. Chim. Phys.*, **1960**, 752.
11. Rigby, H. A., C. J. Danby, and C. N. Hinshelwood, *J. Chem. Soc.*, **1948**, 234.
12. Bovey, F. A., and G. V. D. Tiers, *Forschr. Hochpolymer. Forsch.*, **3**, 139t (1963).
13. Carpenter, D. C., and O. Brockway, *J. Am. Chem. Soc.*, **58**, 1270 (1936); O. Hassel and H. Mark, *Z. Physik. Chem.*, **111**, 357 (1924).

14. Craven, E. C., *J. Appl. Chem.*, **12**, 526 (1962).

15. Jungnickel, J. L., paper presented at ACS Meeting in Miniature, Berkeley Calif., December 1963.

16. Hiroyasu, F., J. Furukawa, T. Saegusa, and A. Kawasaki, *Makromol. Chem.*, **40**, 226 (1960).

17. Schneider, W. G., and H. J. Bernstein, *Trans. Faraday Soc.*, **52**, 13 (1956); N. S. Bayliss, A. R. H. Cole, and L. H. Little, *Austral. J. Chem.*, **8**, 26 (1955).

18. Coomber, D. J., and J. R. Partington, *J. Chem. Soc.*, **1938**, 1444.

19. Alexander, E. A., and J. P. Lambert, *Trans. Faraday Soc.*, **37**, 421 (1941).

20. Brandrup, J., and M. Goodman, to be published.

21. Johnson, K., *Kolloid-Z.* **178**, 161 (1961).

22. Miller, R. L., and L. E. Nielsen, *J. Polymer Sci.*, **46**, 303 (1960).

23. Croxall, W. J., F. J. Glavis, and H. T. Neher, *J. Am. Chem. Soc.*, **70**, 2805 (1948).

24. Laatsch, H., *Ann. Chem.*, **218**, 13 (1883).

25. Weissermel, K., and W. Schmieder, *Makromol. Chem.*, **51**, 39 (1962).

26. Tiers, G. V. D., *J. Phys. Chem.*, **62**, 1151 (1958).

Résumé

On a examiné la configuration du polyacétaldéhyde amorphe, obtenu cationiquement, au moyen de la spectroscopie RMN à haute résolution et à température élevée dans des solvants tels que le diméthylformamide et l'aniline. Nos résultats montrent que le squelette polymérique est constitué de triades séquencées hétérotactiques et isotactiques, les premières étant prédominantes. En utilisant un appareil travaillant à 60 Mc, avec ou sans découplage de spin, nous ne sommes pas à même de détecter des séquences de triades syndiotactiques. De plus le spectre RMN à 60 Mc du poly-α-deutéroacétaldéhyde ne montre l'existence que des deux triades stéréochimiques sus-mentionnées. Néanmoins, l'examen du polyacétaldéhyde à 100 Mc montre l'existence d'un faible épaulement du pic hétérotactique du côté des champs plus bas, qui est probablement dû à une faible teneur en triades syndiotactiques. C'est sur la base de ces découvertes que nous proposons un mécanisme de polymérisation cationique de l'acétaldéhyde. Nous suggérons en effet que l'acétaldéhyde peut exister sous une forme dimérique dans les conditions de polymérisation, conduisant à l'incorporation d'unités mésodimériques au sein de la chaîne en croissance. L'étude du composé modèle, l'éther α,α'-diméthoxyéthylique s'accorde avec ce postulat.

Zusammenfassung

Die Konfiguration von kationisch erzeugtem amorphem Polyacetaldehyd wurde bei hoher Temperatur in Lösungsmitteln wie Dimethylformaid und Anilin mittels Hochauflösungs-NMR-Spektroskopie untersucht. Die Ergebnisse zeigen, dass die Polymerhauptkette aus heterotaktischen und isotaktischen Triadensequenzen aufgebaut ist, wobei die ersteren überwiegen. Mit einem 60-MHz-Instrument mit oder ohne Spinentkopplung konnte keine syndiotaktische Triadensequenz gefunden werden. Ausserdem zeigt das 60-MHz-NMR-Spektrum von Poly-α-deuteroacetaldehyd nur die Anwesenheit der beiden gleichen oben angeführten stereochemischen Triaden. Die Untersuchung von Polyacetaldehyd mit einem 100-MHz-Instrument ergab jedoch, dass an der Seite des heterotaktischen Maximums zu niedrigeren Werten hin eine Schulter vorhanden ist, welche wahrscheinlich auf einen kleinen Gehalt an syndiotaktischen Triaden zurückzuführen ist. Diese Befunde wurden zur Aufstellung eines Mechanismus für die kationische Polymerisation von Acetaldehyd benützt. Es wird angenommen, dass Acetaldehyd unter Polymerisationsbedingungnen in einer dimeren Form vorhanden sein kann, was zu einem bevorzugten Einbau von mesodimeren Einheiten in die wachsende Kette führt. Ergebnisse von Untersuchungen an α,α'-Dimethoxyathyläther als Modellverbindung stimmen mit dieser Annahme überein.

Polyacrylonitrile Prepared in Ethylene Carbonate Solution.   I.   Kinetics at Low Conversion*

L. H. PEEBLES, *Chemstrand Research Center, Inc., Durham, North Carolina*

Synopsis

The kinetics of acrylonitrile polymerization initiated by azobisisobutyronitrile in ethylene carbonate solution were studied at 50 and 60°C. Under these conditions simple solution polymerization kinetics should apply. The initial rate of polymerization was determined by varying the amount of initiator and the monomer concentration. The reaction is found to be first-order in monomer concentration and approximately 0.6-order in initiator concentration. The free radical derived from ethylene carbonate (by abstraction of a proton by a growing chain) apparently can only react with a monomer to start another polymer chain. It does not enter into termination reactions. That is, the solvent acts only as a transfer agent and a diluent and does not affect the rate of polymerization by entering into other reactions. The transfer reactions are relatively unimportant (transfer to monomer is negligible; transfer to solvent is small) as indicated by a study of the degree of polymerization calculated from the intrinsic viscosity. Thus, quite high molecular weight polymer can be obtained. The reaction is first-order to high conversion and is independent of the viscosity of the medium.

INTRODUCTION

The polymerization of acrylonitrile has received considerable study when the polymerization is conducted under homogeneous or heterogeneous conditions. The mechanism of heterogeneous polymerization, where the polymer precipitates as it is formed, is quite complex, and so far it has not been possible to describe adequately the mechanism of heterogeneous polymerization in mathematical terms. The difficulties encountered in the description of the mechanism of heterogeneous polymerization of acrylonitrile are reviewed elsewhere.[1,2] On the other hand, the homogeneous polymerization of acrylonitrile in solution should be a far simpler system. It should be possible to describe the kinetics and mechanism of solution polymerization of acrylonitrile with the same theories that apply to the polymerization of other vinyl monomers.

The kinetics of polymerization of acrylonitrile in ethylene carbonate were studied by Thomas, Gleason, and Pellon.[3] They found that the rate of polymerization was 1.5-order in monomer concentration and 0.6–0.7-order in initiator concentration. At the same time, polymers of high

intrinsic viscosity were obtained. These observations are not consistent with a mechanism of polymerization involving transfer to solvent in reactions where either a highly reactive or a sluggish radical is produced. If transfer produces a reactive radical, then the order with respect to monomer should be 1.0–1.1, while the order with respect to initiator should be 0.5–0.6.[4] If a sluggish radical is produced, both reaction orders should tend to increase, and one would expect a polymer with a lower intrinsic viscosity.[5]

Furthermore, the intrinsic viscosity of the polymer prepared in ethylene carbonate appears to be higher than that of polymers prepared in other solvents[3] under comparable conditions. The ability to prepare polymers of quite high molecular weight in solution permits the study of the possibility of branch formation, especially if these polymers are prepared at high conversion. Studies of the polymerization of acrylonitrile in ethylene carbonate were therefore undertaken at low (~5–10%) and at high (up to 75%) conversion. The kinetic results are reported in this paper, the influence of conversion upon the molecular weight is considered in the second paper of this series,[6] and the molecular parameters of the polymers so produced are reported in the third paper of this series.[7]

THEORETICAL

The usual kinetic scheme for vinyl polymerization by free-radical catalysts is shown in eqs. (1)–(7).

Initiation:

$$\begin{cases} I_2 \xrightarrow{k_1} 2R_c \cdot \\ R_c \cdot + M \xrightarrow{k_1} R_2 \cdot \end{cases} \tag{1}$$

Propagation:

$$\begin{cases} R_2 \cdot + M \xrightarrow{k_2} R_3 \cdot \\ R_s \cdot + M \xrightarrow{k_2} R_{s+1} \cdot \end{cases} \tag{2}$$

Termination:

$$R_s \cdot + R_t \cdot \xrightarrow{k_3} \text{Polymer} \tag{3}$$

Transfer to monomer:

$$R_s \cdot + M \xrightarrow{k_4} P_s + R_1 \cdot \tag{4}$$

Transfer to solvent:

$$R_s \cdot + S \xrightarrow{k_5} P_s + T \cdot \tag{5}$$

Reinitiation by solvent:

$$T \cdot + M \xrightarrow{k_t} R_2 \cdot \tag{6}$$

Solvent termination:

$$T \cdot + R_s \cdot \xrightarrow{k_7} \text{Polymer} \qquad (7)$$

Here, I_2 is the initiator; $R_s \cdot$, radicals containing s units, which include initiator and/or solvent fragments; M, monomer; P_s, polymer containing s units; and $T \cdot$, solvent radicals. The total concentration of radicals is $[R \cdot]$ and is the sum of concentrations of all $R_s \cdot$ radicals.

Reaction (3), can be written as termination by coupling or as termination by disproportionation, where a proton is transferred from one polymeric radical to the other. Termination by disproportionation produces twice as many polymer molecules as termination by coupling and hence is important when considering the molecular weight of the polymer. The constant k_3 is defined by a term $2k_3[R \cdot]^2$ in the rate equation for the variation of $[R \cdot]$ with time.[7] Bamford, Barb, Jenkins, and Onyon[8] as well as Bamford and Tompa[9] prefer to define k_3 by the term $k_3[R \cdot]^2$.

The usual assumption of steady state will be made: that the number of radicals produced equals the number of radicals destroyed and that little or no conversion has occurred. If we further assume that each solvent radical reinitiates the chain, then the rate of polymerization is

$$-d[M]/dt = k_2[M]([R \cdot] + k_4[R \cdot]/k_2 + k_6[T \cdot]/k_2) \qquad (8)$$

In order to have high molecular weight polymer, $(k_4[R \cdot]/k_2 + k_6[T \cdot]/k_2) \ll [R \cdot]$ [c.f. eq. (14)], hence

$$-d[M]/dt = k_2[M][R \cdot] \qquad (9)$$

The value of $[R \cdot]$ can be found from the steady-state relation

$$-d[R \cdot]/dt = 2k_3[R \cdot]^2 - 2fk_1[I_2] \qquad (10)$$

where f is the efficiency of initiation. Hence

$$[R \cdot] = (2fk_1[I_2]/2k_3)^{1/2} \qquad (11)$$

$$-d[M]/dt = [k_2/(2k_3)^{1/2}](2fk_1[I_2])^{1/2}[M] \qquad (12)$$

The reciprocal degree of polymerization is defined as the rate of termination of all species divided by the rate of propagation

$$\frac{1}{\bar{P}_n} = \frac{gk_3[R \cdot]^2 + k_4[R \cdot][M] + k_5[R \cdot][S]}{k_2[R \cdot][M]} \qquad (13)$$

$$= \frac{g(fk_1k_3[I_2])^{1/2}}{[M]} + \frac{k_4}{k_2} + \frac{k_5[S]}{k_2[M]} \qquad (14)$$

where g is a factor whose value is $2 > g > 1$, depending upon the mode of termination, i.e., whether by combination of radicals $(g = 1)$ or by disproportionation $(g = 2)$.

EXPERIMENTAL

Materials

Eastman White Label azobisisobutyronitrile (AIBN) was used either without further purification or was recrystallized at least twice from methanol. No difference was noted between these materials. Jefferson Chemical Company ethylene carbonate was purified by recrystallizing it twice, then distilling at 15 mm. pressure. Monsanto Chemical Company acrylonitrile was freed of inhibitor by washing with $3N$ sulfuric acid, with $3N$ sodium carbonate, and with water, dried with calcium chloride, and then distilled twice at atmospheric pressure—the second time immediately before use.

Polymerization Procedure

Catalyst was added to constricted test tubes prior to addition of ethylene carbonate either by direct weighing or as a solution in acetone, the latter removed at room temperature. The ethylene carbonate was partly outgassed by solidifying slowly under vacuum, then admitting monomer and air. The mixture was frozen in liquid nitrogen, then alternately evacuated and flushed with nitrogen five times, then sealed. The sealed tube was stored in liquid nitrogen until needed. Polymerization was effected at 50 or 60°C. by shaking the tube until it was thoroughly mixed, then allowing the tube to remain completely submerged for the total reaction time. Reaction times are corrected for the time to reach thermal equilibrium. The reaction was stopped by pouring the mixture into well-stirred methanol. The polymer was washed with methanol and dried at 70°C. overnight. In some cases salt had to be added to the methanol–polymer mixture to cause precipitation. The salt was removed by a water wash.

In one case, polymerization was effected in a "ball fall" tube, 1 in. in diameter and 6 in. long, which contained a steel ball. The ball could be raised to the top of the tube and aligned with the axis of the tube by an external magnet. The viscosity of the medium was estimated from the time t required for the ball of density σ and radius r to fall a distance L thru the liquid of density ρ by means of the relation

$$\eta = [2(\sigma - \rho)gr^2t/9L]F \tag{15}$$

where g is the acceleration due to gravity and F is a correction due to wall and end effects (considered unity in the present case).[10]

Intrinsic viscosities of the polymers were determined in freshly distilled dimethylformamide at 25°C. in Cannon-Fenske viscometers. Solvent flow times in excess of 100 sec. were used so kinetic energy corrections were not made. For samples with intrinsic viscosities below 3.0 dl./g., eq. (16) holds to within 0.05 intrinsic viscosity unit.

$$[\eta] = (\eta_{sp}/c)/(1 + 0.24\eta_{sp}) \tag{16}$$

This equation was used to evaluate some of the lower intrinsic viscosities,

RESULTS AND DISCUSSION

Table I gives the conditions of polymerization, the conversion, and the intrinsic viscosity for each sample.

TABLE I

Preparation Conditions for PAN Samples Polymerized in Ethylene Carbonate (EC)

AN, ml.[a]	EC, ml.[b]	AIBN, g.	Time of run, min.	Conversion, %	$[\eta]$, dl./g.
Varying Monomer Concentration at 60°C.					
16.14	33.05	0.2146	30	0.1365	2.56
6.96	42.70	0.2146	30	0.1360	1.60
5.41	44.31	0.2146	30	0.1148	1.36
4.43	45.34	0.2146	30	0.1083	1.14
Varying Initiator Concentration at 60°C.					
9.72	39.79	0.08584	30	0.0747	2.79
10	40	0.0553	62	0.1364	3.10
10	40	0.2196	30	0.1422	2.13
10	40	0.2146	58	0.2564	2.01
10	40	0.0545	115	0.2401	3.03
10	40	0.00337	118	0.0446	5.53
10	40	0.1348	251	0.2257	4.15
Varying Initiator Concentration at 50°C.					
10	40	0.003848	958	0.1848	8.06
10	40	0.003848	464	0.0938	8.20
10	40	0.01539	230	0.1055	6.47
10	40	0.06157	120	0.1204	4.65
10	40	0.1237	90	0.1364	3.81
10	40	0.2570	60	0.1317	3.14
10	40	1.0002	30	0.1360	1.97
Varying Monomer Concentration at 50°C.					
16.23	32.97	0.2538	71	0.1641	4.01
16.23	32.97	0.2539	31	0.0690	4.17
7.00	42.54	0.2549	38	0.0748	2.51
7.00	42.54	0.2543	92	0.1814	2.33
5.62	44.15	0.2549	95	0.0897	1.98
5.62	44.15	0.2542	94	0.2149	1.71
4.60	45.17	0.2530	100	0.2148	1.42

[a] Measured at 25°C.

[b] Measured at polymerization temperature.

The rate of polymerization is plotted against monomer concentration [AN] at 50°C. in Figure 1 at constant initiator concentration. A straight line results which passes through the origin. Figure 2 shows a similar plot of the same data but against monomer concentration to the 1.5 power, as suggested by Thomas et al.[3] The 1.5-order kinetics do not fit as well as first-order kinetics.

A plot of log $(-d[M]/dt)$ versus log $[M]$ would show that an even better straight line would be obtained with an order of monomer concentration of about 1.1. A 10% increase in the order of monomer concentration is considered still to be a normal polymerization in the presence
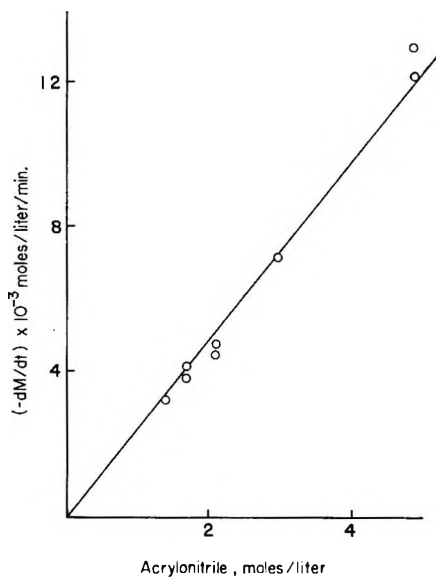
Fig. 1. First order polymerization kinetics of acrylonitrile in ethylene carbonate at 50°. (AIBN) = 3.1 × 10⁻² moles/liter.
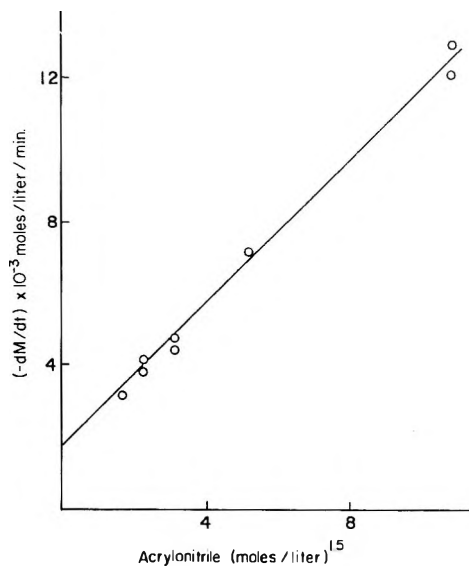
Fig. 2. Three-halves order polymerization kinetics of acrylonitrile in ethylene carbonate at 50°. (AIBN) = 3.1 × 10⁻² moles/liter.
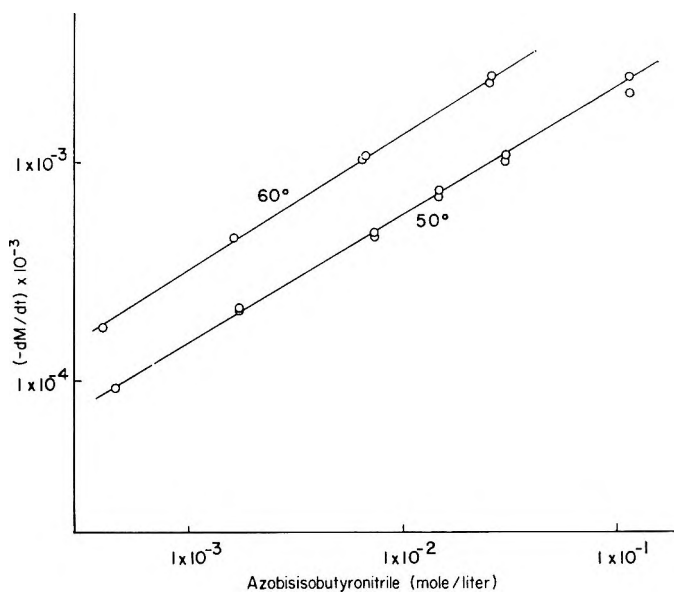
Fig. 3. Dependence of rate of polymerization upon catalyst concentration. Acrylonitrile = 3.0 moles/liter.
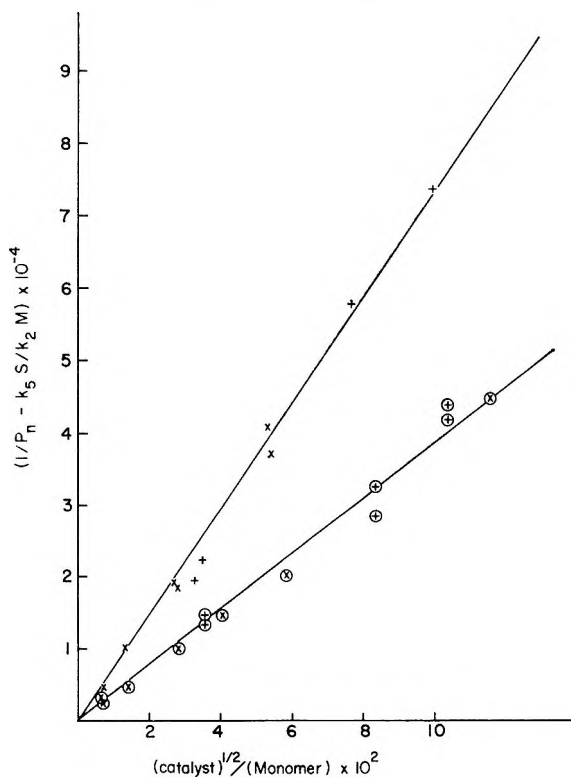
Fig. 4. Dependence of molecular weight upon catalyst and monomer. Concentration: X constant S/M, + I constant, circled values at 50°C.

of a solvent. Figure 3 shows the rate of polymerization versus the initiator concentration on logarithmic coordinates. Slopes of the lines are 0.6 instead of 0.5 as expected. Through the 60°C. data, a line with a slightly more positive slope fits the data better, but it is not known at this time if the difference in order is significant. Therefore, it is assumed that the difference is negligible.

The intrinsic viscosity–molecular weight equation for polyacrylonitrile polymerized in ethylene carbonate is given in Part III of this series.[7] The number-average degree of polymerization was calculated from the intrinsic viscosity by assuming a 2:1 ratio for the weight-average to number-average molecular weight ratio. A straight line results when the reciprocal degree of polymerization is plotted against $([I_2]/[M])^{1/2}$ when the solvent concentration is held constant. From this line, the constants in eq. (14) can be calculated if k_4/k_2 is assumed to be zero. These constants are listed in Table II. In eq. (14), it is arbitrarily assumed that the initiator varies as a 0.5 rather than a 0.6 power, in order that simplified kinetics may be used. Thomas, Gleason, and Pellon[4] have assumed a 0.5 power, even though their data have more scatter than the present data. As a check on the transfer to solvent constant, a series of runs were made at varying monomer concentration and constant initiator concentration. The results are shown in Figure 4. Thomas, Gleason, and Pellon[4] estimated that the chain transfer to monomer constant is 10^{-4} at 50°C.

TABLE II
Kinetic Constants for Polymerization of Acrylonitrile in Ethylene Carbonate

Constant	Value	Temp., °C.	Energy of activation, kcal./mole
Transfer to monomer, k_4/k_2	~ 0	50	
	~ 0	60	
Transfer to solvent, k_5/k_2	0.073×10^{-4}	50	
	0.128×10^{-4}	60	0.11
$-d[M]/dt/[AIBN]^{0.6}[M]$	1.92×10^{-2}	50	
	4.92×10^{-2}	60	20.2

Since a relatively simple mechanism of polymerization appears to exist in this system, it is of interest to examine the effect of higher conversions upon the kinetics. Equation (12) can be integrated to give

$$-\ln (1 - c) = [k_2/(2k_3)^{1/2}] (2fk_1[I_2])^{1/2}t$$

where c is the fractional conversion, $(1 - [M]/[M_0])$, and t is time. Some results are presented in Figure 5. Clearly, first-order kinetics are followed to rather high conversions (71.5%).
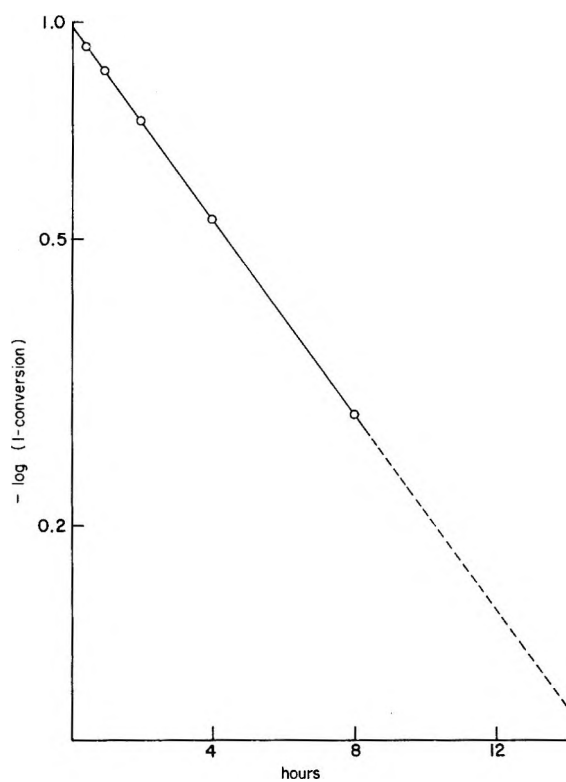
Fig. 5. First-order plot of polymerization of acrylonitrile to high conversion.
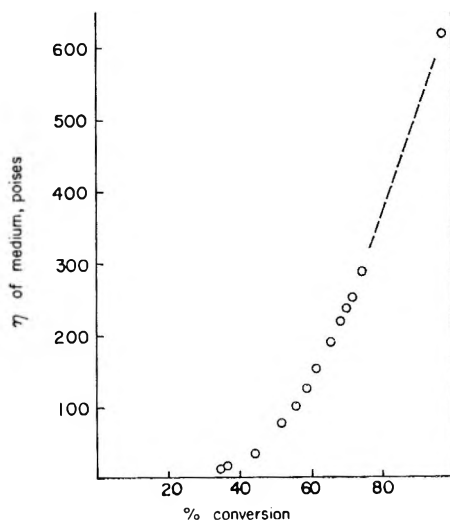
Fig. 6. Viscosity as a function of conversion.

In general, one expects the viscosity of the polymerization medium to influence the termination reaction, via the Tromsdorff or gel effect. In fact, Benson and North[11] feel that under certain circumstances, the termination reaction is controlled even at very low viscosity values around 0.01 poise. To test whether the polymerizations conducted here were being influenced by the viscosity of the medium, a polymerization reaction was conducted in a ball fall tube[10] and the viscosity was measured as a function of polymerization time. For eq. (15) to be exact, t must exceed 20 sec., which was not the case for the present data except for the last two points. Nevertheless, the results are plotted in Figure 6 as calculated viscosity versus conversion. The dotted line is the estimated path of the missing points. Thus, there is no detectable effect of viscosity on the rate of polymerization.

This observation permits calculation of the effect of conversion upon the molecular weight as is considered in the next paper.[6]

CONCLUSION

Thus, it is apparent that in ethylene carbonate the polymerization follows the kinetics of eq. (12) at 50 and 60°C., with the exception of a slightly higher dependence on catalyst concentration. The inconsistencies noted in the beginning of this paper concerning the reactivity of the radical derived from ethylene carbonate are resolved. The ethylene carbonate radical apparently is highly reactive. This fact means that a relatively simple mechanism of polymerization can be used to describe the system.

References

1. Peebles, L. H., in *Copolymerization*, by G. E. Ham, Ed., Interscience, New York, 1964, Chap. 9.
2. Thomas, W. M., *Fortschr. Hochpolymer. Forsch.*, **2**, 401 (1961).
3. Thomas, W. M., E. H. Gleason, and J. J. Pellon, *J. Polymer Sci.*, **17**, 275 (1955).
4. Burnett, G. M., and L. D. Loan, *Trans. Faraday Soc.*, **51**, 219 (1955).
5. Peebles, L. H., J. T. Clarke, and W. H. Stockmayer, *J. Am. Chem. Soc.*, **82**, 4780 (1960).
6. Peebles, L. H., *J. Polymer Sci.*, **A3**, 353 (1965).
7. Peebles, L. H., *J. Polymer Sci.*, **A3**, 361 (1965).
8. Bamford, C. H., W. G. Barb, A. D. Jenkins, and P. F. Onyon, *Kinetics of Vinyl Polymerization by Radical Mechanisms*, Academic Press, New York–London, 1958.
9. Bamford, C. H., and H. Tompa, *J. Polymer Sci.*, **10**, 345 (1953); *Trans. Faraday Soc.*, **50**, 1097 (1954).
10. ASTM Designation D 1343-56, *ASTM Standards*, American Society for Testing Materials, Philadelphia.
11. Benson, S. W., and A. M. North, *J. Am. Chem. Soc.*, **81**, 1339 (1959).

Résumé

La cinétique de polymérisation de l'acrylonitrile initée par l'azo-bis-isobutyronitrile en solution dans le carbonate d'éthylène, a été étudiée à 50 et 60°C. La cinétique habituelle de la polymérisation en solution derrait s'appliquer dans ces conditions. La vitesse in-

itiale de polymérisation est déterminée en faisant varier la quantité d'initiateur et la concentration en monomère. La réaction est du premier ordre par rapport à la concentration en monomère et approximativement du 0.6-ordre par rapport à la concentration en initiateur. Le radical libre provenant du carbonate d'éthylène (parenlèvement d'un proton par une chaîne en croissance) peut apparemment réagir uniquement avec un monomère pour initier une autre chaîne de polymère. Il n'entre pas dans la réaction de terminaison; c'est-à-dire que le solvant agit uniquement comme agent de transfer et comme diluant et n'affecte pas la vitesse de polymérisation en entrant dans d'autres réactions. Les réactions de transfert sont relativement peu importantes (le transfert sur monomère est négligeable, le transfert sur solvant est petit); cela résulte ce l'étude du degré de polymérisation, calculé à partir de la viscosité intrinsèque. Par conséquent des polymères de hauts poids moléculaires peuvent être obtenus. La réaction est du premier ordre à des taux de conversion élevés et est indépendante de la viscosité du milieu.

Zusammenfassung

Die Kinetik der mit Axobisisobutyronitril in Äthylencarbonatlösung gestarteten Acrylnitrilpolymerisation wurde bei 50 und 60°C. untersucht. Unter diesen Bedingungen sollte die einfache Lösungspolymerisationskinetik anwendbar sein. Die Anfangspolymerisationsgeschwindigkeit wurde bei verschiedenen Starter- und Monomer-konzentrationen bestimmt. Die Reaktion ist erster Ordnung in bezug auf die Monomerkonzentration und angenähert von der Ordnung 0,6 in bezug auf die Starterkonzentration. Das vom Äthylencarbonat abgeleitete freie Radikal (Wasserstoffentzug durch eine wachsende Kette) kann offenbar nur mit Monomeren unter Start einer neuen Polymerkette reagieren. Es beteiligt sich nicht an der Abbruchreaktionen. Das Lösungsmittel wirkt also nur als Überträger und Verdünnungsmittel und hat keinen Einfluss auf die Polymerisationsgeschwindigkeit durch etwaige Beteiligung an anderen Reaktionen. Die Übertragungsreaktion hat verhältnismässig wenig Bedeutung (Übertragung zum Monomeren ist vernachlässigbar; Übertragung zum Lösungsmittel ist klein), wie eine Untersuchung des aus der Viskositätszahl berechneten Polymerisationsgrades zeigt. Es kann daher ein ziemlich hohes Molekulargewicht erhalten werden. Die Reaktion ist bis zu hohen Umsätzen von erster Ordnung und von der Viskosität des Mediums unabhängig.

Polyacrylonitrile Prepared in Ethylene Carbonate Solution. II. Kinetics at High Conversion*

L. H. PEEBLES, *Chemstrand Research Center, Inc., Durham, North Carolina*

Synopsis

The first paper in this series has shown that when acrylonitrile is polymerized in ethylene carbonate, the transfer-to-monomer reaction is negligible, and the solvent acts only as a diluent and as a transfer agent. Furthermore, the rate of polymerization is first-order to quite high conversions, even though there is a concomitant high viscosity of the polymerization media. These observations permit calculation of the effect of conversion on the average molecular weight of the polymer. The constants of this calculation were evaluated from low conversion polymerizations and applied to the case of high conversion. The measured weight-average molecular weights as a function of conversion agree with the calculation and indicate that transfer-to-polymer reactions are probably very small. Hence, the extent of branching in polyacrylonitrile prepared in solution is also very small, even at high conversions.

INTRODUCTION

The kinetics of polymerization are rarely studied above a few per cent conversion because, first, the usual assumption of steady state is no longer tenable; second, in undiluted monomer, the rate of polymerization generally accelerates quite rapidly owing to the gel effect or Tromsdorff effect, after a few per cent conversion; and third, interaction with the formed polymer is usually neglected but can be of importance, i.e., it leads to branching reactions. The formation of branches in a polymer is generally assumed to be repressed by polymerization of the monomer in a solvent at low conversion and temperature. As will be seen in the theoretical section, the equations describing the distribution of molecular weights become quite complicated even when just the monomer is allowed to vary with time without allowing the rate of initiation to vary with time. In the work to be described, it will be assumed that a constant rate of initiation exists, even though in fact the rate of initiation varies as $\exp\{-k_1 t\}$ where k_1 is the first-order rate constant for initiator and t is the time. It has already been shown that the rate of polymerization of acrylonitrile (AN) in ethylene carbonate (EC) is not viscosity-dependent over the range of 0.01-600 poises when the solvent-to-monomer ratio is approximately 4.0. It has also been established that the rate of polymerization depends upon the first power of monomer concentration up to rather high conver-

sion.[1] The latter observation shows that the solvent EC enters into the rate expression as a diluent only, and does not complicate the mechanism of polymerization. Thus, the system AN–EC–AIBN (AIBN is the catalyst azobisisobutyronitrile) has the virtues of being a much simpler system than usually encountered. Further, very high molecular weight polymers can be prepared from which it should be possible to detect branch formation if it occurs to an appreciable extent.

MOLECULAR WEIGHT DISTRIBUTIONS AND AVERAGE MOLECULAR WEIGHTS AT HIGH CONVERSION

The derivation of the molecular weight distribution is based on the assumed kinetic model. These distributions contain various functions of the specific rate constants of polymerization, which, if independently evaluated, can then be used to predict the distribution of molecular weights, or various averages of the molecular weight distribution. For the most part, the derivations are adequately described in the literature[2,3] and will not be repeated here. The kinetic scheme is presented in eqs. (1)–(8), where I_2 is the initiator, $R_s\cdot$, denotes radicals containing s units which includes initiator and/or solvent fragments; M is monomer; P_s is concentration of polymer containing s units; $T\cdot$, is solvent radical; and T_2 is a dimerization product of two $T\cdot$ radicals.

Initiation:

$$\begin{cases} I_2 \xrightarrow{k_1} 2R_c\cdot \\ R_c\cdot + M \xrightarrow{k_1} R_2\cdot \end{cases} \tag{1}$$

Propagation:

$$\begin{cases} R_2\cdot + M \xrightarrow{k_2} R_3\cdot \\ R_s\cdot + M \xrightarrow{k_2} R_{s+1}\cdot \end{cases} \tag{2}$$

Termination by recombination:

$$R_s\cdot + R_t\cdot \xrightarrow{k_3} P_{s+t} \tag{3}$$

Termination by disproportionation:

$$R_s\cdot + R_t\cdot \xrightarrow{k_3'} P_s + P_t \tag{3'}$$

Transfer to monomer:

$$R_s\cdot + M \xrightarrow{k_4} P_s + R_1\cdot \tag{4}$$

Transfer to solvent:

$$R_s\cdot + S \xrightarrow{k_5} P_s + T\cdot \tag{5}$$

Reinitiation by solvent:

$$T\cdot + M \xrightarrow{k_6} R_2\cdot \tag{6}$$

Solvent termination:

$$T\cdot + R_s\cdot \xrightarrow{k_7} P_{s+1} \tag{7}$$
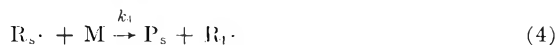
Solvent dimerization:

$$2T\cdot \xrightarrow{k_8} T_2 \tag{8}$$

The preceding paper[1] showed that reaction (7) does not occur appreciably in the polymerization of AN in EC, because the rate of polymerization is dependent upon monomer to the 1.0 power. This reaction therefore will be neglected. In neglecting this reaction, we immediately imply that the solvent acts as a diluent and transfer agent only and does not slow down the rate of polymerization by entering into other reactions. Reaction (8) will be neglected for the sake of mathematical simplicity only. In most kinetic analysis this reaction can be validly neglected except at high dilution. It is also known that transfer-to-monomer reaction (4) does not occur to an appreciable extent in AN polymerization, but this reaction will be retained in the general scheme until it is necessary to neglect it in order to obtain analytical expressions for the distribution functions. Thus, the expressions below are perfectly general, providing that reactions (7) and (8) may be neglected.

Distribution Equation for Invariant Monomer Concentration

In this kinetic scheme, we consider only reactions (1), (2), (3), (3)′, (4), (5), and (6). Then if monomer concentration is not allowed to vary, the molecular weight distribution is given by[1]

$$P_r = \frac{\Delta M}{k_2[M]} (1 - \xi)\xi^{r-1} \left\{ k_4[M] + k_5[S] + \left[\frac{I}{2(k_3 + k_3')} \right]^{1/2} \right.$$

$$\left. \times \left[(r - 1) \frac{(1 - \xi)}{\xi} k_3 + 2k_3' \right] \right\} \quad (9)$$

where

$$\xi = k_2[M]/\{k_2[M] + k_4[M] + k_5[S] + [2I(k_3 + k_3')]^{1/2}\} \quad (10)$$

and ΔM is the amount of monomer converted into polymer, and I is the rate of initiation. Now if termination proceeds by disproportionation only, $k_3 = 0$ and eq. (9) can be written as

$$P_r = \frac{\Delta M}{k_2[M]} (1 - \xi)\xi^{r-1}\{k_4[M] + k_5[S] + (2Ik_3')^{1/2}\}$$

$$= \frac{\Delta M}{k_2[M]} (1 - \xi)^2\xi^{r-1}\{k_2[M] + k_4[M] + k_5[S] + (2Ik_3')^{1/2}\}$$

$$= \Delta M (1 - \xi)^2\xi^{r-1} \quad (11)$$

for long chains, where the first term in braces is by far the largest one. This equation is exactly the same equation which can be derived on a statistical basis (see Flory[4a]) and is known as the "most probable" distribution.

To obtain the weight-average and number-average molecular weights, one needs to recall the definitions of these averages

$$\overline{M}_n = \Sigma N_r W_r/\Sigma N_r = W_0\Sigma r P_r/\Sigma P_r \quad (12)$$

$$\overline{M}_w = \Sigma N_r W_r^2/\Sigma N_r W_r = W_0\Sigma r^2 P_r/\Sigma r P_r \quad (13)$$

where $\bar{M}_n$ and $\bar{M}_w$ are the number-average and weight-average molecular weights, respectively; and W_0 is the molecular weight of the monomer. The weight-average and number-average molecular weights are then, for invariant monomer concentration:

$$\bar{M}_n = \frac{W_0 k_2 [M]}{k_4[M] + k_5[S] + \left[\dfrac{I}{2(k_3 + k_3')}\right]^{1/2} (k_3 + 2k_3')} \tag{14}$$

$$\bar{M}_w = \frac{W_0 2k_2[M]\{k_4[M] + k_5[S] + [I/2(k_3 + k_3')]^{1/2}(3k_3 + 2k_3')\}}{\{k_4[M] + k_5[S] + [2I(k_3 + k_3')]^{1/2}\}^2} \tag{15}$$

Distribution Equation When Monomer Concentration Varies, Transfer to Monomer Zero

In this case, the expression for P_r cannot be found analytically for termination both by recombination and by disproportionation if the transfer-to-monomer reaction is not zero. However, if $k_4 = 0$, then[2]

$$P_r = \frac{1}{r}\left\{\mu - \frac{1-x}{2}\frac{[2I(k_3 + k_3')]^{1/2}}{k_2}\right\}\left\{\left(1 + \frac{\mu}{[M_0]}\right)^{-r}\right.$$
$$- \left(1 + \frac{\mu}{[M]}\right)^{-r}\right\} + \frac{\mu(1-x)}{2}\frac{[2I(k_3 + k_3')]^{1/2}}{k_2}\left\{\frac{1}{[M_0]}\left(1 + \frac{\mu}{[M_0]}\right)^{-r}\right.$$
$$\left.- \frac{1}{[M]}\left(1 + \frac{\mu}{[M]}\right)^{-r}\right\} \tag{16}$$

where

$$\mu = \{k_5[S] + [2I(k_3 + k_3')]^{1/2}\}/k_2 \tag{17}$$

$$x = k_3'/(k_3 + k_3') \tag{18}$$

and the average molecular weights can be obtained by direct summation, which for long chains gives[2]

$$\bar{M}_n = \frac{W_0 k_2([M_0] - [M])}{\ln([M_0]/[M])\{k_5[S] + [I/2(k_3 + k_3')]^{1/2}(k_3 + 2k_3')\}} \tag{19}$$

$$\bar{M}_w = \frac{W_0 k_2([M_0] + [M])\{k_5[S] + [I/2(k_3 + k_3')]^{1/2}(3k_3 + 2k_3')\}}{\{k_5[S] + [2I(k_3 + k_3')]^{1/2}\}^2} \tag{20}$$

These equations are the same as eqs. (14) and (15) in the limit $[M_0] = [M]$ and $k_4 = 0$.

Thus, from eq. (20), as monomer is consumed, the weight-average molecular weight should decrease linearly if the solvent concentration and the rate of initiation are held constant. Further, it should be possible to compare the kinetic results with those obtained from light-scattering measurements on the same polymers.

PREPARATION OF SAMPLES

The polymer samples were prepared as described in Table I of Part I.[1] Light-scattering determinations of the weight-average molecular weight

were determined as described in Part III.[5] The results are tabulated in Table I.

TABLE I
Effect of Conversion on Molecular Weight of PAN

Conversion, %	$[\eta]$, dl./g.[a]	$\bar{M}_w \times 10^{-5}$
6.90	3.21	4.27
6.90	3.18	—
14.81	3.04	4.17
27.13	2.93	3.96
46.78	2.91	4.00
71.53	2.56	3.05

[a] Measured in DMF at 25°C.

EVALUATION OF KINETIC CONSTANTS

The intrinsic viscosity–weight-average molecular weight equation for ethylene carbonate-polymerized polyacrylonitrile in dimethylformamide at 25°C. is[5]

$$[\eta] = 6.98 \times 10^{-4} \, \bar{M}_w^{0.645}$$

Further it is obvious from Figure 1 of Part III[5] that conversion has no effect upon this equation.

Examination of eqs. (14) and (15) shows that the various kinetic constants can be evaluated provided that the mode of termination is either known or assumed, and provided that the conversion is kept sufficiently low. If termination is solely by disproportionation, k_3', $\bar{M}_w/\bar{M}_n = 2$. If termination is solely by recombination, k_3, and further if the transfer terms $k_4[M]$ and $k_5[S]$ are then negligible when compared to the initiation term $Ik_3/2$, then $M_w/M_n = 1.5$. If, however, the transfer terms $k_4[M]$ and $k_5[S]$ predominate, then $\bar{M}_w/\bar{M}_n = 2$ again. For the intermediate case, between the extremes, $\bar{M}_w/\bar{M}_n$ will be between 1.5 and 2.0, and will vary with initial conditions.

In this work, it is first assumed that all termination is either pure disproportionation or pure recombination. The number-average molecular weight was calculated by assuming first that for recombination $\bar{M}_w/\bar{M}_n = 1.5$, calculating the reciprocal number-average degree of polymerization $1/\bar{P}_n$ and plotting $1/\bar{P}_n$ versus $[I_2]^{1/2}/[M]$ to evaluate the kinetic constants, eq. (14) with the assumption that $k_4 = 0$. These constants were then inserted in the $\bar{M}_w/\bar{M}_n$ equation, a new ratio was determined, and new values for the kinetic constants evaluated. The results are shown in Figure 1, where the lower solid line is calculated for termination by recombination. The upper solid line is calculated for termination by disproportionation. The dashed line of Figure 1 is the second calculation for termination by recombination. The data for Figure 1 were obtained from Part I.[1]

From the intercept, $k_5[S]/k_2[M] = 0.29 \times 10^{-4}$, the transfer constant
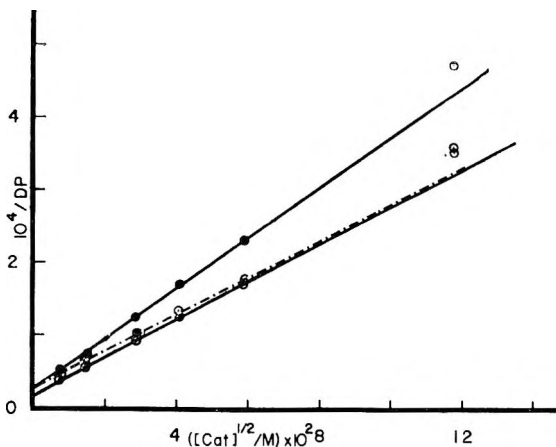
Fig. 1. Evaluation of constants of Equation 4 for acrylonitrile in ethylene carbonate at 50°C. Upper solid line is calculated from termination by disproportionation. The lower solid line is calculated from termination by recombination. The dashed line is the second calculation for termination by recombination.

to ethylene carbonate is found to be 0.073×10^{-4} at 50°C. The slope for disproportionation is $(2fk_1k_3')^{1/2}/k_2 = 3.46 \times 10^{-2}$ (moles/liter)$^{1/2}$ and the slope for recombination is $(fk_1k_3)^{1/2}/k_2 = 2.62 \times 10^{-3}$ (moles/liter)$^{1/2}$. These values will be used in eq. (20) to evaluate the effect of conversion upon molecular weight. The intercepts and slopes are identical to the work reported in the first paper of this series,[1] even though a standard value of 2.0 was taken for $\bar{M}_w/\bar{M}_n$.

EFFECT OF CONVERSION ON THE MOLECULAR WEIGHT

It is seen that either of the two sets of kinetic constants must give the same dependence on the conversion. The dependence is shown in Figure 2, where the ordinate is the calculated molecular weight. The abscissa is the extent of conversion and the data points are taken from Table I. They further are in agreement with the theoretical effect on conversion. Also, there is no apparent effect of conversion upon the intrinsic viscosity-molecular weight equation as shown in Part III.[5] All these facts point to the obvious statement that in a well-behaved system such as the one examined here the results are well behaved.

Bamford, Jenkins, and Johnson[6] and also Bevington and Eaves[7] have shown that termination is by recombination rather than by disproportionation. This is in agreement with the observation that the transfer-to-monomer and the transfer-to-polymer reactions are negligible because all three reactions involve proton transfers.

By comparison with the formulas derived earlier, it is possible, however, to show that if the transfer-to-monomer and the transfer-to-polymer reactions are of equal velocity, then no new molecules would be formed during the course of polymerization owing to initiation of the transfer-to-
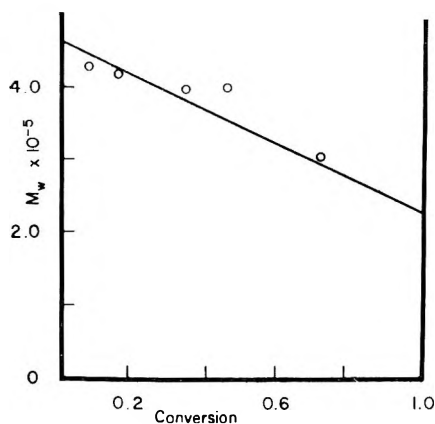
Fig. 2. Influence of conversion upon molecular weight of polyacrylonitrile. The circles are experimental points from Table I. The solid line is that calculated from the results of Figure 1.

polymer type reaction. If these two reactions do occur and are small, the effect on the conversion, similar to Figure 2, cannot be determined experimentally. Furthermore, branching reactions would become appreciable only at high conversion.[4b] If, however, the transfer reactions are appreciable, not only would a different slope be obtained in Figure 2, but also transfer reactions would be observable from such plots as the reciprocal degree of polymerization versus the square root of catalyst concentration divided by monomer. The conclusion is, therefore, that unless transfer to polymer is very different from transfer to monomer, neither reaction occurs appreciably in the solution polymerization of acrylonitrile.

It has been assumed that one reason that stereospecific acrylonitrile could not be obtained is that the hydrogen atom α to the nitrile group is labile and can form an imide with the nitrile as shown in (21)

$$\text{(21)}$$
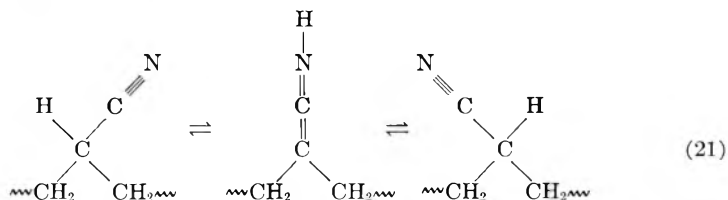
If this hydrogen is labile, then transfer to polymer should occur but it was not evident in this work. Therefore, it must be concluded that the above mechanism does not explain why stereospecific polyacrylonitrile is difficult to obtain.

CONCLUSION

Reactions which involve a transfer of a proton from acrylonitrile, polyacrylonitrile, or the growing free radical to a free radical are at a

minimum in the solution polymerization of acrylonitrile.   If these reactions are neglected in the kinetics of the polymerization, then there is a linear dependence of the weight-average molecular weight upon the extent of conversion.   Measurements on samples obtained at different extents of conversion confirm this dependence.   Hence, there should be very little branch formation in polyacrylonitrile prepared in solution at 50°C.

Mr. R. F. Crafts performed the polymerizations and determined the molecular parameters.

References

1. Peebles, L. H., *J. Polymer Sci.*, **A3,** 341 (1965).
2. Bamford, C. H., W. G. Barb, A. D. Jenkins, and P. F. Onyon, *Kinetics of Vinyl Polymerization by Radical Mechanisms*, Academic Press, New York–London, 1958.
3. Bamford, C. H., and H. Tompa, *J. Polymer Sci.*, **10,** 345 (1953); *Trans. Faraday Soc.*, **50,** 1097 (1954).
4. Flory, P. J., *Principles of Polymer Chemistry*, Cornell Univ. Press, Ithaca, N. Y., 1953, (a) p. 318; (b) p. 385.
5. Peebles, L. H., *J. Polymer Sci.*, **A3,** 361 (1965).
6. Bamford, C. H., A. D. Jenkins, and R. Johnston, *Trans. Faraday Soc.*, **55,** 179 (1959).
7. Bevington, J. C., and D. E. Eaves, *Trans. Faraday Soc.*, **55,** 1777 (1959).

Résumé

Le premier article de cette série montrait que, lors de la polymérisation de l'acrylonitrile dans le carbonate d'éthylène, la réaction de transfert sur monomère est négligeable et le solvant agit seulement comme diluant et comme agent de transfert. De plus la vitesse de polymérisation est du premier ordre jusqu'à des degrés de conversion assez élevés même lorsque le milieu de polymérisation devient très visqueux. Ces observations permettent le calcul de l'effet du degré de conversion sur le poids moléculaire moyen du polymère. Les constantes intervenant dans ce calcul ont été déterminées à partir des données pour la polymérisation à basse conversion et appliquées à des taux de conversion élevés. Le poids moléculaire moyen calculé en fonction du degré de conversion est en accord avec le poids calculé et indique que las réactions de transfert sur polymère sont probablement très peu nombreuses. Donc le degré de ramification du polyacrylonitrile préparé en solution est également très faible même à dex taus de conversion élevés.

Zusammenfassung

In der ersten Mitteilung dieser Reihe wurde gezeigt, dass bei der Polymerisation von Acrylnitril in Äthylencarbonat die Übertragung zum Monomeren vernachlässigbar ist und das Lösungsmittel nur als Verdünnungsmittel und Überträger wirkt. Ausserdem ist die Polymerisationsgeschwindigkeit bis zu recht hohen Umsätzen von erster Ordnung, obwohl das Polymerisationsmedium eine hohe Viskosität entwickelt. Diese Beobachtungen erlauben eine Berechnung des Einflusses des Umsatzes auf das mittlere Molekulargewicht des Polymeren. Die Konstanten für diese Berechnung wurden aus Polymerisationsversuchen bei kleinem Umsatz ermittelt und auf den Fall des hohen Umsatzes angewendet. Der als Funktion des Umsatzes gemessene Gewichtsmittelwert des Molekulargewichts stimmt mit der Berechnung überein und zeigt, dass wahrscheinlich die Übertragung zum Polymeren sehr gering ist. Daher ist das Ausmass der Verzweigung bei in Lösung dargestelltem Polyacrylnitril sogar bei hohem Umsatz ebenfalls sehr klein.

Polyacrylonitrile Prepared in Ethylene Carbonate Solution.   III. Molecular Parameters*

L. H. PEEBLES, *Chemstrand Research Center, Inc., Durham, North Carolina*

Synopsis

The intrinsic viscosity–molecular weight equation for polyacrylonitrile polymerized in ethylene carbonate by an azo catalyst is $[\eta] = 6.98 \times 10^{-4} \bar{M}_w^{0.645 \pm 0.036}$ dl./g. at 25°C. in DMF.   The flexibility of the chain is found to be between that of poly(vinyl acetate) and a polycarbonate.   The intrinsic viscosity decreases as the temperature is increased. This is shown to be due to two processes which occur simultaneously: A decrease in the polymer radius and an increase in the polymer–solvent interaction.   The decrease in the radius overrides the increased solvent attraction.   Comparison of the data with those of Fujisaki and Kobayashi suggests that polymers prepared by the aqueous redox and the homogeneous azo polymerization processes are different.

INTRODUCTION

Previous work on the determination of the weight-average molecular weight of polyacrylonitrile by light-scattering techniques indicated that the polymer contained a considerable amount of branching because of the presence of microgel.[1]   The polymers thus examined were prepared by heterogeneous polymerization carried to quite high conversions.   Recent work[2,3] has shown that homogeneous polymerization of acrylonitrile in ethylene carbonate produces a white polymer with a very low amount of fluorescence in contrast to the more highly colored and more fluorescent solutions examined earlier.   These whiter polymers require fewer corrections and introduce less error in the light-scattering determination of the molecular parameters.

EXPERIMENTAL

The polymers were prepared as described in Part I.[2]   Light-scattering determinations were made in a Brice-Phoenix light-scattering photometer which had been modified according to Dandliker and Kraut[4] to permit ultracentrifugation of the solutions directly in the light-scattering cells. This method effectively eliminates disturbances caused by dust.   The nosepiece slit system was modified so that the phototube did not see beyond the edges of the incident light beam.[5]   The intensity of fluoresced

* Presented in part at the 18th Congress of Pure and Applied Chemistry, Montreal, Canada, August 1961.

light was subtracted from the total observed light intensity by the procedure of Brice, Nutting, and Halwer.[6] The photometer was calibrated by 0.5% Cornell Standard polystyrene in toluene with an assumed turbidity of 0.00352 cm.$^{-1}$ for 436 mμ light. The value of H was calculated to be 2.00×10^{-6}. The Zimm-type diagrams were treated by a least-squares procedure to estimate the value for zero concentration at each angle. These estimates were then used to estimate the intercept at zero angle, again by a least-squares procedure.

Viscosity measurements were performed in Cannon-Fenske viscometers at 25°C. in dimethylformamide (DMF). The solvent flow times were greater than 100 sec., so kinetic energy corrections were not applied.

Dimethylformamide (DMF) was purified by distillation at atmospheric pressure.

TABLE I
Molecular Parameters of PAN Samples Polymerized in Ethylene Carbonate

$[\eta]$, dl./g.	$\bar{M}_w \times 10^5$	R_z, A.	$A_2 \times 10^4$	Conversion, %
Polymers polymerized to low conversion at 50°C.				
7.51	13.8 (14.8)	886 (820)	9.5 (12.3)	10.7
6.80	13.8	878	12.9	10.9
6.14	12.2	812	11.9	11.6
4.20	7.46	618	14.3	12.7
3.21	4.27	436	16.1	6.9
3.04	4.17	430	—	14.8
1.22	1.14	237	21.0	20.4
Polymers polymerized at various conversions at 50°C.				
3.21	4.27	436	16.1	6.9
3.04	4.17	430	15.4	14.8
2.93	3.96	404	18.4	27.1
2.91	4.00	437	—	46.8
2.56	3.05	358	14.7	71.5
Polymers polymerized to low conversion at 60°C.				
8.31	23.0	1144	11.6	12.2
6.14	16.4	948	13.5	11.6
2.79	4.59	464	18.4	7.5
1.57	1.59	216	19.4	25.8
1.19	0.996	246	17.8	10.6
1.09	0.824	207	15.8	23.2
Polymers prepared at 80°C.; each sample reacted for 1 hr.				
5.39	11.6	768	14.8	4.3
5.05	11.3	813	15.1	11.3
2.69	3.96	416	17.6	19.3
2.56	3.06	387	15.8	22.1
1.45	1.48	275	18.4	23.0
Polymer polymerized at 39°C.				
5.32	11.5	797	14.4	10.3

RESULTS

Table I presents the results of this investigation. The z-average radius of gyration was computed from the formula

$$R_z{}^2 = 3\lambda^2 \text{ (slope)}/16n^2\pi^2 \text{ (intercept)} \tag{1}$$

The second virial coefficient, A_2, was evaluated at 90°C.

DISCUSSION

Table I and Figure 1 contain data obtained from polymers prepared at 50, 60, and 80°C. in ethylene carbonate. The intrinsic viscosity-weight-average molecular weight equation* is

$$[\eta] = 6.98 \times 10^{-4} \, \bar{M}_w{}^{0.645\pm0.036} \tag{2}$$

(in deciliters/gram) at 25°C. in DMF.

Figures 2–4 show $(R_z)^2$, $(R_z)^3/[\eta]$, and A_2 plotted against $\bar{M}_w$. In all cases, after eliminating those values below a molecular weight of 3×10^5,
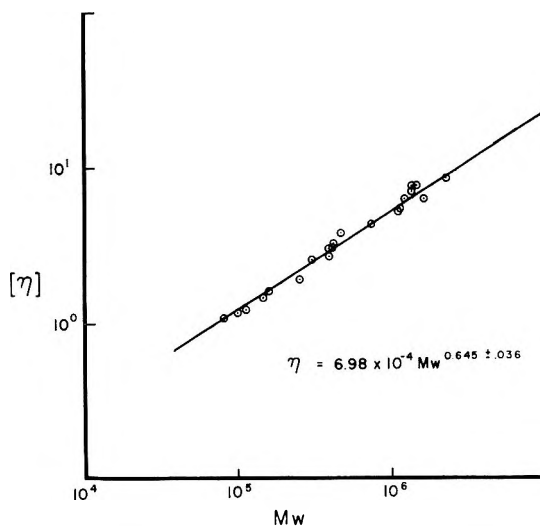
Fig. 1. Intrinsic viscosity–weight-average molecular weight data for polyacrylonitrile prepared in ethylene carbonate.

each plot is reasonably linear in molecular weight. Further, the slope of the $(R_z)^3/[\eta]$ versus $\bar{M}_w$ plot (Fig. 3) after correction for polydispersity,[7] predicts a Flory Φ parameter of 2.5×10^{21} which is in excellent agreement with the general literature. The plot of $R_z{}^2$ versus $\bar{M}_w$ (Fig. 2) does not intersect the origin because $R_z{}^2$ is in fact proportional to $\bar{M}_w{}^{1+\epsilon}$, where

---

* Earlier conclusions on this work were reported in reference 8. In the abstract it was stated that the polymer prepared at 60°C. followed a different viscosity–molecular weight equation from the polymers prepared at 50°C. Examination of the composite data at 50, 60, and 80°C. shows that the earlier conclusion is incorrect.
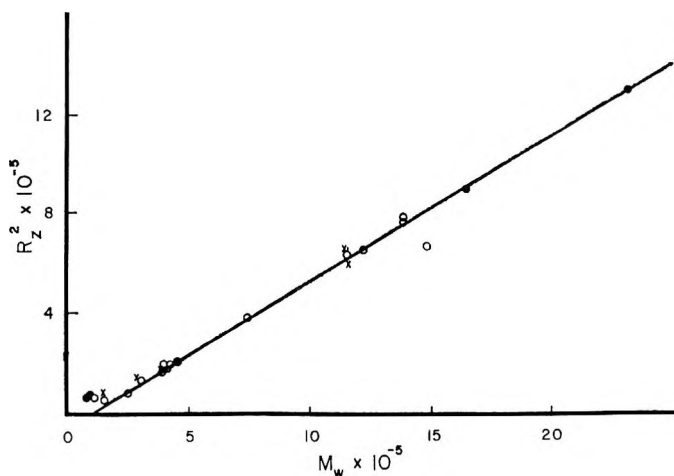
Fig. 2. Dependence of the square radius of gyration upon the molecular weight. Polymers were prepared at 39°, ◊ ; 50°, ○; 60°, ●; 80°, ×.
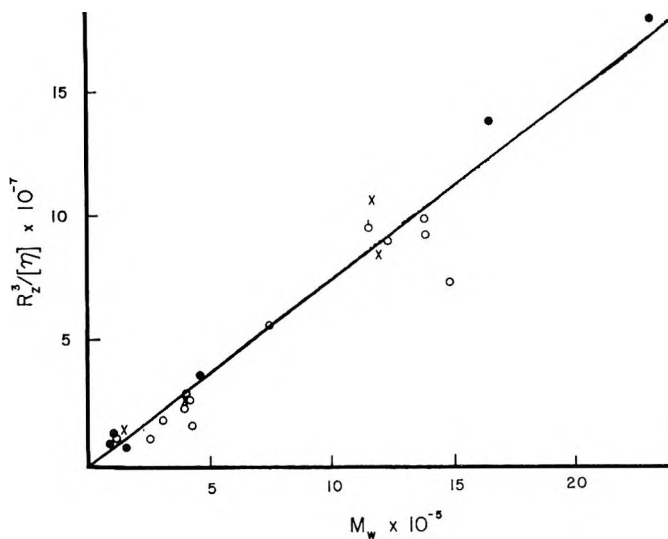
Fig. 3. Dependence of $(R_z)^3/[\eta]$ upon molecular weight. The slope is proportional to the Flory constant Φ. Symbols described under Figure 2.

ϵ differs from zero because the measurements were not made in a theta solvent. The value of ϵ is 0.15 for the data in Table I.

It would be interesting to compute $(R_z^2/\overline{M}_w)_\Theta$ for theta conditions, in order to determine the stiffness of the chain. The values of A_2 and $\overline{M}_w$ are too large to permit direct calculation of either $[\eta]_\Theta$ or $(R_z)_\Theta$ by the theories of Krigbaum,[9] Orofino and Flory,[10] Kurata and Yamakawa,[11] and by Zimm, Stockmayer, and Fixman.[12] Examination of fractions would not give any better results because the primary effect is that of A_2 and $\overline{M}_w$, not of polydispersity.
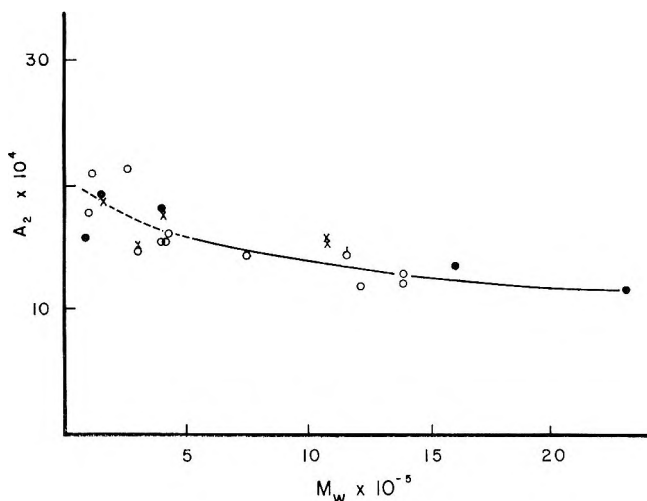
Fig. 4. Dependence of the second virial coefficient upon the molecular weight.

With the above comments kept in mind, it is instructive to compare the calculated root-mean-square separation of the chain ends $(\overline{r_0^2})^{1/2}$ for a series of different polymers at a given and sufficiently low molecular weight under theta conditions. Polycarbonate is a fairly "stiff" molecule but less so than that of the polysaccharides. Poly(vinyl acetate) is considered a fairly flexible molecule. Since R_z is the radius of gyration, it must be converted to r_0 by

$$(\overline{r_0^2})^{1/2} = \sqrt{6}\, R_z(z + 1)/(z + 2) \qquad (3)$$

where z is a measure of the breadth of the molecular weight distribution. For these polymers, z is approximately unity and therefore $(\overline{r_0^2})^{1/2}$ is just $2R_z$. The theory of Zimm, Stockmayer, and Fixman[12] predicts that near theta conditions

$$(\overline{r_0^2})^{3/2} = (\overline{r^2})^{3/2} - 2.2 \times 10^{-24} A_2 \overline{M}_w^2 \qquad (4)$$

where r is in centimeters and A_2 is in cm.³-mole/g.². Since R_z has been shown to depend on $M^{1.15}$, the effect of ϵ must be eliminated by application of eq. (5)

$$(\overline{r^2})_{corr} = (\overline{r^2})[1 + (5\epsilon/6) + (\epsilon^2/6)] \qquad (5)$$

Examination of Table II shows that the stiffness of PAN lies between that of polycarbonate and that of poly(vinyl acetate).*

Essentially the same value $(\overline{r^2})_{corr}$ is obtained by the application of the Stockmayer-Fixman[13] relation

$$[\eta]/M^{1/2} = K_\Theta + 0.51\Phi B M^{1/2}$$

* The author is indebted to Dr. H. A. Ende for pointing out the above approach.

TABLE II
Values of $(\overline{r^2})^{1/2}_{corr}$ for $M_w = 10^5$

Polymer	Solvent	$A_2 \times 10^3$, cm.^{3}-mole/g.^{2}	$(\overline{r^2})^{1/2}$, A.	$(\overline{r^2})^{1/2}_{corr}$, A.
Polycarbonate[a]	Tetrahydrofuran	0.84	460	429
Polycarbonate	Methylene dichloride	1.16	520	488
Cellulose trinitrate[b]	Ethyl acetate	3.3	—	447
	Acetone	2.6	—	376
Polyacrylonitrile	DMF	1.45	413	338
Poly(vinyl acetate)[c]	Butanone	0.5	245	243

[a] Data of Schulz and Horbach.[17]
[b] Data of Krigbaum.[18]
[c] Data of Shultz[7] and Howard.[19]

to the data. Here, K_Θ is the constant in the equation

$$[\eta] = K_\Theta M^{1/2} \alpha^3$$

when the expansion coefficient α is unity, and further

$$K_\Theta = \Phi(\overline{r_0^2}/M)^{3/2}$$

In the present case, for $\Phi = 2.8 \times 10^{21}$, $K_\Theta = 3.46 \times 10^{-3}$, and $B = 1.04 \times 10^{-25}$, all units are expressed in deciliters per gram. The data of Fujisaki and Kobayashi[14] can be analyzed in a similar manner. The results are $K_\Theta = 3.55 \times 10^{-3}$, $B = 4.36 \times 10^{-25}$.

Both sets of data give the same K_Θ value, within experimental error, but different B values. This discrepancy is attributed to the fact that Fujisaki and Kobayashi found a different $[\eta]$–$\overline{M_w}$ relation from our relation.

Hunter[15] has shown that the intrinsic viscosity of PAN decreases with an increase in temperature.

The intrinsic viscosities of two polymers of different molecular weights have been measured at 0 and 60°C. (Table III). Both values of K_Θ are below the average value given earlier for 25°C. but are consistent within themselves; because we are interested in the influence of temperature on K_Θ and not in the best value of K_Θ, the discrepancy is not important for the argument. The value of K_Θ is found to decrease with an increase in temperature whereas the expansion coefficient increases as temperature increases. Thus, there are two opposing effects: an increase in the polymer–solvent interaction, as shown by the increase in α, and a decrease in polymer–polymer repulsion, as shown by the decrease in K_Θ, both of which occur with an increase in temperature. The increasing flexibility of the molecule overrides the expansion coefficient, and hence the intrinsic viscosity decreases with increasing temperature. Thus, at room temperature and below, the PAN molecule is fairly stiff, but becomes more flexible at higher temperatures.

In another paper[16] Fujisaki and Kobayashi present intrinsic viscosities of various fractions of PAN measured in different solvents and at various

TABLE III
Influence of Temperature on Intrinsic Viscosity of PAN in DMF

$[\eta]$, dl./g.	$\bar{M}_w \times 10^6$	Temp., °C.[a]	$[\eta]_\Theta$	α^3
1.56	0.159	0	1.035	1.48
1.31	0.159	60	0.676	1.90
2.97	0.396	0	1.63	1.80
2.62	0.396	60	1.068	2.46

[a] $K_\Theta = 2.6 \times 10^{-3}$ at 0°C., $K_\Theta = 1.7 \times 10^{-3}$ at 60°C.

temperatures. Because the molecular weights of the fractions presented in their tables were calculated from the expression for the viscosity in DMF at 35°C.:

$$[\eta] = 3.17 \times 10^{-4}\bar{M}_w^{0.750}$$

a plot of $[\eta]/M^{1/2}$ versus $M^{1/2}$ is, of course, curved. If the curvature of the data is ignored, their results also show that $\overline{r_0^2}$ decreases and α increases as the temperature of the solution is increased.

The PAN samples used by Fujisaki and Kobayashi were obtained by fractionation of polymers prepared by redox catalysts in aqueous suspension. The polymers in the present study were prepared by an azo catalyst in ethylene carbonate solution. Fujisaki and Kobayashi have suggested that polymers prepared by different procedures may indeed follow different intrinsic viscosity–molecular weight equations. The samples prepared in ethylene carbonate exhibit a higher molecular weight and a higher radius of gyration for a given intrinsic viscosity than the aqueous redox samples. An apparent higher molecular weight could occur because of differences in calibration. However, instrument constants should not influence either the intrinsic viscosity or the radius of gyration. Therefore, it appears that a real difference exists between these samples. The nature of this difference is difficult to visualize because most of the normal causes for this behavior apparently are not important in polyacrylonitrile: (1) no direct evidence exists for variations in the stereoregularity; (2) the amount of both long and short chain branches should be at a minimum because of the kinetics of transfer reactions; (3) variations in the concentration of head-to-head configurations are relatively unimportant in other polymers; (4) possible copolymerization with the solvent can be excluded on the basis of the kinetics and the infrared spectra of the polymer; and (5) any considerable amount of 1,4 polymerization should be apparent from the infrared spectra and should be possible to demonstrate by hydrolysis.

References

1. Peebles, L. H., *J. Am. Chem. Soc.*, **80,** 5603 (1958).
2. Peebles, L. H., *J. Polymer Sci.*, **A3,** 341 (1965).
3. Peebles, L. H., *J. Polymer Sci.*, **A3,** 353 (1965).
4. Dandliker, W. B., and J. Kraut, *J. Am. Chem. Soc.*, **78,** 2380 (1956).
5. Hermans, J. J., and S. Levinson, *J. Opt. Soc. Am.*, **41,** 460 (1951).
6. Brice, B. A., G. C. Nutting, and M. Halwer, *J. Am. Chem. Soc.*, **75,** 824 (1953).
7. Shultz, A. R., *J. Am. Chem. Soc.*, **76,** 3422 (1954).
8. Peebles, L. H., paper presented at 18th International Congress of Pure and Applied Chemistry, Montreal, Canada, August 1961; *Abstracts* No. B4-11.
9. Krigbaum, W. R., *J. Polymer Sci.*, **28,** 213 (1958).
10. Orofino, T. A., and P. J. Flory, *J. Chem. Phys.*, **26,** 1067 (1957).
11. Kurata, M., and H. Yamakawa, *J. Chem. Phys.*, **29,** 311 (1958).
12. Zimm, B. H., W. H. Stockmayer, and M. Fixman, *J. Chem. Phys.*, **21,** 1716 (1953).
13. Stockmayer, W. H., and M. Fixman, *J. Polymer Sci.*, **C1,** 137 (1963).
14. Fujisaki, Y., and H. Kobayashi, *Kobunshi Kagaku*, **19,** 73 (1962).
15. Hunter, W. L., paper presented at American Chemical Society Southeast-Southwest Regional Meeting, Dec. 7, 1961, New Orleans, La.
16. Fujisaki, Y., and H. Kobayashi, *Kobunshi Kagaku*, **19,** 81 (1962).
17. Schulz, G. V., and A. Horbach, *Makromol. Chem.*, **29,** 93 (1959).
18. Krigbaum, W. R., *J. Polymer Sci.*, **28,** 213 (1958).
19. Howard, R. O., Thesis, Mass. Institute of Technology, 1953.

Résumé

L'équation qui relie la viscosité intrinsèque au poids moléculaire du polyacrylonitrile polymérisé dans le carbonate d'éthylène au moyen d'un catalyseur azo est la suivante: $(\eta) = 6.98 \times 10^{-4} \bar{M}_w^{0.645 \pm 0.036}$ dl/g à 25°C dans le DMF. On trouve que la flexibilité de la chaîne se situe entre celle de l'acétate de polyvinyle et d'un polycarbonate. La viscosité intrinsèque diminue par augmentation de la température. Cela est dû à deux processus qui ont lieu simultanément: une diminution du rayon du polymère et une augmentation de l'interaction polymère–solvant. La diminution du rayon est supérieure à l'augmentation d'attraction du solvant. La comparaison des résultats avec ceux de Fujisaki et Kobayashi suggère que les polymères préparés par polymérisation redox en milieu aqueux et par polymérisation avec un catalyseur azo en milieu homogène sont différents.

Zusammenfassung

Die Viskositätszahl-Molekulargewichtbeziehung für in Äthylencarbonat mit einem Azostarter hergestelltes Polyacrylnitril lautet [η] 6,98 $\times$ $10^{-4} \bar{M}_w^{0,645 \pm 0,036}$ dl./g. bei 25°C. in DMF. Die Biegsamkeit der Kette liegt zwischen der von Polyvinylacetat und einem Polycarbonat. Die Viskositätszahl nimmt mit steigender Temperatur ab. Das wird auf zwei gleichzeitig verlaufende Prozesse zurückgeführt. Eine Abnahme des Polymerradius und eine Zunahme der Polymer lösungsmittelwechselwirkung. Die Abnahme des Radius überweigt die erhöhte Lösungsmittelnziehung. Ein Vergleich der Ergebnisse von Fujisaki und Kobayashi zeigt, dass sich die mit einem wässrigen Resoxsystem dargestellten Polymeren von den im homogenen Azopolymerisationsprozess unterscheiden.

An Improved Method of Calculating Copolymerization Reactivity Ratios*

PAUL W. TIDWELL and GEORGE A. MORTIMER, *Monsanto Company, Texas City, Texas*

Synopsis

A nonlinear least-squares method for solving for r_1 and r_2, the copolymerization reactivity ratios, is explained. This new method is superior to all other methods that have been used heretofore in the following ways: (*1*) a unique pair of values is obtained which does not depend on the judgment of the person examining the data; (*2*) this pair of values can be shown mathematically to be the best pair obtainable from the data at hand; (*3*) the errors are quantitatively defined in meaningful terms; and (*4*) the data are checked to see how well they fit the copolymer equation. A basis for selecting experimental conditions which will provide data from which precise values of the reactivity ratios can be obtained is explained, and experimental conditions appropriate for obtaining these precise values over a wide range of r_1, r_2 values are presented in tabular form.

INTRODUCTION

During the course of copolymerization studies at this laboratory and elsewhere,[1] it became evident that the existing methods for computing the copolymerization reactivity ratios were not entirely satisfactory. We were cognizant of the existence of four methods for computing these ratios; for convenience sake we have denoted these methods as (*1*) approximation, (*2*) curve fitting, (*3*) intersection, and (*4*) linearization. While each of these methods is different, they all share the common failing of relying on a subjective weighting of the data in the evaluation of the reactivity ratios. As a consequence of a subjective weighting process, different observers, in evaluating the same data, may obtain similar but different values for the reactivity ratios, even when they use the same method. Further, the existing methods provide no means of establishing how well these reactivity ratios are determined, i.e., they furnish no quantitative error limits for the computed values.

It is the intent of this paper to discuss and illustrate a method for calculating the copolymerization reactivity ratios which circumvents the difficulties inherent in the other methods. We shall also show that this calculation procedure complements the existing and accepted experimental procedures.

EVALUATION OF EXISTING PROCEDURES

In the discussion to follow, we have adopted the following notation (where $u = 1,2$): M_u = the mole fraction of monomer u in the reaction system, m_u = the mole fraction of monomer u in the polymer composed entirely of the two monomers, and r_u = the monomer reactivity ratio.

It is clear that for an equation involving m_1, m_2, M_1, M_2, r_1, and r_2 such as equation (3) below, permuting the subscripts 1 and 2 yields an equation which is equally valid, hence the ensuing discussion will be limited to a single case.

The Approximation Method

The approximation method depends on the fact that at low concentrations of M_2, the composition of the copolymer is almost entirely dependent on r_1. Under these circumstances,

$$r_1 \simeq M_2/m_2 \tag{1}$$

While a single experiment will provide an approximate value for r_1, the limitations of this method are numerous. Extremely sensitive analytical procedures are required to determine the quantity m_2 of the copolymer. If $r_u < 0.1$, or $r_u > 10$, the computed r_u will be seriously biased. The method is also based on the assumption that the system under study obeys the usual copolymerization mechanism, and provides no means of independently evaluating the validity of this assumption. The method is valuable, however, since it permits the experimenter to quickly obtain approximate values for r_1 and r_2 when the Q and e values[2] for one or both of the monomers are unknown.

The Curve-Fitting Method

This method, discussed in detail elsewhere,[3] is based on the copolymer composition equation [eq. (2) below]. It is based on the assumption that if the experimental conditions are such that the monomer concentrations do not change appreciably, and if the polymer is of adequate molecular weight, then eq. (2) can adequately be represented by eq. (3).

$$dM_1/dM_2 = [M_1(r_1M_1 + M_2)]/[M_2(r_2M_2 + M_1)] \tag{2}$$

$$m_1/m_2 = (r_1M_1^2 + M_1M_2)/(r_2M_2^2 + M_1M_2) \tag{3}$$

This method consists of preparing a graph of the observed concentration m_2 in the copolymer versus M_2 and then drawing the curve represented by eq. (3) on the graph for selected values of r_1 and r_2. If in the opinion of the experimenter this curve does not agree with the experimentally obtained points, another pair of values of r_1 and r_2 is selected, and a second curve is drawn. This is done repeatedly until the curve appears to pass through or "near enough to" a sufficient number of the observed points that the experimenter is satisfied with the fit.

One advantage of this method is that it provides the observer with a

visual check on the validity of the assumption that the model describes the observed physical phenomena, since the data used are generally collected over the whole range of monomer compositions. A second advantage is that it provides a qualitative measure of the experimental error even in the absence of repeated runs if one is willing to assume adequacy of the model. Finally in some cases it provides a qualitative measure of how well the reactivity ratios are estimated. Unfortunately the method may require extensive calculations, and, as noted above, provides only a qualitative measure of the precision of the estimates of r_1 and r_2. Further, the observer is required subjectively to weight the data, a task not consistently done even by the same observer.

The Intersection Method

Equation (3) can be rearranged to yield

$$r_1 = r_2(m_1 M_2{}^2/m_2 M_1{}^2) + (M_2/M_1)[(m_1/m_2) - 1] \qquad (4)$$

Treating $m_1 M_2{}^2/m_2 M_1{}^2$ and $(M_2/M_1)[(m_1/m_2)-1]$ as the slope and intercept, one can plot for each experiment a different straight line, where r_1 represents the ordinate and r_2 represents the abscissa. In the absence of experimental error these lines intersect at a point in the r_1, r_2 plane. This method, originated by Mayo and Lewis,[4] has been fully discussed elsewhere[3,5] and has the same limitations as the curve fitting method.

The Linearization Method

Fineman and Ross[6] rearranged eq. (3) to eq. (5):

$$M_1(m_2 - m_1)/M_2 m_1 = (-m_2 M_1{}^2/m_1 M_2{}^2)r_1 + r_2 \qquad (5)$$

Consequently if one graphs $M_1(m_2 - m_1)/M_2 m_1$ versus $-m_2 M_1{}^2/m_1 M_2{}^2$, the slope of the straight line is r_1 and the intercept is r_2. This method has not received as much attention in the literature as the preceding three. Briefly, this method has the same advantages and disadvantages as the intersection and curve fitting methods.

While it is not the primary purpose of this paper to evaluate the various methods of estimating the reactivity ratios, a brief evaluation of the linearization method is given in the Appendix.

NONLINEAR LEAST-SQUARES METHOD

The method we describe below is a modification or extension of the curve fitting method; it differs from the curve-fitting method in that the values of r_1 and r_2 satisfy the criterion that, for the selected values of these ratios, the sum of the squares of the differences between the observed and computed polymer compositions is minimized. In this sense, the values obtained are unique since, for a given body of data, any person or set of persons following the calculation scheme outlined below will arrive at the same values of r_1 and r_2. Further, this method provides a means of evaluat-

ing how well the reactivity ratios have been estimated as well as a means of determining if the data are consistent with the assumption that the copolymerization equation describes the relationship between monomer and polymer composition.

Briefly, the method consists of the following: given initial estimates of r_1 and r_2, a set of computations is performed which, on repetition, rapidly leads to a pair of values of the reactivity ratios which yields the minimum value of the sum of the squares of the differences between the observed and computed polymer composition.

Using the copolymer composition equation in the form due to Skeist,[7] we let m_{2i} = the observed mole fraction of M_2 in the polymer resulting from the ith experimental run, M_{2i} = the initial mole fraction of M_2 used in the ith experiment, $1\text{-}M_{2i} = M_{1i}$ = the initial mole fraction of M_1 used in the ith experiment, $r_1{}^j$ = the jth estimate of r_1, $r_2{}^j$ = the jth estimate of r_2, and $i = 1, 2, 3, \ldots, n$.

Let

$$G^j = G(M_2;\ r_1{}^j\ r_2{}^j) = (r_2{}^j M_2{}^2 + M_2 M_1)/(r_2{}^j M_2{}^2 + 2M_1 M_2 + r_1{}^j M_1{}^2) \quad (6)$$

Then let $G_i{}^j, \partial G_i{}^j/\partial r_1$, and $\partial G_i{}^j/\partial r_2$ be the values of $G(M_2;\ r_1{}^j,\ r_2{}^j)$ and its first partial derivatives evaluated at each of the n experimental runs for the jth set of estimates of r_1 and r_2. Then approximately

$$m_{2i} = G_i{}^j + \partial G_i{}^j/\partial r_1(r_1{}^0 - r_1{}^j) + \partial G_i{}^j/\partial r_2(r_2{}^0 - r_2{}^j) + \epsilon_i \quad (7)$$

where ϵ_i is a random variable with properties as discussed below, and $r_1{}^0$ and $r_2{}^0$ are the expectations of $r_1{}^j$ and $r_2{}^j$, respectively. Then if one computes the least-squares estimates of β_1 and β_2 for the equation

$$d_i = m_{2i} - G_i{}^j = \beta_1 \partial G_i{}^j/\partial r_1 + \beta_2 \partial G_i{}^j/\partial r_2 + \epsilon_i \quad (8)$$

the least-squares estimates, $\hat{b}_1$ and $\hat{b}_2$ of β_1 and β_2, provide corrections such that $r_1{}^{j+1} = r_1{}^j + \hat{b}_1$ and $r_2{}^{j+1} = r_2{}^j + \hat{b}_2$ will (or should) when substituted for $r_1{}^j$ and $r_2{}^j$ in eq. (8) decrease the value of $\Sigma(d_i)^2$.

To this point we have described the well known Gauss-Newton nonlinear least-squares procedure. It is customary, on obtaining the estimates

$$r_1{}^{j+1} = r_1{}^j + \hat{b}_1$$

and

$$r_2{}^{j+1} = r_2{}^j + \hat{b}_2$$

to repeat the above calculations until $\Sigma(d_i)^2$ is reduced to its minimum value, thus obtaining on the last iteration the least-squares estimates $\hat{r}_1$ and $\hat{r}_2$. Unfortunately the rate of convergence of this procedure is often slow, and not infrequently it diverges unless the initial estimates are reasonably close to the least-squares estimates. A modification of the above procedure due to Box[8] assures that, under some very liberal assumptions, the method will converge.[9] Further it has been our observation that the use of this modification in this case greatly accelerates the rate of convergence.

The modification by Box consists of the following:
Evaluate

$$S_h = [\Sigma(d_i)^2]_h$$

for

$$r_1 = r_1{}^j + [(h-1)/2]\hat{b}_1$$

and

$$r_2 = r_2{}^j + [(h-1)/2]\hat{b}_2$$

where $h = 1, 2, 3$.
Let

$$V = 1/2 + (S_1 - S_3)/[4(S_1 - 2S_2 + S_3)]$$

Compute $S_4 = [\Sigma(d_i)^2]_4$ for $r_1 = r_1{}^j + V\hat{b}_1$ and $r_2 = r_2{}^j + V\hat{b}_2$. Then if $S_4 < S_1$, repeat the process using in place of $r_1{}^j$ and $r_2{}^j$ the new estimates $r_1{}^{j+1} = r_1{}^j + V\hat{b}_1$ and $r_2{}^{j+1} = r_2{}^j + V\hat{b}_2$. If $S_4 > S_1$, then reevaluate V after first halving $\hat{b}_1$ and $\hat{b}_2$.

Three iterations of the calculations are illustrated in Table I using the data of Chapin, Ham, and Fordyce[10] for the system, M_1 = vinyl chloride and M_2 = methyl acrylate. A total of five iterations were required to reduce $\Sigma(d_i)^2$ to its minimum value (eight-decimal place accuracy). These results are summarized in Table II, where $r_1{}^j$ and $r_2{}^j$ for $j = 1$ were obtained from the paper by Chapin, Ham, and Fordyce.[10]

It is clear from the data in Tables I and II that after the second iteration only minor adjustments are made in the estimates of r_1 and r_2. Our experience has been that if reasonably good initial estimates are used, three iterations bring one sufficiently close to the least-squares estimates so that additional calculations are seldom justified.

While we have not discussed herein the case where the conversion of monomer to polymer is appreciable, if the extent of the conversion is sufficient to clearly invalidate the assumption that eq. (3) will adequately describe the polymer composition, then, if the final monomer concentrations or the conversion is accurately known, the computed polymer composition for each pair of initial conditions, $M_1{}^0$ and $M_2{}^0$ (expressed as moles), can be obtained from the solution of the following pair of differential equations:

$$-dM_1/d\phi = (r_1)(M_1) + (M_2)$$

and

$$-dM_2/d\phi = (M_2)[1 + (r_2)(M_2)/(M_1)]$$

where ϕ is a dummy integration variable.

Evaluation of the first partial derivatives for this case can be done by numerical methods by utilizing the fact that if $m(M_1{}^0, M_2{}^0, C; r_1, r_2)$ represents the solution of the above set of equations for a particular pair of values

TABLE I

Illustration of the Calculation Scheme

M_1	M_2	m_2	1st Iteration			2nd Iteration			3rd Iteration		
			$10^2(d)$	$\partial G^1/\partial r_1$	$10^2(\partial G^1/\partial r_2)$	$10^2(d)$	$\partial G^2/\partial r_1$	$10^2(\partial G^2/\partial r_2)$	$10^2(d)$	$\partial G^3/\partial r_1$	$10^3(\partial G^3/\partial r_3)$
0.925	0.075	0.441	−1.984 3872	−1.514 2927	1.164 6881	−2.073 1045	−1.452 0092	1.112 8040	−2.033 2361	−1.445 3189	1.109 4550
0.846	0.154	0.699	5.461 0395	−0.864 6152	1.581 0642	4.540 9746	−0.832 0270	1.461 2437	4.510 7696	−0.829 3356	1.454 5748
0.763	0.237	0.753	0.330 0674	−0.476 7343	1.535 6736	−0.794 9410	−0.453 9674	1.375 9614	−0.848 6722	−0.452 3968	1.367 1520
0.674	0.326	0.828	0.756 3530	−0.259 9714	1.331 1106	−0.310 1401	−0.244 6504	1.163 1438	−0.366 2139	−0.243 6752	1.153 8826
0.579	0.421	0.864	−0.731 8432	−0.138 4032	1.080 6690	−1.638 1489	−0.128 8666	0.925 7098	−1.687 8083	−0.128 2820	0.917 1741
0.479	0.521	0.900	−0.929 0538	−0.070 4557	0.831 5158	−1.645 2383	−0.065 0106	0.701 1529	−1.685 3377	−0.064 6845	0.693 9842
0.256	0.744	0.968	0.449 3382	−0.011 7627	0.367 2981	0.115 5395	−0.010 6984	0.309 8731	0.096 4452	−0.010 6362	0.306 2355
0.133	0.867	0.983	−0.031 0805	−0.002 4858	0.179 2849	−0.191 5019	−0.002 2481	0.146 3176	−0.200 7307	−0.002 2343	0.144 5159

	1st Iteration	2nd Iteration	3rd Iteration
$\Sigma(\partial G^j/\partial r_1)^2$	3.359 7667	3.087 4926	3.061 5429
$\Sigma(\partial G^j/\partial r_2)^2$	1.001 9418 × 10^{-3}	8.085 7241 × 10^{-4}	7.984 7157 × 10^{-4}
$\Sigma(\partial G^j/\partial r_1)(\partial G^j/\partial r_2)$	−4.421 8750 × 10^{-2}	−3.909 3209 × 10^{-2}	−3.875 6420 × 10^{-2}
$\Sigma(\partial G^j/\partial r_1)(d)$	−1.909 2007 × 10^{-2}	−1.403 8255 × 10^{-4}	−4.138 8724 × 10^{-7}
$\Sigma(\partial G^j/\partial r_2)(d)$	6.436 8377 × 10^{-4}	2.117 3434 × 10^{-6}	5.550 2101 × 10^{-7}
$\Sigma(d)^2$	3.604 3364 × 10^{-3}	3.108 6694 × 10^{-3}	3.107 4103 × 10^{-3}
b_1	6.615 6633 × 10^{-3}	7.376 9954 × 10^{-4}	−1.224 1012 × 10^{-5}
b_2	9.343 7913 × 10^{-1}	6.185 2830 × 10^{-2}	1.009 4684 × 10^{-4}
S_1	3.604 3364 × 10^{-3}	3.108 6694 × 10^{-3}	3.107 4103 × 10^{-3}
S_2	3.251 2085 × 10^{-3}	3.107 7535 × 10^{-3}	3.107 4099 × 10^{-3}
S_3	3.113 1094 × 10^{-3}	3.107 4134 × 10^{-3}	3.107 4101 × 10^{-3}
V	1.071 1179	1.045 2874	0.574 8503
S_4	3.108 6694 × 10^{-3}	3.107 4103 × 10^{-3}	3.107 4101 × 10^{-3}
r_1^{j+1}	0.090 0855	0.090 8566	0.090 8495
r_2^{j+1}	10.000 830	10.065 484	10.065 542

TABLE II
Results Obtained on Each Iteration on Data
of Chapin, Ham, and Fordyce[10]

j	$r_1{}^j$	$r_2{}^j$	$\Sigma(d_i)^2$
1	0.083	9.0	$3.604\ 3364 \times 10^{-3}$
2	0.090 0855	10.000 830	$3.108\ 6694 \times 10^{-3}$
3	0.090 8566	10.065 484	$3.107\ 4103 \times 10^{-3}$
4	0.090 8495	10.065 542	$3.107\ 4101 \times 10^{-3}$
5	0.090 8459	10.065 593	$3.107\ 4097 \times 10^{-3}$

of the reactivity ratios and conversion, C; and $m(M_1{}^0, M_2{}^0, C; \ r_1 + \Delta r_1, r_2)$ represents another such solution, then

$$\frac{\partial m(M_1{}^0, M_2{}^0, C; \ r_1, r_2)}{\partial r_1}$$

$$\simeq \frac{m(M_1{}^0, M_2{}^0, C; \ r_1 + \Delta r_1, r_2) - m(M_1{}^0, M_2{}^0, C; \ r_1, r_2)}{\Delta r_1}$$

if Δr_1 is sufficiently small. The evaluation of the first partial derivatives with respect to r_2 may be done in a similar fashion. Other methods of obtaining these derivatives, such as Stirling's, may be used to obtain more precise estimates of their numerical values.

Estimation of the Errors

If it can safely be assumed that the model fits the data and that the ϵ_i, the random error components inherent in the observed values of the m_{2i} are independently and approximately normally distributed with constant variance, σ^2, then the least-squares procedure provides a method for establishing approximate joint confidence limits within which the correct values of the reactivity ratios can be asserted to lie with probability 1-α, where α is some number in the interval $0 < \alpha < 1$.

We prefer the joint confidence limits over the simple confidence intervals, since the simple intervals frequently do not clearly convey the message of which pairs of values of the parameters are consistent with the data. This is clearly illustrated in Figure 1, where the area delimited by the rectangle contains the values of r_1 and r_2 that the simple 95% confidence intervals imply are consistent with the data, whereas only those contained within the elliptical figure are considered to be consistent with the data at the stated probability level.

The approximate $100(1 - \alpha)$ per cent joint confidence limits are delimited by the set of values r'_1 and r'_2 which satisfy the equation

$$S_c = [\Sigma(d_i)^2]_{\min} + 2s^2 F_{\alpha(2,h)} \tag{9}$$

where s^2 = an estimate of the experimental error variance, σ^2, having h degrees of freedom, $F_{\alpha(2,h)}$ = the critical value of F taken from the tabled F distribution, and

$$S_c = \Sigma(m_{2i} - G[M_{2i}; \ r'_1, r'_2])^2 \tag{10}$$
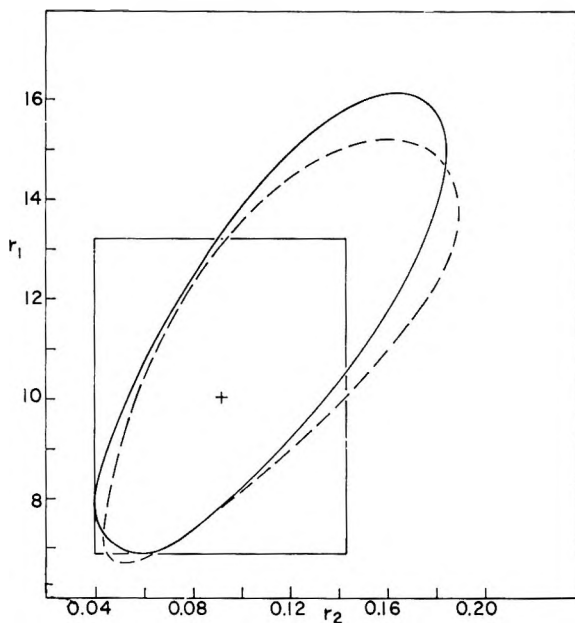
Fig. 1. Confidence limits for the system M_1 = vinyl chloride, M_2 = methyl acrylate: (+) least-squares estimate of r_1, r_2; (———) 95% confidence limits, eq. (9); (- - -) approximate 95% confidence limits, eq. (11).   Data of Chapin, Ham, and Fordyce.[10]
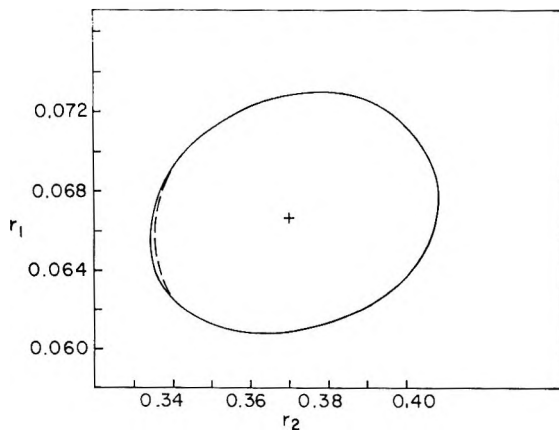
Fig. 2. Confidence limits for the system M_1 = acrylonitrile, M_2 = styrene: (+) least-squares estimate of r_1, r_2; (———) 95% confidence limits, eq. (9); (- - -) approximate 95% confidence limits, eq. (11).   Data of Thompson and Raines.[12]

In the absence of repeated observations and under the assumption that the model adequately represents the data, $s^2 = \Sigma(d_i)^2/(n-2)$ is a legitimate estimate of σ^2 and has $n-2$ degrees of freedom.[11]   Under these conditions

$$F_{\alpha(2,h)} = F_{\alpha(2, n-2)}$$

In general, the joint confidence limits are elliptical figures such as the ones shown in Figures 1, 2, and 3. With functions which are nonlinear in the parameters these confidence limits are not necessarily symmetric about the least-squares estimates. While these limits can be obtained by evaluation of eq. (10), this is clearly laborious. A satisfactory approximation to these confidence limits in this case can be obtained by the procedure outlines below if the data have been obtained under conditions similar to those outlined in the following section on planning of experiments.

TABLE III
Copolymerization Data: This Laboratory

Run no.	M_1	M_2	m_2	Conversion, %
1	0.9977	0.0023	0.0133	6.7
2	0.9972	0.0028	0.0134	6.5
3	0.9811	0.0189	0.0831	9.3
4	0.9763	0.0237	0.1110	9.0
5	0.0637	0.9363	0.8890	1.9
6	0.0613	0.9387	0.8945	3.3
7	0.0115	0.9885	0.9762	~2
8	0.0085	0.9915	0.9820	~2

Let $\ln r_1 = t_1$ and $\ln r_2 = t_2$. Then

$$G(M_2;\ r_1, r_2) = H(M_2;\ t_1, t_2)$$

$$= (e^{t_2}M_2{}^2 + M_1M_2)/(e^{t_2}M_2{}^2 + 2M_1M_2 + e^{t_1}M_1{}^2)$$

Next proceed as directed above taking derivatives with respect to t_1 and t_2 rather than r_1 and r_2. However

$$\partial H(M_2;\ t_1, t_2)/\partial t_u = r_u \partial G(M_2;\ r_1, r_2)/\partial r_u \quad (u = 1,2)$$

consequently the results shown above where the problem was solved in terms of r_1 and r_2 can be utilized. The approximation of the joint confidence limits set out in eq. (9) can therefore be obtained by solving for the values of t'_1 and t'_2 which satisfy eq. (11):

$$(t'_1 - \hat{t}_1)^2 a_{11} + 2(t'_1 - \hat{t}_1)(t'_2 - \hat{t}_2)a_{12} + (t'_2 - \hat{t}_2)^2 a_{22} = 2s^2 F_{\alpha(2,h)} \quad (11)$$

where

$$\hat{t}_u = \ln \hat{r}_u \qquad (u = 1,2)$$

$$a_{11} = (\hat{r}_1)^2 \Sigma(\partial G_i/\partial r_1)^2$$

$$a_{12} = (\hat{r}_1 \hat{r}_2)\Sigma[(\partial G_i/\partial r_1)(\partial G_i/\partial r_2)]$$

$$a_{22} = (\hat{r}_2)^2 \Sigma(\partial G_i/\partial r_2)^2$$

and $\hat{r}_1$ and $\hat{r}_2$ are the least-squares estimates of the reactivity ratios.
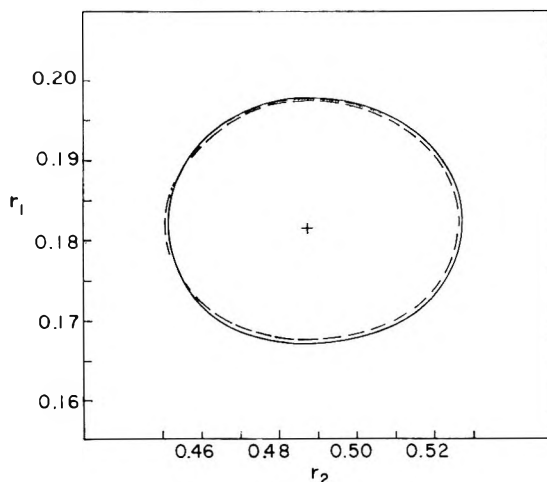
Fig. 3. Confidence limits for the data of Table III: $(+)$ least-squares estimate of r_1, r_2; (———) 95% confidence limits, eq. (9); (- - -) approximate 95% confidence limits, eq. (11)

The adequacy of this approximation of the confidence limits will be dependent to some extent on the magnitude of the experimental error and on the experimental conditions used to generate the data. If the experimental error is reasonably small and the data are collected under approximately the conditions outlined in the section on planning of experiments, then the approximation is remarkably good. This is illustrated in Figures 2 and 3.

While using either the formulation of the copolymer equation in terms of r_1 and r_2 or t_1 and t_2 will yield the same estimates when neither of the r's are zero or close to zero, we prefer the latter, since it applies the natural constraint that both r_1 and r_2 must be greater than zero. We have seen some data in the literature which, without this constraint, give a negative value for one of the reactivity ratios, a state of affairs clearly not consistent with nature. There are other reasons for fitting the data in terms of a function of the parameters, and for a discussion the reader should see the work by Beale.[11]

A computer program to make these calculations, which we shall submit to the IBM users' organization, SHARE, will be formulated with these constraints in the program.

Adequacy of the Model

If experiments have been conducted so that there are p distinct sets of experimental conditions, certain of which have been repeated so that in all there are $n = p + k$ observations, then there exists a simple test for the adequacy of the model in fitting the data. After the last iteration in the least-squares procedure, the quantity $\Sigma(d_i)^2$ represents the sum of the squares of the differences between the observed and predicted mole frac-

tions of the monomer m_2 in the polymer. If the model fits, then under the above assumptions about the nature of the experimental errors the quantity $\Sigma(d_i)^2$ will be distributed approximately as $\chi^2\sigma^2$ with $n - 2$ degrees of freedom. A second sum of squares S_e can be isolated having k degrees of freedom which measures the sum of squares of deviations of the observations from the p means at the distinct experimental conditions which, under the same assumptions, is distributed as $\chi^2\sigma^2$ with k degrees of freedom.

By subtraction we may now obtain a sum of squares S_w which, adopting the usual linear approximation, is distributed as $\chi^2\sigma^2$ with $p - 2$ degrees of freedom. When the model does not fit, $\Sigma(d_i)^2$ and hence S_w will become inflated, but S_e will remain unaffected. Consequently an approximate test for the adequacy of the model is supplied by the ratio

$$k[\Sigma(d_i)^2 - S_e]/[(p - 2)S_e] = [kS_w/(p - 2)S_e]$$

which, when the fit is perfect, is approximately distributed as F with $p - 2$ and k degrees of freedom

PLANNING OF EXPERIMENTS

That not all experimental conditions serve equally well in the evaluation of the reactivity ratios has been noted by other workers.[3] In general, those experimental conditions which generate circular joint confidence limits (or elliptical confidence limits with the axes of the figure parallel to the coordinate axes in an orthogonal r_1, r_2 space) are preferred, since they yield the maximum amount of information with regard to the values of r_1 and r_2. The consequence of a poor choice of experimental conditions is illustrated in Figure 1, while Figure 3 illustrates the results of an excellent choice of experimental conditions.

The data which generated Figure 1 showed considerable scatter, thus illustrating the obvious points that no calculation scheme can get good answers from bad data and that no amount of good planning can overcome the uncertainty generated in the answers by sloppy experimentation. The nonlinear least-squares calculation method can do no more than obtain the most likely values from the data at hand and report the uncertainty in these best or most likely values. Following the guidelines given below will insure circular-type confidence limits, but the magnitude of these limits depends upon the skill of the experimenter.

Some broad rules for determining the concentrations of M_1 and M_2 which lead to precise estimates of the reactivity ratios have been set out in the literature on polymer chemistry.[3] These rules are in general agreement with a criterion used by Box and Lucas[13] in a discussion of the problem associated with the estimation of the parameters of functions which are nonlinear in these parameters. The criterion of Box and Lucas leads to the minimization of the area of the approximate joint confidence limits. Their method, applied in context, requires the finding of the two concentrations

M_{21} and M_{22} of monomer 2 which, for the best available estimates for r, and r_2, maximize the modulus of the determinant D, where

$$D = \begin{vmatrix} \dfrac{\partial G(M_{21};\ r_1, r_2)}{\partial r_1} & \dfrac{\partial G(M_{21};\ r_1, r_2)}{\partial r_2} \\[2ex] \dfrac{\partial G(M_{22};\ r_1, r_2)}{\partial r_1} & \dfrac{\partial G(M_{22};\ r_1, r_2)}{\partial r_2} \end{vmatrix}$$

Some care must be exercised in applying this criterion since it is theoretically possible for the modulus of D to have more than a single extreme, and hence the application of this method under certain circumstances could lead to the selection of a poor set of experimental conditions. However, we have not observed more than a single extreme for the copolymer equation. An alternate procedure which accomplishes the same result but circumvents this possible difficulty requires determining the coordinates of the simplex of maximum volume (area in this case) that can be placed in the envelope generated by graphing the values of $\partial G(M_2;\ r_1, r_2)/\partial r_1$ and $\partial G(M_2;\ r_1, r_2)/\partial r_2$ evaluated on the domain of M_2. This procedure will disclose all the extremes on the domain on which the function is defined. Such a graph is shown in Figure 4, using $r_1 = 0.0908$ and $r_2 = 10.07$, and for this particular case the conditions which maximize D are

$$M_{21} = 0.0343$$

and

$$M_{22} = 0.2024$$

To facilitate future experimental work, we have computed conditions which maximize D for selected values of r_1 and r_2, and these are given in Table IV as mole percentages of M_2. These concentrations have been computed with sufficient accuracy so that estimates of M_{2i} for the reactivity ratios not shown in the table can be obtained by interpolation in terms of $\log[M_{2i}/(1 - M_{2i})]$ and $\log[r_i]$.

While this does not provide exact values, these estimates are sufficiently close to the exact values that the improved estimates of the reactivity ratios are well estimated.

Suppose that preliminary experimental work leads to the estimates of r_1 and r_2 as follows: $r_1 = 1.5$, $r_2 = 0.30$. Then the pair of experimental conditions that should be used to obtain more precise estimates of the reactivity ratios would be found by reading down the left side of the table to $r_1 = 1.5$ and thence across to the column headed by $r_2 = 0.30$, which shows that the appropriate mole percentages of M_2 are $100\ M_{21} = 40.596$ mole-% and $100 M_{22} = 87.976$ mole-%. While Table IV only contains the appropriate mole percentages of monomer 2 when $r_1 \geq r_2$, the experimental conditions when $r_2 > r_1$ can also be obtained from the table by permuting subscripts. Thus if one has preliminary estimates $r_2 = 0.6$ and $r_1 = 0.3$, then the experimental conditions required are obtained as follows.
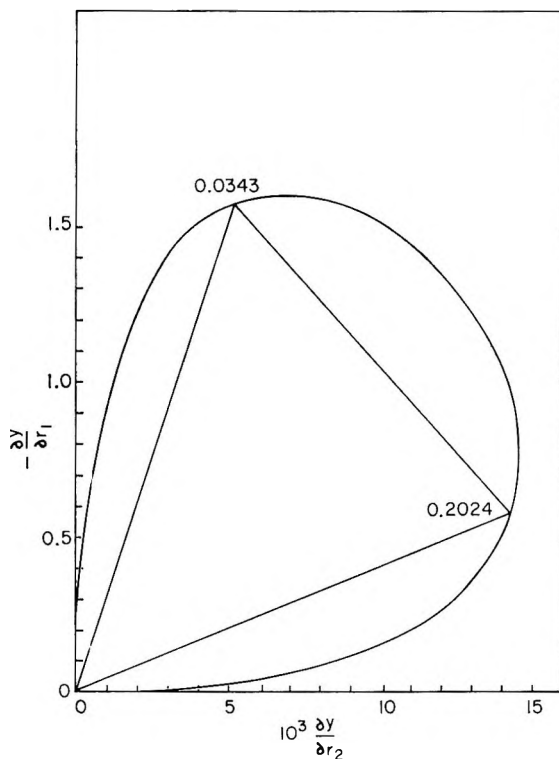
Fig. 4. Simplex of maximum area that can be placed in the envelope generated by the partial derivatives.

Enter the table for $r_1 = 0.6$ and $r_2 = 0.3$. Then $100\ M_{11} = 22.983$ mole-% and $100\ M_{12} = 87.015$ mole-%. Hence for $r_2 = 0.6$ and $r_1 = 0.3$, the two values of the mole percentages of monomer 2 are $100\ M_{21} = 100 - (1 - M_{11}) = 77.017$ mole-% and $100\ M_{22} = 100\ (1 - M_{12}) = 12.985$ mole-%.

A somewhat less exact estimate of the appropriate experimental conditions can be obtained by use of the following:

$$M_{21} \simeq r_1/(2 + r_1)$$

and

$$M_{22} \simeq 2/(2 + r_2)$$

Throughout this section, it has been assumed that reasonable estimates of r_1 and r_2 were available to serve as a starting point. Such initial estimates can be obtained from the Q and e scheme, or by making some preliminary runs. In this laboratory, it is a common practice to make four runs in such a way as to generate a good Fineman-Ross plot, using the full potential of the linearization method. The r values thus obtained are then used to select from Table IV the best set of conditions for further work, and two ad-

TABLE IV

Experimental Conditions (mole-% M_2) Appropriate for the Precise Estimation of the Reactivity Ratios Given Preliminary Estimates

r_1	r_2 0.05	0.10	0.15	0.20	0.30	0.40	0.50	0.60	0.70	0.80	0.90	1.00
0.05	2.441 / 97.559											
0.10	4.767 / 97.558	4.773 / 95.228										
0.15	6.988 / 97.557	6.998 / 95.223	7.007 / 92.993									
0.20	9.110 / 97.555	9.126 / 95.219	9.139 / 92.986	9.150 / 90.849								
0.30	13.082 / 97.553	13.109 / 95.212	13.129 / 92.974	13.140 / 90.840	13.138 / 86.863							
0.40	16.726 / 97.551	16.764 / 95.206	16.785 / 92.968	16.787 / 90.838	16.746 / 86.893	16.655 / 83.346						
0.50	20.081 / 97.549	20.125 / 95.202	20.140 / 92.967	20.123 / 90.845	20.017 / 86.945	19.839 / 83.473	19.614 / 80.386					
0.60	23.179 / 97.547	23.227 / 95.200	23.224 / 92.969	23.178 / 90.862	22.983 / 87.015	22.702 / 83.627	22.369 / 80.637	22.012 / 77.988				
0.70	26.048 / 97.546	26.093 / 95.198	26.064 / 92.976	25.979 / 90.886	25.682 / 87.101	25.283 / 83.797	24.837 / 80.904	24.377 / 78.352	23.919 / 76.081			
0.80	28.714 / 97.544	28.746 / 95.199	28.687 / 92.987	28.553 / 90.916	28.140 / 87.193	27.620 / 83.977	27.063 / 81.177	26.503 / 78.713	25.957 / 76.526	25.435 / 74.565		
0.90	31.196 / 97.543	31.211 / 95.200	31.111 / 93.000	30.923 / 90.952	30.384 / 87.298	29.744 / 84.163	29.079 / 81.447	28.426 / 79.066	27.802 / 76.955	27.208 / 75.061	26.651 / 73.349	

1.00	33.508 / 97.542	33.503 / 95.203	33.356 / 93.017	33.108 / 90.993	32.444 / 87.408	31.684 / 84.352	30.918 / 81.714	30.177 / 79.407	29.479 / 77.363	28.824 / 75.531	28.212 / 73.874	27.639 / 72.361
1.50	43.071 / 97.540	42.882 / 95.234	42.444 / 93.132	41.872 / 91.237	40.596 / 87.976	39.331 / 85.260	38.158 / 82.942	37.085 / 80.921	36.110 / 79.129	35.220 / 77.521	34.405 / 76.062	
2.00	50.192 / 97.543	49.748 / 95.283	48.992 / 93.281	48.122 / 91.512	46.363 / 88.522	44.748 / 86.060	43.309 / 83.964	42.027 / 82.137	40.879 / 80.515	39.845 / 79.055		
2.50	55.680 / 97.549	54.955 / 95.347	53.913 / 93.442	52.804 / 91.784	50.699 / 89.015	48.846 / 86.747	47.233 / 84.816	45.814 / 83.131	44.556 / 81.632			
3.00	60.026 / 97.558	59.028 / 95.418	57.747 / 93.604	56.458 / 92.043	54.106 / 89.454	52.093 / 87.337	50.364 / 85.536	48.855 / 83.961				
3.50	63.542 / 97.571	62.300 / 95.492	60.824 / 93.761	59.400 / 92.285	56.874 / 89.844	54.752 / 87.850	52.943 / 86.153					
4.00	66.441 / 97.585	64.976 / 95.568	63.354 / 93.912	61.830 / 92.508	59.181 / 90.193	56.984 / 88.303						
4.50	68.869 / 97.601	67.214 / 95.643	65.476 / 94.054	63.878 / 92.713	61.143 / 90.505	58.895 / 88.703						
5.00	70.931 / 97.618	69.114 / 95.716	67.256 / 94.188	65.635 / 92.903	62.839 / 90.788							
7.50	77.825 / 97.714	75.521 / 96.049	73.480 / 94.750	71.724 / 93.665								
10.00	81.737 / 97.811	79.251 / 96.321	77.180 / 95.172									
12.50	84.269 / 97.902	81.737 / 96.543	79.695 / 95.502									
15.00	86.054 / 97.985	83.535 / 96.729										
17.50	87.388 / 98.059	84.906 / 96.886										
20.00	88.425 / 98.126	85.997 / 97.021										

ditional runs are made at each of the two best conditions. This is essentially the procedure used to obtain the data of Table III.

It is interesting to note that the experimental conditions required to give precise estimates of the reactivity ratios will in all cases result in polymers containing close to 30% and 70% m_2. Thus, a high degree of accuracy may be obtained inasmuch as polymer analyses can be quite accurate at these levels.

APPENDIX

Some general comments on the difficulties that exist with the various methods of estimating the reactivity ratios are available in the literature.[3,5] To our knowledge, no mathematically rigorous argument has ever been presented with respect to any of the methods,* and we are unable to discover any specific discussion of the method of Fineman and Ross.

Although Fineman and Ross suggest that the method of least squares can be applied to the problem of estimating the reactivity ratios from experimental data, it is clear that this procedure, as they apply it, does not yield results which have the properties usually attributed to least-squares estimates. Further, it is not possible to compute the precision with which the Fineman-Ross "estimates" are determined, since the "dependent variable" in their formula [see eq. (5)] clearly does not have constant variance given some reasonable and rational assumptions about the distribution of the errors in the observed polymer composition. Finally their "independent variable," which in least squares is customarily assumed to be exact, contains a variable which has a stochastic element.

We have used in the past and plan to continue using the Fineman-Ross method to obtain initial estimates for the procedure we describe in the main body of this report. However we consider it to be too poor a method to use in the final evaluation of our hard earned data. We substantiate this assertion below.

While the equations and methods described in the polymer literature are mathematically correct, their difficulties in giving good estimates of the reactivity ratios stem from the fact that they fail to provide for the random variation that is inherent in all experimentally obtained observations.

As a consequence of this fact, these methods can be shown to yield estimates of the reactivity ratios which are less precise than those methods which are designed to cope with random errors; this was adequately illustrated by R. A. Fisher in 1922.[14] Fisher's work leads to the conclusion that those methods which fail to provide for random variations in the observations result, in principle, in the throwing away of a significant portion of the data. This may not be serious if the number of observations is large, however if one has only a few observations, it is difficult to justify the "throwing away" of any observations.

*Note added in proof: After this paper was written, this problem was rigorously treated by Behnken, D. W., *J. Polymer Sci.*, **A2**, 645 (1964).
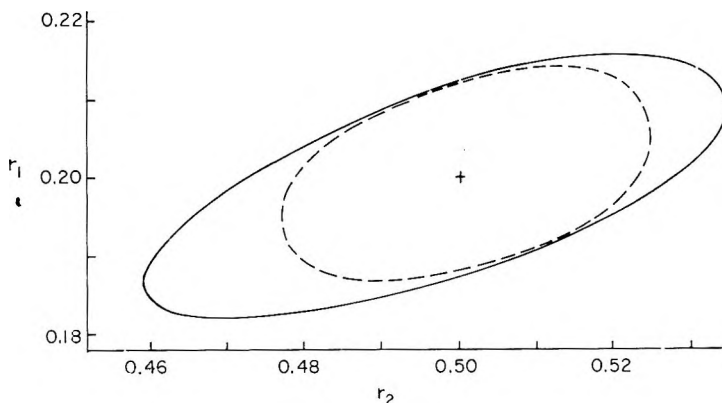
Fig. 5. Approximate 95% confidence limits for the Fineman-Ross and the nonlinear least-squares estimation procedure: (———) Fineman-Ross; (- - -) least squares.

The method described by Fisher is known as the method of maximum likelihood, and the properties of maximum likelihood estimates are discussed in all the standard reference texts on mathematical statistics (see in particular, p. 498 *et seq.* of reference 15). His work also shows that if maximum likelihood estimates can be found, they cannot be improved upon. Under the assumption that the errors in the observations are normally and independently distributed with constant variance, the nonlinear least-squares method we describe above yields maximum likelihood estimates of the reactivity ratios. If the assumption of normality is only approximately correct, the least-squares method still gives estimates which have been shown to have desirable asymptotic properties.[14]

To illustrate, we give the following example. Shown in Figure 5 are the 95% joint confidence limits for the values of r_1 and r_2 for both the nonlinear least-squares method and the Fineman-Ross procedure. While it is possible to obtain the confidence limits for the estimates obtained by the nonlinear least-squares procedure by the method described in the main body of this report, it was necessary to resort to other procedures to obtain these confidence limits for the Fineman-Ross method. The results shown in Figure 5 for the Fineman-Ross procedure were obtained in the following manner.

Computing the values of m_2 for $r_1 = 0.2$, $r_2 = 0.5$, and $M_2 = 0.1$, 0.2, 0.3, 0.4, 0.5, 0.6, 0.7, 0.8, and 0.9, we added to these nine values of m_2 random normal deviates which had mean values equal to zero and a standard error of 0.005. We then computed the estimates of r_1 and r_2 using the least-squares procedure as described by Fineman and Ross. This we repeated 500 times, using on each repetition a new set of random normal deviates, each set of normal deviates having the same mean value and standard error. From the 500 pairs of estimates of the reactivity ratios, we were able to graphically obtain the approximate 95% joint confidence limits shown in Figure 5.

Comparison of the approximate 95% joint confidence limits for the two methods clearly shows the superiority of the nonlinear least-squares procedure.   It should be noted that these limits were obtained for conditions which would be expected to make the Fineman-Ross method look good, i.e., the monomer concentrations were chosen to favor the Fineman-Ross procedure.

While we have chosen not to do the necessary work to illustrate the following assertion, it can readily be seen that the statements made about the Fineman-Ross procedure are also true when applied to the other classical methods of obtaining the reactivity ratios described in the main body of this report.

References

1. Morton, M., and F. R. Mayo, *Unsolved Problems in Polymer Science*, National Academy of Sciences-National Research Council Publication 995, 1962, pp. 9–11.

2. Young, L. J., *J. Polymer Sci.*, **54**, 511 (1961).

3. Alfrey, T., J. J. Bohrer, and H. Mark, *Copolymerization*, Interscience, New York, 1952, pp. 8–23.

4. Mayo, F. R., and F. M. Lewis, *J. Am. Chem. Soc.*, **66**, 1594 (1944).

5. Mayo, F. R., and C. Walling, *Chem. Rev.*, **46**, 191 (1950).

6. Fineman, M., and S. D. Ross, *J. Polymer Sci.*, **5**, 259 (1950).

7. Skeist, I., *J. Am. Chem. Soc.*, **68**, 1781 (1946).

8. Box, G. E. P., *Bull. Inst. Intern. Statistique*, **36**, 215 (1958).

9. Hartley, H. O., *Technometrics*, **3**, 269 (1961).

10. Chapin, E. C., G. E. Ham, and R. G. Fordyce, *J. Am. Chem. Soc.*, **70**, 538 (1948).

11. Beale, E. M. L., *J. Roy. Statist. Soc.*, **B22**, 41 (1960).

12. Thompson, B. R., and R. H. Raines, *J. Polymer Sci.*, **41**, 265 (1959).

13. Box, G. E. P., and H. L. Lucas, *Biometrika*, **46**, 77 (1959).

14. Fisher, R. A., *Phil. Trans. Roy. Soc.* (*London*), **A222**, 309 (1922); reprinted in *Contributions to Mathematical Statistics*, Wiley, New York, 1950.

15. Cramér, H., *Mathematical Methods of Statistics*, Princeton Univ. Press, Princeton, N. J., 1958, p. 498.

Résumé

On expose une méthode non-linéaire des moindres carrés pour résoudre les rapports de réactivité r_1 et r_2 de la copolymérisation.   Cette nouvelle méthode est supérieure à toutes les autres méthodes employées jusqu'ici pour les raisons suivantes: (*1*) on obtient une seule paire de valeurs, qui ne dépend pas du jugement de l'expérimentateur, (*2*) on peut démontrer d'une façon mathématique que cette paire de valeurs est la meilleure que l'on puisse obtenir à partir des résultats, (*3*) les erreurs sont définies quantitativement en termes clairs, (*4*) les résultats sont contrôlés pour voir s'ils correspondent bien à l'équation de la copolymérisation.   On explique aussi une base de sélection des conditions expérimentales qui permet d'obtenir des résultats à partir desquels on peut tirer des valeurs précises pour les rapports de réactivité.   On donne aussi sous forme de tableaux les conditions expérimentales appropriées pour obtenir ces valeurs précises pour un large domaine de valeurs de r_1 et r_2.

Zusammenfassung

Eine nichtlineare Methode der kleinsten Quadrate zur Auflösung nach r_1 und r_2, den Copolymerisationsreaktivitätsverhältnissen, wird entwickelt.   Diese neue Methode ist allen anderen bisher benützten Methoden in folgender Weise überlegen: (*1*) Ein

einziges Wertepaar wird erhalten, welches nicht vom Gutdunken der die Daten auswertenden Person abhängt; (2) es kann mathematische gezeigt werden, dass dieses Wertepaar das beste aus den benützten Daten erhältliche Paar ist; (3) die Fehler werden quantitativ in physikalisch sinnvoller Weise definiert; (4) die Daten werden in bezug auf ihre Anpassung an die Copolymergleichung überprüft. Eine Grundlage zur Auswahl der Versuchsbedingungen, welche Daten, aus denen Werte der Reaktivitätsverhältnisse erhalten werden können, liefern, wird entwickelt, und geeignete Versuchsbedingungen zur Gewinnung dieser genauen Werte in einem weiten Bereich von r_1- und r_2-Werten werden in Tabellenform augegeben.

Probabilistic Model for the Structure of the Microfibril of Cellulose

D. MEJZLER, *Institute for Fibres and Forest Products Research, Ministry of Commerce and Industry, Jerusalem, Israel*

Synopsis

A probabilistic model is presented for the structure of an "ideal" microfibril of cellulose and the distribution of weak bonds along this microfibril is calculated. Exact and asymptotic formulas are derived for the number and weight distributions and for the corresponding averages. The relationship is examined between the model of Kuhn, accepted in theory of random degradation of chain polymers, and the probabilistic model which describes the structure of the ideal microfibril of cellulose.

Introduction

The purpose of this article is to present a probabilistic model for a certain hypothesis concerning the structure of the microfibril of cellulose.[1,2] We should note, however, that we are concerned with an "ideal" microfibril and we do not intend to consider how closely the ideal microfibril approximates the actual one.

According to the hypothesis, the structure of the ideal microfibril resembles that of a brick wall. Let us visualize a monomer having the shape of a cube with a side length of unity, and let us consider a chain molecule having N links (monomers) as a brick of length N. Let us call a combination of p bricks of this kind, with their square faces touching each other, a "row" of length pN (See Fig. 1, where $N = 5$, $p = 3$).

One may regard a microfibril of length pN as a union of a certain number, m, of such rows (see Fig. 2, where $m = 9$).

In a real wall the cement is found between any two adjacent bricks which belong to the same row as well as between any two adjacent bricks belonging to different rows. It is also usually the case that when two bricks belonging to different rows touch each other the end of one will coincide with the middle of the other. For the structure of the microfibril, however, we shall assume that (*a*) the cement is found only between two adjacent bricks which do not belong to the same row, while bricks which belong to the same row are not cemented together; (*b*) the mutual position of two bricks which touch each other and belong to different rows is random in the following sense: denote by 0, 1, ..., $N - 1$ the ends—say the left-hand ones—of each of the monomers of which the brick A is composed. Then the left-hand end of brick B—which touches A but does not belong to the same
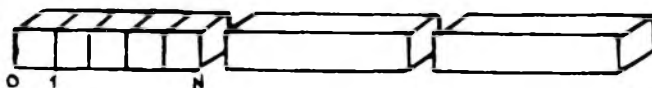
Figure 1.
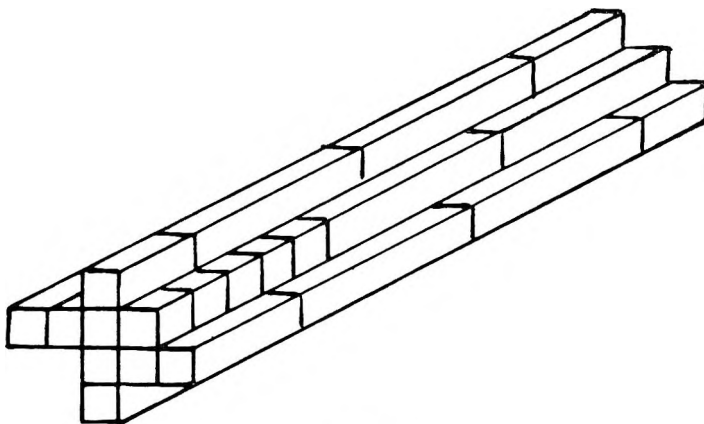
Figure 2.

row—may coincide, with equal probability, with any one of the points $0, 1, ..., N - 1$.

On the two ends of a real wall one may find half bricks. However, in view of assumption (b), at the ends of the ideal microfibril there may appear various different parts of the original brick molecule. It is however clear that the length of any such part is always measured in terms of an integral number of units and that the sum of lengths of the two parts belonging to the same row is always equal to N.

Consider now a microfibril formed by a random union of m rows of length pN, according to assumptions (a) and (b) (Fig. 2). It should be noted that for our purpose the form of the cross section of the microfibril is not important at all: it could be a rectangle, square or any polygon consisting of the unit squares, i.e., of the unit square cross sections of the cube-shaped monomers.

Since the bricks within a single row are not cemented to each other [assumption (a)], the adjacent square-shaped sides will appear, as it were, as "cracks" in the structure. Any cross section of the microfibril which contains at least one crack in its plane will be called a "weak bond," and our purpose is to determine the distribution of weak bonds along the microfibril.

Our problem can be related to various probabilistic schemes. It seems, however, most natural to use the language which is customary in the theory of random degradation of chain polymers, since our problem, as will be seen later, is analogous to that involved in the theory of random degradation. For this reason we shall begin with a short description of one of the models of random degradation. We shall then present the probabilistic formulation of our model and develop the necessary formulas. Finally,

we shall investigate the relationship between our formulas and the corresponding ones used in the theory of random degradation of chain polymers.

Kuhn's Model

The simplest mathematical model for the purpose of describing the degradation process of chain polymers is that of Kuhn.[3] This model deals with an initial chain having $(N + 1)$ links and N bonds. The process of degradation is regarded as a sequence of random trials each of which breaks one of the bonds. It is assumed that the degradation is random, i.e., that all bonds still intact at any one stage of the degradation have the same probability of being broken.

After m trials the initial chain will be converted into $(m + 1)$ chain fragments. If we measure the length n of every chain by the number of its links, then the number distribution of the chains by their length after m trials is given by the formula[4]

$$P(n,m) = \binom{N - n}{m - 1} \Big/ \binom{N}{m} \tag{1}$$

where $P(n,m)$ denotes the expected value of the relative frequency of the chains of length n after m trials. It is more common to use the weight distribution

$$F(n,m) = n \binom{N - n}{m - 1} \Big/ \binom{N + 1}{m + 1} \tag{2}$$

where $F(n,m)$ denotes the expected value of the weight of all the molecules of length n relative to the total weight $(N + 1)$.

The "degree of degradation" is defined by the ratio

$$\alpha = \text{number of bonds broken/initial number of bonds} \tag{3}$$

Therefore, according to our notation

$$\alpha = m/N \tag{4}$$

The fact that N is usually a fairly large number enables us to use simpler formulas, which are obtained from eqs. (1) and (2) by passing to the limit $N \to \infty$ and assuming

$$\alpha = \lim_{N \to \infty} (m/N) \tag{5}$$

This leads to the formulas

$$P(n, \alpha) = \alpha (1 - \alpha)^{n-1} \tag{6}$$

$$F(n, \alpha) = n\alpha^2(1 - \alpha)^{n-1} \tag{7}$$

where $P(n, \alpha)$ and $F(n, \alpha)$ are the limiting expressions for $P(n, m)$ and $F(n, m)$.

The number-average $\bar{n}(\alpha)$ and weight-average $\bar{n}_w(\alpha)$ of the distributions (6) and (7) are given by eqs. (8) and (9), respectively:

$$\bar{n}(\alpha) = 1/\alpha \tag{8}$$

$$\bar{n}_w(\alpha) = (2 - \alpha)/\alpha \tag{9}$$

The Probabilistic Formulation of Our Model

The arrangement of the weak bonds along the microfibril can be described by the distribution of the lengths of the partial microfibrils which are obtained when we cut the original microfibril at each weak bond. We can, therefore, treat the distribution of the weak bonds as if resulting from the degradation of the original microfibril. This distribution is entirely independent of the number p of bricks in a row, because our ideal microfibril is made up of a homogeneous material, i.e., all bricks (molecules) have the same length N. It is therefore sufficient to consider the distribution of the weak bonds along one brick.

Let us consider a segment $[0, N]$, the projection of the brick as a chain of length N and the points $1, 2, ..., N - 1$, as its bonds. Consider now a sequence of random trials in each of which the probability of a given bond being broken is constant and equals $1/N$, in contrast to Kuhn's model, where this probability is a function of the serial number of the trial. In our model we have initially $N - 1$ unbroken bonds and one chain. A trial may or may not result in one bond being broken; if a bond is broken, the number of unbroken bonds decreases by one, while the number of chains increases by one. It follows that the sum of the number of unbroken bonds and the number of chains must remain constant and equal to N.

It is easily seen that our model reflects the structure of the ideal microfibril described in the introduction. Our purpose is to determine the distribution of chains by length and weight after m trials.

It will be noted that our model will still be valid if we consider as weak bonds only those cross sections passing through the cracks on the envelope of the microfibril, and ignore those including the cracks located in the interior. In this case m will denote the number of rows which participate in the envelope of the microfibril (and not the number of all the rows which constitute the microfibril).

Expected Value of the Number of Fragments after m Trials

In our model, unlike in Kuhn's, the number of all the chains after m trials is not defined uniquely: it is a random variable which we denote by $\mu(m)$. As a result of an additional trial, $\mu(m)$ may either increase by one unit or remain unchanged. In other words, the possible values of the random variable δ, defined by

$$\delta = \mu(m + 1) - \mu(m) \tag{10}$$

are 0 and 1. δ assumes the value 1 if and only if as a result of $(m + 1)$th trial one bond out of all bonds still intact after the mth trial is broken. Just before the $(m + 1)$th trial, however, there are $N - \mu(m)$ bonds, therefore, the probability of a bond being broken on this trial is

$$[N - M(m)]/N$$

where $M(m)$ denotes the expected value of $\mu(m)$.   Hence, the expected value $E(\delta)$ of δ is

$$E(\delta) = 1 - M(m)/N$$

We obtain from eq. (10) eq. (11):

$$M(m + 1) - (1 - 1/N)M(m) = 1 \tag{11}$$

This is a linear difference equation of first order.   Its general solution is

$$M(m) = C(1 - 1/N)^m + N$$

where C is a constant independent of m.   Taking into account the initial conditions $M(0) = 1$, we obtain eq. (12):

$$M(m) = (N^{m+1} - (N - 1)^{m+1})/N^m \tag{12}$$

Expected Value of the Number of Fragments of Length n after m Trials

Let us denote by $\sigma(n,m)$ the random variable, number of chains of length n after m trials, and by $S(n,m)$ its expected value.   As a result of one additional trial, there are only four possibilities with respect to $\sigma(n,m)$: it may decrease by one unit, it may remain unchanged, it may increase by one unit or increase by two units.   Therefore, the possible values of the random difference

$$\delta = \sigma(n,m + 1) - \sigma(n,m) \tag{13}$$

are -1, 0, 1, and 2.

The variable δ assumes the value -1 if and only if one of the bonds of any of the $\sigma(n,m)$ chains of length n is broken as a result of the $(m + 1)$th trial. The number of all bonds of all chains of length n, which exist after the mth trial, is

$$(n - 1)\ \sigma(n,m)$$

Therefore, the probability of $\delta = -1$ is

$$(n - 1)S(n,m)/N$$

For δ to assume the value 2 a chain of length $2n$ must be broken at the $(m + 1)$th trial.   Each such chain contains only one bond, the breaking of which will produce two new chains of length n each.   Therefore, the probability of $\delta = 2$ is $S(2n,m)/N$.

In order to have $\delta = 1$ it is necessary to break at the $(m + 1)$th trial a chain of length k, where $k > n$, $k \neq 2n$.   Each of these chains contains two

bonds, the breaking of which will produce an additional chain of length n. Therefore, the probability of $\delta = 1$ is

$$(2/N) \sum_k S(k,m)$$

where the sum runs over all natural values of k which satisfy: $n + 1 \leqslant k \leqslant N$, $k \neq 2n$.

We thus obtain for the expected value $E(\delta)$ the equality

$$E(\delta) = -\frac{(n-1)S(n,m)}{N} + \frac{2}{N} \sum_k S(k,m) + \frac{2}{N} S(2n;m)$$

In view of eq. (13) we have

$$E(\delta) = S(n,m+1) - S(n,m)$$

hence we obtain the equation

$$S(n,m+1) = \frac{N-n+1}{N} S(n,m) + \frac{2}{N} \sum_{k=n-1}^{N} S(k,m) \qquad (14)$$

Thus a difference equation is again obtained. The initial conditions are

$$S(k,0) = 0 \text{ if } 1 \leqslant k \leqslant N-1; \quad S(N,0) = 1 \qquad (15)$$

Using eqs. (14) and (15) we can compute $S(k,m)$ successively for each k and m. It can be shown that $S(n,m)$ is given by the formulas

$$S(n,m) = [(N-n+1)^{m+1} - (N-n-1)^{m+1} - 2(N-n)^{m+1}]/N^m$$
$$\text{if } 1 \leqslant n \leqslant N-1$$
$$S(N,m) = 1/N^m \qquad (16)$$

The formula for $S(N, m)$ is obvious: a chain of length N will be obtained after m trials if and only if in each one of these trials all $(N-1)$ original bonds remain intact. By using the method of complete induction it can be shown that eq. (16) holds also for every n, $1 \leqslant n \leqslant N-1$ (see Appendix).

Distribution of the Chains by Length and Weight: Exact and Asymptotic

The expected value of the relative frequency of chains of length n after M trials is defined by the formula

$$P(n,m) \cong S(n,m)/M(m)$$

(for large values of m)
Hence, by using eqs. (12) and (16) we obtain

$$P(n,m) = \frac{(N-n+1)^{m+1} + (N-n-1)^{m+1} - 2(N-n)^{m+1}}{N^{m+1} - (N-n)^{m+1}}$$
$$\text{if } 1 \leqslant n \leqslant N-1$$

$$P(N,m) = 1/(N^{m+1} - (N-1)^{m+1}) \qquad (17)$$

The expected value of the overall weight of all the molecules of length n relative to the total weight N is defined by

$$F(n,m) = nS(n,m)/N$$

In view of eq. (16) we have

$$F(n,m) = n[(N - n + 1)^{m+1} + (N - n - 1)^{m+1} - 2(N - n)^{m+1}]/N^{m+1}$$

$$\text{if } 1 \leqslant n \leqslant N - 1$$

$$F(N,m) = 1/N^m \tag{18}$$

The mean value $\bar{n}(m)$ of the distribution (17) is conveniently computed by

$$\bar{n}(m) = N/M(m)$$

Using eq. (12) we obtain

$$\bar{n}(m) = N^{m+1}/(N^{m+1} - (N - 1)^{m+1}) \tag{19}$$

Somewhat more complicated is the computation of the mean $\bar{n}_w(m)$ of the distribution (18), which is defined by

$$\bar{n}_w(m) = \sum_{k=1}^{N} kF(k,m)$$

The final formula, which will not be derived here, is

$$\bar{n}_w(m) = (2/N^{m+1}) \sum_{k=1}^{N} k^{m+1} - 1 \tag{20}$$

In problems with which our model is intended to deal, the number N is of the order of thousands of units, so that it is justified to use asymptotic distributions. If we pass to the limit in eqs. (17) and (18), when $N \to \infty$ and assuming that eq. (5) is valid, we obtain for the corresponding limit distributions eqs. (21) and (22):

$$P(n,\alpha) = e^{-(n-1)\alpha}(1 - e^{-\alpha}) \tag{21}$$

$$F(n,\alpha) = ne^{-(n-1)\alpha}(1 - e^{-\alpha})^2 \tag{22}$$

where e is the base of the natural logarithms.

The limiting number-average and weight-average can be obtained either by passing to the limit in eqs. (19) and (20) or directly from eqs. (21) and (22). It can be shown that

$$\bar{n}(\alpha) = 1/(1 - e^{-\alpha}) \tag{23}$$

$$\bar{n}_w(\alpha) = 2/(1 - e^{-\alpha}) - 1 \tag{24}$$

These formulas are more easily handled, if instead of α we introduce the parameter β defined by

$$\beta = 1 - e^{-\alpha} \tag{25}$$

We then have

$$P(n,\alpha) = \beta(1 - \beta)^{n-1} \tag{21'}$$

$$F(n,\alpha) = n\beta^2(1 - \beta)^{n-1} \tag{22'}$$

$$\bar{n}(\alpha) = 1/\beta \tag{23'}$$

$$\bar{n}_w(\alpha) = (2 - \beta)/\beta \tag{24'}$$

Relationship with Kuhn's Formulas

If we compare eq. (21') with eq. (6) we see that in both models the chain length follows a geometric distribution. The definition of the concept "degree of degradation" may be modified to give the same meaning to the parameter α, which appears in eq. (6), and to β, which appears in formula (21').

The magnitude α, as defined by eq. (3), is meaningless in our model because the numerator of fraction (3) is not defined uniquely in our model and is a random variable. Let us now define a parameter γ, "degree of degradation," to replace definition (3) as follows: γ = expected value of the number of bonds broken/initial number of bonds. The magnitude γ is meaningful in both models: it is the reciprocal of the number-average $\bar{n}(\alpha)$.

In Kuhn's model the new definition coincides with the original definition (3), since from eq. (8) we get $\gamma = \alpha$, whereas in our model, according to eq. (23), we have $\gamma = \beta$, where β is defined by eq. (25). On the other hand, with γ so defined, in both models the chain length distribution assumes the same form

$$P(n,\gamma) = \gamma(1 - \gamma)^{n-1}$$

If γ is sufficiently small, there is no practical difference between eqs. (6)–(9) and eqs. (21')–(24'), since

$$\lim_{\alpha \to 0} (\beta/\alpha) = 1$$

The analogy between the chain distribution in the degradation of chain polymers and distribution of weak bonds in the microfibril suggests that the latter problem may be generalized in the same manner as it has been done with the theory of random degradation. Thus for instance the model of Montroll[4,5] does not assume a single chain, but rather a certain distribution $\{p_n\}$ of chains, where p_n denotes the initial relative frequency of chains of length n. A similar generalization of our problem enables us to treat a microfibril built of nonhomogeneous material, viz., the case when the rows of the microfibril are composed of bricks of different lengths. Such treatment may include cases which are closer to the physical reality.

APPENDIX

We shall now prove that (16) is in fact the formula which solves eq. (14) for the initial conditions (15). We may assume that $1 \leqslant n \leqslant N - 1$.

If we insert $m = 0$ in eq. (14), we obtain from (15)

$$S(n,1) = 2/N$$

for all $1 \leqslant n \leqslant N - 1$. The same result follows from eq. (16), if we insert $m = 1$.

Let us therefore assume that (16) is true for a certain m and prove that it is true for $(m + 1)$. From eqs. (14) and (16) we obtain:

$$S(n,m + 1) = \frac{N - n + 1}{N^{m+1}} [(N - n + 1)^{m+1}$$

$$+ (N - n - 1)^{m+1} - 2(N - n)^{m+1}] + \frac{2}{N^{m+1}}$$

$$\times \left[1 + \sum_{k=n+1}^{N-1} (N - k + 1)^{m+1} \right.$$

$$\left. + \sum_{k=n+1}^{N-1} (N - k - 1)^{m+1} - 2 \sum_{k=n+1}^{N-1} (N - k)^{m+1} \right] \quad (26)$$

If we assume $N - k + 1 = t$, we have

$$1 + \Sigma_1 = 1 + \sum_{k=n+1}^{N-1} (N - k + 1)^{m+1} = 1 + \sum_{t=2}^{N-1} t^{m+1} = \sum_{t=1}^{N-1} t^{m+1}$$

Similarly we obtain

$$\Sigma_2 = \sum_{k=n+1}^{N-1} (N - k - 1)^{m+1} = \sum_{t=1}^{N-n-2} t^{m+1}$$

$$\Sigma_3 = \sum_{k=n+1}^{N-1} (N - k)^{m+1} = \sum_{t=1}^{N-n-1} t^{m+1}$$

Hence

$$1 + \Sigma_1 + \Sigma_2 - 2\Sigma_3 = (N - n)^{m+1} - (N - n - 1)^{m+1}$$

Therefore, using eq. (26), we obtain, after elementary transformations,

$$S(n,m + 1) = [(N - n + 1)^{m+2} + (N - n - 1)^{m+2} - 2(N - n)^{m+2}]/N^{m+1}$$

which is identical with eq. (16), if $(m + 1)$ is substituted for m.

References

1. Mark, H., in *Cellulose and Cellulose Derivatives*, E. Ott, H. M. Spurlin, and M. W. Graflin, Eds., Interscience, New York, 1954, p. 250.

2. Meyer, K. H., and L. Misch, *Helv. Chim. Acta*, **20**, 232 (1937).

3. Kuhn, W., *Ber.*, **63**, 1503 (1930).

4. Mejzler, D., J. Schmorak, and M. Lewin, *J. Polymer Sci.*, **46**, 289 (1960).

5. Montroll, E., *J. Am. Chem. Soc.*, **63**, 1215 (1941).

6. Ohad, I., and D. Mejzler, *J. Polymer Sci.*, **A3**, 407 (1965).

Résumé

On présente ici un modèle probable pour la structure d'une microfibrille de cellulose 'idéale' et on a calculé la distribution des liens faibles le long de cette microfibrille. On a obtenu des formules exactes et asymptotiques pour la distribution en nombre et en poids ainsi que pour les moyennes correspondantes. On a examiné la relation entre le modèle de Kuhn, accepté dans la théorie de la dégradation statistique des chaînes polymériques, et le modèle le plus probable qui décrit la structure d'une microfibrille idéale de cellulose.

Zusammenfassung

Ein Wahrscheinlichkeitsmodell für die Struktur einer "idealen" Zellulosemikrofibrille wird aufgestellt, und die Verteilung schwacher Bindungen in dieser Mikrofibrille wird berechnet. Exakte und asymptotische Beziehungen für die Zahlen- und Gewichtsverteilung und für die entsprechenden Mittelwerte werden abgeleitet. Die Beziehung zwischen dem in der Theorie des statistischen Abbaus von Kettenpolymeren angenommenen Modell von Kuhn und dem Wahrscheinlichkeitsmodell, welches die Struktur der idealen Zellulosemikrofibrille beschreibt, wird untersucht.

On the Ultrastructure of Cellulose Microfibrils

I. OHAD and D. MEJZLER, *Department of Biological Chemistry, The Hebrew University of Jerusalem, Israel,* and the *Institute for Fibers and Forest Product Research, State of Israel Ministry of Commerce and Industry, Jerusalem, Israel*

Synopsis

Statistical formulae based on generally accepted models for cellulose microfibril structure were developed to calculate the mean length of microfibril segments which do not contain molecular chain-ends, i.e., "continuous segments." The calculated length of such "continuous segments" for microfibrils of 2–3 mμ cross section, containing molecules of a degree of polymerization from 2×10^3 to 6×10^3, is in the range of 300–1500 A. The relationship between "continuous segments" and crystalline and amorphous regions of cellulose microfibrils is discussed.

Introduction

The width of bacterial cellulose microfibrils (elementary fibrils in the nomenclature of Frey-Wyssling and Mühlethaler[1-3]) was considered until recently to be about 70–300 A.[4-7] Similar dimensions were attributed to cellulose microfibrils from animal[8] and plant sources.[1,9,10]

Using an improved method[11] for the measurement of the lateral dimensions of metal-shadowed bacterial and plant cellulose microfibrils, we were able to show that the above figures are an overestimation, the width of the microfibril being only about 30–35 A. and its thickness about 16–20 A.[12-15] Similar results were obtained for the width of plant microfibrils[2,14,15] and bacterial cellulose[3,14,15] by use of negative staining technique. Thus, it appears to be well established that the cellulose microfibrils from many different sources have a rectangular cross section of about 2–3 mμ.

The arrangement of cellulose molecules inside the microfibril was largely discussed by many authors.[1-3,9,10,16-18] It is now generally accepted that cellulose molecular chains are parallel to the long axis of the microfibril. Adjacent chains overlap over segments of varying length. The lateral order is variable, highly ordered regions being considered as crystalline and less ordered regions as amorphous. The length of crystalline regions is smaller than the length of a single molecule. Consequently, a molecule can traverse regions of alternating crystallinity. The amorphous region is by far more sensitive to acid degradation than the crystalline one.[16,19-21] On the basis of x-ray studies,[22] differential hydrolysis, and electron microscopy,[9,18-20,23] it was concluded that the length of the crystallites is about

600 A. (about 120 monomers) or more. Their width (uncorrected for metal deposited by shadow casting) was estimated from measurements of electron micrographs to be 50–70 A.[19,20]

However, Morehead[19] and Heyn[24,25] have found also crystallites 22–42 A. wide, a value more compatible with the lateral dimensions of cellulose microfibrils as established recently.[2,3,12−15] Similar low values were calculated from x-ray diffraction patterns.[26]

It has been assumed that crystalline regions in the microfibril are surrounded by or embedded within the amorphous material. Since the lateral dimensions of the microfibril are found to contain only about 16–36 molecules in cross section, lateral alternation of crystalline and amorphous material seems unlikely. It appears thus probable that amorphous and crystalline regions alternate only along the length of the fiber. It is also possible that amorphous regions coincide with microfibril regions containing molecular chain-ends.

The aim of this work has been to find out whether the distribution of the molecular chain-ends along a microfibril is related to the crystallite length. For this purpose the mean length of a microfibril region which does not contain chain-ends (which will be referred to as a "continuous segment") has to be calculated. This would be possible with the aid of several assumptions concerning the internal arrangement of cellulose molecules, their number in cross section, and their length.

Results and Discussion

The number of molecules (m) in the cross section of a microfibril can be deduced from its lateral dimensions. In the following calculations we shall use data for m based on lateral dimensions as previously accepted (100–300 A. range) as well as those established by more appropriate techniques (16–35 A. range).[2,3,14,15]

The length of cellulose molecules expressed in number of monomers N, was found by many authors to be in the range of 2,500–10,000.[6,7,27−30] The N values for a given sample show a normal distribution which often has a very narrow range.[28] In the model used below as a basis for our calculations we shall assume that N has a definite constant value.

We further assume that: (1) molecular endpoints are distributed randomly along the microfibril; (2) two parallel chains can be displaced longitudinally toward each other only by a whole monomer unit length (this assumption is based on the general structural feature of the crystallographic unit cell of cellulose microfibrils[31]); (3) there are no gaps between the ends of two consecutive chains situated on the same line along the long axis of the microfibril. The above assumptions concern only an "ideal microfibril" model. Departures from this model will be considered as well.

Based on this model, Mejzler[32] has worked out a formula (1) which enables us to calculate the mean length of a continuous segment as defined above.

Let N be the degree of polymerization of the cellulose molecule, m the number of molecules in the cross section of a microfibril, $P(n,m)$, the relative frequency of a "continuous segment" of length n, and $F(n,m)$, the overall relative weight of the fragments of length n. If N has a large value it is possible to show that the distributions $P(n,m)$ and $F(n,m)$ may be calculated to a close approximation by using the equations:

$$P(n,m) = \beta(1 - \beta)^{n-1} \tag{1}$$

$$F(n,m) = n\beta^2(1 - \beta)^{n-1} \tag{2}$$

where

$$\beta = 1 - e^{-m/N} \tag{3}$$

The mean value of $\bar{n}$ for the distribution of P, and $\bar{n}_w$ for the distribution of F can be calculated by using eqs. (4) and (5):

$$\bar{n} = 1/\beta \tag{4}$$

$$\bar{n}_w = (2 - \beta)/\beta \tag{5}$$

If m/N is a small number, then $\beta = m/N$, and hence $\bar{n}$ and $\bar{n}_w$ can be calculated by more simplified formulae:

$$\bar{n} \doteq N/m \tag{6}$$

$$\bar{n}_w \doteq 2N/m \tag{7}$$

The values $\bar{n}$ and $\bar{n}_w$ for different values of m and N were calculated by means of eqs. (6) and (7); the results are given in Table I.

The structure of cellulose microfibrils may differ in many respects from the model used as the basis for these calculations and we shall now consider to what extent deviations from this model affect the calculated values.

(1) Cellulose samples are polydisperse with regard to the value of N. The relationship between $\bar{n}$ and N for different values of m can be calculated from eq. (4) and is represented in Figure 1. (2) It is not known whether gaps between the ends of two molecules situated on the same long axial

TABLE I
Calculated Values for $\bar{n}$ and $\bar{n}_w$ for Different Values of m and N[a]

m	$N = 2500$		$N = 6000$	
	$\bar{n}$	$\bar{n}_w$	$\bar{n}$	$\bar{n}_w$
16	157	313	375	749
36	69.9	139	167	333
300	8.8	16.7	20.5	40
1000	3.0	5.0	6.5	20

[a] N = degree of polymerization. m = number of molecules in cross section of the microfibril. The values of m and N are taken from the literature,[6-8,13,19,27,28] m being calculated on the basis of lateral dimensions of the microfibril and the cellulose crystallographic unit cell.[31]

line lead to discontinuities, nor what are the lengths of such discontinuities and their distribution. Data obtained so far by means of the negative staining technique[2,3,14,15] support the view that if such discontinuities exist, they are less than about $30 \times 30 \times 30$ A. Considering the rigidity and tensile strength properties of cellulose microfibrils[3,18] and the small number of molecules they contain in cross section, it is conceivable that discontinuities are probably few, not extensive, and therefore can be neglected in the above calculations.
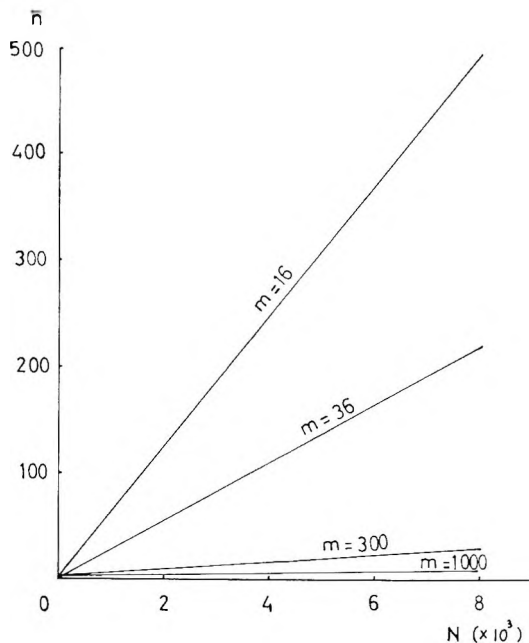
Fig. 1. Relationship between the calculated mean length of a "continuous segment" n and the degree of polymerization N for microfibrils containing different numbers of molecules in cross section m.

The data presented in Table II show good correlation between the length of a "continuous segment" and the crystallites of cellulose microfibrils when the number of molecules in the cross section is small. These results are consistent with the hypothesis that crystalline regions and "continuous segments" are identical.

It was proposed that the amorphous regions which are easily hydrolized by mild acid treatment are distributed randomly along the microfibril length.[21] This would be readily explainable assuming that the hydrolytic cleavage of cellulose microfibrils starts at amorphous regions around randomly distributed chain-ends, since in a microfibril of 2–3 mμ cross section, nearly all the molecules, and therefore nearly all the chain-ends, are on the surface of the microfibril and exposed to hydrolysis.[3,13] Thus the possible identity between crystallites and "continuous segments" as de-

TABLE II
Calculated Length of Continuous Segments ($\bar{n}$) for Microfibrils of Different Lateral Dimensions as Compared with Experimental Data for Crystallite Length

Cross section, A^{2a}	% of molecules on the surface of micro-fibril[a]	m^a	References	$\bar{n}^b$	Crystallite length[c]	References
5×10^2	75–100	16	13	150–375	100	18,20,23
					110–280	33
1.2×10^3	60	36	3	69–167	150–450	26
					60–200	34
10^4	25	300	4–8	8–20		
9×10^4	15	1000	1,10	3–6		

[a] Calculated values from the lateral dimensions of microfibrils as determined from electron micrographs and the crystallographic unit cell of cellulose.[31]

[b] The lower values of $\bar{n}$ are calculated for $N = 2500$; the higher value for $N = 6000$ (Table I).

[c] Length is expressed as degree of polymerization.

TABLE III
Calculated Weight Per Cent p Removed by the Dissolution of a Microfibril Segment of Length a for Different Values of m and N^a

m	N	p					
		$a = 10$	$a = 20$	$a = 30$	$a = 40$	$a = 50$	$a = 60$
16	2500	6.16	11.9	17.4	22.5	—	—
	6000	2.61	5.2	7.7	10.0	12.4	14.7
36	2500	13.2	24.7	—	—	—	—
	6000	5.8	11.2	16.4	21.2	—	—
300	2500	65.5	—	—	—	—	—
	6000	37.2	—	—	—	—	—
1000	2500	95.2	—	—	—	—	—
	6000	75.9	—	—	—	—	—

[a] a and N are expressed in monomer units.

scribed above provides a further basis for the understanding of the initial hydrolysis of cellulose microfibrils.

Assuming that the hydrolysis occurs only at amorphous regions around molecular chain-ends, it is also possible, by using eq. (8), to calculate the weight per cent (p) of cellulose removed after the dissolution of a segment of length a ($-$monomer units).

$$p = 1 - e^{-am/N}[a(e^{m/N} + e^{-m/N}) - (2a - 1)] \tag{8}$$

Table III shows the results of this calculation.

Fig. 2. Schematic model for the arrangement of cellulose molecules in an ideal cellulose microfibril: (cs) "continuous segment"; (ce) chain-ends; (N) length of a molecular chain; (m) number of molecules in cross section of a microfibril; (a) length of a segment dissolved around molecular chain-ends by initial acid hydrolysis.

The number of continuous segments or points of chain ends along a microfibril of length N equals $N/\bar{n}$ and approximates m. The per cent length $p(l)$ removed from this microfibril would be calculated from eq. (9).

$$p(l) = am/N \times 100 \tag{9}$$

Dissolution of about 10% by weight of the cellulose samples during the initial hydrolysis is considered sufficient to remove the amorphous part of the microfibrils.[21,33] Thus the length a of the segment removed by the initial hydrolysis (around the molecular chain ends), as calculated for a microfibril containing up to 36 molecules in cross section having a degree of polymerization of 2×10^3–6×10^3, is about 10–20 monomer units or about 5–28% of the microfibril length. These figures seem reasonable. However, similar calculations for microfibrils of 100–300 A. cross section ($m = 300$–1000) yield unlikely results (Table III). This can be explained if we assume a different arrangement of molecules in the wide microfibrils or what appears to be no less probable, that microfibrils of such lateral dimensions are nonexistent. Though it might appear daring on the basis of results obtained for cellulose microfibrils of bacterial and some plant primary walls to infer that the cross sections of cellulose microfibrils from all sources have similar small dimensions, this is nevertheless a possibility to be envisaged. The same methods were used in measuring the cellulose microfibrils now proved to be about 30 A. wide, as well as microfibrils from many other sources, which are still considered to be 100 A. wide. Assuming an overestimation of width in the latter case as in the former, it is likely that the width of both kinds of microfibrils is identical.

If the distribution of molecular chain-ends is not related to the distribution of amorphous regions and the molecular chain-ends are distributed randomly we would expect the crystallites to contain molecular fragments equal to or shorter than their observed length. This would result in a discrepancy between the mean length of the crystallites as measured from electron micrographs and the value of the degree of polymerization obtained from viscosity measurements after their dissolution. However, it appears that there is a good correlation between data obtained by both methods for a given cellulose sample.[19,23]

The main features of the model describing the molecular arrangement of cellulose chains in an ideal microfibril as used throughout this work are represented schematically in Figure 2.

The identification of the crystalline regions of cellulose microfibrils with "continuous segments" and of the amorphous regions with regions contain-

ing molecular chain-ends is rather tentative. Determination of crystallite length associated with careful measurements of the *true lateral dimensions* of the native cellulose microfibril for samples of different degree of polymerization is now possible. Correlation between the experimental data obtained for crystallite length and the calculated value for "continuous segment" would provide further support for their identity.

References

1. Frey-Wyssling, A., *Die Pflanzliche Zellwand,* Springer-Verlag, Berlin, 1959, p. 12.

2. Mühlethaler, K., *Z. Schweiz. Forstv.,* **30,** 55 (1960).

3. Frey-Wyssling, A., and K. Mühlethaler, *Makromol. Chem.,* **62,** 25 (1963).

4. Mühlethaler, K., *Biochim. Biophys. Acta,* **3,** 527 (1949).

5. Frey-Wyssling, A., and K. Mühlethaler, *J. Polymer Sci.,* **3,** 172 (1946).

6. Rånby, B. G., *Arkiv. Kemi,* 4 (14), 249 (1952).

7. Colvin, J. R., *J. Cell Biol.,* **17,** 105 (1963).

8. Rånby, B. G., *Arkiv. Kemi,* 4 (13), 241 (1952).

9. Preston, R. D., *The Molecular Architecture of Plant Cell Walls,* Chapman and Hall, London, 1952, pp. 89–90.

10. Preston, R. D., in *The Interpretation of Ultrastructure,* R. J. C. Harris, Ed., Academic Press, New York, 1962, p. 325.

11. Ohad, I., D. Danon, and S. Hestrin, *J. Cell Biol.,* **17,** 321 (1963).

12. Hestrin, S., in *Biological Structure and Chemical Function,* 1st International Symp. IUB/IUBS, Vol. 1, Academic Press, 1961, p. 315.

13. Ohad, I., D. Danon, and S. Hestrin, *J. Cell Biol.,* **12,** 31 (1962).

14. Ohad, I., and D. Danon, *J. Israel Chem. Soc.,* **1,** 194 (1963).

15. Ohad, I., and D. Danon, *J. Cell. Biol.,* **22,** 302 (1964).

16. Mark, H., in *Cellulose and Cellulose Derivatives,* E. Ott, H. M. Spurlin, and M. W. Graflin Eds., Interscience, New York, 1954, p. 250.

17. Rånby, B. G., and R. W. Noe, *J. Polymer Sci.,* **51,** 337 (1961).

18. Krässig, H., and W. Kitchen, *J. Polymer Sci.,* **51,** 123 (1961).

19. Morehead, F. F., *Textile Res. J.,* **30,** 549 (1950).

20. Rånby, B. G., *Discussions Faraday Soc.,* **11,** 158 (1951).

21. Sharples, A., *Trans. Faraday Soc.,* **53,** 1003 (1957).

22. Hengstenberg, J., and H. Mark, *Z. Krist.,* **69,** 271 (1928).

23. Rånby, B. G., and Ed. Ribi, *Experientia,* **6,** 12 (1950).

24. Heyn, A. N. J., *Textile Res. J.,* **19,** 163 (1949).

25. Heyn, A. N. J., *J. Am. Chem. Soc.,* **72,** 5768 (1950).

26. Treiber, E., *Die Chemie der Pflanzenzellwand,* Springer-Verlag, Berlin, 1957.

27. Von Husemann, E., and R. Werner, *Makromol. Chem.,* **59,** 43 (1963).

28. Marx-Figini, M., and G. V. Schulz, *Makromol. Chem.,* **62,** 49 (1963).

29. Marx, M., *Makromol. Chem.,* **16,** 157 (1955).

30. Marx, M., *J. Polymer Sci.,* **30,** 119 (1958).

31. Meyer, K. H., and L. Misch, *Helv. Chim. Acta,* **20,** 232 (1937).

32. Mejzler, D., *J. Polymer Sci.,* **A3,** 397 (1965).

33. Nickerson, R. F., and J. A. Habrle, *Ind. Eng. Chem.,* **39,** 1507 (1947).

34. Vogel, A., Ph.D. Thesis, Hochschulle Zürich, Dr. A. Huthig Verlag, Heidelberg, 1953.

Résumé

Des formules statistiques, basées sur les modèles généralement acceptés concernant la structure des microfibrilles de cellulose, ont été développées afin de calculer la longueur moyenne des segments microfibrillaires ne contenant pas de bouts de chaînes moléculaires. La longueur calculée de ces segments pour des microfibrilles d'une section transversale de 2 à 3 mμ et contenant des chainons cellulosiques d'un degré de polymérisation de 2 à 6 $\times$ 10³, se situe entre 300 et 1500 A. Les relations possibles entre ces segments, et les régions cristallines et amorphes des microfibrilles de la cellulose sont envisagées.

Zusammenfassung

Es wurden statistische, auf einem allgemein angenommenen Modell für die Struktur von Zellulosemikrofibrillen beruhenden Formeln entwickelt, um die Länge von Segmenten, die keine Endketten enthalten, zu berechnen. Die ungefähre Länge solcher durchlaufender Ketten von Mikrofibrillen mit etwa 2-3 mμ Durchmesser, welche Moleküle vom Polymerisationsgrad 2–6 $\times$ 10³ enthalten, wurde zu 300 bis 1500 A. berechnet. Die Beziehungen zwischen durchlaufenden Segmenten und kristallinen und amorphen Bereichen von Zellulosemikrofibrillen werden besprochen.

BOOK REVIEWS

N. G. GAYLORD, Editor

Determination of Molecular Weights of High Polymers, Ch'ien Jên-yüan,
Israel Program for Scientific Translations, Jerusalem, 1963. 156 pp.,
$7.00.

Practitioners of the molecular characterization of polymers badly need a good up-to-
date book on this subject. Unfortunately, *Determination of Molecular Weights of High
Polymers* is not such a book. It was written in 1958, in Chinese, translated into Russian
in 1962, and thence into English. Thus, it is now over six years old, and describes
techniques and equipment quite foreign to Western usage.

At first glance, the book creates a favorable impression despite its obvious shortcom-
ings. In general, experimental precautions are described rather well, and the Ap-
pendices contain some useful tabulations of data. But, when one compares *Determina-
tion of Molecular Weights of High Polymers* with the rest of the polymer literature, he
realizes that it can scarcely be recommended even at its relatively modest price.

To begin with, this book is almost the same in age, size, and coverage as P. W. Allen's
Techniques of Polymer Characterization. Despite being written from the British rather
than the American standpoint, Allen's book would without doubt be preferred by most
users in this country for readability, scope, and attention to familiar detail. Thus,
Determination of Molecular Weights of High Polymers fails to stand up to direct com-
petition.

Both books, of course, suffer today from being badly outdated in a rapidly changing
field. Their theoretical treatments are in general still sound, but many instruments and
techniques now widely used are entirely new since 1958, and one must consult the original
literature or recent review articles for more complete coverage.

The reader experienced in molecular characterization practice will probably want a
copy of *Determination of Molecular Weights of High Polymers* to insure completeness of
his library, and he will find a reasonable degree of utility in the book. It can not, how-
ever, be recommended to the novice, student, or casual reader as a modern or accurate
representation of this field.

Fred W. Billmeyer, Jr.

Rensselaer Polytechnic Institute
Troy, New York

Unsaturated Polyesters: Structure and Properties, HERMAN V. BOENIG,
American Elsevier, New York, 1964. x + 222 pp., $10.00.

The present work is an attempt at a comprehensive treatment of the relationship be-
tween the structural diversity of polyester resins and the properties of their cured prod-
ucts. The curing mechanism is discussed in terms of copolymerization principles and
original contributions are made to the problems of the effect of structure on flame re-
tardance and on the properties of coating compositions.

The key chapter, Chapter 6, is 80 pages in length and includes discussion of the rela-
tionship between backbone structure and almost all properties of interest, with the ex-
ception of electrical properties. Chapter 7 covers the effect of the unsaturated mono-

mers on properties of cured products.   In this chapter are mentioned no less than 19 monomers which are of commercial interest.   The book is well indexed.   It is a worthwhile addition to any chemical library and should be extremely useful to those engaged in tailor-making of unsaturated polyester resins.

David S. Hoffenberg

Gaylord Associates, Inc.
Newark, New Jersey

NOTES

Instrument Constant for Dynamic Tensile Modulus Apparatus

In a series of papers we have described an apparatus and a method for the determination of the elastic moduli of thin polymeric films.[1-4] A weight is attached to a 2×60-mm. strip of film, the upper end of which is clamped to a phonograph recording head, which is used to set the system into either longitudinal or transverse vibration. The cross-sectional area of the film is determined in place from the length, the density, and the transverse resonant frequency. The modulus is found from the dimensions of the specimen and the longitudinal resonant frequency.

During recent work in which the elastic modulus of cellophane was studied using this apparatus, it became apparent that the compliance of the recording head used to drive the system was influencing the results of the measurements of the stiffer films to a greater extent than had been suspected. It is the purpose of this communication to indicate how this effect was observed and how the compliance of the recording head was determined, and to correct modulus values previously reported.

Our most recent work on cellophane included measurements on a series of unsoftened films.[5] It was found that the measured moduli of these films decreased considerably with increasing thickness. Furthermore, when the measured modulus was plotted as a function of the quantity, modulus/(transverse frequency $\times$ length)^2, a straight line was obtained. A plot of this type would, however, result if the modulus were considered to be a constant, instead of varying with thickness, and if the spring constant of the apparatus were low enough to influence the result. Since the same result was obtained on a series of measurements made on films of the same gage but with various widths, it was concluded that this effect was due to the compliance of the apparatus.

A direct determination of the spring constant of the apparatus was carried out by hanging weights directly from the end of the clamp mounted in the recording head instead of on the end of a specimen. The resonant frequency of the system was then determined using a series of weights. The spring constant of the recording head was calculated from these results for a series of weights ranging from 24–108 g. The spring constant, k, was found to vary linearly with the reciprocal of the mass, m, according to eq. (1).

$$k \times 10^{-6} \text{dynes/cm.} = 16.69 - 15.83/m \qquad (1)$$

The value of the spring constant for a given mass may be used to correct the apparent modulus values obtained when using that mass to apply tension to the specimen. This is done by using eq. (2).

$$E = E_m(1 - 4\pi^2 f_l^2/k)^{-1} \qquad (2)$$

where E is the actual modulus, E_m is the measured modulus, f_l is the longitudinal frequency, and k is the spring constant of the apparatus.

This method has been used to correct the results reported in our comparison of the dynamic modulus with the Handle-O-Meter stiffness tester.[2,3]

With these results, the logarithm of the stiffness-to-modulus ratio was again plotted as a function of the thickness of the films. The line thus obtained may be represented by eq. (3)

$$S/E = 4.45 \times 10^{-13} t_\mu^{2.5} = 1.23 \times 10^{-9} t^{2.5} \qquad (3)$$

where S is the Handle-O-Meter stiffness in g., t_μ is the thickness in microns, and t is the thickness in mils.

TABLE I
Properties of Films Softened with Glycerol[a]

| Film | Relative humidity, % | E, dynes/cm.², × 10¹⁰ | | |
		Machine direction	Transverse direction	Geometric mean
Control A, unsoftened	15	15.6	9.2	12.0
	35	14.5	8.0	10.8
	81	8.9	4.9	6.6
Control B, unsoftened	15	16.2	10.6	13.1
	35	13.5	8.2	10.5
	81	7.1	4.1	5.4
Glycerol, 7.3%	15	13.1	8.8	10.7
	35	11.3	6.9	8.8
	81	5.3	3.3	4.2
Glycerol, 13.7%	15	11.7	7.3	9.3
	35	10.1	5.9	7.7
	18	3.6	2.0	2.7
Glycerol, 21.3%	15	10.2	6.1	7.9
	35	8.1	4.6	6.1
	81	3.2	1.6	2.3

[a] For further data on these films consult Table I of ref. (2).

The second form of eq. (3) replaces eq. (2a) of ref. (3) and eq. (6a) of ref. (2).   The differences between the values obtained with the corrected and uncorrected equations range from 10 to 20%.   Equation (2b) of ref. (3) and eq. (6b) of ref. (2) should now read for the sample thickness in mils

$$E \times 10^{-9} = 0.813 \, S/t^{2.5}$$

The results obtained on cellophanes softened with glycerol and water reported in ref. (1) have also been corrected.   The corrections for these films ranged from 15% for the softer films to about 70% for the stiffer ones.   These results are shown in Table I. When the logarithm of the corrected compliance* defined as $1/EV_c$, where V_c is the volume of film containing 1g. of cellulose, was plotted as a function of the quantity, x moles of water $+ 2x$ moles of glycerol per 100 g. cellulose, the results are all found to fall close to a single line as before.   This shows that the principal conclusion of ref. (1) still applies; namely, that a mole of glycerol has twice the softening effect of a mole of water.

It should be pointed out that even though this type of correction may be applied to compensate for the effect of the compliance of the apparatus, it is recommended that future apparatus be constructed using a driving device with a lower compliance in order to eliminate or at least to minimize the correction.

References

1. Hansen, O. C., Jr., L. Marker, and O. J. Sweeting, J. Appl. Polymer Sci., 5, 655 (1961).

2. Hansen, O. C., Jr., L. Marker, K. W. Ninnemann, and O. J. Sweeting, Modern Packaging, 36, 121 (1963).

* $V_c^{2/3}$ was used in ref. (1).   Unpublished work in these laboratories, however, indicates that the change in volume on swelling occurs primarily in the direction perpendicular to the plane of the sheet.   Hence, V_c is the more appropriate quantity to account for the effect of swelling.

3. Hansen, O. C., Jr., L. Marker, K. W. Ninnemann, and O. J. Sweeting, *J. Appl. Polymer Sci.*, **7**, 817 (1963).

4. Hansen, O. C., Jr., T. L. Fabry, L. Marker, and O. J. Sweeting, *J. Polymer Sci.*, **A1**, 1585 (1963).

5. Gipstein, Edward, L. Marker, E. Wellisch, and O. J. Sweeting, in press.

ORIN C. HANSEN, JR.
EDWARD GIPSTEIN
LEON MARKER
ORVILLE J. SWEETING

Olin Mathieson Chemical Corp.
New Haven, Connecticut

Steady Flow Viscosity of Aqueous Hydroxyethyl Cellulose Solutions

We have made a limited study of the concentration dependence of the steady flow viscosity of aqueous solutions of high viscosity hydroxyethyl cellulose. The polymer under consideration is available from the Hercules Powder Co., trade name Natrosol 250, viscosity type H, lot number 4429. This polymer at low concentrations yields extremely viscous solutions in water.

The sample was found to contain 2.60 combined ethylene oxide residues per anhydroglucose ring by acetylation analysis[1] and to have an ash content of 1.24% by weight. Measurements were made on solutions in water and in dilute sodium hydroxide over the concentration range of 0.5–3.5 g./100 ml. of solution. All solutions contained 0.1% Dowicide A to protect against the growth of microorganisms.

A horizontal capillary viscometer was used containing a downward right angle bend which was inserted into the solution to be measured. The inside diameter of the capillary was 0.126 cm., and two marks on the horizontal portion were 17.09 and 19.59 cm. from the vertical entrance. Flow times for the solutions between these two markings were determined. Since all flow occurs within the capillary except at the entrance, the capillary length-to-diameter ratio is high, and the solutions are very viscous, kinetic energy corrections are negligible and were disregarded. The capillary was attached to a vacuum system containing a mercury manometer so that flow times at various imposed pressure differentials could be determined. The effective capillary length was found to be 18.62 cm. by timing several Newtonian fluids of known viscosity at 25.0°C. at several applied pressure differentials. The relative viscosities of the aqueous Natrosol solutions at different applied pressures were then calculated from their flow times by using the equations.

$$\eta_{rel}(25°C.) = \text{flow time(sec.)} \times \Delta P(\text{cm.Hg})/0.0625$$

$$\eta_{rel}(48°C.) = \text{flow time(sec.)} \times \Delta P(\text{cm.Hg})/0.0398$$

The entire capillary portion of the instrument was enclosed in an oven which allowed measurements to be made at various temperatures. Samples were conditioned in the oven until temperature equilibrium was reached prior to measurement.

Since aqueous solutions of Natrosol are non-Newtonian and shear thinning, relative viscosities at zero shear (η_0) were obtained by extrapolating the linear η_{rel}^{-1} versus ΔP plots to zero applied pressure.

Log-log plots relating η_0 to concentration C at 25°C. are presented in Figure 1. The equations for these relationships are for H_2O.

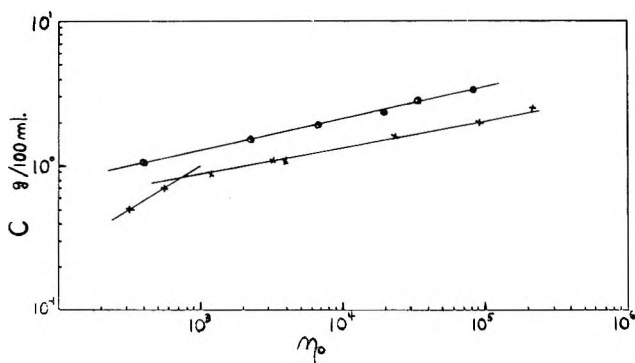$$\eta_0 = 2.15 \times 10^3 C^{5.55}$$

Figure 1.

and for 0.905N NaOH:

$$\eta_0 = 3.30 \times 10^2 C^{4.72}$$

Ferry and co-workers[2-5] have found that for many polymers, above a certain critical concentration, the relative viscosity at zero shear is proportional to C.[5] However, Onogi and co-workers,[6,7] while observing the Ferry relationship for polystyrene, find a C^6 relationship for solutions of polyvinyl alcohol (PVA) above the critical concentration. This discrepancy may be attributed to stronger intermolecular forces in concentrated PVA solutions than in solutions of polystyrene, polyisobutylene, cellulose tributyrate, etc. On the other hand, Ōyanagi and Matsumoto[8] find that PVA solutions do follow the Ferry law.

Because of the extremely high viscosities of our hydroxyethyl cellulose solutions we had to confine our study to a limited concentration range. In water, we observe the normal linear log–log plot with an exponent of 5.55 which is more in accord with the results of Onogi. In dilute sodium hydroxide, a strong hydrogen bond-breaking solvent, the exponent falls to a value of 4.72, which is closer to that of the Ferry relationship. In

TABLE I
Viscosity Data for Natrosol Solutions

System	Concn., g./100 ml.	η_0
H$_2$O, 25°C.	0.5	3.2×10^2
	0.7	5.6×10^2
	0.9	1.19×10^3
	1.1	4.0×10^3
	1.6	2.36×10^4
	2.0	9.09×10^4
	2.5	2.13×10^5
H$_2$O, 48°C.	1.0	1.46×10^3
	2.0	3.01×10^4
	3.0	2.86×10^5
0.905 N NaOH, 25°C.[a]	1.05	4.05×10^2
	1.52	2.28×10^3
	1.90	6.88×10^3
	2.38	1.91×10^4
	2.85	3.36×10^4
	3.34	8.23×10^4

[a] η_{rel} of 0.905 N NaOH at 25°C. was determined to be 1.19.

addition, the absolute values of zero shear viscosities in the dilute alkali are only a small fraction of those in water at the same concentration of polymer. These results affirm that intermolecular forces are very important in determining the viscous behavior of concentrated solutions of polar polymers.

Onogi[7] has shown that the critical concentration is reached much sooner with polar than with nonpolar polymers of the same chain length. With PVA having a chain length of 4400, the critical concentration is still as high as 7–8 wt.-%. With highly viscous Natrosol the Figure 1 discontinuity indicates that the critical concentration in water has decreased to approximately 0.8 wt.-%. In dilute alkali, however, over the concentration range 1–3.3 g./100 ml. we observe no break representative of a critical concentration effect.

From the data obtained at 48°C., apparent activation energies for viscous flow varying from 3.2 kcal. at 1 g./100 ml. up to 8.8 kcal. at the 3 g./100 ml. level are obtained in accord with generally observed results.

Data illustrating the effect of alkali concentration on the relative viscosity at zero shear for a solution containing 1.45 g. of Natrosol/100 ml. are given in Table II.

TABLE II

Effect of Alkali Concentration on η_0

NaOH concn., N	$\eta_0 \times 10^{-3}$
0	17
0.35	3.0
0.69	1.8
1.04	1.4
1.38	1.2
1.72	1.2

Small additions of alkali cause a large decrease in η_0 followed by a smaller change until a normality of 1 is reached. Further increases in alkali concentration produce no effect on η_0.

References

1. Cohen, S. G., and H. C. Haas, *J. Am. Chem. Soc.*, **72**, 3954 (1950).

2. Johnson, M. F., W. W. Evans, I. Jordan, and J. D. Ferry, *J. Colloid Sci.*, **7**, 498 (1952).

3. Ferry, J. D., L. D. Grandine, and D. C. Udy, *J. Colloid Sci.*, **8**, 529 (1953).

4. Plazek, D. J., and J. D. Ferry, *J. Phys. Chem.*, **60**, 289 (1956).

5. Landel, R. F., J. W. Berge, and J. D. Ferry, *J. Colloid Sci.*, **12**, 400 (1957).

6. Onogi, S., I. Hamana, and H. Hirai, *J. Appl. Phys.*, **29**, 1503 (1958).

7. Onogi, S., *J. Appl. Polymer Sci.*, **7**, 847 (1963).

8. Oyanagi, Y., and M. Matsumoto, *J. Colloid Sci.*, **17**, 426 (1962).

HOWARD C. HAAS
PETER J. ELORANTA*

Research Laboratories
Polaroid Corporation
Cambridge, Massachusetts

* Peter J. Eloranta participated in this work as a member of the Thayer Academy, Braintree, Mass., summer program.

INFORMATION FOR CONTRIBUTORS

1. Manuscripts should be submitted to one of the members of the Editorial Board or to the Editorial Office, c/o H. Mark, Polytechnic Institute of Brooklyn, 333 Jay Street, Brooklyn, New York 11201. Those in Europe should be submitted to Professor G. Smets, University of Louvain, Louvain, Belgium. Address all other correspondence to the publishers, Periodicals Division, John Wiley & Sons, Inc., 605 Third Avenue, New York, New York 10016.

2. Manuscripts for publication that have not been published elsewhere, books for review, and all correspondence regarding papers prior to their acceptance should be submitted to the Editorial Office. The editors desire to receive manuscripts based on original research in any phase of the chemistry and physics of large molecules.

3. It is the preference of the editors that papers be published in the English language. However, if the author desires that his paper be published in French or German, it is necessary that a particularly complete and comprehensive synopsis be furnished.

4. Manuscripts should be submitted in duplicate (one *original*, one carbon copy), typed *double space* throughout, on a *heavy* grade of paper, with margins of one inch on both sides.

5. A short synopsis (maximum 200 words) of the main contributions in the paper is required in *triplicate*. This synopsis should be carefully prepared, for it will appear in English, in French, and in German, and is automatically the source of most abstracts. A summary of the whole paper, not the conclusions alone, should form the synopsis.

6. The paper should be reasonably subdivided into sections and, if necessary, subsections. Please refer to any issue of this Journal for examples.

7. The references should be numbered consecutively in the order of their appearance and should be complete, including authors' initials and—for unpublished lectures or symposia—the title of the paper, the date, and the name of the sponsoring society. Please compile references on a separate sheet at the end of the manuscript.

8. Please do not use footnotes to the text. Materials intended for footnotes should be inserted at the appropriate point in the manuscript proper and marked for 'smal type'' (or inserted in the text as parenthetical material).

9. Please supply numbers and titles for all tables. All table columns should have an explanatory heading.

10. It is particularly important that all figures be submitted in a form suitable for reproduction. Good glossy photographs are required for halftone reproductions. For line drawings (graphs, etc.), the figures must be drawn clearly with India ink on heavy white paper, Bristol board, drawing linen, or coordinate paper with a very light blue background. The India ink lettering of graphs must be large, clear, and "open" so that letters and numbers do not fill in when reduced for publication. It is the usual practice to submit drawings that are twice the size of the final engravings; the maximum final size of figures for this journal is $4^1/_2 \times 7^1/_2$ inches.

    It is the author's responsibility to obtain written permission to reproduce material which has appeared in another publication.

    If in doubt about the preparation of illustrations suitable for reproduction, please consult the publisher at the address given above in paragraph *1* and ask for a sample drawing.

11. Please supply legends for all figures and compile these on a separate sheet.

12. Authors are cautioned to type—wherever possible—all mathematical and chemical symbols, equations, and formulas. If these must be handwritten, please write clearly and leave ample space above and below for printer's marks; please use only ink. All Greek or unusual symbols should be identified in the margin the first time they are used. Please distinguish in the margins of the manuscript between capital and small letters of [e alphabet wherever confusion may arise (e.g., k, K, κ). Please underline with a wavy line all vector quantities. Use fractional exponents to avoid root signs.

The nomenclature sponsored by the international Union of Chemistry is requested for chemical compounds. Chemical bonds should be correctly placed, and double bonds clearly indicated. Valence is to be indicated by superscript plus and minus signs.

13. Authors will receive 50 reprints of their articles without charge. Additional reprints can be ordered and purchased by filling out the form attached to the galley proof. Page proofs will not be supplied.

14. No manuscript will be returned following publication unless a request for return is made when the manuscript is originally submitted.

Manuscripts and illustrations not conforming to the style of the Journal will be returned to the author for reworking, thus delaying their appearance.